



**The Jan Mayen microcontinent
and Iceland Plateau:**
Tectono-magmatic evolution and rift
propagation

Anett Blischke



**Faculty of Earth Sciences
University of Iceland
2020**

**The Jan Mayen microcontinent
and Iceland Plateau:**
Tectono-magmatic evolution and rift
propagation

Anett Blischke

Dissertation submitted in partial fulfillment of a
Philosophiae Doctor degree in Geophysics

Advisor

Bryndís Brandsdóttir

PhD Committee

Bryndís Brandsdóttir, University of Iceland
Martyn S. Stoker, University of Adelaide (Australia)
Carmen Gaina, University of Oslo, CEED (Norway)
Freysteinn Sigmundsson, University of Iceland

Opponents

Jenny Collier, Imperial College London (United Kingdom)
Sylvie Leroy, Sorbonne Université, CNRS – ISTeP (France)

Faculty of Earth Sciences
School of Engineering and Natural Sciences
University of Iceland
Reykjavik, May 2020

The Jan Mayen microcontinent and Iceland Plateau: Tectono-magmatic evolution and rift propagation
Dissertation submitted in partial fulfillment of a *Philosophiae Doctor* degree in
Geophysics

Copyright © Anett Blischke 2020
All rights reserved

Faculty of Earth Sciences
School of Engineering and Natural Sciences
University of Iceland
Öskju, Strurlugötu 7
101, Reykjavik
Iceland

Telephone: 525 4000

Bibliographic information:

Anett Blischke, 2020, *The Jan Mayen microcontinent and Iceland Plateau: Tectono-magmatic evolution and rift propagation*, PhD dissertation, Faculty of Earth Sciences, University of Iceland, 336 pp.

Author ORCID: 0000-0001-8854-4499
ISBN: 978-9935-9412-8-2

Printing: Háskólaprent
Reykjavik, Iceland, May 2020

Abstract

This study focused on the tectono-magmatic reconstruction of the Jan Mayen microcontinent (JMMC) and Iceland Plateau Rift (IPR) in context to the breakup and opening processes of the Northeast Atlantic region. Joint interpretation of densely spaced reflection seismic data and other geophysical and geological datasets, has illuminated the complex rift relocations associated with the formation of the JMMC, a narrow section of continental crust that was detached from the central East Greenland margin during the opening of the Northeast Atlantic and activation of the Iceland Plateau Rift. The IPR represents an igneous domain consisting of four distinct stages of rifting (IPR-I to IV) each corresponding to a structural domain. A tectonic-kinematic model was constructed by utilizing structural, volcano-stratigraphic and igneous-province-mapping based on vintage and new geological, geophysical, and geochemical datasets (1960s–2017). Eleven Cenozoic seismic-stratigraphic units, define the stratigraphic framework, bound by ten unconformities and disconformities. Six of these boundaries are regional and reflect discrete tectonostratigraphic phases in the evolution of the Northeast Atlantic region. Eocene to Miocene overlapping ridge segmentation developed during seven distinct tectono-magmatic phases, initially along the Ægir Ridge and subsequently along the northward propagating Iceland Plateau Rift, that interlinked the microcontinent with the anomalous Greenland-Iceland-Faroe ridge, prior to the subaerial formation of Iceland: (1) Pre-breakup to initial breakup phase during Paleocene (~63-56 Ma), characterized by extension, fracture and rift zone formation, followed by plateau basalt emplacement of the North Atlantic igneous province; (2) Syn-breakup during Early Eocene (~55-53 Ma), with stepwise north-to-south development of seaward-dipping reflectors along the microcontinent's north-eastern margin and NV-SE striking fracture zone segments, prior to spreading at the Ægir ridge; (3) Full breakup along the microcontinent's eastern margin and initiation of IPR-I during Early-Mid Eocene (~53-50 Ma); (4) Rift-transfer during Eocene (~49-36 Ma), characterized by SW to NE magmatic propagation within the JMMC domain and forming of the IPR-II segment intersecting IPR-I, contemporary with cessation of spreading at the Ægir ridge; (5) Ridge transfer and tectonic re-arrangement during Late Eocene to Oligocene (~36-25 Ma) was associated with the formation of segment IPR-III, the south-western Jan Mayen igneous province, and the Jan Mayen trough, separating the Jan Mayen southern ridge complex from the main Jan Mayen ridge through SW-NE rift propagation. These events were accompanied by large scale intrusion and flood basalts, in clear proximity to the Iceland hotspot. (6) Final breakup during Late Oligocene (25-22 Ma) with emplacement of a second igneous breakup margin along the western flank of the microcontinent in conjunction with the formation of the IPR-IV and the proto-Kolbeinsey ridge, and the initiation of the proto-Iceland shelf region. (7) Full separation of the JMMC-IPR domains from the central East Greenland margin during Miocene (22-0 Ma) and spreading along the Kolbeinsey ridge. In summary, the initiation of the fanned-shaped Iceland Plateau Rift and the Jan Mayen microcontinent's southern ridge complex was accompanied by crustal breaches and melt incursions that formed several axial rift systems and volcanic ridges. The JMMC-IPR igneous domains portray the complexity of a long-lived (Eocene to Miocene) volcanic margin within an unstable rift-transfer tectonic setting. This region represents a unique analogue Iceland-type crust; the systematic build-up of up to 10-14 km thick oceanic crust and reactivation of pre-existing structural complexes by mantle anomalies; rift-transfer processes; and overlapping sub-aerial and sub-surface igneous activity in conjunction with microplate formation.

Útdráttur

Meginmarkmið þessa verkefnis var að auka skilning okkar á uppruna og þróun Jan Mayen svæðisins (JMMC) og rekbelta Íslandssléttunnar (Iceland Plateau Rift, IPR), í samhengi við opunarferli og reksögu NA-Atlantshafssvæðisins, norðan Íslands. Myndunarsaga JMMC er tvískipt; rek eftir Ægishrygg, við opnun Atlantshafsins, klauf miðhluta Austur-Grænlands frá Noregi, og IPR-rekbeltið innan Íslandssléttunnar, vestan Ægishryggjar, klauf JMMC frá Austur Grænlandi. IPR-rekbeltið skiptist í fjögur aðskilin svæði, í tíma og rúmi. Endurskoðað og ítarlegra líkan af jarðlagafraði, eldvirkni og jarðskorpuhreyfingum svæðisins byggir á samtúlkun jarðfræðilegra, jarðeðlisfræðilegra og jarðefnafræðilegra gagna sem aflað var á árunum 1960 til 2017; fjölgeislafræðingum; endurkast- og bylgjubrotsgögnum; þyngdar-, og segulmælingum, borholugögnum og bergsýnum, sem og samanburði við aðlæg svæði. Jarðlagastafla tertíer- og kvartertímans skiptist í ellefu jarðlagasyrpur sem afmarkast af tíu mismunandi mismislegjum. Sex tengjast stærri, jarðsögulegum atburðum í reksögu Norður-Atlantshafssvæðisins, önnur svæðisbundnari rofmislægjum. Reksaga svæðisins skiptist í sjö tímabil eldvirkni og skerhreyfinga, sem endurspeglar óstöðugleika í jarðskorpuhreyfingum yfir 30 milljón ára tímabil, frá því Atlantshafið opnaðist um Ægishrygg og innan framsækna, skástíga, IPR rekbelteisins. Upprunalega tengdist IPR rekbeltið Grænlands-(Íslands)-Færeyjahrygg en færðist síðan til norðurs, og hóf að éta sig inn í meginlandsskorpu Jan Mayenhryggjar. Samhliða þróun IPR-rekbelteisins, minnkaði rekhraði á sunnanverðum Ægishrygg. Í hnotskurn er þróunarsagan eftirfarandi: (1) Gliðnun innan Laurasíuflekans hófst á paleósentímabilinu (fyrir ~63-56 milljónum ára). Upphaflega myndaðist mikill sigdalur norðan og austan JMMC, sem samanstóð af lægum brotabeltum. Áframhaldandi tog varð til þess að meginlandsskorpan slitnaði og úthafsskorpa myndaðist við öflugt uppstreymi möttulefnis og mikil flæðigos sem mynduðu stór basaltsvæði (North Atlantic Igneous Province). (2) Byrjun eósentímans (fyrir ~55-53 milljónum ára), einkenndist af myndun mikilla flæðibasaltlaga, innan skástígra gosbelta sem þróuðust frá norðri til suðurs eftir norðausturbrún JMMC. Flæðibasaltlögum (seaward dipping reflectors) hallar í átt að Ægishrygg í Noregsdjúpi. Svæðið opnaðist eftir með NV-SA-lægum brotabeltum, hraun runnu á landi og í sjó, með móbergsmýndunum og móbergssetlögum á grunnsævi. (3) Í kjölfar þess að Ægishryggur aðskilur Grænland frá Noregi snemma á eósen (~53-50 Ma), þróast framsækið rekbelti (IPR-I) við suðurenda hryggjarins, og norðurbrún Íslands-Færeyjahryggjarins. (4) Gosbeltaflutningar á mið og seinni hluta eósen (~49-36 Ma) og myndun Íslandssléttunnar. Landrek með innskotavirkni frá SV til NA eftir IPR-I og síðan IPR-II rekásunum innan Íslandssléttunnar, yfirtekur suðurhluta Ægishryggjar, þar sem gliðnun og jarðskorpumyndun minnka til muna. (5) Eósen-ólígósen (~36-25 Ma): IPR-III rekásinn með SV-NA stefnu klífur suðurenda Jan Mayen frá Lyngvahrygg við Hlésum og Suðurhryggir Jan Mayen verða til. Tímabilinu fylgdi aukið uppstreymi kviku til norð-norðausturs, undir áhrifum frá Íslands heita reitnum með tilheyrandi aukningu í innskota- og eldvirkni samfara myndun flæðigossyrpna meðfram sigdölum gosbeltanna. (6) Síð-ólígósen (~25-22 Ma): Landrek meðfram vesturbrún JMMC innan IPR-IV rekássins með flæðigossyrpum, IPR-IV er fyrirrennari Kolbeinseyjahryggjar sem markar upphaf norðausturlandsgrunns Íslands. (7) Míósen til nútíma (22-0 Ma): Með myndun Kolbeinseyjahryggjar slitnar JMMC endanlega frá Grænlandi og úthafsskorpa verður til. Verkefnið hefur varpað nýju ljósi á 30 milljón ára þróunarsögu JMMC, og hvernig suðurhryggirnir urðu til, í framsæknu gosbelti innan Íslandssléttunnar, undir áhrifum af Íslands heita reitnum, sem yfirtók rek á sunnanverðum Ægishrygg. Öflug innskotavirkni og eldvirkni innan skástígra goskerfa, einkenna innviði Íslandssléttunnar og endurspeglar fjölpættar gliðunar- og skerhreyfingar eftir flekaskilunum sem rekja má í endurkastgögnum. Tektónísk þróun rannsóknarsvæðisins er í mörgu lík Íslandi í dag, bæði einkennast af óstöðugum, framsækum rekbeltum, með innskotavirkni í gegnum eldri jarðlagastafla.

Dedication

To my family, friends, advisors and co-workers that made it possible for me to complete this work, with love, encouragement, endless patience and understanding.

"Be passionate about something and lean to that strength."

Michelle Obama

Preface

Understanding the geological evolution of an area of interest is the basis for any exploration assessment and decision making for the Icelandic government tied to their offshore licensing activity. The Jan Mayen microcontinent study was initially focused on the tectonic and volcanic development of the central part of the microcontinent – the Lyngvi ridge and the Jan Mayen southern ridge complex areas. To properly understand their formation, a comprehensive study of the Jan Mayen microcontinent and the Iceland Plateau rift region became necessary, in order to place the local region within the complex setting of the Northeast Atlantic. Consequently, a research project was proposed, which formed the basis for this doctoral work. The resulting project presents an in depth understanding of the microcontinent's structural and magmatic foundation, and the establishment of a tectono- and volcano-stratigraphic framework that enables a clear link to the area's complex geodynamic development. These objectives were achieved through detailed geological and geophysical mapping of the Jan Mayen microcontinent and the Iceland Plateau rift regions, including seismic-stratigraphic analysis of the sedimentary and igneous succession and their correlation to the study area's conjugate margins. Kinematic modelling of the northeast Atlantic region has enabled the Cenozoic evolution of the Jan Mayen microcontinent and the Iceland Plateau rift region to be reconstructed and placed within the context of continental breakup, subsequent plate reorganization, and interlinkage of the Northeast Atlantic rift system to the Iceland mantle anomaly.

This research project was established and its dissertation was written in collaboration between the Institute of Earth Sciences (IES) of the University of Iceland, the Iceland GeoSurvey (ÍSOR), the Centre for Earth Evolution and Dynamics (CEED) at the University of Oslo, the British Geological Survey (BGS) and successively the University of Adelaide. The start of the project ran concurrent with the NAGTEC project, which was a collaboration between the NW European geological surveys, including ÍSOR, and oil companies that produced a tectonostratigraphic atlas of the Northeast Atlantic as well as a comprehensive geological and geophysical database. During that work, the primary database for the project was established by the candidate, who played a key role to assemble and compile data packages for several working groups (WP1: Tectonostratigraphy; WP3: Crustal Structure; WP4: History of Igneous Provinces; or WP5: Data) within the NAGTEC project that concerned matters of the Jan Mayen microcontinent, the Iceland Plateau rift areas, and their links into the conjugate margins. Parallel to the NAGTEC and collaboration projects, was the candidate managing and initiating the first digital offshore database of for Icelandic waters, with the focus on the JMMC-IPR region, a database that is now being steadily expanded for the Icelandic shelf area by a small Icelandic offshore research community. Collaboration projects were pursued at the same time, as it was imminent and necessary to increase data coverage and understanding of the JMMC-IPR area's regional ties to its conjugate margins and oceanic domains. These concerned a high-resolution magnetic survey and analysis of the Ægir ridge by the Norwegian Geological Survey (NGU), and a detailed mapping project of the Jameson Land basin in collaboration with the Geological Survey of Denmark and Greenland (GEUS) and are both specifically acknowledged here. Both, enabling a good data-based comparison the study area and its oceanic domains, and provided a better understanding of the central East Greenland onshore and shelf margin areas.

Table of Contents

List of Figures	xiii
List of Tables.....	xviii
Abbreviations and label keys.....	xix
Acknowledgements	xxi
1 Introduction.....	1
1.1 Research aims and objectives	2
1.2 Outline of the dissertation.....	3
1.3 Previous research and analogues.....	4
1.3.1 Previous research	4
1.3.2 Microcontinents and potential analogue areas.....	8
1.4 The JMMC-IPR study synopsis	10
2 The Jan Mayen microcontinent, Iceland Plateau rift and conjugate margins.....	15
2.1 Structural and stratigraphic framework of the Jan Mayen microcontinent and Iceland Plateau rift	15
2.1.1 Jan Mayen Island igneous complex	17
2.1.2 Jan Mayen and Lyngvi Ridges.....	18
2.1.3 Eastern Jan Mayen igneous complex and fracture zone corridor	18
2.1.4 Jan Mayen basin.....	18
2.1.5 Jan Mayen trough.....	20
2.1.6 Southern ridge complex.....	23
2.1.7 Iceland Plateau rift	23
2.2 Conjugate margins of the Jan Mayen microcontinent.....	25
2.2.1 The Vøring plateau – northeastern igneous conjugate margin	25
2.2.2 Central East Greenland - western igneous conjugate margin.....	28
2.2.3 The Faroe Islands - southeastern igneous conjugate margin.....	30
2.2.4 The mid-oceanic ridge domains.....	33
2.3 Geodynamic development of the JMMC-IPR within the Northeast Atlantic.....	35
2.3.1 Pre-breakup regional setting	35
2.3.2 The JMMC region at breakup.....	36
2.3.3 Iceland Plateau rift propagation	37
2.3.4 The Cenozoic breakup, ocean and microcontinent formation	37
3 Data overview and methods	41
3.1 Description of the data.....	44
3.1.1 Bathymetry	44
3.1.2 Gravity and magnetic data sets	46
3.1.3 Seismic reflection data	47
3.1.4 Seismic refraction data	48

3.1.5	Offshore and onshore geological sample data.....	54
3.1.6	Age analysis and petrochemical data.....	55
3.2	Interpretation methods and applications	58
3.2.1	Structural elements analysis.....	58
3.2.2	Kinematic reconstructions.....	58
3.2.3	Seismic stratigraphy.....	62
3.2.4	Seismic volcano-stratigraphy	63
3.2.5	Unresolved interpretation.....	66
4	Summary	71
4.1	Paper I: The Jan Mayen microcontinent: an update of its architecture, structural development and role during the transition from the Ægir Ridge to the mid-oceanic Kolbeinsey Ridge	71
4.1.1	Summary	71
4.1.2	Main findings	72
4.2	Paper II: The Jan Mayen microcontinent's Cenozoic stratigraphic succession and structural evolution within the NE-Atlantic	73
4.2.1	Summary	73
4.2.2	Main findings	74
4.3	Paper III: Seismic volcanostratigraphic characteristics of the Jan Mayen microcontinent and Iceland Plateau rift system.....	75
4.3.1	Summary	75
4.3.2	Main findings	76
5	Conclusions	77
6	Further work.....	79
	References.....	81
	Publications.....	101
	Paper I	103
	Paper II.....	145
	Paper III.....	183
	Appendix 1: Conference paper, the Iceland Plateau – Jan Mayen volcanic breakup margin	311
	Appendix 2 Seismic reflection survey data overview	325
	Appendix 3 Regional kinematic input data	331

List of Figures

- Figure 1.1. Overview and reference map of the NE-Atlantic region, including active and extinct mid-oceanic ridges, fracture zones and tectonic elements based on Talwani et al., 1977; Einarsson and Sæmundsson (1987); Einarsson (2008); Gernigon et al. (2015), and result presented in papers I, II and III of this dissertation. Bathymetric map from IBCAO 3.0, (Jakobsson et al., 2012). Abbreviations are listed on p.xix-xx.....1
- Figure 1.2. The international commission on stratigraphy chronostratigraphic chart based on Gradstein et al. (2012) and Cohen et al. (2013; updated).6
- Figure 1.3. Correlation chart estimates by Gaina et al. (2017b) comparing plate motion changes within the Northeast Atlantic (see line corresponding coloured points in key map) to Cenozoic regional tectonic events. Seafloor spreading rates and directions. Grey undulating lines indicate changes in spreading rates and/or directions that coincide with postulated compressional dome formation along the Northeast Atlantic continental margins. Abbreviations: AFR – Africa Plate; BAB – back-arc basins; EUR – Eurasia Plate; FAR – Farallon Plate; GRN – Greenland Plate; IND – India Plate; KUL – Kula Plate; LIP S – large igneous province subduction; Medit – Mediterranean region; NAM – North America Plate; PAC – Pacific Plate; Sboff – slab break-off; and VAN – Vancouver Plate.7
- Figure 1.4. Global view of present-day microcontinent locations (modified after Nemčok et al., 2016; Gaina and Whittaker, accepted).9
- Figure 1.5. Comparison of present day Icelandic oblique rift and fracture / transfer zone systems to the oblique opening systems for the greater JMMC-IPR region (Papers I and III): (a) Early Eocene (~49 Ma) reconstruction example during IPR-II rift activity (this study) along the EJMFZ, the IPR-II-IFFZ, and the northernmost extent of the Reykjanes ridge at reconstruction time; (b) Borehole scale structural comparison of the Dalvíkur lineament (the southern segment of the TFZ) (Blischke et al., 2017b); and (c) the Reykjanes Peninsula transfer zone (Einarsson et al., in press). Displayed features: direction of the rift opening – black arrows; direction of the minimum horizontal stress field (σ_{hmin}) – red arrows; direction of the maximum horizontal stress field (σ_{Hmax}) – purple arrows; general fracture zone orientation and opening direction – blue; primary normal fault formation – black dashed lines; and rift parallel strike-slip faults that correspond to each case's locations (a-i – orange, a-ii – pink, and a-iii – green) of insert (a). Abbreviations and label keys are presented on p. xix-xx.13
- Figure 1.6. Greenland-Iceland-Faroe ridge complex crustal thickness estimates through time, by comparing age grid data (Gaina 2014) to crustal thickness data, summarized as cumulative datasets for 1 Ma increments since break-up. This crustal accretion vs. time plot is then compared to the half spreading rate profiles for the Northeast Atlantic analysis by Gaina

et al. (2009), and for the southern part of the Norway basin of the Ægir ridge by Gernigon et al. (2015). It can be shown that the Greenland-Iceland-Faroe ridge complex follows the Northeast Atlantic opening process until the rift reorganization and transfer from the Ægir ridge across to the IPR, and to the Kolbeinsey ridge. After the cessation of the Ægir ridge system, the GIFRC shows a good correlation of increased crustal volume to distinct rift systems, such as the Westffords, the Snæfellsnes–Húnaflói rift zone (SHRZ on Figure 1.1), or the Eastern Volcanic rift zone (EVRZ on Figure 1.1). Crustal volume decreases during potential rift transfer periods. 14

Figure 2.1. Shaded bathymetry (IBCAO 3.0; Jakobsson et al, 2012) structural map of the JMMC-IPR area, with faults, fracture zones and lineaments based on this study (Papers I-III; Blischke et al., 2019). Dark grey shaded area represents the 100 km wavelength filtered Bouguer anomaly level at 95 mGal, by Haase and Ebbing (2014). Chron C24n3n is based on Peron-Pinvidic et al. (2012a) and Gernigon et al. (2015). Western breakup chrons C7 and C6c are from Paper III. Abbreviations are listed on p. xix-xx. 16

Figure 2.2. Present day three-dimensional JMMC volcano-stratigraphic framework, based on Papers II and III. 17

Figure 2.3. Stratigraphic sections of the JMMC based on seismic reflection data (NPD, 2012 and 2013) tied to OBS, sonobuoy, ESP velocity profiles, and available boreholes from Paper III. Magnetic-, free air gravity data (Nasuti and Olesen, 2014; Haase and Ebbing, 2014), and large fracture zone corridor intersections (e.g. Gaina et al., 2009; Kandilarov et al., 2012; Gernigon et al., 2015; and Paper I) plotted above the profiles highlight variations associated with major tectonic and igneous events. Abbreviations are listed on p. xix-xx. 20

Figure 2.4. Present day JMMC volcanic facies and province interpretations in comparison to magnetic (Nasuti and Olesen, 2014), free air gravity and Bouguer gravity data (Haase and Ebbing, 2014). Abbreviations are listed on p. xix-xx. 21

Figure 2.5. Regional chronostratigraphic summary chart emphasizing the relationship between the volcano-stratigraphy of the JMMC in relation to its conjugate igneous margins, sea level changes, and $\delta^{18}O$ data by Van Sickle et al. (2004), Miller et al. (2008), and Murray-Wallace and Woodroffe (2014), Paleogene East Greenland ice-rafted debris occurrences by Tripathi and Darby (2018), ocean gateway interpretations (Stoker et al., 2005a,b; Stürz et al., 2017), Northeast Atlantic spreading direction changes modelled by Gaina et al. (2017a,b), main igneous provinces and rift relocations based on Sæmundsson (1979), Harðarson et al. (1997, 2008), Saunders et al. (2013), Thordarson and Höskuldsson (2008), Brandsdóttir et al. (2015), Geissler et al. (2017), Parson et al. (2017), Hjartarson et al. (2017) and this study. Mid-oceanic ridge systems and orogeny's were modified after

<i>Lundin and Doré (2002). Time scale from Gradstein et al. (2012). Abbreviations are listed on p. xix-xx.</i>	23
<i>Figure 2.6 Examples of 2D seismic reflection profiles tied with magnetic (M) and Bouguer gravity anomaly data (section locations, see Figure 2.7), outlining major fault and fracture zones in relationship to structural and igneous domain elements. Abbreviations are listed on p. xix-xx.</i>	24
<i>Figure 2.7. Volcanic facies and province map of the Jan Mayen microcontinent defined by order of emplacement: Early-Middle Eocene; Late Eocene – Oligocene; and Late Oligocene – Early Miocene, showing the igneous units, such as intrusive and extrusive strata, plateau basalt equivalent, igneous centres, SDRs, hyaloclastite volcanic strata, and flood basalts. Green lines show profile locations in Figure 2.6. IPR phases are listed in detail in Table 2.1. Abbreviations are listed on p. xix-xx.</i>	26
<i>Figure 2.8 Pre-break-up setting of the Northeast Atlantic region around 56-55 Ma based on GPlates (Boyden et al., 2011), showing (a) reconstructed present-day bathymetry, (b) free-air gravity, (c) magnetic anomaly, (d) and crustal thickness data. The JMMC-IPR area is shown with major faults, fractures zones, and lineaments that are based on this study. Bathymetry data is based on IBCAO 3.0; Jakobsson et al. (2012). Features displayed are modified from data and interpretations by Larsen, L.M. et al. (1989, 1999); Osmundsen and Andersen (2001); Torsvik et al. (2001); Foulger et al. (2005); Henriksen (2008); Le Breton et al. (2013); Peron-Pinvidic et al. (2013, 2012a); Gasser (2014); Hopper et al. (2014); Guarnieri (2015); Gernigon et al. (2015); Gaina et al. (2009, 2014, 2017a,b); and á Horni et al. (2017). Abbreviations are listed on p. xix-xx.</i>	27
<i>Figure 2.9 Conjugate margin tectonostratigraphic type sections: (a) Liverpool Land basin; (b) JMMC, (c) Milne land – Geikie plateau – Blosseville Kyst – Liverpool land basin; and (d) Blosseville Kyst – Scoresby Sund – Liverpool Land basin. The sections are tied to ESP velocity profiles, sonobuoy data and available borehole tie points. The pre-breakup section is inferred to contain Paleocene, Mesozoic to Paleozoic strata by direct comparison with the Jameson Land basin and the Blosseville Kyst areas, and seismic refraction data (Hopper et al., 2014; Blischke and Erlendsson, 2018; Papers I – III). Abbreviations are listed on p. xix-xx.</i>	33
<i>Figure 2.10 JMMC chronostratigraphic chart in comparison to regional conjugate margins of this study: (a) Regional chronostratigraphic correlation chart of the JMMC in comparison to the Faroe-Shetland basin area (modified after Ólavsdóttir et al., 2013, 2019; Ritchie et al., 2011; Stoker et al., 2013, 2018; Ellis and Stoker, 2014), the Vøring margin (Hjelstuen et al., 1997, 1999; Lundin et al., 2013), the East Greenland conjugate margin area (Pedersen A.K. et al., 1997; Larsen, M. et al., 1999, 2002, 2005; Larsen, L.M. et al., 1989, 2013; Storey et al., 2004; Japsen et al., 2014; Bonow et al., 2014), and Iceland (Sæmundsson, 1979; Harðarsson, 1997, 2008; and Hjartarson et al., 2014, 2017). Time scale used after Gradstein et al. (2012). Abbreviations are listed on p. xix-xx.</i>	34

<i>Figure 2.11. Reconstructed igneous provinces around Jan Mayen. The positions of Eastern Greenland and the Jan Mayen main tectonic blocks are shown in an absolute position (relative to the mantle) according to kinematic parameters that were computed by carrying out visual fits (in GPlates 2.0.0; https://www.gplates.org) for four groups of basement ridges mapped in this study. Five reconstruction stages are shown in (a) Early Eocene (~55-53 Ma); (b) main breakup phase (~53-50 Ma); (c) syn-breakup to rift propagation phase throughout Eocene (~49-36 Ma); (d) intra rifting phase within the JMMC along the JMT and initiation of the western igneous margin during Late Eocene to Oligocene (~36-25 Ma); and (e) final breakup phase along the western JMMC margin (~25-22 Ma) and the full formation of the Kolbeinsey ridge. Features displayed are modified from data and interpretations by Larsen, L.M. (1985, 1989, 1999, 2013); Larsen, H.C. (1990); and Blischke and Erlendsson (2018). Abbreviations are listed on p. xix-xx.</i>	<i>38</i>
<i>Figure 3.1 Regional project database (Table 3.1) showing seismic reflection (2D MCS (multi-channel data blue lines); 2D SCS (single channel data – green lines)), seismic refraction lines (red lines), borehole data (yellow points), shaded bathymetry (IBCAO 3.0; Jakobsson et al, 2012), and ETOPO1 (Amante and Eakins, 2009).</i>	<i>44</i>
<i>Figure 3.2 An overview of the Jan Mayen database on a hill shaded bathymetry map (Jakobsson et al., 2012), showing (a) 2D MCS lines and cross-sections; (b) boreholes and seabed sampling sites; (c) seismic refraction lines, and multibeam bathymetric maps. For detailed survey information and references see Table 3.1. Abbreviations are listed on p. xix-xx.</i>	<i>45</i>
<i>Figure 3.3 The velocity structure of ESP-125, see insert (a) in comparison with 2D MCS data along the western igneous margin of the JMMC (location is shown on Figure 3.2b) and (b) OBS crustal structure based on Kodaira et al. (1998), for horizon legend see Figure 2.3.</i>	<i>49</i>
<i>Figure 3.4 2D MCS stacking velocity data combined in a 3D grid compilation and highlighted high velocity anomalous areas within the JMMC region. Abbreviations are listed on p. xix-xx.</i>	<i>51</i>
<i>Figure 3.5 Variations in lower crustal velocity within the JMMC and thickness estimates between lowermost seismic reflection event of the “inferred lower crust” and the “R2” event indicate increased magmatic incursions within the IPR domain, SWJMIP, the western igneous margin, NW-JMR – JMI, and close to the segments of fracture zone terminations. Magnetic anomalies data from Haase and Ebbing, (2014). Abbreviations are listed on p. xix-xx.</i>	<i>53</i>
<i>Figure 3.6 The JMMC stratigraphic summary chart of compiled from this study, partly based on DSDP and ODP boreholes (Talwani et al., 1976a-j; Manum et al., 1976a,b,c; Raschka et al., 1976; Nilsen et al., 1978; Thiede et al., 1995; Jansen et al., 1996; Channell et al., 1999a,b; Butt et al., 2001). This</i>	

compilation is used to ties the JMMC's shallow Cenozoic stratigraphy and unconformities to the seismic reflection data.....57

Figure 3.7 GPlate reconstruction of the JMMC-IPR, modified after Gaina et al. (2017b). The different segments and blocks of the JMMC-IPR (inset) were added in this study. Plate boundaries are traced in yellow and isochron interpretations dotted in dark blue (Gaina et al., 2014, 2017b; Nasuti and Olesen, 2014). The path of opening (spreading direction) between the Eurasian plate and Greenland is indicated by green triangles, and across the GIFRC in light blue, with time steps indicated as blue stars. Also shown are flow lines during separation of the JMMC-IPR blocks from the Greenland margin based on this study (pink between East Greenland and JMMC-IPR and in grey between JMMC-IPR and the western Norway shelf margin). The JMMC-IPR block reconstruction and reconstructed time series are listed in Table 3.4 with the corresponding reconstruction times in millions of years (Ma).59

Figure 3.8 Seismic stratigraphy and facies interpretation workflow for the JMMC-IPR areas. Interpretation of lithofacies, geometries and depositional settings based on Seismic reflection and refraction data was tied to geological mapping and petrological data on land. The outcome is a seismic volcano-stratigraphic framework modified after e.g. Mitchum et al. (1977) and Heinz and Aigner (2003).64

Figure 3.9 Examples of volcanic facies types mapped across the JMMC.69

List of Tables

<i>Table 1.1 Overview of selected key research conducted prior to this study for the Jan Mayen microcontinent, Iceland Plateau, and Northeast Atlantic regions.</i>	<i>5</i>
<i>Table 2.1 Summary of the igneous phases of the JMMC-IPR and its conjugate margins.</i>	<i>29</i>
<i>Table 3.1 JMMC-IPR study offshore survey database review and summary. Selected datasets and compilations are marked in column “A” and shown in Figures 3.1 and 3.2.....</i>	<i>42</i>
<i>Table 3.2 ESP-121 to ESP-128 Profile analysis (offset T-Z; Tau-P analysis summary values tied to 2D MCS data) of this study.</i>	<i>50</i>
<i>Table 3.3. An overview of existing DSDP and ODP boreholes and drilled igneous basement, based on data summary in Hopper et al. (2014) and this study. Abbreviations are listed on p. xix-xx.</i>	<i>56</i>
<i>Table 3.4 Finite rotation parameters of various tectonic blocks relative to the Greenland Plate (plate ID 102) (a) modified after Gaina et al. (2017b); (b) – (j) this study. Eastern hemisphere longitudes have positive signs. Abbreviations and label keys are presented on p. xix-xx.</i>	<i>60</i>

Abbreviations and label keys

A		HR	Hatton-Rockall margin and basin
ÆR	Ægir mid-oceanic ridge	HVZ	Hofsjökull volcanic zone
B		I	
BB	Buðli block	IFFZ	Iceland-Faroe fracture zone
BK	Blosseville Kyst	IFR	Iceland-Faroe Islands ridge
BPU	Base Paleogene unconformity	INU	Intra-Neogene unconformity
C		IPR	Iceland Plateau rift
CJMBFZ	Central Jan Mayen basin fracture zone	J	
CNBFZ	Central Norway basin fracture zone	JM	Jan Mayen
COB	Continent ocean boundary	JMB	Jan Mayen basin
D		JMBN	Jan Mayen basin north
DB	Dreki block, Jan Mayen - Southern Rige Complex	JMBS	Jan Mayen basin south
E		JMI	Jan Mayen Island igneous complex
EB	Eggvin bank	JMLB	Jameson land basin
EJMFZ	East Jan Mayen fracture zone	JMMC	Jan Mayen microcontinent
ESP	Expanded spread profile	JMR	Jan Mayen ridge
EVRZ	Eastern volcanic rift zone	JMRN	Jan Mayen ridge north
F		JMSWIP	Jan Mayen southwest igneous province
Fm	Formation	JMT	Jan Mayen trough
FIBG	Faroe Islands basalt group	K	
FP	Faroe Islands plateau	K	Kangerlussuaq area
FSB	Faroe-Shetland basin	KB	Kap Brewster outcrop site
FYR	Fugloy ridge	KD	Kap Dalton outcrop site
G		KR	Kolbeinsey mid-oceanic ridge
GIFRC	Faroe-Iceland-Greenland ridge complex	KRB	Kolbeinsey ridge basin
GP	Geikie Plateau	L	
H		LB	Langabrá block, Jan Mayen - Southern Rige Complex
HB	Hökni block, Jan Mayen - Southern Rige Complex	LLB	Liverpool Land basin
		LLH	Liverpool Land high
		LYR	Lyngvi ridge
		M	
		MB	Møre basin
		ME	Mid-Eocene unconformity

ML	Milne Land	SRCFZ	Southern ridge complex fracture zone
MM	Møre marginal high	SVZ	Snæfellsnes volcanic zone
MMU	Mid-Miocene unconformity	SWJMBFZ	Southwest Jan Mayen basin fracture zone
MOU	Mid-Oligocene unconformity	SWJMIP	Southwest Jan Mayen igneous province
MR	Mohs mid-oceanic ridge		
MSRC	Main block, Jan Mayen - Southern Rige Complex		
N		T	
NAIP	North Atlantic igneous province	TFM	Top flood basalts marker
NJMR	Northern Jan Mayen Ridge block	TFZ	Tjörnes fracture zone
NS	North Sea	TØ	Trail Ø
NVZ	Northern volcanic zone	TPU	Top Paleogene
NWIRZ	Northwest Iceland rift zone	TSDR	Top seaward dipping reflectors
		TVIP	Trail Ø- Vøring igneous complex
O		TR	Treitel ridge
OB	Otur block, Jan Mayen - Southern Rige Complex	TV	Top NAIP plateau basalt volcanics
OBS	Ocean bottom seismograph		
		U	
P		UE1	First Upper Eocene unconformity
PB	Plateau basalt	UE2	Second Upper Eocene unconformity
Proto-KR	Proto-Kolbeinsey ridge		
		W	
R		WJMFZ	Western Jan Mayen fracture zone
RLNRZ	Reykjanes-Langjökull-North Iceland rift zone	WTR	Wyville Thomson ridge
RR	Reykjanes mid-oceanic ridge		
RPOR	Reykjanes Peninsula Oblique Rift	V	
		VB	Vøring basin
S		VM	Vøring margin
SB	Sonobuoy	VT	Vindtoppen formation
SD	Scoresby Sund		
SDR	Seaward dipping reflectors	Ö	
SHRZ	Snæfellsnes-Húnaflói rift zone	ÖSVZ	Öræfajökull-Snæfell volcanic zone
SISZ	South Iceland seismic zone		
SFZ	Spa fracture zone		
SRC	Jan Mayen microcontinent - southern ridge complex		

Acknowledgements

Funding

This research project was conducted at the University of Iceland, funded by the National Energy Authority of Iceland (Orkustofnun) and the Iceland GeoSurvey. I specifically thank the Iceland GeoSurvey and the Earth Sciences department at the University of Iceland for supporting me to finalize this project during its final stages. This project evolved in parallel with the NAGTEC (*Northeast Atlantic Geoscience TEctonostratigraphic Atlas*) and the NORDMIN (*TemaNord 2016:562*) projects. Support from industry sponsors of NAGTEC is gratefully acknowledged, just as the support through the Research Council of Norway through its Centres of Excellence funding scheme, *project number 223272*.

Facilities and data

Data permissions were provided by: Spectrum Ltd. (now TGS), TGS-NOPEC Geophysical Company ASA; the University of Oslo (UiO); the Norwegian Petroleum Directorate (NPD); the Bundesanstalt für Geowissenschaften und Rohstoffe (BGR); and GEUS (Geological Survey of Denmark and Greenland). Additionally, I thank Guðrún Helgadóttir and Páll Reynisson from the Marine Research Institute of Iceland (MRI) and the Naval Hydrographic and Oceanographic Service of France (SHOM) for their data support and cooperation. Crucial and very much appreciated were the visits to the IODP – International Ocean Discovery Program - core sample facility at the Bremen Core Repository, the core age data analysis by Robert Duncan at the OSU Argon geochronology laboratory of the College of Earth, Ocean, and Atmospheric Sciences at Oregon State University, and the geochemical core sample ICP analysis by Sæmundur A. Halldórsson at the geochemistry petrology lab at the University of Iceland and thin section analysis by Helga M. Helgadóttir at the Iceland GeoSurvey.

Advice and support

I am especially grateful to Dr. Þórarinn S. Arnarson, Orkustofnun, for his support and advice. I would also like to say a big thank-you to my project advisors Bryndís Brandsdóttir, Martyn S. Stoker, Carmen Gaina, and Freysteinn Sigmundsson, who have guided me well and shown endless patience and understanding throughout this project. Thanks also goes to my co-authors Bjarni Gautasson, Christian Tegner, Gwenn Peron-Pinvidic, Jana Ólavsdóttir, John R. Hopper, Karl Gunnarsson, Ögmundur Erlendsson, Peter Japsen, Pierpaolo Guarnieri, Sæmundur A. Halldórsson, and Sverre Planke. In addition, the project benefitted from scientific advice through publication reviews by Dieter Franke and Erik Lundin, and discussions with Asbjørn Breivik (CEED, University of Oslo), Lotte M. Larsen (GEUS), John R. Hopper (GEUS), Laurent Gernigon (NGU), Nina Lebedeva-Ivanova (CEED, University of Oslo), and Hans C. Larsen (GEUS/Tongji University).

Family

My heartfelt thanks go out to my family and friends, for their immense support and patience, and put up with endless days of absence throughout this journey.

1 Introduction

This research study aims to increase the understanding of the formation and tectono-magmatic evolution of the Jan Mayen microcontinent (JMMC) and Iceland Plateau rift (IPR) regions (also referred here as the JMMC-IPR) throughout the Cenozoic and in context to the breakup and opening of the Northeast Atlantic Ocean (73°N – 60°N and 5°E – 35°W) (Figures 1.1; 1.2). The JMMC represents a narrow section of continental crust that was detached from the central East Greenland margin during breakup and opening of the Northeast Atlantic since Early Eocene (~55 Ma) (Table 1.1a), described in chapter 2. This chapter provides an outline of the project area, highlights aims and objectives, previous research, primary results and synopsis of this study.

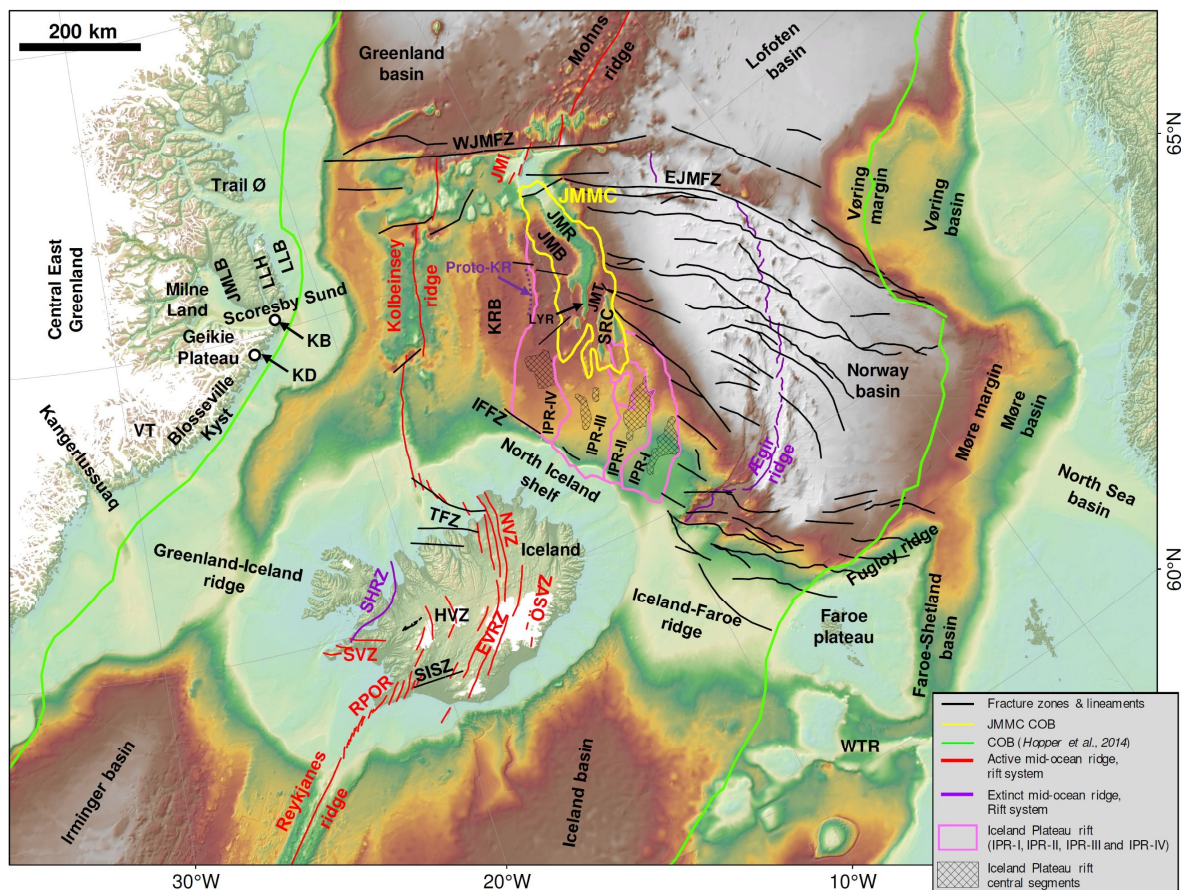


Figure 1.1. Overview and reference map of the NE-Atlantic region, including active and extinct mid-oceanic ridges, fracture zones and tectonic elements based on Talwani *et al.*, 1977; Einarsson and Sæmundsson (1987); Einarsson (2008); Gernigon *et al.* (2015), and result presented in papers I, II and III of this dissertation. Bathymetric map from IBCAO 3.0, (Jakobsson *et al.*, 2012). Abbreviations are listed on p.xix-xx.

1.1 Research aims and objectives

The primary research objective of this study was to establish a comprehensive tectonostratigraphic understanding of the Jan Mayen microcontinent and Iceland Plateau Rift areas. This included addressing sediment-stratigraphy related to tectono-magmatic events and geodynamic processes, since Early Eocene, along the southern half of the JMMC and IPR and how they are related to kinematic modelling of the central East Greenland's Blosseville Kyst, and the Iceland–Faroe fracture zone.

The project was structured around five key tasks, briefly listed below but addressed in detail in the data and methods chapter 4 of the dissertation.

1. Establish a comprehensive regional geological, geophysical, and petrochemical database and compile a bibliography to provide a detailed overview of existing data and interpretations.
2. Define and establish a detailed tectono-magmatic and stratigraphic framework for the JMMC-IPR region; specific sub-tasks include:
 - a. Tie borehole, seafloor samples, and seismic refraction data to vintage and newly acquired seismic reflection data sets.
 - b. Establish a general Cenozoic sedimentary and igneous seismic-stratigraphic framework for the JMMC-IPR region.
 - c. Conduct a stratigraphic comparison with conjugate margins of central East Greenland, SW Norway, Faroe-Shetland, Iceland, and oceanic ridges.
 - d. Model the pre-breakup setting of the JMMC-IPR region in relation to the central East Greenland and Norwegian margin domains.
 - e. Document the different types of igneous activity within the JMMC-IPR and construct a detailed timeline of igneous events.
3. Develop a detailed kinematic reconstruction of the Northeast Atlantic showing the evolution of the JMMC in relation to the general pattern of continental breakup from pre-breakup time to the present day.
4. Investigate the timing and style of igneous activity observed in the JMMC-IPR region in relation to the opening processes of the Northeast Atlantic; particularly the effects of igneous processes on the pre-breakup domains of the JMMC.
5. Assess the interconnection of the JMMC-IPR domains with the IFFZ and the GIFRC in relation to the mantle anomaly – mid-oceanic ridge interlinked systems.

1.2 Outline of the dissertation

The thesis is based on two peer-reviewed and published journal papers (Paper I and II) and one manuscript (Paper III), listed below.

- I. **Blischke, A., Gaina, C., Hopper, J. R., Péron-Pinvidic, G., Brandsdóttir, B., Guarnieri, P., Erlendsson, Ö. and Gunnarsson, K. (2017).** The Jan Mayen microcontinent: an update of its architecture, structural development and role during the transition from the Ægir Ridge to the mid-oceanic Kolbeinsey Ridge. *Geological Society, London, Special Publications*, **447**, 299–337. doi.org/10.1144/SP447.5
- II. **Blischke, A., Stoker, M. S., Brandsdóttir, B., Hopper, J. R., Peron-Pinvidic, G., Ólavsdóttir, J. and Japsen, P. (2019).** The Jan Mayen microcontinent's Cenozoic stratigraphic succession and structural evolution within the NE-Atlantic. *Marine and Petroleum Geology*, **103**, 702-737. doi.org/10.1016/j.marpetgeo.2019.02.008
- III. **Blischke, A., Brandsdóttir, B., Stoker, M. S., Gaina, C., Erlendsson, Ö., Tegner, C., Halldórsson, S. A., Helgadóttir, H. M., Gautason, B., Planke, S. and Hopper, J. R. (in preparation).** Seismic volcanostratigraphic characteristics of the Jan Mayen microcontinent and Iceland Plateau Rift system. To be submitted to *Geochemistry, Geophysics, Geosystems*, Wiley AGU publications.

A regional overview of the study area is presented in Chapter 2, including a summary of its geodynamic evolution. The data and methods section of Chapter 3 provides an overview of the dataset, data interpretation approaches and uncertainties. A summary of the main contributions of each paper, is presented in Chapter 4, along with a summary and conclusions section in Chapter 5, and ongoing and future work outlook in Chapter 6.

A first-author conference paper has been included in Appendix 1, as it shows a smaller-scale structural analysis for the Jan Mayen southern ridge complex that is important to understand the crustal and structural development within an oblique rifting scenario, and highlights further needed work and analysis, specifically in comparison to similar structures and processes across Iceland and the Icelandic shelf region.

Blischke, A., Erlendsson, Ö., Brandsdóttir, B., Hjartardóttir, Á.R. and Gautason, B. (2021). The Iceland Plateau – Jan Mayen volcanic breakup margin: An analogue for axial rift and transfer zone North Iceland. *Proceedings World Geothermal Congress 2021*, 11175, 12.

The two published papers and conference paper are presented in printed format, whereas the third paper (Paper III) is in a manuscript format along with a supplement material section.

1.3 Previous research and analogues

The study area encompasses the Northeast Atlantic (64° N to 72°N and 32°W to 5°E) including the JMMC's continental and igneous conjugate margins of central East Greenland; the central Norwegian shelf with the Møre and Vøring margins; the Faroe-Shetland region and the Greenland-Iceland-Faroe ridge (Figure 1.1). Interpretation of selected sub-areas within the JMMC and their relationship to their conjugate margins became necessary in reference to chronological time and geographical location and are summarized in chapter 2. Table 1.1 provides a detailed list of primary data sets and key research points from the beginning of this project, including joint data analyses, collaboration and co-authored publications.

1.3.1 Previous research

Previous research on tectono-magmatic processes north of Iceland associated with the opening of the Northeast Atlantic show that the tectonic evolution of the IPR and the JMMC regions since Paleocene (Thanetian) has been considerably more complex than along the Reykjanes ridge south of Iceland, or the Mohns ridge north of the Jan Mayen fracture zone (EJMFZ & WJMFZ) (Johnson and Heezen, 1967; Vogt and Avery, 1974; Talwani and Eldholm, 1977; Gairaud et al., 1978; Vogt et al., 1980; Eggen, 1984; Myhre et al., 1984; Srivastava and Tapscott, 1986; Skogseid and Eldholm, 1987; Gudlaugsson et al., 1988; Larsen and Jakobsdóttir, 1988; Åkermoen, 1989; Gunnarsson et al., 1989; Eldholm et al., 1990; Kuvaas & Kodaira, 1997; Hopper et al., 2003; Scott et al., 2005; Breivik et al., 2003; 2008; 2012; Brandsdóttir et al., 2008, 2015; Erlendsson, 2010; Peron-Pinvidic et al., 2012a,b; Gernigon et al., 2012, 2015, 2019; Gaina et al., 2009, 2014, 2017a,b, accepted) (Figure 1.1). The nature of the JMMC as a continental crustal block could until recently only be inferred based on geophysical data, as existing borehole data control is too shallow. Recent seafloor samples recovered rocks with a time range from Permian to Oligocene of Paleogene volcanic, and old metamorphically altered and younger Cenozoic sedimentary rocks (Polteau et al., 2019), which are believed to have been in-situ and not glacial drop stones. Thus, placing the JMMC firmly along the East Greenland conjugate margin with directly comparable lithologies.

Previous studies on the JMMC region focussed on regional scale reconstructions of the NE Atlantic, and were generally included in studies of its conjugate areas (Table 1.1). The primary questions of how the JMMC evolved based on its stratigraphic and volcano-stratigraphic datasets and ridge – mantle interactions, were not thoroughly addressed. The complex tectonics of this region, recorded in the stratigraphy, are linked to pre-existing structural complexities, oblique spreading, crustal block segmentation, and rift propagation within the JMMC-IPR and central NE Atlantic region. Some interpretations of the same geophysical seismic refraction and reconstruction datasets have led to contradicting results, specifically for the Iceland plateau area have been strongly debated. Some consider the southern continuation of the microcontinent, or continental fragments, to lie underneath the Iceland Plateau or even Eastern Iceland (e.g. Breivik et al., 2012; Torsvik et al., 2015; or Gaina et al., 2017b), whereas others have evoked a complex rift system to have intersected the JMMC based on reflection, gravity (Talwani and Udintsev, 1976b; Gairaud et al., 1978; Grønlie et al., 1979) and refraction data (Brandsdóttir et al., 2015).

Table 1.1 Overview of selected key research conducted prior to this study for the Jan Mayen microcontinent, Iceland Plateau, and Northeast Atlantic regions.

<i>Year</i>	<i>Reference</i>	<i>Area</i>	<i>Emphasis</i>
(a) Seismic data and tectonic analysis studies			
1976	Talwani and Udintsev, 1976	Northeast Atlantic and JMMC	Tectonic synthesis of Deep-Sea Drilling Project (DSDP Leg 38)
1978	Gairaud et al., 1978	JMMC	First data analysis.
1979	Gronlie et al., 1979	JMMC-IP	
1984	Eggen, 1984	JMMC	Seismic reflection analysis.
1984	Myhre et al., 1984	JMMC	Seismic reflection and petroleum systems analysis.
1988	Gudlaugsson et al., 1988	JMMC	Seismic reflection and petroleum systems analysis.
1977	Talwani and Eldholm, 1977	Northeast Atlantic	Tectonic synthesis of DSDP Leg 38.
1989	Åkermoen, 1989	JMMC	Seismic reflection and borehole data analysis.
1989	Gunnarsson et al., 1989	JMMC	Seismic reflection and borehole data analysis.
1997	Kuvaas & Kodaira, 1997	Kolbeinsey ridge and JMMC	OBS data acquisition and analysis.
2005	Scott et al., 2005	JMMC and Norway basin	Propagations and retreat of spreading ridges.
2009	Gaina et al., 2009	Northeast Atlantic and JMMC	Comprehensive geodynamic model of the Northeast Atlantic.
(b) Detailed data acquisitions and analysis			
2010	Erlendsson, 2010	JMMC	Mapping of newest 2D seismic reflection data (1985-2001).
2012	Breivik et al., 2012	Norway basin and Iceland Plateau	OBS data analysis of the eastern JMMC volcanic margin.
2012	Peron-Pinvidic et al., 2012a, b	JMMC	Mapping of newest 2D seismic reflection data (1985-2001).
2014	Hopper et al., 2014	Northeast Atlantic	Comprehensive regional database.
2015-2019	Gernigon et al., 2015, 2019	Norway basin and JMMC	High resolution magnetic and reconstruction study.
2018	Blischke and Erlendsson, 2018	East Greenland	East Greenland conjugate seismic reflection data mapping and tie-in to the JMMC-IPR region.
2018	Polteau et al., 2018	JMMC – Southern ridge complex	Seafloor data and analysis.
(c) Conjugate margin stratigraphic constrains			
1985-2014	Larsen, L.M., et al. 1985, 1989, 1999, 2013, 2014	Blosseville Kyst, East Greenland	Plateau basalt and igneous stratigraphy.
1997-1999	Hjelstuen et al., 1997, 1999	Vøring Plateau and margin	Tectono-stratigraphy and Cenozoic evolution.
1997	Pedersen et al., 1997	Blosseville Kyst	Plateau basalt stratigraphy.
1999-2005	Larsen, M. et al., 1999, 2002, 2005	East Greenland	East Greenland stratigraphy.
2008	Henriksen et al., 2008	Greenland	Comprehensive summary of the geology of Greenland.
2011	Ritchie et al., 2011	Faroe-Shetlands	Geology of the Faroe-Shetland basin and adjacent areas.
2013-2019	Ólavsdóttir et al., 2013, 2019	Faroe-Shetlands	Detailed mapping of the Faroe-Shetland area and the Faroe Islands.
2013	Stoker et al., 2013	Faroe-Shetlands and the NW Britain	Cenozoic sediments and tectono-stratigraphy.
2014	Bonow et al., 2014	East Greenland	Burial, uplift and exhumation history of East Greenland during the opening of the Northeast Atlantic.
2014	Ellis and Stoker, 2014	Faroe-Shetlands and Northeast Atlantic	The Faroe-Shetland basin in a regional perspective since the Paleocene for the Northeast Atlantic Ocean.
2014	Hjartarson and Sæmundsson, 2014	Iceland	Iceland's Geology
2014	Japsen et al., 2014	East Greenland	Regional unconformities.
2017	á Horni et al., 2017	Northeast Atlantic	Northeast Atlantic volcano-stratigraphic summary.
2017	Gaina et al., 2017a,b	Northeast Atlantic	Northeast Atlantic regional reconstruction and seamounts.
2017	Geissler et al., 2017	NE Greenland	Northeast Greenland conjugate margin and tectono-magmatic analysis.
2017	Hjartarson et al., 2017	Greenland-Iceland-Faroe ridge complex	Summary of rift development across Iceland and adjacent ridges.
2017	Stoker et al., 2017	Northeast Atlantic	Overview of the Upper Paleozoic–Mesozoic stratigraphy of the Northeast Atlantic region.
2017-2018	Tan et al., 2017, 2018	Eggvin Bank and the western Jan Mayen fracture zone	Seismic refraction, reflection, and gravity data analysis.

Chronostratigraphic chart

Time (Ma)	System / period	Series / Epoch	Stage / Age	Magnetic anomaly (chron)	
0		Holocene	Meghalayan / Northgrippian Greenlandian		
	Quaternary	Pleistocene	Calabrian Gelasian Piacenzian	C1	
5		Pliocene	Zanclean	C2	
	NEOGENE	Miocene	Messinian	C3	
10			Tortonian	C4	
15			Serravallian Langhian	C5	
20			Burdigalian Aquitanian	C6	
25		OLIGOCENE	Chattian	C7 C8 C9	
30			Rupelian	C10 C11 C12	
35			Priabonian	C13 C15/16	
40			Bartonian	C17 C19	
45			Eocene	Lutetian	C20 C21
50				Ypresian	C22 C23
55	PALEOCENE	Thanetian		C24 C25	
60		Selandian	C26		
		Danian	C27 C28 C29		

Figure 1.2. The international commission on stratigraphy chronostratigraphic chart based on Gradstein et al. (2012) and Cohen et al. (2013; updated).

Plate boundary complications associated with cessation of rifting at the southern Ægir Ridge have not, until recently, been studied in any detail. High-resolution geomagnetic data collected for the Jan Mayen fracture zone (EJMFZ) and the Ægir ridge areas reveal irregularities in spreading rates within the Iceland plateau and the Ægir ridge in the Norway basin (Gernigon et al., 2012, 2015). This contrasts with the symmetric magnetic anomalies that can be traced parallel to the Reykjanes ridge and Mohns ridge back to magnetic anomalies chrons C24n2r and C22 respectively (Gaina et al. 2009), highlighting the complexity of the study area.

Prior research of the JMMC-IPR area mostly relied on low coverage and large-scale analysis of seismic data (Table 1.1a). These studies showed the region to be enigmatic and complex, prompting more detailed data analyses, as denser line coverage of seismic reflection and seafloor data became available from 2001 (Table 1.1b).

Stratigraphic constraints were also obtained from published regional correlation charts, established unconformities, and paleogeographic interpretations for the northeast Atlantic region (Table 1.1c). This included regional reconstructions and changes in spreading directions (Gaina et al., 2017b) (Figure 1.3) that were essential to understand the processes that affected the JMMC-IPR area. The Gaina et al. (2017b) model is a key reconstruction within the global framework.

The model presented in this study is based on that model, filling in the reconstruction data gap for the JMMC-IPR area, highlighting major tectonic events represented by five regionally known unconformities within the JMMC-IPR region and identifying a total of 11 unconformities that reflect the local - sub-regional events that are unique to the central NE Atlantic area.

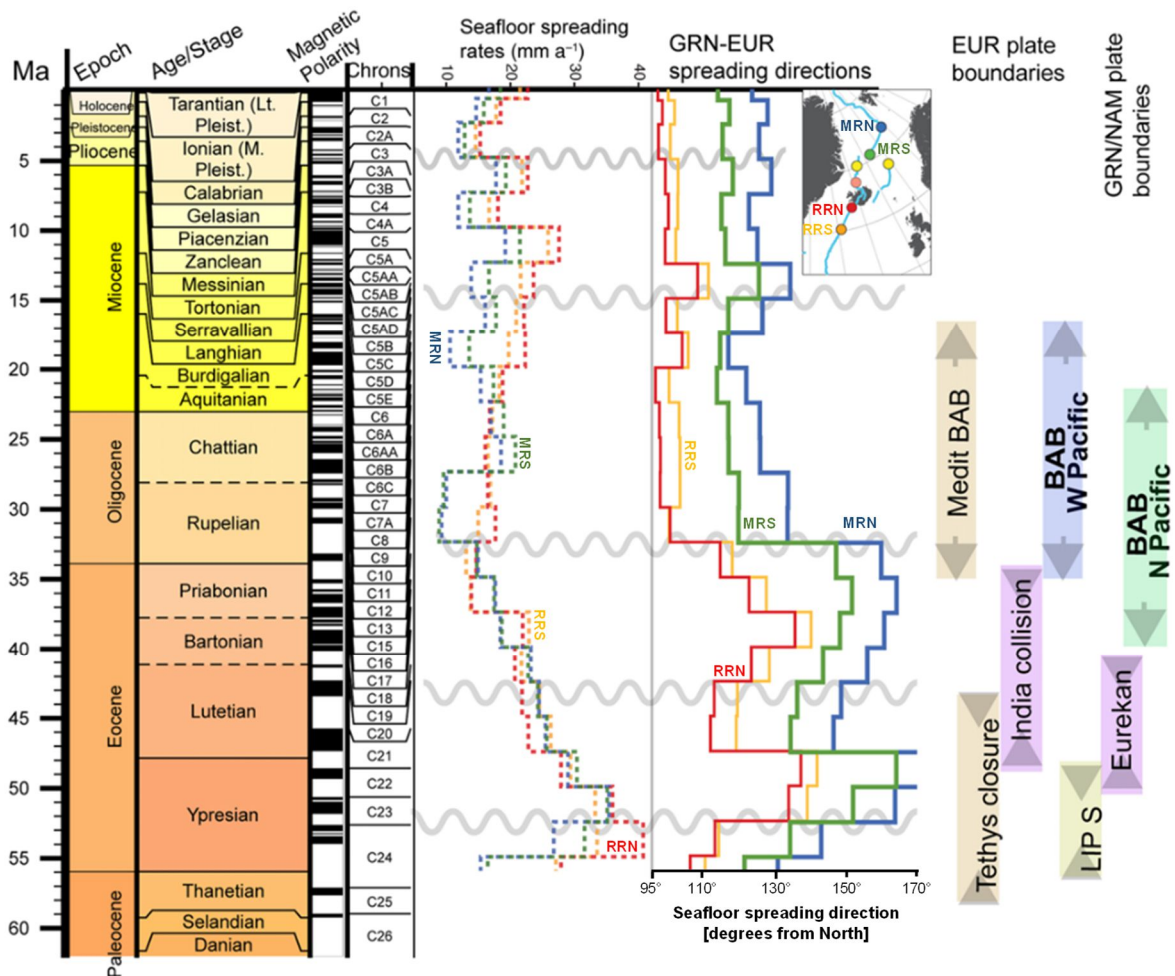


Figure 1.3. Correlation chart estimates by Gaina et al. (2017b) comparing plate motion changes within the Northeast Atlantic (see line corresponding coloured points in key map) to Cenozoic regional tectonic events. Seafloor spreading rates and directions. Grey undulating lines indicate changes in spreading rates and/or directions that coincide with postulated compressional dome formation along the Northeast Atlantic continental margins. Abbreviations: AFR – Africa Plate; BAB – back-arc basins; EUR – Eurasia Plate; FAR – Farallon Plate; GRN – Greenland Plate; IND – India Plate; KUL – Kula Plate; LIP S – large igneous province subduction; Medit – Mediterranean region; NAM – North America Plate; PAC – Pacific Plate; Sboff – slab break-off; and VAN – Vancouver Plate.

1.3.2 Microcontinents and potential analogue areas

Microcontinents are continental fragments that were detached from continental margins during oceanic crust forming and sometimes are moved far out within an oceanic domain. The processes that control microcontinent formations can relate to: (1) relocation of plate boundaries; (2) the proximity of mantle plumes; (3) wrench tectonics; (4) or inherited lithospheric heterogeneities (Gaina and Whittaker, accepted). Often, submerged microcontinents are bathymetrical features that can affected paleogeography, paleo-ocean circulation or biogeography (Gaina and Whittaker, accepted). Nemčok et al. (2016) described microcontinent formation as processes that resulted from: (1) competing wrench faults or rift zones; (2) the presence of horse-tail structure elements; and (3) multiple consecutive tectonic events controlled by different stress regimes, which focuses primarily on the structural/tectonic processes along fracture and wrench fault zone systems.

Both studies mentioned above identified extensional and strike-slip motions, and mid-ocean ridge/rift relocations as key elements for microcontinent formation. Previous studies also suggested that some microcontinents formed close to mantle plumes/hot-spot areas (e.g. Müller et al., 2001) and therefore may be associated with Large Igneous Provinces (LIPs) (Figure 1.4). As JMMC has a continental origin, is surrounded by oceanic lithosphere, but also affected by igneous activity (see section 3.1.4), it can be considered a classical microcontinent formed due to mid-ocean ridge relocation triggered by the proximity of a mantle plume (e.g. Müller et al., 2001). Similar examples may be the Seychelles and Elan Bank in the West and South Indian Ocean, the East Tasman Plateau and Gilbert Seamount Complex in the Tasman Sea, or the Wallaby and Zenith Plateaus in the East Indian Ocean (Müller et al., 2001; Gaina et al., 2003; Nemčok et al., 2016) (Figure 1.4).

Reflecting on the various microcontinent categories and formation processes described by Müller et al. (2001), Nemčok et al. (2016), or Gaina and Whittaker (accepted), the Jan Mayen microcontinent structure and formation follow several general characteristics of a microcontinent: (1) inherited lithospheric heterogeneities (located at the junction of Archean, Caledonian and Mesozoic extensional structural elements); (2) wrench tectonics (located in between the EJMfZ and the IFFZ); (3) competing rift zones (the Reykjanes ridge from the south and the Ægir ridge from the north); and (4) plume-ridge interactions, causing asymmetries of oceanic crust formation and rift propagation (the interaction of the Iceland plume with the IPR, Reykjanes ridge and the Kolbeinsey ridge).

The extensive dataset used in this study does not confirm the model of a Jan Mayen microcontinent that formed as the result of rift transfers along a magma-poor rifted margins (Perón-Pinvidic et al. 2012a), a suggestion based mainly on northern JMMC and its partial Norwegian margin conjugate. A detailed analysis of JMMC western margin and its central East Greenland conjugate margin, specifically the Blosseville Kyst (Larsen, L.M., et al. 1985, 1989, 1999, 2013, 2014; Table 1.1c) significantly contributed to a revised model that confirmed the link to the JMMC formation through several magmatic events.

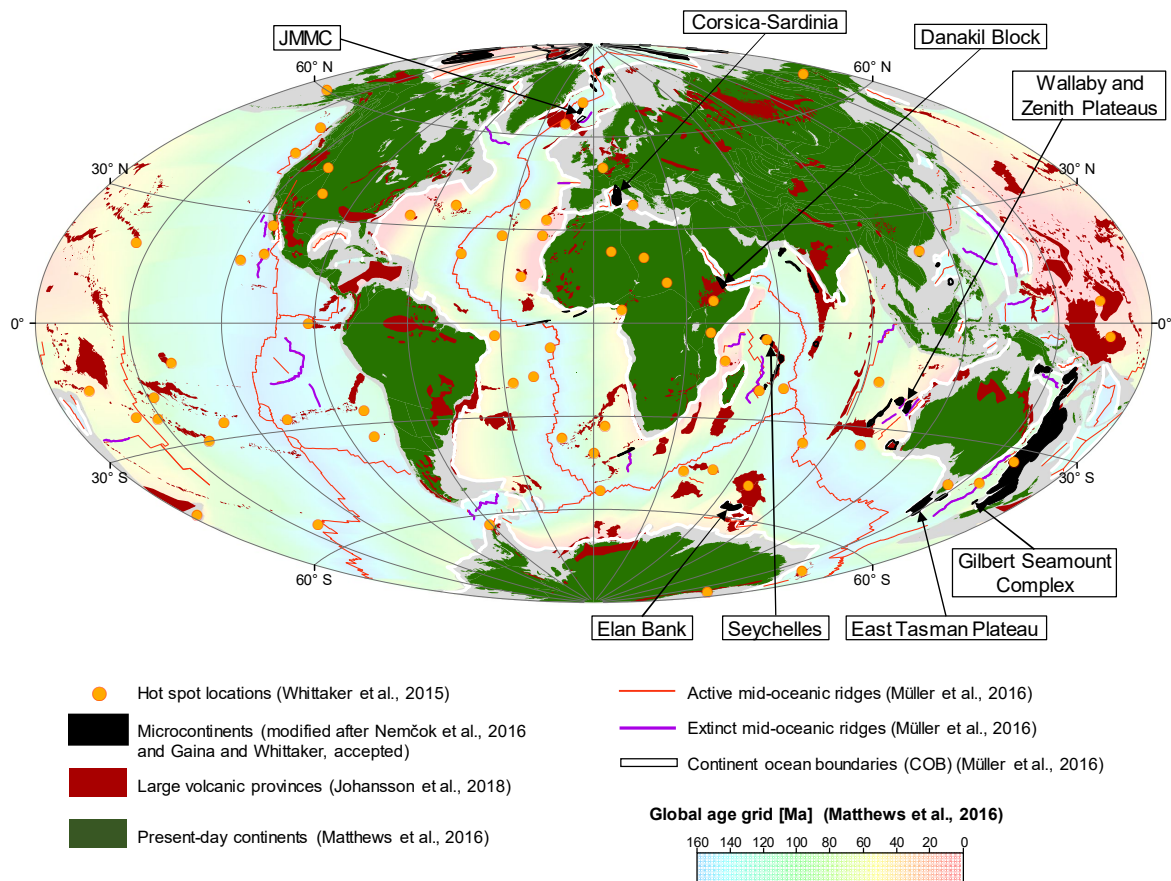


Figure 1.4. Global view of present-day microcontinent locations (modified after Nemčok et al., 2016; Gaina and Whittaker, accepted).

Other microcontinents may have formed due to extension triggered by subduction processes. Some characteristic observed for microcontinent regions linked to passive margins, are also observed in active margin settings. For example, asymmetries in the accretion of oceanic lithosphere due to mid-ocean ridge relocations are observed for both the Jan Mayen microcontinent and Ægir ridge system, and the Corsica-Sardinia block and surrounding oceanic basins (van den Broek et al. 2020). Results from numerical modelling suggest that continental break-up and incipient microcontinent formation in a subduction setting is facilitated by the existence of continental heterogeneities and weak zones, and a rotational kinematic component (van den Broek et al. 2020). The rotational component has been also described for the opening of the Norway Basin and detachment of JMMC from the Norwegian margin (Gaina et al., 2009; Gernigon et al., 2015).

In the case of JMMC-IPR area, a gradual south to north propagation, has resulted in a gradual detachment of JMMC from the main East Greenland margin from Late Eocene to Early Miocene, while the Ægir ridge was still propagating southward. This gradual northward propagation of the IPR formed a narrow impinging wedge from the south into the JMMC domain that caused a counterclockwise rotation of the JMMC blocks away from the East Greenland margin during Mid-Late Oligocene, until it was completely detached at its north-western corner in Early Miocene. During that rotation did the JMMC push into the adjacent

oceanic domain of the Ægir ridge, which specifically can be confirmed by revers structures in the south-eastern domain of the microcontinent and the western extent of the Ægir ridge.

Potential analogues

The JMMC-IPR area appears to be similar to the Elan Bank microcontinent (South Indian Ocean), and Danakil incipient microcontinent (Borissova et al. (2003), Gaina et al. (2007), Nemčok et al. (2016), and Gaina and Whittaker (accepted)). They could be direct analogues since their structure, tectonic framework and history show similar conjugate young continental margins close to a hot-spot within a complex tectonic and rift transfer settings. For example, the Elan Bank has a crustal thickness of at least 16 km consisting of igneous (2–3 km) and continental crust (14 km). It was affected by hot-spot magmatism during the Gondwana breakup, and subsequent microcontinent separation from the Indian plate and Antarctica via a mid-ocean ridge jump (e.g. Borissova et al. 2003) (Figure 1.4).

These key observations appear very similar to the JMMC by comparing the tectono-magmatic development, crustal build-up, evidence of thick lava flows and plateau basalt seen across the JMMC, and high-velocity bodies that appear to surround the microcontinent, the mid-ocean ridge propagation and transfer along both sides of the microcontinent of the Ægir- and Kolbeinsey ridges respectively. A more definitive proof of a temporal plume-related magmatic increase of breakup dynamics can only be given by petrologically sampling the IPR's time transition from IPR stages I to IV and would be part of future research projects.

1.4 The JMMC-IPR study synopsis

In order to address the tectono-stratigraphic and -magmatic processes of the JMMC, and specifically the Iceland Plateau Rift within a spatial reconstruction framework, a comprehensive compilation of different geophysical and geological datasets was necessary, along with comparison with data from the conjugate Mid-Norwegian margin (Vøring and Møre), the Faroe Islands, the Greenland-Iceland-Faroe ridge complex (GIFRC), and especially the north-eastern margin of the Blossville Kyst, central East Greenland (Figure 1.1; Table 1.1c). This assemblage has not previously been demonstrated in such detail for the JMMC-IPR region.

A comprehensive compilation of geophysical and geological data for the JMMC-IPR area, along with assessment and interpretation of structural-, stratigraphic, sedimentary and volcanic development forms the basis of this dissertation. This was accomplished by utilizing gravity- and magnetic anomaly data, multibeam bathymetric data, seismic reflection and refraction data, and borehole and seafloor samples, summarized in detail in chapter 3. Using these datasets, the detailed seismic-stratigraphic analysis of key stratigraphic units, unconformities and other discrete strong reflectors were mapped from vintage (1960's – 2000) and more recent (2001–2012) high-resolution seismic reflection data. These were calibrated with bathymetric seafloor mapping and deep-sea drilling project (DSDP) and ocean drilling program (ODP) borehole, and seafloor sample data control. The use of a dense seismic-reflection and refraction dataset provided a unique opportunity to map intercalated igneous domains and rift zones of the JMMC in 3D, enabling to estimate the volcano-stratigraphic types, their size, distribution and extent of these rift and volcanic

systems, as well as large-scale igneous features, such as deeper-seated intrusions, volcanic complexes, and rift valleys.

Furthermore, were the temporal developments of the IFFZ or the JMFZ key boundaries and may directly relate to pre-existing crustal weak zone that covered the opening of the NE Atlantic in the JMMC-IPR domain. This is an important understanding for the forming of the JMMC. In comparison did the De Geer Transform Fault develop parallel to the JMFZ and its sheared corridor along upper crustal regional extension through strike-slip corridors. This relates directly to the formation of weaker, more brittle crustal deformation zones, and potentially to the reactivation of ancient crustal weakness zones. These weakzones develop an array of opening crustal pathways that developed perpendicular to the at the time acting minimum stress (σ_3) as preferential openings for magmatic material to rise up within the crust. This is seen as a broad corridor across the IFFZ, where several segments of NE-SW en-echelon axial rifts opened up along several strike slip systems that as a whole form the IFFZ (Paper III).

This led to a specifically focus on the IPR domain, as this area has not been clearly represented within the reconstruction model. The IPR domain is located in between the JMMC and the North Iceland shelf, and represents an igneous region consisting of four distinct time stages and igneous domains (IPR-I to IV) between the Early Eocene (Ypresian) and Early Miocene (Aquitanian) (see time scale for reference in Figure 1.2). Each stage corresponding to a distinct igneous and structural domain. This study enabled me to shed new light on the propagating rift domains within the JMMC-IPR region, and tectonic similarities between the Eocene-Miocene rift structures and present-day Iceland became more apparent (Figure 1.5a). Both are characterized by oblique rift systems that open in a none-orthogonal direction where mid-ocean ridge segments are not aligned perpendicular to adjacent transform or fracture zones. Highly obliquely spreading ridges have been recognized globally in relation to slow, intermediate, and super-fast spreading centres. They are described to have been related to reorganizations of plate boundaries and magmatic overpressure, causing spreading obliquity generally up to $\sim 10^\circ$ and in a few cases even up to $\sim 30^\circ$ (e.g. Zhang et al., 2018).

Oblique rift systems characterize present-day Iceland, within the dextral Tjörnes Fracture Zone (TFZ), between the Kolbeinsey Ridge and Northern Rift Zone and in particular along the volcanic systems of the Reykjanes Peninsula, the on land extension of the Reykjanes Ridge (e.g. Einarsson and Sæmundsson (1987); Murton and Parson, 1993; Taylor et al., 1994; Hreinsdóttir et al., 2001; Einarsson (2008); Karson et al., 2018, 2019; Einarsson et al., 2018) (Figures 1.1; 1.5b,c). Surrounding areas respond to the build-up tectonic stresses during oblique opening by brittle crustal fracturing, observed in outcrops (e.g. Karson et al., 2018, 2019), but also in borehole breakout and tensile fracture analysis, as in borehole ARS-39 located just 1 km south of the Dalvíkur lineament, within the TFZ (Figure 1.5b) (Blischke et al., 2017b). In the borehole, the resulting stress field orientation was aligned with the regional stress-field orientation of the TFZ which governed the opening direction of fractures and dykes along near vertical rift parallel strike slip fracture and fault sets.

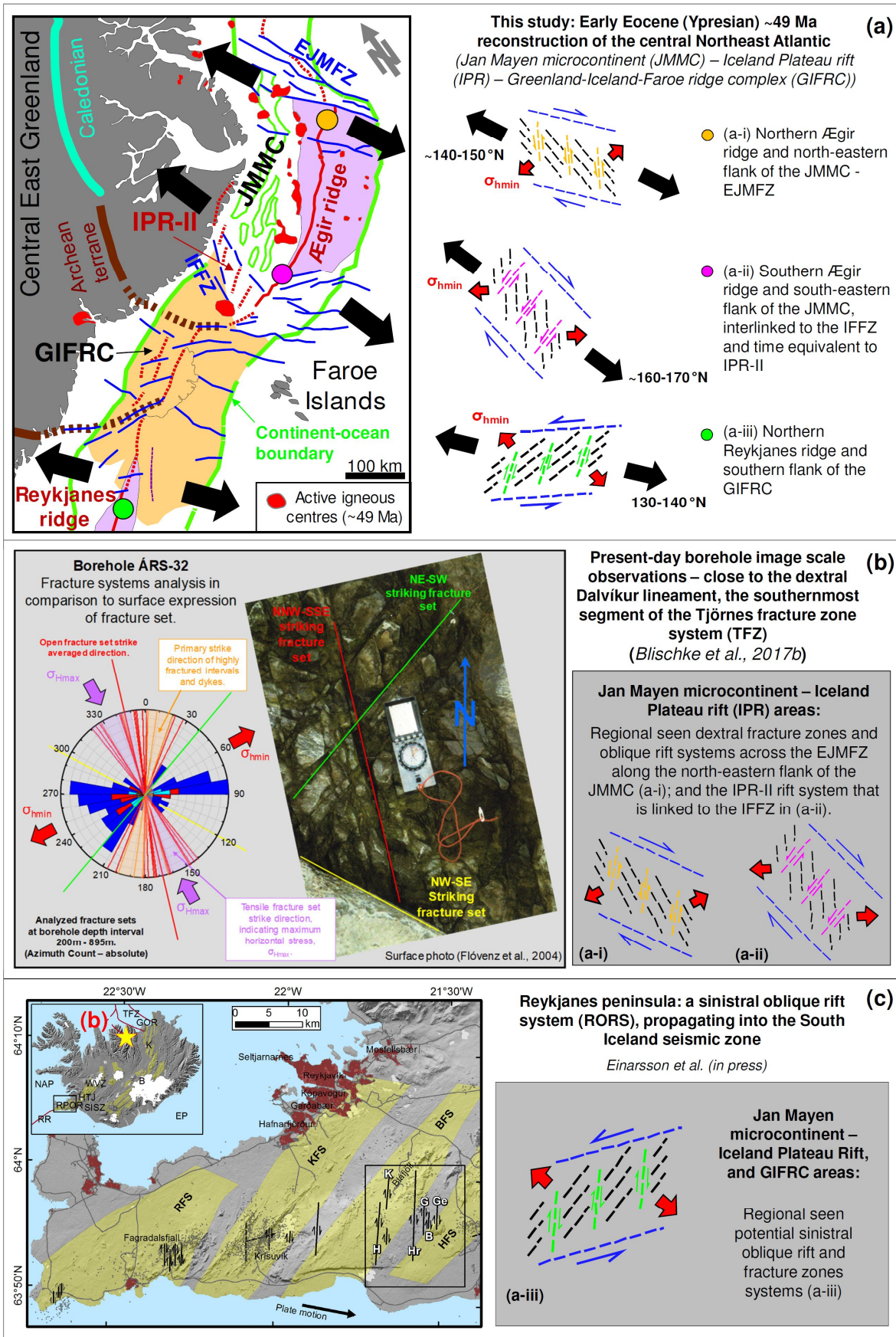


Figure 1.5. Comparison of present day Icelandic oblique rift and fracture / transfer zone systems to the oblique opening systems for the greater JMMC-IPR region (Papers I and III): (a) Early Eocene (~49 Ma) reconstruction example during IPR-II rift activity (this study) along the EJMFZ, the IPR-II-IFFZ, and the northernmost extent of the Reykjanes ridge at reconstruction time; (b) Borehole scale structural comparison of the Dalvíkur lineament (the southern segment of the TFZ) (Blischke et al., 2017b); and (c) the Reykjanes Peninsula transfer zone (Einarsson et al., in press). Displayed features: direction of the rift opening – black arrows; direction of the minimum horizontal stress field (σ_{hmin}) – red arrows; direction of the maximum horizontal stress field (σ_{Hmax}) – purple arrows; general fracture zone orientation and opening direction – blue; primary normal fault formation – black dashed lines; and rift parallel strike-slip faults that correspond to each case's locations (a-i – orange, a-ii – pink, and a-iii – green) of insert (a). Abbreviations and label keys are presented on p. xix-xx.

Present-day mechanisms of fault and fracture development at small and regional scale observations, strengthen the geodynamic reconstruction and interpretation of multiple oblique opening scenarios within the JMMC-IPR region, between the Eastern Jan Mayen fracture zone (EJMFZ) and the Iceland-Faroe fracture zone (IFFZ) (Figure 1.5a), during Eocene to Early Miocene times, as documented in Papers I-III, and Appendix 1. The oblique opening scenarios are linked with documented changes in spreading direction within the NE-Atlantic, throughout the Cenozoic (Paper I-III) (Figure 1.3), as spreading directions appear to have changed since the initial breakup of the Northeast Atlantic ~56-55 Ma, influenced by Cenozoic regional tectonic events (Gaina et al., 2009, 2017b) (Figure 1.3). Seafloor spreading rates and magmatic emplacement also appear to have varied through Cenozoic time based on crustal volume variations across the Greenland-Iceland-Faroe ridge complex (GIFRC) and correlation with ridge transfers and tectono-magmatic changes around the GIFRC (Hjartarson et al., 2017) (Figure 1.6).

This study describes the link between the segmented final rupture of the lithosphere around the JMMC, along deep reaching fault zones, axial rift segments, or along fracture zones. Specifically, where large igneous centres and seaward dipping reflector units (SDR) formed along JMMC's north-eastern margin (SDR definition see Mutter et al., 1982; Larsen et al., 1988; or Planke et al., 1994, 2000), close to fracture zone endpoints or interlinking fracture zone segments. This oblique seafloor opening prompted an en-echelon volcanic ridge emplacement (Paper III). Thus, the north-eastern volcanic margin of the JMMC was formed by a southward propagating Ægir ridge system (e.g. Paper III).

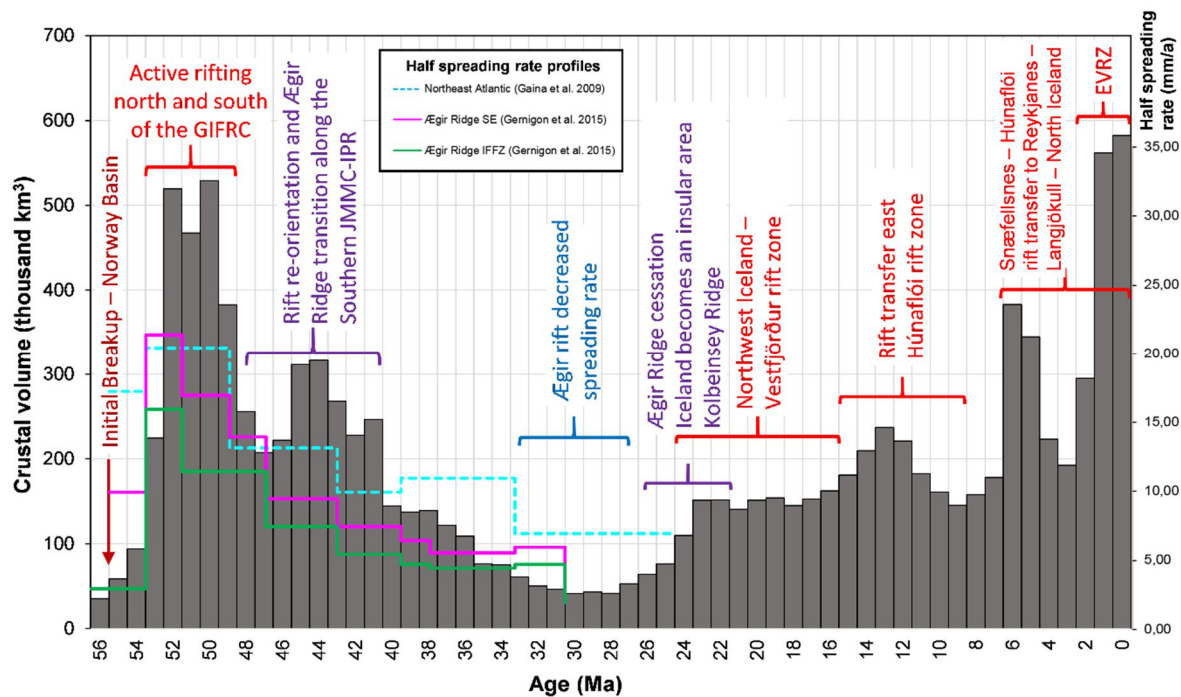


Figure 1.6. Greenland-Iceland-Faroe ridge complex crustal thickness estimates through time, by comparing age grid data (Gaina 2014) to crustal thickness data, summarized as cumulative datasets for 1 Ma increments since break-up. This crustal accretion vs. time plot is then compared to the half spreading rate profiles for the Northeast Atlantic analysis by Gaina et al. (2009), and for the southern part of the Norway basin of the Ægir ridge by Gernigon et al. (2015). It can be shown that the Greenland-Iceland-Faroe ridge complex follows the Northeast Atlantic opening process until the rift reorganization and transfer from the Ægir ridge across to the IPR, and to the Kolbeinsey ridge. After the cessation of the Ægir ridge system, the GIFRC shows a good correlation of increased crustal volume to distinct rift systems, such as the Westfjords, the Snæfellsnes–Húnaflói rift zone (SHRZ on Figure 1.1), or the Eastern Volcanic rift zone (EVRZ on Figure 1.1). Crustal volume decreases during potential rift transfer periods.

Just as the IPR complex represents the southern igneous domain of the JMMC, the Jan Mayen Island igneous complex (JMI), is interlinked with its northern igneous margin (Figure 1.1). Both represent long-lived volcanic margins tied to major fracture zone systems and mantle anomalies within an unstable rift-transfer tectonic setting. Portraying the igneous JMMC-IPR region as a prime example of what is commonly referred to as Iceland type crust, i.e. the systematic build-up of thicker oceanic crust by rift-transfer processes, overlapping sub-aerial and sub-surface igneous activities in conjunction with localized microplate formation is the focus of Paper III.

In-tie with regional observations, the detailed analysis and reconstruction approach for the JMMC-IPR area clarifies the links between structural and igneous domain segmentation during breakup (Papers I-III). Highlighting the JMMC-IPR area as a unique case for a dual breakup system of two rifting complexes that created the JMMC, linked to the oblique IPR system as a precursor to present day Iceland (Paper III).

2 The Jan Mayen microcontinent, Iceland Plateau rift and conjugate margins

The following chapter summarises the structural, stratigraphic and geodynamic setting of the JMMC, its sub-domains, the IPR, and their conjugate margins to give a comprehensive overview and description of the region.

2.1 Structural and stratigraphic framework of the Jan Mayen microcontinent and Iceland Plateau rift

The JMMC – IPR area is approximately 400-450 km long and varies in width from 100 km in the north to 310 km in the south (Figure 2.1). The microcontinent is subdivided into the main Jan Mayen ridge (JMR) with its southern segment referred to as the Lyngvi ridge (LYR), the Jan Mayen basin (JMB), the Buðli block (BB) with the South-western Jan Mayen igneous province, and the Jan Mayen trough (JMT) that separates the JMR from the Jan Mayen southern ridge complex (SRC) (Figure 2.1; 2.2). The SRC complex consists of several segments or blocks that were used within the reconstruction model, these are: the main SRC block (MSRC); the Otur block (OB); the Högni block (HB); the Langabrá block (LB), and the Dreki block (DB) (Figure 2.1). The main northern JMR is well defined, continuous and flat-topped, whereas the SRC is comprised of several smaller ridges that become indistinct towards the south.

Previous JMMC studies focused on mapping the general morphological, gravimetric and magnetic signatures of the JMR (Vogt et al., 1970; Talwani et al., 1976a,b), as a steep-flanked bathymetric horst with water depths varying between 200 and 2500 m that extends south from the Jan Mayen Island (Fitch, 1964; Svellingen and Pedersen, 2003).

Later studies delineated the outline of the microcontinent further south and southeast, primarily focusing on describing structural and tectonic features for geodynamic reconstructions (e.g. Scott et al., 2005; Gaina et al., 2009; Peron-Pinvidic et al., 2012a,b; Gernigon et al., 2012, 2015). However, based on the limited seismic reflection and refraction data sets available at the time, these studies could not address the tectono-stratigraphic and volcanic aspect of the region, in detail, including the excess extension across the southernmost JMMC.

This study focuses on the various segments of the JMMC, specifically addressing the poorly understood area of the IPR. As a result, it became apparent that all of these domains contain more voluminous intrusive and extrusive formations than previously described from seismic reflection data, revealing igneous intrusive and axial rift systems within the wide corridor of

the southernmost JMMC-IPR area, not generated by hyper-extension but rather by extension and the formation of a southern igneous margin (Papers I-III).

Major fracture zone systems mark the boundaries of the JMMC: the eastern and western Jan Mayen fracture zones (EJMFZ; WJMFZ) to the north, and the Iceland-Faroe fracture zone (IFFZ) along the NE Iceland insular shelf and the northern Iceland-Faroe Ridge to its south. These fracture zone systems are linked to the Jan Mayen Island igneous complex that intersects the northernmost extent of the JMMC, at the junction of the eastern and western segments of the Jan Mayen fracture zone system; and the southern Greenland-Iceland-Faroe ridge complex between the north-eastern coastal shelf of Iceland and eastward across the Norwegian Sea, towards the Faroe Islands plateau (FP).

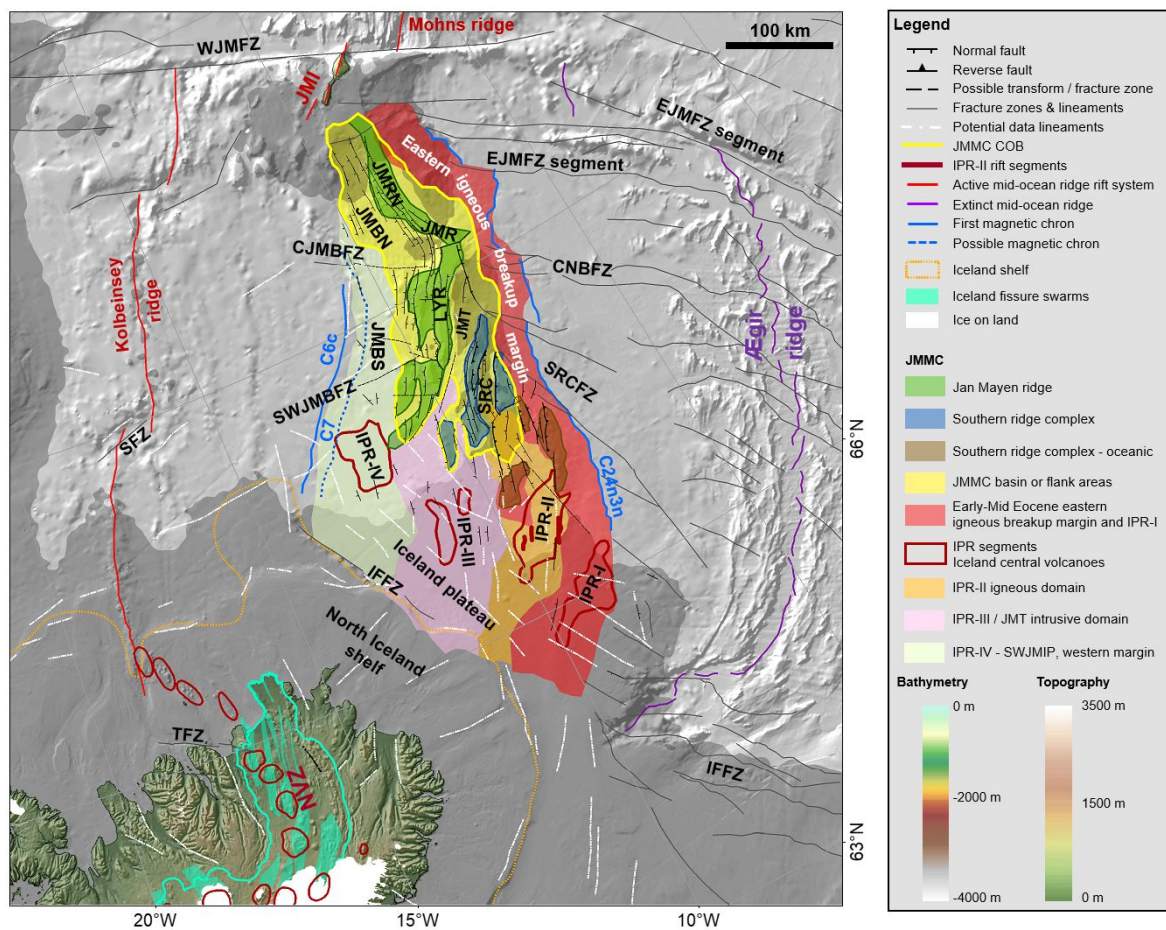


Figure 2.1. Shaded bathymetry (IBCAO 3.0; Jakobsson et al, 2012) structural map of the JMMC-IPR area, with faults, fracture zones and lineaments based on this study (Papers I-III; Blischke et al., 2019). Dark grey shaded area represents the 100 km wavelength filtered Bouguer anomaly level at 95 mGal, by Haase and Ebbing (2014). Chron C24n3n is based on Peron-Pinvidic et al. (2012a) and Gernigon et al. (2015). Western breakup chrons C7 and C6c are from Paper III. Abbreviations are listed on p. xix-xx.

2.1.1 Jan Mayen Island igneous complex

The JMI system, previously described by Kandilarov et al. (2012) as containing 15-25-km thick Iceland-type oceanic crust, highlighted the anomalous nature of the JMI adjacent to the JMR. The thickened JMI crust correlates with the area's 15-21 km crustal thickness estimate based on gravity inversion by Haase and Ebbing (2014) and magnetic highs (Nasuti and Olesen, 2014) (Figures 2.1; 2.3a). These observations and the seismic reflection data analysis of this study indicate that the JMI system is the igneous link between the EJMFZ and WJMFZ domains and is accompanied by deep intrusive structures below the northernmost JMR (Figure 2.3a). West of the JMI domain, a marked decrease in crustal thickness from 13 to 8 km across the Eggvin bank (EB) just south of the WJMFZ (Tan et al., 2017) indicates a waning influence of the JMI along the WJMFZ (Figure 2.4).

The southern extent of the JMI differs in seismic reflection character from the JMR domain itself, where layered reflectors are visible together with typical faulted rift margin structures (Papers II and III). The JMI domain has a poor seismic reflection data resolution, but clearly can be see how younger volcanic structures cut through the thickened oceanic crust and Neogene stratigraphic units (Figure 2.5). The heavily intruded northern end of the JMB and NJMR can be seen on seismic reflection data, where a substantial increase of sills and dykes are intruded into Eocene stratigraphic units (Paper III) (Figure 2.4). The observed increase of dyke and sill intrusions here is substantially greater than along the north-eastern flank of the JMMC adjacent to the JMI.

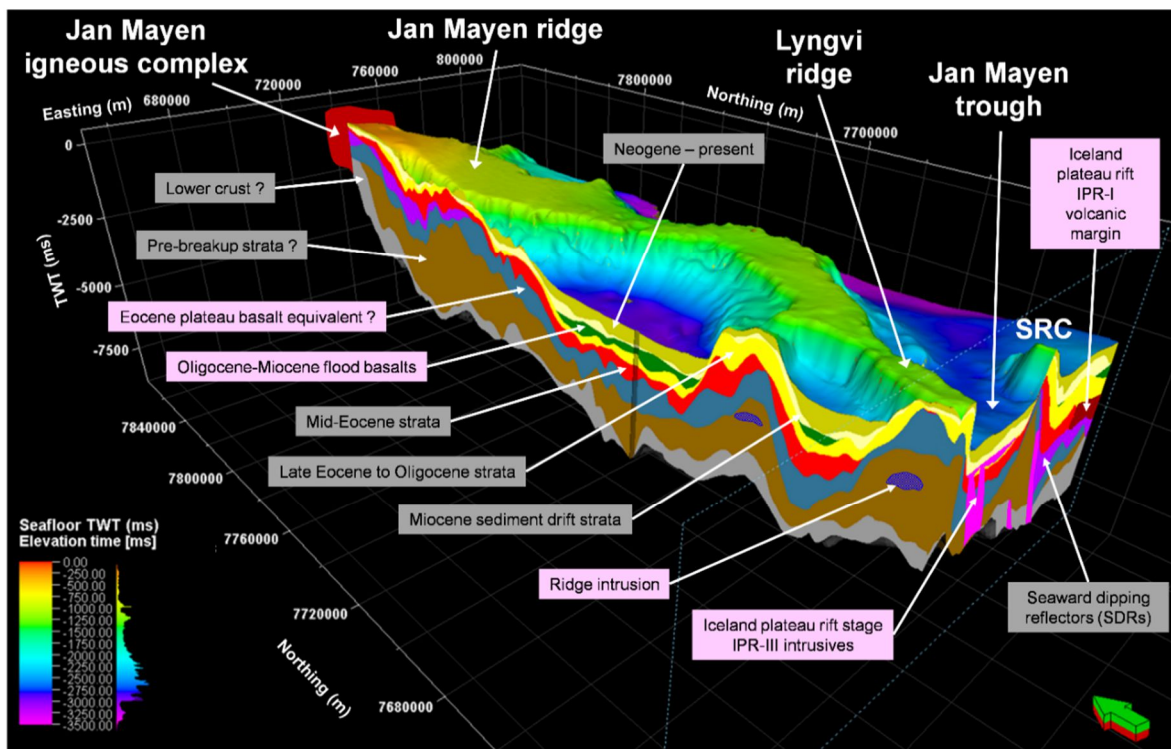


Figure 2.2. Present day three-dimensional JMMC volcano-stratigraphic framework, based on Papers II and III.

2.1.2 Jan Mayen and Lyngvi Ridges

The main JMR extends about 360 km south of the JMI. The Lyngvi Ridge forms the southernmost 130 km of the JMR, just south of the intersection with the central Norway basin fracture zone (CNBFZ on Figures 2.1; 2.3a). The northern end of the JMR is well defined by the adjacent JMI and intersecting EJMFZ and WJMFZ (Figures 2.2; 2.3a). Magnetic anomaly changes are apparent across the JMR in a north to south profile, specifically at the intersection with fracture zones and the IPR-JMT domain. The ridge intersections with the WJMFZ and the CNBFZ is marked by a negative magnetic anomaly, in contrast to the slightly positive anomalies at the EJMFZ intersection. Changes in magnetic polarities across the LYR under strong influence from younger igneous events, specifically across the JMMC's southern boundary and the IPR domain.

Whereas the width of the JMR is 70–80 km, the LYR narrows to about 10 km at its southern tip before disappearing beneath Upper Paleogene and Neogene sediments and lavas (Figure 2.2). The LYR has been more affected by faulting, igneous and rifting activities than the JMR. Internal pre-breakup strata and layering is best observed within the northern segments of the LYR and JMR ridges close to DSDP site 349, described in detail Papers I and II.

2.1.3 Eastern Jan Mayen igneous complex and fracture zone corridor

The eastern margin of the JMR tilts steeply towards the Norway basin almost undisturbed by faulting; in contrast to the western margin that is downfaulted towards the JMB (Papers I and II). However, the eastern margin is intersected by three main fracture zones in the Norway Basin, the EJMFZ, CNBFZ and the Southern ridge complex fracture zone (SRCFZ) (Figures 2.1; 2.3; 2.4 2.6a,b). The main JMR has been periodically eroded during the Cenozoic as recorded by the preservation of various unconformities, which have contributed to the flat-topped character of the ridge (Paper II). The eastern margin is clearly delineated by the increase in Bouguer gravity anomaly and a change in magnetic anomaly pattern, from the relatively magnetically “quite” zone of the adjacent JMR. The wide igneous breakup margin of the JMMC, is clearly distinguishable from the striped anomaly pattern of the Ægir ridge's oceanic domain (Figures 2.3; 2.4). It is important to note that the significant erosion and redeposition downwards the eastern marginal slopes, is not only the result of structural segmentation and major tectonic movements but also the formation of igneous complexes adjacent to fracture zones (Paper III), (Figure 2.6a). The CNBFZ, as an example, terminates within a volcanic margin, seen on seismic refraction and reflection data, and by an offset in the magnetic anomaly data (Figure 2.4). This could be described as a “leaky” fracture zone, as the volcanic complex occupies a lateral space of up to 10 km (Figure 2.6a).

2.1.4 Jan Mayen basin

The JMB is divided into two sub-domains: northern segment (JMBN) west of the JMR, and southern segment (JMBS) west of the LYR (Figures 2.1; 2.3). The entire western flank of the JMMC is strongly faulted into several westward-rotated fault blocks along fault segments that partly extend into the JMB, forming half-graben and small graben structures. Most of the faults and tilted blocks presently mapped have been influenced by post-breakup uplift and tilting.

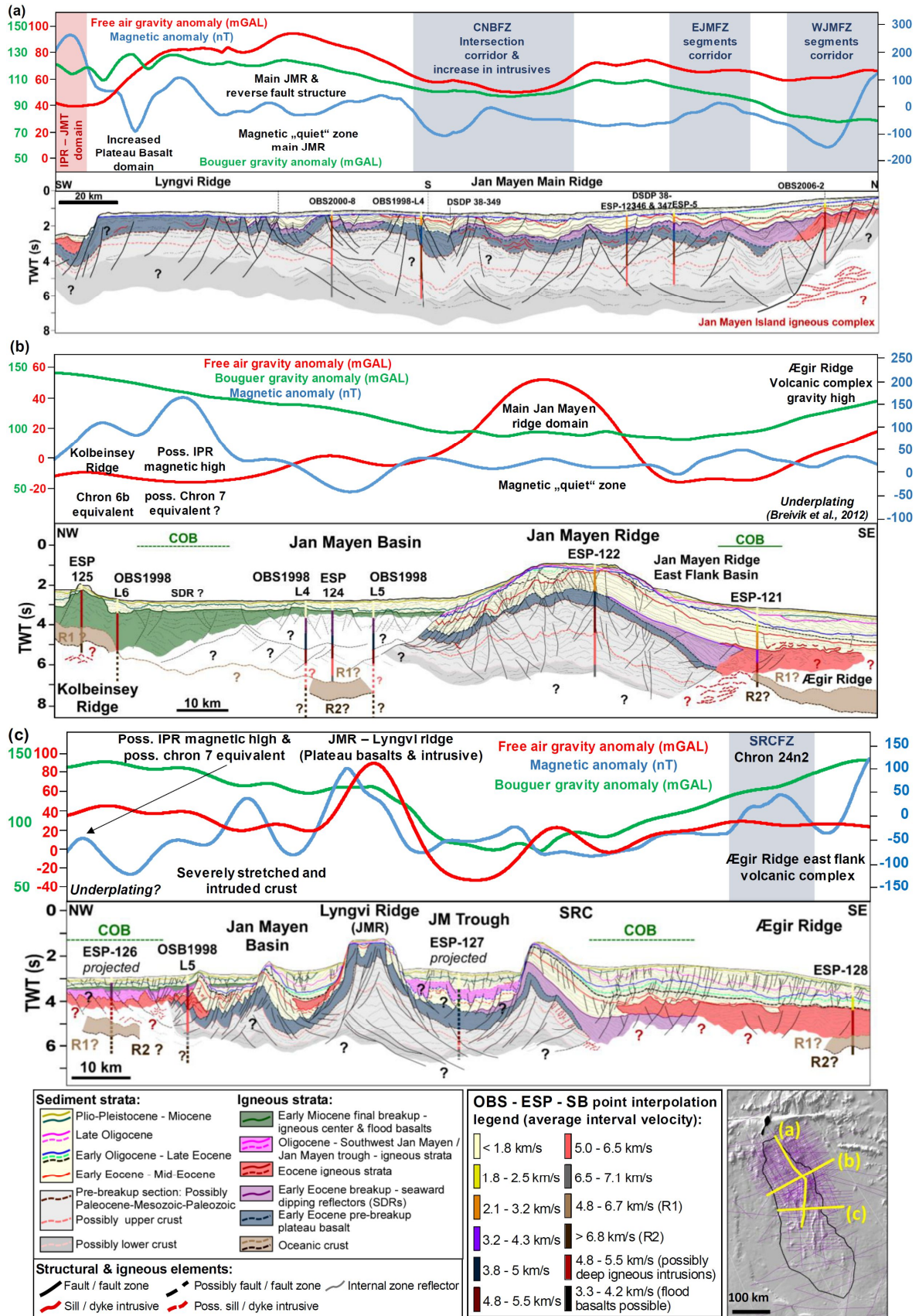


Figure 2.3. Stratigraphic sections of the JMMC based on seismic reflection data (NPD, 2012 and 2013) tied to OBS, sonobuoy, ESP velocity profiles, and available boreholes from Paper III. Magnetic-, free air gravity data (Nasuti and Olesen, 2014; Haase and Ebbing, 2014), and large fracture zone corridor intersections (e.g. Gaina et al., 2009; Kandilarov et al., 2012; Gernigon et al., 2015; and Paper I) plotted above the profiles highlight variations associated with major tectonic and igneous events. Abbreviations are listed on p. xix-xx.

Within the JMB, the crustal thickness varies between 6-12 km based on seismic refraction profiles (Kodaira et al., 1989; Olafsson et al., 1988; Papers II and III). Some traces of the JMB strata can be seen and followed beneath the early Miocene flood basalts (Figure 2.3b and F-Marker on Figure 2.4).

The early Miocene flood basalts represent a flat-lying and almost opaque reflector on seismic reflection data, interpreted as extensive flood basalt lava units of up to 1,3 km thickness within the low areas of both JMBN and JMBS (Paper III). The transition between the tilted blocks of the JMBS and the JMBN is defined by an apparent change of seismic reflection pattern characteristics and fault patterns that are typical for the western margin, where the flood basalts can be seen. This seismic reflection character change is also apparent in more detailed reflection and gravity data (Figures 2.3b,c; 2.4), and interpreted by seismic refraction data analysis as oceanic crust (Paper III).

2.1.5 Jan Mayen trough

The JMT, separating the LYR and the SRC, widens towards the south and southwest with one segment of the SRC embedded within (Figures 2.1; 2.4). Even with the most recent seismic reflection data, it is difficult to clearly define and map underlying deeper structures. A few fault blocks can be seen that are separated by intrusives that appear to align to distinct change in magnetic anomaly, and a narrow south to north alignment of a decrease in Bouguer gravity is apparent within the trough as well (Figures 2.3c; 2.4).

The JMT is covered by a flat-lying and almost opaque reflector in seismic reflection data which is chrono-stratigraphically placed within the Late Oligocene and referred to as F-Marker 2 (Paper III). The main source for this extensive flood basalt within the JMT probably lies within the IPR-III corridor further south and is tied to volcanic complexes and/or fissure zones that intersect the JMT in a north-south direction (Papers I and III) (Figures 2.2-2.4; 2.6). This pattern is also illustrated by the EJMFZ that links into a distinct volcanic complex named (Figure 2.6a) that is clearly observed with similar pattern in seismic reflection data, and magnetic anomaly responses.

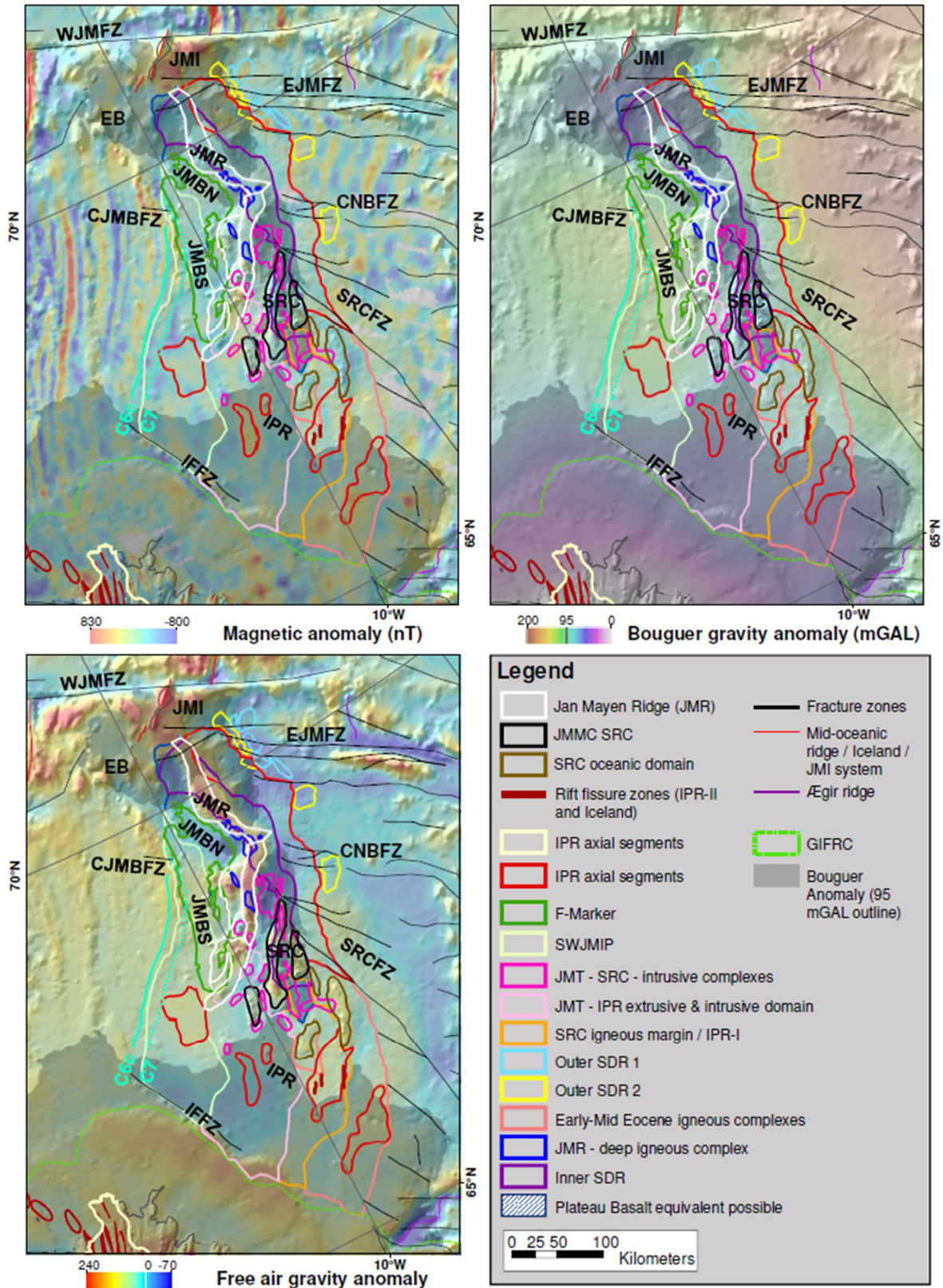


Figure 2.4. Present day JMMC volcanic facies and province interpretations in comparison to magnetic (Nasuti and Olesen, 2014), free air gravity and Bouguer gravity data (Haase and Ebbing, 2014). Abbreviations are listed on p. xix-xx.

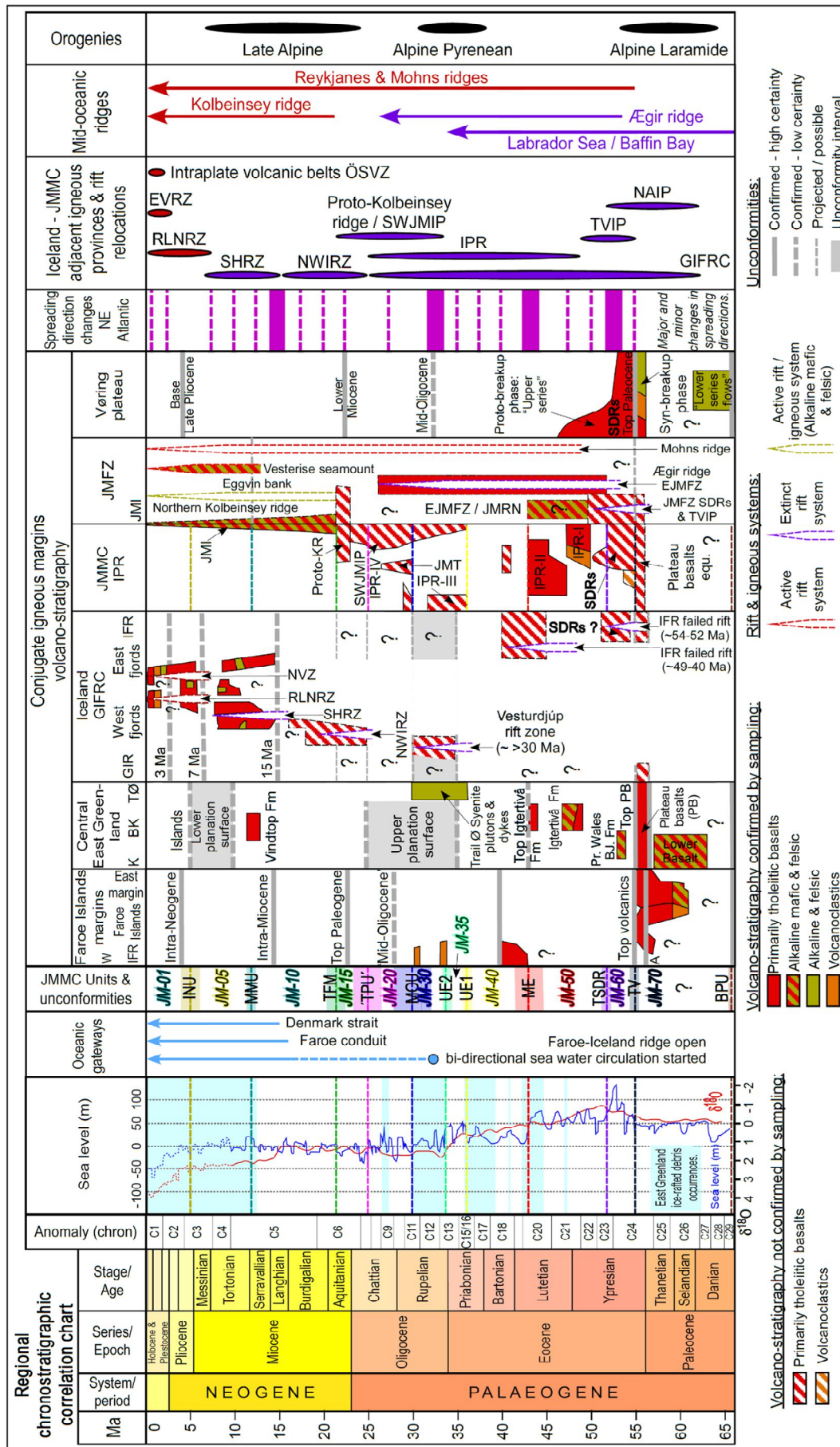


Figure 2.5. Regional chronostratigraphic summary chart emphasizing the relationship between the volcano-stratigraphy of the JMMC in relation to its conjugate igneous margins, sea level changes, and $\delta^{18}O$ data by Van Sickle et al. (2004), Miller et al. (2008), and Murray-Wallace and Woodroffe (2014), Paleogene East Greenland ice-rafted debris occurrences by Tripathi and Darby (2018), ocean gateway interpretations (Stoker et al., 2005a,b; Stürz et al., 2017), Northeast Atlantic spreading direction changes modelled by Gaina et al. (2017a,b), main igneous provinces and rift relocations based on Sæmundsson (1979), Harðarson et al. (1997, 2008), Saunders et al. (2013), Thordarson and Höskuldsson (2008), Brandsdóttir et al. (2015), Geissler et al. (2017), Parson et al. (2017), Hjartarson et al. (2017) and this study. Mid-oceanic ridge systems and orogeny's were modified after Lundin and Doré (2002). Time scale from Gradstein et al. (2012). Abbreviations are listed on p. xix-xx.

2.1.6 Southern ridge complex

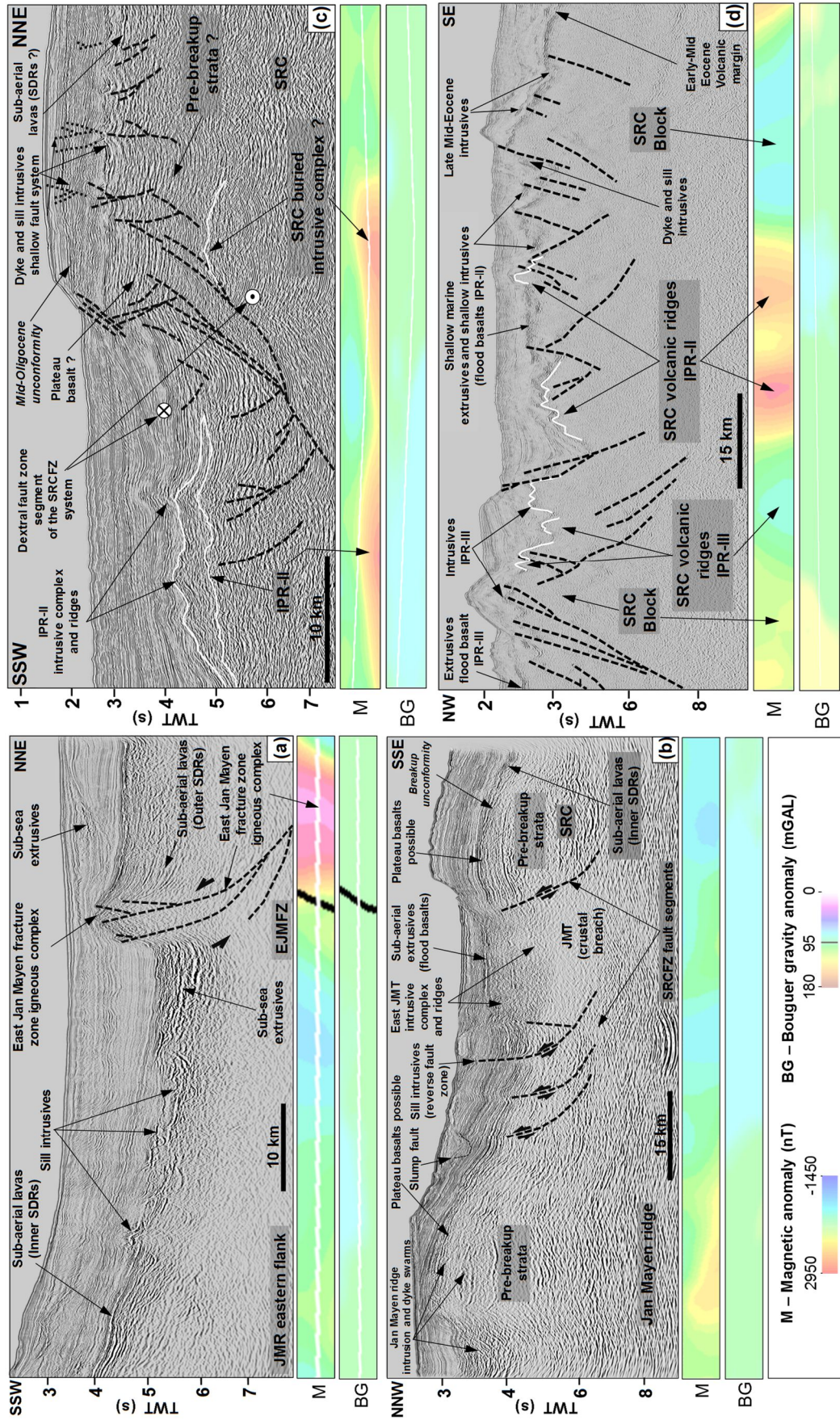
The SRC is a collection of several ridges that were formed during extension and rift transfer along the southern part of the microcontinent (e.g. Talwani et al., 1977; Gaina et al., 2009; Peron-Pinvidic et al., 2012a; Gernigon et al., 2015) and this study (Figures 2.1; 2.2; 2.4). The three northernmost SRC ridges appear similar to the eastern flank of the JMR and are linked to the continental origin of the JMMC (Paper III). The SRC formed initially during the Ægir ridge breakup, by forming a wide igneous margin, which was subsequently broken into several smaller segments.

Several smaller basins, formed in between these segments, are heavily intruded by post-breakup IPR-II and IPR-III sills, dykes, and vent structures along fault and fracture zones (Figure 2.6c,d). These volcanic structures lie within the Lower to Middle Eocene igneous and sedimentary strata and extend in places nearly up to the seafloor, possibly indicating a longer duration of igneous activity (Figure 2.6c).

2.1.7 Iceland Plateau rift

The IPR formed an overlapping spreading system with the southernmost Ægir ridge, tectonically compensating the southwards decrease in spreading rate along the Ægir ridge. Hyper-extended slivers of JMMC crust were intersected by dyke and sill intrusions related to the Mid-Eocene to Late Oligocene formation of the IPRI-IV volcanic ridges and flood basalts (Figures 2.1-2.7). The oblique IPR rifting domain, formed a fan-shaped intersection with the southern ridges of the JMMC by crustal thinning and breaching, where axial rift systems and volcanic ridges would develop (Paper III). The JMMC-type crustal thickness varies between 6 and 22 km, whereas across the IPR segments it varies between 7-15 km. These estimates are based on seismic refraction data and gravity crustal thickness inversions (Haase and Ebbing, 2014; Brandsdóttir et al., 2015). The IPR, south and southeast of the SRC, is primarily of oceanic origin based on the interpretation of seismic refraction velocity data (Brandsdóttir et al., 2015), and detailed seismic reflection, magnetic and gravity data interpretations (Papers I – III).

Figure 2.6 Examples of 2D seismic reflection profiles tied with magnetic (M) and Bouguer gravity anomaly data (section locations, see Figure 2.7), outlining major fault and fracture zones in relationship to structural and igneous domain elements. Abbreviations are listed on p. xix-xx.



2.2 Conjugate margins of the Jan Mayen microcontinent

A comparison of the JMMC-IPR region with the pre- and syn-breakup sequences along the Vøring plateau margin and Møre margin high (offshore Norway), the Blosseville Kyst (onshore East Greenland), and the Faroe-Shetland region is mainly based on available borehole and outcrop data. These north-eastern, southern and western conjugate margins represent tectonostratigraphic regions that underwent a long rifting and basin formation process prior to the breakup of the Northeast Atlantic (Figures 1.1; 2.8-2.10).

The JMMC's north-eastern margin developed as the outermost part of the continental shelf of central East Greenland and is characterized by eastward thickening of Paleogene strata and basaltic lava flows that dip steeply towards the deeper Norway basin. This area is a direct conjugate to the Vøring plateau margin and Møre margin high (Papers I and II) (Figure 2.8).

The southern edge of the microcontinent is less defined and disappears beneath Upper Paleogene to Neogene igneous strata and sediments into the IPR domain, described by Brandsdóttir et al. (2015) and mapped in more detail during this study (Papers I – III). The area is bound by the IFFZ and the NE Iceland coastal shelf (Figures 2.6; 2.7). Previous studies described the southern half of the microcontinent as being covered by extrusives preventing seismic reflection imaging of underlying hyper-extended structures (e.g. Talwani et al., 1976b; Scott et al., 2005; Gaina et al., 2009; Peron-Pinvidic et al., 2012a, b; Gernigon et al., 2012, 2015). This study in contrast highlights the IPR domain as a volcanic margin that intersects the southern JMMC domain from south to north, accompanied by numerous extrusive and intrusive volcanic formations (Papers I – III) that continued into the JMT (Figures 2.6b; 2.7). Furthermore, that the JMMC-IPR region formed the northern-western continuation of the Iceland-Faroe ridge and the Faroe-Shetland region at the time of breakup.

The JMMC's western margin developed due to rifting within the central East Greenland continental shelf with final separation during the formation of the Kolbeinsey ridge. The central East Greenland margin is therefore a key area for understanding the formation of the western margin. Here, the Palaeozoic-Mesozoic sedimentary succession is best seen in the Jameson Land basin and the Liverpool Land high. The Cenozoic succession has been correlated directly to the Liverpool Land basin and Blosseville Kyst with its Paleogene igneous province. The western margin is characterized by tilted extensional fault blocks that formed mainly half-graben structures and a complex of sills or lava flows, which cover the JMBN west of the JMR (e.g. Larsen, L.M. et al., 2013, 2014; Hopper et al., 2014; Blischke and Erlendsson, 2018) (Figures 1.2; 2.8-2.10), and has been tied into the JMMC-IPR in this study.

2.2.1 The Vøring plateau – northeastern igneous conjugate margin

The Vøring plateau is part of the JMMC's north-eastern conjugate margin, a well-studied area of a continental pre- to syn-breakup domain during the Late Cretaceous to Early Paleogene (66-55 Ma) that separated East Greenland from the Norwegian margin (Doré et al., 1999; Faleide et al., 2010; Brekke, 2000; Abdelmalak et al., 2016) (Figures 2.5; 2.8; 2.10).

The Vøring margin igneous province is 100 – 150 km wide and comprises of substantial volumes of submarine to subaerial flood basalts that were extruded prior to, and during breakup and provide excellent analogues for the plateau-basalt-equivalents on the JMMC (e.g. Planke and Eldhom, 1994; Blystad et al., 1995; Doré et al., 1999; Brekke, 2000; Planke et al., 2000; Berndt et al., 2001; Abdelmalak et al., 2016, 2017).

The Vøring plateau contains pre-, syn- and post-breakup volcanics, which are summarized in Figure 2.5 and Table 2.1. They are correlated to the deep plateau-basalt-equivalents of the JMMC area. The pre-breakup sections consist of rhyolitic ignimbrites, tholeiitic basaltic intrusions, basaltic andesite, and dacitic lava flows, which are believed to be the result of the interaction between the continental crust and rising mantle or magmatic underplating that are believed to have resulted in crustal melting (Parson et al., 1989; Meyer et al., 2009). The syn-breakup volcanism was accompanied by the emplacement of large volumes of tholeiitic lavas that coincides with the SDR formation, also correlated to the “Upper Series” and increased sill and dyke emplacement into the nearby basin sediments.

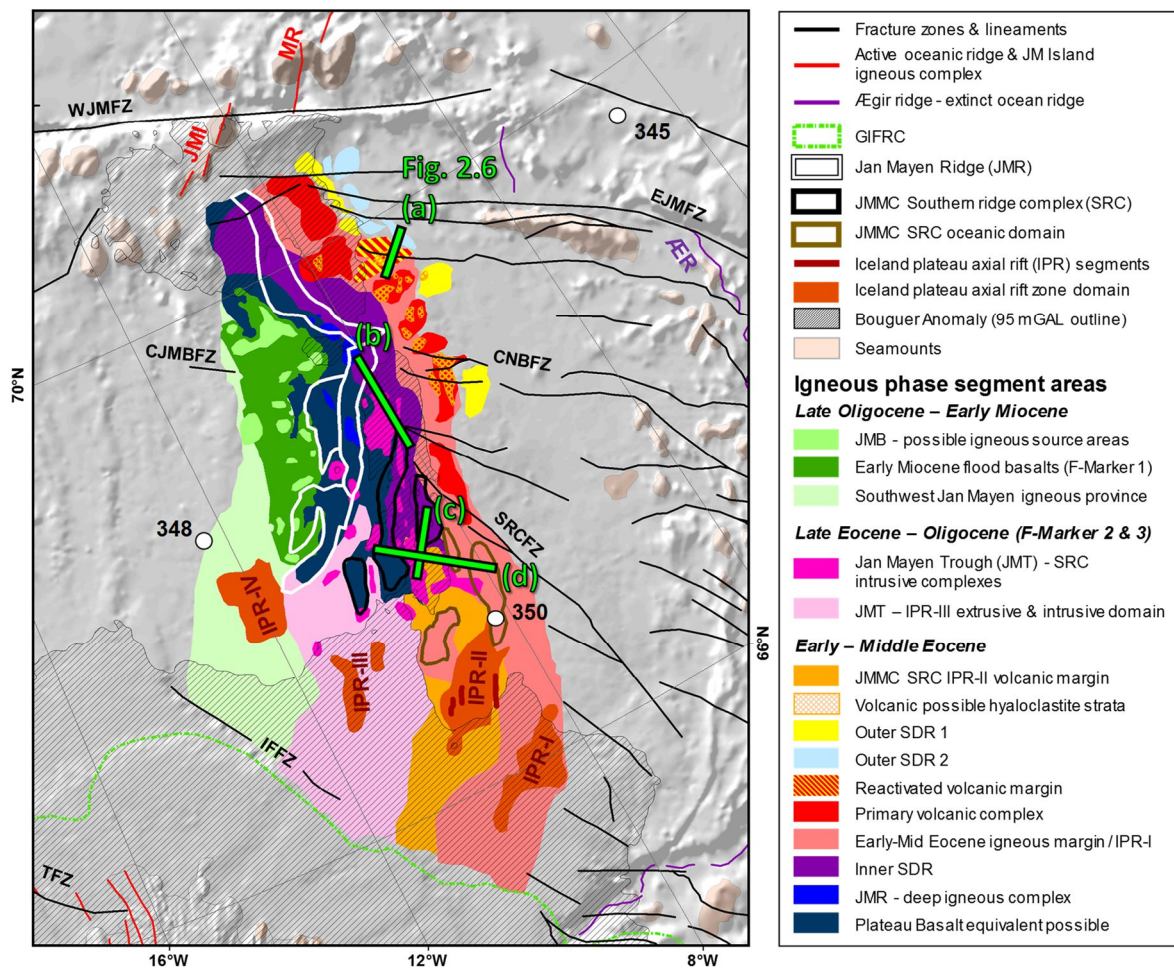


Figure 2.7. Volcanic facies and province map of the Jan Mayen microcontinent defined by order of emplacement: Early-Middle Eocene; Late Eocene – Oligocene; and Late Oligocene – Early Miocene, showing the igneous units, such as intrusive and extrusive strata, plateau basalt equivalent, igneous centres, SDRs, hyaloclastite volcanic strata, and flood basalts. Green lines show profile locations in Figure 2.6. IPR phases are listed in detail in Table 2.1. Abbreviations are listed on p. xix-xx.

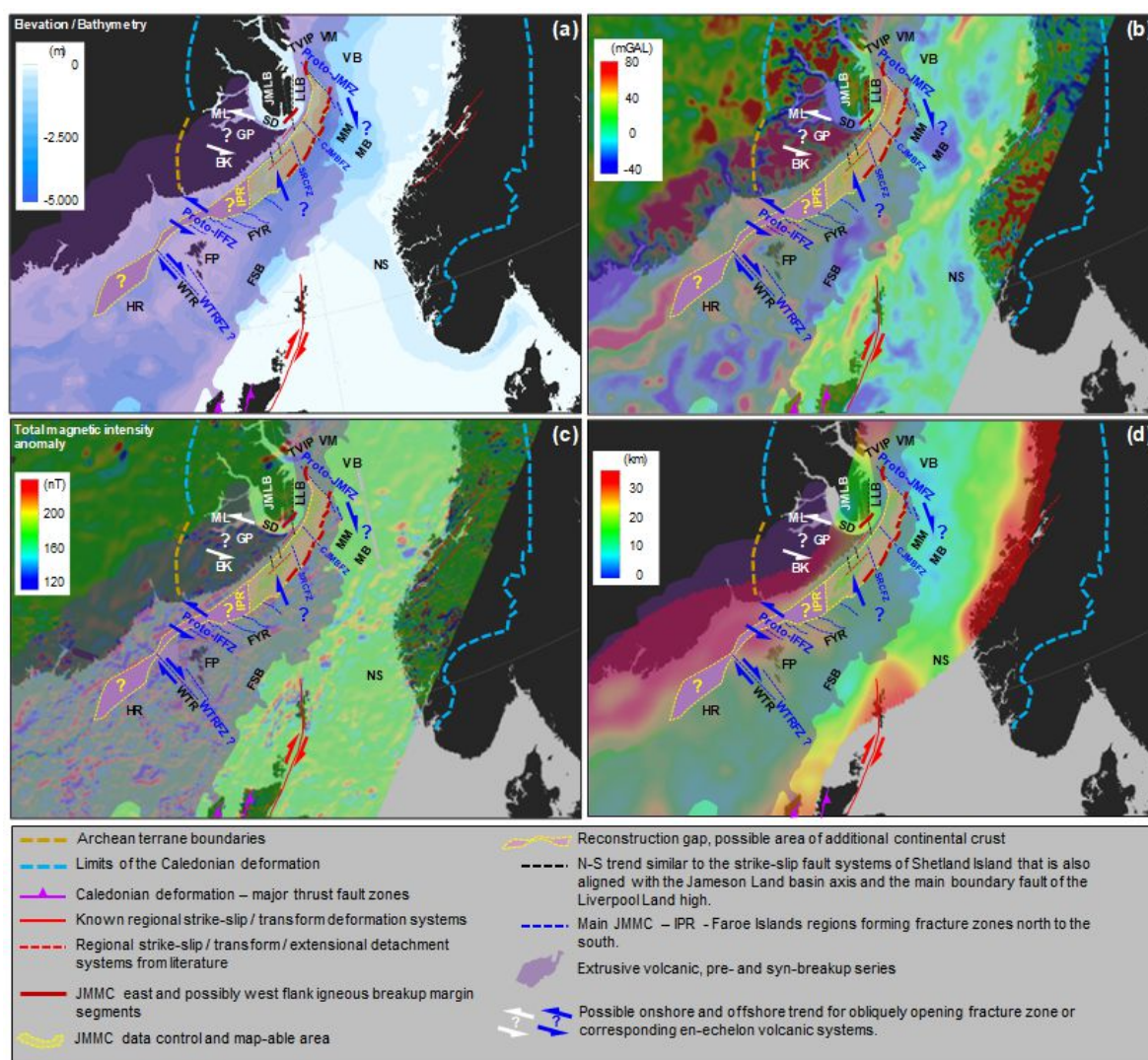


Figure 2.8 Pre-break-up setting of the Northeast Atlantic region around 56-55 Ma based on GPlates (Boyden et al., 2011), showing (a) reconstructed present-day bathymetry, (b) free-air gravity, (c) magnetic anomaly, (d) and crustal thickness data. The JMMC-IPR area is shown with major faults, fracture zones, and lineaments that are based on this study. Bathymetry data is based on IBCAO 3.0; Jakobsson et al. (2012). Features displayed are modified from data and interpretations by Larsen, L.M. et al. (1989, 1999); Osmundsen and Andersen (2001); Torsvik et al. (2001); Foulger et al. (2005); Henriksen (2008); Le Breton et al. (2013); Peron-Pinvidic et al. (2013, 2012a); Gasser (2014); Hopper et al. (2014); Guarnieri (2015); Gernigon et al. (2015); Gaina et al. (2009, 2014, 2017a,b); and á Horni et al. (2017). Abbreviations are listed on p. xix-xx.

This breakup volcanism is preserved as a complex build-up of inner and outer SDR sets and marginal highs along the Vøring continental margin and slope that overlie the lower pre-breakup basalts (e.g. Planke et al., 2000, 2005; Jerram et al., 2009; Wright et al., 2012; Abdelmalak et al., 2016). This complex igneous margin build-up is very similar to JMMC's north-eastern volcanic margin.

Following breakup, volcanic activity continued during the Ypresian (55-46 Ma) with extensive extrusive volcanism and the formation of a subaerial lava escarpment along the western margins of the Vøring and Møre basins (Figures 2.5; 2.10). It also included considerable igneous activity within the basins, accompanied by sills that intruded into the pre-breakup strata (Skogseid et al., 2000; Planke and Eldhom, 1994). Thus, the Vøring margin emplacement model preserves petrological constraints for volcanic margin evolution from Late Paleocene to Early Eocene pre-breakup to post-breakup (Eldholm et al., 1987a,b; Vierick, L.G., 1988; Parson et al., 1989; Viereck et al., 1989; Planke and Eldholm, 1994; Meyer et al., 2009; Abdelmalak et al., 2016) and forms a key potential analogue model of volcanic margin evolution for the JMMC distinguished in four igneous stages (Table 2.1; Figures 2.5; 2.9).

2.2.2 Central East Greenland - western igneous conjugate margin

Central East Greenland, specifically the Blosseville Kyst and Jameson Land basin areas, represent the closest conjugate margin analogue to the western margin of the JMMC prior to the second breakup during Oligocene to Early Miocene (e.g. Pedersen et al., 1997; Larsen, M. et al., 1999; 2002, 2005; Larsen, L.M. et al., 2013, 2014; Hopper et al., 2014; Papers II and III) (Figures 2.5; 2.8-2.10). This area presents a prime onshore type-locality for correlating the extensive pre- and syn-breakup flood basalts and intrusive rock formations along the central East Greenland coast to the JMMC (Table 2.1 and Figure 2.5). Although a substantial section is still visible onshore, the volcanic section is believed to have been eroded by up to 2-3 km since its emplacement (Mathiesen et al., 2000). The present-day estimated onshore record of up-to-6-km-thick Palaeogene volcanics has been subdivided into 4 stages of emplacement that very likely correlate directly across the JMMC and onto the Faroe Islands platform (Larsen, L.M. et al., 1999; Storey Storey et al., 2007; Passey and Jolley, 2009; Papers I and II) (Table, 2.1; Figures 2.5; 2.9).

The area's substantial coastal exposures preserve a record of igneous activity from ~63 Ma, which is referred to as the "Lower Basalt" series around the Kangerlussuaq Fjord region at the southern tip of the Blosseville Kyst. The "plateau basalt" series from around ~56 Ma that is correlated to the main breakup unconformity to a syn-rift volcanic series of the Mid-Eocene (e.g. Nielsen, T.F.D., 1981; Larsen, L.M. et al., 1985, 1989, 2013, 2014; Holm, P.M., 1988; Blichert-Toft, J., 1992, 2005; Pedersen et al., 1997; Tegner et al., 1998; Hansen and Nielsen, 1999; Upton et al., 1995; Brown, 1996; Bernstein, 2000; Momme, 2002; Peate, 2003; Nielsen, T.F.D., 2006; Hoppe et al., 2014) (Figures 2.5; 2.9). The early and primary plateau basalts of the Rømer Fjord, Skrænterne, Milne and Geikie plateau (GP) formations represent massive extrusive flood basalts and lava piles that alternate with thin volcanoclastic layers that covered most of the Blosseville Kyst, Milne Land and Geiki plateau areas (Pedersen et al., 1997) (Table 2.1; Figures 2.8; 2.9). The Early- to Mid-Eocene syn-rift basalts of the Prinsen of Wales Bjerge (~54 – 48 Ma) and Igtertivâ formations (~49 – 43 Ma) discordantly overlie the main plateau basalts.

Table 2.1 Summary of the igneous phases of the JMMC-IPR and its conjugate margins.

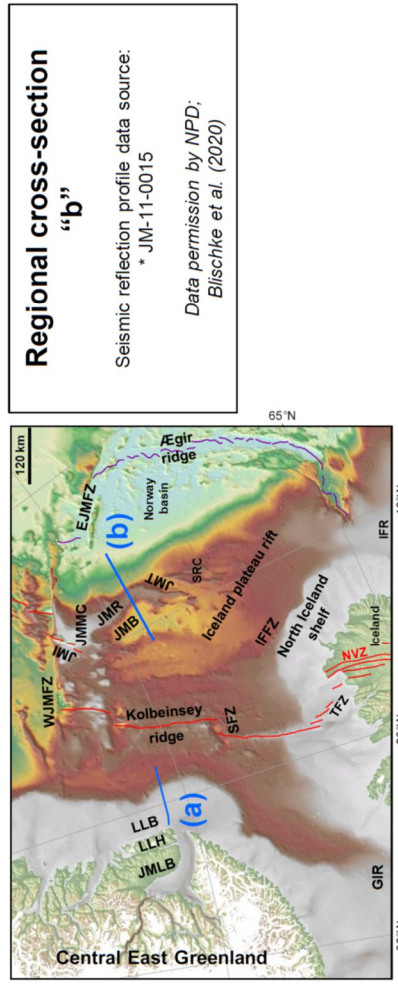
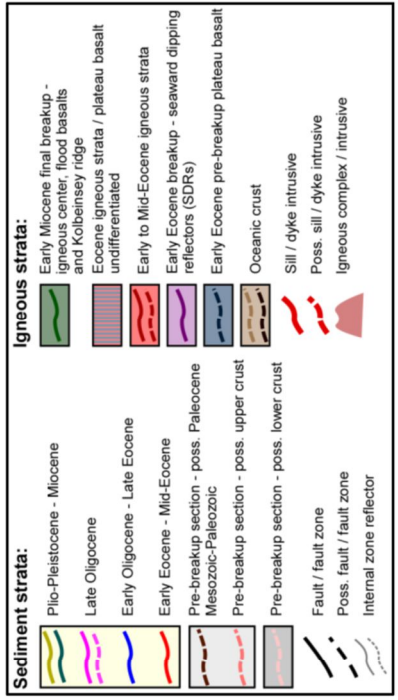
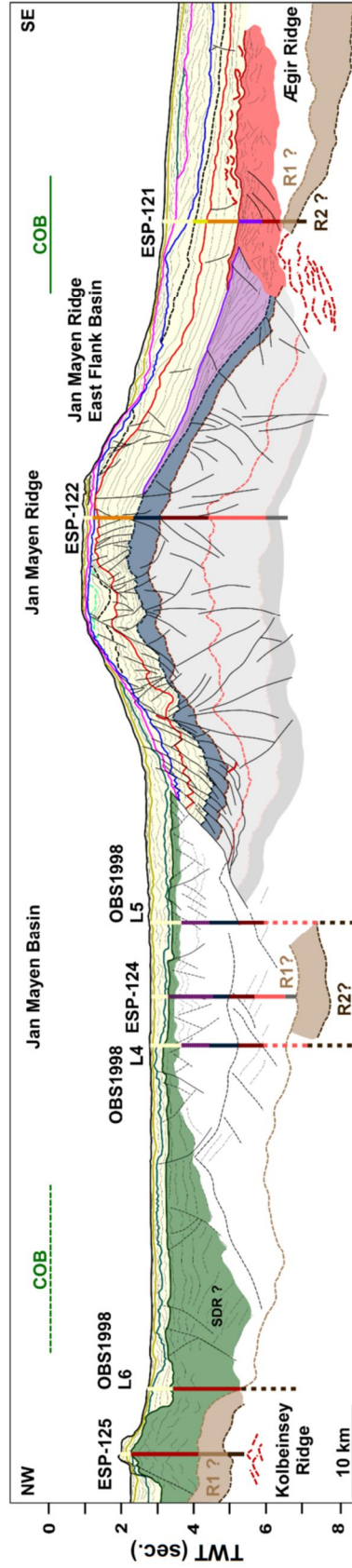
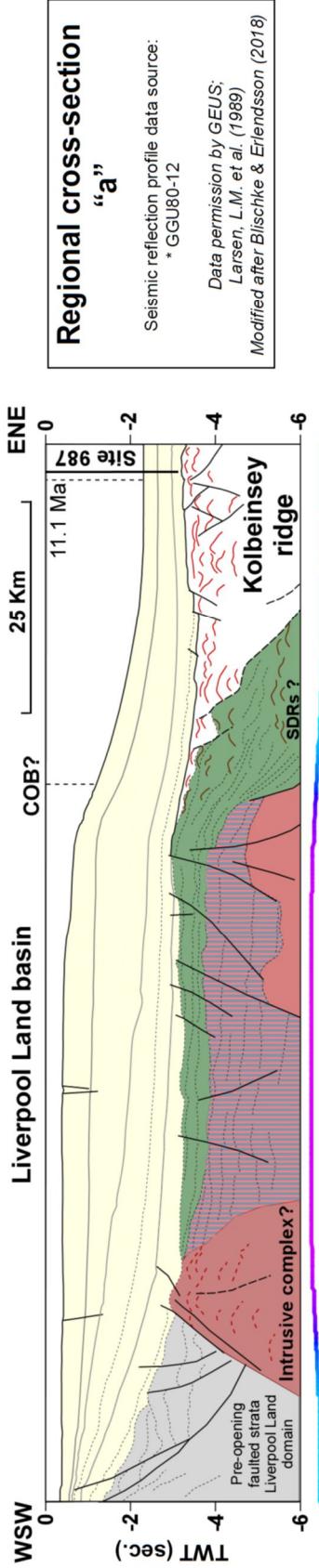
Igneous phases	Time span (Ma)	Seismic stratigraphic unit	Jan Mayen microcontinent Iceland Plateau Rift	Conjugate margins				Vøring plateau
				Time span (Ma)	Central East Greenland	Time span (Ma)	Faroe Islands - Faroe-Shetland basin	
drift / reactivation	since 22	JM-01 JM-05 JM-10	Spreading along the Kolbeinsey ridge with complete separation of the JMMC from the central East Greenland margin.	14-13	" <i>Yndöppnen formation</i> "; transitional to mildly alkaline basalt lavas across the central part of the Blöeseville Kyst and Geikie plateau			
2 nd breakup	~25-22	JM-15	" <i>IPR-IV</i> " forming of the SW Jan Mayen igneous province (<i>SWJMP</i>), the JMMC western igneous margin and the proto-Kolbeinsey ridge along the final breakup axis of the JMMC from Greenland; volcanic ridges and complexes, intrusives, arial extensive flood basalts	~35-21	" <i>Traili Ó igneous province</i> "; syenite intrusions; formed the landward end of the WJMEZ system			
rift propagation	~36-25	JM-35 JM-30 JM-20	" <i>IPR-III</i> " intersects the Jan Mayen southern ridge complex, forming the Jan Mayen trough; volcanic ridges, intrusives, arial extensive flood basalts	49-44	" <i>Igerivá igneous formation</i> "; northeastern shore of the Blöeseville Kyst (e.g. Kap Dalton)	~46.7-39	Post-breakup subaerial basalts across the Iceland-Faroe Ridge	Extensive extrusive formation of a subaerial lava escarpment along the western margins of the Vøring and Møre basins and large scale sill intrusives
syn-rift / rift propagation	~49-36	JM-50 JM-40	" <i>IPR-II</i> " intersected " <i>IPR-I</i> " and the southern extent of the SRC; overlapping spreading system of the IPR segments with the southern <i>Ægir</i> ridge connecting into the northeastern extent of the Greenland-Iceland-Faroe Ridge Complex (GIFRC); axial rift segments, intrusives, flood basalts	~54-48	" <i>Prinsen of Wales Berg formation</i> "; basaltic to felsic volcanics of the syn-breakup phase between central East Greenland and JMMC			
post-breakup	~53-50	JM-50	" <i>JMMC eastern volcanic margin</i> " and " <i>IPR-I</i> "; hyaloclastites and landward flows					
1 st breakup	~55-53	JM-60	" <i>SDRs</i> "; north-to-south development of an inner SDRs along the eastern margin of JMMC; two sets of outer SDRs overlapp the first and inner SDR set, a precursor to the <i>Ægir</i> ridge	~56-55	" <i>Plateau basalts</i> " that discordantly overlie the Caledonian Milne Land basement and " <i>primary breakup plateau basalts</i> " of the Geikie plateau	~56-54.9	" <i>Upper Faroe Islands Basalt Group (Lower FIBG)</i> "; Mainstindur (<4 km thick) and Hmri (>900 m thick) formations; landward and subaerial flood basalts; dominated N-NW of the Faroe Islands, changing into SDRs, connected to the initial opening of the Norway basin	Massive ash deposits; subaerial to subaqueous environment; possible increased sill and dyke intrusions; thermal uplift and subaerial erosion; migration of eruptive centres westwards towards the breakup axis of the Mohn's Ridge; " <i>Upper Series</i> "; large volumes of tholeiitic lavas, SDR formation, increased sill and dyke emplacements
Main breakup (initiation)	~63-55	JM-70	" <i>Plateau basalt equivalent</i> "; possible pre-breakup magmatic intrusions underneath JMR and regional extensive sub-arial flood basalts					
Pre-breakup				~63-57	"Lower Basalts"; early pre-spreading volcanics of the Rømer Fjord and Skrenterne plateau formations; Kangerlussuaq Fjord and southern tip of the Blöeseville Kyst regions	~61-56	" <i>Lower Faroe Islands Basalt Group (Lower FIBG)</i> "; Lopra (~1.1 km thick) and Beinsvørð (~3.3 km thick) formations of volcanoclastic and hyaloclastic to subaerial basaltic lava flows; change from a marine to a subaerial environment	" <i>Lower Series Flows</i> "; rhyolitic ignimbrites, tholeiitic basaltic intrusions, andesite and dacitic lava flow; Late Cretaceous to Paleocene
Stage 7								
Stage 6								
Stage 5								
Stage 4								
Stage 3								
Stage 2								
Stage 1								

Large igneous complexes reside in younger than Eocene sediments alongside the offshore Blosseville Kyst margin associated with the final breakup of the JMMC (Figures 2.5; 2.9). On- and offshore observations have highlighted two younger volcanic phases (Table 2.1; Figure 2.5): one is observed in the Traill Ø (Figure 1.1) region during Late Oligocene to earliest Miocene (~35-21 Ma), which became partially inverted by a syenite pluton, igneous complexes, and dike intrusions that form the landward end of the WJMFZ system (e.g. Gaina et al., 2017; Parsons et al., 2017; Geissler et al., 2017). The second and last volcanic phase occurred during mid-Miocene (13-14 Ma) during another reactivation of the magmatic system, creating the extrusive lavas of the Vindtoppen formation in the central part of the Blosseville Kyst. This formation overlies the mid-Miocene unconformity of the upper plateau and is possibly connected to an old tectono-magmatic reactivation through fracture and fault zones that cross into the Geikie plateau area (Storey et al., 2004; Blischke and Erlendsson, 2018; Paper III) (Figures 2.5; 2.9).

2.2.3 The Faroe Islands - southeastern igneous conjugate margin

The Faroe Islands basalt group (FIBG) which covers almost the entire continental margin of the Faroe Islands, has an estimated stratigraphic thickness of more than 6 km, and comprises a Paleocene – Lower Eocene succession of volcanic rocks that include extensive flood basalts, volcanoclastics, and hyaloclastites (Passey and Jolley, 2009; Passey and Hitchen, 2011; Ólavsdóttir et al., 2017, 2019) (Table 2.1; Figures 2.5; 2.8; 2.10). The FIBG extends westwards onto the Iceland-Faroe ridge, into the Norway basin, and eastwards into the Faroe-Shetland basin and represents the direct conjugate and analogue area to the southern and south-eastern extent of the JMMC-IP region interconnected by the IFFZ.

The volcanic phases of the FIBG were sub-divided into three major stages and stratigraphic units (Table 2.1). The pre-breakup Lower FIBG consists of the Lopra (~1,1 km thick) and Beinisdvørð (~3,3 km thick) formations. The Lower FIBG is dominated at its base by volcanoclastic and hyaloclastic rocks that progressed into subaerial basaltic lava flows within the Beinisdvørð formation, thus indicating a change from a marine to a subaerial environment. Landward, subaerial flood basalts were extruded during the syn-breakup phase and represent the emplacement of the Upper FIBG that consists of the Malinstindur (<4 km thick) and Enni (>900 m thick) formations (Rasmussen and Noe-Nygaard, 1969, 1970; Berthelsen et al., 1984; Ellis et al., 2002; Passey and Bell, 2007; Passey, 2009). These syn-breakup lava successions dominated the area north and northwest of the Faroe Islands, passing laterally into the seaward-dipping reflector succession that is associated with the initial opening of the Norway basin and the formation of the Ægir ridge spreading system. West and northwest of the Faroe Islands, the emplacement of post-breakup subaerial basalts persisted onto the Iceland-Faroe ridge (IFR) during the Mid-Eocene (Talwani et al., 1976f; Kharin et al., 1976; Ólavsdóttir et al., 2017) (Figures 2.5; 2.10).



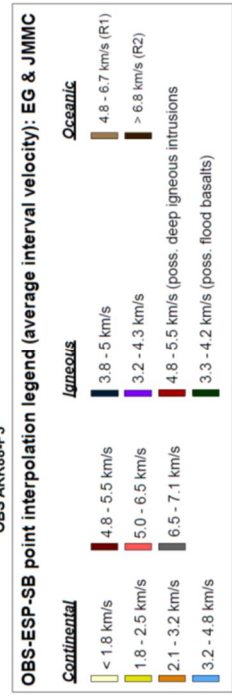
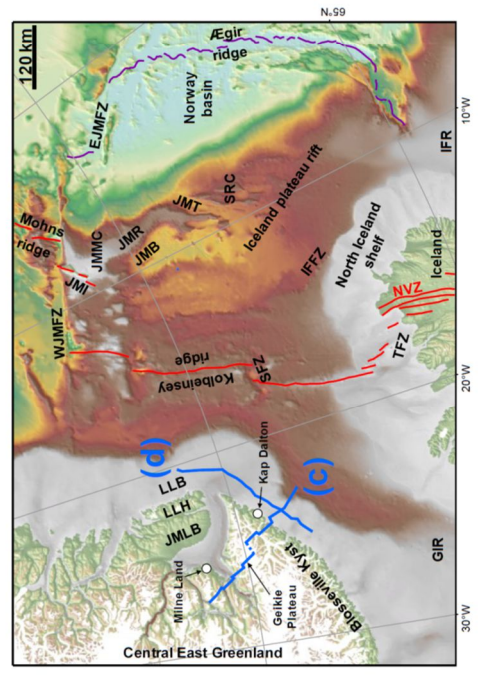
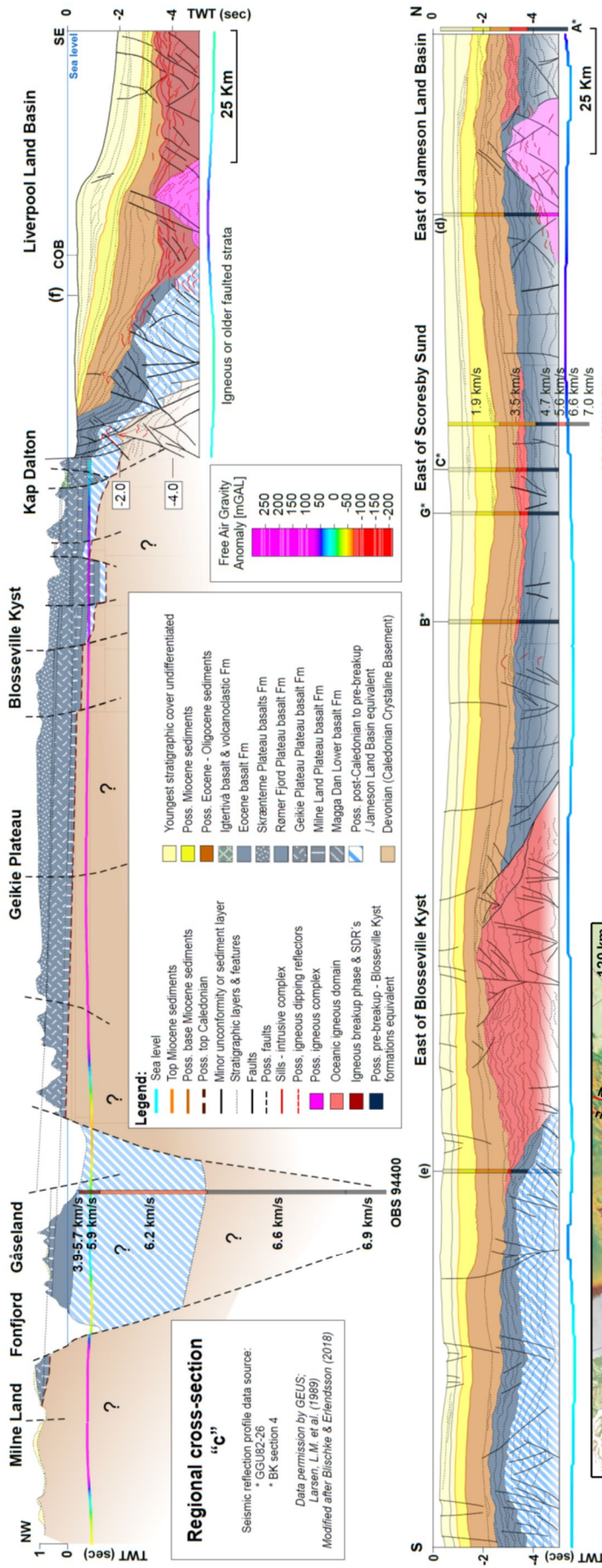


Figure 2.9 Conjugate margin tectonostratigraphic type sections: (a) Liverpool Land basin; (b) JMMC, (c) Milne land – Geikie plateau – Blossville Kyst – Liverpool land basin; and (d) Blossville Kyst – Scoresby Sund – Liverpool Land basin. The sections are tied to ESP velocity profiles, sonobuoy data and available borehole tie points. The pre-breakup section is inferred to contain Paleocene, Mesozoic to Paleozoic strata by direct comparison with the Jameson Land basin and the Blossville Kyst areas, and seismic refraction data (Hopper et al., 2014; Blischke and Erlendsson, 2018; Papers I – III). Abbreviations are listed on p. xix-xx.

2.2.4 The mid-oceanic ridge domains

The three oceanic domains adjacent to the JMMC were formed by different segments of the Northeast Atlantic mid-oceanic ridge system since the Early Eocene (~55 Ma). The Mohs and Ægir ridge systems developed after breakup along the eastern and northern JMMC flanks (Figures 2.5; 2.10), followed by the development of parallel and overlapping rift systems during rift transfer across the southern end of the JMMC and the IPR since the Mid-Eocene (Lutetian, ~49 - 43 Ma). The proto-Kolbeinsey ridge formed during Late Oligocene to earliest Miocene time (~35 – 22 Ma). Between ~35 – 26 Ma, the Ægir Ridge coexisted with the proto-Kolbeinsey Ridge, which led to the final separation of the microcontinent from the central East Greenland margin (e.g. Gaina et al., 2009; Gernigon et al., 2015; Papers I and III). The cessation of spreading at the Ægir Ridge is placed around 26 Ma (Kharin et al., 1976).

2.3 Geodynamic development of the JMMC-IPR within the Northeast Atlantic

This chapter presents a summary of the geodynamic development of the JMMC and existing key publications, addressing the influence of underlying structural trends on rifting and basin formation, as well as the ensuing sedimentary and volcanic response to tectonism throughout the evolution of the JMMC-IPR region (Papers I – III) (Figures 2.5, 2.8, 2.10, 2.11).

2.3.1 Pre-breakup regional setting

Prior to continental breakup, the proto-Northeast Atlantic region was affected by several distinct rifting episodes during the Late Palaeozoic (e.g. Ziegler, 1988; Andersen & Jamtveit, 1990; Stoker et al., 2016). Paper I summarised this evolution within the JMMC region from the post-Caledonian orogenic collapse to the pre-breakup setting in Early Eocene. The initial rifting phases led to rotational block faulting and westwards-tilted half-graben formation along East Greenland towards the JMMC domain, forming terrestrial to shallow marine basins. Deep basins formed by significant crustal thinning along their axial regions include the Jameson Land basin, which was separated by the Liverpool Land high from the JMMC (Figure 2.8 and 2.11). In the latest rifting phase during the Cretaceous, crustal thinning might have included hyperextension (Peron-Pinvidic et al. 2013), resulting in exhumation of deep crust and possibly mantle, as suggested by Osmundsen et al. (2002) and Osmundsen & Ebbing (2008).

The deep and hyperextended basins resulted in over-stretched and highly thinned continental crust, pre-destined for crustal breaches and formation of axial rift segments, specifically along deep reaching structural weak zones. The Norway basin along the JMFZ and along the north-eastern flank of the JMMC domain, prior to the forming of the Ægir ridge are examples of such crustal breaches (Figure 2.8; 2.11) (Gernigon et al., 2019; Paper I). Early volcanism associated with the North Atlantic igneous province (NAIP) during the Paleocene (~63-56 Ma) (Table 2.1), represents the initial attempt to break up the northeast Atlantic region along such underlying structural weak zones. Major fracture zone systems are also related to structurally weakened zones, for example the JMFZ north of the JMMC or the IFFZ south of the JMMC (Paper III).

These fracture zone systems and lineaments gradually developed into strike-slip structures between individual segments that became connected through shearing processes as breakup progressed. The lineaments are well-described by Cianfarra and Salvini (2015) for the regional strike-slip corridor associated with Neogene trans-tensional opening along the “De Geer Transform Fault” in northwest Spitsbergen, which forms the northernmost extent and boundary of the northeast Atlantic. Similar observation can be made for the opening lineaments / fracture zones of the JMFZ and IFFZ (Figure 2.8; 2.11).

Pre- to syn-breakup rifting was accompanied by regionally extensive landward flows of the NAIP, consisting of subaerial and submarine lava flows that were emplaced onto adjacent elevated margins (e.g. á Horni et al. 2017). Infilling of pre-existing basin type areas formed escarpments and hyaloclastite deltas (e.g. Planke et al., 2000, 2005; Gernigon et al., 2012, 2015; Abdelmalak et al., 2016, 2017; Geissler et al., 2017; á Horni et al., 2017; Papers II and III). One area of magmatism was located just southwest of the JMMC, close to the Kangerlussuaq basin and the southern extent of the Blossville Kyst, affecting the entire pre-

breakup region by connecting the central East Greenland, the southwestern Norwegian, and the western Faroe Islands margins (e.g. Tegner et al., 2008; Brooks, 2011) (Figures 2.8).

An area that was interpreted by Mordret (2018) with present day seismic tomography data that showed a 180 km deep reaching mantle anomaly. This mantle anomaly is inferred to be placed right at the intersection of the Caledonian thrust belt and the Archean crustal terrane. Thus, a region that intersects the extended and rifted central East Greenland margin at the southern Blosseville Kyst and Kangerlussuaq region that lay adjacent to the southwest corner of the JMMC-IPR area before breakup time. A juxtaposition area that has been highly volcanically active since Late Paleocene to Early Eocene, and very likely represents one of the focal areas predestined for developing a magma-rich margin, where breakup commenced (Figures 2.7; 2.8; 2.11).

2.3.2 The JMMC region at breakup

During the Early Eocene (56-55 Ma), plate breakup, ridge transfer and intense magmatism occurred along the Kangerlussuaq and southern Blosseville Kyst of central East Greenland (e.g. Tegner et al., 2008; Brooks, 2011; Larsen et al., 2014), including the emplacement of the regionally extensive NAIP plateau basalts (Figure 2.8; 2.11; Table 2.1). The Blosseville Kyst – Kangerlussuaq area has been modelled and linked by Doubrovine et al. (2012) to a plume or hot-spot location between 60 and 55 Ma. This coincides with the starting point of SW-NE-striking magnetic anomalies across the Geikie plateau (Paper III) that terminate at the intersection point between the main Caledonian front and Archaen terrane boundaries. This suggests that deep structurally weak zones might have facilitated the passage of upwelling magmatic material.

In terms of volcanic activity, the pre-breakup phase of the JMMC ended at about 55 Ma with the emplacement of Lower Eocene plateau basalts, deep intrusive complexes, dyke and sills across the microcontinent and the Blosseville Kyst region (Papers I – III) (Figures 2.5; 2.9; 2.11). Farther north, the JMMC was juxtaposed with the Trail-Ø volcanic igneous province (TVIP) and Vøring margin across the Proto-JMFZ to its north and northwest, (Figure 2.8). This area was modelled as a mantle anomaly around 56-54 Ma by Gaina et al. (2017), suggesting a strong fluctuation of the mantle anomaly and implying a much wider area of influence of the mantle anomaly piercing into the overlying weakened structural framework and instigating crustal rupture south and north of the JMMC. It has further been suggested that increased underplating and lower crustal body formations (e.g. Abdelmalak et al., 2017; Gernigon et al., 2019) can be seen underneath the microcontinent, close to the COB's and along the igneous margins (Figures 2.3 and 2.9). Alongside the eastern flank of the JMMC, igneous centres appear to align semi-en-echelon in a left-stepping direction, which would require a linked right-lateral transfer system along the Proto-JMFZ (Figure 2.8). This would explain why the initial breakup margin formed along the north-eastern edge of the microcontinent, which later formed the obliquely opening Ægir ridge and Norway basin, with the Norwegian margin opening in an WNW-ESE direction along the NW-SE striking proto-JMMC fracture zone segments (Paper III) (Figure 2.8). Thus, forming an extensional area south of the Proto-JMFZ with developing igneous centres and a gradually sub-siding eastern JMMC margin, and a developing transpressional region north of the fracture zone with a higher elevated Vøring margin that links to the regionally observed top Paleogene or top volcanic unconformity dated at ~55 Ma (Figure 2.11).

2.3.3 Iceland Plateau rift propagation

As described in section 2.1.7, the IPR consists of a series of rift stages within a propagating rift system with the formation of progressively-younger igneous crust from ESE to WNW within the Iceland Plateau, as can be demonstrated by seismic volcano-stratigraphic analysis of this study, and the variability of crustal thickness (Breivik et al., 2006, 2012; Brandsdóttir et al., 2008, 2015). Younger and overlying flood basalts have left little trace of the IPR rift structures near the seafloor and pre-flood basalt structural features themselves. Except for IPR stages II and III that are visible on seismic reflection data just south of the SRC and within the JMT (Figure 2.11). Thus, the interpreted IPR subsurface structures compensated for the lack of clear linear magnetic anomalies assigned to the IPR stages (I, II, III, and IV).

The IPR propagation and complicated tectonics of the JMMC was complemented by major rift basin formation offshore its conjugate East Greenland margin, especially along the Blosseville Kyst coastline and the Liverpool Land basin (e.g. Larsen, L.M. 1999; Surlyk, 1990, 2003; Stemmerik et al., 1993; Weigel et al., 1995; Butt et al., 2001; Seidler et al., 2004; Larsen, L.M. et al., 2013, 2014) (Figure 2.11a). Rift basin development and IPR propagation occurred in four stages (Figure 2.11b-e). The oblique IPR-I and II systems were linked to the Blosseville Kyst of central East Greenland during the Eocene (52 – 36 Ma) (Figure 2.11a-c). The separation of the JMMC from the central East Greenland margin during Oligocene to Early Miocene (~36 Ma – 21 Ma) (Figure 2.11d,e) was accompanied by extension, the formation of distinct S-N-oriented volcanic ridges and final breakup margin along the southwestern and western extent of the JMMC. Igneous complexes, such as the southwest Jan Mayen igneous province (SWJMIP), were emplaced along the southwestern-western margin of the microcontinent. The IPR stretches into the Jan Mayen basin as part of a buried western Late Oligocene breakup margin. The basin was then covered by regionally extensive flood basalt coming from the west and southwest, probably sourced from the proto-Kolbeinsey ridge system, but also from apparent point sources and potential volcanic complexes within the JMB (Figures 2.1; 2.4; 2.6d; 2.7). The JMMC-IPR transition highlights the complexity of a long-lived, active volcanic margin within an unstable rift-transfer setting, exhibiting both lateral and vertical crustal accretion throughout its formation from Eocene through Early Miocene times (Figure 2.5). This model infers that the anomalously thick oceanic crustal domains formed by overlapping rift systems accompanied by deep and shallow intrusive formations, similar to Iceland-type crustal formation.

2.3.4 The Cenozoic breakup, ocean and microcontinent formation

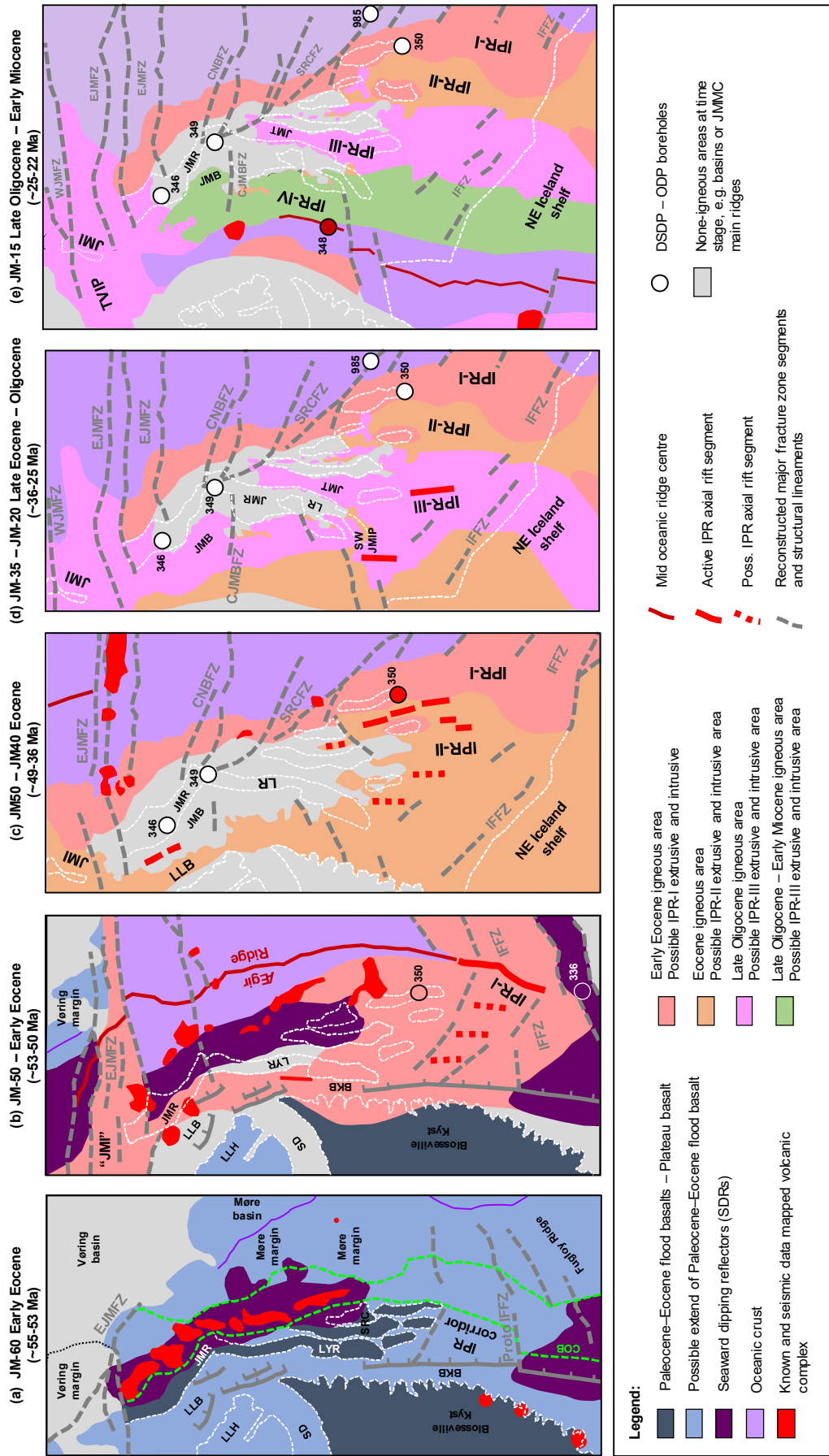
Cenozoic northeast Atlantic breakup and opening processes have been described in previous tectonic reconstructions, primarily based on geochronological work of magnetic anomalies and sparse vintage seismic reflection data (e.g. Talwani and Eldholm, 1977; Nunns, 1982, 1983a,b; Lundin and Doré, 2005; Doré et al., 2008; Gaina et al., 2009; Peron-Pinvidic, 2012a,b; Gernigon et al., 2015) (Figure 2.5; Table 2.1). In this study, the reconstructed geochronology of the Northeast Atlantic region and mapped igneous domains have been substantially updated, and seven major phases influencing the JMMC's breakup history have been identified:

- (1) *Early Paleogene*: Possible pre-breakup magmatic intrusions underneath central East Greenland – JMMC (~63-56 Ma). Initial breakup phase and rupturing of the overlying lithosphere along WNW-ESE striking, pre-existing fracture zones south of the microcontinent, i.e. proto-IFFZ, and along NW-SE striking fracture zones north of the JMMC, i.e. related to the proto-JMFZ system.

During the initial rifting and breakup phase, overlapping igneous systems developed along the divergent plate boundary, with subaerial plateau basalt flows across the Northeast Atlantic, including the JMMC region.

- (2) *Early Eocene*: North-to-south development of an inner, first set of seaward-dipping reflectors along the eastern margin of JMMC. Another two sets of outer seaward-dipping reflectors overlapped the inner SDR set, as a precursor to the formation of the Ægir ridge (~55-53 Ma).
- (3) *Early-Mid Eocene*: Formation of JMMC's eastern volcanic margin that extended into the IPR-I and southernmost extent of the Ægir ridge system (~53-50 Ma).
- (4) *Mid-Late Eocene*: IPR-II segment intersects the IPR-I segment and the southern extent of the SRC. Creation of an overlapping spreading system of the IPR segments with the southern Ægir ridge connecting into the northern extent of the Greenland-Iceland-Faroe ridge complex; axial rift segments, intrusives, flood basalts (~49-36 Ma).
- (5) *Latest Eocene-Oligocene*: The formation of segment IPR-III and the Jan Mayen southern ridge complex, alongside extensions within the Jan Mayen trough, and separation from the main Jan Mayen ridge (~36-25 Ma).
- (6) *Late-Oligocene*: Formation of the western igneous margin of the JMMC, representing the second igneous breakup margin in conjunction with the formation of the south-western Jan Mayen igneous province, the IPR segment IV, the proto-Kolbeinsey ridge, and the initiation of the proto-Iceland shelf region (~25-22 Ma).
- (7) *Early Miocene to present day*: Spreading along the Kolbeinsey ridge with complete separation of the JMMC from the central East Greenland margin (since 22 Ma).

Figure 2.11. Reconstructed igneous provinces around Jan Mayen. The positions of Eastern Greenland and the Jan Mayen main tectonic blocks are shown in an absolute position (relative to the mantle) according to kinematic parameters that were computed by carrying out visual fits (in GPlates 2.0.0; <https://www.gplates.org>) for four groups of basement ridges mapped in this study. Five reconstruction stages are shown in (a) Early Eocene (~55-53 Ma); (b) main breakup phase (~53-50 Ma); (c) syn-breakup to rift propagation phase throughout Eocene (~49-36 Ma); (d) intra rifting phase within the JMMC along the JMT and initiation of the western igneous margin during Late Eocene to Oligocene (~36-25 Ma); and (e) final breakup phase along the western JMMC margin (~25-22 Ma) and the full formation of the Kolbeinsey ridge. Features displayed are modified from data and interpretations by Larsen, L.M. (1985, 1989, 1999, 2013); Larsen, H.C. (1990); and Blischke and Erlendsson (2018). Abbreviations are listed on p. xix-xx.



3 Data overview and methods

The comprehensive database compiled during this study, was based on a larger-scale project database encompassing the entire Northeast Atlantic (Blischke et al., 2017a; Papers I-III) through participation in the NAGTEC project (Hopper et al. 2014). The database includes vintage and new geological and geophysical information acquired between the 1960's and 2017, which was incorporated into the NAGTEC Atlas and the Geological Society of London special publication 447 (Paper I and co-authored publications). The database report (Blischke et al., 2017a) includes a detailed overview of all implemented datasets on 1266 printed pages and is thus only partially included in this dissertation. Data preparations, processing, and interpretations conducted within this study are specifically listed within each data section and specifically flagged in column A of Table 3.1.

The construction of an integrated database involved data from a variety of institutions, including: the National Energy Authority of Iceland (NEA, Orkustofnun); Iceland GeoSurvey; the Marine Research Institute of Iceland (MRI-HAFRO); Spectrum ASA; Tomlinson Geophysical Services - Norwegian Petroleum Exploration Consultants International ASA (TGS-NOPEC); the University of Oslo (UiO); the Norwegian Petroleum Directorate (NPD); the Bundesanstalt für Geowissenschaften und Rohstoffe (BGR); and the Geological Survey of Denmark and Greenland (GEUS). Core samples were obtained from IODP Bremen Core Repository (Germany). Petrological analysis of core samples was undertaken at the Institute of Earth Sciences, University of Iceland and the Iceland GeoSurvey. Core age analysis were carried out at the Argon geochronology laboratory at Oregon State University (OSU, USA).

The seismic, borehole, analogue and interpreted datasets were implemented into the Petrel E&P software platform © by Schlumberger. Petrel is an integrated and interactive interpretation software within three-dimensional mapping tool for geophysical and geological data. Geodynamic plate reconstruction parameters for the relative motion of the JMMC and conjugate margins were calculated using the interactive fitting method of GPlates (www.gplates.org; Boyden et al. 2011). ArcMap, the main component of the © ESRI's ArcGIS suite was used for final data interpretation compilations and database storage.

The geophysical datasets include seismic-reflection and -refraction profiles, gravity and magnetic data, and multibeam bathymetric information. Offshore borehole and seafloor sample data provide geological, geochemical, petrological and age data, whereas analogue studies of the JMMC's conjugate margins provide both onshore and offshore comparative successions. The geophysical database forms the main foundation of this study, as deep borehole data are not available within the entire study area; thus, the age and nature of the geological succession older than Mid-Eocene on the JMMC remains conjectural. Thus, integration of all data types is necessary in order to obtain as best an understanding as possible of the geological succession.

Table 3.1 JMMC-IPR study offshore survey database review and summary. Selected datasets and compilations are marked in column “A” and shown in Figures 3.1 and 3.2.

A	Year	Survey ID	Survey lead	Country	Platform name	Data repository	Data types
	1957		NAVO	USA			Aeromagnetic
X	1961-1971	V2304/V2703/ V2803	L-DGO	USA	Vema/Conrad	NGDC	Bathymetry; Magnetics; Gravity; 2D MCS*1
X	1973	V3010	L-DEO	Norway	Vema/Conrad		Bathymetry; Magnetics; Gravity; 2D MCS
X	1974	DSDP Leg 38	DSDP		Glomar Challenger	IODP	Boreholes
	1975	CEPAN-75	CNEXO	France	Jean Charcot	Ifremer	Bathymetry; Magnetics; Gravity; 2D MCS
	1975	CEPAN-75	CNEXO	France	Jean Charcot	Ifremer	Bathymetry; Magnetics; Gravity; 2D MCS
	1975	CEPAN-75	CNEXO	France	Jean Charcot	Ifremer	Bathymetry; Magnetics; Gravity; 2D MCS
X	1975	BGR-75	BGR	Germany	Longva	BGR	2D MCS
X	1976	BGR-76	BGR	Germany	Explora	BGR	2D MCS
	1976	CGG-76	NPD/CGG	Norway			Aeromagnetic
	1977	IOS-77	UD/IOS	England	Shackleton	NGDC	2D MCS
X	1978	RC2114	L-DGO	USA	Robert Conrad	MGDS	Bathymetry; Magnetics; Gravity; 2D MCS, ESP*3
X	1978	WGC-78		USA	Karen Bravo	Western-Geco	2D MCS
X	1979	J-79	NPD	Norway	GECO alpha	NPD	Bathymetry; Magnetics; Gravity; 2D MCS
X	1980		PAH/SGC	USSR	Akademic Kurchatov		Seafloor sampling
	1983	NGT83/RC2412	L-DGO/BGR	USA/Germany	Prospekta/Conrad		2D MCS wide angle, ESP
	1983	RC2412	L-DEO	Norway	Robert D. Conrad		2D MCS and 2D SCS*2, Gravimeter, Magnetometer, Sonar-Echosounder
	1984	Arktis II/5	UHH	Germany	Polarstern		Refraction seismic
X	1985	JM-85	NPD/NEA	Norway	Malene Østervold	NPD	Bathymetry; Magnetics; Free Air Gravity; Bouguer Gravity; Magnetic; 2D MCS
X	1985	ODP Leg 104	ODP		JOIDES Resolution		Boreholes
X	1986	UiO-86	UiO	Norway	Håkon Mosby	NPD	2D MCS
X	1987	Refranorge IV	IFP	France/Norway	Polarbjorn & Odys Echo	CGG/UiO	ESP; Velocity; Gravity

Table 3.1 continued.

A	Year	Survey ID	Survey lead	Country	Platform name	Data repository	Data types
X	1988	JM-88	NPD/NEA	Norway	Håkon Mosby	NPD	Bathymetry; Magnetics; Gravity; 2D MCS; Sonobuoy
X	1995	JMKR95	UiB/UiH/NEA	Norway/Japan/NEA		UiB	Seismic refraction & 2D MCS
X	1995	ODP Leg 161	L-DGO	Norway/UK/USA	JOIDES Resolution	IODP	Boreholes
X	2000	KRISE 2000	UiB	Norway	Håkon Mosby	UiB	Seismic refraction & 2D MCS
X	2000	OBS2000	UiB	Norway	Håkon Mosby	UiB	Seismic refraction & 2D MCS
X	2001	IS-JMR-01	InSeis	Norway	Polar Princess	CGG/Veritas	2D MCS
X	2002	ICE-02	TGS-NOPEC	Iceland	Zephyr-1	TGS-NOPEC	2D MCS; Gravity
X	2003	EW0307	L-DEO	USA	Maurice Ewing	MGDS	2D MCS; Gravity; Bathymetry Cores
X	2005	JAS-05	NGU/NPD	Norway	Piper Navajo	NGU	Aeromagnetic
X	2006	OBS JM-06	UiB/Geomar	Norway/Germany	G. O. SARS	UiB	Seismic refraction & 2D MCS, gravity, magnetics
X	2008	WI-JMR-08	Wavefield InSeis	Norway	Malene Østervold	Spectrum	2D MCS
X	2008	A8-2008	HAFRO/NEA	Iceland	Arni Fridriksson	HAFRO/NEA	Multibeam
X	2009	JM-85-88	Spectrum	Norway	Re-processing	Spectrum	2D MCS
X	2009	SAR-ICE-2009	NEA	Norway	ENVISAT satellite	Fugro NPA	Satellite Synthetic Aperture Radar (SAR)
X	2010	A11-2010	HAFRO/NEA/NPD	Iceland	Arni Fridriksson	HAFRO/NEA/ NPD/Fugro Geolab	Multibeam; Seafloor sampling
X	2010	B11-2008	HAFRO/NEA	Iceland	Arni Fridriksson	HAFRO/NEA	Benthic survey
X	2011	NPD-11	NPD/UiB	Norway	Harrier Explorer	NPD/PGS	2D MCS; Seafloor sampling
X	2011	JMRS11	VPBR/TGS	Norway	TGS	VPBR/TGS	Seafloor sampling
X	2012	NPD-12	NPD/UiB	Norway	Nordic Explorer	NPD/PGS	2D MCS; Seafloor sampling
X	2012	JAS-12	NGU/NPD/NEA	Norway	Piper Chieftain	NGU/NPD/NEA	Aeromagnetic
X	2016	NARVAL 2016	SHOM	France	R/V Beautemps-Beaupré	SHOM	Multibeam

¹ 2D MCS – Multi-channel seismic reflection data

² 2D SCS – Single channel reflection seismic

³ ESP – Expanded seismic profile

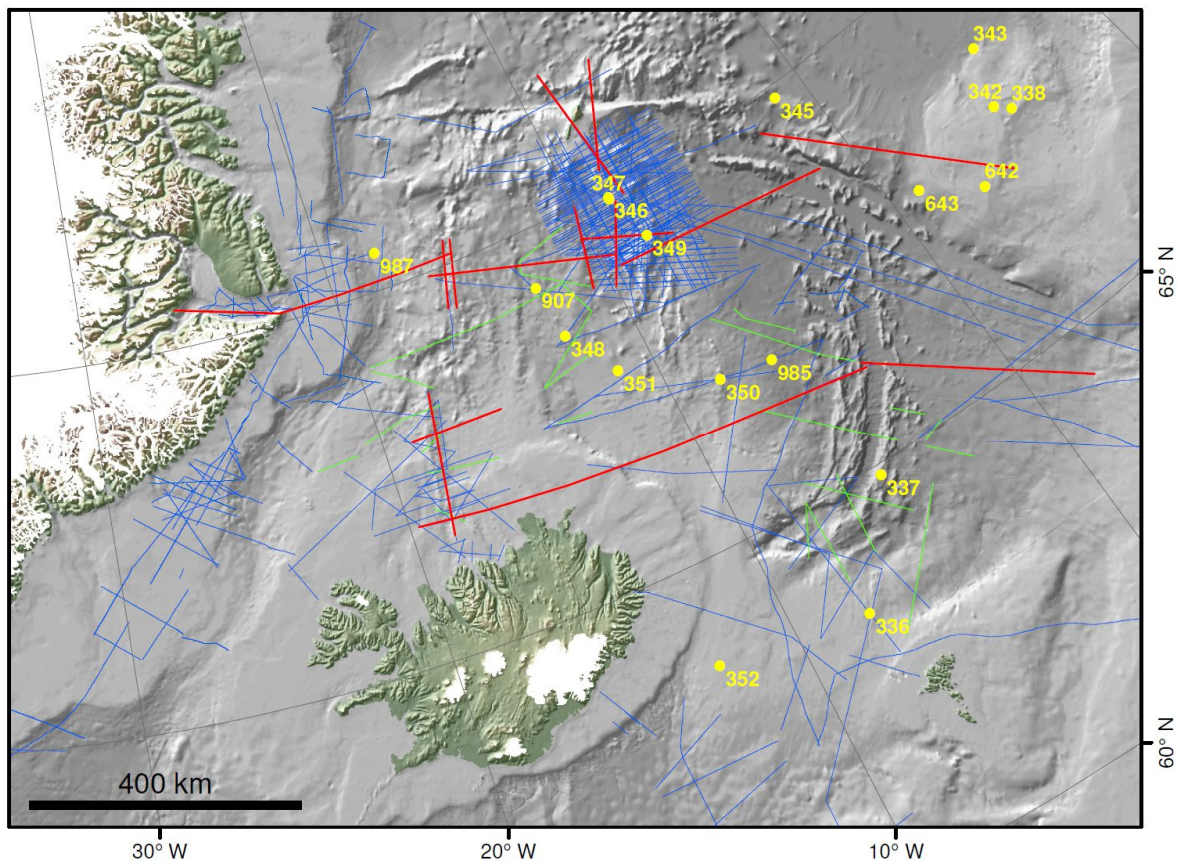


Figure 3.1 Regional project database (Table 3.1) showing seismic reflection (2D MCS (multi-channel data blue lines); 2D SCS (single channel data – green lines)), seismic refraction lines (red lines), borehole data (yellow points), shaded bathymetry (IBCAO 3.0; Jakobsson et al., 2012), and ETOP01 (Amante and Eakins, 2009).

3.1 Description of the data

This study is based on analyses and interpretation of geophysical datasets, including seismic-reflection and -refraction profiles, gravity, magnetic and multibeam bathymetry data. Offshore borehole and seafloor sample data helped constrain geological, geochemical, petrological and stratigraphic age. However, the geological succession older than Mid-Eocene on the JMMC remains conjectural.

3.1.1 Bathymetry

High-resolution multibeam bathymetry data obtained from the international bathymetric chart of the Arctic ocean (IBCAO) Version 3.0 with a 500 m x 500 m resolution (Jakobsson et al., 2012) was used for the regional grid maps (Figures 3.1; 3.2) and tied to ship-track data, required for two-way-travel time-to-depth conversions of the 2D multi-channel seismic (MCS) and single-channel seismic (SCS) data (e.g. Åkermoen, 1989; Gunnarsson et al., 1989; Papers I-III).

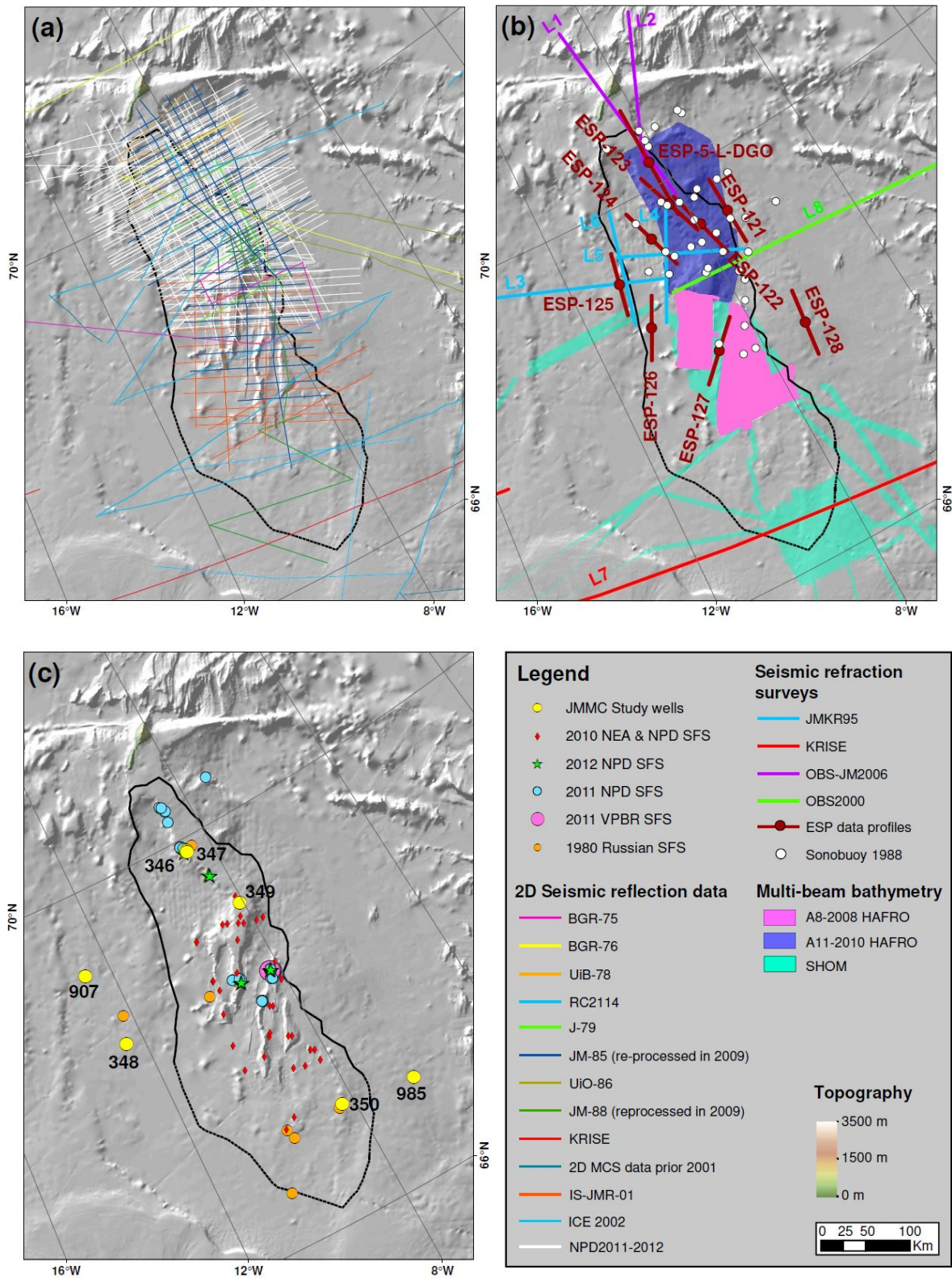


Figure 3.2 An overview of the Jan Mayen database on a hill shaded bathymetry map (Jakobsson et al., 2012), showing (a) 2D MCS lines and cross-sections; (b) boreholes and seabed sampling sites; (c) seismic refraction lines, and multibeam bathymetric maps. For detailed survey information and references see Table 3.1. Abbreviations are listed on p. xix-xx.

Data from three high-resolution multibeam echo-sounder surveys, conducted across the JMMC and IPR in 2008, 2010 and 2016 were merged with the IBCAO regional dataset (Figure 3.2b). The A8-2008 and A11-2010 surveys were planned by NEA, NPD, and MRI-HAFRO, using the research vessel *Árni Friðriksson*. These surveys provided 10,500 km² of 50 m x 50 m resolution bathymetric data, between 790 m and 2210 m depth (Helgadóttir, 2008; Helgadóttir and Reynisson, 2010). The French Hydrographic and Oceanographic Office (SHOM) conducted the NARVAL 2016 cruise using the R/V *Beautemps-Beaupré* across the JMT, SRC and IPR, acquiring 35000 km² of multibeam data with 50 m x 50 m resolution, as well as sub-bottom profiles and magnetic data. The high-resolution bathymetric data provided important information on structural trends and igneous features, such as volcanic cones, axial ridges, and pockmarks interpretations, which combined with the 2D MCS seismic reflection data, has constrained the location of normal faults, strike-slip faults, and slump fault systems along the steep escarpments, in addition to sea-bed and shallow sub-seabed expressions of volcanic activity across of the microcontinent's ridges (Blischke et al., 2017a; Papers I-III).

3.1.2 Gravity and magnetic data sets

Compilation of the extent and depth of sedimentary basins, major tectonic features and variations in crustal segmentation across the study region was based on the NAGTEC gravity data by Haase and Ebbing (2014). The magnetic data implemented in this study was processed and compiled from various magnetic data surveys by Nasuti and Olesen (2014) within the NAGTEC project. The magnetic data was used to constrain the subsurface geology based on anomalies in Earth's magnetic field that effected and preserved the field's orientation of the underlying rocks at its time of emplacement; for example, providing a chronological mapping tool of magnetic anomalies across the ocean floor (see section 3.2.2). The magnetic data also provided information on hidden geological structures, especially in volcanic and metamorphic terrains and structures in non-magnetic sedimentary terrains that were highlighted and described in more detail in the co-authored publication by Gaina et al. (2017a). The potential field data in combination with the seismic data provided a useful interpretive tool to significantly improve and validate the geological and structural configuration, e.g. hidden igneous complexes (Figures 2.4; 2.6).

Gravity and magnetic anomaly mapping lend support seismic data interpretations. Detailed magnetic anomaly datasets from the JMMC and Norway Basin region from surveys JAS-05 and NB-07 and JAS-15 (Gernigon et al., 2012, 2015) were included in the NAGTEC project (Hopper et al., 2014), and combined with line-data acquisitions accompanying the seismic reflection surveys (Blischke et al., 2017a). The magnetic data was crucial determining the breakup boundary along the eastern flank of the JMMC. Traces of several substantial, isolated anomalies can also be seen on the magnetic maps, representing igneous complexes (Figure 2.4).

3.1.3 Seismic reflection data

Analogue single-channel and two-dimensional multichannel seismic reflection data (2D SCS and 2D MCS) constitute the main data analysed in this study (Figures 3.1; 3.2; Table 3.1) This data images the subsurface by recording seismic waves transmitted from a vessel with a controlled sounding source. The transmitted waves, reflected and refracted from the seafloor and layers below the seabed, are recorded by a string of seismic detectors that are towed behind the vessel. As the source and detector positions, the line-up distances and timings are known the data is displayed as two-way-travel time (TWT) along horizontal distance. This data method has been applied since the 1920's (Karcher, 1987; Tóth, 2011). Seismic reflection surveys are conducted from large seismic-acquisition vessels, including 2D single-channel acquisition to up-to-15-km-deep multi-channel recordings. All specific data surveys acquisition details are summarized in an extensive database report by Blischke et al. (2017a; Appendix 2).

Early north Atlantic regional 2D MCS surveys across the JMMC area, mainly BGR-75, BGR-76 (Hinz and Schlüter, 1978), and RC2114 (Talwani et al., 1981; Mutter et al., 1982; Talwani et al., 1978), constrained the transition from the JMMC into the oceanic domain. Two-dimensional MCS and seismic refraction data in combination with onshore geological maps and cross section profiles, together with elevation/bathymetry, gravity and magnetic potential field data along the central East Greenland coast for direct data comparison of the JMMC domain to its direct western margin analogue and are described in detail in Blischke and Erlendsson (2018) (Figure 3.2).

Two-dimensional MCS surveys prior to 2001, available on paper or film had to be imported as images and transferred into the standard segy-data digital format (Blischke et al., 2017a). MSC data from the following surveys were used across the JMMC-IPR study area: BGR75-76, JM-85 and JM-88, IS-JMR-01 (2001), ICE-02 (2002), WI-JMR-08 (2008), NPD-11 (2011), and NPD-12 (2012). Acquisition and processing information by survey, year and company are listed in Appendix 2. All seismic reflection data that covers the JMMC-IPR area was pre-processed, line positions checked, and loaded into a common single geographically projected database during this project. Prior to this project was the candidate involved in the positioning and target prioritisation of the newer surveys of 2008, 2011 and 2012, and correcting the segy-data location and orientation of dataset JM-85 and JM-88 for the Petrobank database system in Norway. Unfortunately, the CEPAN75 survey data could not be imported due to the lack of navigation data.

The JMMC 2D MCS datasets acquired after 2008 are of a higher quality and image deeper into the subsurface. The latest surveys in 2011 and 2012 undertaken by the Norwegian Petroleum Directorate (NPD) considerably improved the imaging quality of the Cenozoic section. These two surveys applied variation to higher-volume source signal, detector streamer length, and separate processing of the long-wave frequency data partition for the deeper sub-basalt sections. This resulted in much improved imaging for the eastern flank and the main JMR and SCR domains but did not fully penetrate the youngest (Late Oligocene – Early Miocene) flood basalt layers of the IPR-III and IPR-IV domains within the JMT and along the southern to western flanks of the JMMC (Figure 2.1).

3.1.4 Seismic refraction data

Seismic refraction-data acquisition is crucial to determine depth and velocity contrasts of the sub-surface. The acquired data builds on the principle that seismic waves have differing densities and thus velocities in varying rock types governed by Snell's law (Kearey and Brooks, 1984). As seismic waves are sent into the subsurface, a portion of its energy is refracted as it crosses an interface between different rock types enabling the determination of intersection time and offset; this further enables the determination of velocity information necessary to convert the 2D MCS from two-way-travel time (TWT) into actual depth data, and can provide information necessary to determine rock type.

Seismic refraction data were used in crustal domain interpretation, constructing seismic-stratigraphic velocity ties to the seismic reflection data, and delineating the extent of the JMMC in comparison with gravity and magnetic anomaly data. Seismic refraction data for the GIFRC and Northeast Atlantic area, compiled within NAGTEC (Funck et al., 2014, 2017) and KRISE (Brandsdóttir et al., 2015) projects, were also made available to this study. For the central East Greenland conjugate margin, existing seismic refraction OBS data interpretations were crucial in tying the seismic reflection data with the surface geology, as described in detail by Blischke and Erlendsson (2018) (Figures 3.1).

Additionally, sonobuoys deployed during the JM-85 seismic-reflection survey and processed by Olafsson and Gunnarsson (1989) were interpreted in order to obtain seismic velocities within the upper layers of the JMMC microcontinent, and better constrain igneous crust with the continent-ocean transition, especially the SDR's along the eastern igneous margin of the JMMC (Papers I-III).

Unpublished expanding spread profiles (ESP-121 to ESP-128) (Figures 3.2a; 3.3) were analysed and interpreted by travel-time-to-offset-ratio (T-X) analysis (e.g. Childs and Cooper, 1978) and by the Tau-P velocity estimation methods of Diebold and Stoffa (1981). The data was available as paper travel-time-to-offset and Tau-P plots only and had to be scanned and interpreted using a high-resolution digitizing tool (<https://apps.automeris.io/wpd/>). The ESP results are presented in Figure 3.3 and Table 3.2.

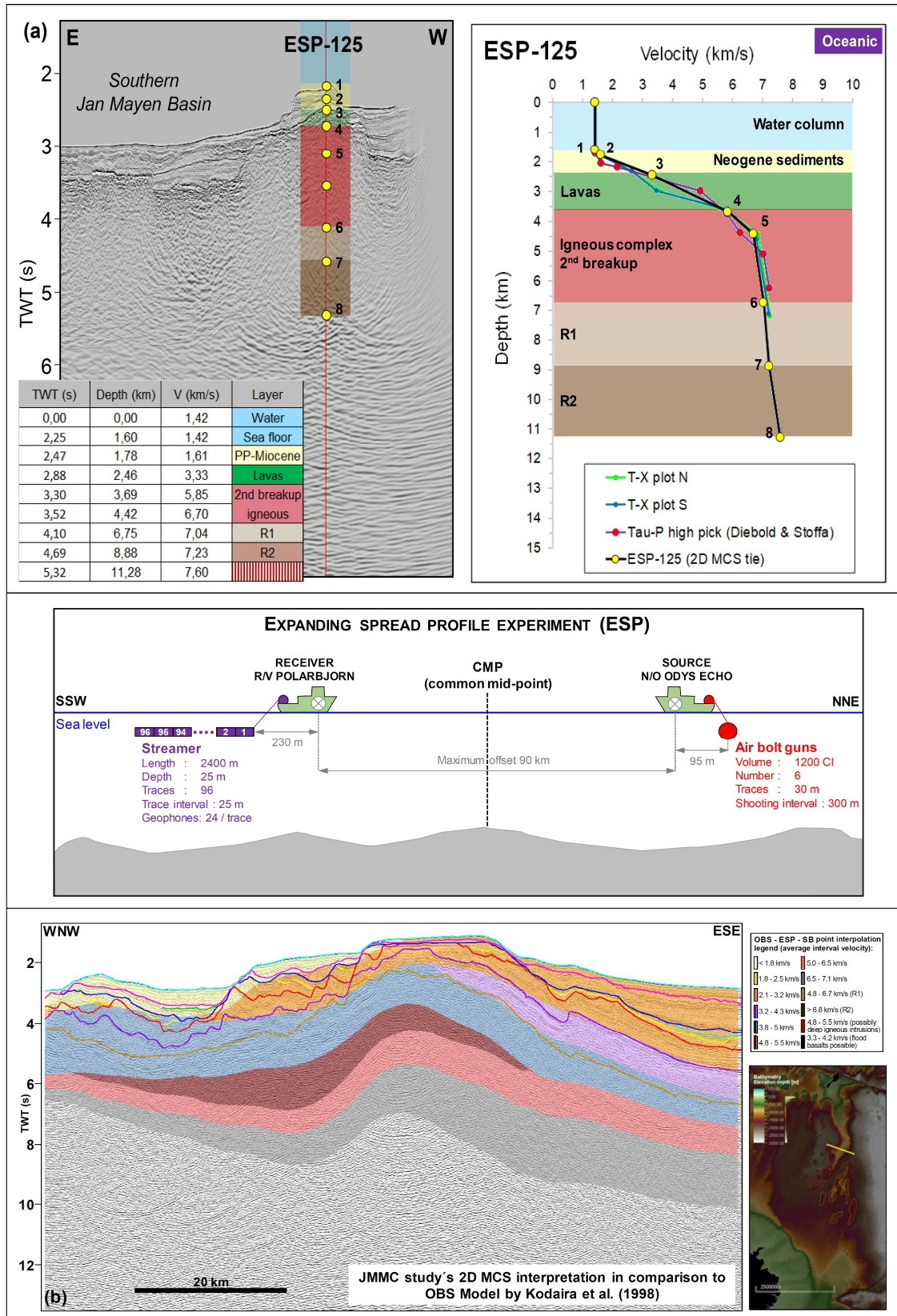


Figure 3.3 The velocity structure of ESP-125, see insert (a) in comparison with 2D MCS data along the western igneous margin of the JMMC (location is shown on Figure 3.2b) and (b) OBS crustal structure based on Kodaira et al. (1998), for horizon legend see Figure 2.3.

Table 3.2 ESP-121 to ESP-128 Profile analysis (offset T-Z; Tau-P analysis summary values tied to 2D MCS data) of this study.

V _{min} (km/s)	V _{max} (km/s)	V _{avg.} (km/s)	V _{avg.} SD* (km/s)	Zone	Comment
1,4	1,5	1,44	0,0	SFL	Sea water
1,4	1,7	1,54	0,1	Plio-Pleistocene	Unconsolidated water saturated sediment
1,4	2,7	1,85	0,3	Miocene	Soft sediment
2,0	4,2	3,35	0,7	2nd BU Basalt	(3.4-4.0) basalt into soft sediment
2,4	3,8	3,03	0,4	Eocene	Consolidated and diagenetically alter sediment
3,4	4,4	3,77	0,3	SDR	Same top pick, used average 4.3 for typical basalt range
3,9	5,8	4,60	0,6	PB	
4,3	5,4	4,99	0,3	PreBreakup	Compacted and metamorph over-printed Mesozoic or Paleozoic sediments
5,3	6,7	5,73	0,5	UC	Caledonian
6,3	7,2	6,64	0,2	LC	Lower crust
7,0	7,8	7,43	0,3	BC	Lower crust (ductile?) to mantle transition
4,8	5,3	5,07	0,3	OC L2	Oceanic basement
5,9	6,8	6,44	0,4	OC L3	Layer R1 on cross-sections
6,8	7,9	7,38	0,4	OC L4	Layer R2 on cross-sections
7,2	8,1	7,72	0,4	BC	Lower crust to mantle transition

*SD – standard deviation

Seismic refraction velocity model and basement tie

As the JMMC is surrounded by igneous domains, delineating its boundary with the volcanic domain was important. To better constrain this region, the 2D seismic reflection dataset was analysed in combination with the available seismic refraction data and crustal velocity models, as well as available borehole control along the ridges. This enabled an interpretation of the nature of acoustic basement and different crustal type domains.

Furthermore, anomalously high 2D MCS-based stacking-velocities were compared to the JMMC structural domains within a 3D grid compiled data set (Figure 3.4). Stacking velocities from the various processed 2D MCS surveys (Appendix 2) were first not included, as the data appeared anomalous and inconsistent by assessing each survey on its own.

However, as all the different vintage stacking velocity data set showed similar anomalously high velocities (>4000 m/s) and normally increasing velocities with increasing depth, they were reconsidered and compared with igneous centres located by other methods across the JMMC, but specifically along the IPR (Figure 3.4). The >4000 m/s anomalies are narrow and appear to align with possible deeper intrusive complexes and volcanic ridges mapped within the SWJMIP, the IPR segments (Figure 3.4), towards the JMI and the microcontinent's northern extent.

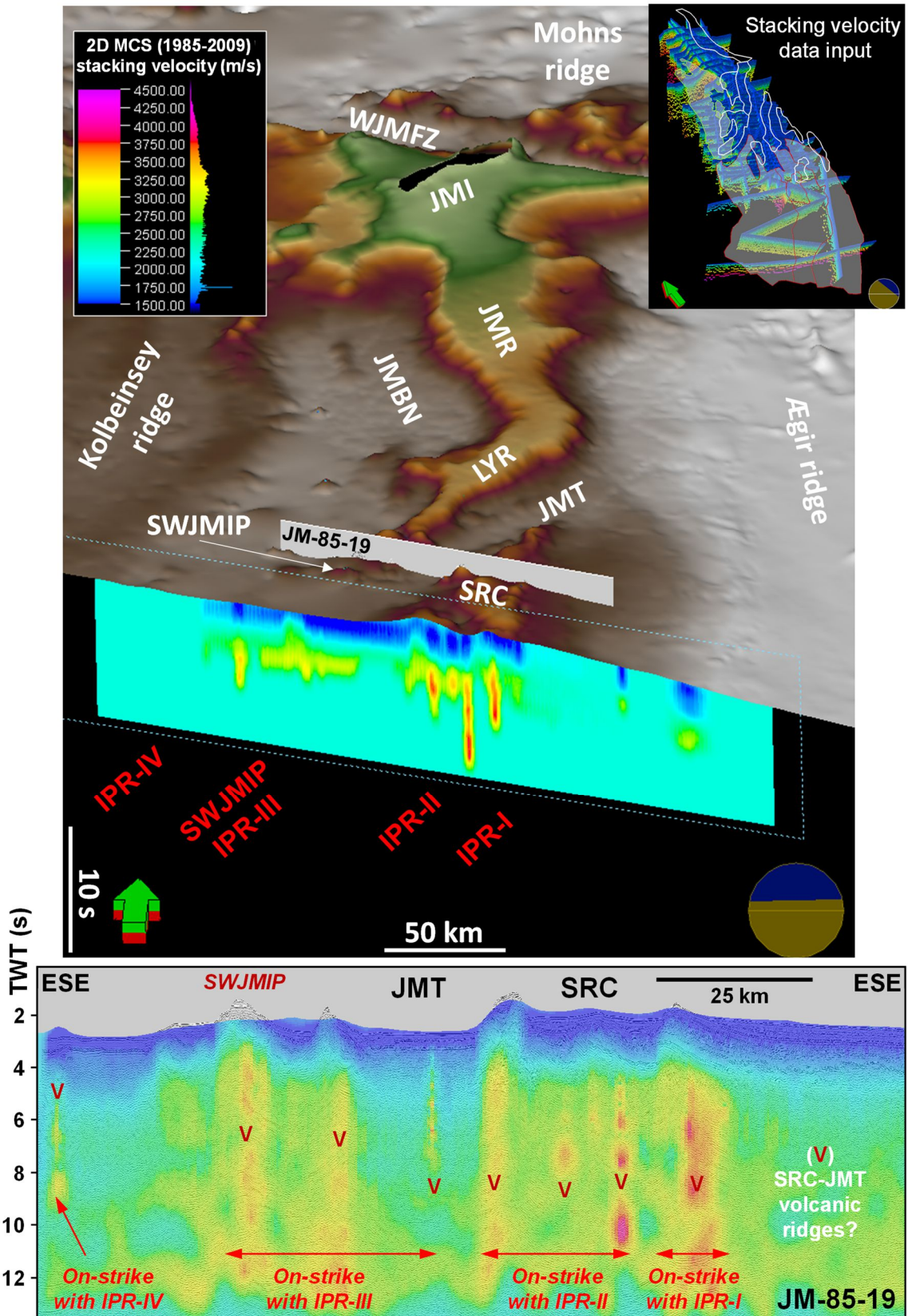


Figure 3.4 2D MCS stacking velocity data combined in a 3D grid compilation and highlighted high velocity anomalous areas within the JMMC region. Abbreviations are listed on p. xix-xx.

Similarly, high velocities (3,3 – 4,2 km/s) are present within the Jan Mayen basin suggesting that the primary western volcanic margin was located right at the western edge of the JMR and not along the western edge of the JMB (Papers I-III) (Figures 2.1; 2.3; 2.7). This provides a better explanation for an igneous source of the areal extensive flood basalts that cover the entire JMB and southwestern region of the JMMC (Figure 3.1e).

The volcanic margins and complexes east of the JMR and SDRs have a much higher velocity range of >4 km/s than the surrounding sedimentary rocks (Figures 2.3b,c; 3.4); thus, being part of the eastern volcanic margin that lies within the oceanic basement domain, covered by a thin low-velocity sedimentary layer (< 2,5 km/s) (Papers II and III). The underlying layer has a velocity range of 4,8 – 6,8 km/s, which most likely corresponds to the oceanic layer 2 (R1-R2 on Figure 2.3; Table 3.2). Seismic reflectors off Norway basinward to the continent ocean boundary and below the “R2” seismic reflection event ($V_p > 6,8$ km/s) are generally chaotic or opaque. These have been interpreted as higher-velocity layers connected to underplating, or lower crustal bodies associated with volcanic margin formation of the JMMC, East Greenland, SW Norway (Møre and Vøring margins) (e.g. Weigel et al., 1995; Breivik and Mjelde, 2003; Breivik et al., 2008, 2012; Faleide et al., 2010; Gernigon et al., 2015; Mjelde et al., 2016; Theissen-Krah et al., 2017; or Zastrozhnov et al., 2018). These higher-velocity layers delineate the transition from the JMMC to the oceanic domain within the volcanic margin and can be observed all around the JMMC domain with apparent localized thickening around fracture zones see Figure 3.5.

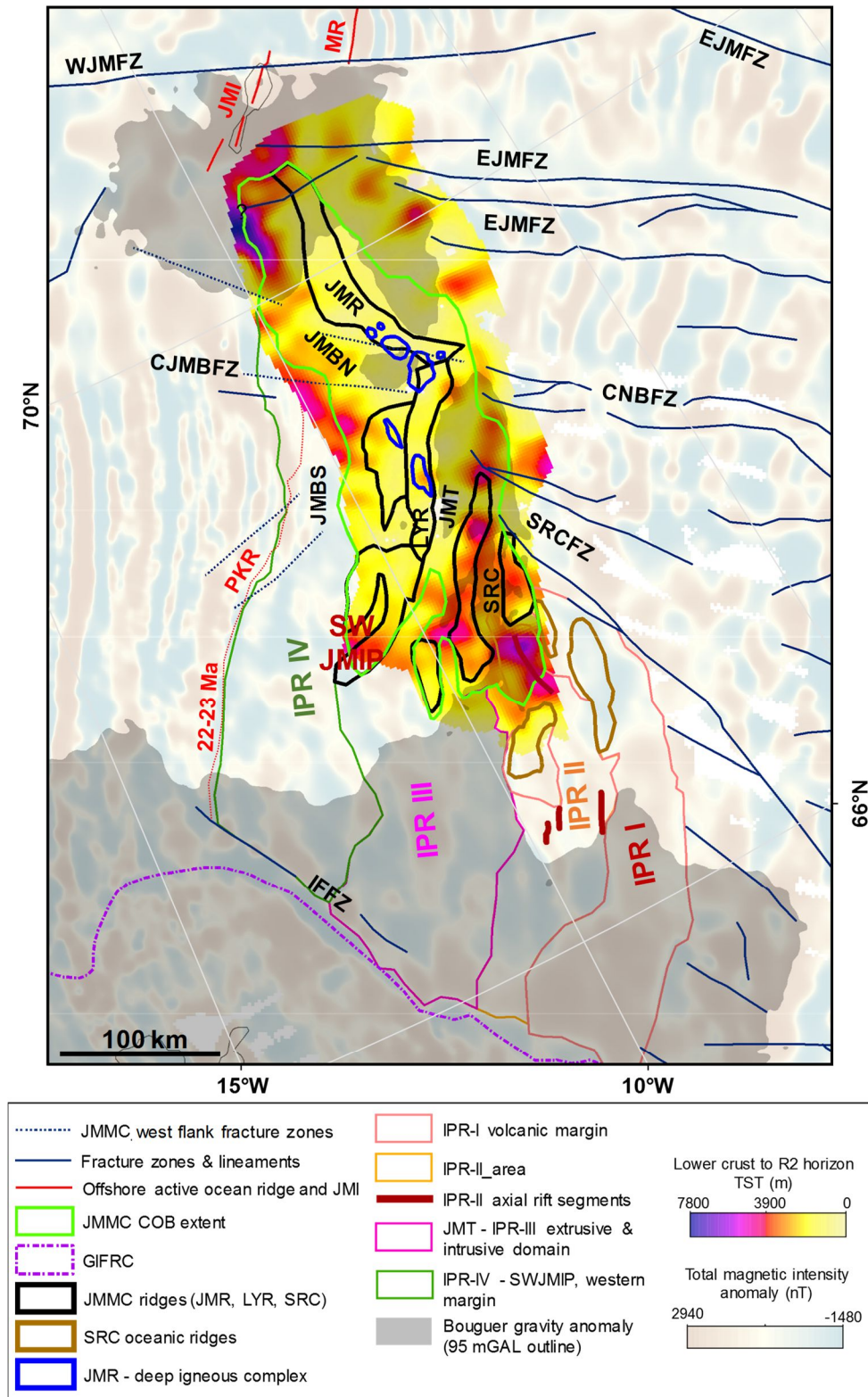


Figure 3.5 Variations in lower crustal velocity within the JMMC and thickness estimates between lowermost seismic reflection event of the “inferred lower crust” and the “R2” event indicate increased magmatic incursions within the IPR domain, SWJMIP, the western igneous margin, NW-JMR – JMI, and close to the segments of fracture zone terminations. Magnetic anomalies data from Haase and Ebbing, (2014). Abbreviations are listed on p. xix-xx.

3.1.5 Offshore and onshore geological sample data

Offshore borehole and seafloor samples are sparse across the Northeast Atlantic region, especially away from the active mid-oceanic ridges (Figures 3.1; 3.2; 3.6). Information from twelve shallow boreholes of Deep-Sea Drilling Program (DSDP, Leg 38) and Ocean Drilling Programs (ODP, Legs 151 and 162) were used in this study, specifically igneous samples in the JMMC area. These boreholes include sites 336, 337, 342, 343, 345, 346, 347, 348, 349 and 350 of DSDP Leg 38 (Talwani and Udintsev, 1976a-j), site 642 of ODP Leg 104 (Eldholm et al., 1974, 1987a,b, 1989), and 985 for ODP Leg 162 (Jansen et al., 1996).

Seafloor sampling campaigns carried out by gravity coring in 1973 by Geodekyan et al. (1980), in 2010 by the NEA, using remote operated vehicle (ROV) directed sampling by the NPD in 2010-2012 (Sandstå et al. 2012), the Volcanic Basin Petroleum Research Group (VBPR) and TGS in 2012 (Polteau et al., 2018) have provided additional data, though the in-situ nature of some of these sample locations remains ambiguous. Dredges and gravity cores acquired by XXX from targeted sites along steep flank areas of the JMMR's western rim, the eastern flank of the Lyngvi ridge, and the north-western flank of the SRC were also included (Figure 3.2).

Geochemical analyses of these JMMC rock samples facilitated a chronostratigraphic and paleo-environmental interpretation which together with the seismic reflection data, added valuable information to the tectonostratigraphic model (Papers I-III).

DSDP Leg 38 sites 348 and 350 were re-viewed and re-sampled from the IODP core data repository in Bremen, Germany as part of this project. Recovered Middle Eocene basalts from 350 at the southeasternmost extent of the SRC, and Lower Miocene basalts from site 348, at the western igneous margin of the microcontinent were reanalysed and $^{40}\text{Ar}/^{39}\text{Ar}$ dated (Paper III), to better constrain the age and geochemical composition of these two boreholes.

Analogue sites comparisons

Data from sedimentary rocks and basement strata older than pre-Mid-Eocene on the JMMC is lacking. Thus, a comparison between the JMMC and its conjugate margins was conducted in order to address interpretation uncertainties regarding the age and character of the basal Cenozoic and pre-Cenozoic strata on the microcontinent. These conjugate areas include the central East Greenland margin and onshore area, the oceanic domains surrounding the JMMC, the mid-Norwegian margin, the Faroe–Shetland region, and the Greenland-Iceland-Faroe ridge complex domain. Detailed reviews and correlations were conducted and discussed in this study and Blischke and Erlendsson (2018).

The geology of the JMMC's western conjugate margin is of importance for correlation purposes as it was part of East Greenland until the Late Oligocene (Figures 2.9; 2.11; 3.1). The Jameson Land basin and the Blosseville Kyst region of central East Greenland have outcrop sites that provide a strong volcano-stratigraphic analogue for the deeper Cenozoic and underlying succession. Along the Blosseville Kyst coastline, lower Palaeogene plateau basalts and shallow-marine deposits are preserved (e.g. Larsen, M. et al., 2002, 2005; Tegner et al., 2008; Larsen, L.M. et al., 2013, 2014), which might represent a direct analogue for the possible plateau basalt and pre-breakup strata of the JMMC.

3.1.6 Age analysis and petrochemical data

Published geochronology data were initially reviewed based on available offshore borehole and onshore data records (e.g. Talwani and Udintsev, 1976a-j; Kharin et al., 1976; Tegner et al., 2008; Larsen, L.M. et al., 2013, 2014; Ganerød et al. 2014). Large error margins and age ranges in K/Ar dating from DSDP Leg 38 boreholes 348 and 350 (Kharin et al., 1976) prompted resampling of their 21 core sections as part of this study (Figure 3.6).

$^{40}\text{Ar}/^{39}\text{Ar}$ analysis

As DSDP site 348 did not fit into the overall geochronologic model by Gaina et al. (2009, 2017b) with an approximate age range between $19,4 \pm 2,2$ Ma to $18,2 \pm 2,4$ Ma (total uncertainty range: 21,6-15,8 Ma) (Kharin et al., 1976) falling outside the geo-chron of that period, it was decided to resample igneous rocks from sites 348 and 350. Eight igneous rock samples were selected and described at the core lab in Bremen (Germany), and sent to the argon geochronology laboratory at the Oregon State University, accompanied by thin sections that were prepared and analyzed at the Iceland GeoSurvey's petrology lab (see supplement material of Paper III). The fine-grained, unaltered 115-513 mg whole-rock basalt samples were analysed at the argon geochronology laboratory from groundmass, with the $^{40}\text{Ar}/^{39}\text{Ar}$ Heine resistance furnace on the MAP 215-50, through incremental heating. Three samples from borehole 348 provided reliable results, and three out of five samples from site 350 could be used. $^{40}\text{Ar}/^{39}\text{Ar}$ data from site 348 gave an age range between $23,19 \pm 0,61$ Ma and $22,15 \pm 0,26$ Ma (total uncertainty range: 23,8-21,89 Ma) providing a firm tie of the geo-chron model to the core data (Paper III).

The K/Ar age range for site 350 displayed great variation, from $50,5 \text{ Ma} \pm 5,5 \text{ Ma}$ to $33,5 \text{ Ma} \pm 2,8 \text{ Ma}$ (total uncertainty range: 56-30,7 Ma) (Kharin et al., 1976). The core was thus resampled, the $^{40}\text{Ar}/^{39}\text{Ar}$ dating gave an age range between $49,28 \text{ Ma} \pm 0,3 \text{ Ma}$ and $44,05 \text{ Ma} \pm 0,21 \text{ Ma}$ (total uncertainty range: 49,58-43,84 Ma), within the geochronological model of IPR-I and IPR-II (Paper III).

Petrochemical data

Seven of the selected samples from the cored igneous section of DSDP sites 348 and 350 were sent and analysed at the University of Iceland ICP laboratory and is described detail in Paper III with its supplementary sections. In addition, the JMMC's conjugate regions were investigated for published petrophysical datasets that would enable comparison between the cored igneous sections and seafloor samples to the volcano-stratigraphic provinces. Information on such datasets was obtained from a number of existing geochemistry databases, including: PETDB (Lamont Doherty Earth Observatory, Columbia University, New York, <http://www.earthchem.org/petdb>); the GEOROC (Max Planck Institute for Chemistry, Mainz, <http://georo~mpch-mainz.gwdg.de/georoc/>); and published data by Grönvold and Mäkipää (1978), Kharin et al. (1976), Tegner, C. (unpublished), and Polteau et al. (2018) (Figure 3.1). For a full reference list, the reader is referred to the geochemistry data analyses and references in the supplementary data of Paper III.

Table 3.3. An overview of existing DSDP and ODP boreholes and drilled igneous basement, based on data summary in Hopper et al. (2014) and this study. Abbreviations are listed on p. xix-xx.

Site name	Latitude	Longitude	Area	Cored section (m)	Igneous drilled section (m)	Age
DSDP Leg 38-336	63.351667	-7.783333	Iceland-Faroe Ridge	515	30,5	Mid-Eocene
DSDP Leg 38-337	64.871667	-5.341833	Aegir Ridge	132.5	19,5	Early Oligocene
DSDP Leg 38-345	69.837167	-1.237667	Jan Mayen Fracture Zone	802	40	Late Oligocene
DSDP Leg 38-346	69.889167	-8.685667	Jan Mayen microcontinent	187	<i>DNR</i>	Late Eocene
DSDP Leg 38-347	69.871833	-8.696667	Jan Mayen microcontinent	190	<i>DNR</i>	Late Eocene
DSDP Leg 38-348	68.503000	-12.462000	Kolbeinsey Ridge	544	17	Early Miocene
DSDP Leg 38-349	69.206833	-8.096667	Jan Mayen microcontinent	320	<i>DNR</i>	Late Eocene
DSDP Leg 38-350	67.055667	-8.294667	Iceland Plateau	388	26	Early-Mid Eocene
DSDP Leg 38-352	63.649500	-12.471000	Iceland-Faroe Ridge	122.5	<i>DNR</i>	Early Oligocene
ODP Leg 151-907	69.249700	-12.698300	Kolbeinsey Ridge	224.1	8	Mid-Miocene
ODP Leg 162-985	66.941500	-6.450200	Aegir Ridge	588	<i>DNR</i>	Late Oligocene
ODP Leg 162-987	70.496450	-17.936467	Liverpool Land Basin	859	<i>DNR</i>	Late Miocene

* *DNR* – Did not reach

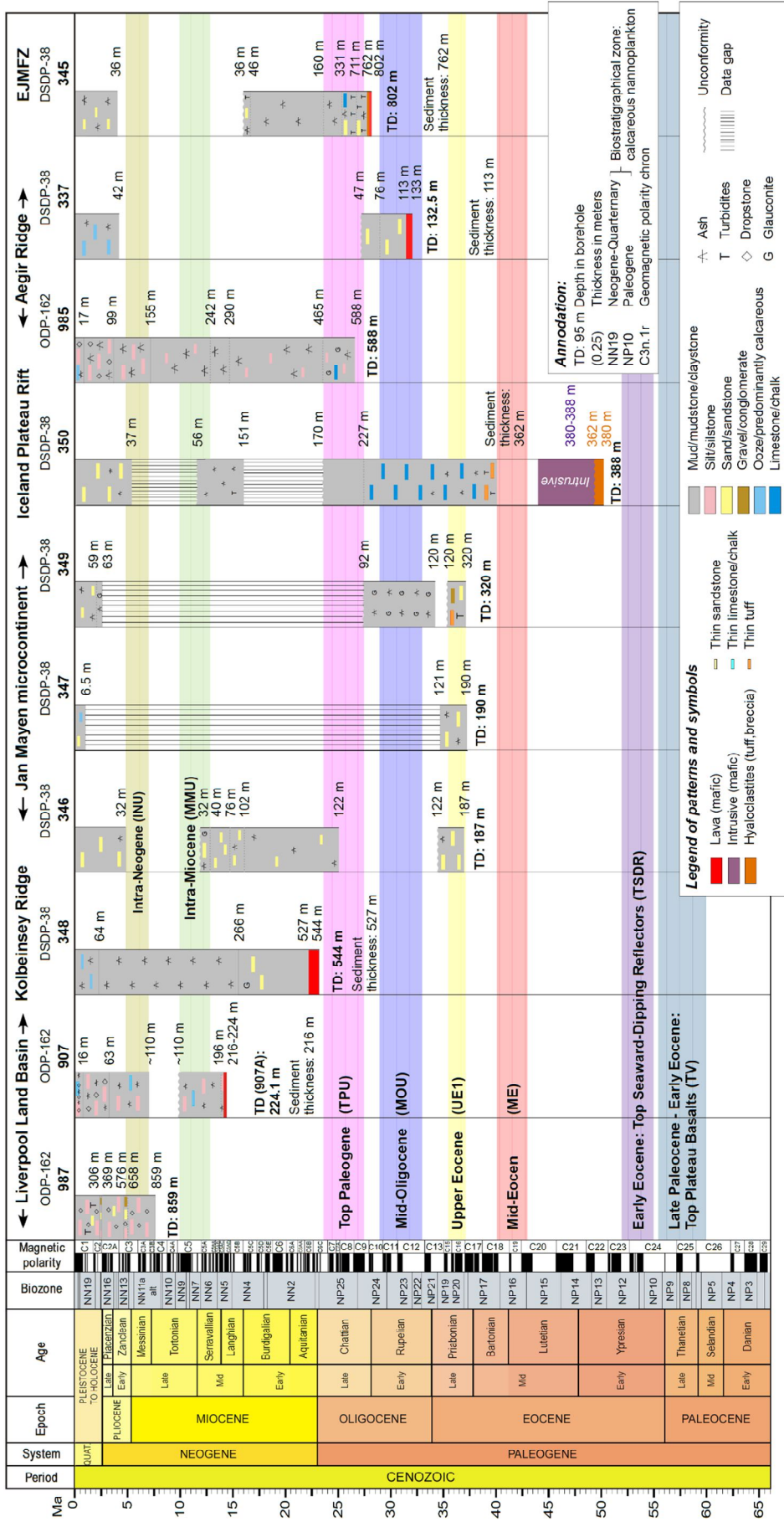


Figure 3.6 The JMMC stratigraphic summary chart of compiled from this study, partly based on DSDP and ODP boreholes (Talwani et al., 1976a-j; Manum et al., 1976a,b,c; Raschka et al., 1978; Thiede et al., 1978; Nilsen et al., 1995; Jansen et al., 1996; Channell et al., 1999a,b; Butt et al., 2001). This compilation is used to ties the JMMC's shallow Cenozoic stratigraphy and unconformities to the seismic reflection data.

3.2 Interpretation methods and applications

Mapped structural elements in the JMMC-IPR, NE Iceland shelf and IFR areas, including rift zones, fracture zones are based on this study. Large-scale fault systems and lineaments are based on published data (e.g. Gaina et al., 2009; Peron-Pinvidic et al., 2012a,b; Gernigon et al., 2012, 2015; Hopper et al., 2014). The main mapped structural features for the JMMC-IPR (Figure 2.1) are based on parameters derived, or inferred, from at least two (preferably three) different potential-field and/or seismic datasets (Papers I and II).

3.2.1 Structural elements analysis

Mapped structural elements include rift zones, fracture zones, large-scale fault systems and lineaments in the JMMC area, which are based on published work (e.g. Gaina et al., 2009; Peron-Pinvidic et al., 2012a,b; Gernigon et al., 2012, 2015; Hopper et al., 2014) and interpretations of this study by delineation of onshore records, bathymetry, free-air gravity anomaly and derivatives, magnetic anomaly, and seismic reflection and refraction datasets. The main mapped structural features for the JMMC-IPR are shown on Figure 2.1, and are based on parameters derived, or inferred, from at least two (preferably three) different potential-field and/or seismic datasets (Papers I and II).

The seismic reflection datasets were used for mapping and identification of structural elements, smaller-scale fault systems, and fault-parallel sill and dyke complexes. Multibeam bathymetry data were used to map structural trends and features at the seafloor. High-resolution bathymetry data in combination with seismic reflection data enabled the differentiation between strike-slip and normal fault systems, and slump faulting along the steep escarpments of the microcontinent's ridges (Papers I-III).

3.2.2 Kinematic reconstructions

Plate-tectonic reconstructions for the relative motion of JMMC with respect to its conjugate margins were obtained using the interactive fitting method of GPlates (www.gplates.org; Boyden et al., 2011; see also Gaina et al., 2009, 2014, 2017b) (Appendix 3). The GPlates application works on the basis of the geographic information system (GIS) functionality by implementing raster-data visualization that can be based on images or 2D grid, line or point datasets, which enables combined interpretation and cross-correlation of various datasets within both plate-tectonic and chronologic contexts. The "GPlates markup language" (GPML) as a custom-designed format for geological and geographic data modified in a plate-tectonic context. The GPML datasets are exported into ArcMap (GIS) compatible formats that enable to interpret and adjust tectonic or paleo-environment maps at a selected geological time, constrained geographically in a coordinate tied mapping project.

Input data for reconstruction of oceanic crustal spreading was primarily based on magnetic anomalies and mapped fracture zones (Figure 3.7), in addition to gravity anomaly data and structural mapping of the study area (Papers I-III). Geo-chron interpretation of the Ægir ridge system was based on the high-resolution magnetic data by Gernigon et al. (2015). The large regional fracture zones are based on Gaina et al. (2014, 2017b) or Gernigon et al. (2015). Larger scale plate-tectonic reconstructions for the relative motion of JMMC were fitted within GIS for each reconstruction stage, using rotation parameters for Greenland relative to Eurasia based on Gaina et al. (2017b), (Appendix 3).

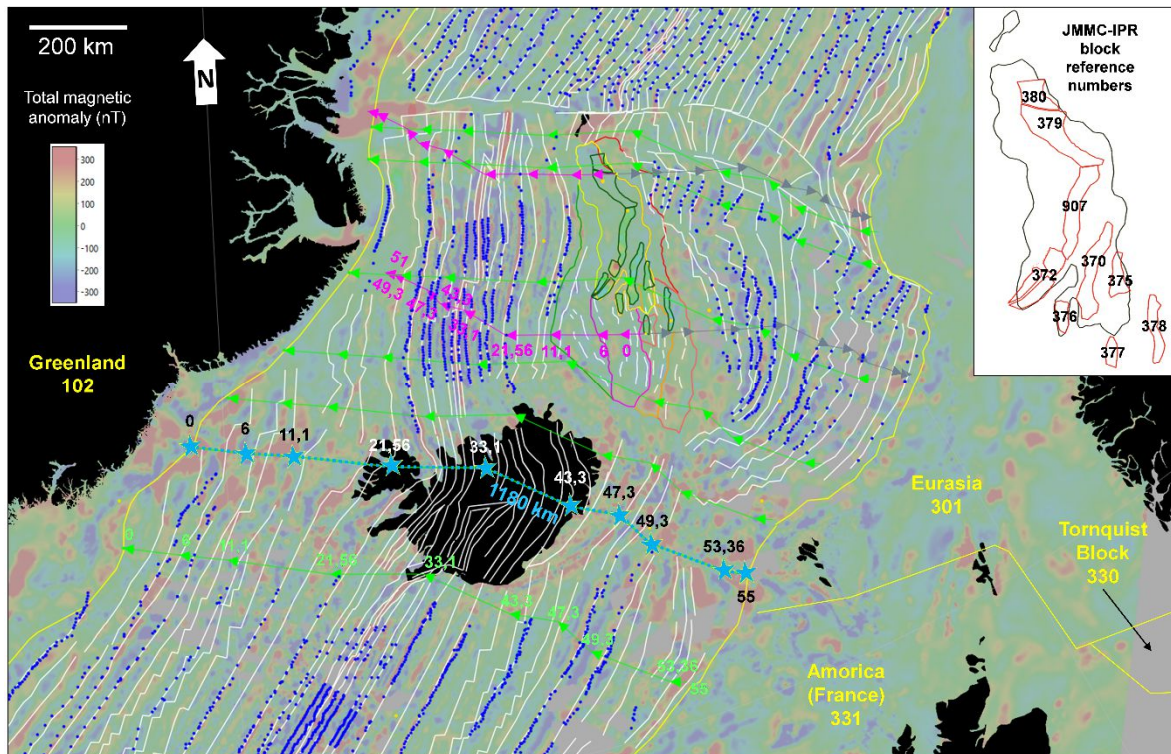


Figure 3.7 GPlate reconstruction of the JMMC-IPR, modified after Gaina et al. (2017b). The different segments and blocks of the JMMC-IPR (inset) were added in this study. Plate boundaries are traced in yellow and isochron interpretations dotted in dark blue (Gaina et al., 2014, 2017b; Nasuti and Olesen, 2014). The path of opening (spreading direction) between the Eurasian plate and Greenland is indicated by green triangles, and across the GIFRC in light blue, with time steps indicated as blue stars. Also shown are flow lines during separation of the JMMC-IPR blocks from the Greenland margin based on this study (pink between East Greenland and JMMC-IPR and in grey between JMMC-IPR and the western Norway shelf margin). The JMMC-IPR block reconstruction and reconstructed time series are listed in Table 3.4 with the corresponding reconstruction times in millions of years (Ma).

More detailed kinematic reconstructions for separate JMMC-IPR tectonic blocks (Figure 3.7; Table 3.4) were tied to the chronostratigraphic succession and best fitting fault and block topography in chronologic order (Papers I-III). Reconstruction parameters used to restore the JMMC blocks to pre-breakup and pre-extension positions are listed in detailed in Table 3.4 with reference to the East Greenland margin, where the JMMC was attached prior to breakup.

Magnetic anomaly picks refer to segments of formed oceanic crust that was magnetised with different polarities of the magnetic field through time as the oceanic crust formed. The temporal motion of the crustal blocks on the Earth's surface follow a great circle path with the axis or rotation pole following a fixed pivot point at the Earth's centre. That is referred to as an Euler pole and was described by Cox and Hart (1986) as the plate tectonic method. Seafloor spreading occurs parallel to the ridges and forms the meridian that intersects at the Euler pole.

Table 3.4 Finite rotation parameters of various tectonic blocks relative to the Greenland Plate (plate ID 102) (a) modified after Gaina et al. (2017b); (b) – (j) this study. Eastern hemisphere longitudes have positive signs. Abbreviations and label keys are presented on p. xix-xx.

Age (Ma)	Chron	Reconstruction Id	Plate / Block name	Rotation		
				Latitude (+°N)	Longitude (+°E)	Angle (°)
Eurasia-Greenland (a)						
6	C3A	301-102	Eurasia-Greenland	67,50	133,10	-1,42
11,1	C5r.1r	301-102	Eurasia-Greenland	67,50	133,10	-2,62
21,56	C6b	301-102	Eurasia-Greenland	71,49	127,45	-5,61
33,1	C13n	301-102	Eurasia-Greenland	68,32	132,27	-7,64
43,3	C20n	301-102	Eurasia-Greenland	57,53	127,90	-8,58
47,3	C21n	301-102	Eurasia-Greenland	53,70	129,00	-9,27
49,3	C22n	301-102	Eurasia-Greenland	55,40	123,50	-10,29
53,36	C24n2r	301-102	Eurasia-Greenland	57,94	119,11	-12,50
55	C24r	301-102	Eurasia-Greenland	56,32	120,51	-12,62
Lyngvi Ridge-JMSWP (b)						
6	C3A	907	Lyngvi Ridge	67,50	133,10	-1,42
11,1	C5r.1r	907	Lyngvi Ridge	67,50	133,10	-2,62
21,56	C6b	907	Lyngvi Ridge	71,49	127,45	-5,61
33,1	C13n	907	Lyngvi Ridge	82,35	14,60	-16,73
43,3	C20n	907	Lyngvi Ridge	83,42	96,81	-10,47
47,3	C21n	907	Lyngvi Ridge	82,65	14,52	-17,16
49,3	C22n	907	Lyngvi Ridge	79,10	-0,52	-24,46
53,36	C24n2r	907	Lyngvi Ridge	79,95	3,23	-21,50
55	C24r	907	Lyngvi Ridge	81,17	3,23	-21,50
Jan Mayen - Southern Rige Complex - main block (c)						
6	C3A	370	JM-SRC main block	67,44	133,06	-1,42
11,1	C5r.1r	370	JM-SRC main block	67,44	133,06	-2,62
21,56	C6b	370	JM-SRC main block	71,43	127,42	-5,62
33,1	C13n	370	JM-SRC main block	82,36	14,85	-16,73
43,3	C20n	370	JM-SRC main block	83,57	102,22	-10,51
47,3	C21n	370	JM-SRC main block	83,19	14,16	-17,19
49,3	C22n	370	JM-SRC main block	79,52	-1,17	-24,49
53,36	C24n2r	370	JM-SRC main block	80,57	0,63	-23,28
55	C24r	370	JM-SRC main block	81,75	4,25	-21,55
Jan Mayen - Southern Rige Complex - Buðli block (d)						
6	C3A	372	Buðli - JMSWIP	67,50	133,10	-1,42
11,1	C5r.1r	372	Buðli - JMSWIP	67,50	133,10	-2,62
21,56	C6b	372	Buðli - JMSWIP	71,49	127,45	-5,61
33,1	C13n	372	Buðli - JMSWIP	82,35	13,91	-16,83
43,3	C20n	372	Buðli - JMSWIP	83,64	98,70	-10,48
47,3	C21n	372	Buðli - JMSWIP	82,74	14,25	-17,17
49,3	C22n	372	Buðli - JMSWIP	79,14	-0,55	-24,47
53,36	C24n2r	372	Buðli - JMSWIP	79,97	-0,04	-23,23
55	C24r	372	Buðli - JMSWIP	81,19	3,16	-21,50
Jan Mayen - Southern Rige Complex - Otur block (e)						
6	C3A	375	JM-SRC Otur	67,55	134,04	-1,42
11,1	C5r.1r	375	JM-SRC Otur	67,54	134,04	-2,62
21,56	C6b	375	JM-SRC Otur	71,54	128,48	-5,62
33,1	C13n	375	JM-SRC Otur	82,51	14,07	-16,74
43,3	C20n	375	JM-SRC Otur	83,53	104,70	-10,53
47,3	C21n	375	JM-SRC Otur	83,38	15,01	-17,21
49,3	C22n	375	JM-SRC Otur	79,67	-0,83	-24,50
53,36	C24n2r	375	JM-SRC Otur	80,87	1,22	-23,31
55	C24r	375	JM-SRC Otur	79,07	-3,65	-27,81

Table 3.4 continued.

Age (Ma)	Chron	Reconstruction Id	Plate / Block name	Rotation		
				Latitude (+°N)	Longitude (+°E)	Angle (°)
Jan Mayen - Southern Rige Complex - Högni block (f)						
6	C3A	376	JM-SRC Högni	67,58	136,07	-1,42
11,1	C5r.1r	376	JM-SRC Högni	67,57	136,08	-2,63
21,56	C6b	376	JM-SRC Högni	71,60	130,72	-5,64
33,1	C13n	376	JM-SRC Högni	82,86	13,09	-16,75
43,3	C20n	376	JM-SRC Högni	83,95	105,80	-10,51
47,3	C21n	376	JM-SRC Högni	83,32	12,88	-17,19
49,3	C22n	376	JM-SRC Högni	79,55	-1,65	-24,49
53,36	C24n2r	376	JM-SRC Högni	80,46	-1,12	-23,26
55	C24r	376	JM-SRC Högni	81,63	2,34	-21,53
Jan Mayen - Southern Rige Complex - Dreki block (g)						
6	C3A	377	JM-SRC Dreki	67,44	133,06	-1,42
11,1	C5r.1r	377	JM-SRC Dreki	67,44	133,06	-2,62
21,56	C6b	377	JM-SRC Dreki	71,43	127,42	-5,62
33,1	C13n	377	JM-SRC Dreki	82,34	14,03	-16,86
43,3	C20n	377	JM-SRC Dreki	81,26	8,49	-18,96
47,3	C21n	377	JM-SRC Dreki	78,46	-2,42	-25,85
49,3	C22n	377	JM-SRC Dreki	76,72	-6,87	-33,24
53,36	C24n2r	377	JM-SRC Dreki	77,43	-6,57	-32,01
55	C24r	377	JM-SRC Dreki	74,89	-10,72	-44,03
Jan Mayen - Southern Rige Complex - Langabru block (h)						
6	C3A	378	JM-SRC Langabru	67,44	133,06	-1,42
11,1	C5r.1r	378	JM-SRC Langabru	67,44	133,06	-2,62
21,56	C6b	378	JM-SRC Langabru	71,43	127,42	-5,62
33,1	C13n	378	JM-SRC Langabru	82,58	15,72	-16,89
43,3	C20n	378	JM-SRC Langabru	81,98	8,69	-19,01
47,3	C21n	378	JM-SRC Langabru	79,01	-2,68	-25,90
49,3	C22n	378	JM-SRC Langabru	77,08	-6,36	-33,28
53,36	C24n2r	378	JM-SRC Langabru	77,97	-5,15	-32,08
55	C24r	378	JM-SRC Langabru	75,54	-9,47	-42,72
Jan Mayen Rige block (i)						
6	C3A	379	JMR	66,48	135,19	-1,44
11,1	C5r.1r	379	JMR	67,02	134,01	-2,64
21,56	C6b	379	JMR	71,32	127,74	-5,63
33,1	C13n	379	JMR	82,42	15,26	-16,87
43,3	C20n	379	JMR	81,04	9,19	-18,99
47,3	C21n	379	JMR	78,53	-2,04	-25,90
49,3	C22n	379	JMR	76,69	-5,69	-33,29
53,36	C24n2r	379	JMR	76,98	-6,37	-32,03
55	C24r	379	JMR	75,88	-8,49	-38,87
Jan Mayen Rige - northern block (j)						
6	C3A	380	N-JMR	66,55	134,22	-1,44
11,1	C5r.1r	380	N-JMR	67,05	133,57	-2,64
21,56	C6b	380	N-JMR	71,33	127,60	-5,63
33,1	C13n	380	N-JMR	80,49	4,51	-20,59
43,3	C20n	380	N-JMR	81,05	9,09	-18,99
47,3	C21n	380	N-JMR	78,52	-1,83	-25,90
49,3	C22n	380	N-JMR	76,68	-5,68	-33,29
53,36	C24n2r	380	N-JMR	76,98	-6,36	-32,03
55	C24r	380	N-JMR	76,00	-8,30	-37,98

Transform- or fracture zones move parallel to the direction of mid-oceanic ridge opening and if reconstructed correctly should always aligned spreading centres of the same paleo-age. These isochrone interpretations can be verified in some cases by borehole data, e.g. DSDP Leg 38 Site 348 or 337. The magnetic anomalies database used in this study was summarised and quality checked by Gaina et al. (2014) based on the geological time scale by Gradstein et al. (2012) and corresponding geomagnetic polarity scale by Ogg (2012). For the NAGTEC project, relative plate motions were considered, and the Eurasian plate was fixed. During this study the NAGTEC regional model was implemented, whereas more localized JMMC-IPR reconstructions were referenced to the East Greenland margin. The JMMC model was developed by finding poles of rotation of the reconstructed areas (whole plates or smaller blocks) and by aligning them best fitting to relevant magnetic anomalies.

Asymmetric spreading along the Ægir Ridge and rift rearrangements within the JMMC-IPR region has complicated previous modelling of the JMMC region (Gernigon et al., 2015; Hjartarson et al., 2017), (Appendix 3). Therefore, one of the main challenges for the JMMC-IPR reconstruction model was to explain this asymmetry, which required more detailed modelling of the seismic, borehole and seafloor data, in order to build a chronostratigraphic and volcano-stratigraphic framework, as regular magnetic anomalies are weak in this region, especially in the IPR area.

A dense set of isochrons was constructed based on magnetic anomaly identifications, mapped fracture zones and other structural elements, and the igneous domains of the JMMC-IPR within the limits of the continent-ocean boundaries (Gaina et al., 2014 regional; Papers I-II JMMC-IPR and IFR) (Figure 3.7). Individual JMMC-IPR tectonic blocks were reconstructed to pre-breakup and pre-extension positions, based on derived rotations at time intervals shown in Table 3.4. They document the trajectory of East Greenland relative to Eurasia, the trajectory for the GIFR region relative to Eurasia, and the path between JMMC-IPR and East Greenland.

3.2.3 Seismic stratigraphy

Correlation of stratigraphic information of available borehole, surface or seafloor sample records, tied to seismic reflection data, form the basis for the seismic stratigraphy and construction of the JMMC regional Cenozoic stratigraphic framework (Paper II). Eleven seismic-stratigraphic units were identified, bound by regional unconformities (Figures 2.5; 2.9; 2.10), defined from discordant seismic reflector relations according to the criteria established by Mitchum et al. (1977). The eleven seismic-stratigraphic units (JM-01–JM-70) establish a stratigraphic framework, based on each unit's characteristic seismic reflection pattern. The correlation of each unit to borehole data, including lithological, biostratigraphic or other stratigraphic data, enabled these seismic reflection units to be mapped across the seismic grid (e.g. Owen, 1987; Vail, 1987; Heinz and Aigner, 2003) (Figure 3.8). Stratigraphic information from DSDP Leg 38 borehole sites 346, 348, 349 and 350, and seafloor samples retrieved by the NPD and VPBR-TGS in 2011, 2012 and 2013, extending back to the Mid-Eocene, provides a controlled framework for seismic units JM-01–JM-50 (Papers I and II) (Figure 3.2); thus, providing key constraints for tying to the seismic reflection data (Papers I-III). This facilitates mapping of unconformities and post basalt stratigraphy across the JMMC. The regional unconformities across the JMMC, which reflect major paleo-environmental and structural changes in its evolution are delineated by mapping key reflectors (Paper II). Major uncertainties in stratigraphic correlation persist in the basins

between the dislocated southern ridge segments and along the collapsed western flank of the JMMC, where borehole control for sections older than Mid-Eocene is lacking. The deeper sub-basalt stratigraphic units are only visible in the central area of the JMMC and around DSDP site 349. Stratigraphic correlation is improved by increased 2D MCS data coverage and thus was substantially improved with the NPD2011 and 2012 survey data interpretation during this study. However, major areas of uncertainty remain, including the JMT, JMB, and the JMBS, where the correlation of stratigraphic units older than Miocene is hindered by the regionally extensive flood basalts which largely obscure the underlying structure and stratigraphic layering (Papers II and III). To reduce these uncertainties, onshore and offshore stratigraphic relationships along the western conjugate margin (Blosseville Kyst in East Greenland) and the Vøring continental margin, to the east, provide information on the basalt stratigraphy that can be inferred to the volcanic horizons on the JMMC's seismic reflection dataset.

3.2.4 Seismic volcano-stratigraphy

Seismic reflection datasets were also used for detailed seismic volcano-stratigraphic characterization, which facilitated mapping and identification of structural elements, sedimentary sequences, SDR sequences, and sill and dyke complexes. Multibeam bathymetry data were used to map structural trends and features at the seafloor. This high-resolution bathymetry data in combination with seismic reflection data enabled us to differentiate not just fault and fracture zone surface intersections, but also igneous complexes and axial rift systems (Paper III). Seismic reflection interpretation utilized to build the Cenozoic seismic-stratigraphic framework for the JMMC area (e.g. Gunnarsson et al., 1989; Paper II), was expanded by more detailed chronostratigraphic appraisal of the igneous succession specifically addressing the seismic volcano-stratigraphy to fully understand the rifting processes within the region. A methodology for the seismic-stratigraphic interpretation of igneous rocks has been systematically developed over the last 20 years, with key papers by Symonds et al. (1998), Planke et al. (2000) and Bischoff et al. (2019), which outline criteria for the recognition and interpretation of volcanic seismic facies. These criteria have been employed in this project whereby seismic volcanic units have been identified by their shape, reflection patterns and boundary reflection signals, and by placing these units into a chronological context (Figures 2.5; 3.8) (Paper III). The JMMC seismic volcano-stratigraphic framework was then compared to conjugate areas and margins and their volcanic seismic facies characteristics, as summarised by various studies, including Larsen, L.M. et al. (2013), Hopper et al. (2014), á Horni et al. (2017), Gaina et al. (2017a), Geissler et al. (2017) and Hjartarson et al. (2017). Key seismic volcanic facies include landward flows, seaward dipping reflector (SDR) sequences, inner and outer SDRs, igneous centres, sill/dyke intrusions, and volcanic vent structures (e.g. Hinz et al., 1981; Planke et al., 2000) (Figure 3.9). These volcanic seismic facies units are summarised below.

JMMC Project workflow

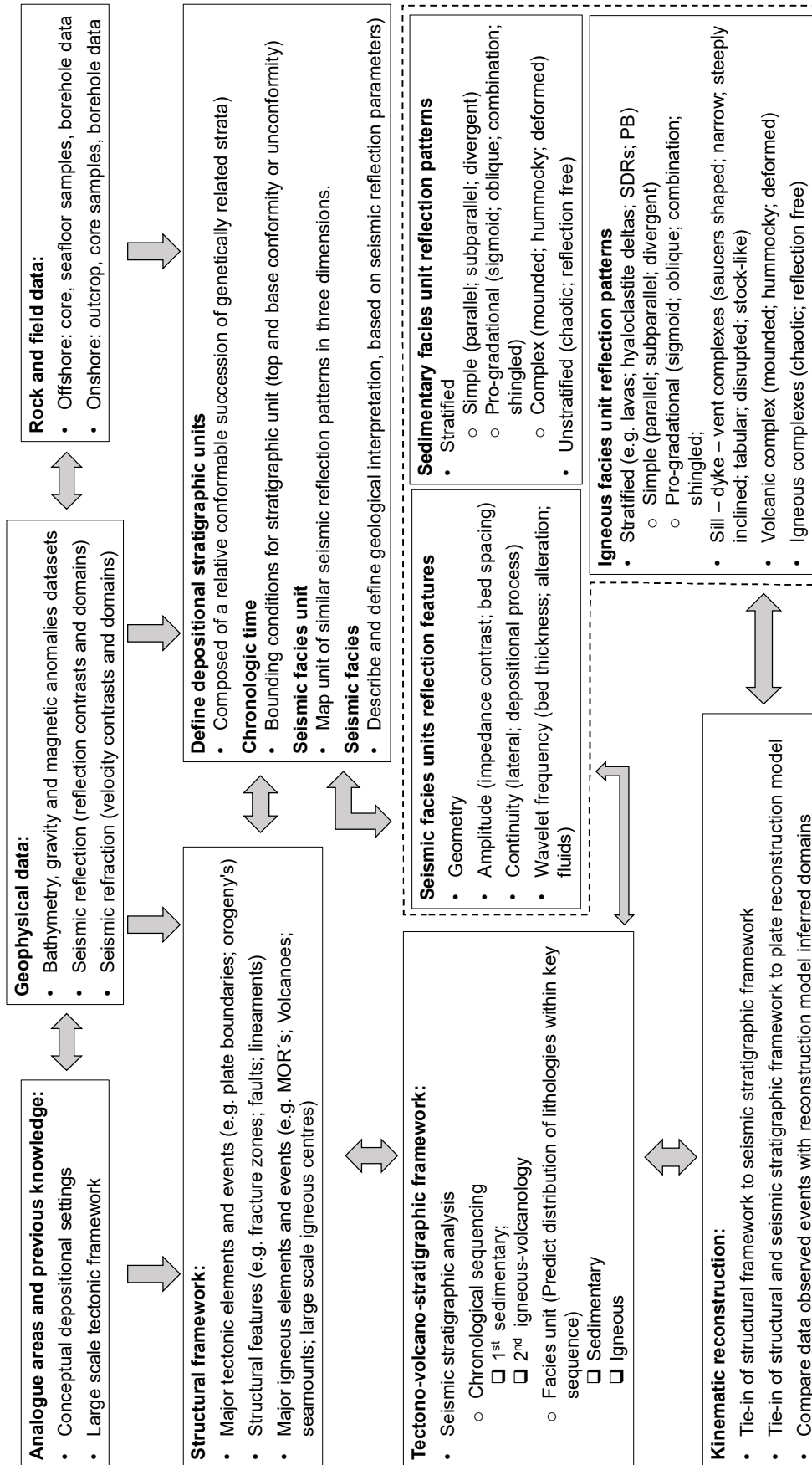


Figure 3.8 Seismic stratigraphy and facies interpretation workflow for the JMMC-IPR areas. Interpretation of lithofacies, geometries and depositional settings based on Seismic reflection and refraction data was tied to geological mapping and petrological data on land. The outcome is a seismic volcano-stratigraphic framework modified after e.g. Mitchum et al. (1977) and Heinz and Aigner (2003).

Landward flows

The layered landward-flow sections underlying the SDR wedges are also referred to as the Early Eocene plateau-basalt-equivalent stratigraphic units that in places can be subdivided into subaerial and submarine lava flows. These lavas have been observed to extend several hundreds of Kilometers from their eruptive centres and close to coastal areas (Self et al., 1997) form strong, relatively smooth and sheet-like seismic reflectors. Their internal reflection character can vary locally but overall displays a sub-parallel character that is commonly wedge-like towards elevated areas or depicts prograding reflectors toward basal areas. Flat-lying high-amplitude basaltic markers within the low areas in between the JMMC ridges are referred to as F-Marker flood basalts.

Seaward dipping reflectors (SDR)

Seaward-dipping reflectors (SDR) form strongly reflective packages that comprise subaerial to shallow-marine flood basalts alternating with rift basin sediments; this interbedding provides good reflection coefficient contrasts. The external geometry of the SDR packages is characterised by distinctive seaward-dipping wedges that commonly display a concave-down form. The formation of SDRs is linked to the initial phase of continental breakup and were first observed and defined by Hinz (1981), Larsen and Jakobsdóttir (1988), and Planke et al. (2000), and mapped for the JMMC in this study (Figure 3.9). These SDR packages were a specific focus for this study as they are commonly associated with axial rifting along the first line of breakup. The inner set of SDR's is linked to an igneous centre referred to as the outer high, which is generally located close to the continent ocean boundary; the determination of the continent ocean boundary around the JMMC was a major objective of this study. The inner SDRs are replaced seaward and in deepening marine conditions by much thinner and poorer developed outer SDR sets that are commonly located at the transition from breakup margin to ocean floor spreading; thus, seaward of the continent ocean boundary (Planke et al., 2000).

Igneous and volcanic complexes

The outer highs are one group of igneous centres that are specified by chaotic internal seismic reflection patterns capped by a strong top reflector. On seismic-reflection profiles, they appear as mounded or sloping features, and can form circular bodies on magnetic or gravity datasets (Figure 3.9). The term 'igneous centre' is also used as a generic description for offshore seamounts, igneous and volcanic complexes that have been active throughout a longer time interval, and which are often linked to faults or fissure zones. Seamounts shown in this study have been mapped for the region and adjacent areas as documented by Epp and Smoot (1989), Hopper et al. (2014), Gaina et al. (2017a) and in Paper III.

Intrusions

Smaller-scale igneous intrusions described in this study represent dykes, sills and connected vent structures, and are generally recognized on seismic reflection data by their often-irregular shape and their strong acoustic impedance contrast with the host sedimentary rocks. These are primarily igneous formations for the JMMC area that have intruded material into the surrounding bedrock under pressure, either as semi-vertical dykes or as sills that are semi-horizontal intrusions (Planke et al., 2005; Smallwood et al., 2001; Smallwood and Maresh, 2002) (Figure 3.9). On seismic-reflection profiles, the sill intrusions within the JMR commonly display relatively short, high amplitude reflections with abrupt terminations (sharp edges) which lie semi-parallel with the stratigraphic layering or along fault planes

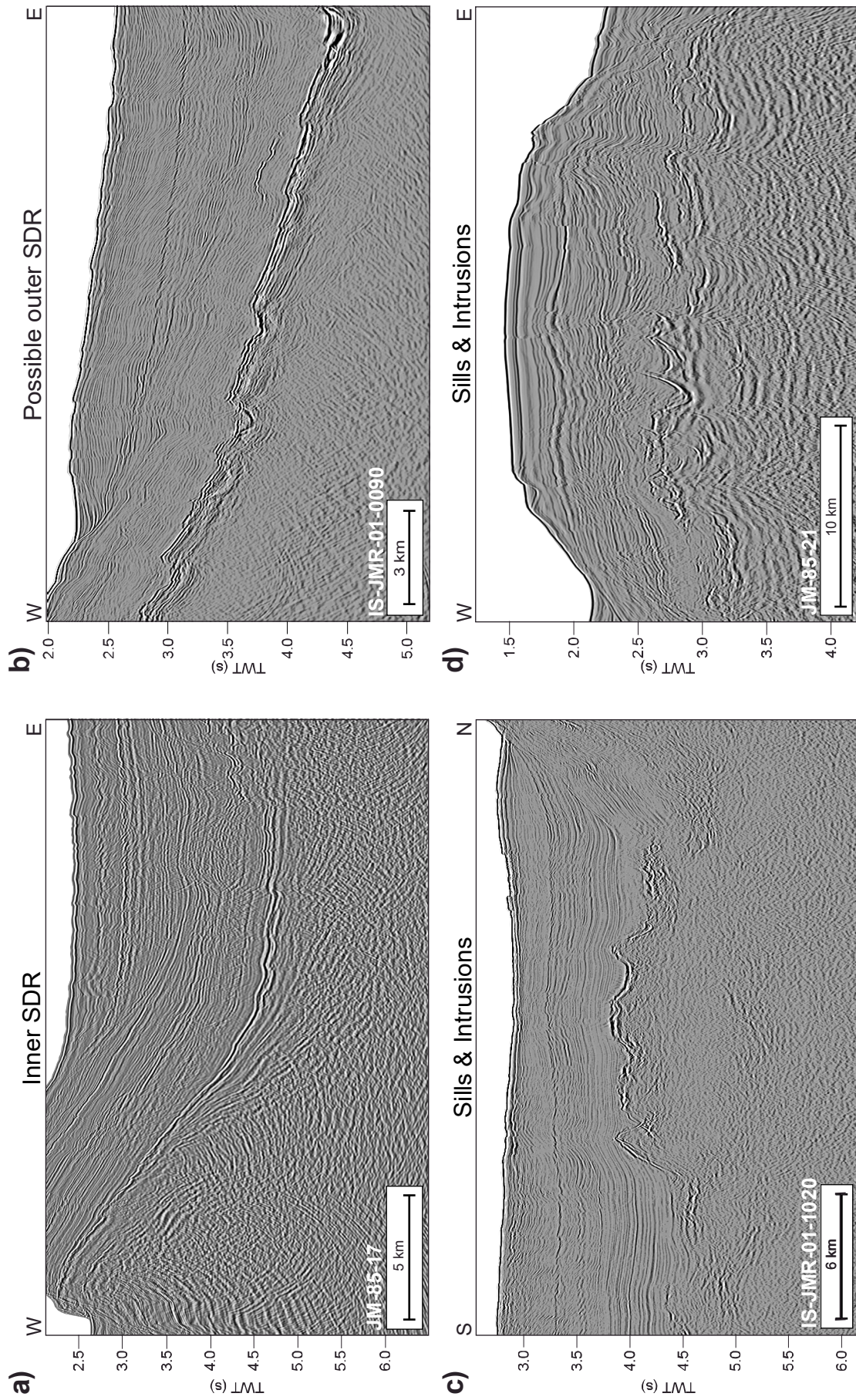
(Figure 3.9). Some sills are more clearly discordant and crosscut the strata as “smiley-shaped” features, interpreted by Planke et al. (2005) as sill intrusions. Sill intrusions can transgress the host strata, i.e. move up or down in relationship to the bedding, sometimes using pre-existing faults (Planke et al., 2005). The morphology of the sill intrusions can be strongly influenced by fault blocks, older igneous formations and deformed strata. These features were mapped consistently across the area, and their presence was used in the determination of the various igneous domains.

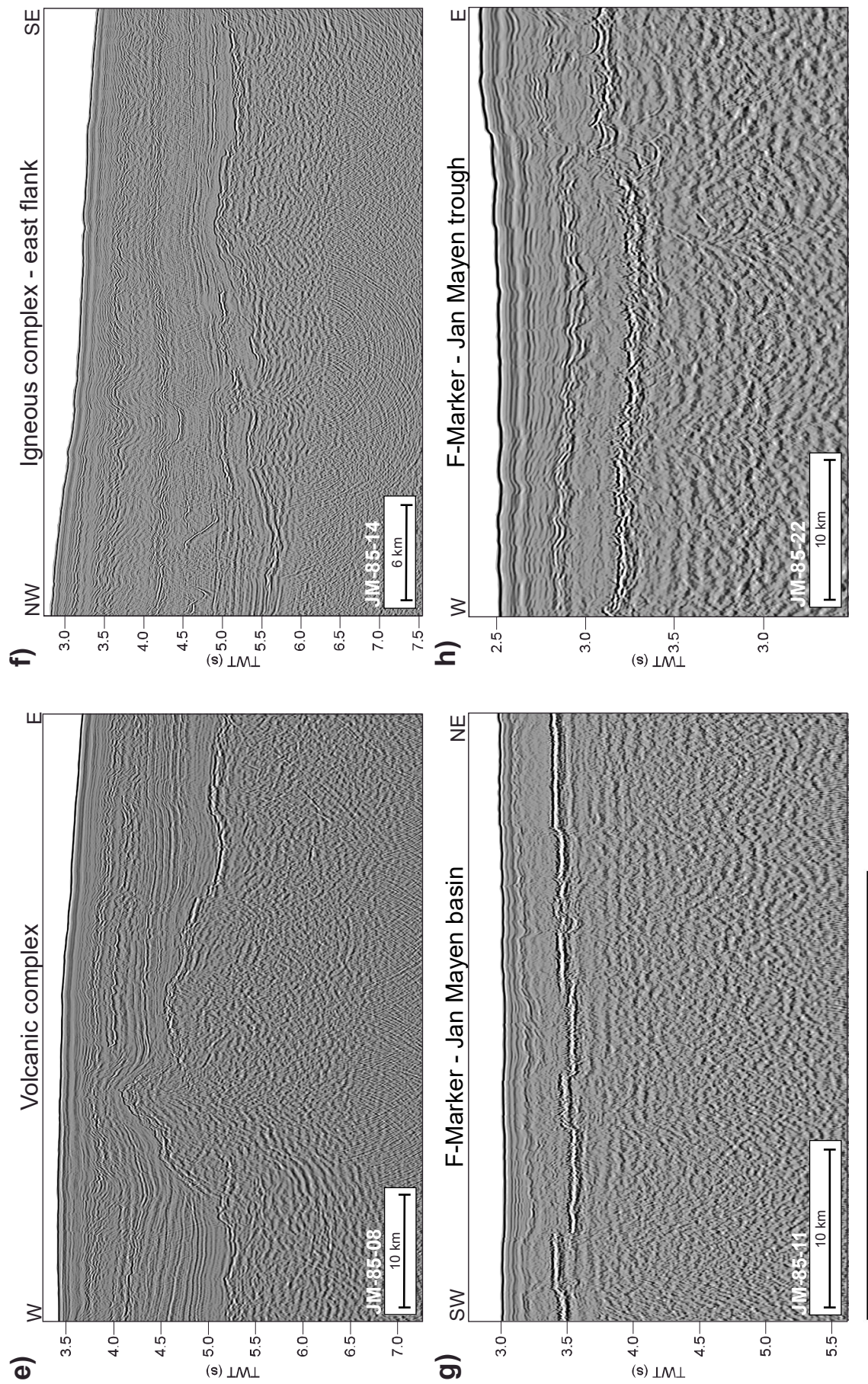
Volcanic ridges – SRC-JMT igneous complexes

Volcanic ridges are clearly visible south and southeast of, and within, the SRC and JMT, where they form domal accumulations of volcanic material. These domal structures have been described in the literature as representing passageways utilised by magma in a volcanic system (Decker and Decker, 2005). In the SRC-JMT area, these structures appear on several seismic-reflection profiles and are interpreted to form volcanic ridges that are related to the rifting and associated volcanism that accompanied the formation of the IPR systems described by Brandsdóttir et al. (2015), this study (Papers I-III), and Erlendsson and Blischke (2018). These volcanic ridges can appear as decentralized structures or along large faults or fault blocks that serve as conduits of rising magma along the fault zones, which leads to deformation and uplift of the fault block. Commonly, a general increase in intrusive activity within the surrounding sedimentary strata is associated with these conduits, lateral to and/or above the conduit structure.

3.2.5 Unresolved interpretation

Intrusive bodies intruded into sedimentary basins are generally very well-imaged by seismic data because of significant acoustic impedance contrasts between the igneous material and the surrounding sediments. However, complex seismic wave scattering and attenuation when travelling through layers of extruded basalt lava flows remains a major issue for seismic exploration (Smallwood and Maresh, 2002). Commonly, seismic signals below highly reflective igneous material is of reduced strength which generally results in poor imaging. This issue has consequences for the JMMC where the widespread igneous activity across the area has resulted in several locations where the image quality and resolution of the sub-basalt geology remains poor or unresolved. This includes the JMMC inter-ridge and flank areas where the Upper Oligocene–Lower Miocene basalts obscure the sub-basalt strata along the southern and western extent of the microcontinent. Elsewhere, seismic reflection data imagery and quality in the deeper parts of JMR are affected by multiple layers of igneous bodies intruded or extruded at various times during the Cenozoic, including the pre-breakup flood basalts, the SDR-basalts, and extrusive and intrusive volcanism associated with the various phases of IPR development (Figure 3.9). In many cases the underlying structures are totally obscured by the igneous strata, and the underlying structure and stratigraphy has had to be interpolated; this is especially the case in those areas that affected by the F-Marker flood basalts.





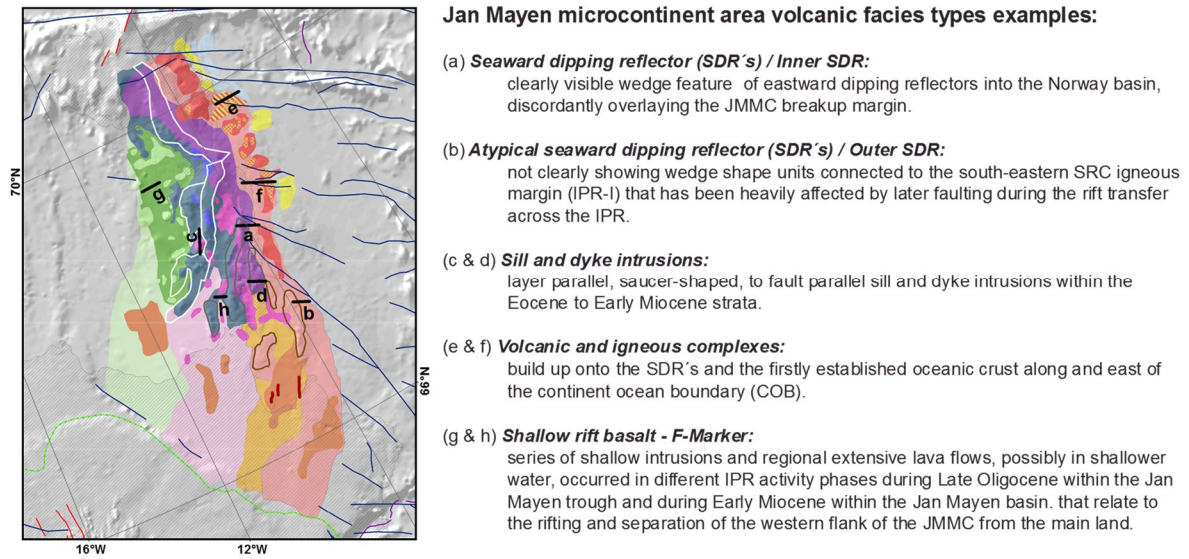


Figure 3.9 Examples of volcanic facies types mapped across the JMMC.

4 Summary

4.1 Paper I: The Jan Mayen microcontinent: an update of its architecture, structural development and role during the transition from the Ægir Ridge to the mid-oceanic Kolbeinsey Ridge

4.1.1 Summary

The aim of paper I was to provide a detailed review of the tectonostratigraphic history of the JMMC and the IPR region based on compilation of existing research projects and provide answers to some of the outstanding research issues based on recently acquired data. The initial phase of this work was based on numerous large scale, regional studies conducted in since the 1960's. Available data was integrated into a kinematic reconstruction of the Northeast Atlantic, including not just the Cenozoic development, but also the pre-Cenozoic development of regional rift basins, remnants of which likely underlie the JMMC. Complex structural patterns along the microcontinent's margins were analysed in comparison with the conjugate East Greenland and Norwegian margins. The new model includes a description of how the southern JMMC structural elements were linked to tectonic features on the Iceland Plateau and Greenland-Iceland-Faroe ridge complex. To establish this, mapping the pre- to post-breakup primary sedimentary strata and igneous complexes was necessary as a first iteration that facilitated a subsequent re-assessment and clearer definition of the igneous and sedimentary domains of the JMMC area throughout its breakup history.

A detailed kinematic model was established explaining the Cenozoic evolution of the JMMC-IPR region in relation to the surrounding oceanic crust. The model is comprised of six main tectonic phases with inferred correlations to major stratigraphic boundaries and unconformities. The initial version of the model is documented in Papers II and III. Structures within the JMMC are consistently oriented similar to major structural lineaments of the surrounding regions, prior to breakup. The main trends are also aligned with the Jameson Land basin and Liverpool Land high, indicating that the JMMC likely forms the southern extension of the Jameson Land basin. Furthermore, it can be demonstrated that the hyper-extended southern domain of the JMMC-IPR region formed an overlapping spreading system with the Ægir ridge system during oblique rift transfer from SE to NW across the Iceland Plateau. The total widening of the IPR domain from about 100 km to 400 km was accompanied by crustal intersection of volcanic rift segments that reached into the north-eastern margin of the Blossville Kyst, where younger rift volcanics are present.

4.1.2 Main findings

Interpretation of new and vintage geophysical data suggests that a significant part of the pre-Paleogene stratigraphic history is preserved below the central area of the Jan Mayen ridge. The conjugate Jameson Land basin, Vøring and Møre basins are direct analogue areas for the JMMC.

The stratigraphy of these basins is well constrained and contains a sedimentary succession that includes Devonian continental sediments, Permo-Triassic continental and marine sequences, Jurassic and Cretaceous shallow- to deep-marine sequences, and Lower Paleocene alluvial to shallow-marine sediments. The breakup and post-breakup igneous sequences have been separated into plateau basalts of likely Paleocene to Early Eocene age, seaward dipping reflector successions, igneous complexes, and sill and dyke intrusions along the flanks of the JMMC. A detailed reconstruction of the Cenozoic evolution of the JMMC and surrounding oceanic crust reveals six tectonic phases that include:

- (1) A pre-breakup stage ending at 56-55 Ma and the emplacement of Lower Eocene plateau basalts across the microcontinent and the Blosseville Kyst region, and continuation into the Faroe-Iceland-East Greenland corridor.
- (2) A first breakup phase that began at 55 Ma (e.g. Gaina et al. 2009) that was associated with the formation of SDRs along the east flank of the JMMC, followed by the initiation of seafloor spreading in the Norway Basin along the Ægir Ridge in the Early Eocene (Chron C24n2r 53.36 Ma) (Gaina et al. 2009; Gernigon et al. 2015).
- (3) An initial intra-JMMC rifting phase around Chron C22n (49.3 Ma) and the establishment of a continuous spreading system in the Norway Basin and formation of the eastern Iceland Plateau.
- (4) The initiation of the southern JMMC rift transition at Chron C21n (47.33 Ma) contemporaneous with oblique seafloor spreading east of JMMC, resulting in the formation of transform systems and uplift along the southern flank of the JMMC.
- (5) A westward rift transfer and initial breakup along the western JMMC around Chron C13n - 33.1 Ma. Oblique mid-oceanic ridge relocation via a southeast to northwest en-echelon rift system occurred along the southern edge of the microcontinent during the Early Oligocene.
- (6) A second breakup phase at Chron C6b (21.56 Ma) with complete cessation of seafloor spreading in the Norway Basin (Gernigon et al. 2015) and the establishment of the Kolbeinsey mid-oceanic ridge as the main mid-ocean spreading centre.

4.2 Paper II: The Jan Mayen microcontinent's Cenozoic stratigraphic succession and structural evolution within the NE-Atlantic

4.2.1 Summary

The paper explores the Cenozoic stratigraphic succession and its linkage to the tectonic and structural evolution of the JMMC-IPR, its conjugate margins as well as the wider Northeast Atlantic region. The JMMC is a key area for stratigraphic correlations and geodynamic development of the Cenozoic Northeast Atlantic and type location for microcontinent formation. Paper II includes a detailed definition and description of the seismic stratigraphy based on new and densely spaced seismic and seafloor sample data coverage; in particular, the recognition of a number of major JMMC-IPR's boundaries and unconformities. Boundaries that correlate to key regional unconformities between the JMMC and adjacent Northeast Atlantic conjugate margins, including onshore regions, such as central East Greenland and the Faroe Islands. This facilitated the most comprehensive (to date), observation-led, regional palaeogeographical reconstruction, laying the framework for the detailed volcanostratigraphic analysis of Paper III of this study.

Paper II addresses the structural evolution of the region between igneous areas of the Greenland-Iceland-Faroe ridge complex in the south and the Jan Mayen igneous complex to the north through tectonics and kinematics from regional and local unconformities. A set of complex pre-existing structural elements, throughout the Cenozoic, and related to the adjacent mid-oceanic ridge systems (Ægir-, Mohn- and Kolbeinsey ridges), the Jan Mayen fracture zone to the north, and the Iceland-Faroe fracture zone to the south, are a testimony to the differential uplift of the JMMC-IPR area. The paper stratigraphically links the Ægir ridge across the IPR south to the Greenland-Iceland-Faroe ridge complex and west into the Blosseville Kyst. The seismic-refraction data was used to compare the JMMC with its conjugate margins, i.e. central East Greenland, the Vøring- and Møre margins of western Norway, and the Faroe-Shetland region, in order to verify and update pre-Cenozoic domains along the continental, transitional and volcanic margins of the JMMC, adjacent oceanic domains, and potential high-velocity lower-crustal features delineating the breakup boundaries basin-ward of the mapped continent-ocean boundary.

This part of the study improved our understanding of the contemporary tectonic activity as breakup ensued, including: rift transfer across the IPR from the Ægir ridge to form the Kolbeinsey ridge system; the uplift processes that were caused by the increased igneous activity and tectonic re-arrangement during the Oligocene, and linked to the formation of the proto-Kolbeinsey ridge; the connection of the Reykjanes ridge to the Mohns ridge; and the initiation of the proto-Iceland shelf by splitting the GIFRC into three segments - the Greenland-Iceland ridge, the proto-Iceland shelf domain, and the Iceland-Faroe ridge.

4.2.2 Main findings

Detailed mapping of the JMMC's Cenozoic sedimentary succession provided a stratigraphic framework revealing individual igneous and tectonic events within the JMMC. The mapping serves as a correlation tool for comparing the geodynamic development of the JMMC with its conjugate margins, as well as changes in sea level and climate. This seismic-stratigraphic framework was based on 2D MCS reflection seismic data, seismic-refraction data, borehole and analogue field data. The study identified ten unconformities and disconformities that subdivide the JMMC's Cenozoic succession into eleven seismic-stratigraphic units (JM-70 to JM-01). The major bounding surfaces include five locally varying unconformities and disconformities (TSDR, UE1, UE2, TFM, MMU), and six regional unconformities (BPU, TV, ME, MOU, TPU, INU). The stratigraphic succession was mapped across the project area and tied to regional events within the northeast Atlantic region, confirming a strong regional tectono-stratigraphic link. Paper II describes six regionally observed tectonic phases have been tied to stratigraphic and major igneous events that include:

- (1) Pre-breakup Paleocene (> 55 Ma) extension represented by seismic unit JM-70, is comprised of terrigenous and marine sedimentary rocks and a thick plateau basalt volcanic succession; no significant sea level changes were noted;
- (2) Early Eocene (~55-52 Ma) syn-breakup (rift-to-drift) and first breakup phase along the eastern margin represented by seismic unit JM-60 that comprises a mixture of intrusives, subaerial lavas, hyaloclastites and non-marine to shallow-marine sedimentary rocks;
- (3) Early to Mid-Eocene (~52-43 Ma) syn-breakup (rift-to-drift) and rift-transfer across the Iceland Plateau rift, represented by seismic unit JM-50 comprising of volcanics and shelf-margin deltaic sediments;
- (4) Late Eocene – Early Oligocene (43-30 Ma) ridge transfer and tectonic re-arrangement in proximity of the Iceland hotspot. The preserved sedimentary record indicates shallow-to deep-marine origin of deposits of stratigraphic units JM-40, JM-35, and JM-30;
- (5) Late Oligocene (30-22 Ma) second breakup phase along the western JMMC igneous margin, in conjunction with the formation of the south-western Jan Mayen igneous province, the proto-Kolbeinsey ridge, and the initiation of the proto-Iceland shelf region that is represented in the seismic stratigraphic records and intrusives between units JM-20 and JM-15;
- (6) Miocene-to-present-day separation phase of the JMMC from East Greenland (since 22 Ma), reflected in seismic stratigraphic units JM-10, JM-05, and JM-01, which record a general deepening and basin-ward shift of the microcontinent's depositional environment.

4.3 Paper III: Seismic volcanostratigraphic characteristics of the Jan Mayen microcontinent and Iceland Plateau rift system

4.3.1 Summary

Paper III addresses the seismic volcano-stratigraphy of the JMMC-IPR, in order to constrain the spatial and temporal evolution of the igneous processes associated with the second breakup from the Greenland margin. It is based on the reconstruction framework presented in Paper I and the detailed chronostratigraphic framework presented in Paper II. The paper also includes more detailed comparison with the igneous successions preserved on the central East Greenland margin (Jameson Land basin, Liverpool Land high and basin, and the Blosseville Kyst), the Mid-Norwegian margin (Vøring- and Møre margins), the Faroe Islands, and the Greenland-Iceland-Faroe ridge complex. Smaller-scale movements of the JMMC ridges in connection to tectono-magmatic processes between the Early Eocene and Early Miocene are also addressed. The distinction of different volcanic facies in the JMMC-IPR was accomplished based on 2D MCS seismic reflection profiles, seismic refraction data, borehole and analogue field data. An investigation of available petrological datasets was undertaken together with a revision of ambiguous age dating of DSDP Leg 38 boreholes sites 350 and 348 to address igneous-province relationships and the timing of volcanic events. Joint interpretation of this data provided a confident fit of the igneous record into the reconstruction and stratigraphic model of the JMMC-IPR's tectono-magmatic evolution, through identification of seismic stratigraphic signatures, such as characteristic of landward flows, SDRs, igneous and volcanic complexes, intrusions (sills, dykes, vent structures) and volcanic ridges. A linkage between the obliquely opening IPR system and the Blosseville Kyst igneous province during Eocene was established based on timing and geochemistry data. Thus, confirming the IPR as an oblique rifting domain that interfingers with the southern ridges of the JMMC due to deep crustal breaches and melt incursions that form several axial rift systems and volcanic ridges.

The delineation and mapping of the second breakup margin along the JMMC's southwestern and western flank during Late Oligocene to Early Miocene portrays a more complex margin than had been previously identified. The breakup was accompanied by emplacement of igneous complexes, forming the Southwest Jan Mayen igneous province, the Proto-Kolbeinsey ridge, and potentially westward dipping SDR units. The second breakup igneous margin relatively wide and interlinked with the opening of the Jan Mayen basin, an igneous domain with massive dyke and sill intrusives and covered by regionally extensive flood basalts during the JMMC's final breakup phase. Deeper understanding of the magmatic evolution of the JMMC-IPR provided the last piece of its volcano-stratigraphic framework puzzle, and in general, the issue of ridge – mantle anomalies that appear to develop along pre-existing structural complex areas, such as the Greenland-Iceland-Faroe ridge complex, where a mid-oceanic ridge systems did not fully develop until Late Oligocene to Early Miocene and formed overlapping rift systems. The non-uniform formation is also represented by the clear north-south asymmetry in SDR formation along the north-eastern to eastern JMMC breakup margin at the initiation of the Ægir rift system. The overall JMMC breakup system is thus preferentially linked to variations in the pre-rift lithospheric structure

and very likely was located above or in vicinity of a thermal mantle anomaly. This conclusion is supported by comparison with other microcontinent analogue areas seen globally, close to mantle plumes, complex pre-breakup crustal configurations, and competing rift systems. The conclusions of paper III have not previously been demonstrated in such detail within the Northeast Atlantic region, where the JMMC represents a key component for understanding such a system in the past as does Iceland today.

4.3.2 Main findings

The paper provides new details on the Northeast Atlantic opening mechanism, based on composite datasets that clearly delineate the JMMC between two breakup centres, the Greenland-Iceland-Faroe ridge complex to its south, and the Jan Mayen Island igneous complex – Jan Mayen fracture zone system to its north. Seven tectono-magmatic and rift-transfer phases were defined, in contrast to the six tectonic and stratigraphic phases described in Papers I and II. These are linked to the rift propagation history of the IPR and are as follows:

- (1) An initial breakup phase characterized by anomalous magmatic activity that followed a SW-NE opening fissure trend along WNW-ESE striking pre-existing fracture zones south and west of the JMMC, here inferred as an oblique opening of the Geikie plateau into the central JMR domain (~63-56 Ma);
- (2) Multiple SDR sets formed along the JMMC eastern igneous margin during syn-breakup in Early Eocene. SSW- NNE striking SDR rift segments propagating northwards in direction represent a precursor for the Ægir ridge mid-oceanic ridge system's development that opened along the NW-SE striking EJMFZ, CNBFZ, and SRCFZ segments (~55-53 Ma);
- (3) Forming of JMMC's eastern breakup margin, the Iceland Plateau rift (IPR-I), and southernmost extent of the Ægir ridge system (~52-50 Ma);
- (4) SW- NE magmatic interaction of the Greenland-Iceland-Faroe ridge complex with the JMMC domain. The IPR-II segment intersecting the IPR-I segment and the southern extent of the SRC domains contemporary with the Ægir ridge. Volcanism was accompanied by axial rift segments, intrusives, flood basalts, shelf-margin deltaic sedimentation within a shallow shelf marine depositional environment (~49-36 Ma).
- (5) SW to NE magmatic incursion from the GIFRC into the JMMC systems creating the IPR-III rift domain, severing the SRC from the main JMR (Lyngvi ridge) forming the JMT and volcanic ridges within the SRC domain (~36-25 Ma);
- (6) The final breakup phase of the JMMC during the formation of the SWJMIP, the IPR-IV segment and western JMMC igneous margin, the proto-Kolbeinsey Ridge and the WJMFZ segments (25-22 Ma);
- (7) Full separation of the JMMC and formation of the Kolbeinsey Ridge between proto-Iceland and the WJMFZ – Jan Mayen island igneous complex at its northern end (since 22 Ma), accompanied by tephra deposits within the Neogene deep marine sediments that possibly were sourced from both primary active volcanic systems.

5 Conclusions

This study of the Cenozoic evolution of the JMMC-IPR region has revealed a protracted history of continental breakup in the Northeast Atlantic Ocean that continues to the present day, constituting a direct link to the formation of Iceland. This contrasts with the hitherto generally accepted model of the North Atlantic breakup and seafloor spreading occurring as a primary event around 56-52 Ma and rifted Greenland from Eurasia.

Focusing on the geodynamic development of the JMMC and the IPR, as a propagating oblique-rift system with associated processes of tectonism, sedimentation and volcanism, has provided new constraints on the regional and sub-regional pattern of continental breakup as a response to long-lived tectono-magmatic interactions, shown as:

- Preserved data record of the sedimentary and igneous succession providing an indicator of the area's response to regional and local tectonic events that can be calibrated with the development of the wider Northeast Atlantic region, not just as the relatively simple west to east transect commonly portrayed, but as a clear north-south asymmetry linked to multi-phased breakup and propagating rifting processes.
- A detailed chronostratigraphic framework based on ten identified unconformities and disconformities linked to tectonic, magmatic and environmental changes, subdividing the Cenozoic succession into eleven seismic stratigraphic units. Five of these are locally varying unconformities and disconformities and six are of regional nature that are linked to the wider Northeast Atlantic region.
- A clear link to JMMC's western margin of the Blosseville Kyst along the central East Greenland conjugate margin and correlation to the plateau basalt and several magmatic events significantly contributed to a revised understanding of a multi-phased igneous margins between the two areas, including their timing and geochemistry suggests an overlapping tectono-magmatic system. A process affecting both margins from the initial emplacement of the NAIP during the Late Paleocene – Early Eocene to the final Oligocene-Early Miocene breakup.
- The role and interlinkage of fracture and rift zone development, with anomalous magmatic activity that followed the pre-breakup extensional structural fabric of the region along weaker and more brittle crustal deformation zones. These weak zones that often form wrench fault system, developed an array of opening crustal pathways perpendicular to the acting minimum stress (σ_3) which acted as preferential openings for magmatic pathways into the crust. In this process en-echelon axial rift segments were formed, which can be seen in these key boundary areas of the JMMC-IPR domain:
 - ⇒ Along the WNW-ESE striking pre-existing fracture zones south and west of JMMC, accompanied by a SW-NE opening fissure trend fabric that linked to the Faroe Islands, the Greenland-Iceland-Faroe ridge domains, and across the IPR as it developed with time.

- ⇒ The WNW-ESE striking proto-EJMFZ linking the Mid-Norwegian margin to the NE Greenland margin, the focal area for the JMI – initial NE-JMMC development and the formation of large igneous centres and seaward dipping reflector units (SDR) close to deep interlinking fracture zone segments, not visible at the surface.
- ⇒ The controversial SW-NE fracture zone, south of the GIFRC, that intersected the WNW-ESE striking trends within the GIFRC domain, creating a crustal weak zone still present across Iceland. Thus, setting the stage for an asymmetric breakup margin right from the breakup of the NE-Atlantic.
- Providing insight into continental break-up, microcontinent formation, and asymmetric oceanic crustal accretion along a passive margin in comparison with active margin microcontinent formation, facilitated by the existence of continental heterogeneities and weak zones, and a rotational kinematic component. These oblique rifting scenarios were initiated by the formation of the Ægir ridge, through the IPR domains, and still exist in present-day Iceland, within the dextral Tjörnes Fracture Zone, the Reykjanes peninsula and South Iceland seismic zone.
- Delineation of the gradual northward propagation of the IPR in four stages (IPR-I to IPR-IV) from Early Eocene to Early Miocene, prior to the formation of the Kolbeinsey ridge. Formation of impinging wedges from the south into the JMMC domain through deep crustal breaches and melt incursions within several axial rift systems and volcanic ridges, representing the westward propagating crustal extension associated with the receding southern Ægir ridge. This process prompted a counterclockwise rotation of the JMMC blocks away from the East Greenland, generating reverse structures within the SRC and adjacent oceanic domain.

These key observations highlight the tectono-magmatic development, crustal build-up, evidence of thick lava flows and plateau basalt across the JMMC. The wedge-shaped characteristics of the IPR suggest an asymmetric plume-ridge interaction within and north of the Iceland region, in contrast to the Reykjanes ridge. High-velocity bodies that surround the JMMC-IPR domain and similarities in the geochemistry of IPR basalts with the NVZ of Iceland lend further support this theory. However, definitive proof of a temporal plume-related magmatic increase in a plume-ridge development can only be confirmed by petrologically sampling the IPR's time transition from IPR stages I to IV and the ridge propagation from the IFR across the IPR, in future research projects.

In summary, the JMMC-IPR study has substantially enhanced our knowledge regarding the non-uniform formation of tectono-magmatic rifted margins and domains that developed through processes not dissimilar to those observed in present-day Iceland. A more detailed model of the initiation and evolution of the oblique IPR propagated rifting domain that inter-fingers with the southern ridges of the JMMC, has been obtained, consisting of several axial rift systems and volcanic ridge formation along over-stretched and breached crustal weak zones. The dual breakup scenario and its association to a series of volcanic zones with links to transfer system has been imaged, and the full opening of the Jan Mayen basin revealed, as an igneous domain with massive dyke, sill intrusive activities, and regionally extensive flood basalts.

6 Further work

One of the primary objectives in wake of this study would be to address propagating rift formations across Iceland, by more detailed mapping of present spreading domains, oblique structures and volcanic zones immediately offshore and within Iceland. The applied methods and data compilations within this study could be used to improve the regional scale understanding of Iceland's onshore and shelf regions by focusing on:

- Acquire new seismic reflection and refraction data around Iceland in order to map in detail subsurface structures with higher resolution than commonly used onshore methods.
- Compilation of all potential field data to better outline the underlying deep intrusive systems, thus adding new information to the tectonostratigraphic reconstruction puzzle of the Northeast Atlantic region since Early Miocene.
- Structurally reconstruct the tectonic trends of key areas in order to distinguish between older structural trends and dominant present-day trends.
- Focus on areas with direct volcanic rift influence vs. oblique rift systems along the northern Icelandic shelf.
- The IPR-GIFRC domains should be investigated in regard to spatially reconstructing hot-spot – ridge interactive domains, as the southern end of the JMMC terminates abruptly against the NE Iceland shelf. Such future work would address hot spot/mantle anomalous crust to ridge proximity interactions through time and observed or modelled lateral and vertical crustal accretion.
- Kinematic investigation, specifically of rotational patterns of known micro-plate onshore and offshore Iceland, could improve our understanding of structural and rift transfer processes as well as the structural and rift fabric across the Iceland region. Located at a hot-spot-rift junction, this region is a key location globally for complex rift transfer zones.

The author of this thesis is a lead proponent on a recently submitted IODP project proposal (IODP Full976) to drill the JMMC-IPR region as an analogue case for axial rift and transfer zone development in relation to the development of the Iceland plume and the greater Northeast Atlantic region is founded on this thesis. The results of this thesis project also strengthened another proposal (GPF 20-2_044) by the Federal Institute for Geosciences and Natural Resources (BGR) to the German Science Foundations to obtain funding for marine data surveying. The plan is to acquire new seismic reflection, refraction, high resolution bathymetry, and potential field data to investigate the crustal fabric and tectonic development of the southern continuation of the Iceland Plateau onto the Iceland Faroe Ridge.

Primary future challenges lie in being able to conduct offshore data acquisition projects to acquire seismic reflection and refraction, high-resolution magnetic, gravity, or bathymetry data in regions with limited data coverage. Future seismic refraction and reflection data acquisitions should target large scale crustal features of the GIFRC.

High resolution bathymetry (multibeam) data acquisition do give a detailed image of the seafloor, highlighting erosional and substrate features, as well as structural elements that reach up to the seafloor. These have to be tied into the subsurface dataset, such as seismic reflection dataset to obtain a realistic structural 3-dimensional interpretation, and the basis for any structural and kinematic modelling analysis.

Emphasising the structural-, volcano-stratigraphic-, and igneous-province-mapping of the JMMC-IPR region, a conference paper (Appendix 1) summarises the complexity of the project area, as a base case to define continued research to apply to the Icelandic margins onto the onshore domains. Improving our understanding of the Iceland onshore and shelf regions by focusing on:

- (1) Primary use of all potential field data to better outline the underlying deep intrusive systems, thus aiding detailed tectonostratigraphic reconstruction of the Northeast Atlantic region and differentiation between observed dominant present-day trends vs. older structural trends that only become apparent by detailed potential field, structure, and age data reconstruction, which are spatially consistent;
- (2) 3D imagery and reconstruction of propagating oblique rift systems, such as the Iceland-Faroe ridge, the northern volcanic zone, or Tjörnes fracture zone domains vs. mid-oceanic ridges, such as Kolbeinsey ridge.

References

- Åkermoen, T. (1989). *Jan Mayen-ryggen: et seismisk stratigrafisk og strukturelt studium*. Cand. scient. thesis, University of Oslo, 174.
- Abdelmalak, M. M., Faleide, J. I., Planke, S., Gernigon, L., Zastrozhnov, D., Shephard, G. E. and Myklebust, R. (2017). The T-Reflection and the deep crustal structure of the Vøring Margin, offshore mid-Norway. *Tectonics*, **36**, 2497–2523.
- Abdelmalak, M.M., Meyer, R., Planke, S., Faleide, J.I., Gernigon, L., Frieling, J., Sluijs, A., Reichart, G.-J., Zastrozhnov, D., Theissen-Kraha, S., Said, A. and Myklebust, R. (2016). Pre-breakup magmatism on the Vøring Margin: Insight from new sub-basalt imaging and results from Ocean Drilling Program Hole 642E. *Tectonophysics*, **675**, 258–274. doi:10.1016/j.tecto.2016.02.037
- Amante, C. and Eakins, B.W. (2009). *ETOPO1 1 Arc-Minute Global Relief Model: Procedures, Data Sources and Analysis*. NOAA Technical Memorandum NESDIS NGDC-24.
- Andersen, T. B. and Jamtveit, B. (1990). Uplift of deep crust during orogenic extensional collapse: a model based on field studies in the Sogn–Sunnfjord area of Western Norway. *Tectonics*, **9**, 1097-1111.
- Berndt, C., Mjelde, R., Planke, S., Shimamura, H. and Faleide, J.I. (2001). Controls on the tectono-magmatic evolution of a volcanic transform margin: the Vøring Transform Margin, NE Atlantic. *Marine Geophysical Research*, **22**(3), 133–152. doi:10.1023/a:1012089532282
- Bernstein, S., Leslie, A.G., Higgins, A.K. and Brooks, C.K. (2000). Tertiary alkaline volcanics in the Nunatak Region, Northeast Greenland: new observations and comparison with Siberian maymechites. *Lithos*, **53**(1), 1-20. doi: 10.1016/S0024-4937(00)00012-8
- Berthelsen, O., Noe-Nygaard, A. and Rasmussen, J. (1984). *The Deep Drilling Project 1980–1981 in the Faeroe Islands*. Føroya Fróðskaparfelag, Tórshavn.
- Bischoff A., Nicol, A., Cole, J. and Gravley, D. (2019). Stratigraphy of Architectural Elements of a Buried Monogenetic Volcanic System. *Open Geosciences*, **11**(1), 581–616. doi:10.1515/geo-2019-0048
- Blichert-Toft, J., Agranier, A., Andres, M., Kingsley, R., Schilling, J.-G., and Albarede, F., (2005). Geochemical segmentation of the Mid-Atlantic Ridge north of Iceland and ridge-hot spot interaction in the North Atlantic. *Geochemistry, Geophysics, Geosystems*, **6**, Q01E19. doi:10.1029/2004GC000788
- Blichert-Toft, J., Leshner, C.E. and Rosing, M.T. (1992). Selectively contaminated magmas of the Tertiary East Greenland macrodiike complex. *Contributions to Mineralogy Petrology*, **110**, 154-172. <https://doi.org/10.1007/BF00310736>
- Blischke, A., Brandsdóttir, B., Erlendsson, Ö., Planke, S. and Gaina, C. (2019). *The Jan Mayen microcontinent and Iceland Plateau volcanic breakup margins*. EGU General Assembly 2019, **21**, EGU2019-14291-1.

- Blischke, A. and Erlendsson, Ö. (2018). *Central East Greenland – conjugate margin of the Jan Mayen microcontinent - Database, structural and stratigraphical mapping project*. Iceland Geosurvey, Reykjavik, report ÍSOR-2018/024.
- Blischke, A., Erlendsson, Ö., Einarsson, G.M., Ásgeirsson, V.L. and Árnadóttir, S. (2017a). *The Jan Mayen Microcontinent Project Database and Seafloor Mapping of the Dreki Area Input Data, Geological and Geomorphological Mapping and Analysis*. Iceland Geosurvey, Reykjavik, report ÍSOR-2017/091.
- Blischke, A., Egilson, Þ., Magnússon, I. Þ., Kristinsson, S. G., Flóvenz, Ó. G. and Gautason, B. (2017b). *Árskógsströnd - Hóla ÁRS-32: Forrannsóknir, borun og mælingar*. Iceland Geosurvey, Reykjavik, report ÍSOR-2017/055.
- Blischke, A., Planke, S., Tegner, C., Gaina, C., Brandsdóttir, B., Halldórsson, S.A., Helgadóttir, H.M. and Koppers, A. (2016). *Seismic volcano-stratigraphic characteristics and igneous province assessment of the Jan Mayen microcontinent, central NE-Atlantic*. American Geophysical Union, Fall Meeting 2016, T33A-3008.
- Blystad, P., Brekke, H., Færseth, R.B., Larsen, B.T., Skogseid, J. and Tærudbakken, B. (1995). *Structural elements of the Norwegian continental shelf. Part II. The Norwegian Sea Region*. NPD Bulletin No. 8. Norwegian Petroleum Directorate.
- Bonow, J.M., Japsen, P. and Nielsen, T.F.D. (2014). High-level landscapes along the margin of southern East Greenland—A record of tectonic uplift and incision after breakup in the NE Atlantic. *Global and Planetary Change*, **116**, 10–29. doi:10.1016/j.gloplacha.2014.01.010
- Borissova, I., Coffin, M.F., Charvis, P. and Operton, S. (2003). Structure and development of a microcontinent: Elan Bank in the southern Indian Ocean. *Geochem. Geophys. Geosyst.*, **4** (9), 1071. doi:10.1029/2003GC000535, 9
- Boyden, J.A., Müller, R.D., Gurnis, M., Torsvik, T.H., Clark, J.A., Turner, M., Ivey-Law, H., Watson, R.J. and Cannon, J.S. (2011). Next-generation plate-tectonic reconstructions using Gplates. In: Keller, G. and Baru, C. (eds). *Geo-informatics: Cyberinfrastructure for the Solid Earth. Sciences*, 95-116. Cambridge: Cambridge University Press.
- Brandsdóttir B., Hooft, E., Mjelde, R. and Murai, Y. (2015). Origin and evolution of the Kolbeinsey Ridge and Iceland Plateau, N-Atlantic. *Geochemistry, Geophysics, Geosystems*, **16**, 612-634. doi:10.1002/2014GC005540
- Brandsdóttir, B. and Menke, W.H. (2008). The seismic structure of Iceland. *Jökull*, **58**, 17-34.
- Breivik, A.J., Mjelde, R., Faleide, J.I. and Murai, Y. (2012). The eastern Jan Mayen microcontinent volcanic margin. *Geophysical Journal International*, **188**(3), 798-818. <https://doi.org/10.1111/j.1365-246X.2011.05307.x>
- Breivik, A.J., Faleide, J.I. and Mjelde, R. (2008). Neogene magmatism northeast of the Aegir and Kolbeinsey ridges, NE Atlantic: Spreading ridge–mantle plume interaction? *Geochemistry, Geophysics, Geosystems*, **9**, Q02004. doi:10.1029/2007GC001750
- Breivik, A.J., Mjelde, R., Faleide, J.I., and Murai, Y. (2006). Rates of continental breakup magmatism and seafloor spreading in the Norway Basin-Iceland plume interaction. *Journal of Geophysical Research*, **111**, B07102. doi:10.1029/2005JB004004
- Breivik, A., and R. Mjelde (2003). *Modeling of profile 8 across the Jan Mayen Ridge*. Technical report, Institute of Solid Earth Physics, University of Bergen, Bergen, Norway.

- Brekke, H. (2000). The tectonic evolution of the Norwegian Sea continental margin with emphasis on the Vøring and Møre basins. In: Nøttvedt, A. et al. (eds) Dynamics of the Norwegian Margin. *Geological Society of London, Special Publications*, **167**, 327-378.
- Brooks, C. K. (2011). The East Greenland rifted volcanic margin. *Geological Survey of Denmark and Greenland Bulletin*, **24**, 96, ISBN 978-87-7871-322-3.
- Brown, P.E., Evans, I.B. and Becker, S.M. (1996). The Prince of Wales Formation - Post-flood basalt alkali volcanism in the Tertiary of East Greenland. *Contributions to Mineralogy and Petrology*, **123**, 424-434. doi:10.1007/s004100050166
- Butt, F.A., Elverhoi, A., Forsberg, C.F. and Solheim, A. (2001). An evolution of the Scoresby Sund Fan, central East Greenland - evidence from ODP Site 987. *Norsk Geologisk Tidsskrift*, **81**, 3-15, ISSN 0277-3791.
- Channell, J.E.T., Smelror, M., Jansen, E., Higgins, S.M., Lehman, B., Eidvin, T. and Solheim, A. (1999b). *Age models for glacial fan deposits off East Greenland and Svalbard (sites 986 and 987)*. Proceedings of the Ocean Drilling Program, Scientific Results.
- Channell, J.E.T., Amigo, A.E., Fronval T., Rack, F., Lehman, B. Raymo, M.E., Jansen E., Blum P. and Herbert, T. (eds) (1999a). *Magnetic stratigraphy at Sites 907 and 985 in the Norwegian-Greenland Sea and a revision of the Site 907 composite section*. Proceedings of the Ocean Drilling Program, Scientific Results, 162, 131-148.
- Childs, J.R. and Cooper, A.K. (1978). *Collection, reduction and interpretation of marine seismic sonobuoy data*. U.S. Geological Survey, Department of interior, report 78-442.
- Cianfarra, P., and Salvini, F. (2015). Lineament Domain of Regional Strike-Slip Corridor: Insight from the Neogene Transtensional De Geer Transform Fault in NW Spitsbergen. *Pure and Applied Geophysics*, **172**(5), 1185–1201. doi:10.1007/s00024-014-0869-9
- Cohen, K. M., Finney, S. C., Gibbard, P. L. and Fan, J.-X. (2013; updated). The ICS International Chronostratigraphic Chart. *Episodes*, **36**, 199-204. doi:10.18814/epiiugs/2013/v36i3/002
- Cox, A. and Hart, R.B. (1986). *Plate tectonics: How it works*. Blackwell Scientific Publications, Palo Alto. ISBN-13: 978-0865423138
- Decker, R. and Decker, B. (2005). *Volcanoes*, 4th ed., W. H. Freeman, 2005, ISBN 0-7167-8929-9.
- Diebold, J.B. and Stoffa, P.L. (1981). The travelttime equation, tau-p mapping, and inversion of common midpoint data. *Geophysics*, **46**(3), 238-254.
- Doré, A.G., Lundin, E.R., Kuszniir, N.J. and Pascal, C. (2008). Potential mechanisms for the genesis of Cenozoic domal structures on the NE Atlantic margin: pros, cons and some new ideas, in The Nature and Origin of Compression in Passive Margins. *Geological Society of London, Special Publication*, **306**(1), 1-26. doi:10.1144/SP306.1
- Doré, A.G., Lundin, E.R., Jensen, L.N., Birkeland, Ø., Eliassen, P.E. and Fichler, C. (1999). *Principal tectonic events in the evolution of the northwest European Atlantic margin*. In: Fleet, A.J., and Boldy, S.A. R (eds) *Petroleum Geology of Northwest Europe: The Geological Society, London, proceedings of the 5th Conference.*, 41-61.
- Dobrovine, P.V., Steinberger, B. and Torsvik, T.H. (2012). Absolute plate motions in a reference frame defined by moving hot spots in the Pacific, Atlantic, and Indian oceans, *Journal of Geophysical Research, Solid Earth.*, **117**, B09101. doi:10.1029/2011JB009072

- Eggen, S.S. (1984). *Jan Mayen-ryggens geologi*. Norwegian Petroleum Directorate contribution 20, 29.
- Einarsson, P., Hjartardóttir, Á. R., Hreinsdóttir, S. and Imsland, P. (2018). The structure of seismogenic strike-slip faults in the eastern part of the Reykjanes Peninsula Oblique Rift, SW Iceland, *Journal of Volcanology and Geothermal Research* (accepted manuscript 2018). <https://doi.org/10.1016/j.jvolgeores.2018.04.029>
- Einarsson, P. (2008). Plate boundaries, rifts and transforms in Iceland. *Jökull*, **58**, 35–58.
- Einarsson, P. and Sæmundsson, K. (1987). *Earthquake epicenters 1982–1985 and volcanic systems in Iceland, map*. In: Sigfússon, Th. (Ed.) *Í hlutarins edli*, Festschrift for Thorbjörn Sigurgeirsson, Menningarsjóður, Iceland.
- Eldholm, O., Skogseid, J., Sundvor, E. and Myhre, A.M. (1990). *The Norwegian-Greenland Sea*. In: The geology of North America, Vol. 1. The Arctic Ocean, ed. by A. Grantz, Johnson, L. and Sweeney, J.F. Geol. Soc. Of Amer., Boulder, Colorado, USA, 351-364.
- Eldholm, O., Thiede, J. and Taylor, E. (1989). *The Norwegian continental margin: Tectonic, volcanic, and paleo-environmental framework*. Proceedings of the Ocean Drilling Program, Scientific Results, 104, 5-26.
- Eldholm, O., Thiede, J., Taylor, E., et al. (1987b). *Shipboard Scientific Party, 1987. Site 642: Norwegian Sea*. In: *Proc. ODP, Initial Reports, 104*, Ocean Drilling Program, College Station, TX, 53–453. doi:10.2973/odp.proc.ir.104.104.1987
- Eldholm, O., Thiede, J., and Taylor, E. (1987a). *Evolution of the Norwegian Continental Margin: Background and Objectives*. In *Proc. ODP, Init. Repts., 104*, Ocean Drilling Program, College Station, TX, 53–453. doi:10.2973/odp.proc.ir.104.101.1987
- Eldholm, O. and Windisch, C. C. (1974). Sediment distribution in the Norwegian-Greenland Sea. *Bulletin of the Geological Society of America*, 85(11), 1661–1676. doi:10.1130/0016-7606(1974)85<1661:SDITNS>2.0.CO;2
- Ellis, D. and Stoker, M.S. (2014). The Faroe–Shetland Basin: a regional perspective from the Paleocene to the present day and its relationship to the opening of the North Atlantic Ocean. In: Cannon, S.J. C. and Ellis, D. (eds) *Hydrocarbon Exploration to Exploitation West of Shetlands*. *Geological Society, London, Special Publications*, **397**. doi:10.1144/SP397.1
- Ellis, D., Bell, B.R., Jolley, D.W. and O'Callaghan, M. (2002). The stratigraphy, environment of eruption and age of the Faroes Lava Group, NE Atlantic Ocean. In: The North Atlantic Igneous Province: Stratigraphy, Tectonic, Volcanic and Magmatic Processes. *Geological Society of London, Special Publication*, **197**, 253-269. doi:10.1144/GSL.SP.2002.197.01.10
- Epp, D., and Smoot, N.C. (1989). Distribution of seamounts in the North Atlantic. *Nature*, **337**, 254-257. doi:10.1038/337254a0
- Erlendsson, Ö. and Blischke, A. (2018). *Review and Assessment of the CNOOC-JMR-2015 2D Seismic Reflection Dataset: Data Quality Check and Preliminary Structural Mapping for the Dreki License Area*. Íslenskar orkurannsóknir, report ÍSOR-2018/083, 93.
- Erlendsson, Ö. (2010). *Seismic Investigation of the Jan Mayen Ridge – with a Close Study of Sill Intrusions*. MSc. thesis, Aarhus University, 111.

- Faleide, J.I., Bjørlykke, K. and Gabrielsen, R.H. (2015). *Geology of the Norwegian continental shelf*. In: Bjørlykke, K (ed.) *Petroleum Geoscience: From Sedimentary Environments to Rock Physics*. New York: Springer, 467-499, ISBN-10 3642341314.
- Fitch, F.J. (1964). *The development of the Beerenberg volcano, Jan Mayen*. Proceedings of the Geologists' Association. doi:10.1016/S0016-7878(64)80002-X
- Foulger, G.R., Natland, J.H. and Anderson, D.L. (2005). A source for Icelandic magmas in re-melted Iapetus crust. *Journal of Volcanology and Geothermal Research*, **141** (2005) pp. 23-44. doi:10.1016/j.jvolgeores.2004.10.006
- Funck, T. Geissler, W.H., Kimbell, G.S., Gradmann, S., Erlendsson, Ö., McDermott, K. and Petersen, U.K. (2017). Moho and basement depth in the NE Atlantic Ocean based on seismic refraction data and receiver functions. *Geological Society of London, Special Publications*, **447**, 171-205. doi:10.1144/SP447.1
- Funck, T., Erlendsson, Ö., Geissler, W.H., Gradmann, S., Kimbell, G.S., McDermott, K. and Petersen, U.K. (2016). A review of the NE Atlantic conjugate margins based on seismic refraction data. *Geological Society of London, Special Publications*, **447**. doi:10.1144/SP447.9
- Funck, T., Hopper, J.R., Fattah, R.A., Blischke, A., Ebbing, J., Erlendsson, Ö., Gaina, C., Geissler, W.H., Gradmann, S., Haase, C., Kimbell, G.S., McDermott, K.G., Peron-Pinvidic, G., Petersen, U., Shannon, P.M. and Voss, P.H. (2014). *Crustal Structure*. In: Hopper, J.R., Funck, T., Stoker, M., Ártíng, U., Peron-Pinvidic, G., Doornenbal, H. and Gaina, C. (eds) *Tectonostratigraphic Atlas of the North-East Atlantic region*. The Geological Survey of Denmark and Greenland (GEUS), Copenhagen, Denmark, ISBN 9781786202789.
- Gaina, C and Whittaker, J. (accepted). *Microcontinents*. In: Encyclopedia of Solid Earth Geophysics. Revised version, ed. H. K. Gupta, Springer, Online ISBN 978-3-030-10475-7.
- Gaina, C., Nasuti, A., Kimbell, G.S. and Blischke, A. (2017b). Break-up and seafloor spreading domains in the NE Atlantic. *Geological Society of London, Special Publications*, **447**. doi:10.1144/SP447.12
- Gaina, C., Blischke, A., Geissler, W.H., Kimbell, G.S. and Erlendsson, Ö. (2017a). Seamounts and oceanic igneous features in the NE Atlantic: a link between plate motions and mantle dynamics. *Geological Society of London, Special Publications*, **447**. doi:10.1144/SP447.6
- Gaina, C. (2014). *Plate Reconstructions and Regional Kinematics*. In: Hopper, J.R., Funck, T., Stoker, M.S., Ártíng, U., Peron-Pinvidic, G., Doornenbal, H. and Gaina, C. (eds.) *Tectonostratigraphic Atlas of the North-East Atlantic Region*. Geological Survey of Denmark and Greenland (GEUS), Copenhagen, Denmark, ISBN 9781786202789.
- Gaina, C., Gernigon, L. and Ball, P. (2009). Palaeocene - Recent plate boundaries in the NE Atlantic and the formation of the Jan Mayen microcontinent. *Journal of the Geological Society*, **166**, 1-16. <https://doi.org/10.1144/0016-76492008-112>
- Gaina, C., Müller, R.D., Brown, B. and Ishihara, T. (2007). Breakup and early sea floor spreading between India and Antarctica. *Geophysical Journal International*, **170**, 151-169. <http://doi.org/10.1111/j.1365-246X.2007.03450.x>

- Ganerød, M., Wilkinson, C.M. and Hendriks, B. (2014). *Geochronology*. In: Hopper, J.R., Funck, T., Stoker, M., Ártíng, U., Peron-Pinvidic, G., Doornenbal, H. and Gaina, C. (eds) *Tectonostratigraphic Atlas of the North-East Atlantic region*. The Geological Survey of Denmark and Greenland (GEUS), Copenhagen, Denmark, ISBN 9781786202789.
- Gairaud, H., Jacquart, G., Aubertin, F. and Beuzart, P. (1978). Jan Mayen Ridge synthesis of geological knowledge and new data. *Oceanologica Acta*, **1**(3), 335–358.
- Gasser, D. (2014). The Caledonides of Greenland, Svalbard and other Arctic areas: status of research and open questions. *Geological Society of London, Special Publications*, **390**(1), 93-129. doi:10.1144/SP390.17
- Geissler, W.H., Gaina, C., Hopper, J.R., Funck, T., Blischke, A., Arting, U., Á Horni, J., Péron-Pinvidic, G. and Abdelmalak, M.M. (2017). Seismic volcanostratigraphy of the NE Greenland continental margin. *Geological Society of London, Special Publications*, **447**. doi:10.1144/SP447.11
- Geodekyan, A.A., Verkhovskaya, Z.I., Sudyin, A.V. and Trotsiuk, V.Ya. (1980). *Gases in Seawater and Bottom Sediments*. In: Udintsev, C.B. (ed) 1980. *Iceland and Mid-Oceanic Ridge – Structure of the ocean-floor*. Academy of Science of the USSR, soviet geophysical committee, report: results of researches on the international geophysical projects., 19-36.
- Gernigon, L., Franke, D., Geoffroy, L., Schiffer, C., Foulger, G.R. and Stoker, M. (2019). Crustal fragmentation, magmatism, and the diachronous opening of the Norwegian-Greenland Sea. *Earth-Science Reviews*. doi:10.1016/j.earscirev.2019.04.011
- Gernigon, L., Blischke, A., Nasuti, A., and Sand, M. (2015). Conjugate volcanic rifted margins, seafloor spreading, and microcontinent: Insights from new high-resolution aeromagnetic surveys in the Norway Basin. *Tectonics*, **34**, 907-933. doi:10.1002/2014TC003717
- Gernigon, L., Gaina, C., Olesen, O., Ball, P., Peron-Pinvidic, G. and Yamasaki, T. (2012). The Norway Basin revisited: From continental breakup to spreading ridge extinction. *Marine and Petroleum Geology*, **35**(1), 1-19. <https://doi.org/10.1016/j.marpetgeo.2012.02.015>
- Govindaraju, K. and Mevelle, G. (1987). Fully Automated Dissolution and Separation Methods for Inductively Coupled Plasma Atomic Emission Spectrometry Rock Analysis. Application to the Determination of Rare Earth Elements. *Journal of Analytical Atomic Spectrometry*, **2**, 615-621. doi:10.1039/ja9870200615
- Gradstein, F.M., Ogg, J.G., Schmitz, M.D. and Ogg, G.M. (2012). *The Geologic Time Scale 2012*, Elsevier Science Limited, Amsterdam, The Netherlands, ISBN 9780444594259.
- Grønlie, G., Chapman, M. and Talwani, M. (1979). Jan Mayen Ridge and Iceland Plateau: origin and evolution. *Norsk Polarinstitutt Skrifter*, **170**(23), 47.
- Grönvold, K. and Mäkipää (1978). *Chemical composition of Krafla lavas 1975-1977*. Nordic volcanological institute, University of Iceland, report 78, 16.
- Guarnieri, P. (2015). Pre-breakup palaeo-stress state along the East Greenland margin. *Journal of the Geological Society of London*, **172**(6). doi:10.1144/jgs2015-053
- Gunnarsson, K., Sand, M. and Gudlaugsson, S.T. (1989). *Geology and Hydrocarbon Potential of the Jan Mayen Ridge*. Orkustofnun, report OS-98014, 143, Reykjavík, Norwegian Petroleum Directorate, report OD-89-91, Stavanger.

- Gudlaugsson, S.T., Gunnarsson, K., Sand, M. and Skogseid, J. (1988). Tectonic and volcanic events at the Jan Mayen Ridge microcontinent. In Morton, A.C. and Parson, L.M. (eds.), 1988, Early Tertiary volcanism and the opening of the NE Atlantic, *Geological Society of London, Special Publication*, **39**, 85–93.
- Haase, C. and Ebbing, J. (2014). *Gravity data*. In: Hopper, J.R., Funck, T., Stoker, M.S., Ártur, U., Peron-Pinvidic, G., Doornenbal, H. and Gaina, C. (eds.) *Tectonostratigraphic Atlas of the North-East Atlantic Region*. Geological Survey of Denmark and Greenland (GEUS), Copenhagen, Denmark, ISBN 9781786202789.
- Halldórsson, S.A., Oskarsson, N., Gronvold, K., Sigurdsson, G., Sverrisdóttir, G. and Steinthorsson, S. (2008). Isotopic-heterogeneity of the Thjorsa lava—implications for mantle sources and crustal processes within the Eastern Rift Zone, Iceland. *Chemical Geology*, **255**(3-4), 305-316. doi:10.1016/j.chemgeo.2008.06.050
- Hansen, H. and Nielsen, T.F.D. (1999). Crustal contamination in Palaeogene East Greenland flood basalts: plumbing system evolution during continental rifting. *Chemical Geology*, **157**(1–2), 89-118. doi: 10.1016/S0009-2541(98)00196-X
- Harðarson, B.S., Fitton, J.G. and Hjartarson, Á. (2008). Tertiary volcanism in Iceland. *Jökull*, **58**, 161–178.
- Harðarson, B.S., Fitton, J.G., Ellam, R.M. and Pringle, M.S. (1997). Rift relocation – a geochemical and geochronological investigation of a palaeo-rift in northwest Iceland. *Earth and Planetary Science Letters*, **153**, 181–196. [https://doi.org/10.1016/S0012-821X\(97\)00145-3](https://doi.org/10.1016/S0012-821X(97)00145-3)
- Heinz, J. and Aigner, T. (2003). Hierarchical dynamic stratigraphy in various Quaternary gravel deposits, Rhine glacier area (SW Germany): Implications for hydrostratigraphy. *International Journal of Earth Sciences*, **92**, 923-938. doi:10.1007/s00531-003-0359-2
- Helgadóttir, G. (2008). *Preliminary results from the 2008 Marine Research Institute multibeam survey in the Dreki area, with some examples of potential use*. Iceland Exploration Conference 2008, Reykjavik, Iceland.
- Helgadóttir, G. and Reynisson, P. (2010). Setkjarnataka, fjölgeisla- og lágtíðni dýptarmælingar á Drekasvæði og Jan Mayen hrygg á rs. Árna Friðrikssyni RE 200 haustið 2010. Hafrannsóknastofnunin, Leiðangursskýrsla A201011, Reykjavík, Ísland.
- Henriksen, N. (2008). *Geological History of Greenland – Four billion years of Earth evolution*. Geological Survey of Denmark and Greenland (GEUS), 272 p, ISBN 978-87-7871-211-0.
- Hinz, K. (1981). An hypothesis on terrestrial catastrophes wedges of very thick oceanward dipping layers beneath passive continental margins; their origin and palaeo-environmental significance. *Geologisches Jahrbuch*, **E22**, 3-28.
- Hinz, K., and Schlüter, H. U. (1978). The North Atlantic - results of geophysical investigations by the Federal Institute for Geosciences and Natural Resources on North Atlantic continental margins. *Erdoel-Erdgas-Zeitschrift*, **94**, 271–280.
- Hjartarson, A., Erlendsson, Ö. and Blischke, A. (2017). The Greenland–Iceland–Faroe Ridge Complex. *Geological Society of London, Special Publications*, **447**. doi:10.1144/SP447.14.
- Hjartarson, A. and Sæmundsson, K. (2014). *Geological map of Iceland – Bedrock map, 1:600 000, Datum: ISN93*. © Iceland GeoSurvey. 1st edition, 2014.

- Hjelstuen, B.O., Eldholm, O. and Skogseid, J. (1999). Cenozoic evolution of the northern Vøring margin. *Geological Society of America Bulletin*, **111**(12), 1792-1807.
[https://doi.org/10.1130/0016-7606\(1999\)111<1792:CEOTNV>2.3.CO;2](https://doi.org/10.1130/0016-7606(1999)111<1792:CEOTNV>2.3.CO;2)
- Hjelstuen, B.O., Eldholm, O. and Skogseid, J. (1997). Vøring Plateau diapir fields and their structural and depositional settings. *Marine Geology*, **144**(1-3), 33-57.
doi:10.1016/s0025-3227(97)00085-6
- Holm, P.M. (1988). Nd, Sr and Pb isotope geochemistry of the Lower Lavas, E Greenland Tertiary Igneous Province, in Early Tertiary Volcanism and the Opening of the NE Atlantic. *Geological Society of London, Special Publication*, **39**, 181-195.
<https://doi.org/10.1144/GSL.SP.1988.039.01.17>
- Hopper, J.R., Funck, T., Stoker, M.S., Ártíng, U., Peron-Pinvidic, G., Doornenbal, H. and Gaina, C. (eds) (2014). *Tectonostratigraphic Atlas of the North-East Atlantic Region*. Geological Survey of Denmark and Greenland, GEUS, Copenhagen, ISBN 9781786202789.
- Hopper, J. R., Dahl-Jensen, T., Holbrook, W.S., Larsen, H.C., Lizarralde, D., Korenaga, J., Kent, G.M. and Kelemen, P. B. (2003). Structure of the SE Greenland margin from seismic reflection and refraction data: Implications for nascent spreading center subsidence and asymmetric crustal accretion during North Atlantic opening. *Journal of Geophysical Research*, **108**(B5), 2269. doi:10.1029/2002jb001996;2269;Artn 2269
- á Horni, J., Hopper, J.R., Blischke, A., Geissler, W., Judge, M., McDermott, K., Erlendsson, Ö., Stewart, M. and Ártíng, U. (2017). Regional Distribution of Volcanism within the North Atlantic Igneous Province. *Geological Society of London, Special Publications*, **447**, 18. doi:10.1144/SP447.18
- Hreinsdóttir, S., Einarsson, P., and Sigmundsson, F. (2001), Crustal deformation at the oblique spreading Reykjanes Peninsula, SW Iceland: GPS measurements from 1993 to 1998, *Journal of Geophysical Research*, **106**(B7), 13803-13816.
<https://doi.org/10.1029/2001JB000428>
- Jakobsson, M., Mayer, L.A., Coakley, B., Dowdeswell, J.A., Forbes, Fridman, S.B., Hodnesdal, H., Noormets, R., Pedersen, R., Rebecco, M., Schenke, H.-W., Zarayskaya, Y., Accettella, A.D., Armstrong, A., Anderson, R.M., Bienhoff, P., Camerlenghi, A., Church, I., Edwards, M., Gardner, J.V., Hall, J.K., Hell, B., Hestvik, O.B., Kristoffersen, Y., Marcussen, C., Mohammad, R., Mosher, D., Nghiem, S.V., Pedrosa, M.T., Travaglini, P.G. and Weatherall, P. (2012). The International Bathymetric Chart of the Arctic Ocean (IBCAO) Version 3.0, *Geophysical Research Letters*. doi: 10.1029/2012GL052219
- Jansen, E., Raymo, M.E., Blum, P. et al. (1996). *Proceedings of the Ocean Drilling Program, Initial Reports, 162*. Ocean Drilling Program, College Station, TX, U.S.A.. doi:10.2973/odp.proc.ir.162.1996
- Japsen, P., Green, P.F., Bonowa, J.M., Nielsen, T.F.D. and Chalmers, J.A. (2014). From volcanic plains to glaciated peaks: Burial, uplift and exhumation history of southern East Greenland after opening of the NE Atlantic. *Global and Planetary Change*, **116**, 91–114. doi:10.1016/j.gloplacha.2014.01.012
- Jerram, D.A., Single, R.T., Hobbs, R.W. and Nelson, C.E. (2009). Understanding the offshore flood basalt sequence using onshore volcanic facies analogues: an example from the Faroe-Shetland basin. *Geological Magazine*, **146**(3), 353-367.
doi:10.1017/S0016756809005974

- Johansson, L., Zahirovic, S. and Müller, R.D. (2018). The interplay between the eruption and weathering of Large Igneous Provinces and the deep-time carbon cycle. *Geophysical Research Letters*, **45**(11), 5380–5389. doi:10.1029/2017GL076691
- Johnson, G. L. and Heezen, B.C. (1967). The morphology and evolution of the Norwegian-Greenland Sea. *Deep Sea Research*, **14**, 755–771.
- Kandilarov, A., Mjelde, R., Pedersen, R.B., Hellevang, B., Papenberg, C., Petersen, C.J., Planert, L. and Flueh, E. (2012). The northern boundary of the Jan Mayen microcontinent, North Atlantic determined from ocean bottom seismic, multichannel seismic, and gravity data. *Marine Geophysical Research*, **33**(1), 55-76. doi:10.1007/s11001-012-9146-4
- Karcher, J. C. (1987). The reflection seismograph: its invention and use in the discovery of oil and gas fields. *The Leading Edge*, **6**(11), 10–19. <https://doi.org/10.1190/1.1439341>
- Karson, J. A., Brandsdóttir, B., Einarsson, P., Sæmundsson, K., Farrell, J. and Horst, A. (2019). Evolution of Migrating Transform Faults in Anisotropic Oceanic Crust: Examples from Iceland. *Canadian Journal of Earth Sciences*, **56**(12), 1297-1308. <https://doi.org/10.1139/cjes-2018-0260>
- Karson, J. A., Farrell, J. A., Chutas, L. A., Nanfíto, A. F., Proett, J. A. and Runnals, K. T. (2018). Rift-Parallel Strike-Slip Faulting Near the Iceland Plate Boundary Zone: Implications for Propagating Rifts. *Tectonics*, **37**, 4567–4594. <https://doi.org/10.1029/2018TC005206>
- Kearey, P. and Brooks, M. (1984). *An Introduction to Geophysical Exploration*. Blackwell Scientific Publications, 296 p, ISBN-10 0632010495.
- Kharin, G.N., Udintsev, G.B., Bogatikov, O.A., Dmitriev, J.I., Raschka, H., Kreuzer, H., Mohr, M., Harre, W. and Eckhardt, F.J., (1976). *K/AR ages of the basalts of the Norwegian-Greenland Sea DSDP Leg 38*. Ocean Drilling Program, College Station, TX, U.S.A. doi:10.2973/dsdp.proc.38.116.1976
- Kodaira, S., Mjelde, R., Gunnarsson, K., Shiobara, H. and Shimamura, H. (1998). Structure of the Jan Mayen microcontinent and implications for its evolution. *Geophysical Journal International*, **132**(2), 383-400. <https://doi.org/10.1046/j.1365-246x.1998.00444.x>
- Kuvaas, B., and S. Kodaira (1997). The formation of the Jan Mayen microcontinent: the missing piece in the continental puzzle between the Møre-Vøring basins and East Greenland. *First Break*, **15**(7), 239–247. doi:10.3997/1365-2397.1997008
- Larsen, H.C. (1990). *The East Greenland shelf*. In: Grant A., Johnson, L., and Sweeney, J.F., (eds.). *The Geology of North America, The Arctic Ocean Region.*, Vol. L, 185-210, Geol. Soc. America, Boulder, Colorado, USA.
- Larsen, H.C., and Jakobsdóttir, S. (1988). Distribution, crustal properties and significance of seawards-dipping sub-basement reflectors off East Greenland. In: Morton, A.C., and Parson, L.M., (eds.). Early Tertiary Volcanism and the Opening of the Northeast Atlantic. *Geological Society of London Special Publication*, **39**, 95-114. doi:10.1144/GSL.SP.1988.039.01.10
- Larsen, L.M., Pedersen, A.K., Tegner, T. and Duncan, R.A. (2014). Eocene to Miocene igneous activity in NE Greenland: northward younging of magmatism along the East Greenland margin. *Journal of the Geological Society*, **171**(4), 539-553. doi:10.1144/jgs2013-118

- Larsen, L.M., Pedersen, A.K., Sørensen, E.V., Watt, W.S. and Duncan, R.A. (2013). Stratigraphy and age of the Eocene Igertivâ Formation basalts, alkaline pebbles and sediments of the Kap Dalton Group in the graben at Kap Dalton, East Greenland. *Bulletin of the Geological Society of Denmark*, **61**, 1-18. <http://hdl.handle.net/1957/42801>
- Larsen, L.M., Waagstein, R., Pedersen, A.K. and Storey, M. (1999). Trans-Atlantic correlation of the Palaeogene volcanic successions in the Faeroe Islands and East Greenland. *Journal of the Geophysical Society*, **156**(6), 1081-1095. doi:<https://doi.org/10.1144/gsjgs.156.6.1081>
- Larsen, L.M., Watt, SW. and Watt, M. (1989). Geology and petrology of the Lower Tertiary plateau basalts of the Scoresby Sund region, east Greenland. *Bulletin (Grønlands geologiske undersøgelse)*, **157**, 164.
- Larsen, L.M. and Watt, W.S. (1985). Episodic volcanism during break-up of the North Atlantic: evidence from the East Greenland plateau basalts. *Earth and Planetary Science Letters*, **73**(1), 105-116. doi:10.1016/0012-821X(85)90038-X
- Larsen, M., Heilmann-Clausen, C., Piasecki, S. and Stemmerik, L. (2005). *At the edge of a new ocean: post-volcanic evolution of the Palaeogene Kap Dalton Group, East Greenland*, in *Petroleum Geology: North-West Europe and Global Perspectives*. Geological Society of London, proceedings of the 6th Petroleum Geology Conference. doi: 10.1144/0060923
- Larsen, M., Piasecki, S. and Stemmerik, L. (2002). The post-basaltic Palaeogene and Neogene sediments at Kap Dalton and Savoia Halvø, East Greenland. *Geology of Greenland Survey Bulletin*, **191**, 103-110.
- Larsen, M., Hamberg, L., Olaussen, S., Preuss, T. and Stemmerik, L. (1999). *Sandstone wedges of the Cretaceous-Lower Tertiary Kangerlussuaq Basin, East Greenland - outcrop analogues to the offshore North Atlantic*. In: Fleet, A.J. and Boldy, S.A.R. (eds) *Petroleum Geology of Northwest Europe*. Geological Society, London, proceedings of the 5th Petroleum Geology Conference.
- Le Breton, E., Cobbold, P.R. and Zanella, A. (2013). Cenozoic reactivation of the Great Glen Fault, Scotland: additional evidence and possible causes. *Journal of the Geological Society*, **170**, 403-415. doi:10.1144/jgs2012-067
- Lundin, E.R., Doré, A.G., Rønning, K. and Kyrkjebø, R. (2013). Repeated inversion and collapse in the Late Cretaceous–Cenozoic northern Vøring Basin, offshore Norway. *Petroleum Geoscience*, **19**, 329-341. doi:10.1144/petgeo2012-022
- Lundin, E.R. and Doré, A.G. (2005). *NE Atlantic breakup: a re-examination of the Iceland mantle plume model and the Atlantic–Arctic linkage*. In: Doré, A.G. and Vining, B.A. (eds) *Petroleum Geology: North-West Europe and Global Perspectives*. Geological Society, London, proceedings of the 6th Petroleum Geology Conference.
- Lundin, E. and Doré, A.G. (2002). Mid-Cenozoic post-breakup deformation in the ‘passive’ margins bordering the Norwegian-Greenland Sea. *Marine and Petroleum Geology*, **19**, 79–93. [https://doi.org/10.1016/S0264-8172\(01\)00046-0](https://doi.org/10.1016/S0264-8172(01)00046-0)
- Manum S.B., Raschka H., Eckhardt F.J., Schrader, H., Talwani, M. and Udintsev, G., e.a. (eds) (1976c). *Site 337 Initial Reports of the Deep Sea Drilling Project*. In: Talwani, M., Udintsev, G., et al. 1976. *Initial Reports of the Deep Sea Drilling Project*. Washington, U.S. Government Printing Office, Volume 38, 117-150.

- Manum, S.B. and Schrader, H.J. (1976b). *Sites 346, 347, and 349*. In: Talwani, M. and Udintsev, G. (eds). *Initial Reports of the Deep Sea Drilling Project*. Washington, U.S. Government Printing Office, Volume 38, 521-594.
- Manum, S.B., Raschka, H. and Eckhardt, F.J. (1976a). *Site 350*. In: Talwani, M. and Udintsev, G. (eds). *Initial Reports of the Deep Sea Drilling Project*. Washington, U.S. Government Printing Office.
- Matthews, K.J., Maloney, K.T., Zahirovic, S., Williams, S.E., Seton, M. and Müller, R.D. (2016). Global plate boundary evolution and kinematics since the late Paleozoic. *Global and Planetary Change*, **146**, 226-250. doi:10.1016/j.gloplacha.2016.10.002
- Mathiesen A., Bidstrup T. and Christinsen F.G. (2000). Denudation and uplift history of the Jameson Land Basin, East Greenland-constrained from maturity and apatite fission track data. *Global and Planetary Change*, **24**, 275-301.
- Meyer, R., Hertogen, J., Pedersen, R. B., Viereck-Götte, L. and Abratis, M. (2009). Interaction of mantle derived melts with crust during the emplacement of the Vøring Plateau, N.E. Atlantic. *Marine Geology*, **261**(1-4), 3-16. <https://doi.org/10.1016/j.margeo.2009.02.007>
- Miller, K.G., Browning, J.V., Aubry, M.-P., Wade, B.S., Katz, M.E., Kulpecz, A.A. and Wright, J.D. (2008). Eocene–Oligocene global climate and sea-level changes: St. Stephens Quarry, Alabama. *Geological Society of America Bulletin*, **120**(1-2), 34–53. doi:10.1130/B26105.1
- Mitchum, RM, Vail, PR and Sangree, JB. (1977). *Seismic stratigraphy and global changes of sea level, part 6: stratigraphic interpretation of seismic reflection patterns in depositional sequences*. In: Payton, CE (Ed): *Seismic Stratigraphy – Applications to Hydrocarbon Exploration*. American Association of Petroleum Geologists, Memoir 26, 117 – 133.
- Mjelde, R., Kvarven, T., Faleide, J.I. and Thybo, H. (2016). Lower crustal high-velocity bodies along North Atlantic passive margins, and their link to Caledonian suture zone eclogites and Early Cenozoic magmatism. *Tectonophysics*, **670**(2016) 16–29. doi:10.1016/j.tecto.2015.11.021
- Mjelde, R., Raum, T., Breivik, A.J., Faleide, J.I. (2008). Crustal transect across the North Atlantic. *Marine Geophysical Research*, **29**, 73–87. doi:10.1007/s11001-008-9046-9
- Mjelde, R., Aurvåg, R., Kodaira, S., Shimamura, H., Gunnarsson, K., Nakanishi, A. and Shiobara, H. (2002). Vp/Vs-ratios from the central Kolbeinsey Ridge to the Jan Mayen Basin, North Atlantic; implications for lithology, porosity and present-day stress field. *Marine Geophysical Researches*, **23**(2), 123-145. doi:10.1023/A:1022439707307
- Mordret, A. (2018). Uncovering the Iceland hot spot track beneath Greenland. *Journal of Geophysical Research, Solid Earth*, **123**, 4922– 4941. doi:10.1029/2017JB015104
- Momme, P., Tegner, C., Brooks, K. and Keays, R. (2002). The behaviour of platinum-group elements in basalts from the East Greenland rifted margin. *Contributions to Mineralogy and Petrology*, **143**(2), 133-153. doi:10.1007/s00410-001-0338-1
- Murray-Wallace, C., and Woodroffe, C. (2014). *Pleistocene sea-level changes*. In: *Quaternary Sea-Level Changes: A Global Perspective*. Cambridge: Cambridge University Press, (256-319). doi:10.1017/CBO9781139024440.007
- Murton, B. J. and Parson, L. M. (1993). Segmentation, volcanism and deformation of oblique spreading centres: A quantitative study of the Reykjanes Ridge. *Tectonophysics* **222**, 237–257. [https://doi.org/10.1016/0040-1951\(93\)90051-K](https://doi.org/10.1016/0040-1951(93)90051-K)

- Mutter, J.C., Talwani, M. and Stoffa, P.L. (1982). Origin of seaward-dipping reflectors in oceanic crust off the Norwegian margin by "subaerial sea-floor spreading". *Geology*, **10**, 3-12. [https://doi.org/10.1130/0091-7613\(1982\)10<353:OOSRIO>2.0.CO;2](https://doi.org/10.1130/0091-7613(1982)10<353:OOSRIO>2.0.CO;2)
- Müller, R.D., Seton, M., Zahirovic, S., Williams, S.E., Matthews, K.J., Wright, N.M., Shephard, G.E., Maloney, K.T., Barnett-Moore, N., Hosseinpour, M., Bower, D.J. and Cannon, J. (2016). Ocean Basin Evolution and Global-Scale Plate Reorganization Events Since Pangea Breakup. *Annual Review of Earth and Planetary Sciences*, **44**, pp. 107. doi:10.1146/annurev-earth-060115-012211
- Müller, D., Gaina, C., Roest, W. and Egholm, D. (2001). A recipe for microcontinent formation. *Geology*, **29**. 203-206. doi:10.1130/0091-7613(2001)029<0203:ARFMF>2.0.CO;2.
- Myhre, A. M., O. Eldholm and E. Sundvor (1984). The Jan Mayen Ridge; present status. *Polar Research*, **2**(1), 47–59. <https://doi.org/10.3402/polar.v2i1.6961>
- Nasuti, A. and Olesen, O. (2014). *Magnetic Data*. In: Hopper, J.R., Funck, T., Stoker, M.S., Árting, U., Peron-Pinvidic, G., Doornenbal, H., Gaina, C. (Eds.), *Tectonostratigraphic Atlas of the North-East Atlantic Region*. Geological Survey of Denmark and Greenland (GEUS), Copenhagen, Denmark, ISBN 9781786202789.
- Nemčok, M., Sinha, S., Dore, A.G., Lundin, E. and Rybár, S. (2016). Mechanisms of microcontinent release associated with wrenching-involved continental break-up; a review. *Geological Society London Special Publications*. **431**. 10.1144/SP431.14.
- Nielsen, T.F.D. and Brooks, C.K. (1981). The E Greenland rifted continental margin: an examination of the coastal flexure. *Journal of the Geological Society*, **138**(5):559. <http://dx.doi.org/10.1144/gsjgs.138.5.0559>
- Nielsen, T.F.D., Turkov, V.A., Solovova, I.P., Kogarko, L.N. and Ryabchikov, I.D. (2006). A Hawaiian beginning for the Iceland plume: Modelling of reconnaissance data for olivine-hosted melt inclusions in Palaeogene picrite lavas from East Greenland. *Lithos*, **92**(1–2), 83-104. doi:10.1016/j.lithos.2006.03.038
- Nilsen, T.H., Kerr, D.R., Talwani, M. and Udintsev, G. e.a. (eds) (1978). *Turbidites, redbeds, sedimentary structures, and trace fossils observed in DSDP Leg 38 cores and the sedimentary history of the Norwegian-Greenland Sea Initial Reports of the Deep Sea Drilling Project*. Washington (U.S. Government Printing Office), Supplement to Volume 38, 259-288.
- Norwegian Petroleum Directorate (2012). *Submarine fieldwork on the Jan Mayen Ridge: integrated seismic and ROV-sampling*. Norwegian Petroleum Directorate, Stavanger, Norway, <http://www.npd.no/en/Publications/Resource-Reports/2013/Chapter-7/>.
- Norwegian Petroleum Directorate (2013). *The Petroleum Resources on the Norwegian Continental Shelf*. Norwegian Petroleum Directorate, Stavanger, Norway, <http://www.npd.no/en/Publications/Resource-Reports/2013/>.
- Nunns, A. (1982). *The structure and evolution of the Jan Mayen Ridge and surroundings regions*. In: Watkins, J.S. and Drake, C.L. (eds). *Studies in Continental Margin Geology*. American Association of Petroleum Geologists, memoir, 193-208.
- Nunns, A.G., Talwani, M., Lorentzen, G.N., Vogt, P.R., Sigurgeirsson, T., Kristjánsson, L., Larsen, H.C. and Voppel, D. (1983a). *Magnetic anomalies over Iceland and surrounding seas, in Structure and Development of the Greenland-Scotland Ridge*. Edited by Bott, M.H.P., Saxov, S., Talwani, M. and Thiede, J., *Plenum*, 661-678.

- Nunns A.G. (1983b). *Plate Tectonic Evolution of the Greenland-Scotland Ridge and Surrounding Regions*. In: Bott M.H.P., Saxov S., Talwani M., Thiede J. (eds). *Structure and Development of the Greenland-Scotland Ridge*. Nato Conference Series (IV Marine Science), vol 8. Springer, Boston, MA. https://doi.org/10.1007/978-1-4613-3485-9_2
- Ólafsson, I. and Gunnarsson, K. (1989). *The Jan Mayen ridge: velocity structure from analysis of sonobuoy data*. Orkustofnun, Reykjavík, report OS-89030/JHD-04.
- Ólavsdóttir, J, Stoker, M.S., Boldreel, L.O., Andersen, M.S., Eidesgaard, Ó.R. (2019). Seismic-stratigraphic constraints on the age of the Faroe Islands Basalt Group, Faroe–Shetland region, Northeast Atlantic Ocean. *Basin Research*, **31**(5), 841-865. doi:10.1111/bre.12348
- Ólavsdóttir, J., Eidesgaard, Ó.R., and Stoker, M.S. (2017). The stratigraphy and structure of the Faroese continental margin. *Geological Society of London, Special Publications*, **447**, 339-356. doi:10.1144/SP447.4
- Ólavsdóttir, J., Andersen, M.S. and Boldreel, L.O. (2013). Seismic stratigraphic analysis of the Cenozoic sediments in the NW Faroe Shetland Basin - Implications for inherited structural control of sediment distribution. *Marine and Petroleum Geology*, **46**, 19-35. doi:10.1016/j.marpetgeo.2013.05.012
- Osmundsen, P.T. and Ebbing, J. (2008). Styles of extension offshore mid-Norway and implications for mechanisms of crustal thinning at passive margins. *Tectonics*, **27**(6), TC6016. <https://doi.org/10.1029/2007TC002242>
- Osmundsen, P.T., Sommaruga, A., Skilbrei, J.R. and Olesen, O. (2002). Deep structure of the Mid Norway rifted margin. *Norwegian Journal of Geology*, **82**(4), 205-224, ISSN 029-196X.
- Osmundsen, P.T. and Andersen, T.B. (2001). The middle Devonian basins of western Norway: sedimentary response to large-scale transtensional tectonics. *Tectonophysics*, **332**(1-2), 51-68. [https://doi.org/10.1016/S0040-1951\(00\)00249-3](https://doi.org/10.1016/S0040-1951(00)00249-3)
- Owen, D.E. (1987). Commentary: usage of stratigraphic terminology in papers, illustrations and talks. *Journal of Sedimentary Petrology*, **57**, 363–372.
- Parsons, A.J., Whitham, A.G., Kelly, S.R.A., Vautravers, B.P.H, Dalton, T.J.S., Andrews, S.D., Pickles, C.S., Strogon, D.P., Braham, W., Jolley, D.W. and Gregory, F.J. (2017). Structural evolution and basin architecture of the Traill Ø region, NE Greenland: A record of polyphase rifting of the East Greenland continental margin: *Geosphere*, **13**(3). 1–38. doi:10.1130/GES01382.1
- Parson, L., Viereck, L., Love, D., Gibson, I., Morton, A. and Hertogen, J. (1989). *The petrology of the lower series volcanics, ODP Site 642*. In: Eldholm, O., Thiede, J., Taylor, E., et al., *Proc. ODP, Scientific Results, 104*, Ocean Drilling Program, College Station, TX, 419–428. doi:10.2973/odp.proc.sr.104.134.1989
- Passey, S.R., and Hitchen, K. (2011). *Cenozoic (igneous)*. In: Ritchie, J.D., Ziska, H., Johnson, H., and Evans, D. (eds). *Geology of the Faroe-Shetland Basin and Adjacent Areas*. BGS Research Report, RR/11/01, Jarðfeingi Research Report, RR/11/01, 209-228, ISBN 978 085272 6433.
- Passey, S.R., and Jolley, D.W. (2009). A revised lithostratigraphic nomenclature for the Palaeogene Faroe Islands Basalt Group, NE Atlantic Ocean. *Earth and Environmental Science Transactions of the Royal Society of Edinburgh*, **99**(3-4), 127-158. <https://doi.org/10.1017/S1755691009008044>

- Passey, S.R. (2009). *Recognition of a faulted basalt lava flow sequence through the correlation of stratigraphic marker units, Skopunarfjørður, Faroe Islands*. In: Varming, T. and Ziska, H. (eds.) *Faroe Islands Exploration Conference: Proceedings of the 2nd Conference*. Annales Societatis Scientiarum Færoensis, Tórshavn, 174-204.
- Passey, S.R. and Bell, B.R. (2007). Morphologies and emplacement mechanisms of the lava flows of the Faroe Islands basalt group, Faroe Islands, NE Atlantic Ocean. *Bulletin of Volcanology*, **70**, 139-156. doi:10.1007/s00445-007-0125-6
- Peate, D.W., Baker, J.A., Blichert-Toft, J., Hilton, D.R., Storey, M., Kent, A.J.R., Brooks, C.K., Hansen, H., Pedersen, A.K. and Duncan R.A. (2003). The Prinsen af Wales Bjerre Formation Lavas, East Greenland: the Transition from Tholeiitic to Alkalic Magmatism during Palaeogene Continental Break-up. *Journal of Petrology*, **44**(2), 279-304. doi:10.1093/petrology/44.2.279
- Pedersen, A.K., Watt, M., Watt, W.S. and Larsen L.M. (1997). Structure and stratigraphy of the Early Tertiary basalts of the Blossesville Kyst, East Greenland. *Journal of the Geological Society, London*, **154**, 565-570. <https://doi.org/10.1144/gsjgs.154.3.0565>
- Peron-Pinvidic, G., Manatschal, G. and Osmundsen, P.T. (2013). Structural comparison of archetypal Atlantic rifted margins: A review of observations and concepts. *Marine and petroleum geology*, **43**, 21-47. doi:10.1016/j.marpetgeo.2013.02.002
- Peron-Pinvidic, G., Gernigon, L., Gaina, C. and Ball, P. (2012a). Insights from the Jan Mayen system in the Norwegian-Greenland Sea - I: mapping of a microcontinent. *Geophysical Journal International*, **191**(2), 385-412. <https://doi.org/10.1111/j.1365-246X.2012.05639.x>
- Peron-Pinvidic, G., Gernigon, L., Gaina, C. and Ball, P. (2012b). Insights from the Jan Mayen system in the Norwegian-Greenland Sea - II: architecture of a microcontinent. *Geophysical Journal International*, **191**(2), 413-435. <https://doi.org/10.1111/j.1365-246X.2012.05623.x>
- Planke, S., T. Rasmussen, S. S. Rey, and R. Myklebust (2005). *Seismic characteristics and distribution of volcanic intrusions and hydrothermal vent complexes in the Vøring and Møre basins*. In: *Petroleum Geology: North-West Europe and Global Perspectives*. Geological Society of London, proceedings of the 6th Petroleum Geology Conference, 833-844.
- Planke, S., Symonds, P.A., Alvestad, E. and Skogseid, J. (2000). Seismic volcanostratigraphy of large-volume basaltic extrusive complexes on rifted margins. *Journal of Geophysical Research, Solid Earth*, **105**(B8), 19335-19351. <https://doi.org/10.1029/1999JB900005>
- Planke, S. and Eldholm, O. (1994). Seismic response and construction of seaward dipping wedges of flood basalts: Vøring volcanic margin. *Journal of Geophysical Research, Solid Earth*, **99**(B5), 9263-9278. doi: 10.1029/94JB00468
- Polteau, S., Mazzini, A., Hansen, G., Planke, S., Jerram, D.A., Millett, J., Abdelmalak, M.M., Blischke, A. and Myklebust, R. (2018). The pre-breakup stratigraphy and petroleum system of the Southern Jan Mayen Ridge revealed by seafloor sampling. *Tectonophysics*, **760**, 152-164. doi:10.1016/j.tecto.2018.04.016
- Raschka, H., Eckhardt, F.J. and Manum, S.B. (1976). *Site 348*. In: Talwani, M. and Udintsev, G. (eds). *Initial Reports of the Deep Sea Drilling Project*. U.S. Government Printing Office, Washington, 595-654.
- Rasmussen, J. and Noe-Nygaard, A. (1970). *Geology of the Faroe Islands (Pre-Quaternary)*. Trans: Henderson G. Geological Survey of Denmark, Copenhagen.

- Rasmussen, J. and Noe-Nygaard, A. (1969). *Beskrivelse til Geologisk Kort over Færøerne i målestok 1:50.000*. C. A. Reitzels Forlag (Jørgen Sandal), København.
- Rey, S.S., Eldholm, O. and Planke, S. (2003). Formation of the Jan Mayen Microcontinent, the Norwegian Sea. *Earth & Space Science News, Transactions of the American Geophysical Union*, **84**, Abstract T31D-0872.
- Ritchie, D.K., Ziska, H., Johnson, H. and Evans, D. (2011). *Geology of the Faroe-Shetland Basin and adjacent areas*. British Geological Survey, research report, RR/11/01, Jarðfeing research report, RR/11/01, ISBN 978 085272 6433.
- Sæmundsson, K. (1979). Outline of the geology of Iceland. *Jökull*, **29**, 7–28.
- Sandstå, N.R., Pedersen, R.B., Williams, R.D., Bering, D., Magnus, C., Sand, M. and Brekke, H. (2012). *Submarine fieldwork on the Jan Mayen Ridge; integrated seismic and ROV-sampling*. Edited Norwegian Petroleum Directorate, <http://www.npd.no/>.
- Saunders, A.D., Fitton, J.G., Kerr, A.C., Norry, M.J. and Kent, R.W. (1997). *The North Atlantic Igneous Province*. In: Mahoney, J.J. and Coffin, M.F. (eds). *Large Igneous Provinces: Continental, Oceanic, and Planetary Flood Volcanism*, American Geophysical Union, Geophysical Monographs, Volume 100, 381-410, ISBN:9780875900827. <https://doi.org/10.1029/GM100p0045>
- Scott, R.A., Ramsey, L.A., Jones, S.M., Sinclair, S. and Pickles, C.S. (2005). *Development of the Jan Mayen microcontinent by linked propagation and retreat of spreading ridges*. In: Wandås, B.T.G., Nystuen, J.P., Eide, E. and Gradstein, F. (eds). *Onshore–Offshore Relationships on the North Atlantic Margin*. Norwegian Petroleum Society, 69-82.
- Seidler, L., Steel, R.J., Stemmerik, L., and Surlyk, F. (2004). North Atlantic marine rifting in the Early Triassic: new evidence from East Greenland. *Journal of the Geological Society*, **161**(4), 583–592. doi:10.1144/0016-764903-063
- Self, S., Thordarson, T. and Keszthelyi, L. (1997). *Emplacement of continental flood basalt lava flows, in Large Igneous Provinces: Continental, Oceanic, and Planetary Flood Volcanism*. In: Mahoney, J.J. and Coffin, M.F. (eds). *Large Igneous Provinces: Continental, Oceanic, and Planetary Flood Volcanism*, American Geophysical Union, Geophysical Monographs, Volume 100, 381-410, ISBN:9780875900827. <https://doi.org/10.1029/GM100p0381>
- Skogseid, J., Planke, S., Faleide, J.I., Pedersen, T., Eldholm, O. and Neverdal, F. (2000). NE Atlantic continental rifting and volcanic margin formation. *Geological Society, London, Special Publications*, **167**(1), 295–326. doi:10.1144/GSL.SP.2000.167.01.12
- Skogseid, J. and Eldholm, O. (1987). Early Cenozoic Crust at the Norwegian Continental Margin and the Conjugate Jan Mayen Ridge. *Journal of Geophysical Research-Solid Earth and Planets*, **92**(B11), 11.471-11.491.
- Smallwood, J. R., and J. Maresh (2002). The properties, morphology and distribution of igneous sills: modelling, borehole data and 3D seismic from the Faroe-Shetland area, in The North Atlantic Igneous Province: Stratigraphy, Tectonic, Volcanic and Magmatic Processes. *Geological Society of London, Special Publication*, **197**(1), 271-306. doi:10.1144/GSL.SP.2002.197.01.11
- Smallwood, J.R., Towns, M.J. and White, R.S. (2001). The structure of the Faeroe-Shetland Trough from integrated deep seismic and potential field modelling, *Journal of the Geological Society*, **158**(3), 409-412. doi:10.1144/jgs.158.3.409
- Srivastava, S.P. and Tapscott, C.R. (1986). *Plate kinematics of the North Atlantic*. (V.P.R. & B.E. Tucholke, Eds.). The Geological Society of America, 379-405.

- Stärz, M., Jokat, W., Knorr, G. and Lohmann, G. (2017). Threshold in North Atlantic-Arctic Ocean circulation controlled by the subsidence of the Greenland-Scotland Ridge. *Nature Communications*, **8**, 15681. doi:10.1038/ncomms15681
- Stemmerik, L., Christiansen, F.G., Piasecki, S., Jordt, B., Marcussen, C., and Nøhr-Hansen, H. (1993). Depositional history and petroleum geology of the Carboniferous to Cretaceous sediments in the northern part of East Greenland. *Norwegian Petroleum Society Special Publications*, **2**, 67-87. doi:10.1016/B978-0-444-88943-0.50009-5
- Stoker, M.S., Holford, S.P. and Hillis, R.R. (2018). A rift-to-drift record of vertical crustal motions in the Faroe–Shetland Basin, NW European margin: establishing constraints on NE Atlantic evolution. *Journal of the Geological Society*, **175**, 263-274. doi:10.1144/jgs2017-076
- Stoker, M.S., Stewart, M.A., Shannon, P. M., Bjerager, M., Nielsen, T., Blischke, A., Hjelstuen, B.O., Gaina, C., McDermott, K. and Ólavsdóttir, J. (2016). An overview of the Upper Palaeozoic–Mesozoic stratigraphy of the NE Atlantic region. *Geological Society, London, Special Publications*, **447**. doi:10.1144/SP447.2
- Stoker, M.S., Leslie, A.B. and K. Smith, K. (2013). A record of Eocene (Stronsay Group) sedimentation in BGS borehole 99/3, offshore NW Britain: Implications for early post-break-up development of the Faroe–Shetland Basin. *Scottish Journal of Geology*, **49**(2), 133–148. doi:10.1144/sjg2013-001
- Stoker, M.S., Praeg, D., Hjelstuen, J.S., Laberg, J.S., Nielsen, T., and Shannon, P.M., (2005b). Neogene stratigraphy and the sedimentary and oceanographic development of the NW European Atlantic margin. *Marine and Petroleum Geology*, **22**(9), 977–1005. doi:10.1016/j.marpetgeo.2004.11.007
- Stoker, M.S., Hout, R.J., Nielsen, T., Hjelstuen, J.S., Laberg, J.S., Shannon, P.M., Praeg, D., Mathiesen, A., van Weering, T.C.E. and McDonnell, A.M. (2005a). Sedimentary and oceanographic responses to early Neogene compression on the NW European margin. *Marine and Petroleum Geology*, **22**(9), 1031–1044. doi:10.1016/j.marpetgeo.2005.01.009
- Storey, M., Duncan, R. and Tegner, C. (2007). Timing and duration of volcanism in the North Atlantic Igneous Province: Implications for geodynamics and links to the Iceland hotspot. *Chemical Geology*, **241**(3-4), 264-281. doi:10.1016/j.chemgeo.2007.01.016
- Storey, M., Pedersen, A.K., Stecher, O., Bernstein, S., Larsen, H.C., Larsen, L.M., Baker, J.A. and Duncan, R.A. (2004). Long-lived postbreakup magmatism along the East Greenland margin; evidence for shallow-mantle metasomatism by the Iceland Plum. *Geology*, **32**(2), 173-176. doi: 10.1130/g19889.1
- Surlyk, F. (2003). *The Jurassic of East Greenland: a sedimentary record of thermal subsidence, onset and culmination of rifting*. In: Ineson, J.R. and Surlyk, F. (eds). The Jurassic of Denmark and Greenland. *Geological Survey of Denmark and Greenland Bulletin*, **1**, 659-722.
- Surlyk, F. (1990). *Timing, style and sedimentary evolution of Late Paleozoic-Mesozoic extensional basins of East Greenland*. In: Hardman, R.F.P. and Brooks, J. (eds). Tectonic events responsible for Britain's oil and gas reserves. *Geological Society, London, Special Publications*, **55**, 107-25.
- Svellingen, W. and Pedersen, R. (2003). Jan Mayen: A result of ridge-transform-micro-continent interaction. *Geophysical Research Abstracts*, **5**, 12993.

- Symonds, P.A., Planke, S., Frey, Ø. and Skogseid, J. (1998). *Volcanic evolution of the western Australian continental margin and its implications for basin development*. In: Purcell, R.R. (ed), *The Sedimentary Basins of Western Australia*, 33-54, Perth.
- Talwani, M., Mutter, J. and Eldholm, O. (1981). The Initiation of Opening of the Norwegian Sea. *Oceanologica Acta*, SP, 23-30.
- Talwani, M., Udintsev, G., Mirlin, E., Beresnev, A.F., Kanayev, V.F., Chapman, M., Groenlie, G. and Eldholm, O. (1978). Survey at sites 346, 347, 348, 349, and 350, the area of the Jan-Mayen Ridge and the Icelandic Plateau. Initial Reports of the Deep Sea Drilling Project. doi:10.2973/dsdp.proc.38394041s.127.1978
- Talwani, M. and Eldholm, O. (1977). Evolution of the Norwegian-Greenland Sea. *Geological Society of America Bulletin*, **88**, 969-999.
- Talwani, M., Udintsev, G.B., Bjoerklund, K., Caston, V.N.D., Faas, R. W., van Hinte, J.E., Kharin, G.N., Morris, D.A., Mueller, C., Nilsen, T.H., Warnke, D.A., White, S.M., Manum, S.B. and Schrader, H.-J. (1976j). Sites 336 and 352. Initial Reports of the Deep Sea Drilling Project, Vol.38, 595-654. Publisher: Texas A & M University, Ocean Drilling Program, College Station, TX, United States. ISSN: 0080-8334 CODEN: IDSDA6. doi:10.2973/dsdp.proc.38.102.1976
- Talwani, M., Udintsev, G.B., Bjoerklund, K., Caston, V.N.D., Faas, R. W., van Hinte, J.E., Kharin, G.N., Morris, D.A., Mueller, C., Nilsen, T.H., Warnke, D.A., White, S.M., Manum, S.B. and Schrader, H.-J. (1976i). Site 337. Initial Reports of the Deep Sea Drilling Project, Vol.38, 595-654. Publisher: Texas A & M University, Ocean Drilling Program, College Station, TX, United States. ISSN: 0080-8334 CODEN: IDSDA6. doi:10.2973/dsdp.proc.38.103.1976
- Talwani, M., Udintsev, G.B., Bjoerklund, K., Caston, V.N.D., Faas, R. W., van Hinte, J.E., Kharin, G.N., Morris, D.A., Mueller, C., Nilsen, T.H., Warnke, D.A., White, S.M., Manum, S.B. and Schrader, H.-J. (1976h). Sites 338-343. Initial Reports of the Deep Sea Drilling Project, Vol.38, 595-654. Publisher: Texas A & M University, Ocean Drilling Program, College Station, TX, United States. ISSN: 0080-8334 CODEN: IDSDA6. doi:10.2973/dsdp.proc.38.104.1976
- Talwani, M., Udintsev, G.B., Bjoerklund, K., Caston, V.N.D., Faas, R. W., van Hinte, J.E., Kharin, G.N., Morris, D.A., Mueller, C., Nilsen, T.H., Warnke, D.A., White, S.M., Manum, S.B. and Schrader, H.-J. (1976g). Site 345. Initial Reports of the Deep Sea Drilling Project, Vol.38, 595-654. Publisher: Texas A & M University, Ocean Drilling Program, College Station, TX, United States. ISSN: 0080-8334 CODEN: IDSDA6. doi:10.2973/dsdp.proc.38.106.1976
- Talwani, M., Udintsev, G.B., Bjoerklund, K., Caston, V.N.D., Faas, R. W., van Hinte, J.E., Kharin, G.N., Morris, D.A., Mueller, C., Nilsen, T.H., Warnke, D.A., White, S.M., Manum, S.B. and Schrader, H.-J. (1976f). Site 348. Initial Reports of the Deep Sea Drilling Project, Vol.38, 595-654. Publisher: Texas A & M University, Ocean Drilling Program, College Station, TX, United States. ISSN: 0080-8334 CODEN: IDSDA6. doi:10.2973/dsdp.proc.38.108.1976
- Talwani, M., Udintsev, G.B., Bjoerklund, K., Caston, V.N.D., Faas, R. W., van Hinte, J.E., Kharin, G.N., Morris, D.A., Mueller, C., Nilsen, T.H., Warnke, D.A., White, S.M., Manum, S.B. and Schrader, H.-J. (1976e). Site 350. Initial Reports of the Deep Sea Drilling Project, Vol.38, 655-682. Publisher: Texas A & M University, Ocean Drilling Program, College Station, TX, United States. ISSN: 0080-8334 CODEN: IDSDA6. doi:10.2973/dsdp.proc.38.109.1976

- Talwani, M., Udintsev, G. B., Bjoerklund, K., Caston, V. N. D., Faas, R. W., van Hinte, J. E., Kharin, G. N., Morris, D. A., Mueller, C., Nilsen, T. H., Warnke, D. A., White, S. M., Manum, S. B. and Schrader, H.-J. (1976d). Initial Reports of the Deep Sea Drilling Project, Vol.38, 655-682. Publisher: Texas A & M University, Ocean Drilling Program, College Station, TX, United States. ISSN: 0080-8334 CODEN: IDSDA6. doi:10.2973/dsdp.proc.38.109.1976
- Talwani, M., Udintsev, G.B., Bjoerklund, K., Caston, V.N.D., Faas, R. W., van Hinte, J.E., Kharin, G.N., Morris, D.A., Mueller, C., Nilsen, T.H., Warnke, D.A., White, S.M., Manum, S.B., Schrader, H.-J. (1976c). Sites 346, 347, and 349. Initial Reports of the Deep Sea Drilling Project, Vol.38, 521-594. Publisher: Texas A & M University, Ocean Drilling Program, College Station, TX, United States. ISSN: 0080-8334 CODEN: IDSDA6. doi:10.2973/dsdp.proc.38.107.1976
- Talwani, M., Udintsev, G. and Shirshov, P.R. (1976b). Tectonic synthesis. In: Talwani, M. and Udintsev, G. (eds). Initial Reports of the Deep Sea Drilling Project. Volume 38, U.S. Government Printing Office, Washington, 1213-1242.
- Talwani, M., Udintsev, G. and White, S.M. (1976a). Introduction and explanatory notes, Leg 38, Deep Sea Drilling Project. In: Talwani, M. and Udintsev, G. (eds). Initial Reports of the Deep Sea Drilling Project. Volume 38, U.S. Government Printing Office, Washington, 3-19.
- Tan, P., Sippel, J., Breivik, A.J., Meeßen, C. and Scheck-Wenderoth, M. (2018). Lithospheric control on asthenospheric flow from the Iceland plume: 3-D density modeling of the Jan Mayen-East Greenland Region, NE Atlantic. *Journal of Geophysical Research, Solid Earth*, **123**(10), 9223-9248. doi:10.1029/2018JB015634
- Tan, P., Breivik, A.J., Trønnes, R.G., Mjelde, R., Azuma, R. and Eide, S. (2017). Crustal structure and origin of the Eggvin Bank west of Jan Mayen, NE Atlantic. *Journal of Geophysical Research, Solid Earth*, **122**, 43–62. doi:10.1002/2016JB013495
- Taylor, B., Crook, K. and Sinton, J. (1994). Extensional transform zones and oblique spreading centers. *Journal of Geophysical Research, Solid Earth*, **99**, 19707–19718. <https://doi.org/10.1029/94JB01662>
- Tegner, C., Brooks, C.K., Duncan, R.A., Heister, L.E. and Bernstein, S. (2008). ^{40}Ar – ^{39}Ar ages of intrusions in East Greenland: Rift-to-drift transition over the Iceland hotspot. *Lithos*, **101**(3), 480-500. doi:10.1016/j.lithos.2007.09.001
- Tegner, C., Leshner, C.E., Larsen, L.M. and Watt, W.S. (1998). Evidence from the rareearth-element record of mantle melting for cooling of the Tertiary Iceland plume. *Nature*, **395**(6702), 591-594. doi:10.1038/26956
- Theissen-Krah S., Zastrozhnov, D., Abdelmalak, M.M., Schmid, D.W., Faleide, J.I. and Gernigone, L. (2017). Tectonic evolution and extension at the Møre Margin – Offshore mid-Norway. *Tectonophysics*, **721**(721), 227–238. doi:10.1016/j.tecto.2017.09.009
- Thiede, J., Firth, J.V. et al. (eds) (1995). Site 907. Ocean Drilling Program, College Station, TX, proceedings of the Ocean Drilling Program, Initial Reports, 151, 57-111.
- Thordarson, T. and Höskuldsson, Á. (2008). Postglacial volcanism in Iceland. *Jökull*, **58**, 197-228.
- Torsvik, T.H., Amundsen, H.E.F., Trønnes, R.G., Doubrovine, P.V, Gaina, C., Kuszniir, N. J., et al. (2015). Continental crust beneath southeast Iceland. *Proceedings of the National Academy of Sciences of the United States of America*, **112**(15), E1818-27. <https://doi.org/10.1073/pnas.1423099112>

- Torsvik, T.H., Mosar, J. and Eide, E.A. (2001). Cretaceous-Tertiary geodynamics: a North Atlantic exercise. *Geophysical Journal International*, **146**(3), 850–866.
<https://doi.org/10.1046/j.0956-540x.2001.01511.x>
- Tóth T. (2011) *Single and Multichannel Seismics*. In: Gupta H.K. (eds) *Encyclopedia of Solid Earth Geophysics*. Encyclopedia of Earth Sciences Series. Springer, Dordrecht.
https://doi.org/10.1007/978-90-481-8702-7_210
- Tripati, A. and Darby, D. (2018). Evidence for ephemeral middle Eocene to early Oligocene Greenland glacial ice and pan-Arctic sea ice. *Nature Communications*, **9**(1038), 2041–1723. doi:10.1038/s41467-018-03180-5
- Upton, B.G.J., Emeleus, C.H., Rex, D.C. and Thirlwall, M.F. (1995). Early Tertiary magmatism in NE Greenland. *Journal of the Geological Society*, **152**(6), 959–964. doi:10.1144/gsl.jgs.1995.152.01.13
- Vail, P.R. (1987). *Seismic Stratigraphy Interpretation Using Sequence Stratigraphy: Part 1: Seismic Stratigraphy Interpretation Procedure*. In: Ball, A.W. (ed). *AAPG Studies in Geology*, **27**(1), 1–10, ISBN 9781588611932.
- van den Broek, J.M., Magni, V., Gaina, C. and Buiter, S.J.H. (2020). The formation of continental fragments in subduction settings: The importance of structural inheritance and subduction system dynamics. *Journal of Geophysical Research: Solid Earth*, **125**, e2019JB018370. <https://doi.org/10.1029/2019JB018370>
- Van Sickel, W.A., Kominz, M.A., Miller, K.G., Browning, J.V. (2004). Late Cretaceous and Cenozoic sea-level estimates: backstripping analysis of borehole data, onshore New Jersey. *Basin Research*, **16**, 451–465. doi:10.1111/j.1365-2117.2004.00242.x
- Viereck, L.G., Hertogen, J., Parson, L.M., Morton, A.C., Love, D. and Gibson, I.L. (1989). *Chemical stratigraphy and petrology of the Vøring Plateau: theoleiitic lavas and interlayered volcanoclastic sediments at ODP Hole 642E*. In: Eldholm, O., Thiede, J., Taylor, E., et al., Ocean Drilling Program, College Station, TX, *Proc. ODP, Scientific Results*, **104**, 367–396. doi:10.2973/odp.proc.sr.104.135.1989
- Vogt, P.R., Johnson, G.L. and Kristjansson, L. (1980). Morphology and Magnetic-Anomalies North of Iceland. *Journal of Geophysics-Zeitschrift für Geophysik*, **47**(1-3), 67.
- Vogt, P. R., & Avery, O. E. (1974). Detailed magnetic surveys in the northeast Atlantic and Labrador Sea. *Journal of Geophysical Research*, **79**(2), 363–389. Retrieved from <http://onlinelibrary.wiley.com/doi/10.1029/JB079i002p00363/abstract>
- Vogt, P.R., Anderson, C.N., Bracey, D.R. and Schneider, E.M. (1970). North Atlantic Magnetic Smooth Zones. *Journal of Geophysical Research*, **75**(20), 3955–3968.
<https://doi.org/10.1029/JB075i020p03955>
- Weigel, W., Flüh, E., Miller, H., Butzke, A., Deghani, A., Gebhardt, V., Harder, I., Hepper, J., Jokat, W., Kläschen, D., Schübler, S. and Zhao-Groekart, Z. (1995). Investigations of the East Greenland continental margin between 70° and 72° N by deep seismic sounding and gravity studies. *Marine Geophysical Research*, **17**(2), 167–199. doi:10.1007/bf01203425
- Whittaker, J., Afonso, J., Masterton, S., Müller, R., Wessel, P., Williams, S. and Seton, M. (2015). Long-term interaction between mid-ocean ridges and mantle plumes. *Nature Geoscience*, **8**(6), 479–483. doi: 10.1038/ngeo2437

- Wright, T.J., Sigmundsson, F., Pagli, C., Belachew, M., Hamling, I., Brandsdóttir, B., Keir, D., Pedersen, R., Ayele, A., Ebinger, C., Einarsson, P., Lewi, E. and Calais, E. (2012). Geophysical constraints on the dynamics of spreading centres from rifting episodes on land. *Nature Geoscience*, **5**, 242-250. doi:10.1038/ngeo1428
- Zhang, T., Gordon, R. G. and Wang, C. (2018). Oblique seafloor spreading across intermediate and superfast spreading centers. *Earth and Planetary Science Letters*, **495**, 146–156. <https://doi.org/10.1016/j.epsl.2018.05.001>
- Zastrozhnov, D., Gernigon, L., Gogin, I., Abdelmalak, M.M., Planke, S., Faleide, J.I., Eide, S. and Myklebust, R. (2018). Cretaceous-Paleocene Evolution and Crustal Structure of the Northern Vøring Margin (Offshore Mid-Norway): Results from Integrated Geological and Geophysical Study. *Tectonics*, **37**. doi:10.1002/2017TC004655
- Ziegler, P.A. (1988). *Evolution of the Arctic-North Atlantic and the Western Tethys*. American Association of Petroleum Geologists, Memoir 43, ISBN 9781629811338. <https://doi.org/10.1306/M43478>

Publications

Paper I

The Jan Mayen microcontinent: an update of its architecture, structural development and role during the transition from the Ægir Ridge to the mid-oceanic Kolbeinsey Ridge

Blischke, A., Gaina, C., Hopper, J. R., Péron-Pinvidic, G., Brandsdóttir, B., Guarnieri, P., Erlendsson, Ö. and Gunnarsson, K. (2017)

Geological Society, London, Special Publications, 447, first published on February 3, 2017, 299–337

<https://doi.org/10.1144/SP447.5>.

Copyright © The Authors 2017

The Jan Mayen microcontinent: an update of its architecture, structural development and role during the transition from the Ægir Ridge to the mid-oceanic Kolbeinsey Ridge

A. BLISCHKE^{1*}, C. GAINA², J. R. HOPPER³, G. PÉRON-PINVIDIC⁴, B. BRANDSDÓTTIR⁵, P. GUARNIERI³, Ö. ERLENDSSON⁶ & K. GUNNARSSON⁶

¹*Iceland GeoSurvey, Branch at Akureyri, Rangárvöllum, 602 Akureyri, Iceland*

²*Centre for Earth Evolution and Dynamics, University of Oslo, Sem Sælands vei 24, PO Box 1048, Blindern, NO-0316 Oslo, Norway*

³*Geological Survey of Denmark and Greenland, Øster Voldgade 10, DK 1350 Copenhagen, Denmark*

⁴*Geological Survey of Norway, Postboks 6315 Sluppen, Trondheim 7491, Norway*

⁵*Institute of Earth Science, Science Institute, University of Iceland, Askja, Sturlugata 7, 101 Reykjavík, Iceland*

⁶*Iceland GeoSurvey, Grensásvegi 9, 108 Reykjavík, Iceland*

*Corresponding author (e-mail: Anett.Blischke@isor.is)

Abstract: We present a revised tectonostratigraphy of the Jan Mayen microcontinent (JMMC) and its southern extent, with the focus on its relationship to the Greenland–Iceland–Faroe Ridge area and the Faroe–Iceland Fracture Zone. The microcontinent’s Cenozoic evolution consists of six main phases corresponding to regional stratigraphic unconformities. Emplacement of Early Eocene plateau basalts at pre-break-up time (56–55 Ma), preceded the continental break-up (55 Ma) and the formation of seawards-dipping reflectors (SDRs) along the eastern and SE flanks of the JMMC. Simultaneously with SDR formation, orthogonal seafloor spreading initiated along the Ægir Ridge (Norway Basin) during the Early Eocene (C24n2r, 53.36 Ma to C22n, 49.3 Ma). Changes in plate motions at C21n (47.33 Ma) led to oblique seafloor spreading offset by transform faults and uplift along the microcontinent’s southern flank. At C13n (33.2 Ma), spreading rates along the Ægir Ridge started to decrease, first south and then in the north. This was probably complemented by intra-continental extension within the JMMC, as indicated by the opening of the Jan Mayen Basin – a series of small pull-apart basins along the microcontinent’s NW flank. JMMC was completely isolated when the mid-oceanic Kolbeinsey Ridge became fully established and the Ægir Ridge was abandoned between C7 and C6b (24–21.56 Ma).



Gold Open Access: This article is published under the terms of the CC-BY 3.0 license.

The Jan Mayen microcontinent (JMMC) is a structural entity encompassing the Jan Mayen Ridge and the surrounding area, including the Jan Mayen Basin, the Jan Mayen Basin South, the Jan Mayen Trough and the Southern Ridge Complex (SRC) (Fig. 1; Table 1). The JMMC is bordered to the north by the east and west segments of the Jan Mayen Fracture Zone and the volcanic complex of Jan Mayen Island (Svellingén & Pedersen 2003). To the south, it is bordered by the NE coastal shelf of Iceland, to the east by the Norway Basin and to the west by the Kolbeinsey Ridge. Early descriptions of the JMMC considered only the Jan Mayen

Ridge (Vogt *et al.* 1970; Talwani *et al.* 1976a), a steep-flanked bathymetric horst structure with water depths varying between 200 and 2500 m that extends south from Jan Mayen Island. However, based on modern datasets, it is now accepted that the microcontinent is much larger than this and encompasses a number distinct, structurally controlled tectonic features that were formed by a succession of tectonic and volcanic events (e.g. Scott *et al.* 2005; Gaina *et al.* 2009; Peron-Pinvidic *et al.* 2012a, b; Gernigon *et al.* 2012). In total, the JMMC is 400–450 km long, and varies in width from 100 km in the north to 310 km in the south.

From: PÉRON-PINVIDIC, G., HOPPER, J. R., STOKER, M. S., GAINA, C., DOORNENBAL, J. C., FUNCK, T. & ÁRTING, U. E. (eds) *The NE Atlantic Region: A Reappraisal of Crustal Structure, Tectonostratigraphy and Magmatic Evolution*. Geological Society, London, Special Publications, **447**, <http://doi.org/10.1144/SP447.5>

© 2016 The Author(s). Published by The Geological Society of London.

Publishing disclaimer: www.geolsoc.org.uk/pub_ethics

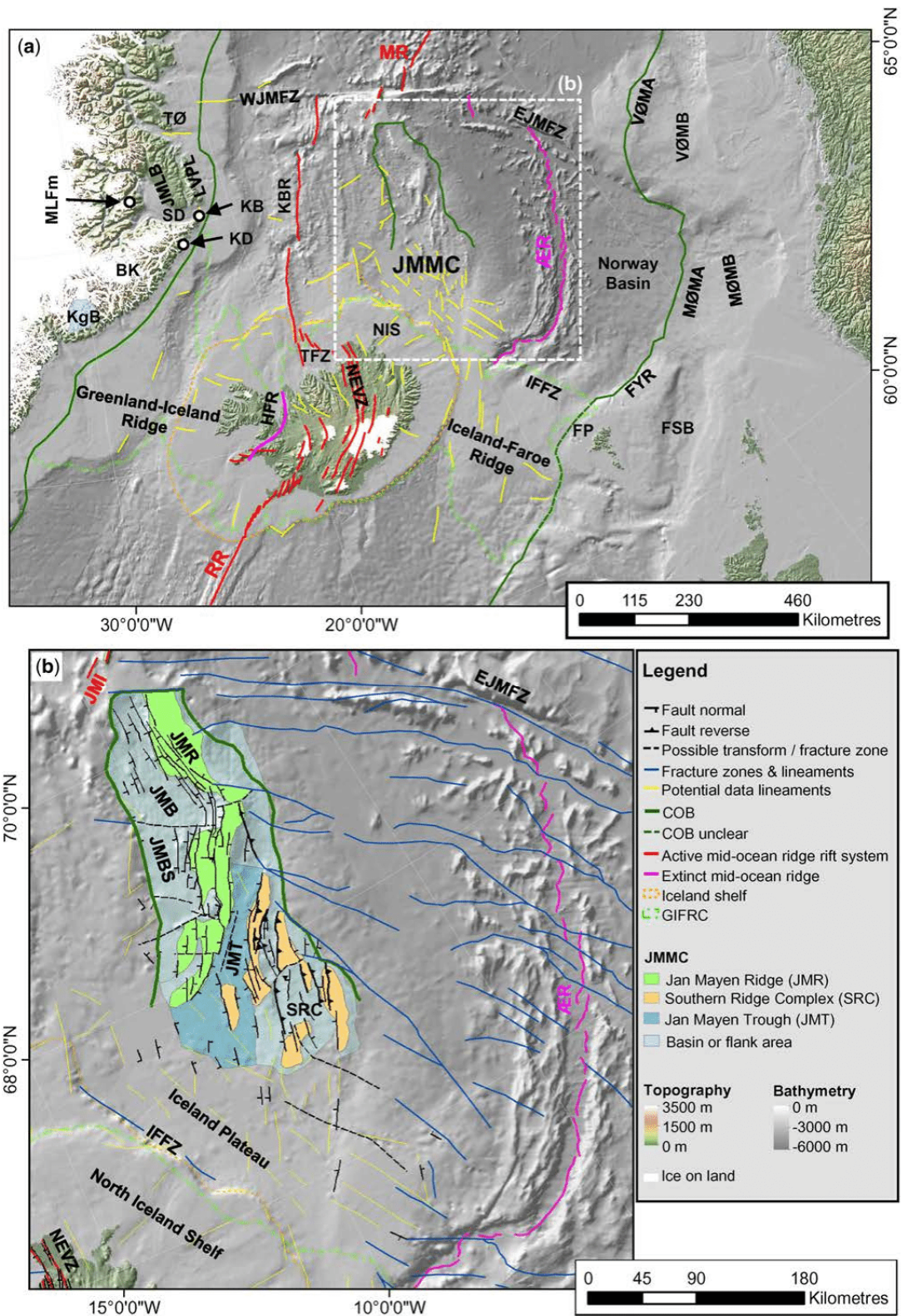


Fig. 1. Overview map (a) of the study area with the location of structural elements identified on potential field data. Structural elements map (b) for the JMMC study with mapped faults, fractures zones and lineaments based on this study and modified after Peron-Pinvidic *et al.* (2012a) and Gernigon *et al.* (2015) (for label keys, see Table 1). The background image is shaded bathymetry (IBCAO 3.0: Jakobsson *et al.* 2012; Amante & Eakins 2009).

THE JMMC: THE ÆGIR RIDGE TO THE KOLBEINSEY RIDGE

Table 1. Explanation of structural element abbreviations and label key, modified after Gunnarsson et al. (1989), Jóhannesson (2011), Hjartarson & Sæmundsson (2014), Hopper et al. (2014) and Magnúsdóttir et al. (2015)

Abbreviation and label key		
General features:	Central NE Atlantic:	
COB Continent–ocean boundary	JMMC Jan Mayen microcontinent	IB Iceland Basin
SDR Seawards-dipping reflector	BR Buðli Ridge	
Mid-oceanic ridges:	EFBN Jan Mayen East Flank Basins North	GIFRC Faroe–Iceland–Greenland Ridge Complex
ÆR Ægir mid-oceanic ridge	EFBS Jan Mayen East Flank Basins South	GIR Greenland–Iceland Ridge
MR Mohn’s mid-oceanic ridge	HC/JMWIP Hakarennna Channel/Jan Mayen West Igneous Province South	HFR Húnaflóa Rift
KBR Kolbeinsey mid-oceanic ridge	HR Högni Ridge	ICE Iceland onshore
RR Reykjanes mid-oceanic ridge	JMT/HT Jan Mayen Trough/Hléssund Trough	IFR Iceland–Faroe Island Ridge
JMI Jan Mayen Island System	JMB Jan Mayen Basin	NEVZ Northeast Volcanic Zone
Transfer systems and fracture zones:	JMRN Jan Mayen Ridge North	
EJMFZ East Jan Mayen Fracture Zone	LYR Lyngvi Ridge	Central Norway Margin:
IFFZ Iceland–Faroe Fracture Zone	SFB/JMBS Sörlahryggur Flank Basin/Jan Mayen Basin South	MØMA Møre Marginal High
MIRFTS Mid-Iceland Rift Transfer System	SHR Sörlahryggur Ridge	MØMB Møre Basin
SISZ South Iceland Seismic Zone	WIPN Jan Mayen West Igneous Province North	VØMA Vøring Marginal High
TFZ Tjörnes Fracture Zone		VØMB Vøring Basin
WJMFZ West Jan Mayen Fracture Zone	SRCCC Jan Mayen microcontinent–Southern Ridge Complex (SRC) – continental crust	
Central East Greenland Margin:	FR Fáfñir Ridge	Faroe Islands Atlantic Margin:
BK Blossville Kyst	OR Otur Ridge	FYR Fugloy Ridge
JMLB Jameson Land Basin		FP Faroe Platform
KD Kap Dalton outcrop site	SRCTC Jan Mayen microcontinent–Southern Ridge Complex – transitional crust	FSB Faroe–Shetland Basin
KB Kap Brewster outcrop site	DR Dreki Ridge	
KgB Kangerlussuaq Basin	LR Langabrún Ridge	
LVPL Liverpool Land High	ORS Otur Ridge southern spur	
ML Fm Milne Land Formation outcrop site	TR Treitel Ridge	
SD Scoresby Sund		
TØ Trail Ø	NIS North Iceland Shelf	
	IP Iceland Plateau	
	IPR Iceland Plateau Rift	

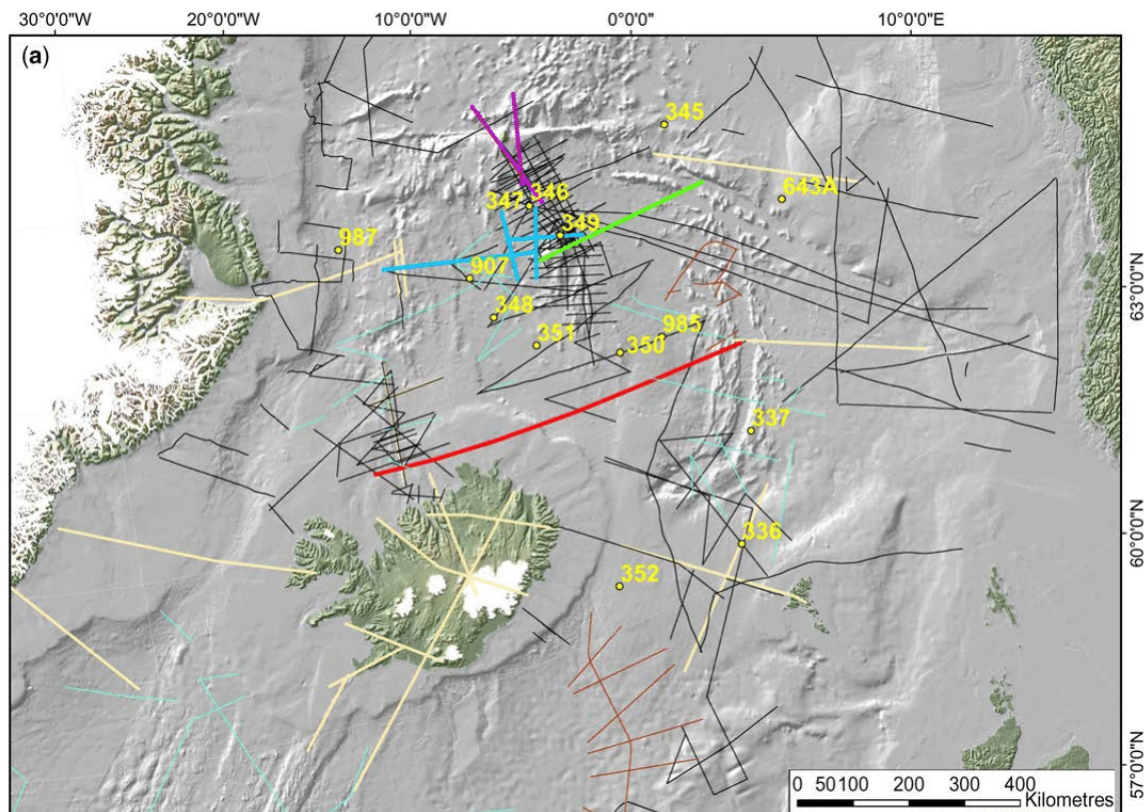


Fig. 2. Regional map showing shaded bathymetry (Amante & Eakins 2009; Jakobsson *et al.* 2012) and (a) refraction and reflection seismic lines and boreholes. Legend see Figure 2b.

The microcontinent is bounded on all sides by oceanic crust, although its southern limit remains poorly constrained. This is due, in part, to sparse data coverage south of 68° N (Fig. 2), but also to the occurrence of numerous intrusive and extrusive volcanic rocks that limit seismic imaging of the underlying features. Previous interpretations of the continent–ocean transition (COT) along the JMMC margins were mainly based on magnetic and/or gravity data (e.g. Vogt *et al.* 1970; Talwani & Eldholm 1977; Åkermoen 1989; Doré *et al.* 1999; Lundin & Doré 2002; Rey *et al.* 2003; Gaina *et al.* 2009; Gernigon *et al.* 2012) and seismic reflection data (Gunnarsson *et al.* 1989; Scott *et al.* 2005; Peron-Pinvidic *et al.* 2012a, b). Breivik *et al.* (2012) considered crustal velocity information from wide-angle data with potential field data to derive the location of the COT.

The purpose of this paper is to establish a detailed tectonic and stratigraphic framework for the JMMC based on a new regional database of geological and geophysical data. The analysis includes interpretation of new seismic reflection data, as well as recent geological findings, from on- and offshore central East Greenland (e.g. Larsen *et al.* 2013; Guarnieri 2015). This study has been facilitated by

the interpretation of recently acquired commercial seismic reflection data that were made available for the project, together with older seismic reflection and refraction data collected offshore Iceland since the early 1970s (Fig. 2). Revised ^{39}Ar – ^{40}Ar dates of East Greenland basalt samples (e.g. Tegner *et al.* 2008; Larsen *et al.* 2013), and an improved coverage of magnetic data and interpretations (CAMP-GM: Gaina *et al.* 2011; Gernigon *et al.* 2015), are also considered. Pre- and post-break-up sedimentary strata and igneous complexes, together with volcanostratigraphic seismic characterization, have been revisited, together with a reassessment of the seawards-dipping reflector sequences (SDRs), igneous complexes, sill and dyke intrusions, and hydrothermal vent complexes.

The JMMC margins are compared to the conjugate margins: the central East Greenland margin and the Møre margin off Norway (Blystad *et al.* 1995). The western JMMC margin is linked to central East Greenland, where the Palaeozoic–Mesozoic Jameson Land Basin is located (JMLB: Henriksen 2008) (Fig. 1). The segmentation and extent of the southern area of the JMMC and its link to the oblique opening of the Norway Basin are also considered. Finally, the question of how the igneous

THE JMMC: THE ÆGIR RIDGE TO THE KOLBEINSEY RIDGE

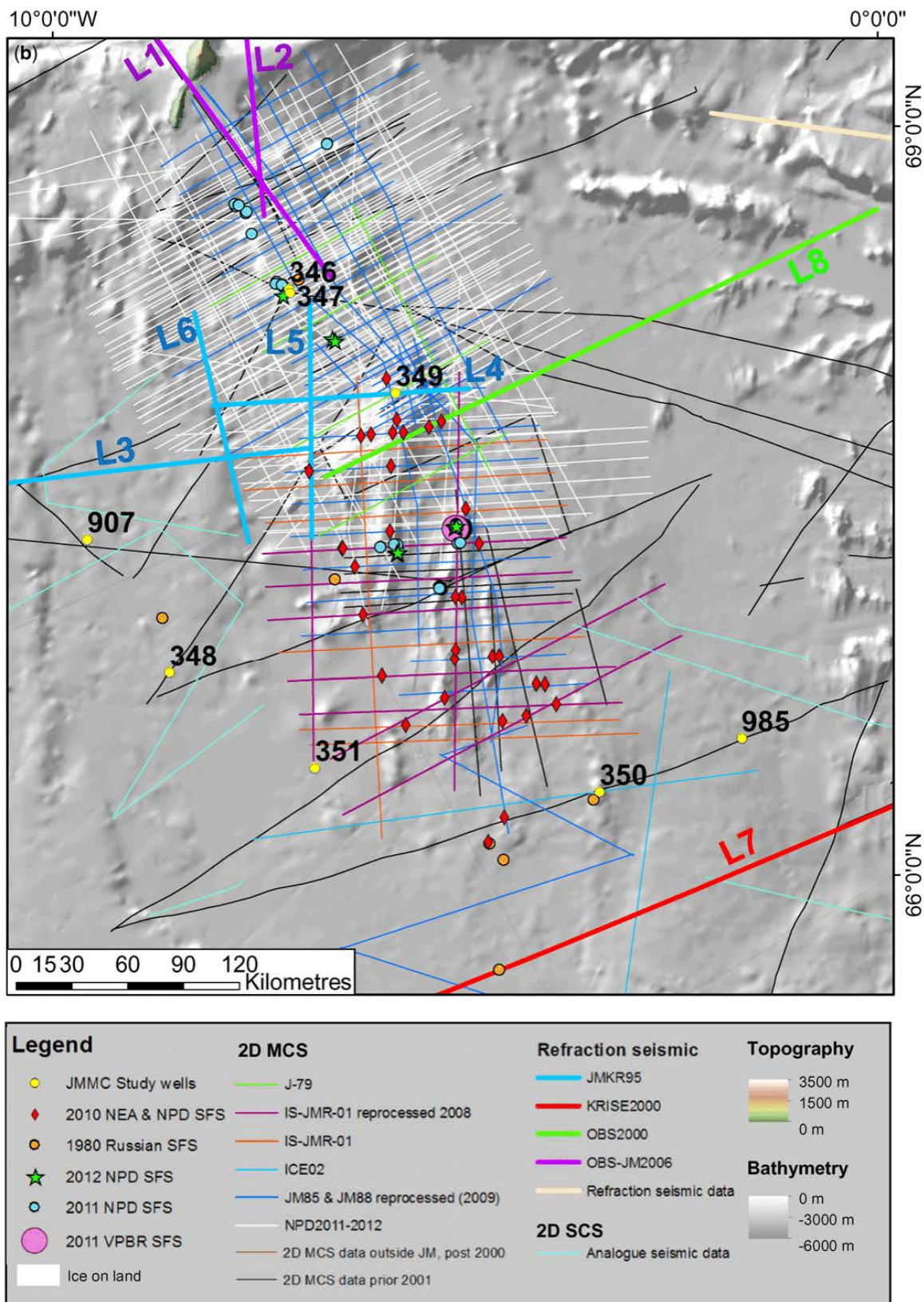


Fig. 2. (b) seabed sampling sites (NEA, National Energy Authority, Iceland; NPD, Norwegian Petroleum Directorate (2013); Spectrum ASA; TGS; SFS seafloor samples; VBPR, Volcanic Basin Petroleum Research AS).

THE JMMC: THE ÆGIR RIDGE TO THE KOLBEINSEY RIDGE

events along the southern half of the JMMC are related to the Blossville Kyst, the Iceland–Faroe Fracture Zone system that forms the NE limit of the Greenland–Iceland–Faroe Ridge Complex (GIFRC) (Árting 2014), and the Iceland Plateau (Fig. 1; Table 1) is addressed. The new interpretation has been used to model the detailed kinematics of the JMMC from pre-break-up time to the present day.

Geological setting of the central NE Atlantic

Several distinct rifting episodes and the subsequent break-up of the supercontinent Pangea led to the formation of a series of segmented rifted margins along the North Atlantic Ocean (Ziegler 1988). Extensional episodes are recognized from Devonian and Carboniferous times, initiated by the collapse of the Caledonian mountain belt (e.g. Andersen & Jamtveit 1990). Devonian onshore rift basins along East Greenland (Henriksen 2008) and SW Norway (Osmundsen & Andersen 1994, 2001; Osmundsen *et al.* 2002) are well documented, including their complex relationship to large-scale transtensional tectonics (Osmundsen & Andersen 2001). These basins are interpreted to extend in the central and northern part of the NE Atlantic during the Carboniferous, and were not affected by the Variscan Orogeny (Hopper *et al.* 2014), which occurred at the same time and influenced the NE and SE regions of the NE Atlantic, the North Sea and northern Europe (Pharaoh *et al.* 2010). During the Permian and Triassic periods, the entire NE Atlantic region was subjected to extension (e.g. Doré *et al.* 1999; Brekke 2000). At that time, a first rifting phase led to minor rotational block faulting and westwards tilted half-graben along East Greenland (Seidler 2000), forming terrestrial to shallow marine basins that discordantly covered the old Devonian–Carboniferous basin (Stemmerik 2000). The entire NE Atlantic system went through two major rifting phases during the Late Jurassic and a major Cretaceous rifting phase from the late Early Cretaceous (Aptian–Albian) to Late Cretaceous (Lundin & Doré 1997, 2011; Stoker *et al.* 2016), leading to significant crustal thinning in the central parts of the corridor and forming deep basins. The Cretaceous rifting phase may have included a hyper-extension (Peron-Pinvidic *et al.* 2013), resulting in

exhumation of deep crust and possibly mantle, as suggested by Osmundsen *et al.* (2002) or Osmundsen & Ebbing (2008).

During Late Paleocene and pre-break-up time, early volcanism associated with the North Atlantic igneous province occurred. Regionally extensive landwards flows consisting of subaerial and submarine lava flows onto adjacent elevated margins were emplaced during this time (Horni *et al.* 2016). Infilling of pre-existing basin areas formed escarpments and hyaloclastite deltas (Planke *et al.* 2000; Horni *et al.* 2016). Intense magmatism occurred at this time just SW of the JMMC, close to the Kangerlussuaq Basin and the southern extent of the Blossville Kyst (e.g. Tegner *et al.* 2008; Brooks 2011). Magmatic margins formed during the Early Eocene (56–55 Ma), in association with final rupture of the lithosphere and the onset of seafloor spreading of the NE Atlantic (e.g. Talwani & Eldholm 1977). The resulting North Atlantic continental margins contain SDR sequences observed on seismic reflection data (Hinz 1981). The break-up process was also accompanied by the emplacement of sill and dyke complexes into the margin flank areas. Oceanic crust was first formed in the Norway Basin at the end of chron C25 or the beginning of C24r (c. 55 Ma) forming the Ægir mid-oceanic ridge (e.g. Talwani & Eldholm 1977; Gaina *et al.* 2009).

The JMMC structure and stratigraphy observed between its eastern and western margins is profoundly segmented. A first-order boundary within the microcontinent is between the Jan Mayen Ridge and the SRC. Updated datasets suggest that the JMMC internal segmentation is probably related to the complex multistage seafloor spreading processes on both sides of the microcontinent.

Published plate tectonic reconstructions indicate a westwards migration of the plate boundary from the Norway Basin towards the Kolbeinsey mid-oceanic ridge (Nunns 1983a, b; Nunns *et al.* 1983; Lundin & Doré 2005; Doré *et al.* 2008; Gaina *et al.* 2009), suggesting a gradual separation of the microcontinent from East Greenland during the Early Miocene (Talwani & Eldholm 1977; Gunnarsson *et al.* 1989). Larsen *et al.* (2013) suggested that early rifting between the JMMC and East Greenland coast may have occurred from 49 to 44 Ma, with a direction semi-parallel to the Ægir mid-oceanic ridge system. This event generated increased igneous activity and structural deformation along the NE extent of the Blossville Kyst (Fig. 1).

Fig. 3. The JMMC stratigraphic summary chart, partly based on DSDP and ODP boreholes (Talwani *et al.* 1976a, b; Manum & Schrader 1976; Manum *et al.* 1976a, b; Raschka *et al.* 1976; Nilsen *et al.* 1978; Thiede *et al.* 1995; Jansen *et al.* 1996; Channell *et al.* 1999a, b; Butt *et al.* 2001). This is used to tie the known shallow Cenozoic stratigraphy and unconformities to the seismic reflection data (see the type section in Fig. 4). The Pliocene–Pleistocene correlation marker is based on sedimentary core records (Talwani *et al.* 1976a, b).

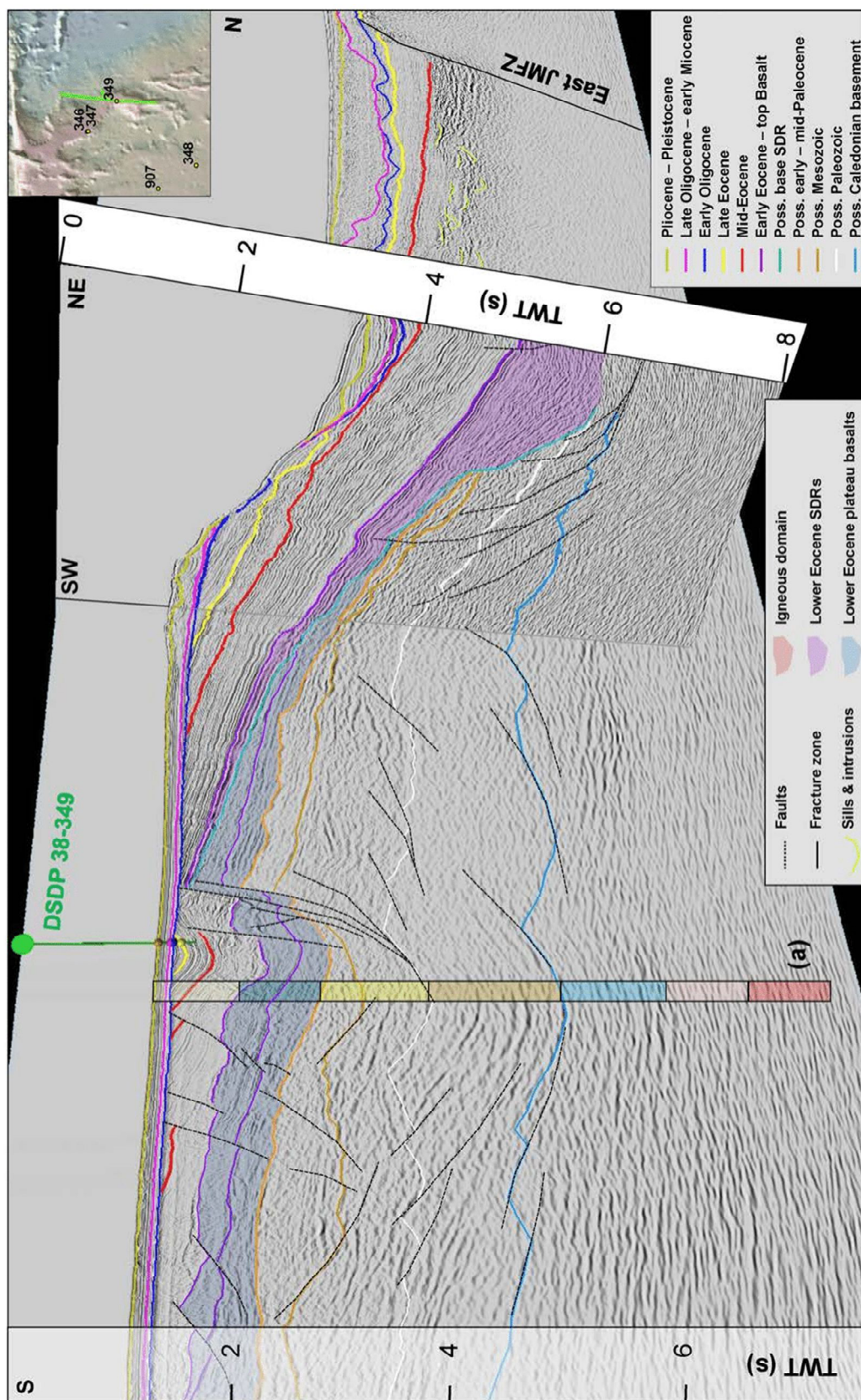


Fig. 4. Type section showing sedimentary basins below the Cenozoic succession and the seismic refraction velocity interval interpretation intersection (a) (Table 3). The SDR sequence (purple) is interpreted to overlie a thick basalt sequence (blue) that is likely to be equivalent to the plateau basalts exposed on East Greenland. The east–west line is courtesy of Spectrum ASA, and the north–south line is courtesy of NPD.

THE JMMC: THE ÆGIR RIDGE TO THE KOLBEINSEY RIDGE

Data overview and methods

Geophysical datasets consist of magnetic and gravity anomaly compilations (Haase & Ebbing 2014; Nasuti & Olesen 2014) (Fig. 2), 2D multichannel seismic reflection data (2D MCS data) and seismic refraction data (Johansen *et al.* 1988; Olafsson & Gunnarsson 1989; Kodaira *et al.* 1998; Brandsdóttir *et al.* 2015). Eight shallow Ocean Drilling Program (ODP) and Deep Sea Drilling Program (DSDP) boreholes (legs 38, 151 and 162) (Eldholm & Windish 1974; Talwani & Udintsev 1976; Eldholm *et al.* 1987, 1989) provide some of the few samples from the JMMC (Figs 2–5). Results from seafloor sampling campaigns carried out in 1973 by Geodekyan *et al.* (1980), in 2010 by the National Energy Authority of Iceland (OS) and the Norwegian Petroleum Directorate (NPD), in 2012 by the NPD (Sandstå *et al.* 2012), and in 2012 by the Volcanic Basin Petroleum Research (VBPR) and TGS (Polteau *et al.* 2012) were also taken into account. Finally, recently revised ^{40}Ar – ^{39}Ar dating of East Greenland coastal basalts and onshore unconformities within the igneous successions of the Blosseville Kyst area are considered (Larsen *et al.* 2013).

Seismic reflection data includes only a few 2D multichannel surveys from before 2001, of which the JM-85-88 results were reprocessed in 2009. More recent surveys include IS-JMR-01 (2001), ICE-02 (2002), WI-JMR-08 (2008), NPD-11 (2011) and NPD-12 (2012) (Fig. 2; Table 2). The reprocessed dataset was used for detailed volcanostratigraphic seismic characterization, which facilitated mapping and identification of structural elements, sedimentary sequences, SDR sequences, and sill and dyke complexes. Multibeam bathymetry data were used to map structural trends and features at the seafloor. This high-resolution bathymetry data in combination with seismic reflection data enabled us to differentiate strike-slip from normal fault systems and slump faulting along the steep escarpments of the microcontinent's ridges.

There are no deep drill holes on the JMMC. For this reason, the older history and stratigraphic correlations are inferred by comparison to better-known analogue areas along the conjugate margins, in particular the Jameson Land Basin (Surlyk *et al.* 1973; Surlyk & Noe-Nygaard 2001; Surlyk 1977, 1978, 1990, 1991, 2003; Henriksen 2008), and the mid-Norway Møre and Vøring margins (e.g. Brekke *et al.* 1999; Osmundsen *et al.* 2002; Faleide *et al.* 2010) (Fig. 1a; Table 1).

Correlation of stratigraphic information to seismic reflection data

Information from DSDP Leg 38 (sites 346, 348, 349 and 350) and from seafloor samples retrieved by the

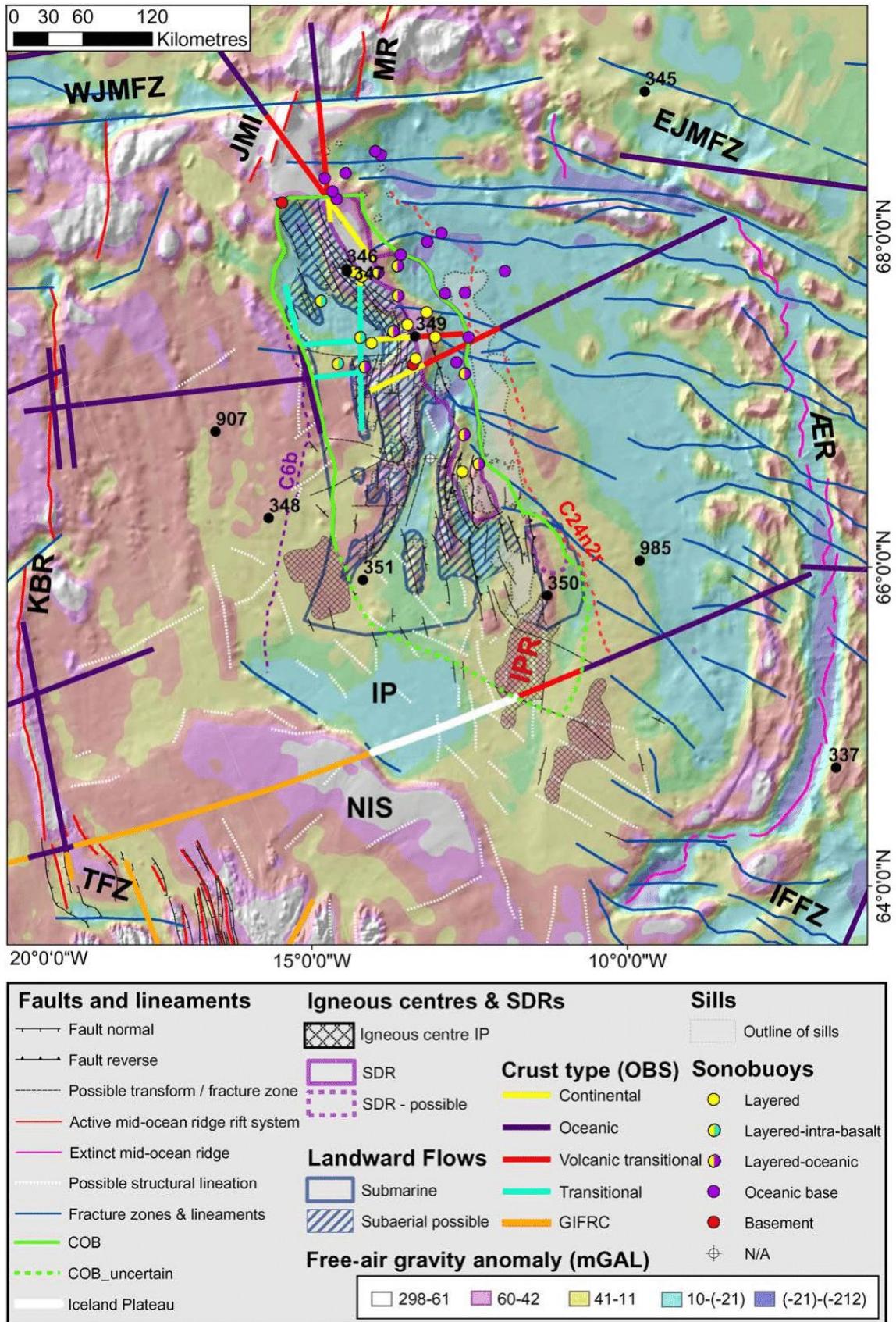
NPD in 2011, 2012 and 2013 (Fig. 2b; Table 2) provide key constraints for tying it to the seismic reflection data along the central part of the JMMC (Fig. 3). This permits mapping of unconformities and post-basalt stratigraphy across the JMMC (Figs 4, 5 & 6). Some uncertainties in local stratigraphic correlations still exist, notably along the collapsed western flank of the JMMC and between the dislocated southern ridges. The sub-basalt sequences are only visible in the central area of the JMMC and around DSDP Leg 38 site 349. Seismic reflection data in vicinity of this drill site has been interpreted as possible Mesozoic and Palaeozoic strata based on comparisons to the Jameson Land Basin (Blischke *et al.* 2014a).

In addition to the well ties, onshore and offshore stratigraphic relationships along the western conjugate margin (Blosseville Kyst in East Greenland) provide information on the basalt stratigraphy that can be used for interpreting volcanic horizons on the seismic reflection dataset. This will be discussed in detail in the following section on 'Stratigraphic setting'.

Basement tie on reflection data using velocity interpretations

Significant uncertainty surrounds the full extent of the JMMC, primarily to the south but also to the east and west. Of particular focus here is the southern extent of the JMMC towards the Icelandic Shelf (Fig. 1). Talwani & Eldholm (1977) and Brandsdóttir *et al.* (2015) suggested that the JMMC terminates south of the SRC (Fig. 5). However, other studies propose severely stretched and fragmented continental crust and/or exhumed altered mantle for the southernmost part of the JMMC (Gaina *et al.* 2009; Breivik *et al.* 2012; Peron-Pinvidic *et al.* 2012a; Gernigon *et al.* 2015; Torsvik *et al.* 2015). Sparse data in combination with the inherent non-uniqueness of geophysical modelling and interpretation makes this particularly challenging. To better constrain this region, the 2D seismic reflection dataset was analysed in combination with the available seismic refraction data and crustal velocity models, as well as available well control along the ridges. This enabled an interpretation of the nature of acoustic basement and different crustal type domains (Figs 4 & 5).

Seismic refraction velocity model. Three ocean-bottom seismometer (OBS) experiments have been carried out for the larger JMMC area (Fig. 2; Table 2). The JMKR-95 survey included east–west- and SW–NE- orientated profiles (Kodaira *et al.* 1998), with profile JMKR95-L4 crossing the Jan Mayen Ridge just south of DSDP borehole



THE JMMC: THE ÆGIR RIDGE TO THE KOLBEINSEY RIDGE

Leg 38 site 349. Line 8 of the OBS2000 survey lies 30 km south of that same borehole, crossing the SW end of the JMMC and the NW end of the EJMFSZ (Mjelde *et al.* 2002, 2007; Breivik *et al.* 2012). The southern extent of the JMMC onto the Iceland Plateau was investigated as part of the KRISE survey in 2000 (Brandsdóttir *et al.* 2015) (L7 on Fig. 2b). A third survey in 2006 focused on the northern region of the JMMC, consisting of a NW–SE (L1) and a north–south profile (L2) across Jan Mayen Island (Kandilarov *et al.* 2012). Refraction data from all these surveys were used to constrain the southern extent of the JMMC.

Sonobuoys deployed during a 1985 seismic reflection survey provide velocity information for the upper layers of the microcontinent (Olafsson & Gunnarsson 1989). Based on these, we were able to better constrain the igneous crust of the JMMC, especially the area within the SDR sequences. Each sonobuoy location was assigned to a velocity-profile domain and incorporated into the volcanic facies map (Table 2; Fig. 5). Distinct velocity-profile domains are defined: layered, layered-intra-basalt, layered-oceanic, oceanic basement and basement of the microcontinent. The layered domain corresponds to velocity layers within the range 1.7–3.2 km s⁻¹, which are interpreted as post-break-up sediments; velocity layers between 3.9 and 5.5 km s⁻¹ across the crest area of the JMMC, and distinct velocity interval breaks, are, however, most likely to correspond to pre-break-up sedimentary sections that correlate directly to seismic refraction data. The layered-intra-basalt domain corresponds to 270–470 m-thick basaltic layers (4–5 km s⁻¹) within the post-break-up sedimentary section (1.8–2.5 km s⁻¹) of the Jan Mayen Basin. A distinct velocity domain within the SDR area of the eastern flank is termed the layered-oceanic domain. The oceanic basement domain is characterized by thin low-velocity sediment layers (<2.5 km s⁻¹) on top of a high-velocity layer (4–5 km s⁻¹) that gradually and smoothly increases towards the base (5–6 km s⁻¹). These oceanic basement velocity domains were also compared to seismic refraction data interpretations (Breivik *et al.* 2012). One velocity profile at the crest of the JMMC is inferred to represent continental crust, as an abrupt velocity layer increase to 5.5 km s⁻¹ was recorded

below the thin post-break-up sediment cover (1.9–2.2 km s⁻¹).

Seismic velocities derived from wide-angle data were used as a basis for the depth and stratigraphic thickness estimations across the JMMC (Figs 4, 5, 6 & 7; Table 3). Relatively high-velocity values (4.4–5.6 km s⁻¹) have been assigned to the deeper layers above the acoustic basement where reflectivity is observed and interpreted as older pre-Cenozoic sedimentary sequences. This is similar to what is observed along the conjugate Norwegian Shelf, where the Mesozoic–Palaeozoic sections are usually interpreted to range between 4 and 5.5 km s⁻¹ (Mjelde *et al.* 2008, 2009).

Stratigraphic setting

The following subsections summarize the interpretations of the Palaeozoic–Cenozoic succession over the JMMC. The total thickness of interpreted sediments is variable across the area and may reach up to 18 km along the eastern flank of the JMMC. The microcontinent contains several major unconformities and related structures that are linked to the complex tectonomagmatic processes on both sides.

A type section was constructed to provide a framework for mapping unconformity horizons and stratigraphic geometries along the JMMC (Figs 4 & 8). The section is based on bathymetric, borehole and seismic refraction data, combined with a dense grid of seismic reflection data. The section is orientated north–south along the strike of the Lyngvi Ridge, a central and stable block of the JMMC (Fig. 4, LYR in Fig. 8; Table 1).

The presence of Palaeogene volcanic rocks on the JMMC makes it difficult to interpret older strata below on seismic sections. Some local uncertainties in stratigraphic correlations still exist, notably along the microcontinent's collapsed western flank and between the dislocated southern ridges. Sub-basalt sequences are only visible within the central area of the microcontinent in the vicinity of DSDP Leg 38 site 349, where seismic reflection and refraction data have been compared to the Mesozoic and Palaeozoic strata of the Jameson Land Basin area of the East Greenland margin.

Fig. 5. Volcanic facies map based on the interpretation of seismic reflection and refraction data and information from wells, in addition to free-air gravity anomaly data (DTU2010; Andersen 2010). Refraction information includes velocity profile interpretations of wide-angle data and crustal-type interpretations (modified after Funck *et al.* 2014), as well as sonobuoy velocity profile interpretations (Olafsson & Gunnarsson 1989). Magnetic anomalies C6b and C24n2r are from Gernigon *et al.* (2015), showing the onset of oceanic seafloor spreading east and west of the JMMC. The extent of landwards flows labelled 'subaerial possible' refers to the pre-break-up plateau basalt extent over the area. The areas labelled 'submarine' areas are interpreted primarily by mapping the F-reflector (Gunnarsson *et al.* 1989) and are inferred as being related to the second break-up phase during Late Oligocene.

Table 2. JMMC database and results that have been reviewed. Data and studies that have been used in this study are marked in column 'A'

A	Year	Survey ID	Survey lead	Country	Platform name	Data repository	Data types
	1957						Aeromagnetic
X	1961–1971	V2304/V2703/V2803	NAV0 L-DGO	USA USA	Vema/Conrad	NGDC	Bathymetry; magnetics; gravity; 2D multichannel reflection seismic (2D MCS) Bathymetry; magnetics; gravity; 2D MCS
X	1973	V3010	L-DEO	Norway	Vema/Conrad		Boreholes
X	1974	DSDP Leg 38	DSDP		Glomar Challenger		Bathymetry; magnetics; gravity; 2D MCS
	1975	CEPAN-75	CNEOX	France	Jean Charcot	Ifremer	Bathymetry; magnetics; gravity; 2D MCS
	1975	CEPAN-75	CNEOX	France	Jean Charcot	Ifremer	Bathymetry; magnetics; gravity; 2D MCS
	1975	CEPAN-75	CNEOX	France	Jean Charcot	Ifremer	Bathymetry; magnetics; gravity; 2D MCS
X	1975	BGR-75	BGR	Germany	Longva	BGR	2D MCS
X	1976	BGR-76	BGR	Germany	Explora	BGR	2D MCS
	1976	CGG-76	CGG	Norway			Aeromagnetic
	1977	IOS-77	UD/IOS	England	Shackleton	NGDC	2D MCS
X	1978	RC2114	CGG-76	USA	Robert Conrad	MGDS	Bathymetry; magnetics; gravity; 2D MCS2D MCS
X	1978	WGC-78	L-DGO	USA	Karen Bravo	Western-Geco	2D MCS
X	1979	J-79	NP	Norway	GECO alpha	NPD	Bathymetry; magnetics; gravity; 2D MCS
X	1980	RC2114	PAH/SGC	USSR	Akademic Kurchatov		Seafloor sampling
X	1983	RC2412	L-DGO/BGR	USA/Germany	Prospekta/Conrad		2D MCS, ESP, WA, CDP
	1983	RC2412	L-DEO	Norway	Robert D. Conrad		2D MCS and single-channel reflection seismic (2D SCS), gravimeter, magnetometer, sonar-echosounder
	1984	Arktis II/5	UHH	Germany	Polarstern	NPD	Refraction seismic
X	1985	JM-85	NP/NEA	Norway	Malene Østervold		Bathymetry; magnetics; free air gravity; Bouguer gravity; magnetic; 2D MCS
X	1985	ODP Leg 104	ODP		JOIDES Resolution		Boreholes
X	1986	UfO-86	UfO	Norway	Håkon Mosby	NPD	2D MCS
X	1987	ESP	IPP	France			ESP; velocity; gravity
X	1988	JM-88	NP/NEA	Norway	Håkon Mosby	NPD	Bathymetry; magnetics; gravity; 2D MCS; sonobuoy
X	2000	KRISE 2000	UiB	Norway	Håkon Mosby	UiB	2D MCS
X	2001	IS-JMR-01	InSeis	Norway	Polar Princess	CGGVeritas	2D MCS
X	2002	ICE-02	TGS-NOPEC	Iceland	Zephyr I	TGS-NOPEC	2D MCS; gravity
X	2003	EW0307	L-DEO	USA	Maurice Ewing	MGDS	2D MCS; gravity
X	2005	JAS-05	NGU/NPD	Norway	Piper Navajo	NGU	Aeromagnetic
X	2006	OBS JM-06	UiB/Geomar	Norway/Germany	G. O. SARS	UiB	2D MCS; gravity; magnetics
X	2008	WF-JMR-08	Wavefield InSeis	Norway	Malene Østervold	Spectrum	2D MCS
X	2008	A8-2008	HAFRO/NEA	Iceland	Ami Fridriksson	HAFRO/NEA	Multibeam
X	2009	JM-85-88	Spectrum	Norway	Re-processing	Spectrum	2D MCS
X	2009	SAR-ICE-2009	NEA	Norway	ENVISAT satellite	Fugro NPA	Satellite Synthetic Aperture Radar (SAR)
X	2010	A11-2010	HAFRO/NEA/NPD	Iceland	Ami Fridriksson	HAFRO/NEA/ NPD/Fugro	Multibeam; seafloor sampling
	2010	B11-2008	HAFRO/NEA	Iceland	Ami Fridriksson	Geolab	Benthic survey
X	2011	NPD-11	NP/UiB	Norway	Harrier Explorer	NPD/PGS	2D MCS; seafloor sampling
X	2011	JMRS11	VPBR/TGS	Norway	TGS	VPBR/TGS	Seafloor sampling
X	2012	NPD-12	NP/UiB	Norway	Nordic Explorer	NPD/PGS	2D MCS; seafloor sampling
X	2012	JAS-12	NGU/NPD/NEA	Norway	Piper Chieftrain	NGU/NPD/NEA	Aeromagnetic

THE JMMC: THE ÆGIR RIDGE TO THE KOLBEINSEY RIDGE

The Palaeozoic

Sub-basalt structures and inferred velocities along the JMMC (Fig. 4) are comparable to the Upper Palaeozoic–Lower Mesozoic rocks of the Jameson Land Basin and Traill Ø (Fig. 1a) areas onshore East Greenland, as well as of the Møre and Vøring basins offshore Norway (e.g. Surlyk *et al.* 1973; Surlyk & Noe-Nygaard 2001; Brekke *et al.* 1999; Osmundsen *et al.* 2002; Surlyk 2003; Henriksen 2008; Faleide *et al.* 2010). The inferred Palaeozoic section on the JMMC is thinner and more condensed in comparison to the East Greenland and Møre–mid-Norway areas. It can be inferred that the JMMC was at that time in a structurally higher position, corresponding to a shallow platform domain between the adjacent Jameson Land and Møre basins. Small sub-basin structures below the Cenozoic section are potentially linked to the region south of the Jameson Land Basin (Fig. 4). It remains uncertain whether older Palaeozoic, in particular Devonian and/or Carboniferous rocks similar to those that crop out along the NW edge of the Jameson Land Basin, underlie the northernmost part of the JMMC.

The Mesozoic

The interpreted Mesozoic–Paleocene interval of the JMMC has a velocity range of between 3.9 and 5.0 km s⁻¹ (Table 3) (Kodaira *et al.* 1998; Kandilarov *et al.* 2012). These are similar to velocities interpreted for Mesozoic sequences in the Møre Basin, where pre-Cretaceous–Lower Cretaceous sections show a range of values between 3.85 and 5.35 km s⁻¹ (Mjelde *et al.* 2008, 2009). Since sub-units within the Mesozoic layers cannot be identified, an average value of 4.4 km s⁻¹ is used for a time-depth conversion.

Although controversial, a seafloor sample has been interpreted to contain evidence of a Jurassic oil seep (Polteau *et al.* 2012) (NPD 2012) (Fig. 2b). Waxy bitumen samples from Cenozoic basalts on the Faroe Islands and the Isle of Skye in Scotland have also been associated with mature source rocks (Laier *et al.* 1997; Laier & Nytoft 2004).

The Jameson Land Basin contains deltaic and lacustrine facies of Early Jurassic age that became increasingly influenced by marine processes during Mid–Late Jurassic, including deposits of a black organic-rich mudstone of the Hareelv Formation (Surlyk 2003), which is consistent with the regional setting of the NE Atlantic (Stoker *et al.* 2016). Thus, a trend towards a Mesozoic marine setting in the JMMC area can be inferred from regional structural observations. That would suggest a phase of southwards and eastwards crustal thinning during the Jurassic, which, in turn, may have resulted

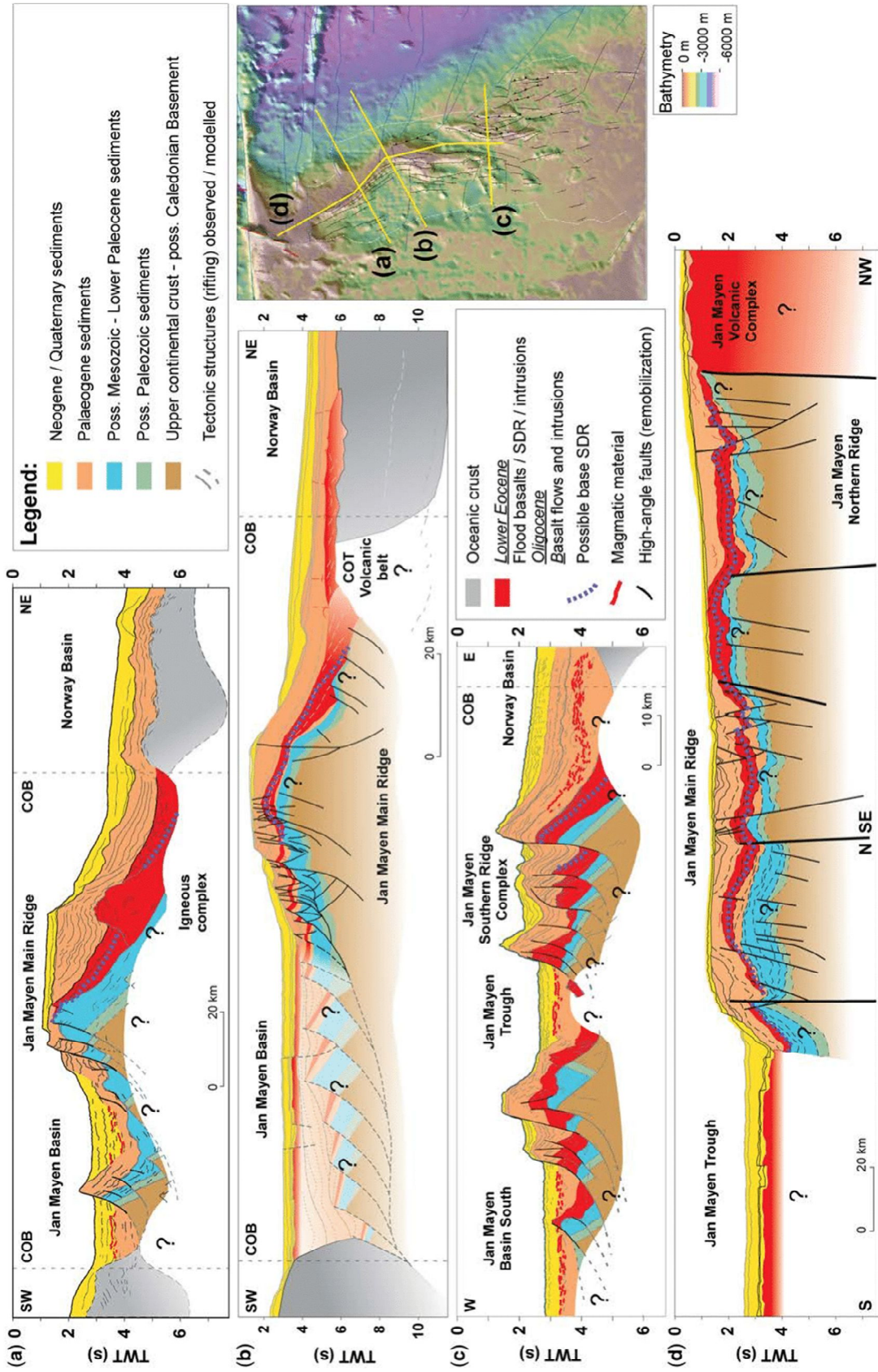
in a general subsidence of the region and the development of marine conditions (Peron-Pinvidic *et al.* 2012b).

The presence of a thin, Lower Cretaceous sedimentary succession across the JMMC seems probable according to results from a structural and stratigraphic comparison with the conjugate margins and the interpretation of the local seismic refraction data (Figs 4–6). During the Cretaceous, regional extension occurred throughout much of the NE Atlantic region (Stoker *et al.* 2016). Thick, deep-marine, sag-type basins formed during this process, including the Danmarkshavn and Thetis basins (Lundin & Doré 1997; Doré *et al.* 1999; Lundin & Doré 2011), the Traill Ø–Hold with Hope area of NE Greenland, and the Norwegian Vøring and Møre basins (Brekke 2000; Osmundsen *et al.* 2002; Faleide *et al.* 2010, 2010; Peron-Pinvidic *et al.* 2012b). However, all of the above-mentioned basins had their main extensional to hyperextensional phase during the Mesozoic, whereas the Jameson Land Basin had a main opening phase and faulting during the Palaeozoic (Henriksen 2008). Such hyperextension cannot be seen along central Eastern Greenland or the JMMC area, and possibly formed the western shelf margin of the Vøring basin.

The Cenozoic

Cenozoic sedimentary succession. The pre-break-up Cenozoic sedimentary succession was inferred by comparing onshore geological data from East Greenland to offshore areas of Scoresby Sund and Blosseville Kyst and the seismic reflection data of the JMMC. The post-break-up successions are derived from borehole data and seismic reflection data across the microcontinent, tied to the main unconformity horizons of the post-break-up succession (Figs 3, 4, 6 & 7). Mapping thickness intervals of the Cenozoic sequence along the ridge flanks and in-between the ridge segments enabled us to indicate areas of sediment deposition due to subsidence. Depositional settings for the Cenozoic strata are constrained by borehole data interpretations and onshore analogue comparisons.

Pre-break-up Cenozoic strata. *In situ* Paleocene dinoflagellate cyst assemblages were found in the uppermost pre-volcanic/pre-break-up sequences at the Blosseville Kyst area (Nøhr-Hansen & Piasecki 2002) (Figs 4, 6 & 7), which is the closest conjugate segment to the JMMC. This sequence corresponds to the upper marine sections of the Ryberg Formation in the Kangerlussuaq Basin (KgB on Fig. 1a) (Soper *et al.* 1976; Nøhr-Hansen *et al.* 2002), representing a regional marker that most likely also covered the JMMC area in the Paleocene. Dark mudstones of the Kap Brewster site (KB on Fig. 1a)



THE JMMC: THE ÆGIR RIDGE TO THE KOLBEINSEY RIDGE

contain reworked Cretaceous dinoflagellate cysts, indicating an age range between the late Danian to early Selandian (Nøhr-Hansen *et al.* 2002). Analogue areas for Lower Paleocene deposits include the Hold with Hope and Wollaston Foreland formations in Northeast Greenland (Larsen *et al.* 1999; Nøhr-Hansen 2003, 2012), and the Vøring and Møre basins offshore Norway (Brekke 2000; Faleide *et al.* 2010).

Post-break-up Cenozoic strata. The post-break-up Cenozoic sedimentary section is thickest along the microcontinent's eastern flank (Figs 5, 6 & 8), but has been eroded to a large extent across the highest sections of the ridges (e.g. the Lyngvi Ridge). Based on data from DSDP Leg 38 boreholes located on the northern Jan Mayen Ridge (Talwani *et al.* 1976b; Talwani & Eldholm 1977), the Cenozoic succession has been subdivided into a Lower Paleocene–Lower Oligocene unit, unconformably overlain by an Upper Oligocene–Quaternary unit (Figs 6 & 7).

The stratigraphic thickness of post-break-up sediments varies from 0 to 4200 m along the eastern flank of the JMMC (Fig. 8). The Cenozoic units consist predominantly of mudstone, whereas the Lower Paleocene–Lower Oligocene unit includes thin sand and muddy sand beds, which might have been deposited by turbidity currents on the JMMC shelf edge (Figs 3 & 7). The Upper Oligocene–Miocene units probably represent erosional sediments from the JMMC highs, redeposited into the surrounding lows. This can be seen around the highs of the SRC and its small sub-basins and in the borehole records (Talwani *et al.* 1976b; Talwani & Eldholm 1977). Above the Mid-Upper Miocene hiatus, Pliocene–Pleistocene deep-marine sediments are present across the microcontinent (Fig. 3). These youngest sediments are cut by deep-sea current features, causing localized erosion along the ridge segments, and were affected by gravitational slumping and faulting from the steep ridge flanks.

During the Pleistocene, several glacial events removed about 1 km of the Iceland Plateau basalts (Walker 1964) and much of the JMMC. The eroded sediments were likely to have been deposited into newly formed basins within the Iceland Plateau (Figs 5 & 9b), between the Iceland shelf and the SRC.

The Cenozoic igneous sequence

The Lower Palaeogene volcanic succession probably includes two major units: the pre-break-up plateau basalt sequence; and the break-up SDR sequence along the eastern flank of the JMMC (Planke *et al.* 2000) (Figs 4, 6 & 7). The southern and central part of the JMMC appear to be covered by Early Eocene plateau basalts, with a layered character of distinct lava-flow events interpreted as landwards flows (Planke *et al.* 2000). Apparent erosional effects at the top of these formations are probably filled with Lower Eocene sediments.

The pre-break-up igneous formations. The plateau basalt equivalent section on the JMMC is subdivided into two major units and appears to increase in thickness from north to south towards the SRC (Fig. 7c). A possible base of the plateau basalts was tied to the velocity model from refraction data (Kodaira *et al.* 1998). From this, an igneous stratigraphic thickness of approximately 1100 m is estimated across the crest of the JMMC. There are indications that the plateau basalt sequence continues to be downfaulted towards the south (Fig. 4), implying the formation of a topographical low south of the SRC (Figs 10 & 11a). This would possibly correlate with the very thick basalt sections in the Kangerlussuaq Basin, at the southernmost extent of the Blosseville Kyst, and the NW area of the Faroe Islands Platform (FP on Fig. 1a). In these regions, the main pre-break-up to break-up phase plateau basalts are well exposed onshore. The succession is estimated to be more than 6 km thick towards the southern extent of the Blosseville Kyst and the Kangerlussuaq area (Brooks 2011), but is progressively younger and dramatically thinner to the north in Scoresby Sund and Jameson Land Basin (Larsen *et al.* 1999, 2014). Based on age dating of exposed dykes that have similar ages to the plateau basalts (Larsen *et al.* 2014), it is inferred that the plateau basalts covered the Jameson Land Basin but were subsequently eroded away. The thickness of the eroded section is estimated at 2–3 km (Mathiesen *et al.* 2000).

The break-up igneous formations. During break-up (54–55 Ma), a magma-rich margin formed along the eastern flank of the JMMC with thick sequences of onlapping lava flows forming SDRs (Figs 4, 5 & 7).

Fig. 6. JMMC tectonostratigraphic type sections that are based on seismic reflection and refraction data interpretations, tied to shallow borehole data only. Possible Palaeozoic–Mesozoic formations of the JMMC are inferred from the structural and stratigraphic setting in comparison to the East Greenland analogue areas (Hamann *et al.* 2005). Seismic velocity models from refraction data are consistent with interpretation. Modified from Peron-Pinvidic *et al.* (2012a, b) and Blischke *et al.* (2014b). The volcanic margin is clear (see the sections in a–c) along the eastern flank of the microcontinent. The magmatic anomaly poor western margin that was formed during the second break-up (d) appears as a sharp boundary along the western margin of the microcontinent.

Jan Mayen microcontinent - General Stratigraphic Chart

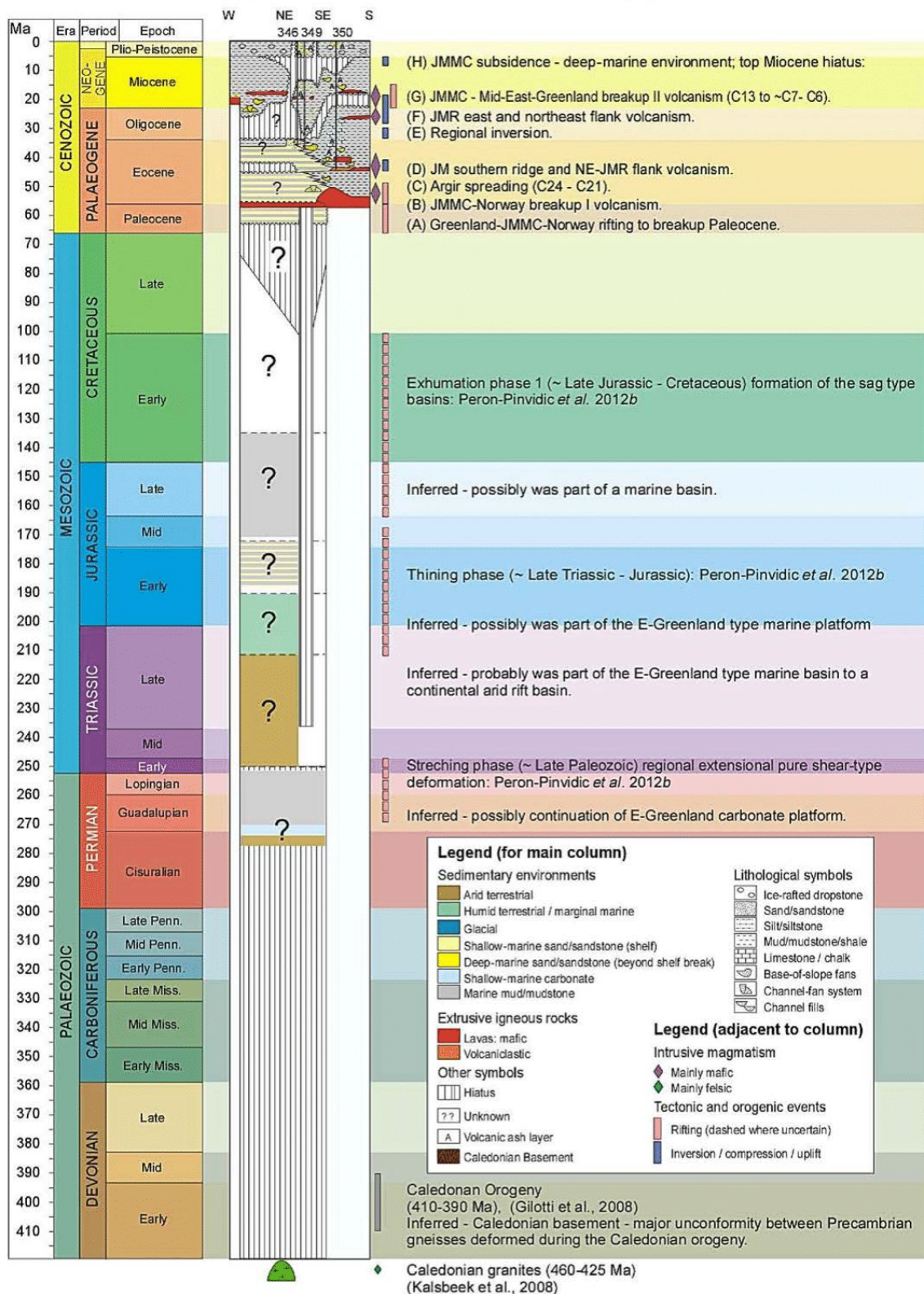


Fig. 7. Tectonostratigraphic chart of the JMMC region based on borehole data, seismic interpretation and analogue studies (Talwani & Eldholm 1977; Åkermoen 1989; Gunnarsson *et al.* 1989; Rey *et al.* 2003; Harðarsson *et al.* 2008;

THE JMMC: THE ÆGIR RIDGE TO THE KOLBEINSEY RIDGE

These SDRs are considered to be subaerial lava flows onlapping higher terranes, stacking onto previous flows as rifting and seafloor spreading initiated along the margins (Hinz 1981; Mutter *et al.* 1982; Planke *et al.* 2000; Berndt *et al.* 2001). The SDRs along the eastern flank onlap westwards onto the crest of the main ridge and the SRC: they are up to 4–6 km thick at the NE end of the JMMC, thinning from north to south.

*The Mid-Eocene–Neogene
volcanostratigraphy*

The Eocene sedimentary succession is intruded by many sills and dykes, especially along the eastern and SE flanks, coinciding with the Early–Middle Eocene time (49–44 Ma). During this period, igneous activity affected the entire southern extent of the microcontinent. The occurrence of a series of ridge jumps from east to west across the Iceland Plateau have been suggested by several authors (e.g. Gaina *et al.* 2009; Brandsdóttir *et al.* 2015) (Figs 5 & 9). The youngest substantial igneous event on the JMMC is expressed as a flat-lying, opaque reflection in seismic data, the so called ‘F-Reflector’ (Gunnarsson *et al.* 1989), which covers most of the northern Jan Mayen Basin, the western margin of the JMMC (Fig. 6b, c) and much of the Jan Mayen Trough (Figs 5 & 6d). This reflection is believed to correspond to regionally extensive composite sheets of flat-lying lava flows and intrusive rocks that covered the underlying structures in very shallow and unconsolidated wet sediment possibly during the Late Oligocene (28–22 Ma) (Gunnarsson *et al.* 1989). This corresponds to the time of plate boundary relocation from the Ægir mid-oceanic ridge to the Kolbeinsey mid-oceanic ridge (Gaina *et al.* 2009). No SDR type formations are observed along the JMMC western margin. Since the complete separation from the East Greenland margin, only the northern extent of the JMMC has been

affected by volcanic activity, which is related to the present-day Jan Mayen Island volcanic system.

**Kinematic reconstruction of the central
NE Atlantic region**

A series of detailed kinematic reconstructions for the JMMC tectonic blocks and surrounding areas is presented in Figures 10 and 11. Plate reconstruction parameters for the relative motion of the JMMC and conjugate margins were calculated using an interactive fitting method using GPlates (<http://www.gplates.org>; Boyden *et al.* 2011; see also Gaina *et al.* 2016). Rotation parameters for Greenland relative to Eurasia are based on Gaina *et al.* (2016). The geographical extent of the individual JMMC tectonic blocks was guided by the interpretation of Peron-Pinvidic *et al.* (2012a) and Gernigon *et al.* (2015).

The model includes six stages: (1) the pre-break-up stage ending at 56–55 Ma; (2) the break-up stage at chron C24n2r (53.36 Ma) equivalent to chron C24B of Gunnarsson *et al.* (1989), associated with the formation of a wide volcanic margin; (3) an early intra-JMMC rifting phase around C22n (49.3 Ma); (4) a fully established intra-JMMC rift phase and the beginning of rift transfer from east to west around C21n (47.33 Ma); (5) westwards rift transfer and the initial western JMMC margin break-up phase around C13n (33.1 Ma); and (6) the complete isolation of JMMC by establishing the Kolbeinsey mid-oceanic ridge around C6b (21.56 Ma).

*Structural elements included in plate tectonic
reconstructions*

We combined magnetic and gravity anomaly data interpretations with other structural, geological and geophysical data for defining several distinct

Fig. 7. (Continued) Gilotti *et al.* 2008; Kalsbeek *et al.* 2008; Gaina *et al.* 2009; Erlendsson 2010; Gernigon *et al.* 2012, 2015; Peron-Pinvidic *et al.* 2012a, b; Stoker *et al.* 2016). The chronostratigraphic scheme is based on Gradstein *et al.* 2012. The pre-break-up stratigraphic section is inferred from seismic data and analogue comparisons, primarily the Jameson Land Basin, East Greenland. (a) Greenland–JMMC–Norway rifting to break-up. (b) JMMC–Norway break-up I volcanism: emplacement of the plateau basalts, SDR, dyke complexes. (c) Aegir spreading (C24–C21): extension along the JMMC–mid-East Greenland rift. (d) JM southern ridge and NE–JMR flank volcanism. (e) Regional inversion causing an erosional hiatus across the main ridges, localized erosion into surrounding lows as marine fan–turbidite deposits, and minor reverse faulting. (f) JMR east and NE flank volcanism. (g) JMMC–mid-East Greenland break-up II volcanism (C13; c. C7–C6): the formation of composite sheets of flat-lying, shallow intrusions and lavas into shallow soft sediment (the F-reflector), and fault-connected dykes and sill intrusions simultaneously with the establishment of oceanic crust from the Kolbeinsey mid-oceanic ridge and formation of the Jan Mayen Basin. At this time, erosion along the Southern Ridge Complex occurred. (h) JMMC subsidence and establishment of a deep-marine environment. The Kolbeinsey mid-oceanic ridge continues to establish itself as the main spreading centre. Sedimentary sequences include ash layers. The top Miocene hiatus was possibly caused by regional uplift in conjunction with west to east migration of the main rift axis on Iceland.

Table 3. Reflection seismic interval velocity estimates used for building a time-depth conversion model based on refraction data interpretations

Seismic intervals	OBS model (Kodaira <i>et al.</i> 1998)	OBS model (Kandilarov <i>et al.</i> 2012)	Velocity data used for time-depth conversion	Estimated stratigraphic thickness across the JMMC	Estimated stratigraphic thickness OBS model Figure 4 intersection
	P-wave model layer	V_p (km s^{-1})	V_p (km s^{-1})	Thickness ranges (km)	TST estimate (km)
Seabed					
Plio-Pleistocene			1.49	0–3.2	0.95
Late Oligocene–Early-Miocene			1.8	0.1–1.1	0.06
Early Oligocene			2.0	0–1.05	0.09
Late Eocene			2.3	0–2.05	0.29
Mid-Eocene					
Basalts–Early Eocene			3.0	0–2.84	0.65
Early–Mid Paleocene			4.0	0–6	1.48
Possible Mesozoic			4.4	0–4.5	2.25
Possible Palaeozoic					
			5.2	0–4	3.82
<i>Estimated stratigraphic and igneous section thickness above Caledonian basement:</i>					
Possible Caledonian Basement			5.6	0–15	8.64
Continental lower crust – sub-basalt			6.8	0–10	2.79
					2.96
<i>Estimated stratigraphic, igneous section, and crustal stratigraphic thickness:</i>					
					14.4

Displayed are the possible stratigraphic thickness ranges across the highly variable mapped JMMC, and one specific stratigraphic thickness profile for the reflection seismic data intersection with the OBS model by Kodaira *et al.* (1998).

THE JMMC: THE ÆGIR RIDGE TO THE KOLBEINSEY RIDGE

structural elements that constitute independent kinematic model blocks (isochrons and rotation model, see Gaina *et al.* 2016). Interpreted fault and transfer systems are linked to stratigraphic thickness changes, mapped unconformities, age data control from borehole data and other geological information. Reconstructions include the present-day coastline for better reference (Figs 10 & 11).

We have compiled a number of structural lineaments in the JMMC area, which are based on published work, bathymetry, free-air gravity anomaly and derivatives, magnetic anomaly (Hopper *et al.* 2014), and seismic reflection data. These proposed structural lineaments (Fig. 1a) are based on features that can be inferred from at least two, and preferably three, different potential datasets.

We consider several observations that may give information on how the JMMC evolved during the multiphased break-up. Along the eastern margin, Palaeogene rocks dip steeply towards the Norway Basin (Fig. 6) and exhibit normal faulting associated with rapid subsidence within the northern and southern eastern-flank basin (EFBN and EFBS in Fig. 8; Table 1), in association with SDR emplacement and the early establishment of the Ægir mid-oceanic ridge system. The western margin, along the Jan Mayen Ridge North, the Sörlahryggur Flank Basin and the Sörlahryggur Ridge (JMRN, SFB, SHR in Fig. 8; Table 1), displays a more gentle west-facing listric normal fault system (Fig. 6), where rotated crustal blocks are downfaulted towards the Jan Mayen Basin (JMB in Fig. 8; Table 1) along major detachment faults. This indicates a distinct phase of extension and basin formation before the final break-up of the JMMC to the west. In addition, some minor reverse faulting occurred along the SE segments within the SRC, including the Fáfñir Ridge, the Otur Ridge, the Otur Ridge southern spur, the Langabrún Ridge and the Dreki Ridge (FR, OR, ORS, LR and DR in Figs 6 & 8; Table 1), as a result of regional inversion during the Late Eocene–Early Miocene.

Stratigraphic unconformities represent major tectonostratigraphic markers. Several major and small-scale unconformities in the JMMC stratigraphy have been described (Figs 3, 4 & 7). Three unconformities are present within Eocene sections: (1) an Early Eocene main break-up unconformity at C24 (56–53 Ma); (2) a main Middle Eocene unconformity at C19–C20 (47–41 Ma) associated with the initiation of ridge transition from the Ægir mid-oceanic ridge to extension concentrated further west; and (3) an unconformity of the Late Eocene age at chron C15 (*c.* 35 Ma). Following these Eocene events, two major erosional events affected the microcontinent during the Oligocene. An unconformity that marks a major truncation surface at 33 Ma (C12–C11) can be observed across

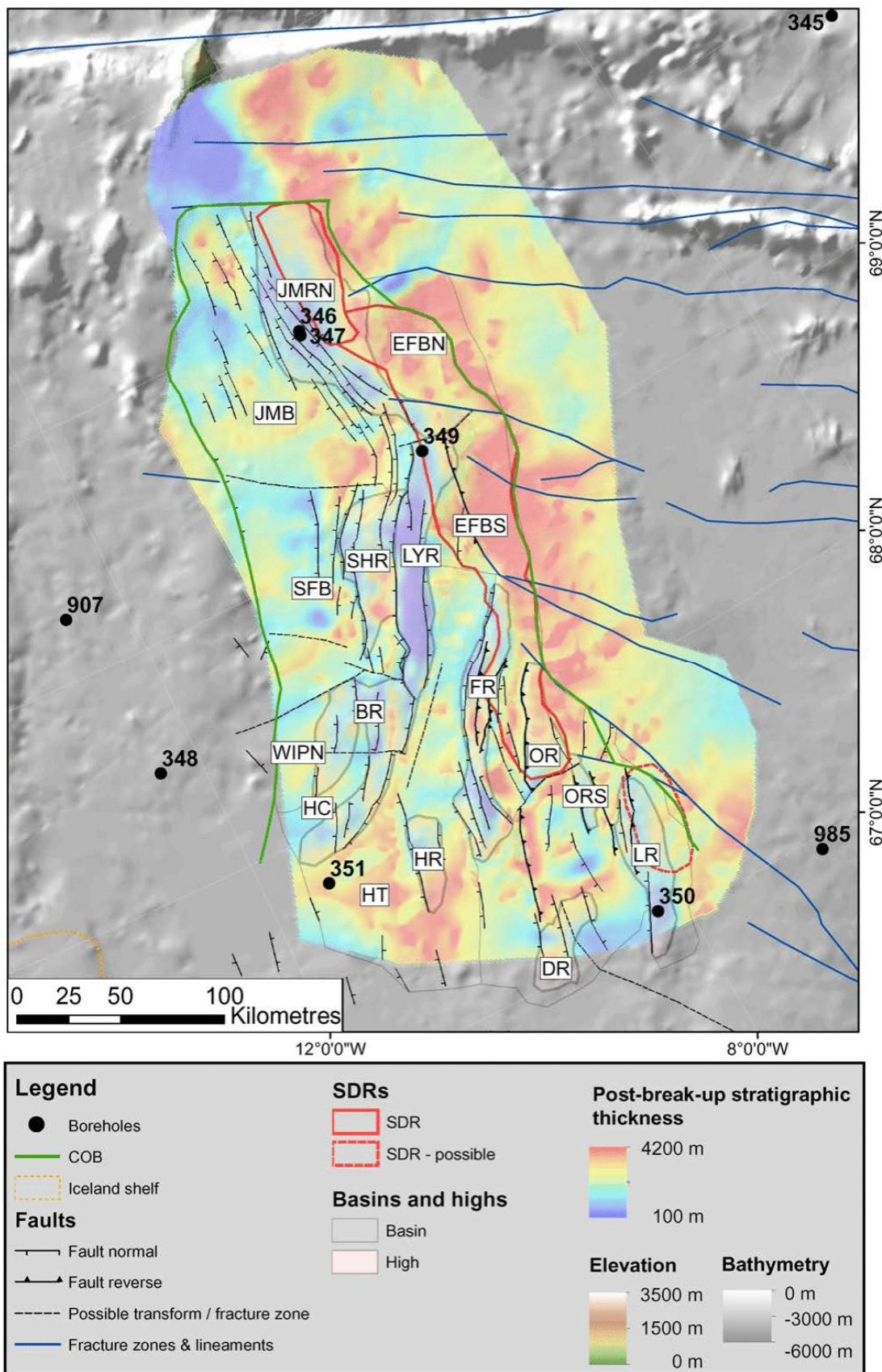
all ridge areas of the microcontinent and correlates to a change in the seafloor spreading direction along the Ægir mid-oceanic ridge axis before the cessation of the mid-oceanic ridge (Gernigon *et al.* 2015) (Fig. 11d). This transtensional phase resulted in small-scale reverse faulting across the SRC. A second unconformity marks a major hiatus in the Late Oligocene, which corresponds to the complete cessation of the Ægir mid-oceanic ridge. The microcontinent was isolated completely, as the Kolbeinsey mid-oceanic ridge became fully established along the western margin at chron C6b (22–21 Ma) (Fig. 11e).

Pre-break-up stage ending around 56–55 Ma

Major structural elements and subdivisions of the JMMC at pre-break-up time align fairly well with published regional trends and lineaments interpreted on the NE Atlantic continental margins (Hamann *et al.* 2005; Tsikalas *et al.* 2005, 2008; Vogt & Jung 2009; Gaina *et al.* 2009, 2013; Gernigon *et al.* 2012, 2015) (Fig. 10). Three main trends are observed (Fig. 10): (1) a north–south trend similar to the strike-slip fault systems of the Shetland Islands, which is also aligned with the Jameson Land Basin axis and the main boundary fault of the Liverpool Land High; (2) an east–west trend parallel to the strike-slip fault system proposed by Guarnieri (2015), forming the northern limit of the Faroe–Shetland region; and (3) a SE–NW trend that separates the JMMC from the Vøring margin to the north and the Faroe Islands region to the south. The latter two subdivisions also form the boundaries of several gaps in the reconstructions shown by Gaina *et al.* (2016).

At pre-break-up time, the JMMC was most probably a 40–100 km-wide crustal fragment, with stratigraphic and crustal geometries corresponding to the conjugate central East Greenland margin (Gaina *et al.* 2009; Gernigon *et al.* 2015) (Figs 1a, 10 & 11). The JMMC was bounded to the north by the proto-Jan Mayen Fracture Zone (proto-JMFZ in Fig. 10). The northern segment of the microcontinent near the proto-JMFZ that could be mapped shows stratigraphic and structural similarities with the Scoresby Sund and Blosseville Kyst areas.

The NNW–SSE-orientated axis of the Jameson Land Basin terminates abruptly at the Blosseville Kyst (Engkilde & Surlyk 2003), with no major east–west-striking fault structures marking its southern boundary in the Scoresby Sund area. This indicates that a deep basin may continue south underneath the Blosseville Kyst. The kinematic models here suggest that the central and southern JMMC were attached to that part of East Greenland prior to break-up, with the NNW–SSE-striking Liverpool Land high lining up with



THE JMMC: THE ÆGIR RIDGE TO THE KOLBEINSEY RIDGE

the northern Lyngvi Ridge, the central high of the JMMC (Fig. 8).

The southern boundary is less clear, but was probably influenced by the large-scale transform system proposed by Guarnieri (2015). This, in turn, was linked to the development of the Greenland–Iceland–Faroe Ridge Complex, a subdomain of the North Atlantic Igneous Province. The GIFRC forms a complex WNW–ESE-striking ridge structure that includes the Greenland–Iceland Ridge, the entire Iceland shelf and the Iceland–Faeroe Ridge.

The southernmost part of the microcontinent, where East Greenland links to the Faroe Platform and the Hatton Bank, remains far more uncertain owing to a lack of data constraints (Breivik *et al.* 2012; Brandsdóttir *et al.* 2015; Gernigon *et al.* 2015; Torsvik *et al.* 2015). Still, the stratigraphic mapping of the JMMC (event B in Fig. 7) suggests a potential link between the southern extent of the JMMC and the pre-break-up/break-up successions along the Blossville Kyst of central East Greenland margin, the NW margin of the Faroe Platform and the northern edge of the Iceland Faroe Ridge (Figs 10 & 11a). The interpretation of seismic reflection data across the central part of the JMMC indicates two possible Early Eocene plateau basalt-equivalent sections that appear to increase in thickness from north to south (Fig. 4).

A gap in our pre-break-up reconstruction situated to the south of the JMMC is assumed to have been filled by either stretched continental crust (Torsvik *et al.* 2015) and/or pre-break-up formations of Palaeozoic–Early Paleocene age, similar to those known from onshore East Greenland and the Norwegian shelf margin (Brekke 2000).

Break-up stage around C24n2r (53.36 Ma)

The break-up stage (Fig. 11a and event (C) in Fig. 7) is marked by large-scale extrusive volcanism leading to the formation of the plateau basalts onshore East Greenland (Storey *et al.* 2007a, b). The plateau basalts mapped extend from East Greenland and across the Faroe Islands area. They have an estimated thickness of more than 6 km in East Greenland (Brooks 2011 and over 7 km at the Faroe Islands (Árting 2014).

The main structural elements of the JMMC are parallel to the overall trends of the basins and highs of the surrounding regions, except for the

east Jan Mayen Fracture Zone, which appears to be linked to an initial rift centre just at the NW edge of the JMMC, as proposed by Gaina *et al.* (2009). This coincides with the formation of SDR sequences along the eastern margin, which reach a stratigraphic thickness of 4–6 km at the northeasternmost flank (Figs 4 & 5).

Early Eocene (53.36 Ma) volcanism marks the establishment of the Ægir mid-ocean ridge system at C24n2r (e.g. Gernigon *et al.* 2015), separating the mid-Norwegian Vøring and Møre basins from the Central East Greenland margin. Large igneous complexes were mapped on seismic reflection data along the eastern flank of the JMMC located close to fracture/fault zones (Figs 7a, b & 9). These complexes most probably formed after the initial emplacement of SDR sequences, cutting through that sequence and the initial oceanic crust, forming a 40–80 km-wide volcanic margin (Fig. 5) as Eocene sediments onlap and fill in those features.

Initial intra-JMMC rifting phase around C22n (49.3 Ma)

The initial intra-JMMC rifting phase at chron C22n (49.3 Ma; Fig. 11b) is marked by the southwards propagation of the Ægir mid-oceanic ridge and the establishment of a continuous spreading system in the Norway Basin. The EJMFZ extends from the Mohn's mid-oceanic ridge, which was established to the NE of the JMMC at C24 and separated the Vøring margin from the NE Greenland margin. A distinct rift segment can be seen along the SE margin of the JMMC, forming the eastern extent of the Iceland Plateau, here referred to as Iceland Plateau rift I (IPR-I; Fig. 11b, c). During the Lower Eocene, thick sediment wedges formed along the central eastern and NE flank of the microcontinent (Figs 7 & 8).

An uneven north to south change in spreading rate from intermediate to slow (Gernigon *et al.* 2015) led to oblique spreading within the Norway Basin, initiating a V-shaped mid-oceanic ridge structure and a counterclockwise rotation of the JMMC. This resulted in extension of the entire southern half of the microcontinent and the formation of small ridge segments. This extension widened the area across the southern half of the microcontinent from the original 100 km to approximately 150 km. This also explains the crustal

Fig. 8. Post-break-up stratigraphic thickness map includes estimates from the Lower Eocene (top SDR/flood basalts) to present day. The main ridges are heavily eroded and have only a very thin sediment cover. The low areas along the east flank show a very thick stratigraphic section. The thicker stratigraphic sections along the west flank of the ridge are related to the Jan Mayen Basin, as well as to several lows between the main structural highs. The stratigraphic thinning towards the Jan Mayen Island volcanic complex to the north and towards the south, and the area of borehole 350, where the Iceland Plateau Rift is proposed. For an explanation of abbreviations, see Table 1.

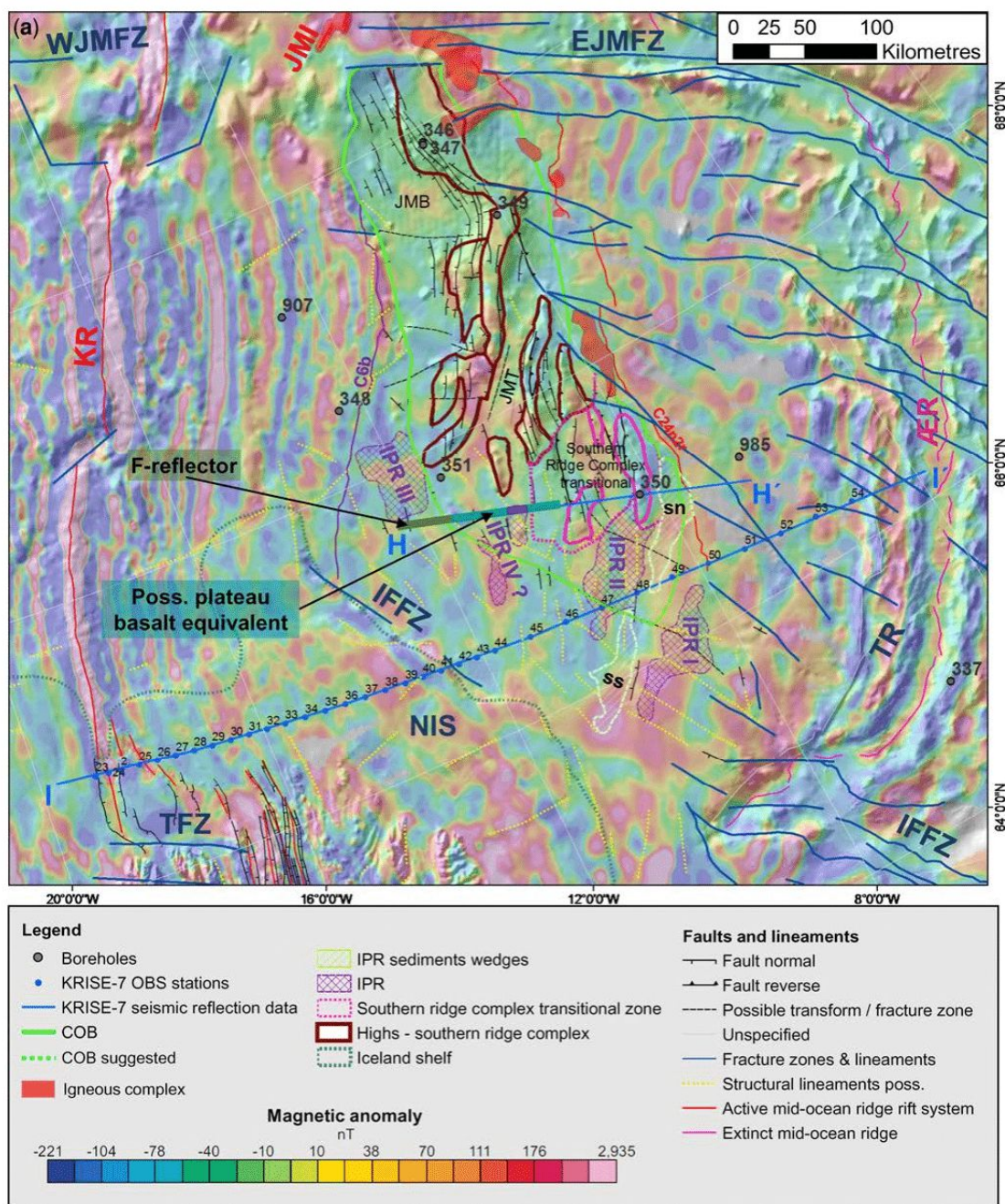


Fig. 9. Structure and volcanic elements map (a) of the JMMC and the Iceland Plateau. The proposed Iceland Plateau rifts I, II and III (IPR I, IPR II and IPR III) are interpreted on seismic reflection data. Gravity and magnetic anomalies are linked to segments of older microcontinent transitional crust 'Southern Ridge Complex transition', pre-break-up plateau basalts segments and youngest second break-up volcanics 'F-marker'. The Iceland Plateau rift II was described by Brandsdóttir *et al.* (2015) based on interpretation of seismic refraction data. The sediment wedges (sn and ss) correspond to observations on seismic refraction data (in b) and correlate to negative gravity anomalies west of the COB. Interpreted profiles.

thinning trend from north to south that has been observed on refraction data in the JMMC area (Kandilarov *et al.* 2012).

The Ægir mid-oceanic ridge system did not directly link up with the Reykjanes mid-oceanic

ridge system to the south. Instead, the link to the Reykjanes mid-oceanic ridge was marked by a complex system of transforms and off-ridge volcanic systems that formed an Iceland-type oceanic crust within the proto-GIFRC (Árting 2014). In order to

THE JMMC: THE ÆGIR RIDGE TO THE KOLBEINSEY RIDGE

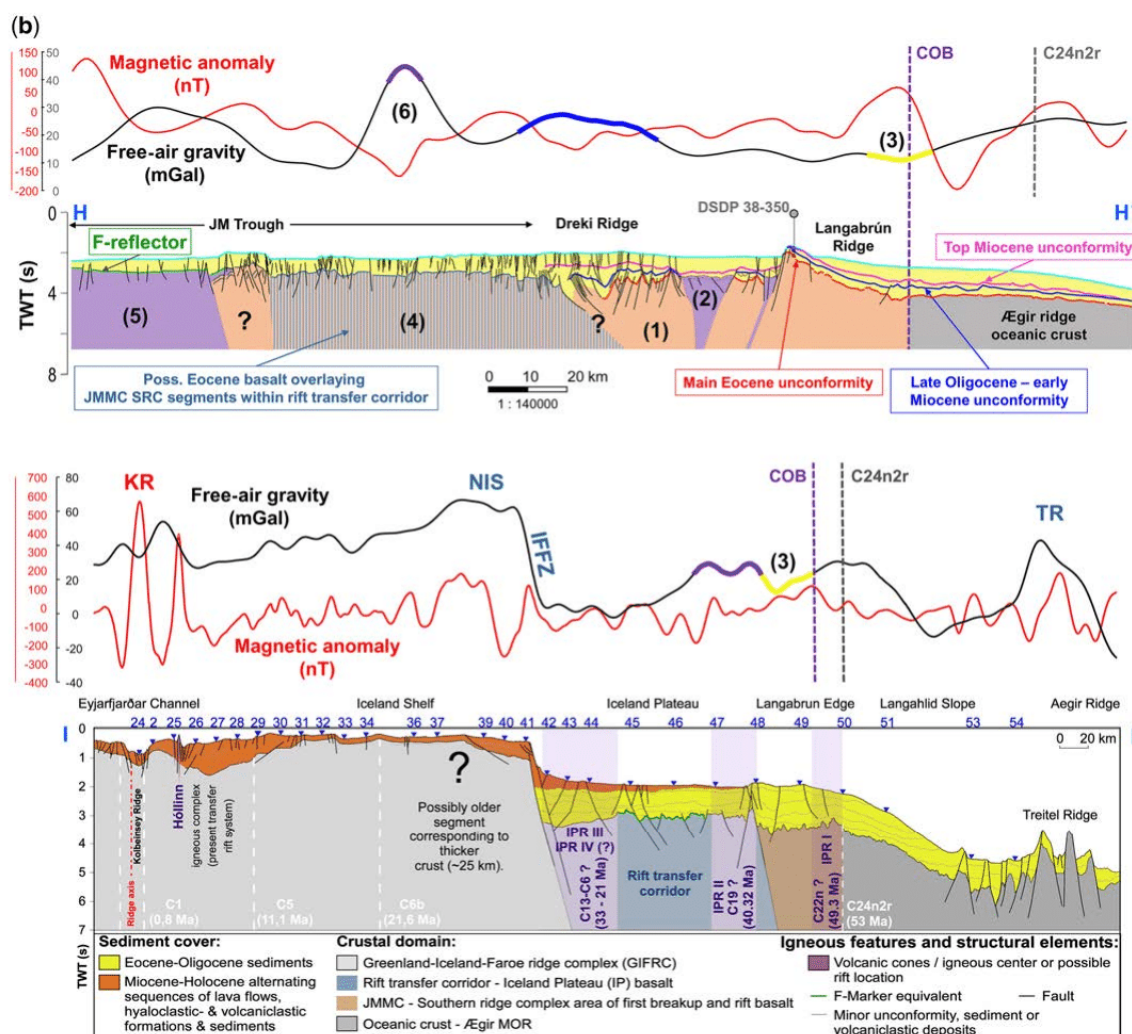


Fig. 9. (b) I–I' from Brandsdóttir *et al.* (2015) and H–H' across the SRC. The H–H' profile based on TGS seismic reflection data crosses the southernmost area where the SRC is clearly observed and ties to DSDP site 350. Section H–H' has several areas marked to explain the subdivision of the mapped structures: (1) The Dreki Ridge transfer system (possibly active from the Mid-Eocene to Oligocene with Miocene infill). (2) A graben structure that separated the Eocene ridges of the SRC. The strike of the graben is parallel to the Iceland Plateau rift II structure. (3) A sediment wedge that is thickest close to the COB. This is observed along the entire eastern edge of the JMMC and helps to define the COB location. (4) Areas where deep faulting appears absent and structures are distinctly different from elsewhere. A basalt cover is indicated, possibly equivalent to the plateau basalts. (5) A typical section where the F-reflector is observed and is connected to IPR III. (6) A positive gravity anomaly that might be related to another possible rift complex, but not confirmed on seismic reflection data. A clear signature on the magnetic anomaly data (Fig. 9a) south of intersection H–H' is observed, however. Section I–I' shows the Iceland Plateau rift between the Langabrunn Edge and the Iceland Shelf. It includes a segment of thick crust between the C6 magnetic chron just west of the youngest rift system on NE Iceland (the Eyjarfjarðar Channel/Kolbeinsey mid-oceanic ridge).

maintain a spatial balance within the reconstruction, the areas of the Iceland Plateau and East Iceland must have been involved in this early stage of break-up, forming new basaltic crust and possibly SDR overlying older crust segments that remain as segments in-between off-mid-oceanic ridge volcanic segments (Erlendsson & Blischke 2013; Blischke *et al.* 2014b).

Fully established intra-JMMC rift phase and the beginning of rift migration around C21n: 47.33 Ma

The oblique seafloor spreading direction recorded by the Norway Basin oceanic crust caused large strike-slip/transfer fault systems that affected the eastern flank of the microcontinent (event D on

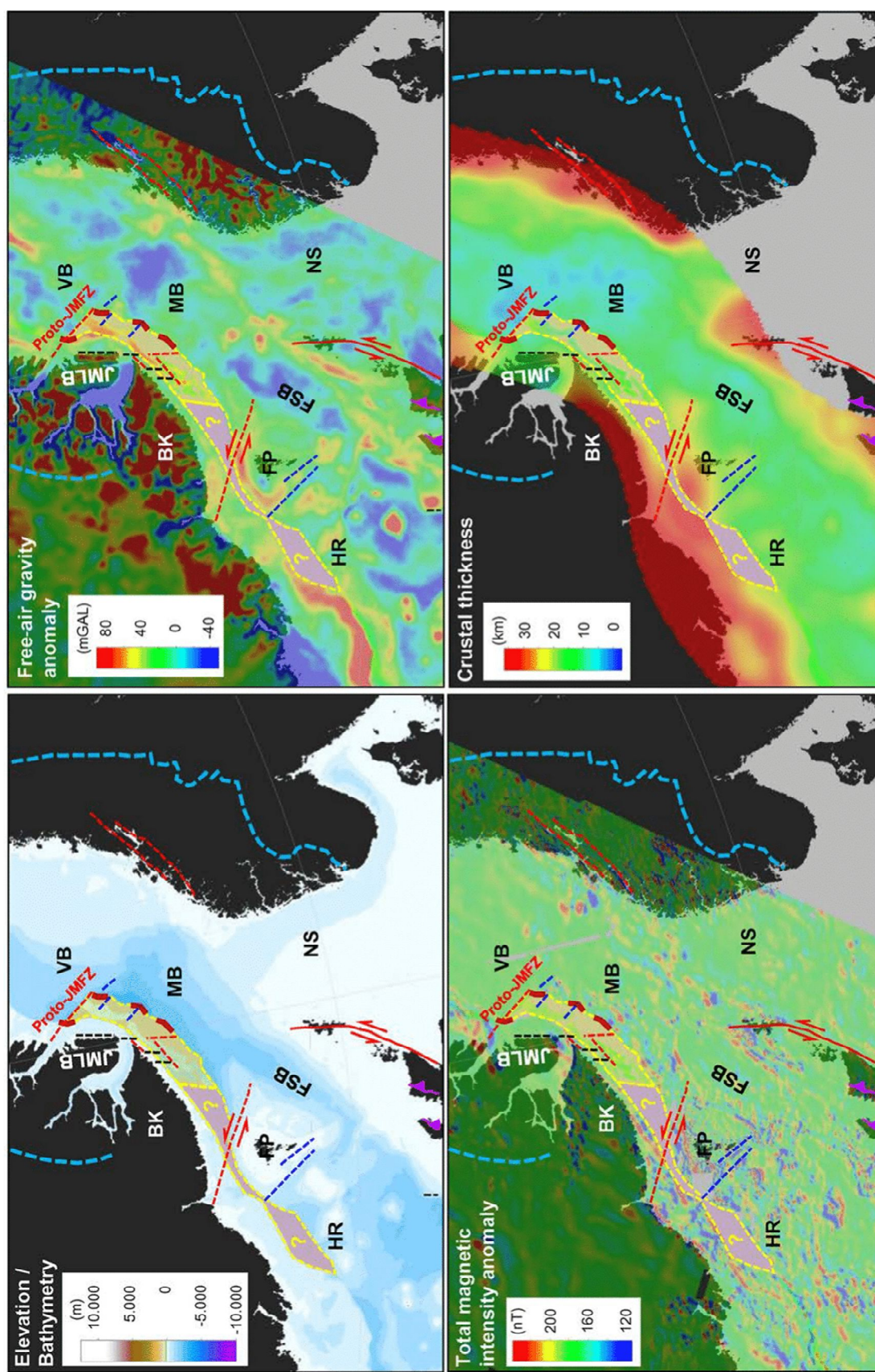


Fig. 10. Continued

THE JMMC: THE ÆGIR RIDGE TO THE KOLBEINSEY RIDGE

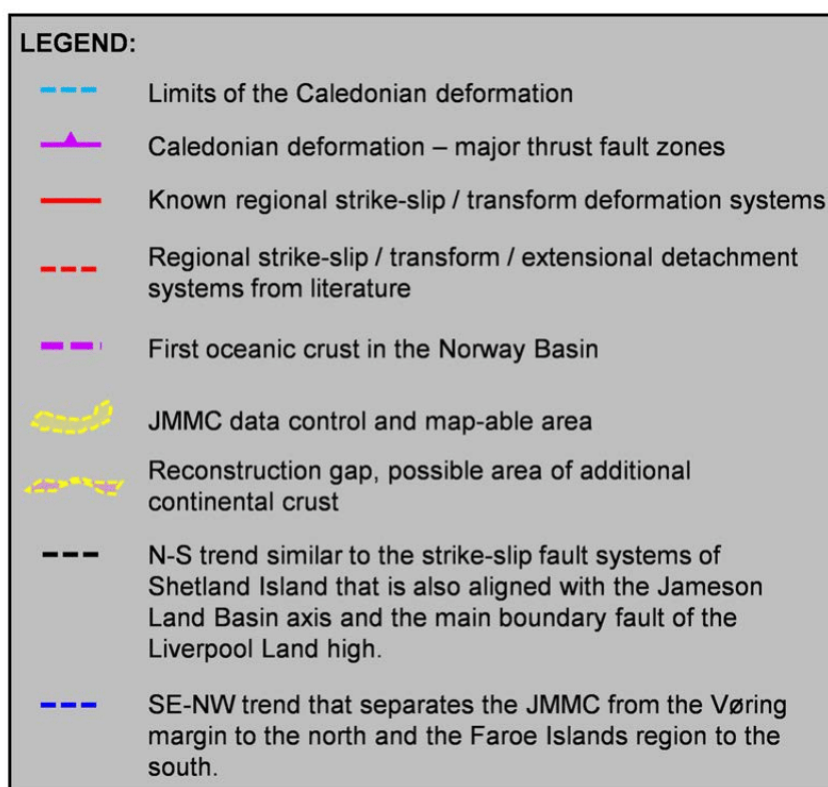


Fig. 10. Pre-break-up setting of the central NE Atlantic region, showing reconstructed present-day bathymetry, magnetic, gravity and crustal thickness data. Crustal thickness is based on the gravity inversion (Funck *et al.* 2014). The reconstruction is at pre-break-up stage ending at 56–55 Ma and is fixed to the European Plate. Features displayed are modified from data, and interpretations by Osmundsen & Andersen (2001), Torsvik *et al.* (2001), Foulger *et al.* (2005), Henriksen (2008), Gaina *et al.* (2009), Boyden *et al.* (2011), Peron-Pinvidic *et al.* (2012a, 2013), Gasser (2014), Hopper *et al.* (2014), Gernigon *et al.* (2015), Guarnieri (2015) and Torsvik *et al.* (2001, 2015). Regions marked are: BK, Blosseville Kyst; FP, Faroe Plateau; FSB, Faroe–Shetland Basin; HR, Hatton–Rockall margin and basin; JLB, Jameson Land Basin; MB, Møre Basin; NS, North Sea; VB, Vøring Basin.

Fig. 7) and subdivided the JMMC into the northern Jan Mayen Ridge and the SRC. The Ægir mid-oceanic ridge appears to terminate at the GIFRC (Fig. 11c).

A series of en echelon magnetic anomalies across the Iceland Plateau, referred to as the Iceland Plateau Rift System (Fig. 11c), is interpreted as marking the onset of a propagating rift system towards the Ægir mid-oceanic ridge (Figs 5 & 9). A NW–SE-striking fault system that links up to the Iceland–Faroe Fracture Zone and terminates the north–south fault trend of the SRC, marks the southern extent of the microcontinent. The NW–SE-striking fault system is in direct alignment with the volcanically active area of the Blosseville Kyst (F on Fig. 11c), where a major coast-parallel dyke swarm belonging to the Igtertivå Formation magmatism is thought to have been caused by a regional extensional event at 49–44 Ma (Larsen *et al.* 2013).

This event is also marked by a distinct unconformity, where the base consists of sediments that are dated to 49.09 ± 0.48 Ma and the top is formed by sediments intercalated with lava flows of the Bopladsdalen Formation, which are dated to 43.77 ± 1.08 Ma (Larsen *et al.* 2013). This Late–Middle Eocene time interval (49–44 Ma) coincides with an increase in observed sills and intrusions within the sediment stratigraphy (Fig. 8) of the JMMC area.

Westwards rift transfer and the initial western JMMC margin break-up phase around C13n: 33.1 Ma

By chron C13n (33.2 Ma), the Norway Basin seafloor spreading had changed from slow to ultra-slow spreading (Gernigon *et al.* 2015), while, on

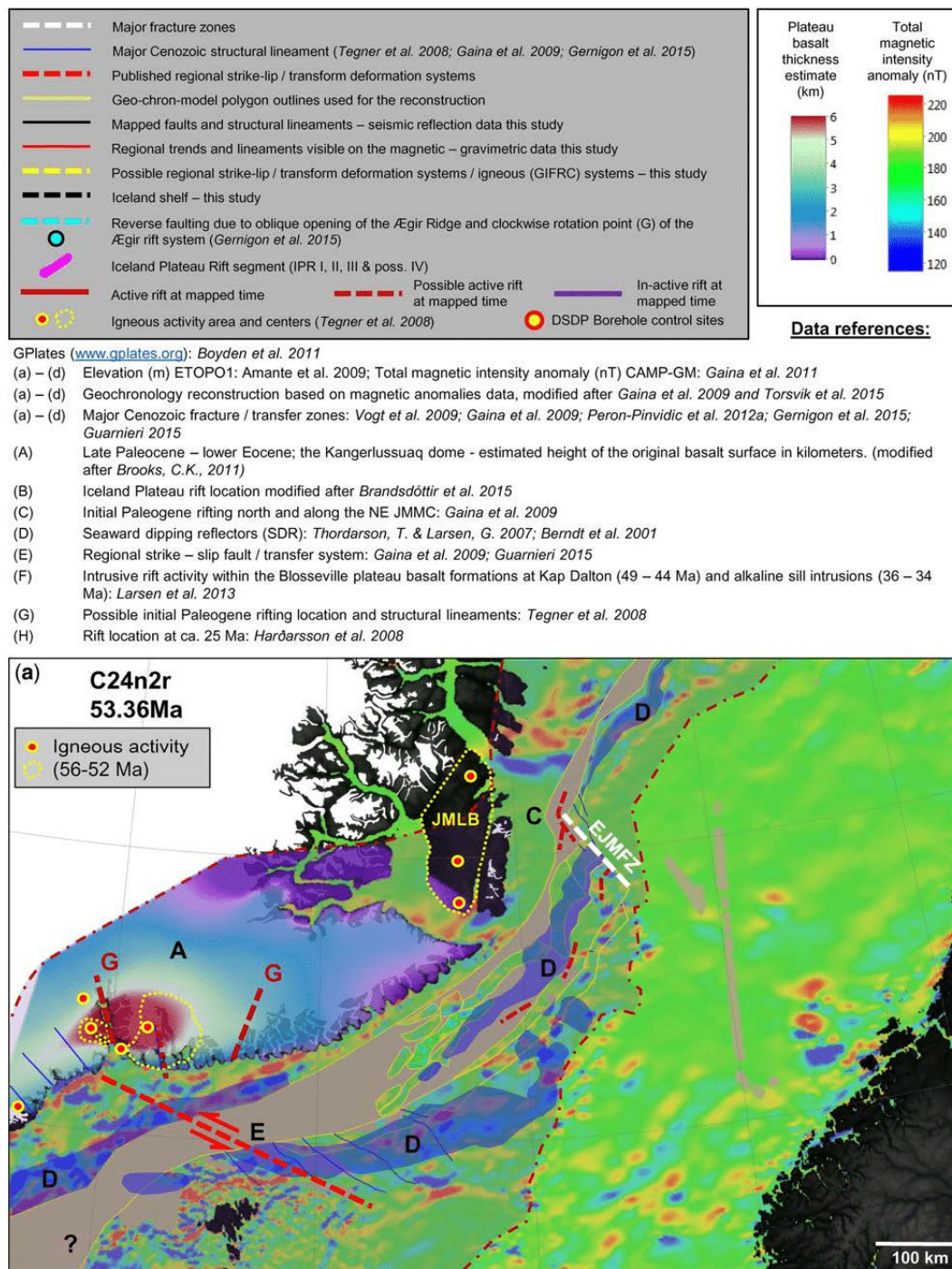


Fig. 11. Central NE Atlantic plate reconstructions relative to the European Plate: (a) break-up stage around chron C24n2r (53.36 Ma).

the western part of the JMMC, the proto-Kolbeinsey mid-oceanic ridge was forming. Two igneous complexes were identified on seismic reflection and gravity data, and are here referred to as the Iceland Plateau rift II and III systems (Figs 9 & 11d). Iceland Plateau rift II is located parallel to magnetic

anomaly C19n (40.32 Ma) and forms the eastern shelf limit of Iceland (Brandsdóttir et al. 2015). Iceland Plateau rift III is observed on seismic reflection, gravity and magnetic anomaly data, and appears to have affected the nearby Hakarennna Channel (HC in Fig. 9). This area of the

THE JMMC: THE ÆGIR RIDGE TO THE KOLBEINSEY RIDGE

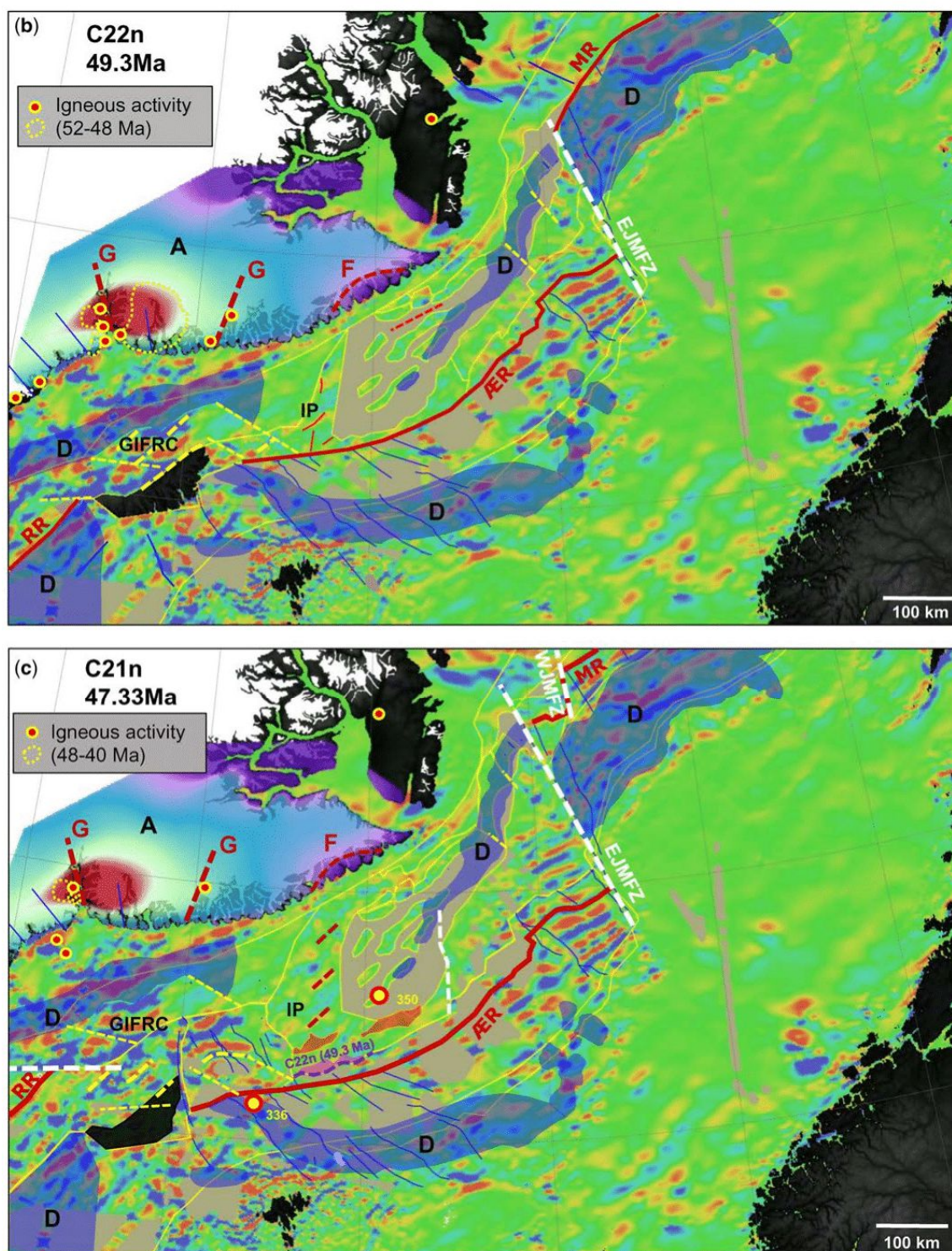


Fig. 11. (b) initial intra-JMMC rifting phase around chron C22n (49.3 Ma); (c) fully established seafloor spreading east of JMMC rift phase and beginning of intra-JMMC rift migration around chron C21n (47.33 Ma).

microcontinent was located parallel to the offshore Blosseville Kyst region at chron C13n, and lines up with observed offshore igneous centres (Árting

2014). This is interpreted as clear evidence that the rift transition had reached the SW corner of the JMMC by chron C13n.

THE JMMC: THE ÆGIR RIDGE TO THE KOLBEINSEY RIDGE

During this phase, the Jan Mayen Basin and Jan Mayen Trough (HT in Fig. 8; Table 1) both developed as a consequence of Middle Eocene and Late Oligocene–Early Miocene extension prior to the establishment of the Kolbeinsey mid-oceanic ridge (Peron-Pinvidic *et al.* 2012b). The Jan Mayen Basin was initiated as a series of small pull-apart basins along the NW flank of the JMMC (Fig. 11d, e). These small basins spatially compensated for the rapid extension occurring during this second break-up phase (Fig. 6a, b). Rotation and compression along the SE JMMC, initiated in the previous phase, probably continued until the cessation of seafloor spreading in the Norway Basin. This resulted in inversion structures that are also observed in the stratigraphic record in the form of the Lower Oligocene unconformity across the microcontinent's ridges (Figs 3 & 6, event E in Fig. 7).

Extension of the SRC widened the area to about 310 km. The nature of the basement at depth still remains unconstrained, but can be interpreted in terms of highly stretched and probably very thin continental crust. This thin crust is covered by thick basalt formations emplaced since break-up. During rift transfer, the area was intersected by the Iceland Plateau rift systems that separated the stretched composite crust into segments, forming a transitional crust between continental crust and the oceanic crust of the Iceland Plateau. These basalt formations are probably Late Oligocene–Early Miocene and filled the topographical lows between the main structures along the Jan Mayen Ridge. They are indicated by the F-Marker on seismic reflection data (Figs 5 & 6).

Complete isolation of the JMMC by establishing the Kolbeinsey mid-oceanic ridge around C6b: 21.56 Ma

The final separation of the JMMC occurred around C6b at 21.56 Ma (e.g. Gernigon *et al.* 2015) (Fig. 11e), when the Kolbeinsey mid-oceanic ridge reached the JMFZ and the plate boundary in the Greenland Sea. This phase coincides with the initiation of Iceland as an insular province and the formation of the GIFRC by increased igneous activity (Harðarsson *et al.* 2008). The offshore area NW of Iceland, and the onshore and offshore areas of East Iceland, began to form the Icelandic Plateau basalts continuously throughout the Late Miocene (Walker 1964; Sæmundsson 1979; Thordarson & Larsen 2007).

Rift propagations have been shown to occur in a NW direction within the Iceland Plateau–GIFRC area up to the Late Miocene (7.2–5.3 Ma). At around 7 Ma, a northeastwards oceanic rift relocation occurred (Jóhannesson & Sæmundsson 2009) from the Húnaflóa rift centre (HFR on Fig. 1) in

the NW of Iceland to the NE volcanic zone. As a consequence of substantially increased volcanic activity, new land formed and the GIFRC has been documented to have been located above or close to sea level (Denk *et al.* 2011). Well data from the highest ridges of the JMMC show a Mid–Late Miocene hiatus with marine sedimentation continuing only from the Pliocene onwards (Fig. 3).

During the Quaternary, the JMMC has only been affected by occasional volcanic activity of the Jan Mayen Island volcanic system, located at the northern edge of the JMMC, and gravitational erosion from the escarpment areas of the steep ridge flanks. In the Pleistocene, several glacial events removed about 1 km of the Iceland Plateau basalt (Walker 1964). The opposite occurred for the area between the Iceland Shelf and the SRC, indicating that the JMMC was subsiding during this last phase, presumably due to lithospheric cooling.

Discussion

The central focus of this contribution is the detailed development of the Jan Mayen microcontinent and its relationship to the surrounding areas to enable a better understanding of the full extent of the continental crust and its age and history. Central goals include:

- (1) Establishing a detailed tectonic and stratigraphic framework for the JMMC:
 - (a) the pre-break-up section and the JMMC relationship to the surrounding areas, in particular the East Greenland and Norway margins;
 - (b) the stratigraphic and igneous record during first break-up;
 - (c) the stratigraphic and igneous record during mid-oceanic ridge transfer.
- (2) To develop a detailed kinematic model of the JMMC from pre-break-up time to the present day, in particular with respect to the second break-up phase and the formation of a microcontinent.
- (3) To assess the Iceland–Faroe Fracture Zone (IFFZ) and the southern extent of the JMMC, in particular the connection to the Greenland–Iceland–Faroe Ridge Complex along the IFFZ, and the Iceland Plateau.

(1a) Stratigraphic records of the pre-break-up section

Where the JMMC type section intersects the seismic refraction profile line 4 of Kodaira *et al.* (1998) (Fig. 4), the pre-break-up sedimentary section, defined as the interval between the basalt and acoustic basement, is approximately 6 km thick. The

velocity model indicates that this interval is characterized by velocities of 3.9–5.3 km s⁻¹ (Kodaira *et al.* 1998). Palaeozoic–Mesozoic sequences in the Jameson Land Basin along East Greenland also show seismic velocities in the range between 3.5 and 5.5 km s⁻¹ (Fechner & Jokat 1996), assuming similar velocities along the central eastern flank of the microcontinent, where the pre-break sections appear thickest and may reach up to 9 km thick.

Overall, the Lyngvi Ridge seismic profile is similar in structural character to the Jameson Land Basin, which is 3–5 s deep at its centre and contains up to 12–16 km of pre-break-up sedimentary sequences (Henriksen 2008) with multiple unconformities, complex faulting patterns and deep intrusive events (Blischke *et al.* 2014b).

(1b) Stratigraphic and igneous records during first break-up

The Early Eocene flood basalts, SDRs and igneous centres along the eastern flank of the JMMC are located within an interpreted volcanic-transitional crust consisting of stretched continental crust modified by significant volcanism. The earliest clear oceanic crust produced by the Ægir mid-oceanic ridge spreading centre is indicated by the onset of regular magnetic anomalies (chron C24n2r in Fig. 5) (Gernigon *et al.* 2015). The average thickness of oceanic crust in the Norway Basin is about 5.3 km ± 1 km (Breivik & Mjelde 2003), in contrast to the much thicker 6–10 km (Kandilarov *et al.* 2012) oceanic crust close to the Jan Mayen Island volcanic complex (JMI) and the west Jan Mayen Fracture Zone (WJMFZ in Fig. 5). The crustal thickness of the central area of the microcontinent (Fig. 6b) is 15–18 km based on refraction data (JMKR-95 in Figs 2 & 5), whereas the continental crust under the main Jan Mayen Ridge, close to wells 346 and 347, reaches up to 20 km (Kandilarov *et al.* 2012).

The break-up-related basaltic layers interpreted here along the JMMC are assumed to be correlative to the central East Greenland margin. Nøhr-Hansen (2003) and Larsen *et al.* (2013) reported that the landwards flows (Planke *et al.* 2000) of the plateau basalts overlie Lower Paleocene sediments at Kap Brewster and Kap Dalton (KB and KD on Fig. 1a), and mark an erosional horizon interpreted here as equivalent to the break-up conformity of the central JMMC (Figs 3 & 4).

Further to the west, the Milne Land Formation (56.36 ± 0.25 Ma) of the main plateau basalts discordantly overlies Precambrian gneiss (Storey *et al.* 2007b), marking the break-up unconformity for the north Blosseville Kyst and Scoresby Sund region. At break-up time (*c.* 55 Ma), this region

was located approximately 400 km to the NE of the Faroe Island Plateau basalts.

The Faroe Islands, which have been covered by more than 7 km-thick landward basalt flows (Passey & Jolley 2009; Passey & Hitchen 2011; Ártung 2014), is conjugate to the Kangerlussuaq Basin, located at the southernmost extent of the Blosseville Kyst. This plateau basalt succession has often been assumed to have had a similar stratigraphic thickness across the entire area further to the north, which would have included the proto-Jan Mayen microcontinent area. Seismic reflection data (Fig. 4; Table 3), however, indicate a thinner basaltic section of approximately 1.1–1.5 km over the central part of the JMMC. As noted earlier, the Jameson Land Basin may have been covered by thick flood basalts and 2–3 km of basalt may have been removed (Mathiesen *et al.* 2000). The same may have occurred here. By inference, the flood basalts associated with SDR formation probably covered the entire JMMC and may have been continuous with the flood basalts of the Blosseville Kyst area.

(1c) Stratigraphic and igneous records during mid-oceanic ridge transfer

Along the Blosseville Kyst area, the lower Igtertivâ Formation (C22: *c.* 49 Ma) coincides with the beginning of rift transfer away from the Ægir mid-oceanic ridge (F in Fig. 11b), which is followed by a hiatus between the lower (C22–C21: 49–47 Ma) and the upper Igtertivâ Formation (C20: *c.* 44 Ma) (Larsen *et al.* 2014). As only the Mid-Eocene (chron C20) unconformity (Fig. 3) is observed along the eastern flank of the microcontinent, it is assumed that the area was again above sea level from 49 to 44 Ma, eroding all pre-chron C22 deposits. The rift transfer processes may have contributed to some thermal uplift along the SW and southern flanks of the microcontinent, accompanied by emplacement of igneous complexes and sill intrusions primarily into the Lower Eocene strata along the NE and SE flanks of the JMMC. This is also seen in borehole data (DSDP 38-350: Fig. 3), and on seismic reflection and refraction data (Figs 4–6).

Along the southern flank of the microcontinent, increased magmatism most probably coincided with volcanism within the Greenland–Iceland–Faroe Ridge Complex region. The Eocene sediment succession shows many intrusive sills and dykes, especially along the eastern and SE flanks. These intrusions are primarily located within the Lower Eocene sediment sequences, possibly coinciding emplacement within the Mid-Eocene time interval (49–44 Ma). This time interval correlates well with the increased igneous activity observed along the East Greenland coast (Larsen *et al.* 2014) and

THE JMMC: THE ÆGIR RIDGE TO THE KOLBEINSEY RIDGE

may indicate a regional event, and, furthermore, may explain the major unconformity that has been observed along the JMMC in the Mid-Eocene (Figs 3, 4 & 7).

(2) The second break-up phase and the formation of a microcontinent

This second break-up phase between the western edge of the JMMC and the central East Greenland margin is most probably a magma-starved break-up due to the lack of SDR sequences and large-scale magmatic activity. A gradual rift propagation is observed beginning at chron C21 (Fig. 11c) accompanied by large-scale extension of the SRC, crustal thinning across the Iceland Plateau and a listric normal faulting along the western flank (Fig. 5). Extension rates were probably very small, consistent with a reduced magma supply. Lundin *et al.* (2014) suggested that this is likely in areas near the tip of a propagating rift and eventual normal oceanic-crust accretion.

The youngest regionally extensive igneous event indicated on seismic reflection data on the JMMC (Gunnarsson *et al.* 1989) is referred to as the 'F-Reflector', and covers an area of approximately 18 400 km² along the western and the SW to southern flanks of the Jan Mayen Ridge and within the Jan Mayen Trough (JMT in Fig. 5). This igneous formation is interpreted as shallow-marine landwards flows emplaced during chrons C13–C6b (33–21.56 Ma), possibly sourced from fissure-type volcanic complexes south and west of the microcontinent. Small lava deltas located on the SW extent of the JMMC on seismic reflection data indicate south–north to SW–NE flow directions.

During the second break-up event, the central East Greenland region was most probably the main sediment source, along with the Jan Mayen ridges and highs. The Jan Mayen Basin, including local low areas along the SW flank of the microcontinent, was filled with sediments sourced from the west as the microcontinent separated from the East Greenland margin (Fig. 8; Table 1). The southern area of the microcontinent towards the Iceland Plateau must have been elevated from the Mid-Oligocene, as the overall sediment stratigraphic thickness decreased from north to south and the Late Oligocene unconformity (Fig. 3) is observed on highs of the SRC (Fig. 6c).

After the Kolbeinsey mid-oceanic ridge had completely separated the microcontinent from East Greenland, the sediment supply was greatly reduced. Intra-Neogene unconformities within the oceanic sediments are observed away from the JMMC, and the occurrence of mounded onlapping sediment packages are observed on the flanks of the Jan Mayen Ridge. These attest to processes of

erosion and deposition associated with deep-water bottom currents, which were common around the NE Atlantic region from the Mid-Miocene onwards (e.g. Bohrmann *et al.* 1990; Howe *et al.* 1994; Davies *et al.* 2001; Stoker *et al.* 2005). Borehole information (Talwani *et al.* 1976b; Talwani & Eldholm 1977) and interpretation of seismic reflection data show that these sediment sequences are very thin, deep marine, and form thick contourite deposits. Beginning in the Mid-Miocene, the sediment supply direction was from the North Iceland Shelf (NIS) area to the south. Sediment was supplied into the Ægir to Kolbeinsey rift transfer corridor of the Iceland Plateau (Fig. 5) and into the Hléssund Trough (HS in Fig. 8; Table 1), the southernmost extension of the Jan Mayen Trough.

(3) The Iceland–Faroe Fracture Zone and the southern extent of the JMMC

To understand the development of the southernmost part of the JMMC, the present-day development of the onshore areas of Iceland are considered, where complex transfer zones link the Reykjanes and Kolbeinsey mid-oceanic ridges to the main spreading axis (Sæmundsson 1974; Magnúsdóttir *et al.* 2015). These transfer systems result in an echelon orientated volcanic ridge segments, here referred to as flank systems (e.g. the Snæfellsnes and Örfafjökull volcanic zones: e.g. Hards *et al.* 1995; Prestvik *et al.* 2001; Einarsson 2008; Jakobsson *et al.* 2008). The present-day spreading axis is apparently migrating east via ridge jumps (Arting 2014). These observations serve as an analogue to understand how the left-lateral Greenland–Faroe Transfer System described by Guarnieri (2015) might have developed in time (Figs 10 & 11).

This transfer system between the Norway Basin and Kolbeinsey mid-oceanic ridge system that passes south of the JMMC and north of the Iceland–Faroe Ridge has been described previously (e.g. Vogt & Jung 2009; Gernigon *et al.* 2015). The interpretations of the wide-angle data along KRISE Line 7 (Brandadóttir *et al.* 2015) (Figs 2 & 5), which extends from the Kolbeinsey mid-oceanic ridge to the Ægir mid-oceanic ridge, are important in this context. The western part of the profile crosses the Kolbeinsey mid-oceanic ridge and the NIS, which is part of the GIFRC. The crustal thickness ranges from 12 to 14 km near the Kolbeinsey Ridge, increasing gradually across the Iceland Shelf up to 25 km. Crustal thickness decreases abruptly down to around 8 km across the Iceland Plateau corridor and across the NIS shelf break, with a major fault escarpment dipping NE. Within the volcanic transitional area of the Iceland Plateau Rift (IPR), the crustal thickness again increases to 12 km. The oceanic crust towards the Ægir

mid-oceanic ridge is relatively thin, at only 4–5 km thick. A domain characterized by velocity variations in lower-crustal structures across the Iceland Plateau is interpreted as an extinct spreading centre that is part of the Iceland Plateau Rift, which was active at the same time as the Aegir Ridge prior to the initiation of the Kolbeinsey Ridge. The spreading rate during that time decreased along the Aegir Ridge, as more and more of the extension was being taken up further west.

From the Iceland Plateau to the JMMC, a clear change in fault and lineament trends occurs based on the bathymetry and potential field datasets. These trends range from a north–south direction on the JMMC to a NW–SE trend on the Iceland Plateau. The latter trend is in alignment with the structural trend of the Iceland–Faroe Fracture Zone (IFFZ in Figs 1a & 5) and both trends correlate with magnetic anomalies. The junction of those two trends is suggested to mark the most likely southern boundary of the microcontinent as a structural entity. The boundary is probably a volcanic transitional-type crust that incorporates slivers of continental crust along with formed new volcanic crustal accretion. Gernigon *et al.* (2015) proposed a major SE–NW regional dextral strike-slip system from the Aegir mid-oceanic ridge to the centre of the microcontinent at the northern limit of the SRC. This system lies parallel to the Iceland Plateau corridor and the Iceland–Faroe Fracture Zone. In the Dreki Ridge area (Fig. 9a, b), where the segmentation of the SRC is clearly visible, a subdivision of the lineaments can be made. Here, distinct segments are likely to relate to pre-break-up segments of continental crust. Segments of possible Lower Eocene plateau basalts are intersected by possible oceanic crust. If the Iceland Plateau corridor represents a broad dextral SE–NW strike-slip fault zone, then the minimum horizontal stress lies approximately east–west, allowing faults to open and propagate in a north–south direction, which is parallel to the magnetic lineation in that area. These transtensional oblique rift systems were volcanically active and may be similar to the oblique rift segments observed today where the Reykjanes Ridge connects across Iceland to the Eastern Volcanic Zone (Clifton & Schlische 2003; Clifton & Kattenhorn 2005), and within the Northeastern Volcanic Zone (Khodayar 2014) on Iceland (NEVZ on Fig. 1a).

Conclusions

The objective of this study was to construct a detailed tectonostratigraphic history of the Jan Mayen microcontinent with a focus on the southernmost area. This was then integrated into kinematic reconstructions of the central NE Atlantic to better understand the Cenozoic development and the

implications for the pre-Cenozoic development of regional rift basins, remnants of which probably underlie the JMMC. Complex structural patterns are observed along the microcontinent's margins, as well as the conjugate East Greenland and Norwegian margins on either side. The new model includes a description of how the southern JMMC structural elements were linked to tectonic features on the Iceland Plateau and Greenland–Iceland–Faroe Ridge Complex.

Mapping the pre- to post-break-up sedimentary strata and igneous complexes together with volcanostratigraphic seismic characterization has facilitated a reassessment and clearer definition of the igneous v. sedimentary domains of the JMMC area throughout its break-up history. The main results include:

- Interpretation of new and vintage geophysical data suggests that a significant pre-Palaeogene stratigraphic history is preserved. However, without deep borehole data, the age of possible sedimentary successions are speculative. Nevertheless, the conjugate Jameson Land and Møre basins are considered to be direct analogue areas for the JMMC. These basins are well constrained, and contain a sedimentary succession that includes Devonian continental sediments, Permo-Triassic continental and marine sequences, Jurassic and Cretaceous shallow- to deep-marine sequences, and Lower Paleocene alluvial to shallow-marine sediments.
- The break-up and post-break-up igneous sequences were separated into plateau basalts of probable Paleocene–Early Eocene age, seawards-dipping reflector sequences, igneous complexes, and sill and dyke intrusions along the flanks of the JMMC.
- A consistent kinematic model for the Cenozoic evolution of the JMMC and surrounding oceanic crust that consists of six main phases is proposed. The boundaries between these phases correlate to major unconformities and related structures. Important events include:
 - (1) A pre-break-up stage ending at 56–55 Ma and the emplacement of Lower Eocene plateau basalts across the microcontinent and the Blosseville Kyst region, with an apparent thickening of the basalt sequences to the south, possibly continuing into the Faroe–Iceland–East Greenland corridor. The structures of the JMMC are consistently orientated with major structural lineaments of the surrounding regions prior to break-up. The main trends are aligned with the Jameson Land Basin and Liverpool Land high. The JMMC probably forms the southern extension of the Jameson Land Basin.

THE JMMC: THE ÆGIR RIDGE TO THE KOLBEINSEY RIDGE

- (2) A first break-up phase that began at 55 Ma (e.g. Gaina *et al.* 2009) and was associated with the formation of SDR along the east flank of the JMMC, followed by the initiation of seafloor spreading in the Norway Basin along the Ægir Ridge in the Early Eocene (chron C24n2r 53.36 Ma) (Gaina *et al.* 2009; Gernigon *et al.* 2015).
- (3) An initial intra-JMMC rifting phase around chron C22n (49.3 Ma) and the establishment of a continuous spreading system in the Norway Basin and forming the eastern extent of the Iceland Plateau, here referred to as Iceland Plateau rift I (IPR-I; Fig. 11b, c). Initial extension of the entire southern half of the microcontinent occurred, widening it from originally 100 km to approximately 150 km. This eventually led to early stage break-up in the Iceland Plateau area, forming new Lower Eocene volcanic formations (volcanic breccia, intrusions and SDR sequences) along the SE flank of the Southern Ridge Complex (SRC).
- (4) The initiation of the southern JMMC rift transition at chron C21n (47.33 Ma) contemporaneous with oblique seafloor spreading east of the JMMC, causing the formation of transform systems and uplift along the southern flank of the JMMC. Volcanic activity occurred along the NE margin of the Blossville Kyst (Larsen *et al.* 2014).
- (5) A westwards rift transfer and initial break-up along the western JMMC around chron C13n–33.1 Ma. Oblique mid-oceanic ridge relocation via a SE–NW en echelon rift system occurred from the southern extent of the microcontinent during the Early Oligocene. Significant volcanism affected the SW area of the JMMC, referred to here as the Iceland Plateau rift III, which can be linked to the Blossville Kyst margin. Oblique extension occurred along the NW flank of the JMMC, resulting in the opening of the Jan Mayen Basin and a series of small pull-apart basins and igneous intrusions with little to no evidence of SDR formation.
- (6) A second break-up phase at chron C6b (21.56 Ma) with complete cessation of seafloor spreading in the Norway Basin (Gernigon *et al.* 2015) and the establishment of the Kolbeinsey mid-oceanic ridge as the main mid-ocean spreading centre.

The extension of the southern half of the JMMC has been quantified from the original 40–100 km width up to a width of 310 km during the Early Eocene. The SRC is overprinted by volcanic extrusive complexes that consist

primarily of Early Eocene basalt flows, which are interpreted as being similar to the plateau basalts exposed along the Blossville Kyst of Greenland. These are overlapped by clear and well-developed SDRs associated with the final opening of the Norway Basin. Multiple phases of intrusive events appear to have affected the eastern flank of the microcontinent during the Eocene and the southern part of the JMMC during the Late Eocene–Early Oligocene.

- The Iceland–Faroe Fracture Zone across the Iceland Plateau has been mapped as an echelon transfer system from the Ægir Ridge to the Kolbeinsey Ridge. Detailed mapping of the southern extent of the JMMC supports the Gaina *et al.* (2009) model in which mid-oceanic ridge propagation occurred directly south of the microcontinent, beginning in the latest Early Eocene (49.3 Ma) and continuing throughout the Eocene. This formed at least three rift-flank systems on the Iceland Plateau. These rift flanks are referred to as Iceland Plateau rift IPR-I, IPR-II and IPR -III (Brandsdóttir *et al.* 2015).

This work is part of a PhD project at the University of Iceland, the National Energy Authority of Iceland (Orkusstofnun) and the Iceland GeoSurvey, with data permissions provided by: Spectrum ASA, TGS; the University of Oslo (UiO); the Norwegian Petroleum Directorate (NPD); the Bundesanstalt für Geowissenschaften und Rohstoffe (BGR); and GEUS (Geological Survey of Denmark and Greenland). This project benefitted from the NAG-TEC project. Support from the following industry sponsors of NAG-TEC is gratefully acknowledged (in alphabetical order): Bayerngas Norge AS; BP Exploration Operating Company Ltd; Bundesanstalt für Geowissenschaften und Rohstoffe (BGR); Chevron East Greenland Exploration A/S; ConocoPhillips Skandinavia AS; DEA Norge AS; Det norske oljeselskap ASA; DONG E&P A/S; E.ON Norge AS; ExxonMobil Exploration and Production Norway AS; Japan Oil, Gas and Metals National Corporation (JOGMEC); Maersk Oil; Nalcor Energy – Oil and Gas Inc.; Nexen Energy ULC, Norwegian Energy Company ASA (Noreco); Repsol Exploration Norge AS; Statoil (UK) Ltd; and Wintershall Holding GmbH. C.G. acknowledges support from the Research Council of Norway through its Centres of Excellence funding scheme, project number 223272. In addition, the authors would like to thank Dr Nina Lebedeva-Ivanova and Dr Asbjørn Breivik (CEED, UiO), and Dr Laurent Gernigon (NGU) for all their help, advice and patience throughout this project. Reviews from Dieter Franke, Erik Lundin and the editor, Martyn Stoker, greatly improved this manuscript.

References

- ÅKERMOEN, T. 1989. *Jan Mayen-ryggen: et seismisk stratigrafisk og strukturelt studium* (The Jan Mayen Ridge: a seismic stratigraphic and structural study.). Cand. scient. thesis, University of Oslo.

- AMANTE, C. & EAKINS, B.W. 2009. *ETOPOI 1 Arc-Minute Global Relief Model: Procedures, Data Sources and Analysis*. NOAA Technical Memorandum NESDIS NGDC-24.
- ANDERSEN, O.B. 2010. The DTU10 gravity field and mean sea surface. Paper presented at the *Second International Symposium of the Gravity Field of the Earth (IGFS2)*, 20–22 September 2010, Fairbanks, Alaska, USA.
- ANDERSEN, T.B. & JAMTVEIT, B. 1990. Uplift of deep crust during orogenic extensional collapse: a model based on field studies in the Sogn–Sunnfjord area of Western Norway. *Tectonics*, **9**, 1097–1111.
- ÁRTING, U. 2014. Regional volcanism. In: HOPPER, J.R., FUNCK, T., STOKER, M., ÁRTING, U., PERON-PINVIDIC, G., DOORNENBAL, H. & GAINA, C. (eds) *Tectonostratigraphic Atlas of the North-East Atlantic Region*. GEUS, Copenhagen, Denmark, 223–290.
- BERNDT, C., MJELDE, R., PLANKE, S., SHIMAMURA, H. & FALÉIDE, J.I. 2001. Controls on the tectono-magmatic evolution of a volcanic transform margin: the Vøring Transform Margin, NE Atlantic. *Marine Geophysical Researches*, **22**, 133–152.
- BLISCHKE, A., ERLENDSSON, Ö. & ÁRNADÓTTIR, S. 2014a. *CRUSMID-3D – NORDMIN Status Report 2014 – Crustal Structure and Mineral Deposit Systems: 3D-modelling of Base Metal Mineralization in Jameson Land and Nickel Mineralization in Disko-Nuussuaq*. ÍSOR-2014/056. Closed Report for the Geological Survey of Denmark and Greenland and the National Energy Authority of Iceland, 184–194.
- BLISCHKE, A., HJARTARSON, A., ERLENDSSON, Ö., ÁRNADÓTTIR, S. & PERON-PINVIDIC, G. 2014b. The Iceland margin, Jan Mayen microcontinent, and adjacent oceanic areas. In: HOPPER, J.R., FUNCK, T., STOKER, M., ÁRTING, U., PERON-PINVIDIC, G., DOORNENBAL, H. & GAINA, C. (eds) *Tectonostratigraphic Atlas of the North-East Atlantic Region*. GEUS, Copenhagen, Denmark.
- BLYSTAD, P., BREKKE, H., FÆRSETH, R.B., LARSEN, B.T., SKOGSEID, J. & TØRUBAKKEN, B. 1995. *Structural Elements of the Norwegian Continental Shelf, Part II. The Norwegian Sea Region*. Norwegian Petroleum Directorate Bulletin, **8**.
- BOHRMANN, G., HENRICH, R. & THIEDE, J. 1990. Miocene to Quaternary paleoceanography in the Northern North Atlantic: variability in carbonate and biogenic opal accumulation. In: BLEIL, U. & THIEDE, J. (eds) *Geological History of the Polar Oceans: Arctic Versus Antarctic*. NATO Science Series C, **308**, 647–675.
- BOYDEN, J.A., MÜLLER, R.D. ET AL. 2011. Next-generation plate-tectonic reconstructions using Gplates. In: KELLER, G. & BARU, C. (eds) *Geoinformatics: Cyberinfrastructure for the Solid Earth Sciences*. Cambridge University Press, Cambridge, 95–116.
- BRANDSDÓTTIR, B., HOOFT, E., MJELDE, R. & MURAI, Y. 2015. Origin and evolution of the Kolbeinsey Ridge and Iceland Plateau, N-Atlantic. *Geochemistry, Geophysics, Geosystems*, **16**, 612–634.
- BREIVIK, A. & MJELDE, R. 2003. *Modelling of Profile 8 Across the Jan Mayen Ridge*. Report of the Institute of Solid Earth Physics, University of Bergen, Bergen, Norway.
- BREIVIK, A.J., MJELDE, R., FALÉIDE, J.I. & MURAI, Y. 2012. The eastern Jan Mayen microcontinent volcanic margin. *Geophysical Journal International*, **188**, 798–818.
- BREKKE, H. 2000. The tectonic evolution of the Norwegian Sea continental margin with emphasis on the Vøring and Møre basins. In: NØTTVEDT, A. (ed.) *Dynamics of the Norwegian Margin*. Geological Society, London, Special Publications, **167**, 327–378, <http://doi.org/10.1144/GSL.SP.2000.167.01.13>
- BREKKE, H., DAHLGREN, S., NYLAND, B. & MAGNUS, C. 1999. The prospectivity of the Vøring and Møre basins on the Norwegian Sea continental margins. In: FLEET, A.J. & BOLDY, S.A.R. (eds) *Petroleum Geology of Northwest Europe: Proceedings of the 5th Conference*. Geological Society, London, 261–274, <http://doi.org/10.1144/0050261>
- BROOKS, C.K. 2011. *The East Greenland Rifted Volcanic Margin*. Geological Survey of Denmark and Greenland Bulletin, **24**.
- BUTT, F.A., ELVERHOI, A., FORSBERG, C.F. & SOLHEIM, A. 2001. An evolution of the Scoresby Sund Fan, central East Greenland – evidence from ODP Site 987. *Norsk Geologisk Tidsskrift*, **81**, 3–15.
- CHANNELL, J.E.T., AMIGO, A.E. ET AL. (eds). 1999a. Magnetic stratigraphy at Sites 907 and 985 in the Norwegian–Greenland Sea and a revision of the Site 907 composite section. In: RAYMO, M.E., JANSEN, E., BLUM, P. & HERBERT, T.D. (eds) *Proceedings of the Ocean Drilling Program, Scientific Results*, Volume **162**. Ocean Drilling Program, College Station, TX, 131–148.
- CHANNELL, J.E.T., SMELROR, M., JANSEN, E., HIGGINS, S.M., LEHMAN, B., EIDVIN, T. & SOLHEIM, A. 1999b. Age models for glacial fan deposits off East Greenland and Svalbard (sites 986 and 987). Paper presented at *Proceedings of the Ocean Drilling Program, Scientific Results*, College Station TX (Integrated Ocean Drilling Program Management International, Inc.), 162.
- CLIFTON, A.E. & KATTENHORN, S.A. 2005. Structural architecture of a highly oblique divergent plate boundary segment. *Tectonophysics*, **419**, 27–40.
- CLIFTON, A.E. & SCHLISCHE, R.W. 2003. Fracture populations on the Reykjanes Peninsula, Iceland: Comparison with experimental clay models of oblique rifting. *Journal of Geophysical Research*, **108**, 2074.
- DAVIES, R., CARTWRIGHT, J., PIKE, J. & LINE, L. 2001. Early Oligocene initiation of North Atlantic Deep Water formation. *Nature*, **410**, 917–920, <http://doi.org/10.1038/35073551>
- DENK, T., GRÍMSSON, F. & KVACEK, Z. 2011. The Miocene floras of Iceland and their significance for Late Cainozoic North Atlantic biogeography. *Botanical Journal of the Linnean Society*, **149**, 369–417.
- DORÉ, A.G., LUNDIN, E.R., JENSEN, L.N., BIRKELAND, Ø., ELIASSEN, P.E. & FICHLER, C. 1999. Principal tectonic events in the evolution of the northwest European Atlantic margin. In: FLEET, A.J. & BOLDY, S.A.R. (eds) *Petroleum Geology of Northwest Europe: Proceedings of the 5th Conference*. Geological Society, London, 41–61, <http://doi.org/10.1144/0050041>
- DORÉ, A.G., LUNDIN, E.R., KUSZNIR, N.J. & PASCAL, C. 2008. Potential mechanisms for the genesis of

THE JMMC: THE ÆGIR RIDGE TO THE KOLBEINSEY RIDGE

- Cenozoic domal structures on the NE Atlantic margin: pros, cons and some new ideas. In: JOHNSON, H., DORÉ, T.G., GATLIFF, R.W., HOLDSWORTH, R.W., LUNDIN, E. & RITCHIE, J.D. (eds) *The Nature and Origin of Compression in Passive Margins*. Geological Society, London, Special Publications, **306**, 1–26, <http://doi.org/10.1144/SP306.1>
- EINARSSON, P. 2008. Plate boundaries, rifts and transforms in Iceland. *Jökull*, **58**, 35–58.
- ELDHOLM, O. & WINDISH, C.C. 1974. Sediment distribution in the Norwegian-Greenland Sea. *Geological Society of America Bulletin*, **85**, 1661–1676.
- ELDHOLM, O., THIEDE, J. ET AL. 1987. *Proceedings of the ODP Initial Reports*, Volume **104**. Ocean Drilling Program, College Station, TX.
- ELDHOLM, O., THIEDE, J. & TAYLOR, E. 1989. The Norwegian continental margin: tectonic, volcanic, and paleo-environmental framework. In: ELDHOLM, O., THIEDE, J. ET AL. *Proceedings of the Ocean Drilling Program, Scientific Results*, Volume **104**. Ocean Drilling Program, College Station, TX, 5–26.
- ENKILDE, M. & SURLYK, F. 2003. Shallow marine syn-rift sedimentation: Middle Jurassic Pelion Formation, Jameson Land, East Greenland. In: INESON, J.R. & SURLYK, F. (eds) *The Jurassic of Denmark and Greenland*. Geological Survey of Denmark and Greenland Bulletin, **1**, 813–863.
- ERLENDSSON, Ö. 2010. *Seismic Investigation of the Jan Mayen Ridge – with a Close Study of Sill Intrusions*. Aarhus University, Aarhus, Denmark.
- ERLENDSSON, Ö. & BLISCHKE, A. 2013. *Haffréttarmál: hljóðendurvarps- og bylgjubrotsmælin-gar: skýrsla um stöðu mála á úrvinnslu og túlkun gagna* (Law of the sea: seismic reflection and refraction database and interpretation status report.). Report ÍSOR-2013/067. ÍSOR (Iceland GeoSurvey), Reykjavík, Iceland.
- FALEIDE, J.I., BJØRLYKKE, K. & GABRIELSEN, R.H. 2010. Geology of the Norwegian continental shelf. In: BJØRLYKKE, K. (ed.) *Petroleum Geoscience: From Sedimentary Environments to Rock Physics*. Springer, New York, 467–499.
- FECHNER, N. & JOKAT, W. 1996. Seismic refraction investigation on the crustal structure of the western Jamson Land Basin, East Greenland. *Journal of Geophysical Research*, **101**, 15,867–15,881.
- FOULGER, G.R., NATLAND, J.H. & ANDERSON, D.L. 2005. A source for Icelandic magmas in re-melted Iapetus crust. *Journal of Volcanology and Geothermal Research*, **141**, 23–44.
- FUNCK, T., HOPPER, J.R. ET AL. 2014. Crustal structure. In: HOPPER, J.R., FUNCK, T., STOKER, M., ÁRTING, U., PERON-PINVIDIC, G., DOORNENBAL, H. & GAINA, C. (eds) *Tectonostratigraphic Atlas of the North-East Atlantic Region*. Geological Survey of Denmark and Greenland (GEUS), Copenhagen, Denmark.
- GAINA, C., GERNIGON, L. & BALL, P. 2009. Palaeocene–Recent plate boundaries in the NE Atlantic and the formation of the Jan Mayen microcontinent. *Journal of the Geological Society, London*, **166**, 601–616, <http://doi.org/10.1144/0016-76492008-112>
- GAINA, C., WERNER, S.C., SALTUS, R., MAUS, S. & THE CAMP-GM GROUP 2011. Circum-arctic mapping project: new magnetic and gravity anomaly maps of the arctic. In: SPENCER, A.M., EMBRY, A.F., GAUTIER, D.L., STOUPOKOVA, A. & SØRENSEN, K. (eds) *Arctic Petroleum Geology*. Geological Society, London, Memoirs, **35**, 39–48, <http://doi.org/10.1144/M35.3>
- GAINA, C., TORSVIK, T.H., VAN HINSBERGEN, D., MEDVEDEV, S., WERNER, S.C. & LABAILS, C. 2013. The African Plate: A history of oceanic crust accretion and subduction since the Jurassic. *Tectonophysics*, ISSN 0040-1951.604, s4–25. doi:10.1016/j.tecto.2013.05.037
- GAINA, C., NASUTI, A., KIMBELL, G.S. & BLISCHKE, A. In review. Break-up and seafloor spreading domains in the NE Atlantic. In: PERON-PINVIDIC, G., HOPPER, J.R., STOKER, T., GAINA, C., DOORNENBAL, H., FUNCK, T. & ÁRTING, U. (eds) *The NE Atlantic Region: A Reappraisal of Crustal Structure, Tectonostratigraphy and Magmatic Evolution*. Geological Society of London, London, Special Publications, **447**.
- GASSER, D. 2014. The Caledonides of Greenland, Svalbard and other Arctic areas: status of research and open questions. In: CORFU, F., GASSER, D. & CHEW, D.M. (eds) *New Perspectives on the Caledonides of Scandinavia and Related Areas*. Geological Society of London, London, Special Publications, **390**, 93–129, <http://doi.org/10.1144/SP390.17>
- GEODEKYAN, A.A., VERKHOVSKAYA, Z.I., SUDYIN, A.V. & TROTSIUK, V.YA. 1980. Gases in seawater and bottom sediments. In: UDINTSEV, C.B. (ed.) *Iceland and Mid-Oceanic Ridge: Structure of the Ocean-Floor*. National Research Council, Reykjavik, Iceland, 19–36.
- GERNIGON, L., GAINA, C., OLESEN, O., BALL, P., PERON-PINVIDIC, G. & YAMASAKI, T. 2012. The Norway Basin revisited: from continental breakup to spreading ridge extinction. *Marine and Petroleum Geology*, **35**, 1–19.
- GERNIGON, L., BLISCHKE, A., NASUTI, A. & SAND, M. 2015. Conjugate volcanic rifted margins, seafloor spreading, and microcontinent: insights from new high-resolution aeromagnetic surveys in the Norway Basin. *Tectonics*, **34**, 907–933.
- GILOTTI, J.A., JONES, K.A. & ELVEVOLD, S. 2008. Caledonian metamorphic patterns in Greenland. In: HIGGINS, A.K., GILOTTI, J.A. & SMITH, M.P. (eds) *The Greenland Caledonides: Evolution of the Northeast Margin of Laurentia*. Geological Society of America, Memoirs, **202**, 201–225.
- GRADSTEIN, F.M., OGG, J.G., SCHMITZ, M.D. & OGG, G.M. 2012. *The Geologic Time Scale 2012*. Elsevier, Amsterdam.
- GUARNIERI, P. 2015. Pre-breakup palaeo-stress state along the East Greenland margin. *Journal of the Geological Society, London*, **172**, 727–739, <http://doi.org/10.1144/jgs2015-053>
- GUNNARSSON, K., SAND, M. & GUDLAUGSSON, S.T. 1989. *Geology and Hydrocarbon Potential of the Jan Mayen Ridge*. Orkustofnun, Reykjavik Report OS-98014 & Norwegian Petroleum Directorate, Stavanger, OD-89-91.
- HAASE, C. & EBBING, J. 2014. Gravity data. In: HOPPER, J.R., FUNCK, T., STOKER, M.S., ÁRTING, U., PERON-PINVIDIC, G., DOORNENBAL, H. & GAINA, C. (eds) *Tectonostratigraphic Atlas of the North-East Atlantic Region*. Geological Survey of Denmark and Greenland (GEUS), Copenhagen, Denmark.

- HAMANN, N.E., WITTAKER, R.C. & STEMMERIK, L. 2005. Geological development of the Northeast Greenland shelf. In: DORÉ, A.G. & VINING, B.A. (eds) *Petroleum Geology: North-West Europe and Global Perspectives – Proceedings of the 6th Petroleum Geology Conference*. Geological Society, London, 887–902, <http://doi.org/10.1144/0060887>
- HARDS, V.L., KEMPTON, P.D. & THOMPSON, R.N. 1995. The heterogeneous Iceland plume: new insights from the alkaline basalts of the Snaefell volcanic centre. *Journal of the Geological Society, London*, **152**, 1003–1009, <http://doi.org/10.1144/GSL.JGS.1995.152.01.21>
- HARÐARSSON, B., FITTON, J. & HJARTARSON, Á. 2008. Tertiary volcanism in Iceland. *Jökull*, **58**, 161–178.
- HENRIKSEN, N. 2008. *Geological History of Greenland – Four Billion Years of Earth Evolution*. Geological Survey of Denmark and Greenland (GEUS), Copenhagen, Denmark.
- HINZ, K. 1981. A hypothesis on terrestrial catastrophes wedges of very thick ocean-ward dip-ping layers beneath passive continental margins; their origin and palaeo-environmental significance. *Geologisches Jahrbuch*, **E2**, 3–28.
- HJARTARSON, A. & SÆMUNDSSON, K. 2014. *Geological Map of Iceland – Bedrock Map, 1:600 000, Datum: ISN93*. Iceland GeoSurvey, Reykjavík.
- HOPPER, J.R., FUNCK, T., STOKER, M.S., ÁRTING, U., PERON-PINVIDIC, G., DOORNENBAL, H. & GAINA, C. (eds). 2014. *Tectonostratigraphic Atlas of the North-East Atlantic Region*. Geological Survey of Denmark and Greenland (GEUS), Copenhagen.
- HORNI, J., HOPPER, J.R. ET AL. 2016. Regional distribution of volcanism within the North Atlantic Igneous Province. In: PÉRON-PINVIDIC, G., HOPPER, J., STOKER, M.S., GAINA, C., DOORNENBAL, H., FUNCK, T. & ÁRTING, U. (eds) *The North-East Atlantic Region: A Reappraisal of Crustal Structure, Tectono-Stratigraphy and Magmatic Evolution*. Geological Society, London, Special Publications, **447**, xx–xx, <http://doi.org/10.1144/SP447>?
- HOWE, J.A., STOKER, M.S. & STOW, D.A.V. 1994. Late Cenozoic sediment drift complex, northeast Rockall Trough, North Atlantic. *Palaeoceanography*, **9**, 989–999.
- JANSEN, E., RAYMO, M.E. ET AL. 1996. *Proceedings of the Ocean Drilling Program. Initial Reports, Volume 162*. Ocean Drilling Program, College Station, TX.
- JAKOBSSON, M., MAYER, L. ET AL. 2012. The International Bathymetric Chart of the Arctic Ocean (IBCAO) Version 3.0. *Geophysical Research Letters*, **39**, <http://doi.org/10.1029/2012GL052219>
- JAKOBSSON, S.P., JÓNASSON, K. & SIGURDSSON, I.A. 2008. The three igneous rock series of Iceland. *Jökull*, **58**, 117–138.
- JÓHANNESON, H. 2011. *Örnefnagjöf á landgrunninu og utan þess. III. Drekasvæðið, Rep. JHJ-2011-012*, 6 pp., National Energy Authority of Iceland, Reykjavík, Iceland.
- JÓHANNESON, H. & SÆMUNDSSON, K. 2009. *Geological Map of Iceland. 1:600,000. Tectonics*. 1st edn. Icelandic Institute of Natural History, Reykjavík.
- JOHANSEN, B., ELDHOLM, O., TALWANI, M., STOFFA, P.L. & BUHL, P. 1988. Expanding spread profile at the northern Jan Mayen Ridge. *Polar Research*, **6**, 95–104.
- KALSBECK, F., HIGGINS, A.K., JEPSEN, H.F., FREI, R. & NUTMAN, A.P. 2008. Granites and granites in the East Greenland Caledonides. In: HIGGINS, A.K., GILOTTI, J.A. & SMITH, M.P. (eds) *The Greenland Caledonides: Evolution of the Northeast Margin of Laurentia*. Geological Society of America, Memoirs, **202**, 227–249.
- KANDILAROV, A., MJELDE, R. ET AL. 2012. The northern boundary of the Jan Mayen microcontinent, North Atlantic determined from ocean bottom seismic, multi-channel seismic, and gravity data. *Marine Geophysical Research*, **33**, 55–76.
- KHODAYAR, M. 2014. *Shift of Þeistareykir Fissure Swarm in Tjörnes Fracture Zone: Case of Pull-apart on Strike-slip?* Technical report, ISOR-2014/074, LV-2014-144, Iceland GeoSurvey for Landsvirkjun (National Energy Company of Iceland), Reykjavík, Iceland.
- KODAIRA, S., MJELDE, R., GUNNARSSON, K., SHIOBARA, H. & SHIMAMURA, H. 1998. Structure of the Jan Mayen microcontinent and implications for its evolution. *Geophysical Journal International*, **132**, 383–400.
- LAIER, T. & NYTOFT, H.P. 2004. Waxy bitumen in basalts – Skye and Faroe Islands, North Atlantic. *Geochimica et Cosmochimica Acta*, **68**, (11), Supplement 234.
- LAIER, T., NYTOFT, H.P., JØRGENSEN, O. & ISAKSEN, G.H. 1997. Hydrocarbon traces in the Tertiary basalts of the Faeroe Islands. *Marine and Petroleum Geology*, **14**, 257–266.
- LARSEN, L.M., WAAGSTEIN, R., PEDERSEN, A.K. & STOREY, M. 1999. Trans-Atlantic correlation of the Palaeogene volcanic successions in the Faeroe Islands and East Greenland. *Journal of the Geophysical Society*, **156**, 1081–1095.
- LARSEN, L.M., PEDERSEN, A.K., SØRENSEN, E.V., WATT, W.S. & DUNCAN, R.A. 2013. Stratigraphy and age of the Eocene Igtertivâ Formation basalts, alkaline pebbles and sediments of the Kap Dalton Group in the graben at Kap Dalton, East Greenland. *Bulletin of the Geological Society of Denmark*, **61**, 1–18.
- LARSEN, L.M., PEDERSEN, A.K., TEGNER, T. & DUNCAN, R.A. 2014. Eocene to Miocene igneous activity in NE Greenland: northward younging of magmatism along the East Greenland margin. *Journal of the Geological Society, London*, **171**, 539–553, <http://doi.org/10.1144/jgs2013-118>
- LUNDIN, E.R. & DORÉ, A.G. 1997. A tectonic model for the Norwegian passive margin with implications for the NE Atlantic: early Cretaceous to break-up. *Journal of the Geological Society, London*, **154**, 545–550, <http://doi.org/10.1144/gsjgs.154.3.0545>
- LUNDIN, E.R. & DORÉ, A.G. 2002. Mid-Cenozoic post-breakup deformation in the ‘passive’ margins bordering the Norwegian-Greenland Sea. *Marine and Petroleum Geology*, **19**, 79–93.
- LUNDIN, E.R. & DORÉ, A.G. 2005. NE Atlantic breakup: a re-examination of the Iceland mantle plume model and the Atlantic–Arctic linkage. In: DORÉ, A.G. & VINING, B.A. (eds) *Petroleum Geology: North-West Europe and Global Perspectives – Proceedings of the 6th Petroleum Geology Conference*. Geological Society, London, 739–754, <http://doi.org/10.1144/0060739>

THE JMMC: THE ÆGIR RIDGE TO THE KOLBEINSEY RIDGE

- LUNDIN, E.R. & DORÉ, A.G. 2011. Hyperextension, serpentinization, and weakening: a new paradigm for rifted margin compressional deformation. *Geology*, **39**, 347–350.
- LUNDIN, E.R., REDFIELD, T.F. & PERON-PINDIVIC, G. 2014. Rifted continental margins: geometric influence on crustal architecture and melting. *In*: PINDELL, J., HORN, B. *ET AL.* (eds) *33rd Annual GCSSEPM Foundation Bob F. Perkins Conference. Sedimentary Basins: Origin, Depositional Histories, and Petroleum Systems*. Gulf Coast Section SEPM, Houston, TX, 18–53.
- MAGNÚSDÓTTIR, S., BRANDSDÓTTIR, B., DRISCOLL, N. & DETRICK, R. 2015. Postglacial tectonic activity within the Skjálfandadjúp Basin, Tjörnes Fracture Zone, offshore Northern Iceland, based on high resolution seismic stratigraphy. *Marine Geology*, **367**, 159–170. <http://doi.org/10.1016/j.margeo.2015.06.004>
- MANUM, S.B. & SCHRADER, H.J. 1976. Sites 346, 347, and 349. *In*: TALWANI, M. & UDINTSEV, G. (eds) *Initial Reports of the Deep Sea Drilling Project*, Volume **38**. United States Government Printing Office, Washington, DC, 521–594.
- MANUM, S.B., RASCHKA, H. & ECKHARDT, F.J. 1976a. Site 350. *In*: TALWANI, M. & UDINTSEV, G. (eds) *Initial Reports of the Deep Sea Drilling Project*, Volume **38**. United States Government Printing Office, Washington, DC.
- MANUM, S.B., RASCHKA, H., ECKHARDT, F.J., SCHRADER, H., TALWANI, M. & UDINTSEV, G. 1976b. Site 337 initial reports of the Deep Sea Drilling Project. *In*: TALWANI, M., UDINTSEV, G. *ET AL.* (eds) *Initial Reports of the Deep Sea Drilling Project*, Volume **38**. United States Government Printing Office, Washington, DC, 117–150.
- MATHIESEN, A., BIDSTRUP, T. & CHRISTINSEN, F.G. 2000. Denudation and uplift history of the Jameson Land Basin, East Greenland-constrained from maturity and apatite fission track data. *Global and Planetary Change*, **24**, 275–301.
- MJELDE, R., AURVÅG, R., KODAIRA, S., SHIMAMURA, H., GUNNARSSON, K., NAKANISHI, A. & SHIOBARA, H. 2002. Vp/Vs-ratios from the central Kolbeinsey Ridge to the Jan Mayen Basin, North Atlantic; implications for lithology, porosity and present-day stress field. *Marine Geophysical Researches*, **23**, 123–145.
- MJELDE, R., ECKHOFF, I. *ET AL.* 2007. Gravity and S-wave modelling across the Jan Mayen Ridge, North Atlantic; implications for crustal lithology. *Marine Geophysical Researches*, **28**, 27–41.
- MJELDE, R., BREIVIK, A.J., RAUM, T., MITTELSTAEDT, E., ITO, G. & FALEIDE, J.I. 2008. Magmatic and tectonic evolution of the North Atlantic. *Journal of the Geological Society, London*, **165**, 31–42, <http://doi.org/10.1144/0016-76492007-018>
- MJELDE, R., RAUM, T., KANDILAROV, A., MURAI, Y. & TAKANAMI, T. 2009. Crustal structure and evolution of the outer Møre Margin, NE Atlantic. *Tectonophysics*, **468**, 224–243.
- MUTTER, J.C., TALWANI, M. & STOFFA, P.L. 1982. Origin of seaward-dipping reflectors in oceanic crust off the Norwegian margin by 'subaerial sea-floor spreading'. *Geology*, **10**, 3–12.
- NASUTI, A. & OLESEN, O. 2014. Magnetic data. *In*: HOPPER, J.R., FUNCK, T., STOKER, M.S., ÁRTING, U., PERON-PINDIVIC, G., DOORNENBAL, H. & GAINA, C. (eds) *Tectonostratigraphic Atlas of the North-East Atlantic Region*. Geological Survey of Denmark and Greenland (GEUS), Copenhagen, Denmark, 41–51.
- NILSEN, T.H., KERR, D.R., TALWANI, M. & UDINTSEV, G. 1978. Turbidites, redbeds, sedimentary structures, and trace fossils observed in DSDP Leg 38 cores and the sedimentary history of the Norwegian–Greenland Sea. *In*: *Initial Reports of the Deep Sea Drilling Project. Supplement to Volume 38*. United States Government Printing Office, Washington, DC, 259–288.
- NØHR-HANSEN, H. 2003. Dinoflagellate cyst stratigraphy of the Palaeogene strata from the wells Hellefisk-1, Ikermiut-1, Kangâmiut-1, Nukik-1, Nukik-2 and Qulleq-1, offshore West Greenland. *Marine and Petroleum Geology*, **20**, 987–1016.
- NØHR-HANSEN, H. 2012. Palynostratigraphy of the Cretaceous-Lower Palaeogene sedimentary succession in the Kangerlussuaq Basin, southern East Greenland. *Review of Palaeobotany and Palynology*, **178**, 59–90.
- NØHR-HANSEN, H. & PIASECKI, S. 2002. Paleocene sub-basaltic sediments on Savoia Halvø, East Greenland. *Geology of Greenland Survey Bulletin*, **191**, 111–116.
- NORWEGIAN PETROLEUM DIRECTORATE 2012. *Submarine Fieldwork on the Jan Mayen Ridge: Integrated Seismic and ROV-Sampling*. Norwegian Petroleum Directorate, Stavanger, Norway, <http://www.npd.no/en/Publications/Presentations/Submarine-fieldwork-on-the-Jan-Mayen-Ridge/>
- NORWEGIAN PETROLEUM DIRECTORATE 2013. *The Petroleum Resources on the Norwegian Continental Shelf*. Norwegian Petroleum Directorate, Stavanger, Norway, <http://www.npd.no/en/Publications/Resource-Reports/2013/>
- NUNNS, A. 1983a. The structure and evolution of the Jan Mayen Ridge and surroundings regions. *In*: WATKINS, J.S. & DRAKE, C.L. (eds) *Studies in Continental Margin Geology*. American Association of Petroleum Geologists, Memoirs, **34**, 193–208.
- NUNNS, A.G. 1983b. Plate tectonic evolution of the Greenland-Scotland Ridge and surrounding regions. *In*: BOTT, M.H.P., SAXOV, S., TALWANI, M. & THIEDE, J. (eds) *Structure and Development of the Greenland–Scotland Ridge*. Plenum, New York, 11–30.
- NUNNS, A.G., TALWANI, M. *ET AL.* 1983. Magnetic anomalies over Iceland and surrounding seas. *In*: BOTT, M.H.P., SAXOV, S., TALWANI, M. & THIEDE, J. (eds) *Structure and Development of the Greenland-Scotland Ridge*. Plenum, New York, 661–678.
- OLAFSSON, I. & GUNNARSSON, K. 1989. *The Jan Mayen Ridge: Velocity Structure from Analysis of Sonobuoy Data*. OS-89030/JHD-04. Orkustofnun, Reykjavík.
- OSMUNDSEN, P.T. & ANDERSEN, T.B. 1994. Caledonian compressional and late-orogenic extensional deformation in the Staveneset area, Sunnfjord, Western Norway. *Journal of Structural Geology*, **16**, 1385–1401.
- OSMUNDSEN, P.T. & ANDERSEN, T.B. 2001. The middle Devonian basins of western Norway: sedimentary response to large-scale transtensional tectonics. *Tectonophysics*, **332**, 51–68, [http://doi.org/10.1016/S0040-1951\(00\)00249-3](http://doi.org/10.1016/S0040-1951(00)00249-3)

- OSMUNDSEN, P.T. & EBBING, J. 2008. Styles of extension offshore mid-Norway and implications for mechanisms of crustal thinning at passive margins. *Tectonics*, **27**, TC6016.
- OSMUNDSEN, P.T., SOMMARUGA, A., SKILBREI, J.R. & OLESEN, O. 2002. Deep structure of the Mid Norway rifted margin. *Norwegian Journal of Geology*, **82**, 205–224.
- PASSEY, S. & HITCHEN, K. 2011. Cenozoic (igneous). In: RITCHIE, J.D., ZISKA, H., JOHNSON, H. & EVANS, D. (eds) *Geology of the Faroe-Shetland Basin and Adjacent Areas*. British Geological Survey and Jarðfeingi Research Report RR/11/01 British Geological Survey, Keyworth, Nottingham, 209–228.
- PASSEY, S.R. & JOLLEY, D.W. 2009. A revised lithostratigraphic nomenclature for the Palaeogene Faroe Islands basalt Group, NE Atlantic Ocean. *Earth and Environmental Science, Transactions of the Royal Society of Edinburgh*, **99**, 127–158.
- PERON-PINVIDIC, G., GERNIGON, L., GAINA, C. & BALL, P. 2012a. Insights from the Jan Mayen system in the Norwegian-Greenland Sea – I: mapping of a microcontinent. *Geophysical Journal International*, **191**, 385–412.
- PERON-PINVIDIC, G., GERNIGON, L., GAINA, C. & BALL, P. 2012b. Insights from the Jan Mayen system in the Norwegian-Greenland Sea – II: architecture of a microcontinent. *Geophysical Journal International*, **191**, 413–435.
- PERON-PINVIDIC, G., MANATSCHAL, G. & OSMUNDSEN, P.T. 2013. Structural comparison of archetypal Atlantic rifted margins: a review of observations and concepts. *Marine and Petroleum Geology*, **43**, 21–47.
- PHARAOH, T.C., DUSAR, M. ET AL. 2010. Tectonic evolution. In: DOORNENBAL, J.C. & STEVENSON, A.G. (eds) *Petroleum Geological Atlas of the Southern Permian Basin Area*. European Association of Geoscientists & Engineers, Houten, The Netherlands, 25–57.
- PLANKE, S., SYMONDS, P.A., ALVESTAD, E. & SKOGSEID, J. 2000. Seismic volcanostratigraphy of large-volume basaltic extrusive complexes on rifted margins. *Journal of Geophysical Research*, **105**, 19335–19351.
- POLTEAU, S., MAZZINI, A., TRULSVIK, M. & PLANKE, S. 2012. *JMRS11 – Jan Mayen Ridge Sampling Survey 2011*. VBPR-TGS, Commercial Report, February 2012.
- PRESTVIK, T., GOLDBERG, S., KARLSSON, H. & GRÖNVOLD, K. 2001. Anomalous strontium and lead isotope signatures in the off-rift Örefajökull central volcano in southeast Iceland: evidence for enriched endmember(s) of the Iceland mantle plume? *Earth and Planetary Science Letters*, **190**, 211–220.
- RASCHKA, H., ECKHARDT, F.J. & MANUM, S.B. 1976. Site 348. In: TALWANI, M. & UDINTSEV, G. (eds) *Initial Reports of the Deep Sea Drilling Project*, Volume **38**. United States Government Printing Office, Washington, DC, 595–654.
- REY, S.S., ELDHOLM, O. & PLANKE, S. 2003. Formation of the Jan Mayen Microcontinent, the Norwegian Sea. *Eos, Transactions of the American Geophysical Union*, **84**, Abstract T31D-0872.
- SANDSTÅ, N.R., PEDERSEN, R.B., WILLIAMS, R.D., BERING, D., MAGNUS, C., SAND, M. & BREKKE, H. 2012. *Submarine fieldwork on the Jan Mayen Ridge; integrated seismic and ROV-sampling*. Norwegian Petroleum Directorate, Stavanger, Norway, <http://www.npd.no/>
- SÆMUNDSSON, K. 1974. Evolution of the Axial Rifting Zone in Northern Iceland and the Tjörnes Fracture Zone. *Geological Society of America Bulletin*, **85**, 495–504.
- SÆMUNDSSON, K. 1979. Outline of the geology of Iceland. *Jökull*, **29**, 7–28.
- SCOTT, R.A., RAMSEY, L.A., JONES, S.M., SINCLAIR, S. & PICKLES, C.S. 2005. Development of the Jan Mayen microcontinent by linked propagation and retreat of spreading ridges. In: WANDÅS, B.T.G., NYSTUEN, J.P., EIDE, E. & GRADSTEIN, F. (eds) *Onshore–Offshore Relationships on the North Atlantic Margin*. Norwegian Petroleum Society, Oslo, 69–82.
- SEIDLER, L. 2000. Incised submarine canyons governing new evidence of Early Triassic rifting in East Greenland. *Palaeogeography, Palaeoclimatology, Palaeoecology*, **161**, 267–293.
- SOPER, N.J., HIGGINS, A.C., DOWNIE, C., MATTHEWS, D.W. & BROWN, P.E. 1976. Late Cretaceous-early Tertiary stratigraphy of the Kangerdlugssuaq area, east Greenland, and the age of opening of the northeast Atlantic. *Journal of the Geological Society, London*, **132**, 85–104, <http://doi.org/10.1144/gsjgs.132.1.0085>
- STEMMERIK, L. 2000. Late Palaeozoic evolution of the North Atlantic margin of Pangea. *Palaeo-geography Palaeo-climatology. Palaeoecology*, **161**, 95–126.
- STOKER, M.S., PRAEG, D. ET AL. 2005. Neogene evolution of the Atlantic continental margin of NW Europe (Lofoten Islands to SE Ireland): anything but passive. In: DORÉ, A.G. & VINING, B.A. (eds) *Petroleum Geology: North-West Europe and Global Perspectives – Proceedings of the 6th Petroleum Geology Conference*. Geological Society, London, **6**, 1057–1076, <http://doi.org/10.1144/0061057>
- STOKER, M.S., STEWART, M. ET AL. 2016. An overview of the Upper Paleozoic–Mesozoic stratigraphy of the NE Atlantic region. In: PÉRON-PINVIDIC, G., HOPPER, J., STOKER, M.S., GAINA, C., DOORNENBAL, H., FUNCK, T. & ÁRTING, U. (eds) *The North-East Atlantic Region: A Reappraisal of Crustal Structure, Tectono-Stratigraphy and Magmatic Evolution*. Geological Society, London, Special Publications, **447**, first published online August 11, 2016, <http://doi.org/10.1144/SP447.2>
- STOREY, M., DUNCAN, R.A. & SWISHER, C.C., III. 2007a. Paleocene-Eocene thermal maximum and opening of the Northeast Atlantic. *Science*, **316**, 587–589.
- STOREY, M., DUNCAN, R.A. & TEGNER, C. 2007b. Timing and duration of volcanism in the North Atlantic Igneous Province: implications for geodynamics and links to the Iceland hotspot. *Chemical Geology*, **241**, 264–281.
- SURLYK, F. 1977. *Stratigraphy, Tectonics and Palaeogeography of the Jurassic, Eiments of the Areas North of Kong Oscars Fjord, East Greenland*. Bulletin Grønlands Geologiske Undersøgelse, **123**.
- SURLYK, F. 1978. *Submarine Fan Sedimentation Along Fault Scarps On Tilted Fault Blocks*

THE JMMC: THE ÆGIR RIDGE TO THE KOLBEINSEY RIDGE

- (*Jurassic–Cretaceous Boundary, East Greenland*). Bulletin Grønlands Geologiske Undersøgelse, **128**.
- SURLYK, F. 1990. Timing, style and sedimentary evolution of Late Paleozoic–Mesozoic extensional basins of East Greenland. In: HARDMAN, R.F.P. & BROOKS, J. (eds) *Tectonic Events Responsible for Britain's Oil and Gas Reserves*. Geological Society, London, Special Publications, **55**, 107–125. <http://doi.org/10.1144/GSL.SP.1990.055.01.05>
- SURLYK, F. 1991. Tectonostratigraphy of North Greenland. In: PEEL, J.S. & SØNDERHOLM, M. (eds) *Sedimentary Basins of North Greenland*. Bulletin Grønlands Geologiske Undersøgelse, **160**, 25–47.
- SURLYK, F. 2003. The Jurassic of East Greenland: a sedimentary record of thermal subsidence, onset and culmination of rifting. In: INESON, J.R. & SURLYK, F. (eds) *The Jurassic of Denmark and Greenland*. Geological Survey of Denmark and Greenland Bulletin, **1**, 659–722.
- SURLYK, F. & NOE-NYGAARD, N. 2001. Cretaceous faulting and associated coarse-grained marine gravity flow sedimentation, Traill Ø, East Greenland. In: MARTINSEN, O.J. & DREYER, T. (eds) *Sedimentary Environments Offshore Norway – Paleozoic to Recent*. Norwegian Petroleum Society, Special Publications, **10**, 293–319.
- SURLYK, F., CALLOMON, J.H., BROMLEY, R.G. & BIRKELUND, T. 1973. *Stratigraphy of the Lower Jurassic–Lower Cretaceous Sediments of Jameson Land and Scoresby Land, East Greenland*. Bulletin Grønlands Geologiske Undersøgelse, **105**.
- SVELLINGEN, W. & PEDERSEN, R. 2003. Jan Mayen: a result of ridge-transform-micro-continent interaction. *Geophysical Research Abstracts*, **5**, 12993.
- TALWANI, M. & ELDHOLM, O. 1977. Evolution of the Norwegian-Greenland Sea. *Geological Society of America Bulletin*, **88**, 969–999.
- TALWANI, M. & UDINTSEV, G. (eds). 1976. *Initial Reports of the Deep Sea Drilling Project*, Volume **38**. United States Government Printing Office, Washington, DC.
- TALWANI, M., UDINTSEV, G. & SHIRSHOV, P.R. 1976a. Tectonic synthesis. In: TALWANI, M. & UDINTSEV, G. (eds) *Initial Reports of the Deep Sea Drilling Project*, Volume **38**. United States Government Printing Office, Washington, DC, 1213–1242.
- TALWANI, M., UDINTSEV, G. & WHITE, S.M. 1976b. Introduction and explanatory notes, Leg 38, Deep Sea Drilling Project. In: TALWANI, M. & UDINTSEV, G. (eds) *Initial Reports of the Deep Sea Drilling Project*, Volume **38**. United States Government Printing Office, Washington, DC, 3–19.
- TEGNER, C., BROOKS, C.K., DUNCAN, R.A., HEISTER, L.E. & BERNSTEIN, S. 2008. ^{40}Ar – ^{39}Ar ages of intrusions in East Greenland: rift-to-drift transition over the Iceland hotspot. *Lithos*, **101**, 480–500.
- THIEDE, J., FIRTH, J.V. ET AL. 1995. Site 907. In: MYHRE, A.M., THIEDE, J. ET AL. (eds) *Proceedings of the Ocean Drilling Program, Initial Reports*, Volume **151**. Ocean Drilling Program, College Station, TX, 57–111.
- THORDARSON, T. & LARSEN, G. 2007. Volcanism in Iceland in historical time: volcano types, eruption styles and eruptive history. *Journal of Geodynamics*, **43**, 118–152.
- TORSVIK, T.H., MOSAR, J. & EIDE, E.A. 2001. Cretaceous–Tertiary geodynamics: a North Atlantic exercise. *Geophysical Journal International*, **146**, 850–866.
- TORSVIK, T.H., AMUNDSEN, H.E.F. ET AL. 2015. Continental crust beneath southeast Iceland. *Proceedings of the National Academy of Sciences of the United States of America*, **112**, 1818–1827.
- TSIKALAS, F., ELDHOLM, O. & FALÉIDE, J.I. 2005. Crustal structure of the Lofoten-Vesterålen continental margin, off Norway. *Tectonophysics*, **404**, 151–174.
- TSIKALAS, F., FALÉIDE, J.I. & KUSZNIR, N.J. 2008. Along-strike variations in rifted margin crustal architecture and lithosphere thinning between northern Vøring and Lofoten margin segments off mid-Norway. In: ROSENBAUM, G., WEINBERG, R.F. & REGENAUER-LIEB, K. (eds) *Geodynamics of Lithospheric Extension*. *Tectonophysics*, **458**, 68–81.
- VOGT, P.R. & JUNG, W.Y. 2009. Treitel ridge: a unique inside corner hogback on the west flank of extinct Aegir spreading ridge, Norway basin. *Marine Geology*, **267**, 86–100.
- VOGT, P.R., ANDERSON, C.N., BRACEY, D.R. & SCHNEIDER, E.M. 1970. North Atlantic Magnetic Smooth Zones. *Journal of Geophysical Research*, **75**, 3955–3968.
- WALKER, G.P.I. 1964. Geological investigations in eastern Iceland. *Bulletin of Volcanology*, **27**, 351–363.
- ZIEGLER, P.A. 1988. *Evolution of the Arctic-North Atlantic and the Western Tethys*. American Association of Petroleum Geologists, Memoirs, **43**.

Paper II

The Jan Mayen microcontinent's Cenozoic stratigraphic succession and structural evolution within the NE-Atlantic

Blischke, A., Stoker, M. S., Brandsdóttir, B., Hopper, J. R., Peron-Pinvidic, G., Ólavsdóttir, J. and Japsen, P. (2019)

Marine and Petroleum Geology, Volume 103, May 2019, Pages 702-737

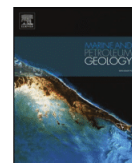
<https://doi.org/10.1016/j.marpetgeo.2019.02.008>

Copyright © The Authors 2019



Contents lists available at ScienceDirect

Marine and Petroleum Geology

journal homepage: www.elsevier.com/locate/marpetgeo

Research paper

The Jan Mayen microcontinent's Cenozoic stratigraphic succession and structural evolution within the NE-Atlantic

Anett Blischke^{a,b,*}, Martyn S. Stoker^c, Bryndís Brandsdóttir^a, John R. Hopper^d, Gwenn Peron-Pinvidic^e, Jana Ólavsdóttir^f, Peter Japsen^d^a Institute of Earth Sciences, Science Institute, University of Iceland, Askja, Sturlugata 7, 101, Reykjavík, Iceland^b Iceland GeoSurvey, Branch at Akureyri, Rangárvöllum, 603, Akureyri, Iceland^c Australian School of Petroleum, University of Adelaide, Adelaide, South Australia 5005, Australia^d Geological Survey of Denmark and Greenland (GEUS), Øster Voldgade 10, DK1350, Copenhagen K, Denmark^e Geological Survey of Norway (NGU), Postboks 6315 Sluppen, 7491, Trondheim, Norway^f Jarðfeingi, Jóhannesar Paturssonargöta 32-34, Postsmoga 3059, FO 100, Tórshavn, Faroe Islands

ARTICLE INFO

Keywords:

Cenozoic
Dual-breakup
Hiatus
Kinematic model
Iceland plateau
Jan Mayen microcontinent
Seismic stratigraphy
Unconformity

ABSTRACT

Cenozoic seismic-stratigraphic units of the Jan Mayen microcontinent (JMMC) are presented in context with kinematic modelling of plate reorganisation correlation with conjugate margins, and their chrono-stratigraphic correlations. Our model of development of the microcontinent, from continental breakup to present-day, is based on the interpretation of new and legacy geological and geophysical data. From these data, we have established eleven Cenozoic seismic-stratigraphic units (JM-70 to JM-01) separated by ten locally varying unconformities and disconformities, six of which are regional and reflect discrete tectonostratigraphic phases in the evolution of the Jan Mayen region. These six main phases are: (1) pre-breakup Paleocene (> 55 Ma) extension represented by seismic unit JM-70, which comprises terrigenous and marine sedimentary rocks and a thick plateau basalt volcanic succession; (2) Early Eocene (~55–52 Ma) syn-breakup (rift-to-drift) represented by seismic unit JM-60 and comprises a mix of intrusive igneous rocks, subaerial lavas and hyaloclastites, and non-marine to shallow-marine sedimentary rocks; (3) Early to Mid-Eocene (~52–43 Ma) syn-breakup (rift-to-drift) and rift-transfer across the Iceland plateau rift, represented by seismic unit JM-50 that comprises volcanic rocks and shelf-margin deltaic sediment succession; (4) Late Eocene – Early Oligocene (43–30 Ma) ridge transfer and tectonic re-arrangement in proximity of the Iceland hotspot represented in the rock record by shallow-to deep-marine deposits preserved as units JM-40, JM-35, and JM-30; (5) in the Late Oligocene (30–22 Ma), a second breakup occurred along the western JMMC igneous margin, together with the formation of the south-western Jan Mayen igneous province, the proto-Kolbeinsey ridge, and the initiation of proto-Iceland all, of which, is represented in the rock record by seismic units JM-20 and JM-15; and, (6) Miocene-to-present-day separation of the JMMC from East Greenland (since 22 Ma), which is represented by seismic units JM-10, JM-05, and JM-01 that reflect a general deepening of the microcontinent.

1. Introduction

In previous studies of the Jan Mayen microcontinent (JMMC) (Fig. 1), the main focus of research has been on the reconstruction of a detailed tectonostratigraphic model based largely on its relation to its conjugate margins, including the central East Greenland and Møre margins, and the central Norwegian shelf (Talwani and Eldholm, 1977; Åkermoen, 1989; Gunnarsson et al., 1989; Henriksen, 2008; Peron-Pinvidic et al., 2012a, b; Gernigon et al., 2012, 2015; Gaina et al., 2009, 2017; Blischke et al., 2017a). In this study, we focus specifically on the

Cenozoic stratigraphy preserved on the JMMC to generate a structural and tectonic model of the microcontinent and surrounding oceanic crust. Our seismic-stratigraphic mapping is based on new and vintage geological and geophysical data, collected offshore Iceland since the early 1970's, including seismic reflection and refraction data, IODP borehole control, seafloor samples, and multibeam seafloor data (Figs. 2 and 3 & Table 1). Stratigraphic constraints are further provided by published regional correlation charts, established unconformities, and paleogeographic interpretations for the central northeast Atlantic region (e.g. Pedersen et al., 1997; Larsen et al., 1999a,b; 2002, 2005;

* Corresponding author. Institute of Earth Sciences, Science Institute, University of Iceland, Askja, Sturlugata 7, 101, Reykjavík, Iceland.
E-mail addresses: anb@isor.is, anb24@hi.is (A. Blischke).

<https://doi.org/10.1016/j.marpetgeo.2019.02.008>

Received 8 November 2018; Received in revised form 5 February 2019; Accepted 7 February 2019

Available online 27 February 2019

0264-8172/ © 2019 Elsevier Ltd. All rights reserved.

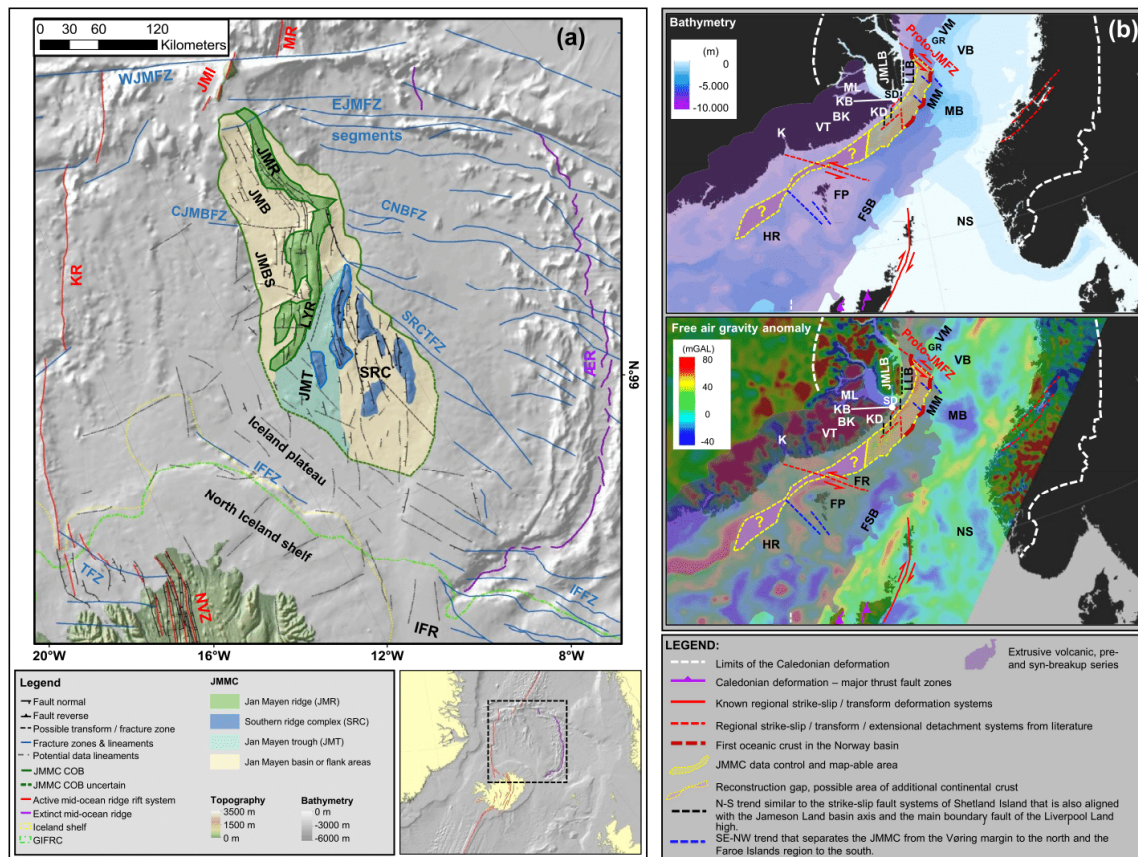


Fig. 1. Overview map (a) of the JMMC with mapped faults, fracture zones and lineaments based on this study and Blischke et al. (2017a). Background is shaded bathymetry (IBCAO 3.0; Jakobsson et al., 2012). Abbreviations: CJMBFZ – central Jan Mayen basin fracture zone, CNBFZ – central Norway basin fracture zone, EJMFZ – East Jan Mayen fracture zone segments, GR – Gjallar ridge, IFFZ – Iceland-Faroe fracture zone, JMB – Jan Mayen basin, JMBS – Jan Mayen basin south, JMI – Jan Mayen Island complex, JMR – Jan Mayen ridge, JMT – Jan Mayen trough, MR – Mohn's ridge, KR – Kolbeinsey ridge, LYR – Lyngvi ridge, NVZ – Northern volcanic zone, SRC – Southern ridge complex, SRCTFZ – Southern ridge complex transfer fracture zone, TFZ – Tjörnes fracture zone, WJMFZ – Western Jan Mayen fracture zone, ÆR – Ægir ridge. The pre-breakup setting of the central Northeast Atlantic region is shown on insert (b) with reconstructed present day bathymetry and free air gravity data at around 56–55 Ma using GPlates (Boyden et al., 2011): BK – Blossville Kyst, FP – Faroe Plateau, FR – Fugloy ridge, FSB – Faroe-Shetland basin, HR – Hatton-Rockall margin and basin, JLB – Jameson Land basin, K – Kangerlussuaq, KB – Kap Brewster, KD – Kap Dalton, I.L.B – Liverpool Land basin, MB – Møre basin, MM – Møre margin, NS – North Sea, SD – Scoresby Sund, VB – Vøring basin, VM – Vøring margin, VT – Vindtoppen formation. Features displayed are modified from data and interpretations by Larsen, L.M. et al. (1989, 1999); Osmundsen and Andersen (2001); Foulger et al. (2005); Henriksen (2008); Le Breton et al. (2013); Peron-Pinvidic et al. (2013, 2012a); Gasser (2014); Hopper et al. (2014); Guarnieri (2015); Gernigon et al. (2015); Blischke et al. (2016); Gaina et al. (2009, 2017a,b) and á Horni et al. (2017).

Ritchie et al., 2011; Larsen et al., 2013, 2014; Ólavsdóttir et al., 2013; Japsen et al., 2014; Stoker et al., 2013; Ellis and Stoker, 2014; Bonow et al., 2014; or Hjartarson et al., 2017).

The study area is approximately 400–450 km long and varies in width from 100 km in the north to 310 km in the south, encompassing the Jan Mayen ridge (JMR) and surrounding areas, i.e. the Jan Mayen basin (JMB), Jan Mayen basin south (JMBS), Jan Mayen trough (JMT), and the southern ridge complex (SRC) (Fig. 1). The northern boundary of the microcontinent is formed by the east and west segments of the Jan Mayen fracture zone (EJMFZ and WJMFZ) and the Jan Mayen Island volcanic complex (JMI) (Svelling and Pedersen, 2003). The north-eastern coastal shelf of Iceland, the Iceland-Faroe fracture zone (IFFZ), and the Iceland plateau (IP) form the southern boundary, whereas the Norway basin (NB) limits the microcontinent to the east, and to the west it is bounded by the Kolbeinsey ridge (KR). Earliest interpretations of the JMMC describe the Jan Mayen ridge (Vogt et al.,

1970; Talwani et al., 1976b) as a steeply-flanked bathymetric horst structure extending south from the Jan Mayen Island with a varying water depth between 200 and 2500 m. Later studies delineated the outline of the microcontinent further south and southeast, describing structurally controlled tectonic and volcanic features of the JMT and SRC with the occurrence of numerous intrusive and extrusive volcanic rocks that limit seismic imaging of the underlying features (e.g. Scott et al., 2005; Gaina et al., 2009; Peron-Pinvidic et al., 2012a, b; Gernigon et al., 2012, 2015; Blischke et al., 2017a).

1.1. Regional geological setting

The structure and stratigraphy of the JMMC has been shaped by two separate rifting and breakup events on either side of the microcontinent related to a westward transfer of rifting process from the Ægir ridge (ÆR), east of the JMMC, to the Kolbeinsey ridge rift system, to the west

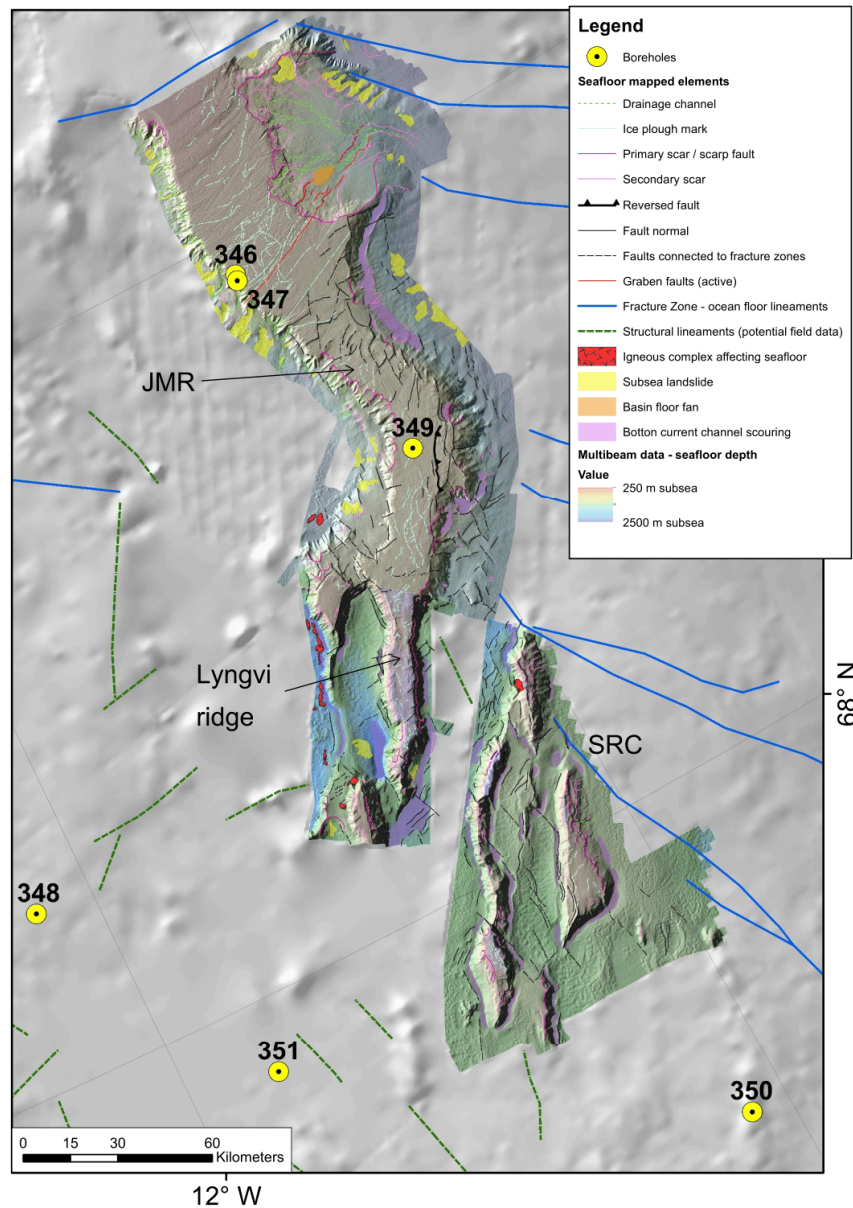


Fig. 2. Structural and sedimentary features of the JMJC. Background image is shaded bathymetry (IBCAO 3.0; Jakobsson et al., 2012), and foreground 50 × 50 m gridded multi-beam bathymetry data Iceland Marine Institute, Nation Energy Authority of Iceland, and Norwegian Petroleum Directorate in 2008 & 2010 (Blischke et al., 2017b).

(Fig. 1a). During Early Eocene (56–55 Ma) breakup and ridge transfer, intense magmatism occurred along the Kangerlussuaq (K) and southern Blossville Kyst (BK) coasts of East Greenland (e.g. Tegner et al., 2008; Brooks, 2011; Larsen et al., 2014), including the emplacement of the regionally extensive plateau basalts that are part of the North Atlantic igneous province (NAIP) (Fig. 1b). Seafloor spreading in the Northeast Atlantic followed the final rupturing of the lithosphere around the end of chron C25 or beginning of C24r (~55 Ma) (e.g. Talwani and Eldholm, 1977) and resulted in the formation of seaward-dipping

reflectors observed on seismic reflection data (Hinz, 1981; Planke et al., 2000; Geissler et al., 2017; á Horni et al., 2017) along the continental margins, and subsequently the formation of oceanic crust within the Norway basin, forming the Ægir mid-oceanic ridge (e.g. Talwani and Eldholm, 1977; Gaina et al., 2009, 2017).

These processes have been described in various tectonic reconstructions, primarily based on geochronological work (Nunns, 1983a, b, c; Lundin and Doré, 2005; Doré, 2008; Gaina et al., 2009). More recently, higher-resolution reconstruction was generated by

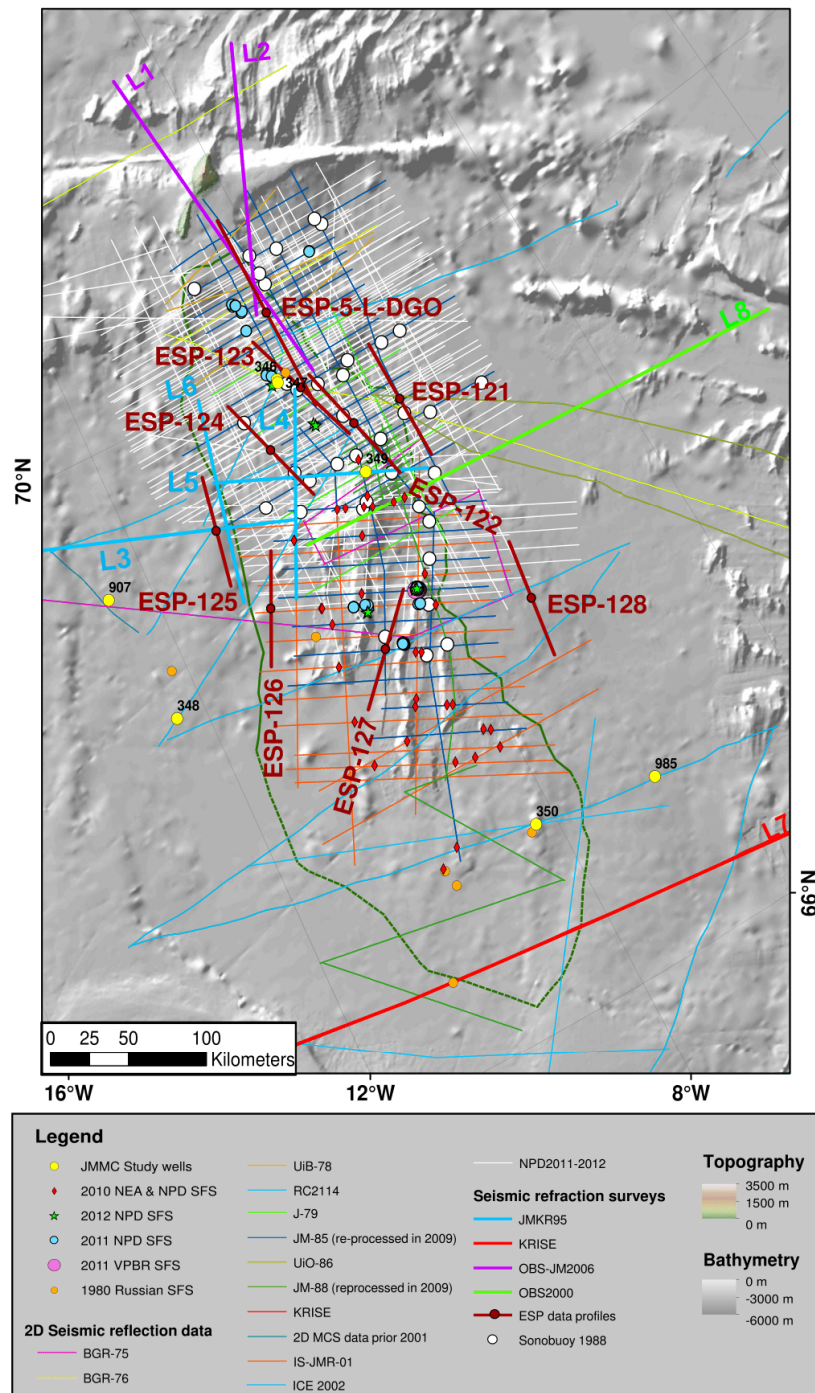


Fig. 3. Study database (Table 1) and shaded bathymetry map (Jakobsson et al., 2012) showing location of refraction and reflection seismic lines, boreholes and seabed sampling sites (National Energy Authority of Iceland, Iceland; Norwegian Petroleum Directorate; Spectrum ASA; TGS; SFS seafloor samples; Volcanic Basin Petroleum Research AS).

Table 1
JMMC study database (Blischke et al., 2017a; Norwegian Petroleum Directorate, 2013), reviewed and selected data and studies (Fig. 3).

Year	Survey ID	Survey lead	Country	Platform name	Data repository	Data types
1974	DSDP Leg 38	DSDP		Glomar Challenger	IODP	Boreholes
1975	BGR-75	BGR	Germany	Longva	BGR	2D MCS
1976	BGR-76	BGR	Germany	Explora	BGR	2D MCS
1978	RC2114	L-DGO	USA/Norway	Robert Conrad	MGDS	Bathymetry; Magnetics; Gravity; 2D MCS/2D MCS; ESP-5
1979	J-79	NPD	Norway	GECO alpha	NPD	Bathymetry; Magnetics; Gravity; 2D MCS
1980		PAH/SGC	USSR	Akademic Kurchatov		Seafloor sampling
1985	JM-85	NPD/NEA	Norway	Malene Østervold	NPD	Bathymetry; Magnetics; Free Air Gravity; Bouguer Gravity; Magnetic; 2D MCS
1986	UiO-86	UiO	Norway	Håkon Mosby	NPD	2D MCS
1986	ESP	IFP	France/Norway	Polarbjørn & Odys Echo	CGG/UiO	Refranorge IV; ESP; Velocity; Gravity
1988	JM-88	NPD/NEA	Norway	Håkon Mosby	NPD	Bathymetry; Magnetics; Gravity; 2D MCS; Sonobuoy
1995	JMKR95	UiB/UiH/NEA	Norway/Japan/NEA		UiB	Seismic refraction & 2D MCS
1995	ODP Leg 161	L-DGO	Norway/UK/USA	JOIDES Resolution	IODP	Boreholes
2000	KRISE	UiB	Norway	Håkon Mosby	UiB	Seismic refraction & 2D MCS
2000	OBS2000	UiB	Norway	Håkon Mosby	UiB	Seismic refraction & 2D MCS
2001	IS-JMR-01	InSeis	Norway	Polar Princess	CGG/Veritas	2D MCS
2002	ICE-02	TGS-NOPEC	Iceland	Zephyr 1	TGS-NOPEC	2D MCS; Gravity
2006	OBS JM-06	UiB/Geomar	Norway/Germany	G. O. SARS	UiB	Seismic refraction & 2D MCS, gravity, magnetics
2008	WI-JMR-08	Wavefield InSeis	Norway	Malene Østervold	Spectrum	2D MCS
2008	A8-2008	HAFRO/NEA	Iceland	Arni Fridriksson	HAFRO/NEA	Multibeam
2009	JM-85-88	Spectrum	Norway	Re-processing	Spectrum	2D MCS
2010	A11-2010	HAFRO/NEA/NPD	Iceland	Arni Fridriksson	HAFRO/NEA/NPD/Fugro Geolab	Multibeam; Seafloor sampling
2010	B11-2008	HAFRO/NEA	Iceland	Arni Fridriksson	HAFRO/NEA	Benthic survey
2011	NPD-11	NPD/UiB	Norway	Harrier Explorer	NPD/PGS	2D MCS; Seafloor sampling
2011	JMRS11	VPBR/TGS	Norway	TGS	VPBR/TGS	Seafloor sampling
2012	NPD-12	NPD/UiB	Norway	Nordic Explorer	NPD/PGS	2D MCS; Seafloor sampling

implementing local structural and stratigraphic mapping results based on denser spaced seismic reflection and refraction data sets as well as potential field, borehole and seafloor data (Peron-Pinvidic, 2012a, b; Gernigon et al., 2015; Blischke et al., 2017a). On this basis, the Cenozoic tectono-magmatic evolution of the JMMC and surrounding oceanic crust was divided into six main phases (Fig. 4), which are summarised (in ascending chronological order) as follows:

1. The JMMC was affected by a pre-breakup stage ending at 56–55 Ma with the emplacement of Lower Eocene plateau basalts across the microcontinent and the Blosseville Kyst region (Blischke et al., 2017a). The main structures of the JMMC were in alignment with major structural lineaments of the surrounding regions prior to breakup, with the Jameson Land basin and Liverpool Land high along the central East Greenland coast, and with the IFFZ along the southern extension of the JMMC.
2. The first breakup began around 55 Ma along the north-eastern to eastern flank of the JMMC and formed a series of seaward-dipping reflectors (SDRs) that marked the initiation of seafloor spreading in the Norway basin along the Ægir ridge in the Early Eocene (chron C24n2r 53.36 Ma) (Gaina et al., 2009; Gernigon et al., 2015; Blischke et al., 2017a).
3. A renewed phase of rifting during chron C22n (49.3 Ma) established a continuous Ægir ridge spreading system within the Norway basin and formed the eastern margin of the Iceland plateau, southeast of the JMMC.
4. The initiation of a rift transition occurred around chron C21n (47.33 Ma) from the south-eastern to the southern extent of the known JMMC, which is interpreted to have been caused by the oblique seafloor spreading of the Ægir ridge system to the east of the JMMC. This oblique spreading system is believed to have caused the formation of transform systems and uplift along the southern flank

of the JMMC that correspond to volcanic activity along the north-eastern margin of the Blosseville Kyst (Larsen et al., 2014; Blischke et al., 2017a).

5. A westward shift of volcanic activity along the southern and south-western JMMC initiated the second breakup phase focused along the western margin of the JMMC during Early Oligocene (around chron C13n, 33.1 Ma). The south-western area of the JMMC was heavily affected by volcanism linked to the Iceland plateau rift (IPR) system that was located adjacent to the conjugate Blosseville Kyst margin with known igneous centres close to the continent ocean boundary (Gaina et al., 2017a; Blischke et al., 2017a).
6. The onset of full spreading as a consequence of the second breakup phase of the JMMC led to the establishment of the Kolbeinsey mid-oceanic ridge system along the western margin of the microcontinent, and the cessation of seafloor spreading in the Norway basin between 30 Ma and 26 Ma (Gaina et al., 2009; Gernigon et al., 2015) around chron C6b (21.56 Ma).

In this study, we investigate the stratigraphic and sedimentary response to these key tectono-magmatic events, thereby enabling a regional seismic-stratigraphic framework to be established across the JMMC. The study is conducted at a scale that provides a primary stratigraphic unit analysis, which are tied to units composed of a relatively conformable succession of genetically related strata and bound by either unconformities or conformities, reflecting tectono-stratigraphic changes (Mitchum et al., 1977).

2. Data overview and methods

For this study, we have utilised an integrated dataset, including bathymetry, seismic reflection, seismic refraction, onshore and offshore sampling, magnetic, gravity, and crustal thickness (e.g. Vogt et al.,

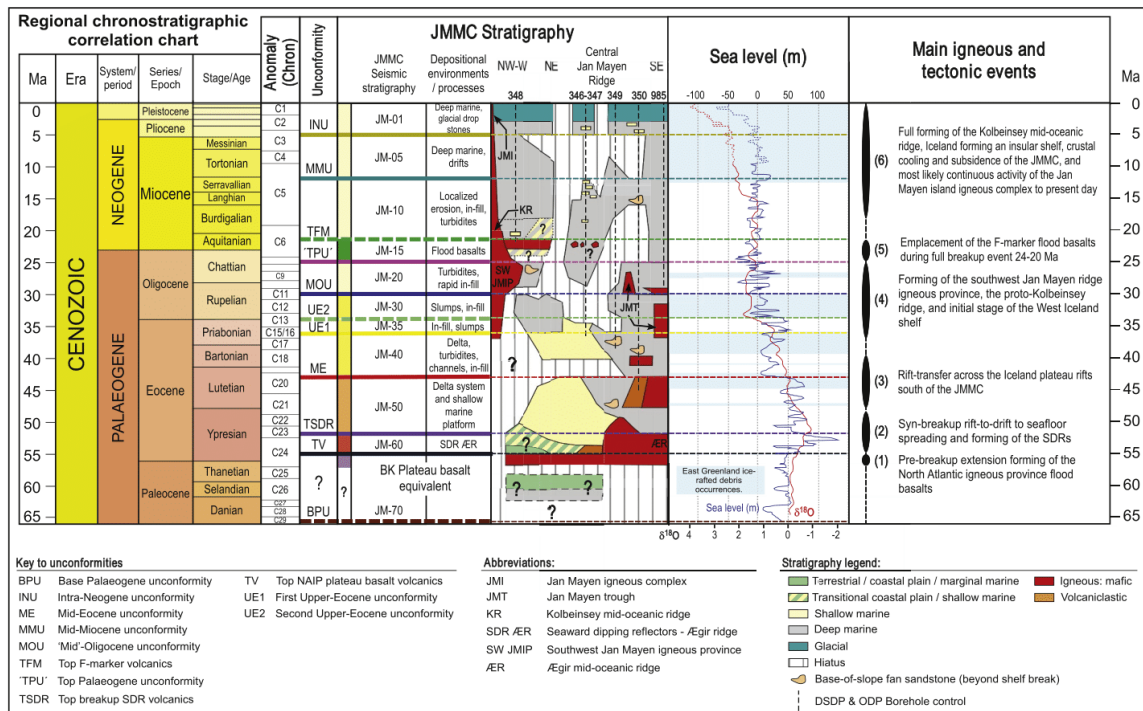


Fig. 4. Chronostratigraphic chart of the JMMC based on DSDP borehole data (Talwani et al., 1976a, b; Manum and Schrader, 1976; Schrader et al., 1976; Manum et al., 1976a, b; Raschka et al., 1976; Nilsen et al., 1978; Thiede et al., 1995; Jansen et al., 1996; Channell et al., 1999a, b; Butt et al., 2001) summarised in Blischke et al. (2017a), constrained by interpretation of the Jan Mayen seismic reflection and refraction data. The main igneous events are marked as (1) pre-breakup extension forming of the NAIP flood basalts; (2) syn-breakup rift-to-drift to seafloor spreading and forming of the SDRs; (3) rift-transfer across the Iceland plateau rifts south of the JMMC; (4) forming of the southwest Jan Mayen ridge igneous province, the proto-Kolbeinsey ridge, and initial stage of the West Iceland shelf; (5) emplacement of the F-marker flood basalts during full breakup event 24-21 Ma; and (6) full forming of the Kolbeinsey mid-oceanic ridge, Iceland forming an insular shelf, crustal cooling and subsidence of the JMMC, and most likely continuous activity of the Jan Mayen island igneous complex to present day. Time scale from Gradstein et al. (2012), average sea level change and $\delta^{18}O$ data by Van Sicken et al. (2004), Miller et al. (2008), and Murray-Wallace and Woodroffe (2014). Palaeogene East Greenland ice-rafted debris occurrences by Tripati and Darby (2018), and borehole location reference see Fig. 3.

1970; Talwani and Eldholm, 1977; Åkermoen, 1989; Doré et al., 1999; Lundin and Dóre, 2002; Rey et al., 2003; Gaina et al., 2009; Gernigon et al., 2012; Hopper et al., 2014; Haase and Ebbing, 2014; Nasuti and Olesen, 2014; Funck et al., 2016, 2017; Blischke et al., 2017a) in order to establish a detailed Cenozoic stratigraphic framework for the JMMC that documents its development from continental breakup to present-day. In addition, we established plate reconstructions, tied into this framework, which were calculated using an interactive fitting method utilising GPlates (www.gplates.org; Boyden et al., 2011; see also Gaina et al., 2017b) for the relative motion of the JMMC to its conjugate margins. A summary of the database is presented below together with our methodology for constructing the Cenozoic stratigraphic framework.

2.1. Implemented data

2.1.1. Bathymetry

The international bathymetric chart of the Arctic ocean (IBCAO) Version 3.0 with a 500 m × 500 m resolution (Jakobsson et al., 2012) was overlain by the JMMC bathymetric map compilation based on two-dimensional multichannel seismic reflection data (2D MCS) (Åkermoen, 1989; Gunnarsson et al., 1989; Blischke et al., 2017a). The A8-2008 and

A11-2010 multibeam echo-sounder surveys were planned by the national energy authority of Iceland (NEA), the Norwegian Petroleum Directorate (NPD) and the Marine Research Institute of Iceland (MRI) that surveyed on the MRI research vessel Árni Friðriksson. The resulting 10,500 km² bathymetric and seabed composition maps, in 50 m × 50 m resolution and a depth range between 790 m and 2210 m (Fig. 2) (Helgadóttir, 2008; Helgadóttir and Reynisson, 2010; Blischke et al., 2017a), have illuminated structural trends and features at the seafloor, which in combination with seismic reflection data enabled us to distinguish normal fault, strike-slip fault, or slump fault systems along the steep escarpments of the microcontinent's ridges (Blischke et al., 2017a).

2.1.2. Seismic reflection data

Seismic reflection data used in this study are listed in Table 1 and their coverage is illustrated in Fig. 3. They include the following surveys: JM-85-88, re-processed in 2009, IS-JMR-01 (2001), ICE-02 (2002), WI-JMR-08 (2008), NPD-11 (2011), and NPD-12 (2012). Some early north Atlantic regional 2D MCS surveys that cross the JMMC area, mainly BGR-75, BGR-76 (Hinz and Schlüter, 1978), and RC2114 (Talwani et al., 1981; Mutter et al., 1984), constrained the transition from the JMMC into the oceanic domain. The 2D MCS JMMC datasets

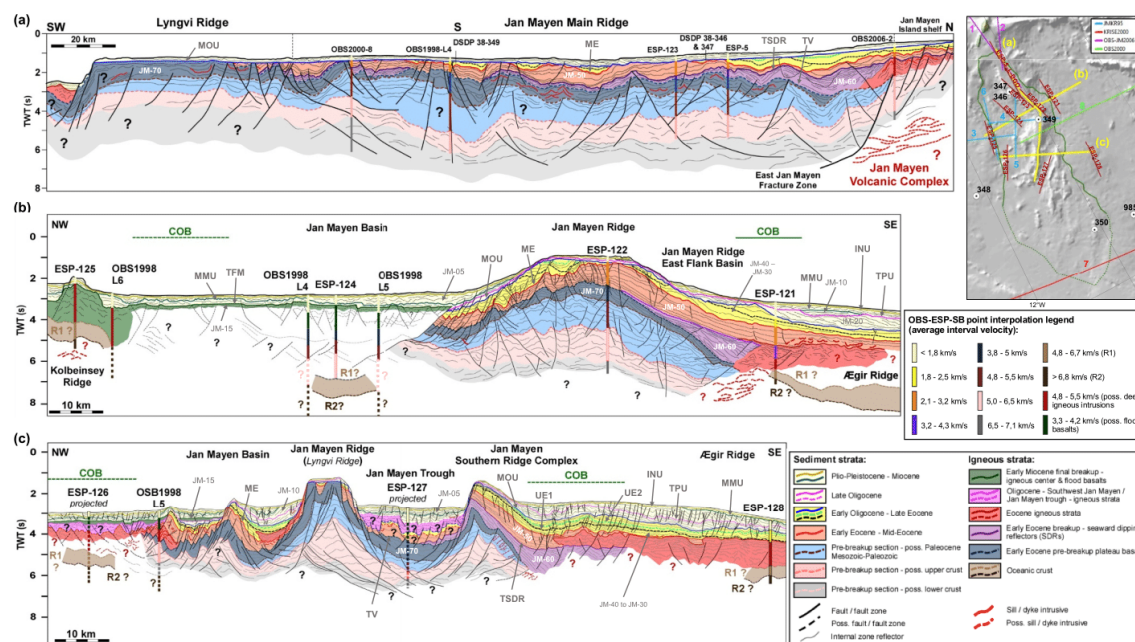


Fig. 5. Detailed tectonostratigraphic type sections of the JMMC based on seismic reflection data surveys NPD-2011 and NPD-2012, see Table 1, tied to ESP velocity profiles, sonobuoy (SB) data and available borehole tie points. The pre-breakup section is inferred to contain Paleocene, Mesozoic to Paleozoic strata by direct comparison with the Jameson Land basin and the Blossesville Kyst areas and seismic refraction data (Hopper et al., 2014; Blischke et al., 2017a;). The detailed geoseismic sections present a clearer image of the internal structure of the Cenozoic sediments (Peron-Pinvidic et al., 2012a, b and Blischke et al., 2017a), and the sub-basalt strata, indicating a much more significant volcanism along the northern and western margin of the microcontinent, (sections (b) and (c)), in line with pre-2001 acquired seismic reflection datasets. Corresponding sequences and unconformities are listed. Corresponding seismic-stratigraphic units and unconformities are listed in Fig. 4.

acquired and reprocessed since 2008, have higher data quality and deeper section imaging. The latest surveys in 2011 and 2012, conducted by the NPD improved the imaging quality of the Cenozoic section considerably, but did not fully penetrate the youngest (Late Oligocene – Early Miocene) flood basalt layers on the western and southern flanks of the microcontinent (Fig. 5b and c).

2.1.3. Offshore and onshore geological sample data

Several shallow boreholes were drilled by the deep-sea drilling program (DSDP Leg 38) (Talwani and Udintsev, 1976a–e) and the ocean drilling program (ODP Leg 162) (Jansen et al., 1996) in the JMMC region. DSDP sites 346, 347, 349 and 350 penetrated into the Cenozoic section on the Jan Mayen ridge and Middle Eocene basalts on the southern ridge complex. Oligocene and younger deposits were cored in the adjacent basin at DSDP site 348 and ODP site 985 (Talwani and Udintsev, 1976a–e; Jansen et al., 1996; Blischke et al., 2017a). Separate seafloor sampling campaigns were carried out in 1973 by Geodekyan et al. (1980), in 2010 by the NEA of Iceland and NPD, in 2012 by NPD (Sandsta et al., 2012, 2013), and in 2012 by the Volcanic Basin Petroleum Research AS (VBPR), and TGS (Polteau et al., 2012). These operations targeted sample sites along steep flank areas of the JMMC's western rim, the eastern flank of the Lyngvi ridge, and the north-western flank of the southern ridge complex (Fig. 3).

The lack of samples from the older sedimentary strata and basement of the JMMC prompted us to review the geology of the western conjugate margin of the JMMC, including the Jameson Land basin and the Blossesville Kyst region of East Greenland, where outcrops provide a potential stratigraphic analogue for the deeper Cenozoic and underlying succession. The lower Palaeogene plateau basalts and shallow-

marine deposits preserved along the East Greenland coastline (e.g. Larsen et al., 2002, 2005; Larsen et al., 2013, 2014) might correlate with the basal Cenozoic rocks of the JMMC (Blischke et al., 2017a).

2.1.4. Seismic refraction data

The structure and extent of the JMMC has been the focus of several ocean bottom seismic (OBS) and expanded seismic profiling (ESP) refraction surveys and experiments since 1985 (Johansen et al., 1988; Eldholm and Grue, 1994; Kodaira et al., 1998; Mjelde et al., 2002, 2007; Breivik et al., 2012; Kandilarov et al., 2012; Brandsdottir et al., 2015). Additionally, sonobuoys deployed during the JM-85 seismic-reflection survey provided velocity information of the upper layers of the JMMC microcontinent (Olafsson and Gunnarsson, 1989) (Table 2), which better constrained the igneous crust of the continent-ocean transition, and especially the area within the SDR's (Blischke et al., 2017a).

The eastern and western extent of the JMMC is fairly well constrained by the east-west and southwest-northeast oriented profiles of the JMCR-95 survey (Kodaira et al., 1998), and the southwest-northeast profile of the OBS2000 survey (Mjelde et al., 2002, 2007; Breivik et al., 2003; 2008, 2012) which crosses the south-western end of the JMMC, and the north-western end of the EJMFZ (Fig. 3). The northern extent of the JMMC is also well constrained by the OBS-JM2006 survey (Kandilarov et al., 2012). The southern extent of the JMMC into the Iceland plateau has been debated (Brandsdottir et al., 2015) leading to the suggestion that the termination of the JMMC south of the SRC, which also coincides with changes in the character of the 2D MCS data as well as the mapped structures for that region (Talwani et al., 1977; Blischke et al., 2017a). A severely stretched and fragmented continental

Table 2

Reflection seismic interval velocity estimates used for building a time-depth conversion model based on refraction data interpretations. Displayed are the possible stratigraphic velocity ranges across the highly variable mapped JMMC, based on OBS, sonobuoy, and ESP data estimates (modified after Johansen et al., 1988; Olafsson and Gunnarsson, 1989; Kodaira et al., 1998; and Kandilarov et al., 2012) in comparison to the microcontinent conjugate margins (Eldholm and Grue, 1994; Weigel et al., 1995; Morgan et al., 2000; Smallwood et al., 2001; Raum et al., 2002; Mjelde et al., 2008; Osmundsen and Ebbing, 2008; Parkin and White, 2008; White and Smith, 2009; Ritchie et al., 2011; and Funck et al., 2014, 2016).

Seismic intervals	OBS model estimates JMMC & Kolbeinsey Ridge		OBS model estimates JMMC & Jan Mayen Fracture Zone	OBS model estimates Jameson Land basin, Liverpool Land High & Basin	Velocity data estimates JMMC (ESP & Sonobuoy)	OBS model estimates More & Vøring margins	OBS model estimates Faroe-Shetland area
	P-wave model layer	V _p (km/s)	V _p (km/s)	V _p (km/s)	V _p (km/s)	V _p (km/s)	V _p (km/s)
<i>Sediments</i>							
Seabed	Water depth		-	1.6	1.44	-	-
Plio-Pleistocene	Cenozoic sediments		1.7 - 2.2	1.6 - 2.3	< 1.8	1.8	1.8 - 2.5
Late Oligocene - Early-Miocene							
Early Oligocene							
Late Eocene							
Early-Mid-Eocene	2.0 - 3.5		2.2 - 3.2	-	1.8 - 2.5	1.8 - 2.4	2.4 - 3.3
Early-Mid Paleocene	Poss. Lower Paleocene - Mesozoic		3.9 - 5.0	4.4 - 5.7	2.1 - 3.2	2.4 - 3.3	2.5 - 3.5?
Poss. Mesozoic			3.9 - 4.7	4.3 - 5.0	4.3 - 5.0	Cretaceous 3.1 - 4.2	3.5 - 5.77
Poss. Paleozoic			5.0 - 5.3	5.0 - 5.5	5.0 - 5.5	Pre-Cretaceous 4.2 - 5.35	
<i>Igneous</i>							
T-Marker poss. flood basalts and sediments - poss. Late Oligocene Poss. deep igneous intrusives - poss. Eocene	4.6 - 5.0		-	-	3.3 - 4.2 4.8 - 5.5	-	-
Basalts (SDRs) - Early Eocene	4.0 - 5.0		3.2 - 4.1	4.0 - 4.8	3.2 - 4.3 3.8 - 5.0	4.6 - 5.0	4.4 - 5.2
Basalts (Plateau basalts) - Early Eocene							
<i>Crustal types</i>							
Poss. Caledonian Basement	Cont. upper crust	5.5 - 6.7	5.5 - 6.5	5.8 - 6.8	5.7 - 6.7	6.1 - 6.5	6.0 - 6.3
Poss. continental lower crust - sub-basalt - Underplating	Cont. lower crust	6.7 - 6.8	6.5 - 7.2	6.8 - 7.6	6.7 - 7.2	6.5 - 7.3	6.4 - 7.3
Poss. oceanic crust - Layer 2 (R1)	Oceanic crust Layer 2	2.5 - 6.6	5.8 - 6.4	5.6 - 6.4	4.8 - 6.7	4.6 - 5.7	4.8 - 6.0
Poss. oceanic crust - Layer 3 (R2)	Oceanic crust Layer 3	6.6 - 7.6	6.7 - 8.0	6.8 - 8.0	6.8 - 7.9	6.7 - 7.7	6.8 - 7.6

crust has been proposed for the southernmost part of the JMMC and its continuation beneath Iceland (e.g. Gaina et al., 2009; Breivik et al., 2012; Peron-Pinvidic et al., 2012a; Gernigon et al., 2015; Torsvik et al., 2015).

The unpublished ESP velocity data (ESP-121 to ESP-128 on Fig. 3) were analysed within this study by travel-time-to-offset-ratio analysis (e.g. Childs and Cooper, 1978) and by the Tau-P velocity estimation methods of Diebold and Stoffa (1981). The resulting average velocity values were tied into the existing seismic-reflection correlation datasets, assigning associated velocity values to actual velocity-facies-domains in combination with the compiled OBS survey and sonobuoy velocity results, shallow offshore borehole, seafloor, and the JMMC 2D MCS reflection database (Fig. 5 & Table 2). The velocity ranges of the microcontinent and its adjacent areas were also compared to known velocity structures of central East Greenland, the Norwegian shelf and the Faroe-Shetland region (Table 2). These data provide the basis for building a time-depth conversion model that has been utilised to correlate the deeper stratigraphic levels of the JMMC (cf. Fig. 5).

2.2. Construction of the stratigraphic framework

The construction of a regional Cenozoic stratigraphic framework was primarily based on interpretation of the 2D MCS reflection data. We identified eleven seismic-stratigraphic units bounded by regional unconformities (Fig. 4), which were defined from discordant seismic reflector relations according to the criteria established by Mitchum et al. (1977). These units, prefixed by the letters JM and numbered (in descending stratigraphic order) from 01 to 70, are regarded as physical units with informal stratigraphic status. Their temporal or genetic significance remains open to interpretation based on correlation to litho-, bio- or other stratigraphic data (e.g. Owen, 1987 or Vail, 1987). Correlation of key reflectors bounding these seismic units indicates the presence of regional unconformities that we interpret to represent major changes in the evolution of the JMMC (Table 3). On the Jan Mayen ridge and the southern ridge complex, the seismic-stratigraphic scheme was geologically calibrated down to the Middle Eocene (units JM-01–JM-50) through correlation with the DSDP and ODP boreholes

(Blischke et al., 2017a). The stratigraphic interpretation of the pre-Middle-Eocene succession is based on the integration of seismic-refraction and -reflection data and outcrop information from the East Greenland and the Vøring continental margins. This includes speculation on the lower Palaeogene volcanic stratigraphy (units JM-60 – JM-70) based on its similarity to the Blossville Kyst region of East Greenland, as well as the possibility of Mesozoic and Palaeozoic rocks beneath the Jan Mayen ridge using the proven succession in the Jameson Land basin as an analogue.

Major uncertainties in stratigraphic correlations persist in the basins between the dislocated southern ridge segments and along the collapsed western flank of the JMMC, where borehole control for sections older than Middle Eocene is lacking. Nevertheless, our proposed correlations in these areas were substantially improved by the NPD2011 and 2012 surveys. In the Jan Mayen trough, Jan Mayen basin, and the southern Jan Mayen basin the correlation of strata older than Miocene is hindered due to the regionally extensive basaltic cover, below which structures are only faintly visible (Fig. 5).

3. Results

3.1. JMMC's conjugate margins comparison

Although the focus of the study is the Cenozoic stratigraphy, and in the absence of deep borehole control, it was essential to assess and compare the geophysical datasets of the pre-breakup intervals of the JMMC that form the base of all interpreted structures, to the known conjugate margins of the microcontinent. A consistent correlation with the conjugate margins was established using seismic-refraction velocity data ranges, especially in relation to the upper and lower crust, where the change in velocity data corresponds with a strong seismic reflection event for the lower crust (Fig. 5 & Table 2). A good correlation exists between East Greenland's Jameson Land basin, with a velocity range of 4.4–5.7 km/s for its Jurassic to 'Caledonian' stratigraphic section, and the velocity range of 4.3–5.5 km/s for the Jan Mayen ridge area (Weigel et al., 1995; Funck et al., 2014, 2016) (Table 2). The More & Vøring margin and basin velocity ranges corresponds to the deeper section of

Table 3
Summary of key Cenozoic dis- & unconformities on and around the JMMC.

Unconformity	Description	Age & approximat time range
Intra-Neogene (INU)	Distinct reflector character change interface that is tied to borehole, seismic reflection, and offset area inference datasets. The unconformity overlies dipping and partially eroded Miocene drift sediment strata, and is overlain by infill, parallel primarily Plio-Pleistocene sediments.	Messinian ^{b, c, e, f} 5 Ma ± 2 Ma
Intra-Miocene (MMU)	Not as distinct visible boundary if reflector sequence changes of dip directions above and below the unconformity that is primarily tied to borehole records and offset areas inference. The unconformity is only partially visible along the eastern ridge flanks and across the top F-marker area of the western and southwestern flank areas.	Serravallian-Langhian ^{a, c, e} 12 Ma ± 1 Ma
Top F-marker flood basalts (TFM)	Strong reflector along the microcontinent's west and southwest flank areas, indicating an irregular to planar, partially faulted and erosive surface with a distinct change in seismic refraction velocity. The reflector is overlain by faulted, parallel to on- and down-lapping earliest Miocene infill sediments.	Aquitainian ^{a, b, c, d, e} ~ 22 Ma ± 2 Ma
Top Palaeogene ('TPU')	Distinct reflector sequence change alongside the Jan Mayen and Lyngvi ridges and main flank areas. Angular erosion surface along the eastern flanks and often merged as a composite unconformity with the Mid-Oligocene unconformity across the high ridge areas, and overlain Miocene sediment drift deposits that on- and down-lap onto the unconformity.	Upper Chattian ^{b, c, d} 23 Ma ± 3 Ma
Mid-Oligocene (MOU)	Strong reflector across entire JMMC area. Forms an angular, planar, erosion surface on Jan Mayen ridge, truncating older folded and dipping strata; irregular surface on flanks of ridge and in adjacent basins, which is progressively buried beneath younger deposits.	Chattian-Rupelian ^{b, c, d, e} 30 Ma ± 4 Ma
Eocene-Oligocene boundary (UE2)	Not as a distinct reflector sequence change alongside the Jan Mayen and Lyngvi ridges and main eastern flank areas, but tied to borehole control and intermediate sea level change. The unconformity appears eroded by the next following unconformity in high ridge but also reversed flank areas. Parallel infill reflectors underlay the UE2 unconformity along the top region of the Jan Mayen ridge, but change into irregular slumped patterns, and locally faulted slump erosion surface along the ridge flank areas.	Rupelian-Priabonian ^{a, c, e, f} ~ 34 Ma ± 1 Ma
Upper Eocene (UE1)	Not as distinct reflector sequence change alongside the Jan Mayen and Lyngvi ridges and main eastern flank areas. Parallel deltaic forest or infill reflectors overlaying the ME unconformity along the top region of the Jan Mayen ridge, irregular, slumps, and locally faulted erosion surface truncating underlying Mid Eocene strata along the ridge flank areas that are overlain by on- and down-lapping, or slumped strata of the latest Eocene/possibly earliest Oligocene.	Priabonian ^{b, e} 36 Ma ± 1 Ma
Mid-Eocene (ME)	Strong and distinct reflector beneath Jan Mayen and Lyngvi ridges and main flank areas. Irregular and locally faulted erosion surface truncating underlying Early Eocene strata; overlain by on- and down-lapping Upper Eocene to Oligocene strata across the highest areas of the Jan Mayen & Lyngvi ridges.	Upper Lutetian ^{b, c, d, e, f} 43 Ma ± 3 Ma
Top Seaward-Dipping Reflectors (TDSR)	Strong reflector along the eastern flanks of the Jan Mayen ridge and the northern extend of the southern ridge complex. Angular erosion surface that on-laps onto the underlying Plateau Basalt sequence; onlapped and down-lapped by easterly-pro-grading Eocene deposits.	Early-Mid Ypresian ^{b, c, d, e, f} 52 Ma ± 1 Ma
Top Basalt (TV)	Strong reflector beneath Jan Mayen and Lyngvi ridges. Angular erosion surface that truncates the underlying plateau basalt sequence; progressively buried by westward pro-grading SDR's on eastern flank of Jan Mayen ridge, onlapped and down-lapped by easterly pro-grading Eocene deposits.	Earliest Ypresian ^{b, c, d, e, f} 55 Ma ± 1 Ma
Base Palaeogene (BPU)	Strong reflector beneath Jan Mayen and Lyngvi ridges. Irregular and locally faulted erosion surface truncating underlying (inferred) Mesozoic strata; overlain predominantly by pre-breakup plateau basalts.	'Paleocene' undefined ^{c, d, e}

^a DSDP-ODP borehole data.

^b Magnetostratigraphic data.

^c Inferred on basis of regional correlation, including outcrop and offshore observations (East Greenland, Vøring continental margin and slope, Iceland, Faroe Islands, or Faroe-Shetland basin areas).

^d Seismic refraction data.

^e Seismic reflection data correlation grid.

^f Distinct to intermediate sea level change.

the pre-Cretaceous with 4.2–5.35 km/s (Raum et al., 2002; Mjelde et al., 2008, 2009; Osmundsen and Ebbing, 2008). In the Scotland/Faroe-Shetland area a velocity range of 3.5–5.77 km/s correlates with the Devonian to Recent stratigraphic section (Morgan et al., 2000; Smallwood et al., 2001; Parkin and White, 2008; White and Smith, 2009; Ritchie et al., 2011; Funck et al., 2016).

3.1.1. The Cenozoic

The shallowest sedimentary domain corresponds to the interval velocity range of < 1.8 km/s, correlating to the section from the uppermost part of the Upper Oligocene up to the seafloor, including the topmost section of glacial sediments (Table 2). This interval corresponds to the second breakup event for the JMMC region and its syn- and post-breakup sediment cover. This is underlain by Upper Eocene to Lower Oligocene rocks, with a velocity range of 1.8–2.5 km/s, which represent the interval between about 43 Ma to 30 Ma during the rift transfer from east to west across the IPR south of the JMMC. The Ægir ridge syn- and post-breakup deposits of Early to Mid-Eocene age have slightly higher velocities of 2.1–3.2 km/s, corresponding to equivalent rocks (with velocity range of 2.4–3.3 km/s) in the Møre basin (Osmundsen and Ebbing, 2008). This sedimentary sequence is missing

or not specified for the Jameson Land, Blossville Kyst, and Scoresby Sund regions, where onshore outcrops are primarily Jurassic and older, overlain by very small patches of Lower Cretaceous and Paleocene rocks, Lower Eocene volcanic strata, and younger sediments within the Scoresby Sund and Liverpool Land basin (LLB) areas (Surlyk et al., 1973, 1991; Weigel et al., 1995; Larsen et al., 1999a,b, 2002, 2005; Larsen et al., 2013, 2014).

As the JMMC is surrounded by igneous domains, delineating the microcontinental boundary with the volcanic domain is important. The areas of SDRs along the east flank of the JMMC and the basaltic sections that cover the JMR ridge area have a similar velocity range of 3.2–4.3 km/s (Table 2), whereas the plateau basalts are slightly higher with 3.8–5.0 km/s. The volcanic margins and complexes east of the JMR and SDRs have a much higher velocity range of 4.8–5.5 km/s (Figs. 5 and 6; Table 2). The eastern volcanic margin follows the oceanic basement domain, which is characterised by a high velocity layer of 4–5 km/s that is covered by a thin low-velocity sedimentary layer (< 2.5 km/s). The section below, comprising both volcanic-margin and oceanic domain has a velocity of 4.8–6.8 km/s, which might correspond to the oceanic layer 2 (R1-R2 in Fig. 5). Below the "R2" seismic reflection event, velocities > 6.8 km/s are associated with

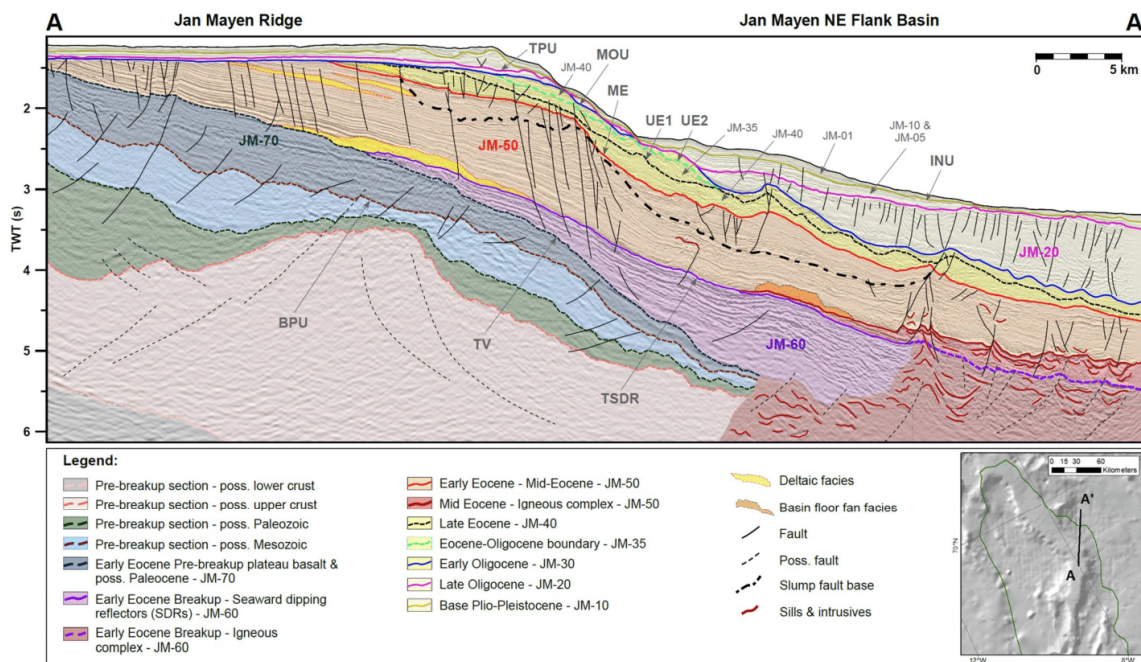


Fig. 6. Northeast flank stratigraphic type section based the seismic reflection data (NPD, 2012) tied to the JMMC regional correlation grid. The Eocene shelf system can be seen as a layered seismic pattern section with prograding delta system and basin floor fan like features in the lowermost part of the Early-Mid Eocene seismic unit JM50, and within the uppermost preserved section of that unit indicating a regression of the system. The Mid-Late Eocene to Early Oligocene seismic units (JM40, JM35 & JM30) are preserved as slumps along an instable shelf margin with slump faulting and entire blocks that moved downslope and chaotic seismic patterns. Up to the Upper Oligocene a very distinct erosional surface can be observed at the top of the ridge, channel forming along the slope and rapid sediment deposition across the basinal plain with features similar to submarine creep zones (Shillington et al., 2012 or Li et al., 2016). These units are then covered by layered and sediment drift patterns within the Miocene unit JM20), and deep sea current channels and layered sediment patterns of the Plio-Pleistocene to present unit (JM10 to Seafloor). Corresponding seismic-stratigraphic units and unconformities are listed in Fig. 4.

irregular seismic reflectors adjacent to the continent ocean boundary (COB), and these have been interpreted as higher-velocity layers connected to under-plating, or lower crustal bodies (LCBs) associated with volcanic margins of the JMMC, East Greenland, Møre and Vøring (Fig. 5) (e.g. Weigel et al., 1995; Breivik and Mjelde, 2003; Breivik et al., 2008, 2012; Faleide et al., 2010; Gernigon et al., 2015; Mjelde et al., 2016; Theissen-Krah et al., 2017; or Zastrozhnov et al., 2018). The higher-velocity layers delineate the transition from the JMMC to the oceanic domain within the volcanic margin (Fig. 5).

As similarly high velocities were observed within the Jan Mayen basin (Fig. 5), this has implications for the western extent of the main extended ridge segments of the JMMC, which had, in previous studies, been extended across the JMB to the COB (e.g. Gunnarsson et al., 1989; Peron-Pinvidic et al., 2012a; or Blischke et al., 2017a). The velocity profiles however, imply that the JMB is primarily a volcanic margin that correlates to observed flood basalt marker within the JMB, also referred to as the “F-marker” (Blischke et al., 2016, 2017a). This marker horizon is correlative with the second breakup event of the JMMC from the central East Greenland mainland, and was emplaced into the sedimentary section (1.8–2.5 km/s) of the Jan Mayen basin, Jan Mayen trough and along the southern extent of the JMMC. This layer corresponds to a 270–470 m thick basaltic section with a velocity range of 3.3–4.2 km/s within the JMB (Fig. 5b and c; Fig. 6; Fig. 8 and Table 2).

3.2. The JMMC Cenozoic stratigraphic framework

Talwani et al. (1976a, 1977) originally divided the Cenozoic succession on the northern Jan Mayen ridge into a Lower Paleocene to

Lower Oligocene unit and an Upper Oligocene to Quaternary unit separated by an angular ‘Mid’-Oligocene unconformity (MOU), which was caused by extensive erosion of the ridge, creating its characteristic flatlying topography (Figs. 5 and 6).

Based on the 2D MCS reflection data, we have identified eleven unconformities and disconformities (Fig. 4; Table 3), thus subdividing the Cenozoic succession into eleven (JM-01 – JM-70) seismic-stratigraphic units: units JM-01 – JM-15 represents the Neogene succession, whereas units JM-20 – JM-70 represents the Palaeogene strata (Fig. 4). The characteristics and form of these boundaries are expressed as distinct erosion surfaces, or surfaces with onlap or downlap (Figs. 5 and 6). The geometry and stratigraphic range of the Cenozoic succession (Figs. 4–6) reveal a maximum thickness of the Eocene and younger succession (JM-50–JM-01) of 4200 m along the eastern flank of the JMMC (Blischke et al., 2017a).

3.2.1. Uncertainties

The greatest uncertainty concerns the age of the bounding surfaces of the early Palaeogene volcanic rocks, i.e. the base of the Palaeogene (BPU); the top of the plateau basalts (TV); and the top of the seaward-dipping reflectors (TSDR) (Fig. 5). The TV unconformity is an important seismic marker, as it is easily recognised on seismic reflection and velocity data and can be correlated across the central Northeast Atlantic region. The top of the SDR is an important marker for the JMMC and marks the final opening stage of the Ægir ridge spreading processes (~52 Ma) (Gaina et al., 2009; Gernigon et al., 2015).

Other surfaces, such as the boundaries separating seismic units JM-40/JM-35 and JM-35/JM-30, represent more localised events along the

eastern flank of the JMMC, and might relate to episodic slumping. Across the flat-topped areas of the ridges several unconformities converge and/or are cut out by the MOU unconformity. In the Jan Mayen Basin, the F-marker is a very strong, flat-lying, opaque reflective horizon, which is interpreted as comprising composite sheets of lava flows. This reflector hinders interpretation of the underlying Cenozoic basinal stratigraphy.

3.3. The JMMC Cenozoic seismic-stratigraphic units

3.3.1. Unit JM-70 (Paleocene)

Seismic unit JM-70 is bounded by the Base Palaeogene (BPU) and Top Basalt (TV) unconformities (Fig. 5; Table 3). On seismic reflection profiles, its internal acoustic character comprises a strong, laterally continuous pattern of parallel-bedded reflectors, which are clearly visible in the upper part of the unit and enables it to be mapped across the microcontinent's ridges and along their flank areas. In the lower part of the unit, localised half-graben structuration is observed especially on northwest-southeast-trending seismic reflection data (Fig. 6). The unit is approximately 1100 m thick on the crest of the Jan Mayen ridge thickening southwards to approximately 3300 m on the southernmost extent of the Lyngvi ridge (Blischke et al., 2017a) (Fig. 5a). The Lyngvi ridge appears to have been exposed the highest along the north-south profile of the main Jan Mayen ridge, as the ridge has been affected by the main MOU and no SDR or younger pre-Neogene sediments sections preserved. Thus, the original stratigraphic thickness of unit JM-70 is uncertain. To the north, the unit onlaps the Jan Mayen igneous complex but thins into the Jan Mayen NE flank basin where it is eroded beneath the Top Basalt unconformity and progressively onlapped and buried by the westerly-prograding seaward-dipping reflectors of unit JM-60 (Fig. 6).

Seismic-refraction velocity data for unit JM-70 (cf. Table 2) are comparable to the plateau basalts that crop out along the East Greenland coastline. This interpretation is supported by the acquisition of vesicular olivine-rich silica-depleted basaltic rock samples recovered from the seabed along the east flank of the Lyngvi ridge and the west flank of the Jan Mayen SRC (Norwegian Petroleum Directorate, 2012; Polteau et al., 2012, 2018; Sandstå et al., 2012, 2013; Blischke et al., 2017b) (Fig. 3). Unfortunately, no dating of these samples has been obtained as they are too altered for reliable results. Nevertheless, Sandstå et al. (2012, 2013) have interpreted the entire succession as a Paleocene (possibly Lower Eocene) basalt formation, whereas Polteau et al. (2012, 2018) assigns these rocks to the Palaeogene–Cretaceous boundary, which is located at the foot of the fault escarpment from which the samples were obtained. Although the sampling profile lies well within the outcrop area of the escarpment, marked by high-amplitude responses on the multibeam data, uncertainty remains regarding the in-situ nature of the samples as the entire block from which the samples were recovered might well be allochthonous (Blischke et al., 2017b). The presence of sedimentary rocks within unit JM-70, deposited prior to the breakup and rifting event of the Ægir ridge system across the JMMC remains unproven by borehole data. However, comparing this interval with analogue sites of the central East Greenland coast, e.g. Kangerlussuaq, Kap Dalton and Savoia Halvø areas, or seafloor samples of the western flank of the SRC, and the by seismic reflection data well imaged parallel stratification, does underline the presence of a by the TV unconformity truncated JM-70 unit of lower impedance sediments and higher acoustic impedance landward flow lavas (Larsen et al., 1999a,b, 2002, 2005; Larsen et al., 2013; or Polteau et al., 2018) (Figs. 6 and 11). Whereas the upper part of the unit is dominated by parallel-bedded plateau basalts (Fig. 9a), seismic-reflection profiles across the JMMC show the BPU and lower part of unit JM-70 to be cut and offset by a series of faults which resulted in rotation of fault blocks and local development of half-grabens (Fig. 6).

3.3.2. Unit JM-60 (Early Eocene)

Seismic unit JM-60 discordantly overlies the plateau basalts of unit JM-70, and forms a wedge-shaped deposit several kilometers thick that onlaps and thins westwards, eventually pinching-out onto the Top Basalt unconformity (TV in Fig. 4 and Table 3) on the Jan Mayen ridge (Figs. 5 and 6). Its internal reflection configuration displays a hummocky to lenticular pattern that represents a topographic build-up of stacked deposits. These deposits have previously been interpreted as primarily volcanic in origin comprising a stacked accumulation of subaerial basaltic wedges that are alternating with primarily terrestrial sediments, and often deepening into a marginal marine to shelf setting and alternating lava flows and sediments. Examples of these have been described or even drilled by Pálmason (1980, 1986) or Larsen and Saunders (1998) for the south-east Greenland margin and onshore Iceland. Here specifically for ODP Leg 152 boreholes 915–918 show the transition from terrestrial to marginal marine and shelf settings (Larsen and Saunders (1998)). Furthermore, were SDR units described on seismic reflection data by Hinz (1981), Mutter et al. (1982), Planke et al. (2000) for the western Norwegian margin that are comparable wedge shaped and dipping units flanking the eastern margin of the JMMC.

The upper boundary of unit JM-60 is defined by the Top Seaward-Dipping Reflectors unconformity (TSDR in Fig. 4 and Table 3), which terminates at the intersection with the TV unconformity upslope and the Early-Mid Eocene igneous complex downslope, close to the continent ocean boundary (Figs. 5 and 6). The TSDR surface is defined by a strong seismic reflector, which is down-lapped by reflectors of the overlying unit JM-50.

The SDRs are generally assumed to have been formed during initial breakup (55–53 Ma), based on magnetic anomaly geo-chronologic analysis (Gaina et al., 2009), and the breakup unconformity along the East Greenland coast (Larsen et al., 2014). The approximate timing of the unconformity is set towards the end of the breakup volcanism, synchronous with the first continuous magnetic anomaly of the Ægir rift system around 52 Ma, which is based on high-resolution magnetic anomaly geo-chronological mapping of the Norway basin (Gernigon et al., 2015).

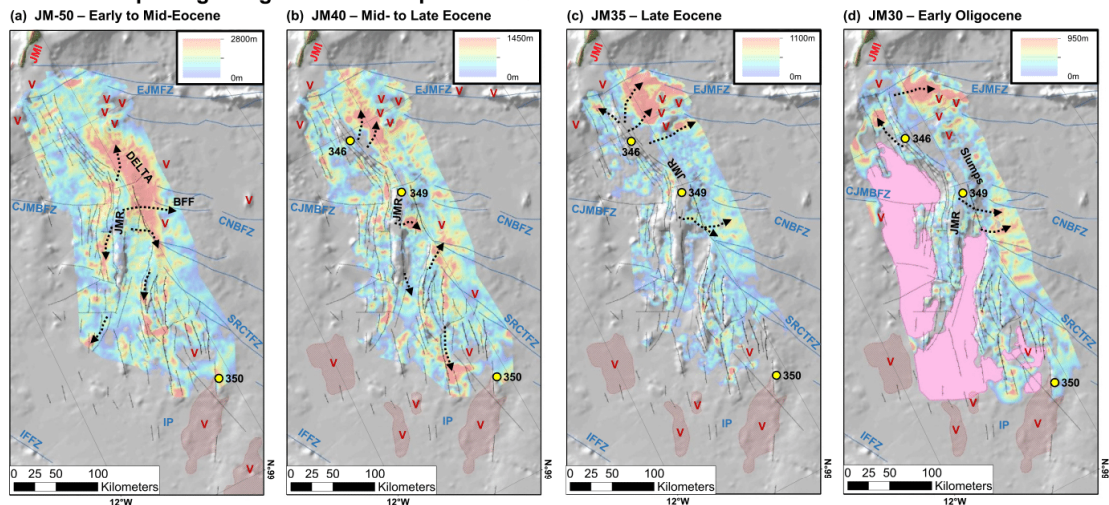
The SDRs are best developed along the central eastern flank of the microcontinent and have a slightly lower seismic-refraction velocity range than the underlying plateau basalts of unit JM-70 (Figs. 5 and 6; Table 2). These basalts are interpreted as subaerial lava flows that onlap onto higher terranes and stack onto previous lava flows as rifting and seafloor spreading progressed along the margins (Hinz, 1981; Mutter et al., 1982; Planke et al., 2000; Buck, 2017). The basalt wedges are of uneven thickness along the margin but appear to be thickest in the vicinity of large igneous systems; up-to-4–6-km-thick basaltic wedges are observed on the north-eastern flank, thinning and disappearing to the south (Blischke et al., 2016, 2017a) (Figs. 5 and 6).

3.3.3. Unit JM-50 (Early- to Mid-Eocene)

Seismic unit JM-50 down-laps onto the erosion surfaces of the TV and TSDR unconformities; its upper boundary is marked by the planar-to-irregular Mid-Eocene (ME) unconformity (Figs. 5 and 6; Table 3). The latter has been dated as 43 ± 3 Ma based on seafloor samples recovered from the north-western Jan Mayen ridge (NPD, 2012; Sandstå et al., 2012), and the SRC (Talwani et al., 1976a-e; NPD, 2012; Polteau et al., 2018). Unit JM-50 can be traced across the JMMC but is best preserved on the eastern flank of the Jan Mayen ridge, where a section thickness of up to 2.8 km is preserved (Fig. 7a), becoming increasingly eroded across the JMMC ridges, especially the main Jan Mayen and Lyngvi ridges (Fig. 8). To the east, the unit onlaps the igneous complex of the Ægir ridge system (Figs. 5 and 6).

The internal acoustic character of unit JM-50 comprises a variable configuration, including parallel/sub-parallel, prograding and

Post breakup – Ægir ridge and Iceland plateau rift transition



Breakup & post breakup phase – Kolbeinsey ridge

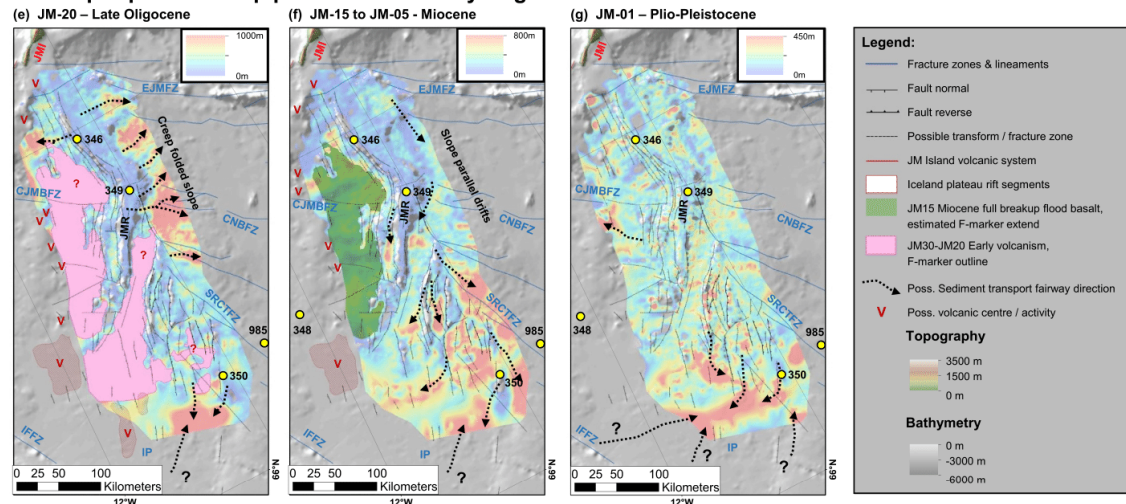


Fig. 7. True stratigraphic thickness map series based on the regional JMMC correlation model for each mapped interval of the post breakup section of the Ægir ridge and Iceland plateau rift transition (a)–(d), and the breakup and post breakup phase of the forming of the Kolbeinsey ridge (e)–(g). The time intervals are tied to offset borehole data (Talwani et al., 1976a–e; Blischke et al., 2017a) and approximated for the top Early Eocene basalt series of SDR's and plateau basalts of the Bløseville Kyst (Larsen et al., 2013, 2014). Well visible are the volcanic centres to the east and northeast during the opening of the Ægir ridge and increased extension along the EJMFBZ (East Jan Mayen fracture zone) north of the central Norway basin fracture zone (CNBFBZ), and the slump and canons forming along the eastern flank during the Mid-Late Eocene (JM40 & JM35) and Lower Oligocene (JM30). During the Kolbeinsey ridge breakup and post breakup phase, sediment depocentres are forming due to rapid subsidence along the eastern ridge flank, and primarily forming towards the south with a possible infill of erosional volcanoclastics from the south and the elevated Iceland terrain. Additional abbreviations: CJMBFBZ – central Jan Mayen basin fracture zone, CNBFBZ – central Norway basin fracture zone, Iceland plateau rift system (IP), IFFZ – Iceland-Faroe fracture zone, JMI – Jan Mayen igneous complex, and SRCTFZ – Southern ridge complex transfer fracture zone.

mounted seismic-reflection patterns albeit disrupted by later faulting. This combination of seismic facies units is interpreted collectively as a shelf-margin system, which includes prograding packages and basin-floor fan deposits which characterise the unit along the eastern margin of the Jan Mayen ridge; the parallel/sub-parallel facies predominates along the western flank of the JMMC and the southern ridges and probably represents marine shelf platform sediments (Figs. 5 and 6). On the basis of the upwards-repetition of prograding packages we infer that during this interval a shelf-margin delta system formed along the central eastern to north-eastern flank of the microcontinent (Fig. 7a).

Evidence of instability along this palaeo-shelf-margin is indicated by a significant slide or slump deposit characterised by contorted reflections, which represents a partial collapse of the shelf-margin (Fig. 6). The basal surface of the slide or slump is marked by a distinct reflection.

Sample data, including core samples from DSDP borehole 350 and seafloor samples, include quartz-rich breccias, sandstone, and inter-bedded shale and siltstone, together with slump deposits (Talwani et al., 1976a–e, 1977; Sandstå et al., 2012, 2013). The core data analysis indicates a shelf-margin to basin floor environment during Early-Mid Eocene that is interpreted by a sedimentary succession of a progression

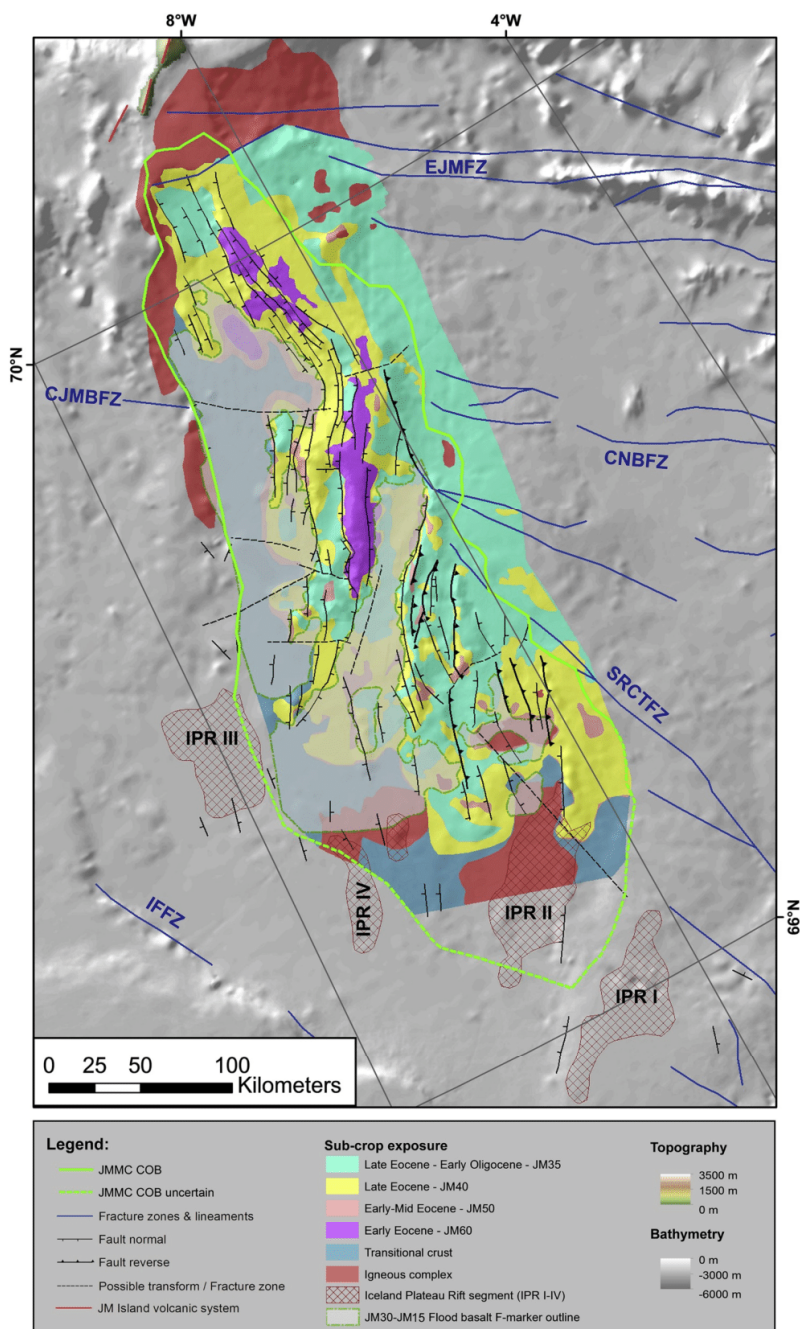


Fig. 8. Base Oligocene subcrop map at horizon JM30. Well visible are the ridge highs with the exposed Early Eocene SDR and possible plateau basalts and the volcanic margins of the Iceland plateau rift to the south, the Jan Mayen igneous complex to the north, and the formation of the Kolbeinsey ridge system and volcanic margin to the west and northwest. The area of the southern ridge complex is clearly elevated, so is the central part of the ridge and the areas to the east-northeast at the beginning of the Oligocene, which fits well with the ridge transfer from the Ægir ridge via the Iceland plateau rift system to the western margin of the JMMC. Additional abbreviations: C-JMBFZ – Central Jan Mayen basin fracture zone, CNBFBZ – Central Norway basin fracture zone, EJMFBZ – East Jan Mayen fracture zone, Iceland plateau rift systems (IPR-I to IPR-IV), IFFZ – Iceland-Faroe fracture zone, JMI – Jan Mayen igneous complex, and SRCTFZ – Southern ridge complex transfer fracture zone.

from relatively coarse-grained sediments at the base, to fine-grained sediments in the centre, and a return to coarser grained deposits at the top of that interval right above the basalts (Talwani et al., 1976b). These were interpreted as slump deposits, succeeded by well-developed proximal turbidites, grain-and boundary-flow deposits, which indicate a relative proximity to the sediment source. The environment of

deposition is considered to have been close to a steep submarine slope, or in the vicinity of a submarine canyon (Nilsen et al., 1978).

Here it is suggested that the JMMC was probably topographically high during the Paleogene and structurally instable, as the Eocene sedimentary section recorded contorted layering and faulting in the mudstones underlying the turbidites, as well as within the lower

turbidites sections (Nilsen et al., 1978). Thus, implying that the JMMC originally was attached to the eastern Greenland continental margin, and most likely formed a fault-bounded marginal basin such as the inner Vøring Plateau, underlain by transitional crust rather than clearly continental or oceanic crust (Nilsen et al., 1978).

3.3.3.1. Early-Mid-Eocene igneous complex. Igneous sills and dykes are locally intruded into the sedimentary succession of unit JM-50, derived from igneous complexes along the eastern and south-eastern flanks of the microcontinent (Figs. 5 and 6). The igneous complexes are characterised by high-amplitude irregular seismic reflective patterns and an increase in seismic velocities (Figs. 5–6 and Table 2). Both extrusive and intrusive events are associated with these igneous complexes: lava flows on the eastern flank overlap the SDRs of unit JM-60, whilst sills and dykes are observed above these igneous centres, along faults, or forming saucer-shaped seismic patterns within unit JM-50 on the eastern flank of the Jan Mayen ridge (Fig. 5b and c and 6).

A little altered diabasic dyke intrusion encountered in borehole DSDP 38–350, on the southern edge of the JMMC, provided an ^{40}Ar – ^{39}Ar age range of ~49–44 Ma. This dyke was emplaced within a highly altered basalt tuff breccia section, close to the Iceland Plateau Rift II (IPR II) (Figs. 4–7a and 8) (Manum et al., 1976a, b; Blischke et al., 2016, 2017a). The apparently much older basaltic tuff breccia section has a high iron content, which is typical for the northern Atlantic volcanic province, and are considered to be closely related to the Paleogene-Neogene plateau-basalt of East Iceland and Faroe Islands (Kharin, 1976). Schilling (1976) reported that the fresh basalt sample from site 350 showed light rare earth enrichment and similarities to the Vøring Plateau, or to the basalt compositions of the lower and middle Faeroe basalt series.

The apparent igneous re-activation of the Early-Mid Eocene igneous complex indicate a more complex picture of the igneous activities in this area with the older samples representing the “true basement” of lava flows related to the initial sea-floor spreading, and the younger, fairly unaltered samples give indications for later small intrusions that occurred during the transition of the rift centre from the Aegir Ridge to the Kolbeinsey Ridge during the Late Eocene to Early Oligocene (Talwani et al., 1976b). The later igneous activity appears to coincide with the alteration and partial lithification of the overlying sediment that often occur during sill or dyke intrusions. Our studies age re-assessment of the core data in combination with recent 2D seismic data moved the igneous activity earlier into the Early-Mid Eocene and ties to the mapped Iceland Plateau rift centres, as an intersecting spur into the southern domain of the SRC (Figs. 7a and 8).

3.3.4. Unit JM-40 (Mid- to Late Eocene)

Seismic unit JM-40 is primarily preserved along the eastern and western flanks of the Jan Mayen ridge, having been largely eroded from the crest of the ridge (Figs. 5 and 6). The unit locally exceeds 1 km thickness, especially on the NE flank of the ridge (Fig. 7b) and is bounded at its base by the irregular Mid-Eocene unconformity, and at its top by the Upper Eocene (UE1) unconformity (Table 3).

The internal acoustic character of unit JM-40 is variable especially on the NE flank of the Jan Mayen ridge where parallel-to-prograding reflectors pass basin-ward into a more chaotic and contorted configuration (Fig. 6). This geometry and seismic-facies arrangement is comparable to the underlying unit JM-50, and most probably represents a renewed phase of shelf-margin progradation followed by its partial collapse and slumping. On the western flank of the Jan Mayen ridge, the continuity of unit JM-40 is strongly disrupted by faulting (Fig. 5), though remnants of parallel-to-prograding reflections are locally observed within the faulted half-grabens.

Lithological information for unit JM-40 is derived from boreholes and seafloor samples (e.g. Talwani et al., 1976a–e, 1977; Sandstå et al., 2012, 2013). DSDP sites 346 and 347 proved massive, extensively bioturbated sandy mudstone that locally graded into conglomerate,

breccia, sandstone and mudstone from the main Jan Mayen ridge and its northern ridge segments (Fig. 5). The interval is locally calcareous and turbiditic with ash lamination present within the section, indicating volcanic activity at the time within shelf-margin sediments. Farther south along the Jan Mayen ridge, DSDP site 349 sampled well-developed turbidite intervals consisting of abundant pebbly mudstones and very thick turbidite deposits that displayed Bouma divisions, sedimentary slumping structures, and prominent erosional interfaces (Nilsen et al., 1978). The section comprising primarily of terrigenous sourced material, is locally bioturbated, contains pyrite nodules and calcareous layers are common as well, records of zeolites indicate influence of geothermal fluid circulation, which correlates to the intervals harder composition and related drilling and core recover difficulties.

A mixture of bioturbated mudstone, claystone, limestone, breccia and sandstone interbedded with ash and calcareous zones have been recorded at DSDP site 350, within the Jan Mayen SRC. Moreover, pyrite concretions are recorded within the fine-grained sediments, and proximal turbidite deposits, comprising terrigenous material, and lithified breccias.

3.3.5. Unit JM-35 (Latest Eocene / Earliest Oligocene)

The distribution of seismic unit JM-35 is largely confined to the eastern flank of the Jan Mayen ridge, as well as downfaulted accumulations within small grabens that underlie the crest of the ridge (Figs. 5 and 6). The unit is thickest on the NE flank of the Jan Mayen ridge, where it locally reaches up to 1.1 km thickness (Fig. 7c). Its base is marked by the UE1 unconformity; its top is bounded by the UE2 unconformity (Table 3).

The internal acoustic character of unit JM-35 displays a parallel to sub-parallel configuration below the crest of the Jan Mayen ridge, which passes laterally into irregular contorted and chaotic patterns on the eastern slope of the ridge, characteristic of slumping (Fig. 6). The unit is locally cut by faults. A parallel, even-bedded, commonly wavy reflection configuration is preserved in small basins or grabens beneath the crest of the Jan Mayen ridge.

On the Jan Mayen ridge, DSDP borehole 346 indicates that this unit consists primarily of massive, extensively bioturbated terrigenous mudstone and sandy mudstone, with subordinate amounts of sandstone and claystone, and minor amounts of volcanic ash towards the northern part of the main ridge (Nilsen et al., 1978). The section was generally unstratified, contained no visible sedimentary structures or trace fossils. The lowermost interval consists of thinly parallel-stratified, very fine to fine-grained sandstone, siltstone and mudstone. Thus, placing the area within a shallow marine to terrigenous depositional environment. Farther the south, DSDP borehole 350 proved mudstone, claystone, limestone, breccia, siltstone and sandstone, with interlayered ash layers and calcareous zones, indicating a change to a more distal deeper marine depositional character with increased water depth, or decrease in sediment transport energy (Talwani et al., 1976d–e).

3.3.6. Unit JM-30 (Early Oligocene)

On the Jan Mayen ridge, seismic unit JM-30 is only sporadically preserved as downfaulted accumulations in localised half-graben structures. More extensive accumulations are present on the slopes of the ridge, particularly the NE flank of the ridge where the unit is up to 950 m thick (Fig. 7d). The base of unit JM-30 is marked by the UE2 unconformity on the upper part of the slope on the NE flank of the Jan Mayen ridge, though this boundary is less distinct farther basin-wards (e.g. Fig. 6). The top of the unit is defined by the Mid-Oligocene unconformity (MOU); a pronounced, flat-lying, angular unconformity that created the distinctive flat-topped topography observed on seismic-reflection profiles, that characterises the main Jan Mayen ridge as well as the highest parts of the SRC (Figs. 5 and 6; Table 3). This major unconformity is also recognised in borehole and seafloor records (Talwani et al., 1976a, 1977; Sandstå et al., 2012, 2013; Blischke et al., 2017a). On the crest of the Jan Mayen ridge, the MOU truncates most of the

underlying strata, the disposition of which is revealed in the sub-crop map in Fig. 8. On the eastern flank of the Jan Mayen ridge, the MOU-equivalent surface is marked by the top of unit JM-30 slumped deposits, and can be traced towards the Ægir Ridge; to the west, the continuity of the MU is disrupted by numerous faults on the western flank of the Jan Mayen ridge, and/or down-warped in the adjacent basins, e.g. Jan Mayen basin (Figs. 5 and 6).

On the eastern flank of the Jan Mayen ridge, unit JM-30 displays contorted to chaotic seismic-reflection patterns characteristic of slumped deposits (Fig. 6). Elsewhere, subparallel, even patterns are observed, though commonly disrupted on the western faulted margin of the ridge. On the crest of the Jan Mayen ridge, DSDP borehole 349 recovered primarily massive mud and a few sandy mudstone layers with significant amounts of volcanic ash and glauconite from unit JM-30. This sedimentary unit's depositional environment is not clear, but presumably located within a hemipelagic setting with some reworking, as well as erosion of older strata that may have supplied most of the detritus along a steeper and instable slope, as sediments were intense to moderately deformed and locally mottled (Talwani et al., 1976a-e). In the area of the SRC, DSDP borehole 350 proved mudstone, claystone and limestone, with subordinate sandstone beds; however, an absence of volcanic ash beds was noted (Talwani et al., 1976d; Sylvester, 1975, 1978). As proximal turbidite layer are described and are less frequent, a changed in depositional character to a more distal environment is apparent, which is supported by the finer-grained and layered character of these sediments, and the abundance of benthic foraminifera species belonging to the bathyal region close to the continental shelf (Moreno-Vásquez, 1995). This indicates either a water depth increased, and a decrease in transport energy setting, both preventing sediment influx.

3.3.7. Unit JM-20 (Late Oligocene)

Seismic unit JM-20 occurs primarily on the flanks of the Jan Mayen ridge and in the adjacent basins, where it locally reaches up to 1 km thick in the NE and in the far south; in contrast, a discontinuous veneer is preserved on the top of the ridge (Fig. 7e). The base of the unit is marked by the MOU; its top corresponds to the Top Palaeogene unconformity ('TPU') (Figs. 5 and 6; Table 3). On the crest of the Jan Mayen ridge, the TPU is marked by a flat-lying, angular, erosional surface which locally merges with the MOU to form to a composite unconformity across the highest parts of the ridge. On the eastern flank of the Jan Mayen ridge, and towards the Ægir Ridge, its correlative surface is marked by a deep-water erosion surface; on the western flank of the ridge, it is locally disrupted by faulting (Figs. 5 and 6).

The internal acoustic character of the slope-to-basinal succession is variable ranging from subparallel, even to wavy reflections, to hummocky and progradational, as well as massive and opaque (Figs. 5 and 6). Internal faulting commonly disrupts the continuity of the reflections to the east of the Jan Mayen ridge, but few faults seem to penetrate the TPU (Fig. 6). On the crest of the Jan Mayen ridge, the unit comprises a flat-lying, parallel reflection configuration, overlaying the MOU unconformity, which has been tested in DSDP borehole 346, whereas boreholes 347 and 349 have missing sections for this interval. Site 346 proved to contain primarily as terrigenous to transitional interpreted sourced mud and sandy mudstone that containing only trace amounts of sponge spicules and a few ash layers. The mudstone and sandy mudstone were extensively and thoroughly bioturbated, and contained no identifiable trace fossils (Talwani et al., 1976a-e, 1977). Siliceous microfossils were generally rare and poorly preserved, including a few corroded foraminifera.

DSDP site 350 suggests that terrigenous-sourced clay and mudstone, containing quartz, mica, chlorite- and kaolinite-rich clay, and silty and glauconitic clay, were also deposited at the south-easternmost extent of the SRC at this time (Talwani et al., 1976c; Jansen et al., 1996). Turbidite layers have been noted in the lower section of this unit and became less frequent up-section, indicating a change to a more distal deposition setting. The unit is interbedded with alternating layers of

unconsolidated and indurated to lithified sediments together with sporadic ash layers further up the borehole within this unit, where bioturbations become less predominant (Talwani et al., 1976a-e; Sylvester, 1978; Jansen et al., 1996). Difficult was the microfossil diagnostic, as this interval was practically barren of foraminifera, recording only a few fish teeth, faecal pellets, and radiolarians (Schrader et al., 1976).

Erosional channels were observed along the eastern slope of the JMMC coinciding with slope instability and slumping of entire blocks down-slope. This was accompanied by infilling into local lows along the slope and onto the basin plain. Further down the slope, sediment deposits were piling onto the slope with seismic-reflection characteristics suggestive of submarine creep zones (Shillington et al., 2012 or Li et al., 2016). These creep zones are indicators of massive sedimentation of divergent, partially prograding fills, and small-scale faulting, represented by disrupted seismic reflectors, suggesting tilting of the microcontinent from west to east, with subsequent erosion of high areas and re-deposition down the shelf slopes. The Jan Mayen trough and basin possibly contain a mixture of terrigenous to shallow marine platform sediments intersected by extrusive and intrusive rock formations that are poorly imaged due to the overlain younger flood basalt strata of unit JM-15 (Figs. 4, 5c, 7e and 10b).

3.3.8. Unit JM-15 (Early Miocene)

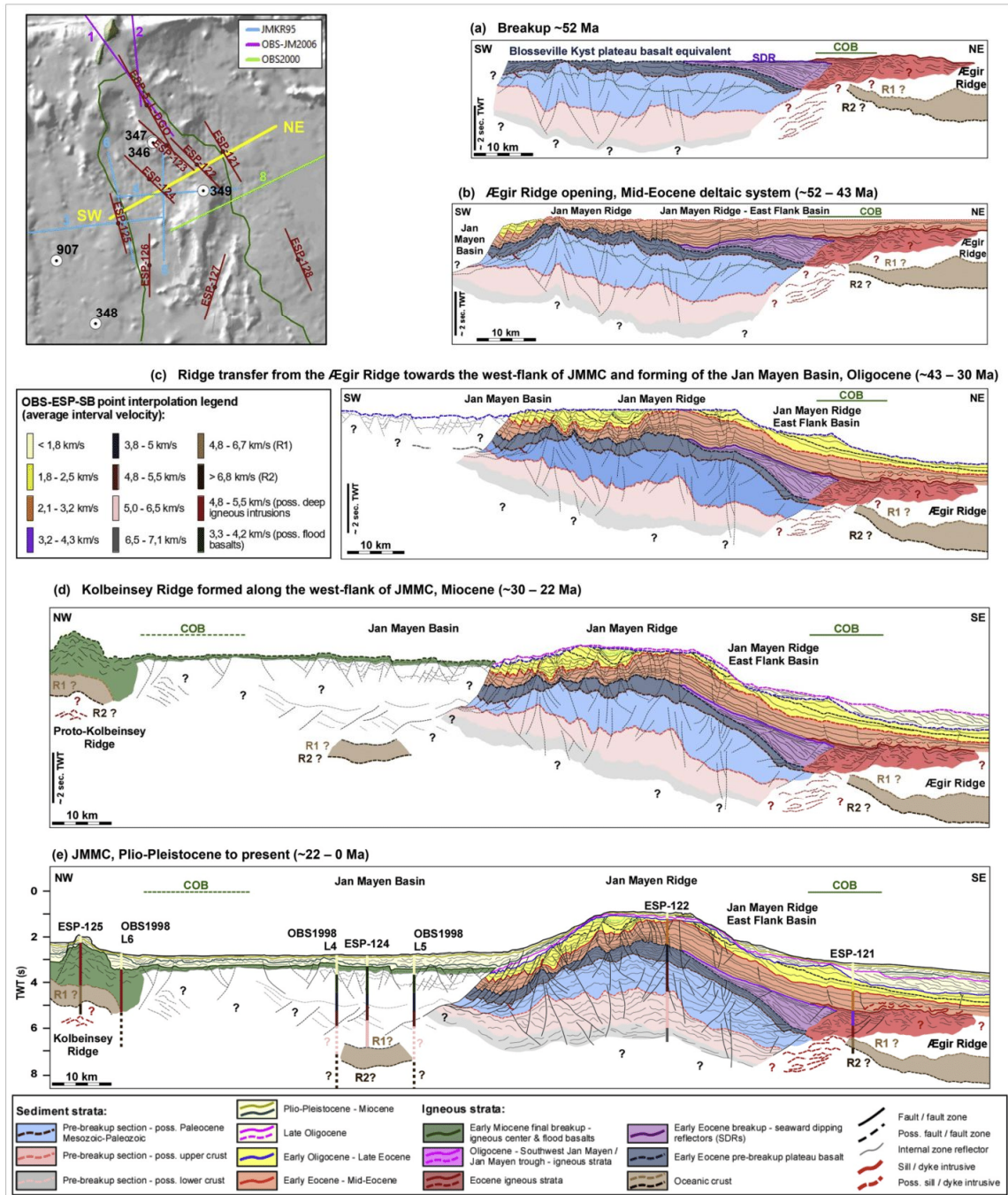
Seismic unit JM-15 is primarily represented to the extrusion of flood basalts within the Jan Mayen basin, the top of which is marked by the F-reflector (TFM) and can be traced over an area of approximately 18,400 km² (Gunnarsson et al., 1989). The TFM has a velocity range of 3.3–4.2 km/s, and is expressed as a flat-lying, opaque reflective horizon, which represents a regionally extensive igneous event, dated as Early Miocene (Table 3), across the western-to south-western areas of the JMMC (Figs. 5, 6 and 7f; Table 3). Correlative sedimentary deposits have seismic reflection unit's regional extent is difficult to determine, presenting rather localised thin parallel layered infill sections. The unit has been sampled in DSDP boreholes 346, 348, 985, and partially in site 350. Boreholes 347 and 349 have no core recovery and missing sections. Borehole 348 is located west of the JMMC COB within the initial oceanic domain of the Kolbeinsey Ridge. The basement basalt in the well was re-dated by Ar³⁹/Ar⁴⁰ dating for 21–22 Ma (Blischke et al., 2016) that corresponds much better to the magnetic anomalies interpretations of anomaly C6a by Talwani et al., 1976b) and Gaina et al., (2009). Paleotologically the basalt overlying sediment interval corresponds to the age Early Miocene to possibly Oligocene (Schrader et al., 1976). However, the possible Oligocene interpretation is based on a single foraminifera species marker, which makes the Oligocene age interpretation quite uncertain, and possibly could have been from re-worked sediment or contamination at this site (Talwani et al., 1976e).

The cored sediments in borehole 346 on the main JMR consists of transitional siliceous mud, minor sandy mud, and a few ash layers. The section contained primarily sponge spicules, which made an age assignment uncertain, but was placed within the Late Oligocene to Early-Miocene cored section (Talwani et al., 1976c) with known age description for the sections above and below to place the Oligocene to Miocene boundary. Here specifically were used the Oligocene section that is supported by a few corroded foraminifera and dinoflagellates, and the Miocene diatoms section abundant in sponge spicules that was interpreted as an indication for displaced sediments within a shallow water environment (Schrader et al., 1976; Talwani et al., 1976c). Likewise, is the comparable interval in borehole 350 difficult to determine regarding its age and consists of localised bioturbated clay and mudstone with interlayered volcanic ash and streaks of muddy chalk. (Talwani et al., 1976d). The cored section is barren of foraminifera or siliceous microfossils and was just as for borehole 346 assigned as intermittent section around the Oligocene – Miocene transition placing this section into the timeframe of JM-15.

3.3.9. Unit JM-10 (Early to Mid-Miocene)

Seismic unit JM-10 is best developed in the Jan Mayen basin and around the southern JMMC, including the Jan Mayen trough and the SRC (Figs. 5 and 6). It is commonly variable in thickness between 100 and 400 m in the Jan Mayen basin, where the base of the unit is marked

by the F-marker, and its top is marked by the Intra-Miocene unconformity (MMU); the latter being defined where there is a clear discordance between underlying and overlying reflectors (Table 3). Elsewhere the top and base of the unit is less well-defined. The F-marker is not present south and east of the Jan Mayen ridge, and the



(caption on next page)

Fig. 9. Central JMMC seismic reflection data (NPD, 2012) SE-NE line data reconstruction through the main ridge phases tied to offset ESP velocity data and interpreted crustal type profiles that were compared to velocity data calibrations (Blischke et al., 2017a). The first phase (a) illustrates the initial breakup phase and volcanic margin of the Ægir ridge with an erosional plain towards the west. The second phase shown (b) refers to the opening of the Ægir ridge and the forming of the east flank basin during the Early to Mid-Eocene, and the apparent subsidence and graben forming along the western flank of the microcontinent. During (c) the time of ridge transfer from the Ægir ridge system to the Iceland plateau rift and initial forming of the western volcanic margin with flood basalts (F-marker), the entire microcontinent tilts to the east and northeast forming an unstable eastern flank slope with slumps and erosion along the crest of the ridge. Volcanic activity moves to the west in (d) forming a distinct volcanic margin and subsidence along the eastern flank due to the cooling of the Ægir ridge area with rapid sediment transport along that flank (also see in Fig. 7 (b)). During the last stage in (e) subsidence occurred for the basin areas, specifically within the Jan Mayen basin, and current erosional features affected the ridge plateau top and flank regions. An uneven JMMC extend into the basin can be estimated for the sub-basalt (F-marker) areas for the Jan Mayen basin area seen in (d) and (e).

MMU is difficult to interpret on the NE flank of the ridge. In the ocean basin south-east of the SRC, unit JM-10 is of the order of 500 m thick but it is generally thin-to-absent on the crest of the Jan Mayen ridge and its NE flank (Figs. 5 and 6).

The internal acoustic character of unit JM-10 is variable, including subparallel, even and wavy reflections, as well as lenticular and mounded configurations (Fig. 5). On the western side of the Jan Mayen ridge there is a hint of progradation into the Jan Mayen basin (Fig. 5c).

On the Jan Mayen ridge and west of the COB, DSDP sites 346 and 348 proved siliceous, glauconitic, volcanoclastic mudstone to sandy mudstone with subordinate interbedded ash layers that are interpreted to lie within a transitional and deeper marine depositional environment. This transitional location also is reflected by a few thin consolidated sand banks within the Miocene sediment series that are interpreted to most likely have been sourced marine sediments (Talwani et al., 1976c,e). Similarly, to stratigraphic unit JM-15, were the samples near barren or poorly preserved microfossils besides a few marine benthonic diatoms or radiolarian specimens that placed this uncertain or also as “unzoned” referred section into the late Early Miocene to early Mid-Miocene range (Talwani et al., 1976c). Farther south, close to the SRC, DSDP site 350 recovered deeper marine interbedded, bioturbated mudstone and claystone, interlayered with volcanic ash. The sediments of site 350 were overall extremely poor in microfossils and samples contained a lot of ash. The sampled Miocene section contained a few silicoflagellates that were used to assign the age range (Talwani et al., 1976d).

3.3.10. Unit JM-05 (Late Miocene)

Seismic unit JM-05 occurs mainly on the flanks of the Jan Mayen ridge and in the adjacent basins where it is up to several hundred metres thick (Fig. 5); it is largely absent from the crest of the ridge where this interval is marked by an erosional hiatus (Blischke et al., 2017b). The base of the unit is marked by the MMU (where identified); its top is bounded by the Intra-Neogene unconformity (INU), which is an erosion surface over most of the area, including on shallow ridges and in deeper water (Fig. 4; Table 3). In the basins, the internal acoustic character commonly displays a subparallel, even-to-wavy, reflection configuration; however, on the flanks of the basins, the unit is commonly mounded or plastered against the slope with the internal reflections displaying upslope progradation (Figs. 5 and 6). This seismic reflection configuration is characteristic of contourite drift deposits (cf. Stow et al., 2002), which reflect processes of erosion and deposition associated with deep-water bottom currents, and which were strongly developed in the NE Atlantic from the Mid-Miocene onwards (e.g. Bohrmann et al., 1990; Howe et al., 1994; Stoker et al., 2005a; Davies et al., 2001). DSDP borehole 348 and ODP site 985, west and east of the Jan Mayen ridge, respectively, recovered predominantly mudstones with subordinate thin sandstone, siltstone, calcareous beds, and an increase of pelagic biogenic siliceous oozes (Talwani et al., 1976a, 1977). The unit is interlayered with volcanic ash beds and calcareous nannoplankton and foraminifera are rare but present, indicating an open and deeper marine environment.

3.3.11. Unit JM-01 (Plio-Pleistocene to present)

Seismic unit JM-01 forms a veneer (mostly < 100 m thick) across most of the area, though it may locally be several hundred metres thick

south of the SRC (Figs. 5, 6 and 7g). The base of the unit is marked by the INU; its top is marked by the present-day sea-bed. On seismic profiles, it commonly displays subparallel, even-to-wavy reflections in the basins but – as with the underlying unit JM-05 – may develop a mounded form around the margins of the basins, with internal reflections characteristically onlapping and locally prograding upslope. Lateral variation in the thickness of the deep-water deposits (e.g. Fig. 6) attests to the ongoing action of differential erosion and deposition due to bottom-current activity. On the steeper slopes of the Jan Mayen ridge, such bottom currents have caused localised erosion and slumping. On the crest of the Jan Mayen ridge, the irregular topography created by the INU was infilled and buried by unit JM-01. The layered seismic reflectors are cut by deep-sea current features, causing localised erosion along the ridge segments and by gravitational slumping and faulting from the steep ridge flanks (Figs. 2 and 7g).

DSDP boreholes across the region, together with sea-floor samples, prove a predominantly muddy, clayey to oozy lithology, with variable amount of silty and sandy interbeds, volcanic ash, glauconite, diatom-stones and manganese crusts (Talwani et al., 1976a, 1977; Sandstå et al., 2012, 2013). The stratigraphic unit has good micro-paleontology controls of radiolarians, globigerina, pachyderma, foraminifera, and deep water benthonic species that support the deep marine setting for the area.

The occurrence of reworked cold water nannoplankton and pollen suggest that the more topographically elevated northern part of JMR was located under permanent ice cover with low organic production and receiving little ice-rafted material (Talwani et al., 1976c; Dzinoridze et al., 1978).

The submerged south-eastern extend of the SCR within the Norway basin domain recorded in borehole ODP Leg 162 site 985 (Jansen et al., 1996) an uppermost section of this unit that ties to the glacial events of the Quaternary. Good records of interbedded layers of grey clay, nannofossil ooze with foraminifers, dark grey to brown nannofossil clays that testify to the cyclicity and interbedded nature of the sediments and their glacial to interglacial origin and milder conditions in between the glacial phases. Additionally, were iceberg-derived dropstones of pre-Cenozoic erosive material good indicators for the glacial periods as well.

4. The JMMC's tectonostratigraphic framework

The stratigraphical observations presented above provide a basis upon which to assess the tectonic effects on the Cenozoic succession in the JMMC. In the following sub-sections, a summary of the tectonostratigraphical framework is presented, with a focus on the following time intervals (in ascending stratigraphic order): (1) the Early to Mid-Eocene following the 1st breakup (~52–43 Ma); (2) the ridge transfer period and re-organisation in the Late Eocene–Early Oligocene (43–30 Ma); (3) the formation of the western JMMC igneous margin and 2nd breakup (30–22 Ma); and, (4) the separation stage of the microcontinent from East Greenland (22 Ma to present). The description of this evolutionary sequence of events is accompanied by a set of reconstruction profiles across the JMMC (Fig. 9) together with a series of schematic palaeogeographical maps (Fig. 10).

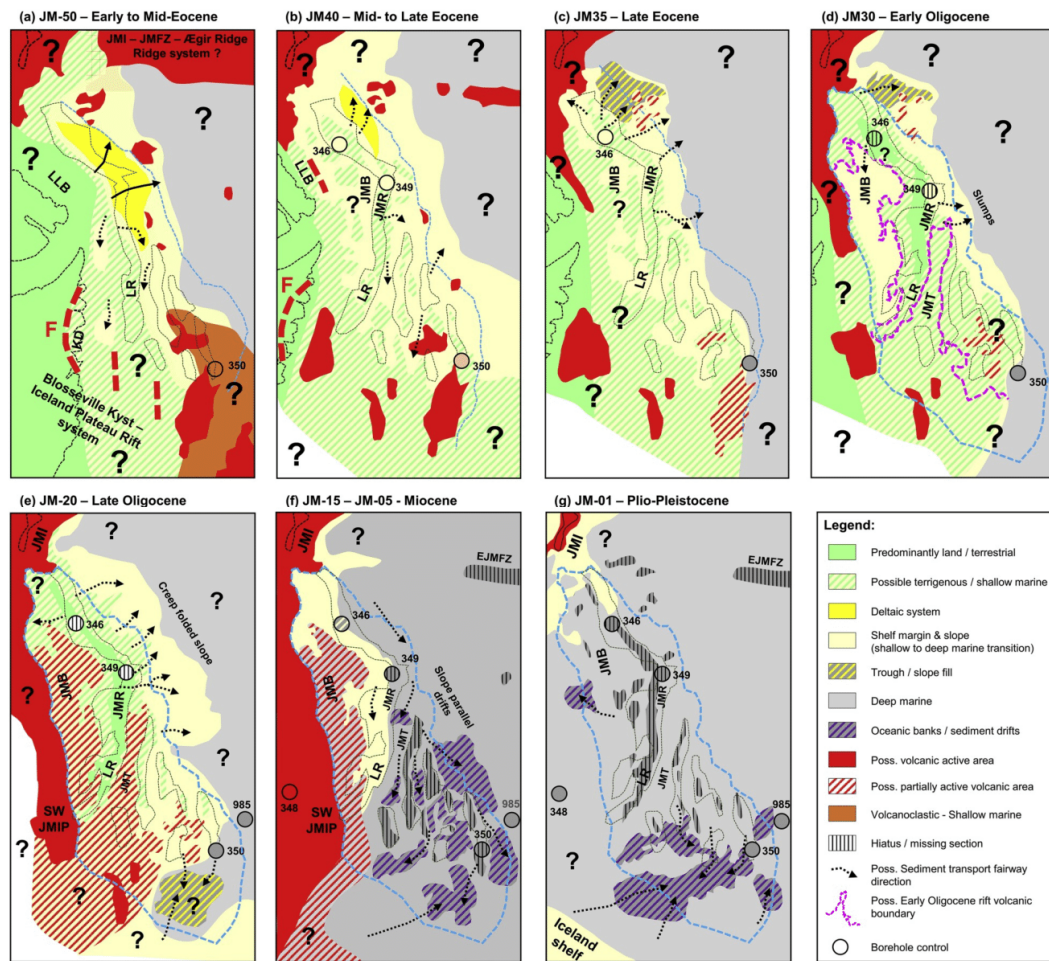


Fig. 10. Series of schematic paleo-geographical maps showing the inferred spatial and temporal development of the JMMC area that are primarily tied to borehole data control, seismic reflection, and stratigraphic thickness distribution map data interpretations (Fig. 7). The map series is tied to the established JMMC seismic-stratigraphic framework (Fig. 4): (a) JM-50 – Early to Mid-Eocene; (b) JM40 – Mid-to Late Eocene; (c) JM35 – Late Eocene; (d) JM30 – Early Oligocene; (e) JM-20 – Late Oligocene; (f) JM-15 – JM-05 – Miocene; and (g) JM-01 – Plio-Pleistocene. Abbr.: F – Lower Igertivá formation and intrusives (~49 Ma); JMB – Jan Mayen basin; JMI – Jan Mayen igneous complex; JMR – Jan Mayen ridge; JMT – Jan Mayen trough; KD – Kap Dalton; LLB – Liverpool Land basin; LR – Lyngvi ridge; SW JMIP – southwest Jan Mayen igneous province.

4.1. Early to Mid-Eocene tectonostratigraphy (~52-43 Ma)

Igneous activity associated with breakup and rifting at the Ægir Ridge spreading centre, characterised the northern, eastern and south-eastern margin of the microcontinent during this time interval, with the main direction of sediment transport being due northeast and east (Fig. 10a). The northern extent of the microcontinent from the Jan Mayen igneous complex, along the eastern EJMZFZ, appears to have been volcanically active throughout this period, represented by oceanic crust of the Ægir Ridge system, and increased igneous activity specifically along the northern and north-eastern edge of the JMMC (Figs. 5, 7a and 10a).

As the Ægir Ridge developed (~52-43 Ma), the eastern flank of the JMMC began subsiding. Accommodation space was created into which an ENE to NE prograding delta system of unit JM-50 built-out into and along the central north-eastern slope of the microcontinent. Synchronously-formed graben and half-graben structures along the

western flank of the JMMC is indicative of extension along the western rim of the Jan Mayen ridge but also within the SRC (Figs. 7a and 9a,b and 10a). Throughout this interval, the JMMC region appears to have been a transitional terrestrial-to-shallow-marine environment, flanking the deeper marine realm of the Norway basin to the east (Fig. 10a).

The south-eastern margin of the JMMC appears to have been near the shoreline or in a shallow-marine environment as indicated by terrigenous sediments with ash layers and hyaloclastite rocks in DSDP borehole 350. This nearshore-to-shallow-marine embayment formed part of a distinct volcanic margin, flanking the early Ægir rift and overlying the breakup SDRs section (Figs. 5 and 10a).

Mid-Eocene igneous activity along the southern JMMC is represented by dyke intrusions in borehole DSDP 350 with an ⁴⁰Ar-³⁹Ar age between ~49 and 44 Ma, emplaced within a highly-altered tuff-breccia, close to the Iceland Plateau Rift II (IPR II), observed as intersecting spurs within the SRC (Figs. 7a and 8) (Manum et al., 1976a, b; Blischke et al., 2016, 2017a). The rift transfer and associated igneous

activity appear to coincide with extension along the microcontinent's western margin, with formation of listric half-graben structures in the Jan Mayen basin and possibly small marine embayment areas (Figs. 9b and 10a).

4.2. Ridge re-organisation during Late Eocene – Early Oligocene (43–30 Ma)

As the Norway basin widened by spreading at the Ægir Ridge, the eastern flank of the JMMC continued to subside and deepen to the east and northeast. As a consequence of this process, a steep and unstable shelf slope formed with large blocks detaching themselves from the shelf and sliding downslope along slump fault detachment surfaces. Contorted and chaotic seismic-reflection patterns are observed within units JM40 to JM30, as a result of sliding and/or slumping, sediment reworking and redeposition, submarine channelling, and canyon formation (Figs. 5 and 7b–d). This slope failing process is especially well visible at the north-easternmost edge of the JMMC (Figs. 2 and 7b), where the slump-fault escarpments are still fully exposed at seafloor today and slump deposits were mapped on seismic reflection data.

Higher-spreading rates between ~43 and 30 Ma in the northern domain of the oblique Ægir Ridge, north of the central Norway basin fracture zone (CNBFZ) (Gernigon et al., 2015; Blischke et al., 2017a) (Fig. 1), was associated with enhanced subsidence, reflected by the thicker sediment cover and channel infills along the north-eastern and eastern flank of the JMMC. The basin infill is thickest adjacent to the EJMZF, where rapid subsidence is represented by seismic reflectors overlapping the JMR and volcanic centres (Fig. 7b–d and 9c).

Throughout this interval, the JMR is interpreted to have formed an elevated area. The relative planarity of the ME, UE1 and UE2 unconformities beneath the crest of the JMR (Fig. 6), prior to later tilting and erosion, suggests a shallow shelfal setting, which is supported by borehole data that proved terrigenous-to-shallow-marine deposits in this part of units JM-40 to JM-30 (Fig. 10b–d). Relative sea level was also generally lower during this interval (Fig. 4). The overall former distribution of the JM-40 to JM30 units on the JMR is unclear, due to their truncation by the MOU unconformity (Figs. 5, 6 and 9); however, stratigraphic reconstruction of seismic profile data (e.g. Fig. 9) has helped us to cross-correlate the stratigraphy and depositional environments between the flank areas across the ridges.

Along the collapsing western flank of the microcontinent the Jan Mayen basin continued to deepen, represented by a progressive increase in stratigraphic thickness in the half-graben structures near the central Jan Mayen basin fracture zone (CJMBFZ) (Fig. 7b and c). These half-graben structures can be seen on the Mid-Oligocene sub-crop (Fig. 8) extending half way into the Jan Mayen basin, underneath the younger, possibly Early to Late Oligocene, flood basalts and intrusive rocks (Fig. 9c). Although this interpretation is uncertain, an overall thinning of the microcontinental domain from east to west is observed suggesting a transition into a younger and igneous-dominated domain within the western segment of the Jan Mayen basin (Fig. 5b and c; 8; 9c & 10d), thereby forming a transitional crustal segment in response to increased igneous activity within the basin from the Early Oligocene onward.

In contrast to the north-eastern flank, the southern domain of the JMMC was uplifted in response to oblique spreading of the Ægir Ridge, as well as its decreased spreading rates in its southern domain. The oblique-spreading process was compensated by an anti-clockwise rotation of the southern ridge system along the SRC transfer fracture zone (SRCTFZ) (Gaina et al., 2009; Gernigon et al., 2015; Blischke et al., 2017a). Extension within the Jan Mayen trough and the southern half of the SRC generated compression in the northern part of the complex, causing minor reverse faulting. The fan-like pattern of extensional processes of the SRC and the Jan Mayen trough triggered a northward propagation of volcanic activity across the Iceland plateau rift segments (IPR-1 to IV on Fig. 8) breaching the stretched and fractured crust of the

SRC in numerous places (Fig. 7d). An overall thinning of the sediment cover towards the south and southwest suggests that the SRC as well as the main Jan Mayen ridge was probably uplifted. Increased igneous activity is supported by frequent ash layers within the mudstone and siltstone deposits in DSDP site 350 (Talwani et al., 1976a, 1977; Blischke et al., 2017a).

4.3. Formation of the western JMMC igneous margin and 2nd breakup (30–22 Ma)

The western volcanic margin of the microcontinent was developed by spreading at the nascent Kolbeinsey ridge, fully separating the JMMC domain from the central East Greenland shelf, as the Ægir ridge became extinct (~30–26 Ma) (Gaina et al., 2009; Gernigon et al., 2015). Cessation of spreading within the Norway basin caused cooling and subsidence along the eastern and south-eastern margins of the JMMC.

The increased igneous activity and formation of volcanic centres along the western and south-western margins of the JMMC is placed within the chronological time window of unit JM-20, specifically for the area of the Jan Mayen trough, the southwest Jan Mayen igneous province (SWJMIP), and along the western margin of the Jan Mayen basin (Figs. 4 and 5b,c, 7e and 9c–d). The volcanic centres and probable associated extrusive lava formations of this volcanic margin filled the topographical low areas along the Jan Mayen trough and the Jan Mayen basin (Fig. 10e). The increase of igneous activity along the microcontinent's western edge probably caused a thermal anomaly, subsequently resulting in uplift of the area that can be seen on seismic reflection and borehole data as the distinct MOU erosional surface (Fig. 4; Table 3). A hiatus that spans across the top of the Jan Mayen ridge, Lyngvi and most SRC ridges, and marks the acme of uplift (Figs. 7b–d, 8 and 10e). The MOU erosional marker could represent a combination event of both processes uplift and sea-level low changes, as it is placed at 30 ± 4 Ma which would include sea-level low changes at about 28 Ma (Fig. 4; Table 3).

The uplift of the JMMC appears to correspond to an eastward tilt of the main Jan Mayen ridge, as sediments were redeposited from the truncated and eroded crest of the ridge into the Norway basin. The south-western margin of the microcontinent, towards the SWJMIP, was probably elevated as well from the Mid-Oligocene, as the overall sediment thickness decreased in contrast to the subsiding south-eastern IPR segments, where an increase in sediment accumulation is indicated by preserved fill within troughs and small basins across the south of the SRC (Figs. 7e and 10e). Eastward tilting, erosion and redeposition along the eastern slope of the JMMC is further suggested by the occurrence of erosional channels, which may have acted as conduits for sediment transport and apparent rapid sediment deposition across the basin plain. These sediments show features similar to submarine creep zones that indicate unconsolidated sediment emplacement onto an instable and still subsiding slope (Shillington et al., 2012 or Li et al., 2016), (Figs. 5 and 6).

The proto-Kolbeinsey ridge was fully established by approximately 22 Ma (e.g. Gaina et al., 2009; Gernigon et al., 2015; Blischke et al., 2016). The F-marker flood basalts and associated intrusions (Figs. 7f and 10f) most likely represent regionally extensive composite sheets of flat-lying, lava flows and intrusive rocks emplaced along the western JMMC margin and Jan Mayen basin, possibly during the latest Oligocene to earliest Miocene (~25–22 Ma), covering the underlying unconsolidated, shallow-marine sediments (Gunnarsson et al., 1989; Blischke et al., 2017a) (Fig. 4). This volcanic margin includes the southwest Jan Mayen igneous province, which might be related to the source of the F-marker, as well as internal igneous sources along fault or fissure zones within the Jan Mayen basin (Fig. 5b and c, 7f and 9d,e). However, there is currently no direct borehole evidence to confirm the igneous origin of the F-marker; however, $^{40}\text{Ar}/^{39}\text{Ar}$ dating of igneous samples from DSDP borehole 348 indicates that a phase of volcanism did occur between 23 and 22 Ma (Blischke et al., 2016, 2017a), which is

well aligned to the geo-chron model of Gaina et al. (2009). Volcanic activity of the Jan Mayen Island volcanic system also affected the microcontinent's northern and north-western margin at this time, which formed an elevated volcanic margin with little-to-no sediment cover (Fig. 7f).

4.4. Spreading at the Kolbeinsey ridge (22 Ma to present)

Following the subsidence of the eastern flank of the JMMC and its SRC into a deeper marine environment, caused by the cooling of the Ægir and IPR systems, the microcontinent itself started to subside in response to the cooling of the more distal Kolbeinsey ridge system (Fig. 10g). Unit JM-10 reflects a deeper-marine setting with decreased sediment supply, localised erosional highs, and sediment accumulation within the Jan Mayen basin and Jan Mayen trough, as well as distal turbidite and sediment-drift deposits along the south-eastern flank of the JMMC and SRC (Figs. 4 and 5b,c, 7f, 9e and 10f).

With the JMMC now occupying a central position within a newly formed ocean, there was a shift of the overall drainage pattern from west-east (Fig. 10e) to a more ridge parallel and ocean current dominated north-south direction (Fig. 10f). The Miocene (JM-10–JM-05) sediment thickness increases towards the southeast and south with an indication of a distal source from the southwest, in the direction of the newly-forming Iceland shelf area. Prominent ash layers within DSDP boreholes 348, 349 and 350, and ODP site 985 indicate the presence of continuous volcanic activity in the western and south-eastern part of the region (Fig. 10f).

The most recent major environmental change relates to sea-level drop associated with the onset of widespread glaciation during the Plio-Pleistocene (unit JM-01 to seafloor) (Fig. 4). The stratigraphic record of borehole 346 on the northern Jan Mayen ridge indicates terrigenous sandy and muddy deposits interbedded with shallow-water siliceous and glauconitic sandy mud, and volcanic ash layers most probably derived from the Jan Mayen Island igneous system (Talwani et al., 1976c) (Fig. 10g). The occurrence of reworked cold water nannoplankton and pollen suggest that the northern JMR was located under permanent ice cover with low organic production and receiving little

ice-rafted material (Talwani et al., 1976c; Dzinoridze et al., 1978). High-resolution seabed bathymetry data show ice-sheet striation marks across the northernmost section of the microcontinent and iceberg plough marks across the main Jan Mayen ridge (Fig. 2). These observations suggest that the northernmost area of the JMR was located either close to sea level and a local ice-sheet across the JMI existed with sea-level curve data indicating a distinct drop at the time (Fig. 4); or the area was located right at the edge of a thick ice-sheet at a deeper sea-level that left the glacial striation marks. The JMI with the presently active Beerenberg volcano (Fitch, 1964) related to the thermal uplift as well, as an uplift process combination for the northernmost area of the JMMC. The area being still active at present and juxtaposed to the intersection of the EJMFZ and the JMI complex with at seafloor visible subsea landslides and active graben faulting (Fig. 2).

Farther south along the Jan Mayen ridge and towards the SRC, the JM-01 unit covers the underlying topography and its predominantly parallel seismic reflection configuration suggests that it has not been significantly disturbed by submarine glacial processes (Figs. 2, 6 and 7b). South of the SRC, sediment thickness increases into a topographically lower area (Figs. 7g and 10g). These sediments consist of cyclical, interbedded units of glacial-marine mud and clays with iceberg-derived drop-stones, sandy mud and silt, scattered admixtures of volcanic ash layers, and foraminiferal ooze indicative of intermittent, milder conditions in between the glacial phases (Talwani et al., 1976a, b; Jansen et al., 1996).

5. Regional correlation to JMMC

The Cenozoic stratigraphic framework of the JMMC is here compared with equivalent successions in adjacent areas, including the East Greenland margin, the Vøring margin, Iceland, the NW Faroe Margin, and the Faroe-Shetland margin. Established stratigraphic schemes exist for all these areas, and a stratigraphic-range chart for the Cenozoic succession across this part of the NE Atlantic region is presented in Fig. 11. The JMMC's adjacent margins are presented as summary sections of their specific tectono-stratigraphy in this section, followed by a consideration of the potential implications for regional stratigraphic

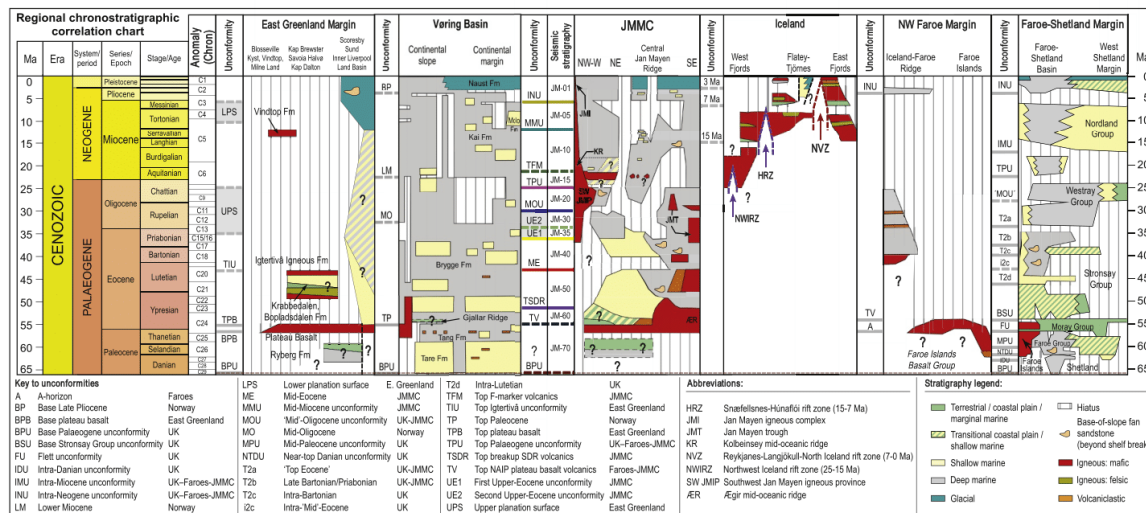


Fig. 11. Regional chronostratigraphic correlation chart of the JMMC in comparison to the Faroe-Shetland basin area (modified after Ólavsdóttir et al., 2013; Ritchie et al., 2011; Stoker et al., 2013, 2018; Ellis and Stoker, 2014), the Vøring margin (Hjelstuen et al., 1997, 1999; Lundin et al., 2013), the East Greenland conjugate margin area (Pedersen et al., 1997; Larsen et al., 1999a,b, 2002, 2005, 1989, 2013; Storey et al., 2004; Japsen et al., 2014; Bonow et al., 2014), and Iceland (Sæmundsson, 1979; Harðarson et al., 1997, 2008; and Hjartarson et al., 2017). Time scale used after Gradstein et al. (2012).

correlation and palaeogeography across this region, including the JMMC.

5.1. Adjacent NE Atlantic margins

5.1.1. Central East Greenland margin

A comparable structural setting for the JMMC exists along the Blossville Kyst area, central East Greenland, to which the micro-continent was still firmly attached prior to breakup and represents the closest analogue. Here specifically the onshore analogue site locations of Kap Brewster, Kap Dalton, Jameson Land basin, Kangerlussuaq basin, Milne Land, Savoia Halvø, and Vintop are of interest and were summarised (Pedersen et al., 1997; Larsen et al., 1999a,b; 2002, 2005, 2013; Hopper et al., 2014; Japsen et al., 2014; Bonow et al., 2014; Rotevatn et al., 2018) (Figs. 1b and 11). Offshore central East Greenland stratigraphic sections of marine to deep marine, and glacial depositional environments, are primarily based on seismic reflection data interpretations and have very little age constrain (Hopper et al., 2014) (Fig. 11).

Important sites, such as Kap Brewster show small rotated fault blocks within the uppermost pre-volcanic/pre-breakup succession containing possibly upper Danian to lower Selandian dark mudstones, which correspond to the marine sections of the Ryberg Formation in the Kangerlussuaq basin farther south-west (Soper et al., 1976; Nøhr-Hansen and Piasecki, 2002) (Fig. 11). Furthermore, are Lower Paleocene deposits present at Hold with Hope and Wollaston Foreland in Northeast Greenland (Larsen et al., 1999a,b; Nøhr-Hansen, 2003, 2012). Primarily preserved along the central East Greenland coast are the extensive breakup flood basalts and intrusive rock formations that overlie the main breakup unconformity base plateau basalt (BPB) and are exposed at surface marking the top plateau basalt unconformity (TPB) (Larsen et al., 1989; Upton et al., 1995) (Fig. 11).

Syn-rift successions are known at Kap Dalton, such as the terrigenous to shallow marine Krabbedalen and Bopladsdalen Formation that were preserved within the syn-breakup mafic and felsic Igertivå igneous outcrops (49–44 Ma) that form a local secondary top basalt unconformity (TIU) (Larsen et al., 1989, 2013) (Fig. 11). Offshore mapping indicates the continuation of a shallow shelf platform of syn-rift units with a distinct Late Paleogene unconformity (Blischke & Erlendsson, 2018) that could correspond the onshore upper planation surface (UPS) described by (Japsen et al., 2014; Bonow et al., 2014). The UPS formed as the result of an episode of late Eocene uplift and erosion that affected the Blossville Kyst region beginning between 40 and 35 Ma (Japsen et al., 2014).

The Miocene (13–14 Ma) and youngest igneous transitional to mildly alkaline onshore outcrop of central East Greenland is the Vindtoppen formation with isotopic evidence of Archaean contaminations (Storey et al., 2004). The formation overlies the UPS and the plateau lavas in the central part of the Blossville Kyst (Figs. 1b and 11).

This UPS surface is overlain by a more than 2 s (TWT) thick Neogene eastward-pro-gradating sedimentary succession across the Liverpool Land basin and Scoresby Sund offshore area (Larsen, 1990; Hamann et al., 2005). Within the offshore succession, the Miocene-Pliocene boundary was drilled by borehole ODP leg 162 site 987 that reached to about ~7.5 Ma old sediments, but did not reach into the oceanic crustal basement with an inferred age of ~10–11 Ma (Jansen et al., 1996; Channell et al., 1999a,b; Butt et al., 2001), closely located to magnetic anomaly 5 (Vogt, 1986; Gaina et al., 2017b). This Mid-Late Miocene unconformity is close to the base of the by Japsen et al. (2014) and Bonow et al. (2014) described lower planation surface (LPS) onshore (Fig. 11), an unconformity formed as the result of an episode of late Miocene uplift and erosion that affected the Blossville Kyst region beginning at ~10 Ma (Japsen et al., 2014). A surface that is close to the base of the youngest Neogene-Plio-Pleistocene primarily glacial sediment successions for the central East Greenland margin.

5.1.2. Vøring margin

The Vøring margin is part of the JMMC conjugate Norwegian margin to the east and northeast and represents the best studied analogue in comparison to the northeastern extend of the JMMC domain. The area went through the same continental breakup processes around the Paleocene and Eocene boundary that separated East Greenland from the Norwegian shelf (Eldholm et al., 1987, 1989; Doré et al., 1999; Faleide et al., 2010; Brekke, 2000).

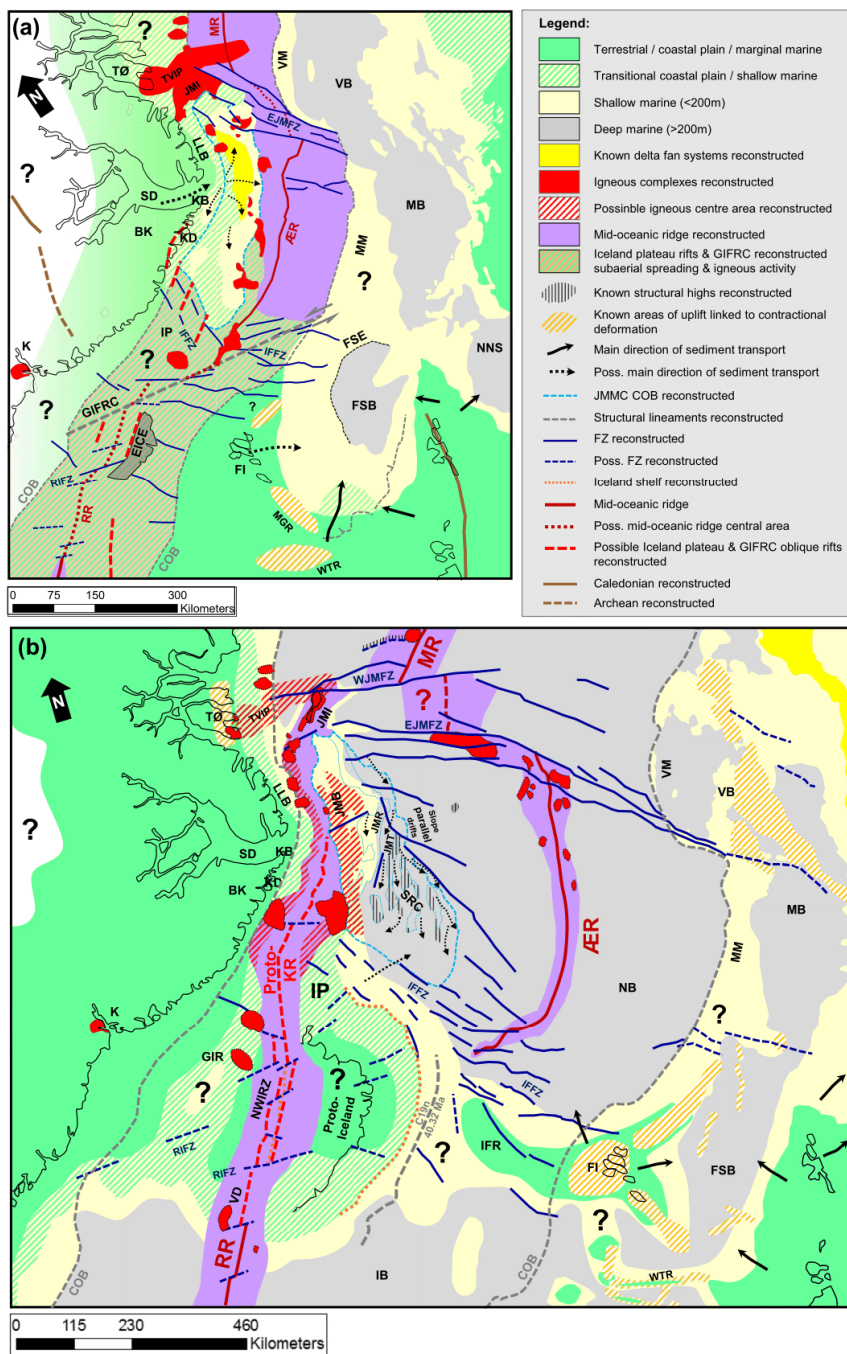
Shallow to deep marine Paleocene sediments are present along the Vøring and Møre margins that became increasingly deeper marine due east into the basins Vøring and Møre offshore Norway (Brekke, 2000; Faleide et al., 2010), and is bound by the base Paleocene unconformity (BPU on Fig. 11). Clear evidence of volcanism with interbedded volcanoclastic tuffs and extrusive and intrusive rock formations are present in borehole and seismic reflections records, such as seen in the Tare or Tang formations along the Vøring continental margin and basin (e.g. Dalland et al., 1988; Hjelstuen et al., 1999; Brekke, 2000; Lundin et al., 2013) (Fig. 11).

Especially the Vøring continental slope consists of a complex record of breakup volcanism and a complex build-up of seaward-dipping reflectors that show igneous activity from the pre-breakup extrusive rock formations that are part of the NAIP during Thanetian (57–55 Ma) and form the top plateau basalt breakup unconformity (Planke and Eldholm, 1994; Blystad et al., 1995; Doré et al., 1999; Brekke, 2000; Planke et al., 2000) (TP on Fig. 11). This was followed by post-breakup volcanism of the earliest Eocene during Ypresian (55–46 Ma) of extensive extrusive volcanism and the forming of a subaerial lava escarpment along the western basin margins of the Vøring and Møre basins, accompanied by considerable continued basin ward igneous activity emplacing sill intrusive rock formations into the pre-breakup strata (Skogseid et al., 2000; Planke and Eldholm, 1994) (Fig. 1b).

Uplift and faulting effected the Vøring margin, i.e. Gjallar ridge that was located on-strike with the JMMC before breakup, into the Paleocene time that can be seen as localised terrestrial platform areas that most likely represented the sediment source areas for the surrounding local graben areas and depositional centres of the westernmost Vøring basin (Hjelstuen et al., 1999) (Fig. 11). The flank areas of the Vøring margin to the north and south, such as the outer Møre margin are covered with breakup volcanic rock formations that obscure the pre-breakup stratigraphy of the Late Cretaceous to Paleocene. However, it has been documented that the Paleocene stratigraphic succession is thinning towards the westernmost Møre margin high, or even locally absent for its highest elevated areas, i.e. indicate stratigraphic thickness mapping results of the Tang formation that locally uplifted areas appear to be present, similarly to the locally exposed Gjallar ridge area of the Vøring margin (Hjelstuen et al., 1999; Brekke, 2000).

The post breakup Eocene to earliest Miocene succession is bound by the regionally seen top basalt and the lower Miocene unconformities (Hjelstuen et al., 1999) (TP and LM on Fig. 11). The succession is built of primarily of deep and open marine depositions varying in thickness with a general trend to thin across the underlying structural highs of the margins that include compressional domes that are estimated to have formed during middle Eocene to early Oligocene (Doré et al., 2008). Thus being the initial stage of localised forming of structural highs, as the entire mid-Norwegian shelf margin was overall subsiding after final breakup, but was locally affected by uplift that is believed to be associated with doming events between mid-Eocene and mid-Miocene and large scale tilting of the margins (Praeg et al., 2005; Doré et al., 2008). Such a doming process appear to correspond to the locally seen hiatuses across ridge areas of the Vøring margin and on-lapping successions at the Eocene to Oligocene boundary (Brekke, 2000) (MO on Fig. 11).

Across the Vøring margin and basin the succession is represented by the open marine Brygge formation primarily consisting of claystone, siltstone, thin sandstone banks, limestone and marls (Dalland et al., 1988) (Fig. 11). Increased deep water influences were observed along



(caption on next page)

Fig. 12. Breakup reconstruction of the possible sediment-fairway maps for the central Northeast Atlantic for the (a) end of main breakup phase (~49 Ma) and beginning of final breakup (~30–22 Ma) phase of the JMMC. The maps are a compilation of this study for the JMMC area and modified after Blischke et al. (2017a, 2018). For the central Northeast Atlantic conjugate regions paleo-geographic map and interpretations were included and modified based on Eldholm and Windisch (1974); Doré et al. (1999, 2008); Hopper et al. (2003, 2014); Berger and Jokat (2009); Gaina et al. (2009), Gaina et al. (2016), Gaina et al. (2017a,b); Roberts et al. (2009); Eidvin et al. (2014); Ellis and Stoker (2014); Stoker et al. (2005a, 2013, 2018); Gernigon et al. (2015); Døssing et al. (2016); Kimbell et al. (2016); Mudge (2015); Hjartarson et al. (2017) and Morlighem et al. (2017). Abbreviations: ÆR – Ægir ridge, BK – Blosseville Kyst, COB – Continental ocean boundary, EICE – East Iceland area, EJMFZ – East Jan Mayen fracture zone, FI – Faroe Islands, FSB – Faroe-Shetland basin, FSE – Faroe-Shetland escarpment, GIR – Greenland-Iceland ridge, GIFRC – Greenland-Iceland-Faroe ridge complex, IB – Iceland basin, IFFZ – Iceland-Faroe fracture zone, IFR – Iceland-Faroe ridge, IP – Iceland plateau, JMB – Jan Mayen basin, JMI – Jan Mayen igneous complex, JMR – Jan Mayen ridge, JMT – Jan Mayen trough, K – Kangerlussuaq, KB – Kap Brewster; KD – Kap Dalton; LLB – Liverpool Land basin, MB – Møre basin, MM – Møre margin, MGR – Munkagrannur ridge, MR – Mohn's ridge, NB – Norwegian basin, NNS – Northern North Sea, NWIRZ – Northwest Iceland rift zone, RIFZ – Reykjanes-Iceland fracture zone, RR – Reykjanes ridge, SD – Scoresby Sund, SRC – Jan Mayen southern ridge complex, TØ – Trail Ø, TVIP – Traill Ø-Vøring igneous complex, VM – Vøring margin, VB – Vøring basin, VD – Vesturdjúp, WJMZ – West Jan Mayen fracture zone, and WTR – Wyville Thomson ridge.

the western extends of the Vøring and Møre margins that are dominated by calcareous ooze and stratigraphic thicknesses vary between 50 m and 1,3 km passing the shelf edges (Dalland et al., 1988; Hjelstuen et al., 1999).

The next following succession for the Vøring margin is regionally known as the middle Miocene to lower Pliocene succession, includes the open marine Kai and Molo formations, and is bound by the lower Miocene and base Late Pliocene unconformities (Dalland et al., 1988; Brekke, 2000; Eidvin et al., 2007) (LM and BP on Fig. 11).

The Kai formation forms a base unconformity (Stoker et al., 2005a,b) that lines up with the lower Miocene hiatus across the margin that is believed to correspond to the mid-Miocene tectonic uplift and associated bottom-current erosional processes. In general does the formation vary in composition and depositional depth, and consists of contourites deposits along the continental margin (Bryn et al., 2005; Laberg et al., 2005; Stoker et al., 2005a; b).

The Molo formation is time equivalent to the Kai formation but represents the basin ward sandstone dominated formations of a deltaic system of longshore drift and coastal deposits from the east and northeast towards the Vøring margin that was caused by a regional uplift of mid-Norway during middle Miocene (Eidvin et al., 2007) (Figs. 11 and 12b).

The uppermost succession across the Vøring margin and continental slope consists of the regionally extensive and up to 1.8 km thick predominantly glacial Naust formation of a 150 km westward prograding shelf systems (Dalland et al., 1988; Brekke, 2000; Rise et al., 2005, 2010; Ottesen et al., 2009). The base of this succession is formed by the regional known hiatus between mid-late Pliocene (e.g. Brekke, 2000, 2005; Stoker et al., 2005a; b) (BP on Fig. 11). Basin ward and west of the continental slopes are seen primarily hemi-pelagic sediments and contourites along the deep sea topographic rises (Rise et al., 2005; Laberg et al., 2005).

5.1.3. Iceland

The forming of Iceland is directly related to the junction of multiple rift systems across the Greenland-Iceland-Faeroes ridge complex and increased volcanism that link the Reykjanes ridge to the south and the Kolbeinsey ridge to the north, and forms the direct southern margin of the JMMC domain.

The oldest (> 15 Ma) known and dated onshore geological rock record of Iceland have been found along the northwest coast of the Westfjords, around 14 Ma along the Iceland's eastern coast, and about 12 Ma in central north Iceland (Sæmundsson et al., 1980; McDougall et al., 1984; Harðarson et al., 1997; Pringle et al., 1997; Jóhannesson and Sæmundsson, 1998) (Fig. 11). Deeper rock formation can only be implied, as they are buried underneath younger volcano-stratigraphic sections, with the oldest provinces of present day Iceland consisting of up to 35 km thick crust in East Iceland, and about 25–30 km thick crust along West Iceland (Menke et al., 1996; Staples et al., 1997; Brandsdóttir and Menke, 2008).

The adjacent insular shelf margin to the north-west of Iceland was very likely formed by the extinct Northwest Iceland rift zone, which is

estimated to have been active between 15 and 25 Ma and represents the oldest and Mid-Miocene known volcano-stratigraphic section of Iceland marked by a top hiatus at around 15 Ma (Harðarson et al., 1997, 2008) (NWIRZ on Fig. 11). Spreading activity shifted again from the Icelandic northwestern shelf area to the Snæfellsnes-Húnaflói rift zone that is interpreted to have been active for about 8–10 Ma until 7 Ma (Harðarson et al., 2008) (HRZ on Fig. 11). This rift transition is well marked by an Iceland wide hiatus, also referred to as the 7 Ma unconformity (Sæmundsson, 1979; Harðarson et al., 1997, 2008; and Hjartarson et al., 2017). Subsequently spreading shifted again at around 7 Ma and formed the present day active Reykjanes-Langjökull-North-Iceland rift zone and the rift zone (NVZ on Fig. 11), indicating a broadly southeast shift of ridge centre activity by the process of rift-jumps (Hjartarson et al., 2017). This process of rift transfer is ongoing and can be observed in south Iceland, where a new rift propagation is in progress for the last 2–3 Ma, forming the eastern volcanic zone by segmenting older pre-existing crust and forming micro-plates in the process (Sæmundsson, 1979; Einarsson, 2008).

The primarily onshore mapped stratigraphic record of Iceland for the Mid-Miocene to Quaternary consists primarily of volcanic extrusive and intrusive rock formations of primarily mafic composition and secondarily felsic compositions that is emplaced within the Neogene strata and close to central volcanic systems (Fig. 11). Onshore preserved sediment sections that are found locally in between volcanic strata can be up to 200–500 m thick and represent 5–10% of the total volcano-stratigraphic section (Sæmundsson, 1979; Grimsson and Simonarson, 2008). On- and offshore areas, where sediment strata reaches to at least up to 2 km thickness, are specifically known along the north Iceland shelf and the Flatey-Tjörnes sedimentary stratigraphic sequence (Fig. 11). The Tjörnes peninsula onshore exposures are up to 500 m thick, consist of paralic-shallow marine sandstones that are interlayered by terrestrial mudstone, muddy sandstone and lignite, and are interrupted by sporadic extrusive lava emplacement events (Eiriksson, 1981; Simonarson and Eiriksson, 2008). Icelandic sedimentary rocks in general are of mixed compositions from terrestrial to lacustrine-shallow marine facie types (Grimsson and Simonarson, 2008) that are formed by thin-bedded shale, mudstone, siltstone, or slump-turbiditic deposits, and prograding coarser deltaic deposits of sandstone and conglomerate. Leave imprints, seeds, stems, fossilised tree branches and rare faunal remains can be found within the lacustrine beds (Grimsson and Simonarson, 2008; Denk et al., 2011).

The Flatey-Tjörnes area is a good type location for the overlying increased glacial sediment record (Fig. 11), marking the onset of cooling towards the end of the Pliocene. During the Pleistocene, several glacial events removed approximately 1 km of the Iceland plateau basalts (Walker, 1964), the eroded deposits, of which, were likely deposited into newly formed basins off the Iceland shelf, such as the Iceland plateau area to the north-east (Figs. 7g, 10g and 11).

5.1.4. NW Faroe margin

The Cenozoic succession on and around the Faroe Islands is dominated by the Faroe Islands Basalt Group (FIBG) which comprises a thick

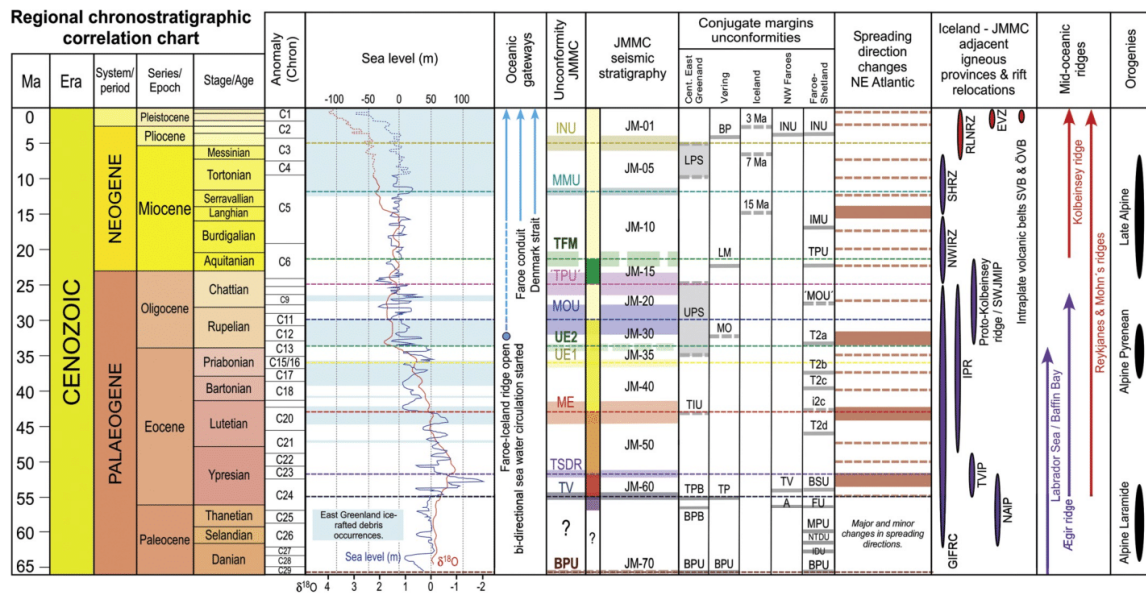


Fig. 13. Chronostratigraphic summary chart of the JMMC unconformities (Fig. 4 and Table 3) in correlation to unconformities of adjacent margins (Fig. 11), sea level changes and $\delta^{18}\text{O}$ data by Van Sickle et al. (2004), Miller et al. (2008), and Murray-Wallace and Woodroffe (2014), Paleogene East Greenland ice-rafted debris occurrences by Tripathi and Darby (2018), ocean gateway interpretations (Stoker et al., 2005a,b; Stürz et al. 2017), NE Atlantic spreading direction changes modelled by Gaina et al. 2017a,b), main igneous provinces and rift relocations after Sæmundsson (1979), Harðarson et al. (1997, 2008), Saunders et al. (2013), Thordarson and Höskuldsson (2008), Brandsdóttir et al. (2015), Blischke et al. (2017a), Geissler et al. (2017), and Hjartarson et al. (2017), mid-oceanic ridge systems and orogenies modified after Lundin and Doré 2002. Key of igneous provinces and rift relocations: GIFRC – Greenland-Iceland-Faroe ridge complex, IPR – Iceland plateau rift zone, NAIP – North Atlantic igneous province, SWJMIP – Southwest Jan Mayen igneous province, TVIP – Trill Ø-Vøring igneous complex; Iceland: EVZ – Eastern volcanic zone, NWIRZ – Northwest Iceland rift zone, RLNRZ – Reykjanes-Langjökull-North Iceland rift zone, SHRZ – Snæfellsnes-Húnaflói rift zone, SVB – Snæfellsnes intraplate volcanic belt, and ÖVB – Öraefi intraplate volcanic belt. Time scale from Gradstein et al. (2012).

(> 6 km) succession of Paleocene–Lower Eocene volcanic rocks, which covers almost the entire Faroes continental margin (Passey and Jolley, 2009; Passey and Hitchen, 2011). The FIBG extends westwards onto the Iceland-Faroe Ridge (IFR) and eastwards into the Faroe-Shetland basin (Fig. 11) and is juxtaposed with the former spreading ridge – the Ægir Ridge – just north of the area. The lower part of the FIBG, the Lopra Formation, is dominated by volcanoclastic and hyaloclastic rocks that contain microfossils indicative of a marine environment (Ellis et al., 2002), whereas the middle and upper parts of the group are dominated by subaerial basaltic lava flows assigned to the Beinivörð, Malinstindur and Enni formations (Rasmussen and Noe-Nygaard, 1969, 1970; Berthelsen et al., 1984; Passey and Bell, 2007; Passey, 2009). The terrestrial basaltic formations are separated by three sedimentary and volcanoclastic units: the Prestfjall and Hvannhagi formations, which lie between the Beinivörð and Malinstindur formations, and the Sneis Formation, which separates the Malinstindur and Enni Formations (Passey and Jolley, 2009). The Prestfjall Formation comprises a thin coal-bearing sedimentary unit that correlates with the A-horizon; at present, this is only regional seismic reflector identified within the FIBG and separates the pre-breakup Mid-to Late Paleocene (Selandian–Thanetian, ~61–56 Ma) Lopra and Beinivörð formations from the overlying syn-breakup Early Eocene (early Ypresian, ~56–54.9 Ma) Malinstindur and Enni formations (Mudge, 2015; Ólavsdóttir et al., In Prep.). The A-horizon is broadly correlated with the Flett unconformity (see section 5.5) in the Faroe-Shetland basin (Fig. 11).

North of the Faroe Islands, the syn-breakup lava succession passes into the seaward-dipping reflector succession associated with the former spreading system of the Ægir Ridge. To the NW, the FIBG extends onto the IFR, though its relationship to the volcanic rocks of this ridge remains unclear as younger (Middle Eocene: dated as

41.5 ± 2.5 Ma) subaerial basalts were proved at DSDP site 336 on its northern flank (Talwani et al., 1976; Ólavsdóttir et al., 2017) (Figs. 11 and 13). These basalts were subsequently transgressed by Upper Eocene–Oligocene marine mudstones in a shelf-to-upper-slope environment, though the crest of the IFR likely remained subaerial; a scenario that probably persisted into the early Neogene as evidenced by a significant Miocene hiatus (Stoker and Varming, 2011; Ellis and Stoker, 2014). Northwards, beyond the drill site, a substantial Oligocene – Pleistocene shelf-margin wedge prograded into the Norway basin (Nielsen and van Weering, 1998).

5.1.5. Faroe-Shetland margin

The structural framework of the Faroe-Shetland margin is dominated by the Faroe-Shetland basin, a semi-enclosed basin (to the south) throughout much of the Palaeogene but developed into a through-going deep-water conduit from the early Neogene (Stoker et al., 2005a) (Fig. 12). The Cenozoic rock record in the Faroe-Shetland basin is punctuated by a series of unconformities that reflect a persistent tectonic instability throughout the Palaeogene–early Neogene interval (Stoker et al., 2018). It may be no coincidence that this interval spans the prolonged history of breakup associated with the JMMC, as described in section 4. Key phases of development are as follows:

- The Paleocene pre-breakup rifting phase (late Danian–Thanetian, ~63–56 Ma) was characterised by the formation of a series of sag and fault-controlled sub-basins (Dean et al., 1999; Lamers and Carmichael, 1999). Coeval borderland uplift events (rift-pulses) led to an episodic influx of coarse clastic sediment preserved as unconformity-bounded cyclical accumulations of shelf, shelf-margin and basinal deposits of the Shetland and Faroe groups (Ebdon et al.,

1995; Goodwin et al., 2009; Mudge, 2015) (Fig. 11). Rifting and extension was accompanied by volcanism associated with the Lopra and Beinivørð formations of the FIBG (Mudge, 2015; Ólavsdóttir et al., 2017).

- The latest Paleocene uplift, erosion and formation of the Flett unconformity (Fig. 11) at about 56 Ma marked a major regression that, in the southern part of the Faroe-Shetland basin, was characterised by a change from largely marine to coastal plain and terrestrial sedimentation of the Moray Group (Ebdon et al., 1995). This change was coeval with the extrusion of flood basalts of the syn-breakup Malinstindur and Enni formations of the FIBG, between about 56 and 55 Ma (Mudge, 2015). Extensive tuffs in the upper part of the Moray Group (Balder Formation) probably mark the instigation of discontinuous sea-floor spreading along the northern margin of the Faroe-Shetland region during chron C24r (early Ypresian, 55–54 Ma) (Passey and Jolley, 2009).
- The syn-breakup phase continued during the Early–Mid-Eocene (early/mid-Ypresian–early Lutetian, ~54–46 Ma) and represents the rift-to-drift transition (Stoker et al., 2018). An alternating, cyclical succession of coastal plain, deltaic and shallow-marine deposits preserved in the lower part of the Stronsay Group (Fig. 11) attest to tectonic instability throughout this interval linked, in part, to episodic uplift of the Munkagrannur and Wyville Thomson ridges, on the southern flank of the Faroe-Shetland basin (Ólavsdóttir et al., 2010, 2013; Stoker et al., 2013) (Fig. 12).
- The early Mid-Eocene (chron C21) instigation of continuous sea-floor spreading in the Norway basin marked the onset of the post-breakup phase on the Faroe-Shetland margin. In the Faroe-Shetland basin, this change was marked by the initiation of a series of Mid–Late Eocene (mid-Lutetian–Priabonian, ~46–35 Ma) uplift events linked to the continued growth of structures, such as the Wyville Thomson and Munkagrannur ridges, the instigation of inversion domes within the basin, and the tilting of the West Shetland margin (Ritchie et al., 2008; Ólavsdóttir et al., 2010, 2013; Stoker et al., 2013). This tectonic activity resulted in the formation of a set of subaerial and submarine unconformities (T2d, i2c, T2c, T2b) that reflect the episodic uplift, erosion and re-deposition of the contemporary Eocene basin-fill (Stoker et al., 2013, 2018) (Fig. 11).
- The late Palaeogene–early Neogene interval (~35–15 Ma) witnessed a major change in the shape of the Faroe-Shetland region, and arguably marked the instigation of the present-day physiography of the continental margin (Fig. 12b). In the latest Eocene/Early Oligocene, tectonic movements linked to compression and/or rapid differential subsidence (sagging) led to the basinward collapse of the Late Eocene shelf-margin, west of Shetland, and the general disposition of the Eocene succession, which was folded about the axes of the Wyville Thomson, Munkagrannur and Fugloy ridges forming the T2a unconformity (Stoker et al., 2013) (Fig. 11). This regional surface was variably overlapped by Oligocene and Lower Miocene basinal sequences, which were themselves deformed by compressional stresses that persisted throughout this interval creating the angular submarine discordances of the Top Palaeogene unconformity and the Intra-Miocene unconformity; the latter marking the early Mid-Miocene culmination of widespread inversion and fold growth (Johnson et al., 2005; Stoker et al., 2005b; Ritchie et al., 2008).
- Mid-Miocene–Pleistocene sedimentation in the Faroe-Shetland basin was dominated by deep-water sediment-drift deposits (Stoker et al., 2005a). Early Pliocene uplift and tilting of the West Shetland and East Faroe margins accompanied by basinal subsidence resulted in a major seaward progradation of the shelf-slope wedges as well as deep-marine erosion during a reorganisation of bottom current patterns (Andersen et al., 2000; Stoker et al., 2005a; Ólavsdóttir et al., 2013). This late Neogene deformation formed the Intra-Neogene unconformity (late Early Pliocene, ~4 Ma) (Fig. 11). Mid- and Late Pleistocene sedimentation was dominated by shelf-wide

glaciations which enhanced the shelf-slope prograding wedges (Stoker et al., 2005c).

6. Regional stratigraphic correlations

Based on the above data, we are able to make some general regional observations regarding the Cenozoic development of the JMMC and adjacent areas in terms of regional stratigraphic correlation, palaeogeography, and structural development (Figs. 11–13).

Using the charts in Fig. 11, two palaeogeographic maps have been constructed in Fig. 12 representing the two breakup phases for the JMMC that are set within the wider context of the NE Atlantic: (1) End of first breakup phase at ~49 Ma; and (2) Beginning of final breakup phase at ~30–22 Ma. On the palaeogeographic maps, structural trends, igneous complexes, fracture and rift zones, are based on present-day features mapped on potential field data, and a detailed kinematic reconstruction model (Blischke et al., 2017b). Parallel rift-systems line-up during reconstruction of anomalous magnetic trends in relation to the Iceland Plateau Rift and the formation of the Greenland-Iceland-Faroe ridge complex (GIFRC). The latter is specifically connected to lateral crustal thickness changes, mapped subaerial rift systems based on the distribution of SDRs for the region, and reconstructed igneous centres. All observations and correlations were then summarised in Fig. 13 to highlight the series of structural, magmatic, spreading directional changes, and climate change events that affected the central NE Atlantic area in correlation to JMMC during the Cenozoic.

6.1. Paleocene to earliest Eocene rifting and breakup time

The Cenozoic sedimentary record can be reconstructed based on the compiled dataset and analogue comparisons from rifting to breakup time during Paleocene and the earliest Eocene, primarily during the emplacement of the plateau basalts and the SDRs, which both belong to the NAIP (63–52 Ma) (Figs. 11–13). In the case for JMMC can this be compared to the analogue area of onshore central East Greenland, the offshore areas west and north of the JMMC, such as the conjugate Vøring and Møre basins of Norway (Brekke, 2000; Faleide et al., 2010), and the analogue areas due southeast and east are the Møre and Faroe-Shetland margins, where good seismic data and offshore deep well control exists (e.g. Pedersen et al., 1997; Larsen et al., 1999a,b, 2002, 2005; Brekke et al., 1999; Ritchie et al., 2011; Stoker et al., 2013, 2018; Ellis and Stoker, 2014; Larsen et al., 2013; Ólavsdóttir et al., 2013; Japsen et al., 2014; Bonow et al., 2014) (Figs. 4, 9a and 11 and 13).

The reconstructed microcontinent aligns adjacent to central East Greenland's coastline during pre-breakup time: thus, similarities in the overall stratigraphic succession should be expected (Figs. 10a, 11 and 13). The areas of the Jameson Land basin and Liverpool Land high reconstruct adjacent to the northern section of the Jan Mayen ridge and are believed to have been covered by pre-breakup and plateau basalt sequences as well (e.g. Blischke et al., 2017b). The geology along the Blossville Kyst coast line serves as a direct analogue area for the microcontinent, specifically the Lyngvi Ridge area and the southern half of the JMMC, as they realign parallel to each other (Fig. 1b).

6.1.1. Pre-breakup units and regional unconformities

The regionally known base Cenozoic unconformity BPU can be observed in the JMMC data as well (Figs. 6, 11 and 13), where a paleo-surface with seismic reflector dip changes of the possible Mesozoic section below the unconformity and the overlying Paleogene section creates a discontinuity across the JMMC, which has also been observed in the Kap Brewster location (Soper et al., 1976; Nøhr-Hansen and Piasecki, 2002) (Figs. 4–6, 9 & 11). The unconformity is clearly visible across the main Jan Mayen and the Lyngvi ridges and was confirmed by velocity contrast of seismic refraction data profiles for OBS and ESP datasets, as no borehole data exists to confirm this marker (Fig. 5 & Table 2).

The JMMC's pre-breakup unit JM-70 shows marked similarities in seismic-reflection character that is dominated by parallel-bedded plateau basalts across the JMMC (Fig. 9a), and to the velocity range to the Blossville Kyst area's Lower Paleocene plateau basalts (Table 2). Reviewing a JMMC example in comparison to the possible Early Eocene pre-breakup plateau basalt with its underlying Paleocene sedimentary section, small eastward dipping wedges above the possible Mesozoic top marker can be seen (Fig. 6) that are similar to the Kap Brewster analogue location. Here small rotated fault blocks in the uppermost pre-volcanic/pre-breakup rocks are noted, reflecting the extension of the area before breakup. The half-graben sediments consist of possibly upper Danian to lower Selandian dark mudstones that correspond to the marine sections of the Ryberg Formation in the Kangerlussuaq basin (Soper et al., 1976; Nøhr-Hansen and Piasecki, 2002).

Similarly, in the Faroe-Shetland region the occurrence of pre-breakup rifting, subsidence and the formation of fault-controlled sub-basins is documented to have occurred during the Paleocene (late Danian–Thanetian, ~63–56 Ma) (Dean et al., 1999; Lamers and Carmichael, 1999). Furthermore, the presence of Lower Paleocene deposits have been reported at Hold with Hope and Wollaston Foreland of Northeast Greenland (Larsen et al., 1999a,b; Nøhr-Hansen, 2003; 2012), and in the Vøring and Møre basins offshore Norway (Hjelstuen et al., 1999; Brekke, 2000; Faleide et al., 2010). Considering that these areas are the closest conjugated segments for the microcontinent, this would imply that the Paleocene pre-breakup rocks also extend regionally across the JMMC.

The upper-bounding unconformity of unit JM-70 – TV – represents the main breakup unconformity for the JMMC. Regionally, several latest Paleocene to earliest Eocene unconformities correlate well to this breakup marker, i.e. TPB, TP, TV or BSU for the earliest Eocene (c. 55–54 Ma) (Figs. 11 and 13). Here the regional breakup unconformity of Early Eocene is described as top volcanics (TV), or top plateau basalts (TP or TPB), which can be seen on seismic reflection, outcrop and borehole data across the region, on the central East Greenland shore, across the Vøring margin, JMMC, and the NW Faroe, and Faroe-Shetland margins (Fig. 11 and Table 3).

The base of these plateau basalt and pre-breakup volcanic rocks (BPB on Figs. 11 and 13), mark the lower boundary of the main regionally-observed igneous event of the NAIP. This pre-breakup base unconformity is confirmed for the East Greenland margin, and can be seen as a seismic reflection marker across the high and well imaged areas of the JMR as well (Figs. 5 and 6). A chrono-stratigraphic areal mapped distribution of the various units of the NAIP has not yet been fully resolved, but differences in the timing of igneous activities for each area can be seen from comparison of each conjugate margin area of the microcontinent (Fig. 11). The pre-breakup plateau basalt section can be seen consistently across the entire region (Figs. 1b and 11), although the igneous activity was active longer in the Faroe-Shetland region since c. 61 Ma, 57–55 Ma along the Vøring margin, and since 56 Ma for the central East Greenland margin marked by the BPB unconformity (Figs. 11 and 13).

In regards to the sub-aerial plateau basalts are those well exposed along the central East Greenland coast of the Blossville Kyst and overlie Lower Paleocene terrigenous sediments that are visible at the Kap Brewster and Kap Dalton locations, and Precambrian gneiss at the Milne land location (KB, KD & ML on Fig. 1b) (Nøhr-Hansen, 2003; Storey et al., 2007 & Larsen et al., 2013, 2014). These sediment and basalt units are believed to have subsequently been eroded by up to 2–3 km stratigraphic thickness, which is based on age-dating of basaltic intrusions and burial depth-based apatite fission track analysis (Mathiesen et al., 2000; Larsen et al., 2013; Japsen et al., 2014; Bonow et al., 2014).

Across the JMMC the mapped central East Greenland pre-breakup plateau basalt-equivalent section increases in stratigraphic thickness towards the south. This is even noticeable as these rocks have been more greatly affected by erosion across the Lyngvi ridge than across the

JMR further north (Fig. 5a). Towards the north are the plateau basalts on-lapping onto the Jan Mayen igneous complex that was closest located to the Vøring margin via the Proto-JMFZ (Figs. 1b and 5a). This north to south stratigraphic thickness increases of the plateau basalt strata has been observed from the southern area of the Blossville Kyst to the Kangerlussuaq basin, and the north-western area of the Faroe Islands platform (Brooks, 2011). The total plateau basalt succession is estimated to increase to 6–7 km towards the Kangerlussuaq area, but becomes younger and dramatically thinner to the north in Scoresby Sund and Jameson Land basin due to regional on-lap to a high area and subsequent erosion (Larsen et al., 1999a,b, 2014; Passey and Jolley, 2009; Passey and Hitchen, 2011; Árting et al., 2014). Thus, pinpointing to the main initial focal points of initial breakup initiation areas between East Greenland and the Faroe margin, and the Proto-JMFZ - Vøring shelf margin with the JMMC located in between as an elevated terrain.

6.1.2. Early Eocene syn-breakup

Prior to breakup, the area was uplifted along the microcontinents eastern volcanic margin, with the plateau basalt section exposed to erosion by forming a clear unconformity (TV on Figs. 4 and 11), but reversed during breakup and gradually sub-siding along its eastern margin during the formation of the SDR's and recorded shallower marine Early to Mid-Eocene pro-grading deltaic systems that form unit JM-60 (Figs. 6 and 10a). Initiation of seafloor spreading has been established for the Traill Ø–Vøring- Møre-Faroe-Shetland margin to lie within chron C24r during early Ypresian (55–54 Ma) (e.g. Passey and Jolley, 2009; Gaina et al., 2009; Gernigon et al., 2015). This time span correlates with the JMMC's main breakup base unconformity (TV) to the East Greenland top plateau basalt unconformities (TPB) and the Vøring margin top Paleocene - basalt unconformity (TP) (Figs. 11 and 13). In the Faroe-Shetland region, the initiation of the syn-breakup phase is marked by the A-horizon and the FU, though the onset of limited ocean spreading essentially correlates with the TV and BSU.

Full breakup along the eastern margin of the JMMC occurred from 55 to 52 Ma along an elevated eastern margin with the Ægir ridge SDR's units on-lapping onto the microcontinent's TV unconformity (Figs. 5 and 9a) (Gaina et al., 2009; Gernigon et al., 2015). The SDR's were identified primarily for the central and northern part of the JMMC, where most of the SDR forming occurred (Fig. 5) becoming more complex towards the JMI with its counterpart along the Vøring margin (Fig. 11) (Blischke et al., 2016a). The modelled change of Eurasia-Greenland's spreading rate and direction (c. 54–52 Ma) by Gaina et al. (2017a,b) corresponds to the JMMC's main mid-oceanic rift initiation unconformity "TSDR" (c. 52 Ma) (Figs. 11 and 13).

6.1.3. Palaeostructural and geographical considerations

Old structural trends and their intersection create potential zones of weak crust, where mid-oceanic ridge segments or hot-spot upwelling are likeliest to break through (Schiffert et al., 2018), which in turn causes localised thermal uplift of the affected area, such as the areas south and north of the JMMC that are marked as the GIFRC, IPR (Blischke et al., 2017b; Hjartarson et al., 2017), Traill Ø–Vøring igneous complex (TVIP) (Geissler et al., 2017; Gaina et al., 2017b), and the JMI areas in Fig. 12a. These are the areas suggested to be the sites of initial breakup that affected the surrounding regions by localised large igneous activity, which overlay modelled Iceland hot spot locations for breakup time Rogozhina et al. (2016) and Mordret (2018). These observations are based on hot spot track, heat flow, and 3-D shear wave velocity modelling that indicate a broad lineament of magmatic intrusions in Greenland's crust. These regions are predestined for differential uplift, which in turn cause linked structural processes and erosion, changing sediment path-ways and distributions that are not correlative to global sea-level changes. Thus a detailed review of the sediment record clearly functions as a gage, where and when igneous and structural activities occurred around the larger JMMC region. As the

JMMC is “sandwiched” in between these two active and uplifted regions, the stratigraphic record does reflect this in the form of a stratigraphic thinning towards the north and the south and the development of a depositional low in the central part of the microcontinent (Figs. 5, 9a and 10a and 12a).

In comparison to global and North Atlantic region modelled sea level changes and $\delta^{18}\text{O}$ data by Van Sickle et al. (2004) and Miller et al. (2008) the top of the SDR's (TSDR on Figs. 4, 11 and 13) correlate best with the maximum Eocene thermal optimum and flooding event (~52 Ma). Furthermore no significant sea level change could be seen for the Paleocene-Eocene thermal maximum (PETM) event, which is interpreted as a short lived but rapid warming event around ~55.5 Ma (Bowen et al., 2015). Nevertheless, the data show a good correlation between major extrusive volcanic activity and climate changes within the NE Atlantic region for the pre-breakup and breakup phase.

6.2. Early to Mid-Eocene from breakup to rift-to-drift

The rift-to-drift transition of the Ægir mid-oceanic ridge within the Norway basin was forming an oblique spreading system by ~49 Ma (Gaina et al., 2009; Gernigon et al., 2015; Blischke et al., 2017a) (Fig. 12a), however, the first definitive and continuous spreading anomaly was not achieved until chron C21 (late Ypresian–early Lutetian, ~48–46 Ma) (Gaina et al., 2009; Ellis and Stoker, 2014; Blischke et al., 2017b). Volcanic activity continued along the microcontinents northern and eastern margins, and along the Iceland Plateau rift to the southeast to south of the microcontinent. North of the JMMC, the igneous system Traill Ø–Vøring igneous complex continued to be active (Geissler et al., 2017), connecting the East Greenland igneous province to the Vøring igneous domain between 52 Ma to 49 Ma. These areas align side by side to the JMI at ~49 Ma and form the north-western edge of the eastern Jan Mayen fracture zone located within a marginal marine environment along the east Greenland shelf, into marine and deeper marine depositional settings along the Vøring margin. Along the JMMC's western margin a transition to a shallow marine area developed, and south of JMMC forms the IPR and the GIFRC as subaerial ridge complex that align with the terrestrial and subaerial margin of the Faroe margin, and the terrestrial to shallow marine area of the Faroe-Shetland margin (Figs. 11 and 12a).

6.2.1. Rift-to-drift units and adjacent margins

The JMMC's primarily shallow marine unit JM-50 includes marginal marine to deltaic sections, and its shallow marine to subaerial volcanics (Fig. 12a). Here specifically, the microcontinents top Mid-Eocene unconformity (ME; c. 43 ± 3 Ma) aligns with the top of the Igertivá igneous formation and its unconformity (TIU) (Japsen et al., 2014), and with a series of unconformities in the FSB within the 46–40 Ma time span (T2c, i2c, and T2d on Figs. 11 and 13), which reflect high-frequency differential vertical motions and growth of inversion domes, indicating that these areas were all variably and episodically exposed above sea level during the Mid-Eocene (Lutetian–Bartonian) (Stoker and Varming, 2011; Stoker et al., 2013, 2018). In the western part of the FSB, Ólavsdóttir et al. (2013) identified a ‘Mid-Eocene’ hiatus which they tentatively correlated with T2c. The Vøring margin did not show a correlation for that distinct ME unconformity within a time range of 46–40 Ma except small high ridge areas along the outermost continental slope crest (Hjelstuen et al., 1997, 1999).

Strong similarities can be seen by comparing the seismic characteristics of the JMMC's unit JM-50 with the FSB terrestrial to shallow marine deposits of the Stronsay Group with alternating succession of deltaic and shallow-marine sediments (Figs. 4 and 11). The Munkagrinnur Ridge Delta is part of that group and prograded northwards into the Faroe-Shetland basin (Ólavsdóttir et al., 2010), as the JMMC deltaic system prograded in an easterly to north-easterly direction into the Norway basin, being located at the opposite end of the newly forming ocean basin. Several phases of prograding deltaic systems

within the JM-50 might also relate to short-lived global cooling episode (c. 50.3 Ma) that occurred abruptly and has been recorded in many regions as a low-stand and re-sedimentation deposition period (Payros et al., 2015).

Along JMMC's western margin a transitional to shallow marine area developed (Figs. 9b and 10a,b), which can be tied to small infill grabens preserved along the northernmost part of the Bløseville Kyst, at Kap Dalton and Savoia Halvø. A transgression from terrestrial to shallow marine sediments can be observed within the Bopladsdalen formation of the Kap Dalton Group which correlates to the same age range of the JMMC Early to Mid-Eocene deposits (Larsen et al., 2005) (Figs. 11 and 12a), suggesting that the paleo-shoreline lay on top and across parts of the Bløseville Kyst region which probably served as the main source area for the JMMC Lower-Mid Eocene delta system (Fig. 12a). The higher parts of the Bløseville Kyst and the southern flank of the microcontinent formed an embayment, where increased magmatism along the IPR's is observed as well as increased igneous activity of the central East Greenland coast (Larsen et al., 2014). Here the microcontinents southern extend corresponds to the lower part of the Igertivá formation, mapped at Kap Dalton (KD) (~49 Ma) on the conjugate East Greenland margin (Larsen et al., 2014) (Fig. 11), and coincides with the initiation of rift-transfer from the Ægir Ridge to the IPR (F on Fig. 10a). A rift transfer that is located within a phase of an overall change in spreading direction and decrease in seafloor spreading rate within the NE Atlantic domain, which is described by Gaina et al. (2017a,b) (Fig. 13), and does correlate to the main mid-Eocene hiatus and unconformity ME.

To the south of JMMC, the GIFRC links the Ægir and Reykjanes Ridge systems through a complex fracture zone region and off-ridge volcanic systems, connecting the Ægir Ridge with the Iceland plateau rift segments, onto the Bløseville Kyst, including segments of present day East Iceland (Fig. 12a). The seismic reflection characteristics for this area indicate SDR's, igneous complexes, and older crustal segments that formed an Iceland type oceanic crust within the proto-GIFRC (Arting et al., 2014; Blischke et al., 2017a; Hjartarson et al., 2017). The area has been shown as a sub-aerial volcanic region, corresponding to the terrestrial depositional environment of the Faroe Islands (Stoker et al., 2005a, 2018) (Fig. 11). The actively expanding GIFRC and IPR areas thus appear to have had a direct effect on the basin development within the JMMC and the FSB throughout the Early to Mid-Eocene interval (Figs. 11 and 12a).

6.2.2. Palaeogeography

Even though the central northeast Atlantic region went through an active igneous (e.g. GIFRC or IPR on Fig. 13) and structural re-arrangement during the formation of the active spreading systems, is it not certain that the formation of the regional ‘Mid-Eocene’ unconformity was solely due to local or regional uplift processes. A global sea level drop of nearly 60 m occurred during the Mid-Eocene (Fig. 4) (Van Sickle et al., 2004); thus, the possibility that the ‘ME’ unconformity is at least in part a response to this drop in sea level, as well as other factors, such as a cooling climate after the Eocene thermal maximum (45–42 Ma: as supported by ice-rafted debris (IRD) in the Northeast Atlantic region: Tripathi and Darby, 2018) (Fig. 4), cannot be discounted.

Still a structural alignment of the palaeogeography appears reasonable, as paleogeographic reconstruction of the Faroe-Shetland basin (FSB) illustrates an en-echelon NNE orientation of the JMMC embayment area across the central Northeast Atlantic with NE sediment transport direction and primary sediment influx from the east and south into shallow seas (Andersen et al., 2000; Stoker et al., 2013, 2018) (Fig. 12a). The main local uplift and source areas are related to episodic uplift of the Munkagrinnur Ridge (Ólavsdóttir et al., 2010, 2013) in line with the structural direction of the Faroe Islands and the Iceland plateau rift zone. The Wyville Thomson Ridge grew during this time as well (Ritchie et al., 2008; Tuitt et al., 2010) following the structural

grain of the developing fracture zones of the Reykjanes ridge (RIFZ on Fig. 12a). This being part of the extensive terrestrial region south of the FSB is part of the terrestrial and subaerial North Atlantic land bridge between Greenland and Scotland (Denk et al., 2011; Stoker et al., 2013, 2018), which is supported by paleo-current modelling of lagoon circulation conditions for the areas north of the land bridge in the Greenland and Norwegian seas during middle to upper Eocene (Stärz et al., 2017).

Furthermore, base-Eocene paleo-bathymetric modelling results by Roberts et al. (2009) represent the differentiation from coastal plain to deep marine environment for the Vøring and Møre basins and the Norwegian shelf, where the traditionally used structural segmentation of the area was not used, as that reflects the underlying pre-Cenozoic conditions (Brekke, 2000; Hopper et al., 2014). Unsurprisingly, the Vøring and Møre basins follow the structural trend segmentation of the EJMFC separating the two basins, with the Møre basins indicating a much broader shallow marine margin.

6.3. Central NE-Atlantic rift-transfer and re-organisation phase

Mid-Eocene to Early Oligocene (43 ± 3 Ma to 30 ± 4 Ma in Table 3) indicates a period of instability and change within the central NE Atlantic that is imprinted within the stratigraphic record of the JMMC and manifested by structural tilting and slope instability and down-slope slumping along the microcontinents eastern slope (Figs. 9c and 10c,d, 11 and 12b). This is accompanied by several unconformity events not just for the JMMC (UE1, UE2, and MOU on Figs. 11 and 13) but also along the adjacent margins, including: the T2b and T2a unconformities in the Faroe-Shetland region, which reflect tilting of the West Shetland margin and subsidence of the FSB, respectively (e.g. Stoker et al., 2013, 2018); the onshore upper planation surface (UPS), a composite unconformity along the central East Greenland coast (Japsen et al., 2014; Bonow et al., 2014) that is correlating closest to the MOU of JMMC; and the mapped MO hiatus of the central Vøring continental margin (Hjelstuen et al., 1997, 1999; Lundin et al., 2013).

6.3.1. Rift-transfer units and adjacent margins

The microcontinent units JM-40, JM-35, and JM-30 consist of shallow-marine to slope, and deep marine deposits intruded by volcanic rocks, and are indicative of a gradually-deepening Norway basin towards the east and northeast, accompanied by slump deposits down an increasingly unstable shelf (Figs. 9c and 10b-d, 11). Especially apparent is the increased volcanic influence during the Late Eocene and Early Oligocene along the southern and western JMMC margin into shallow marine to transitional marine areas (Fig. 10b-d).

Several glaciation events have been recorded across East Greenland and the Arctic during this period (Tripathi and Darby, 2018); thus, glacio-eustatic falls in sea level might, at least in part, be responsible for the upper boundary of unit JM-35 (UE2). This was followed by extensive erosion across the area (Figs. 11 and 13) marked by the major erosive boundary (MOU: top unit JM-30) of this period. Whilst the JMMC's MOU correlates to the end of a glaciation period, it does not correlate to as sharp a drop in sea level as for UE2 and may therefore, reflect uplift caused by the increased igneous activity and tectonic re-arrangement during the Early Oligocene.

6.3.2. Tectono-magmatic processes influencing palaeogeography

The mid-Alpine Pyrenean orogeny occurred at the same time as this phase of the NE Atlantic opening; thus, the NW European plate margin essentially formed a buffer zone under compressional stress between the ocean spreading ridge to the northwest and the orogenic belt to the southeast (Figs. 12b and 13) (e.g. Lundin and Doré, 2002; Ritchie et al., 2008). At the same time, spreading activity ceased within the Labrador Sea – Baffin Bay area (Lundin and Doré, 2002), accompanied by changes in spreading direction, a decrease in seafloor-spreading rate north of JMMC within the Mohn's ridge, and an increase south of the

microcontinent within the northernmost extend of the Reykjanes ridge that reached into the GIFRC (Gaina et al., 2017b). Around ~33 Ma, spreading rates and direction between Greenland and the Eurasian plate changed drastically from NNW-SSE to WNW-ESE also due to global plate motion changes (Gaina et al., 2017b), forcing a rearrangement of the active spreading centres. This observation correlates to the initiation of the proto-Kolbeinsey ridge – south-western Jan Mayen igneous province (SWJMIP on Fig. 10e and f and 11, 12b and 13) and time period that is associated with the modelled linking of the Iceland hot-spot with the mid-oceanic ridge system around 35–30 Ma as a distinct event (Dubrovine et al., 2012). A time period, where terrestrial to shallow marine conditions were dominating close to the central East Greenland coast and very likely elevated area of proto-Iceland as well (Fig. 12b) that formed elevated domains, whereas the Norway basin and Mohn's ridge were dominated by open deep marine environment conditions.

By way of contrast, Parnell-Turner et al. (2014) suggested that the Iceland plume influenced the area periodically from 55 to 35 Ma by V-shaped ridge formation every 3 Ma, and from 35 Ma to present the periodicity changed about every 8 Ma. However, even though it could be attempted to tie these observations to the apparently regular occurring changes in spreading directions for the NE Atlantic by Gaina et al. (2017), simply pulsing does not explain the major changes and unconformities that are linked to regionally effecting tectonic and paleoclimate change events (Fig. 13).

A change from terrestrial to shallower and open marine conditions can be seen for the Faroe margin, specifically the IFR area as well (Fig. 12b). According to Denk et al. (2011), the land-bridge from Greenland to NW Scotland was probably mostly intact during the Oligocene with small shallower marine pathways developing in between islands. This can be supported by sea water circulation changes from estuarine to an open bi-directional circulation around 33–32 Ma that is based on ocean gateway modelling by Stärz et al. (2017), though stratigraphic and structural evidence from the Faroe-Shetland region suggests that a fully-connected deep-water gateway was not established until the early Mid-Miocene (Stoker et al., 2005a,b). The GIR on the other hand appears to have remained under terrestrial to shallow marine influence (Fig. 12b), based on the complete hiatus onshore East Greenland (Japsen et al., 2014; Bonow et al., 2014) (UPS on Fig. 11), and on seismic reflection data well visible unconformities along the central East Greenland shelf (Blischke & Ögmundsson, 2018).

6.4. Regional ties to JMMC's western margin breakup settings

The Kolbeinsey mid-oceanic ridge is known to have been fully established by magnetic anomaly C6 (22–21 Ma) (e.g. Gaina et al., 2009; Blischke et al., 2017a) finalizing the initial western JMMC margin breakup phase that began earlier, around ~33–30 Ma (Figs. 10f and 12b) with an east to west rift transfer, as the Ægir ridge went into ultra-slow spreading and cessation mode (Gernigon et al., 2015; Gaina et al., 2017b) (Fig. 13). This can be demonstrated by the emplacement and increased activity of a string of igneous complexes along the microcontinents western margin, such as the SWJMIP (Fig. 10e and f and 11) that was accompanied by increased dyke and sill intrusive formations, and flood basalt within the JMB with its local TFM unconformity. That time marks the full breakup of the JMMC from the central East Greenland and ties nearly to the Lower Miocene (LM) unconformity of the Vøring margin and the top Paleogene unconformity of the Faroe-Shetland margin (Fig. 10e and f, 12b and 13). The Norwegian LM unconformity represents the lower Miocene hiatus across the margin that is believed to correspond to the initiation of the mid-Miocene tectonic uplift, changing the bathymetric layout that is associated bottom-current erosional processes (Stoker et al., 2005a,b).

Whereas the western JMMC was influenced by the developing igneous margin, the crest of the Jan Mayen ridge was subjected to erosion and the formation of its characteristic flat-topped topography. This flat-

lying, angular, erosional surface corresponds to the TPU, locally merging with the MOU unconformity, which lines up with broad hiatus of the UPS along the central East Greenland coast (Fig. 13). In contrast along the microcontinents eastern to southern flanks developed the slope-to-basinal, turbidite succession of unit JM-20 that is the result of rapid deposition of proximal eroded sediments due west (Fig. 10e), and evidence of the eastward tilting of the JMMC due to localised tectono-magmatic processes along its western flank.

6.4.1. Tectono-magmatic processes influencing palaeogeography

Global plate motion changes are also believed to have triggered spreading rates and directions to change drastically from a NNW-SSE to WNW-ESE between Greenland and the Eurasian plate (~33–21 Ma) just before the onset of the late Alpine orogeny (Gaina et al., 2017b; Blischke et al., 2017a) (Fig. 13). This process forced a rearrangement of active spreading centres within the NE Atlantic domain, as well as causing reactivation and compression along the south-eastern JMMC domain, and generated inversion structures within the SRC highs that may correspond to the MOU and the TPU unconformities. These may broadly correlate to the UPS unconformity of central East Greenland, and possibly to the 'MOU' unconformities of the Faroe Islands and the Faroe-Shetland margins (Figs. 1, 4 and 112b and 13).

Inversion structures occur across the IFR, the Faroe-Island plateau, the FSB that most likely reacted to the movement along the IFFZ, the expansion of proto-Iceland, and along the Jan Mayen fracture zone as the Kolbeinsey ridge became connected to the Mohn's ridge system (e.g. Ritchie et al., 2008; Hopper et al., 2014; Blischke et al., 2016; Stoker et al., 2018). The Traill Ø region became partially inverted, accompanied with syenite pluton and dike intrusions that form the landward end of the WJMFZ system (Parsons et al., 2017) (Fig. 12b). Along the EJMFZ, the inversion structures are aligned with the Vøring basin.

Reconstructed magnetic and gravimetric anomalies during the ~33 to 21 Ma period suggest that several rift and flank rift segment systems were active across the GIFRC (Blischke et al., 2017a), possibly offset by SW-NE striking fracture zone segments (RIFZ on Fig. 12b). Increased igneous activity west and southwest of JMMC, from the north-western Iceland rift zone (Harðarson et al., 2008) or the igneous complex of the Vesterdjúp (Hjartarson et al., 2017) reconstruct in alignment with the Reykjanes and proto-Kolbeinsey ridges, indicating breakup and rifting across the GIFRC, separating the domain into three segments, the Greenland-Iceland ridge (GIR), the proto-Iceland domain, and the Iceland-Faroe ridge (Fig. 12b). The reconstructed present-day western shelf margin (Blischke et al., 2017a) aligns as being centred within this rift zone, which is broader than the Mohn's ridge or the Reykjanes ridge corridors, and close to the proposed initial proto-Iceland rift zone at approximately 25 Ma, suggested by Harðarson et al. (2008). Thus, correlating to increased igneous activity from the Traill Ø region, along the Proto-Kolbeinsey ridge and the western JMMC margin, across the GIFRC, and the Reykjanes ridge, where increased numbers of igneous complexes and seamounts have been mapped (Gaina et al., 2017a), including the EJMFZ, or Ægir ridge systems (Fig. 12b). This scenario of active multiple igneous complexes and rift zones reflect a localised anomaly effecting primarily the central NE Atlantic, and does tie well into the modelled link of the Iceland hot-spot with the mid-Atlantic rift zone, just as seen on Iceland today.

The reconstructed terrain includes northeast and east Iceland, thus being the oldest terrains of present-day Iceland. The reconstructed eastern Icelandic shelf edge aligns with segments of the NW-SE trending IFFZ corridor, close to the extinct ~40 Ma Reykjanes ridge rift zone. The suggested SW-NE trending fracture zone (RIFZ) across the proto-Iceland region appears to precede today's south Iceland and central Iceland transfer system (Fig. 12b), whereas the NW-SE trend of the IFFZ appears to precede the present day north Iceland fracture zone trends, e.g. Tjörnes fracture zone (TFZ on Fig. 1a).

With the establishment of a continuous mid-oceanic rift system west of JMMC, its eastern flank, together with the Ægir ridge and the

Norway basin cooled and subsided, creating a pre-dominantly deep marine environment, e.g. seen in borehole data and slope parallel drift deposits based on seismic reflection data (Fig. 12b). Similarly, the 'structural highs' of the FSB area that formed during Eocene to Early Oligocene had by Late Oligocene-Early Miocene subsided beyond 200 m water depth (Stoker et al., 2005a, 2018), developing a part of a deeper-water oceanic margin. The main structural process in the Faroe-Shetland region at this time involved an intensification of differential uplift and subsidence, which had been developing throughout the whole period of protracted JMMC breakup but culminated at the climax of full breakup, creating its current bathymetric expression. Thus, the combination of inferred land areas and areas of contractional uplift provide a good indication of this 'developing' bathymetry (IFR and FI on Fig. 12b). The IFR land-bridge started to subside during Late Oligocene to early Neogene time, although some connectivity may have lasted via a series of island stepping-stones prior to a fully developed deep-water gateway in the early Mid-Miocene (Stoker et al., 2005a; Ellis and Stoker, 2014), and full oceanic connectivity between the Norway and Iceland basins (Fig. 12b).

6.5. Separation stage of the microcontinent from East Greenland

During the Neogene to Pleistocene the microcontinent subsided after cessation and cooling of the Ægir and IPR systems, and moved further away from the Kolbeinsey ridge (Fig. 10f and g), resulting in a transition from marine to deep and open marine conditions across the JMMC. This was followed by a dominance of newly formed ocean current deposits, a shift of the overall drainage pattern from west-east to north-south along the microcontinent ridge topography, accompanied by localised small to large slump erosion and deposits. Generally, changes of ocean current pattern across the central NE Atlantic are reported during Mid-Miocene to Pleistocene that resulted in the present-day bathymetric ocean basin and oceanographic systems.

In general, Miocene sediment thicknesses of units JM-10 to JM-05 increase towards the southeast and south, with an indication of a distal source from the southwest that include tephra deposits within the deep marine sediments, suggestive of consistent and ongoing volcanic activity to the north and south of the JMMC with the formation of the subaerial volcanic terrain of Iceland and the JMI.

During Plio-Pleistocene the JMMC's uppermost unit (JM-01) reflects an influx of terrigenous materials, most probably due to continental-glacial conditions of nearby land masses and localised erosional highs, such as the northern Iceland shelf area at this time. A clear sea-level drop can be seen that is associated with the onset of widespread glaciation during the Plio-Pleistocene (unit JM-01 to seafloor) (Figs. 4 and 13). This correlates as well with erosional events across Iceland during the Pleistocene, where several glacial events removed approximately 1 km of the Iceland plateau basalts (Walker, 1964), the eroded deposits, of which, were likely deposited into newly formed basins off the Iceland shelf, such as the Iceland plateau area to the north-east (Figs. 7g and 10g). A glacial ice shelf probably covered the northernmost JMMC with well visible striation marks (Fig. 2), whereas overall the JMMC remained under deep sea environment during glaciation with predominantly ice-berg scarp marks and drop stone in the uppermost stratigraphic section and the seafloor.

6.5.1. Tectono-magmatic processes influencing palaeogeography

Regional Mid-Miocene unconformity development is represented by the MMU across the JMMC, in Iceland c. 15 Ma, and the IMU (early Mid-Miocene) in the Faroe-Shetland region. Thus, the regional marker occurred in the interval from c. 17–13 Ma and may represent the culmination of widespread inversion and fold growth (Johnson et al., 2005; Stoker et al., 2005b; Ritchie et al., 2008), as well as the instigation of the 'modern' deep-water oceanic circulation system in the NE Atlantic as manifested by onset of deposition of major contourite drifts (Laberg et al., 2005).

Even though no basin wide Norwegian margin unconformity is reported, a regional uplift of mid-Norway during middle Miocene is well described by Eidvin et al. (2007) that was accompanied by longshore drift and coastal deposits into a deltaic system towards the Vøring margin (Figs. 11 and 12b). These stratigraphically seen processes are aligned with the Late Alpine orogeny, the last major change in overall spreading direction within the NE Atlantic, and rift transfer from the NWIRZ to the Snaefellsnes-Húnaflói rift zone (SHRZ) (Fig. 13) as a tectono-magmatic combined regional event. Interestingly enough this time correlate with the youngest igneous transitional to mildly alkaline on-shore outcrop of the Blossville Kyst's Vindtoppen formation (13–14 Ma) (Storey et al., 2004) as well, suggesting a more regional pulse of increased igneous activity within the central NE Atlantic.

During Late Miocene–Pliocene (c. 7–3 Ma) a more regional line up of locally seen unconformities is apparent from the INU ($\sim 5 \pm 2$ Ma) of JMMC, to the LPS (~ 10 –5 Ma) of central East Greenland, the BP (~ 5 –4 Ma) of the Vøring margin, and the INU (~ 4 Ma) unconformity of the Faroe Islands and Faroe-Shetland margin (Fig. 13). The INU hiatus represents NE Atlantic-wide marker and reorganisation of the bottom-current circulation pattern, which is expressed by a widespread deep-water erosion surface followed by renewed growth of contourite drifts (Laberg et al., 2005; Stoker et al., 2005a).

In the Iceland region, two unconformities are recorded from this time interval: 1) the so-called 7 Ma hiatus that is tied to the rift transfer from the SHRZ to the present day Reykjanes-Langjökull-North Iceland rift zone (RLNRZ); and 2), a second rift transfer at c. 3 Ma that started to form the eastern volcanic zone of Iceland (EVZ) (Fig. 13). However, no unconformity has been located for the 5–4 Ma events that were seen in the adjacent margins. No major orogeny or major shift in spreading direction is noted for this time, indicating the Iceland igneous and hot-spot system has a major influence on its surrounding margins and central NE Atlantic topography. Thus possibly also relating to the continued intra-plate developing volcanic zones across Iceland, such as the Snaefellsnes intraplate volcanic belt, or the ÖVB – Öræfi intraplate volcanic belt (Fig. 13), which reflects the complexity of the multiple rift systems across the Greenland-Iceland-Faroes ridge complex at present day and represents a prime example for the primarily sub-aerial volcanic processes active since the initial forming of the GIFRC. Still, in order to fully understand these complex processes of plume-rift interactions, Iceland-wide age dating has to be made available during future research projects to set the various rift forming processes and related hiatus events in chronological order.

7. Conclusions

The importance of this study was to map out paleo-facies sedimentary processes related to the development of the JMMC and their stratigraphic correlation to sea level changes. In addition, we have attempted to demonstrate, for the first time, a direct link between observed regional unconformities and palaeogeographic development, thereby highlighting the complexity of the multiple rift processes that affected the central Northeast Atlantic region prior to the formation of present-day Iceland.

Addressing a region that is “sandwiched” in between two active igneous focal areas that were predestined for differential uplift through time due to its location within a set of complex pre-existing structural weak zones (i.e. JMFZ to the north; IFFZ to the south), mid-oceanic ridges (i.e. Mohn's ridge to the north, Ægir ridge to the east, Reykjanes ridge to the south, and Kolbeinsey ridge to the west), flank rift systems (IPR, GIFRC and present day Iceland), and their link to the Iceland hot-spot dynamics.

The project resulted in a good demonstration to compare and assign JMMC's seismic refraction velocity data to its conjugate margin areas, such as central East Greenland, Norway (Vøring and Møre margin), and the Faroe-Shetland region. Thus, verify and update the microcontinent's pre-Cenozoic domains of continental, transitional to volcanic margins,

oceanic domains, and potential high velocity lower crustal features aligning the JMMC breakup boundaries to its Cenozoic stratigraphy. Indicating that the volcanic margin within the JMB terminates the JMMC domain close to its main western boundary faults, shows the microcontinent's southern and south-western termination against the IPR and SWJMIP, and its northern volcanic margin of the JMI.

Detailed mapping of the JMMC's sediment record functioned as a gage to pinpoint, where and when igneous and structural activities occurred on the JMMC and its conjugate margin, in comparison to sea level and climate changes. This resulted in a seismic-stratigraphic model, based on 2D MCS reflection, seismic refraction, borehole, and analogue field data, identifying ten unconformities and discontinuities that subdivide the JMMC's Cenozoic succession into eleven seismic units (JM-70 to JM-01).

Units JM-70 to JM-20 were identified for the Paleogene, and units JM-15, JM-10, JM-05, and JM-01 for the Neogene succession that were furthermore linked to 6 regional observed main igneous and tectonic events, which are briefly described and tied to regional stratigraphic events, within the central northeast Atlantic region:

- (1) Pre-breakup extension succession of JM-70 of the Paleocene (> 55 Ma) and earliest Eocene (56–55 Ma):
 - Bound by the BPU and TV unconformities
 - Consisting of terrigenous to transitional marine sediments and plateau basalts of the NAIP.
 - No significant sea level change could be seen close to the Paleocene-Eocene thermal maximum (PETM), which is interpreted as a short lived but rapid warming event around ~ 55.5 Ma.
 - Plateau basalt section of the JMMC has increased stratigraphic thickness towards the south, on-lapping onto the Jan Mayen ridge northward similar to the Blossville Kyst in East Greenland.
- (2) Syn-breakup (rift to drift) phase of unit JM-60 during Early Eocene (Lower Ypresian) (~ 55 –52 Ma):
 - Bound by the regionally seen TV (TPB, TP, or BSU) and locally on the JMMC seen TSDR unconformities.
 - SDR's and local igneous systems sourced intrusives, lavas and hyaloclastites, terrestrial to shallow marine environment across JMMC, regionally linked to GIFRC, and Vøring margin.
 - Substantial global sea level rise during the Eocene thermal optimum (~ 52 Ma) accompanied with increased marine depositional environment along the JMMC flanks.
- (3) Syn-breakup (rift to drift) and rift transfer across the Iceland plateau rifts south of JMMC, unit JM-50 during Early to Mid-Eocene (~ 52 –43 Ma):
 - Locally bound by the TSDR and regionally seen ME (TIU) unconformities.
 - Volcanics and transitional, shallow to marine sedimentary successions with well-established east to north-east prograding delta system along the JMMC east flank.
 - Reconstructed en-echelon NNE orientation of the JMMC and Faroe-Shetland basin (FSB) embayment areas with NE sediment transport direction and primary sediment influx from the east and south into shallow seas.
 - Extensive terrestrial region of the GIFRC as part of the terrestrial and subaerial North Atlantic land bridge between Greenland and Scotland, supported by paleo-current modelling of lagoon circulation conditions for the areas north of the land bridge in the Greenland and Norwegian seas during middle to upper Eocene
 - Around ~ 50.3 Ma a global short-lived cooling episode occurred abruptly that has been recorded in many regions as a low-stand and re-sedimentation deposition period, which could account for the top basalt (PB and SDR) unconformity across the high JMMC ridge areas.
 - The top (unit JM-50) bounding ME unconformity is not just reflecting the local igneous influence along the JMI and EJMZ

- (north of JMMC), or the IPR (south of JMMC), but rather an overall regionally sea level drop at the end of a series of glaciation event that has been recorded across East Greenland and Arctic and effected the entire region.
- (4) Ridge transfer and re-organisation, units JM-40, JM-35, and JM-30 during Late Eocene – Early Oligocene (43–30 Ma):
- Bound by regionally seen ME (TIU) and the MOU unconformities.
 - Shallow marine to slope, and deep marine deposits intersected by volcanic intrusives, gradually deepening into the Norway basin towards east and northeast, accompanied by slump deposits down an increasingly unstable shelf. Increased volcanic influence during Late Eocene to Early Oligocene along the southern and western JMMC margin into shallow marine to transitional marine areas.
 - Several glaciation events have been recorded across East Greenland and Arctic during this period, probably accounting for the upper boundary of unit JM-35 (UE2), as a sharp drop in sea level accompanies this boundary that was followed by extensive erosion across the area.
 - The main erosional boundary (MOU: top unit JM-30) of this period correlates to the end of a glaciation but does not correlate to a sharp drop in sea level, and therefore reflects the uplift caused by the increased igneous activity and tectonic re-arrangement during Early Oligocene, also being linked to the Iceland hotpot proximity to the GIFRC.
- (5) *Western JMMC igneous margin and 2nd breakup, forming of the south-western Jan Mayen igneous province, proto-Kolbeinsey ridge, and initial stage of the West Iceland shelf, unit JM-20 during Late Oligocene (30–22 Ma):*
- Bound by unconformities MOU, TPU as regional unconformities, and TFB as a JMMC local unconformity.
 - Distinct depositional domain difference between the subsiding deep marine Norway basin to the east, and the uplifting western and southwestern region in reference to JMMC with much increased volcanics, terrigenous, transitional to shallow marine deposits, with accompanied mass sediment transport along JMMC east flank.
 - West to east structural tilt of the JMR, as probably for the GIFRC area as well, as the GIR appears to have remained under terrestrial to shallow marine influence.
 - Cessation of the Ægir ridge, formation of the proto-Kolbeinsey ridge, connecting the Reykjanes ridge to the Mohn's ridge, and initiation of proto-Iceland separating GIFRC into three segments, the Greenland-Iceland ridge (GIR), the proto-Iceland domain, and the Iceland-Faroe ridge.
 - Phase was accompanied by a change in spreading rates and direction between Greenland and the Eurasian plate that caused inversion structures across the region (IFR, FP, FSB), as proto Iceland expanded.
 - Western Jan Mayen fracture zone formed and connected the Kolbeinsey with the Mohn's ridge, probably causing inversion and intrusive activity along the northern JMMC and the Traill Ø region. Along the EJMfZ, the inversion structures are aligned with the Vøring basin.
- (6) *Separation stage of the microcontinent from East Greenland (22 Ma to present)*
- JMMC moved into deep marine environment, dominated by newly formed ocean current deposits, shift of the overall drainage pattern from west-east to north-south, localised small to large slump erosion and deposits.
 - Cooling of the Ægir and IPR systems, JMMC area started subsiding, cooling with increased distance to the Kolbeinsey ridge system.
 - Tephra deposits within the deep marine sediments indicate consistent volcanic activity to the north and south of the JMMC, and increased sediment deposition into the low area between the

Iceland shelf and SRC.

- Glacial ice cover across the northernmost JMMC, whereas overall remained the JMMC under deep sea environment during glaciation the Plio-Pleistocene times.

In summary there is not just one explanation and correlation that can cause uplift or depositional settings changes, but different process appears interlinked, such global climate and sea level changes, rift tectonics, or the Iceland hot spot affecting rift propagations that in turn affect the structural and igneous processes and the overlaying topography with changing depositional and sedimentary processes.

Acknowledgements

This research project is conducted at the University of Iceland and funded by the National Energy Authority of Iceland (Orkustofnun) and the Iceland GeoSurvey. We specifically commemorate Dr. Þórarinn S. Arnarson, Orkustofnun, for his support and advice. Data permissions were provided by Spectrum ASA, TGS; the University of Oslo (UiO), the Bundesanstalt für Geowissenschaften und Rohstoffe (BGR), and GEUS (Geological Survey of Denmark and Greenland). We thank Guðrún Helgadóttir and Páll Reynisson, Marine Research Institute of Iceland (MRI), for making the multibeam and backscatter data available and the Norwegian Petroleum Directorate (NPD) for use of their 2D multichannel reflection data sets from 2011 & 2012.

Appendix A. Supplementary data

Supplementary data to this article can be found online at <https://doi.org/10.1016/j.marpetgeo.2019.02.008>.

References

- á Horni, J., Hopper, J.R., Blischke, A., Geissler, W., Judge, M., McDermott, K., Erlendsson, Ö., Stewart, M., Ártung, U., 2017. Regional Distribution of Volcanism within the North Atlantic Igneous Province. Geological Society, London, Special Publications 447, 18. <https://doi.org/10.1144/SP447.18>.
- Ártung, U., et al., 2014. In: D. H., G. C., Hopper, J.R., Funck, T., Stoker, M., Ártung, U., Peron-Pinvidic, G. (Eds.), Regional Volcanism - Tectonostratigraphic Atlas of the North-East Atlantic Region. Geological Survey of Denmark and Greenland (GEUS), Copenhagen, Denmark.
- Åkermoen, T., 1989. Jan Mayen-ryggen: et seismisk stratigrafisk og strukturelt studium. Cand. scient. thesis. University of Oslo, pp. 174.
- Andersen, M.S., Nielsen, T., Sørensen, A.B., Boldreel, L.O., Kuijpers, A., 2000. Cenozoic sediment distribution and tectonic movements in the Faroe region. *Glob. Planet. Chang.* 24, 239–259.
- Berger, D., Jokat, W., 2009. Sediment deposition in the northern basins of the North Atlantic and characteristic variations in shelf sedimentation along the East Greenland margin. *Mar. Petrol. Geol.* 26, 1321–1337. <https://doi.org/10.1016/j.marpetgeo.2009.04.005>. (2009).
- Berthelsen, O., Noe-Nygaard, A., Rasmussen, J., 1984. The Deep Drilling Project 1980–1981 in the Faroe Islands. Føroya Frøðskaparfelag, Tórshavn.
- Blischke, A., Planke, S., Tegner, C., Gaina, C., Brandsdóttir, B., Halldórsson, S.A., Helgadóttir, H.M., Koppers, A., 2016. Seismic volcano-stratigraphic characteristics and igneous province assessment of the Jan Mayen microcontinent, central NE-Atlantic. In: T33A: Accretion Modes, Structure, and Processes at Slow- and Ultra-slow Spreading Mid-Ocean Ridges II Posters, T33A-3008, AGU Fall Meeting, San Francisco, 12–15 December 2016.
- Blischke, A., Gaina, C., Hopper, J.R., Péron-Pinvidic, G., Brandsdóttir, B., Guarnieri, P., Erlendsson, Ö., Gunnarsson, K., 2017a. The Jan Mayen microcontinent: an update of its architecture, structural development and role during the transition from the Ægir Ridge to the mid-oceanic Kolbeinsey Ridge. In: Péron-Pinvidic, G., Hopper, J.R., Stoker, M.S., Gaina, C., Doornenbal, J.C., Funck, T., Ártung, U.E. (Eds.), The NE Atlantic Region: A Reappraisal of Crustal Structure, Tectonostratigraphy and Magmatic Evolution, vol. 447. Geological Society, London, Special Publications, pp. 299–337. <https://doi.org/10.1144/SP447.5>.
- Blischke, A., Erlendsson, Ö., Einarsson, G.M., Ásgeirsson, V.L., Árnadóttir, S., 2017b. The Jan Mayen Microcontinent Project Database and Seafloor Mapping of the Dreki Area Input Data, Geological and Geomorphological Mapping and Analysis. Prepared for Orkustofnun National Energy Authority of Iceland, ISOR-2017/055, Iceland.
- Blischke, A., Erlendsson, Ö., Guarnieri, P., Brandsdóttir, B., Gaina, C., 2018. Structural links between the Jan Mayen Microcontinent and the central East Greenland coast prior to, during, and after breakup. In: NGWM2018 – The 33rd Nordic Geological Winter Meeting 2018. The Geological Society of Denmark, Copenhagen.
- Blischke, A., Erlendsson, Ö., 2018. Central East Greenland – conjugate margin of the Jan

- Mayen microcontinent - Database, structural and stratigraphical mapping project. Prepared for Orkustofnun (OS) technical report. 95 pls., 2 maps, Appendices 1 to 5, ISOR-2018-024.
- Blystad, P., Brekke, H., Færseth, R.B., Larsen, B.T., Skogseid, J., Tærudbakken, B., 1995. Structural elements of the Norwegian continental shelf. Part II. The Norwegian Sea Region. Norwegian Petroleum Directorate NPD Bulletin No. 8.
- Bohrmann, G., Henrich, R., Thiede, J., 1990. Miocene to Quaternary Paleocyanography in the Northern North Atlantic: Variability in Carbonate and Biogenic Opal Accumulation. Geological History of the Polar Oceans: Arctic versus Antarctic 308, 647–675 of the series NATO ASI Series.
- Bonow, J.M., Japsen, P., Nielsen, T.F.D., 2014. High-level landscapes along the margin of southern East Greenland—A record of tectonic uplift and incision after breakup in the NE Atlantic. *Glob. Planet. Chang.* 116, 10–29. <https://doi.org/10.1016/j.gloplacha.2014.01.010>.
- Bowen, G.J., Maibauer, B.J., Kraus, M.J., Röhl, U., Westerhold, T., Steimke, A., Gingerich, P.D., Wing, S.L., Clyde, W.C., 2015. Two massive, rapid releases of carbon during the onset of the Palaeocene–Eocene thermal maximum. *Nat. Geosci.* 8, 44. Nature Publishing Group. <https://doi.org/10.1038/ngeo2316>.
- Boyden, J.A., Müller, R.D., Gurnis, M., Torsvik, T.H., Clark, J.A., Turner, M., Ivey-Law, H., Watson, R.J., Cannon, J.S., 2011. Next-generation plate-tectonic reconstructions using Glades. In: Keller, G., Bar, C. (Eds.), *Geo-informatics: Cyberinfrastructure for the Solid Earth Sciences*. Cambridge University Press, Cambridge, pp. 95–116.
- Brandsdóttir, B., Menke, W.H., 2008. The seismic structure of Iceland. *Jokull* 58, 17–34.
- Brandsdóttir, B., Hoof, E., Mjelde, R., Murai, Y., 2015. Origin and evolution of the Kolbeinsey Ridge and Iceland Plateau, N-Atlantic. *Geochem. Geophys. Geosyst.* 16, 612–634.
- Breivik, A., Mjelde, R., 2003. Modeling of profile 8 across the Jan Mayen Ridge. Rep. Institute of Solid Earth Physics, University of Bergen, Bergen, Norway.
- Breivik, A.J., Faleide, J.I., Mjelde, R., 2008. Neogene magmatism northeast of the Aegir and Kolbeinsey ridges, NE Atlantic: Spreading ridge–mantle plume interaction? *Geochem. Geophys. Geosyst.* 9, Q02004.
- Breivik, A.J., Mjelde, R., Faleide, J.I., Murai, Y., 2012. The eastern Jan Mayen micro-continent volcanic margin. *Geophys. J. Int.* 188 (3), 798–818.
- Brekke, H., 2000. The tectonic evolution of the Norwegian Sea continental margin with emphasis on the Vøring and Møre basins. In: In: Nøttvedt, A. (Ed.), *Dynamics of the Norwegian Margin*, vol. 167. Geological Society, London, Special Publications, pp. 327–378.
- Brekke, H., Dahlgren, S., Nyland, B., Magnus, C., 1999. The prospectivity of the Vøring and Møre basins on the Norwegian Sea continental margins. In: Fleet, A.J., Boldy, S.A.R. (Eds.), *Petroleum Geology of Northwest Europe: Proceedings of the 5th Conference*. Geological Society, London, pp. 261–274.
- Brooks, C.K., 2011. The East Greenland rifted volcanic margin. *Geol. Surv. Den. Greenl. Bull.* 24, 96.
- Bryn, P., Berg, K., Stoker, M.S., Hafliðason, H., Solheim, A., 2005. Contourites and their relevance for mass wasting along the Mid-Norwegian Margin. *Mar. Petrol. Geol.* 22 (1–2), 85–96. <https://doi.org/10.1016/j.marpetgeo.2004.10.012>.
- Buck, W.R., 2017. The role of magmatic loads and rift jumps in generating seaward dipping reflectors on volcanic rifted margins. *Earth Planet. Sci. Lett.* 466, 62–69. <https://doi.org/10.1016/j.epsl.2017.02.041>.
- Butt, F.A., Elverhoi, A., Forsberg, C.F., Solheim, A., 2001. An evolution of the Scoresby Sund Fan, central East Greenland - evidence from ODP Site 987. *Nor. Geol. Tidsskr.* 81, 3–15.
- Channell, J.E.T., Amigo, A.E., Fronval, T., Rack, F., Lehman, B., Raymo, M.E., Jansen, E., Blum, P., Herbert, T., 1999a. Magnetic stratigraphy at Sites 907 and 985 in the Norwegian-Greenland Sea and a revision of the Site 907 composite section. *Proc. Ocean Drill. Progr. Sci. Results* 162, 131–148.
- Channell, J.E.T., Smelror, M., Jansen, E., Higgins, S.M., Lehman, B., Eidvin, T., Solheim, A., 1999b. Age models for glacial fan deposits off East Greenland and Svalbard (sites 986 and 987). In: Paper presented at Proceedings of the Ocean Drilling Program, Scientific Results.
- Childs, J.R., Cooper, A.K., 1978. Collection, reduction and interpretation of marine seismic sonobuoy data. U.S. Geological Survey, Department of Interior Open file report 78-442.
- Dalland, A., Worsley, D., Ofstad, K., 1988. A lithostratigraphic scheme for the Mesozoic and Cenozoic succession offshore mid- and northern Norway. *Norwegian Petroleum Directorate Bulletin* 4, 87.
- Davies, R., Cartwright, J., Pike, J., Line, L., 2001. Early Oligocene initiation of North Atlantic Deep Water formation. *Nature* 410, 917–920. <https://doi.org/10.1038/35073551>.
- Dean, K., McLachlan, K., Chambers, A., 1999. Rifting and the development of the Faeroe-Shetland Basin. In: Fleet, A.J., Boldy, S.A.R. (Eds.), *Petroleum Geology of Northwest Europe: Proceedings of the 5th Conference*. Geological Society, London, pp. 533–544.
- Denk, R., Grimsson, F., Zetter, R., Simonarson, L.A., 2011. Late Cainozoic Floras of Iceland: 15 million years of vegetation and climate history in the Northern North Atlantic. *Igass* 2014. <https://doi.org/10.1007/s13398-014-0173-7.2>.
- Diebold, J.B., Stoffa, P.L., 1981. The traveltimes equation, tau-p mapping, and inversion of common midpoint data. *Geophysics* 46 (3), 238–254 12 figures, 1 table.
- Doré, A.G., Lundin, E.R., Jensen, L.N., Birkeland, Ø., Eliassen, P.E., Fichler, C., 1999. Principal tectonic events in the evolution of the northwest European Atlantic margin. In: Fleet, A.J., Boldy, S.A.R. (Eds.), *Petroleum Geology of Northwest Europe: Proceedings of the 5th Conference*. The Geological Society, London, pp. 41–61.
- Doré, A.G., Lundin, E.R., Kuszniir, N.J., Pascal, C., 2008. Potential mechanisms for the genesis of Cenozoic domal structures on the NE Atlantic margin: pros, cons and some new ideas. In: In: Johnson, H., Doré, T.G., Gatliff, R.W., Holdsworth, R.W., Lundin, E., Ritchie, J.D. (Eds.), *The Nature and Origin of Compression in Passive Margins*, vol. 306. Geological Society of London, pp. 1–26 Special Publication.
- Dossing, A., Japsen, P., Watts, A.B., Nielsen, T., Jokat, W., Thybo, H., Dahl-Jensen, T., 2016. Miocene uplift of the NE Greenland margin linked to plate tectonics: Seismic evidence from the Greenland Fracture Zone, NE Atlantic. *Tectonics* 35, 257–282. <https://doi.org/10.1002/2015TC004079>.
- Dobrovine, P.V., Steinberger, B., Torsvik, T.H., 2012. Absolute plate motions in a reference frame defined by moving hot spots in the Pacific, Atlantic, and Indian oceans. *J. Geophys. Res.-Sol. Ea.* 117, B09101. <https://doi.org/10.1029/2011JB009072>.
- Dzinoridze, R.N., Jousé, A.P., Koroleva-Golikova, G.S., Kozlova, G.E., Nagaeva, G.S., Petrushevskaya, M.G., Strelnikova, N.I., 1978. Diatom and radiolarian cenozoic stratigraphy. In: Norwegian basin; dsdp leg 38, paper presented at Initial Reports of the Deep Sea Drilling Project. U.S. Government Printing Office, Washington.
- Ebdon, C.C., Granger, P.J., Johnson, H.D., Evans, A.M., 1995. Early Tertiary evolution and sequence stratigraphy of the Faeroe-Shetland Basin: implications for hydrocarbon prospectivity. In: In: Scrutton, R.A., Stoker, M.S., Shimmield, G.B., Tudhope, A.W. (Eds.), *The Tectonics, Sedimentation and Palaeoceanography of the North Atlantic Region*, vol. 90. Geological Society, London, Special Publications, pp. 51–69.
- Eidvin, T., Bugge, T., Smelror, M., 2007. The Molo Formation, deposited by coastal progradation on the inner Mid-Norwegian continental shelf, coeval with the Kai Formation to the west and the Utsira Formation in the North Sea. In: *Norsk Geologisk Tidsskrift*, vol. 87. pp. 75–142.
- Eidvin, T., Riis, F., Rasmussen, E.S., 2014. Oligocene to Lower Pliocene deposits of the Norwegian continental shelf, Norwegian Sea, Svalbard, Denmark and their relation to the uplift of Fennoscandia: A synthesis. *Mar. Petrol. Geol.* 56, 184–221. 2014. <https://doi.org/10.1016/j.marpetgeo.2014.04.006>.
- Einarsson, P., 2008. Plate boundaries, rifts and transforms in Iceland. *Jokull* 58, 35–58.
- Eiriksson, J., 1981. Lithostratigraphy of the upper Tjörnes sequence, North Iceland: The Breiðavík Group. *Acta Nat. Isl.* 29, 1–37.
- Eldholm, O., Grue, K., 1994. North Atlantic margins: Dimensions and production rates. *J. Geophys. Res.* 99 (B2), 2955–2968.
- Eldholm, O., Windisch, C.C., 1974. Sediment distribution in the Norwegian-Greenland Sea. *Bull. Geol. Soc. Am.* 85 (11), 1661–1676. [https://doi.org/10.1130/0016-7606\(1974\)85%3e1661:SDITNS%3c2.0.CO;2](https://doi.org/10.1130/0016-7606(1974)85%3e1661:SDITNS%3c2.0.CO;2).
- Eldholm, O., Thiede, J., Taylor, E., 1987. Evolution of the Norwegian Continental Margin: Background and Objectives. In: Proceedings of the Ocean Drilling Program, vol. 104 Initial Reports. Ocean Drilling Program. <https://doi.org/10.2973/odp.proc.ir.104.101.1987>.
- Eldholm, O., Thiede, J., Taylor, E., 1989. The Norwegian continental margin: Tectonic, volcanic, and paleo-environmental framework. *Proc. Ocean Drill. Progr. Sci. Results* 104, 5–26.
- Ellis, D., Bell, B.R., Jolley, D.W., O'Callaghan, M., 2002. In: Jolley, D.W., Bell, B.R. (Eds.), *The stratigraphy, environment of eruption and age of the Faroes Lava Group, NE Atlantic Ocean* Retrieved from. <http://sp.lyellcollection.org/content/197/1/253.abstract>.
- Ellis, D., Stoker, M.S., 2014. The Faroe-Shetland Basin: a regional perspective from the Paleocene to the present day and its relationship to the opening of the North Atlantic Ocean. In: In: Cannon, S.J.C., Ellis, D. (Eds.), *Hydrocarbon Exploration to Exploitation West of Shetlands*, vol. 397 Geological Society, London, Special Publications. <https://doi.org/10.1144/SP397.1>.
- Faleide, J.I., Bjørlykke, K., Gabrielsen, R.H., 2010. Geology of the Norwegian continental shelf. In: Bjørlykke, K. (Ed.), *Petroleum Geoscience: From Sedimentary Environments to Rock Physics*. Springer, New York, pp. 467–499.
- Fitch, F.J., 1964. The development of the Beerenberg volcano, Jan Mayen. *Proc. Geol. Assoc.* 75 (2), 133–165. [https://doi.org/10.1016/S0016-7878\(64\)80002-X](https://doi.org/10.1016/S0016-7878(64)80002-X).
- Foulger, G.R., Natland, J.H., Anderson, D.L., 2005. A source for Icelandic magmas in remelted Iapetus crust. *J. Volcanol. Geoth. Res.* 141, 23–44 (2005).
- Funck, T., Hopper, J.R., Fattah, R.A., Blischke, A., Ebbing, J., Erlendsson, Ö., Gaina, C., Geissler, W.H., Gradmann, S., Haase, C., Kimbell, G.S., McDermott, K.G., Peron-Pinvidic, G., Petersen, U., Shannon, P.M., Voss, P.H., 2014. Crustal Structure. In: Hopper, J.R., Funck, T., Stoker, M., Ártung, U., Peron-Pinvidic, G., Doornenbal, I.I., Gaina, C. (Eds.), *Tectonostratigraphic Atlas of the North-East Atlantic region*. The Geological Survey of Denmark and Greenland (GEUS), Copenhagen, Denmark, pp. 340.
- Funck, T., Erlendsson, Ö., Geissler, W.H., Gradmann, S., Kimbell, G.S., McDermott, K., Petersen, U.K., 2016. In: Péron-Pinvidic, G., Hopper, J.R., Stoker, M.S., Gaina, C., Doornenbal, J.C., Funck, T., Ártung, U.E. (Eds.), *A review of the NE Atlantic conjugate margins based on seismic refraction data. The NE Atlantic Region: A Reappraisal of Crustal Structure, Tectonostratigraphy and Magmatic Evolution*, vol. 447 Geological Society, London, Special Publications. <http://doi.org/10.1144/SP447.9>.
- Funck, T., Geissler, W.H., Kimbell, G.S., Gradmann, S., Erlendsson, Ö., McDermott, K., Petersen, U.K., 2017. Moho and basement depth in the NE Atlantic Ocean based on seismic refraction data and receiver functions. In: In: Péron-Pinvidic, G., Hopper, J.R., Stoker, M.S., Gaina, C., Doornenbal, J.C., Funck, T., Ártung, U.E. (Eds.), *The NE Atlantic Region: A Reappraisal of Crustal Structure, Tectonostratigraphy and Magmatic Evolution*, vol. 447. Geological Society, London, Special Publications, pp. 171–205. <http://doi.org/10.1144/SP447.1>.
- Gaina, C., Gernigon, L., Ball, P., 2009. Palaeocene - Recent plate boundaries in the NE Atlantic and the formation of the Jan Mayen microcontinent. *J. Geol. Soc.* 166, 1–16.
- Gaina, C., Blischke, A., Geissler, W.H., Kimbell, G.S., Erlendsson, Ö., 2017a. Seamounts and oceanic igneous features in the NE Atlantic: a link between plate motions and mantle dynamics. *Special Publications*. vol. 447 Geological Society, London. <https://doi.org/10.1144/SP447.6> first published on September 8, 2016.
- Gaina, C., Nasuti, A., Kimbell, G.S., Blischke, A., 2017b. Break-up and seafloor spreading domains in the NE Atlantic. *Special Publications*. vol. 447 Geological Society, London. <https://doi.org/10.1144/SP447.12> first published on February 3, 2017.
- Gasser, D., 2014. The Caledonides of Greenland, Svalbard and other Arctic areas: status of research and open questions. *Geological Society, London, Special Publications* 390,

- 93–129 2014.
- Geissler, W.H., Gaina, C., Hopper, J.R., Funck, T., Blischke, A., Arting, U., & Horni, J., Péron-Pinvidic, G., Abdelmalak, M.M., 2017. Seismic volcanostratigraphy of the NE Greenland continental margin. In: Péron-Pinvidic, G., Hopper, J.R., Stoker, M.S., Gaina, C., Doornenbal, J.C., Funck, T., Ártung, U.E. (Eds.), *The NE Atlantic Region: A Reappraisal of Crustal Structure, Tectonostratigraphy and Magmatic Evolution*, vol. 447 Geological Society, London, Special Publications. <https://doi.org/10.1144/SP447.11>.
- Geodekyan, A.A., Verkhovskaya, Z.I., Sudyin, A.V., Trotsiuk, V.Ya., 1980. Gases in Seawater and Bottom Sediments. In: Udintsev, C.B. (Ed.), *Iceland and Mid-Oceanic Ridge – Structure of the ocean-floor*. Academy of Science of the USSR, soviet geophysical committee, results of researches on the international geophysical projects, pp. 19–36 1980.
- Gernigon, L., Gaina, C., Olesen, O., Ball, P., Peron-Pinvidic, G., Yamasaki, T., 2012. The Norway Basin revisited: From continental breakup to spreading ridge extinction. *Mar. Petrol. Geol.* 35, 1–19.
- Gernigon, L., Blischke, A., Nasuti, A., Sand, M., 2015. Conjugate volcanic rifted margins, seafloor spreading, and microcontinent: Insights from new high-resolution aeromagnetic surveys in the Norway Basin. *Tectonics* 34, 907–933.
- Goodwin, T., Cox, D., Trueman, J., 2009. Paleocene sedimentary models in the sub-basalt around the Munkagrunnur–East Faroes Ridge. *Faroe Islands Exploration Conference: Proceedings of the 2nd Conference*. Ann. Soc. Sci. Faroensis - Suppl. 50, 267–285.
- Gradstein, F.M., Ogg, J.G., Schmitz, M.D., Ogg, G.M., 2012. *The Geologic Time Scale 2012*. Elsevier, Amsterdam.
- Grimsson, F., Simonarson, L.A., 2008. Upper Tertiary non-marine environments and climatic changes in Iceland. *Jokull* 58, 303–314.
- Guarnieri, P., 2015. Pre-breakup palaeo-stress state along the East Greenland margin. *Journal of the Geological Society of London First published on August 20, 2015*.
- Gunnarsson, K., Sand, M., Gudlaugsson, S.T., 1989. Geology and Hydrocarbon Potential of the Jan Mayen Ridge. Orkustofnun. OS-98014, report. pp. 143 5 appendices incl. 9 maps Reykjavik and Norwegian Petroleum Directorate, Stavanger, OD-89-91, 156 pp.
- Haase, C., Ebbing, J., 2014. Gravity Data. In: Hopper, J.R., Funck, T., Stoker, M.S., Ártung, U., Peron-Pinvidic, G., Doornenbal, H., Gaina, C. (Eds.), *Tectonostratigraphic Atlas of the North-East Atlantic Region*. GEUS, Copenhagen, Denmark.
- Hamann, N.E., Whittaker, R.C., Stemmerik, L., 2005. Geological development of the Northeast Greenland Shelf. In: Doré, A.G., Vining, B.A. (Eds.), *Petroleum Geology: North-West Europe and Global Perspectives—Proceedings of the 6th Petroleum Geology Conference*. 887–902.
- Harðarson, B.S., Fitton, J.G., Ellam, R.M., Pringle, M.S., 1997. Rift relocation – a geochemical and geochronological investigation of a palaeo-rift in northwest Iceland. *Earth Planet. Sci. Lett.* 153, 181–196.
- Harðarson, B.S., Fitton, J.G., Hjartarson, Á., 2008. Tertiary volcanism in Iceland. *Jokull* 58, 161–178.
- Helgadóttir, G., 2008. Preliminary results from the 2008 Marine Research Institute multibeam survey in the Dreki area, with some examples of potential use. In: *Iceland Exploration Conference 2008*. Reykjavik, Iceland.
- Helgadóttir, G., Reynisson, P., 2010. Setjarnataka, fjölgeisla- og lágtíðniðýptarmælingar á Drekasvæði og Jan Mayen hrygg á rs. Árna Friðrikssyni RE 200 haustið 2010. Prepared for Orkustofnun og Norsku Olfustofnunina, Hafrannsóknastofnunin, Leiðangurskýrsla A201011, hluti 1 og 2, 17. ágúst–15. september 2010, Reykjavík, Ísland.
- Henriksen, N., 2008. Geological History of Greenland – Four billion years of Earth evolution. *Geological Survey of Denmark and Greenland (GEUS)*, pp. 272.
- Hinz, K., 1981. An hypothesis on terrestrial catastrophes wedges of very thick oceanward dipping layers beneath passive continental margins; their origin and palaeo-environmental significance. *Geologisches Jahrbuch*, E2 3–28.
- Hinz, K., Schlüter, H.U., 1978. The North Atlantic - results of geophysical investigations by the Federal Institute for Geosciences and Natural Resources on North Atlantic continental margins. *Erdöl-Erdgas-Zeitschrift* 94, 271–280.
- Hjartarson, A., Erlendsson, Ö., Blischke, A., 2017. Special Publications. The Greenland–Iceland–Faroe Ridge Complex, vol. 447 Geological Society, London. <https://doi.org/10.1144/SP447.14> first published on . Accessed date: 14 December 2016.
- Hjelstuen, B.O., Eldholm, O., Skogseid, J., 1997. Vøring Plateau diapir fields and their structural and depositional settings. *Mar. Geol.* 144 (1–3), 33–57. [https://doi.org/10.1016/s0025-3227\(97\)00085-6](https://doi.org/10.1016/s0025-3227(97)00085-6).
- Hjelstuen, B.O., Eldholm, O., Skogseid, J., 1999. Cenozoic evolution of the northern Vøring margin. *GSA Bulletin* v111 (12), 1792–1807 13 figures.
- Hopper, J.R., Dahl-Jensen, T., Holbrook, W.S., Larsen, H.C., Lizarralde, D., Korenaga, J., Kent, G.M., Kelemen, P.B., 2003. Structure of the SE Greenland margin from seismic reflection and refraction data: Implications for nascent spreading center subsidence and asym-metric crustal accretion during North Atlantic opening. *J. Geophys. Res.* 108 (B5), 2269. <https://doi.org/10.1029/2002jb001996>. 2269;Artn 2269.
- Hopper, J.R., Funck, T., Stoker, M.S., Ártung, U., Peron-Pinvidic, G., Doornenbal, H., Gaina, C. (Eds.), 2014. *Tectonostratigraphic Atlas of the North-East Atlantic Region*. Geological Survey of Denmark and Greenland, GEUS, Copenhagen, pp. 338.
- Howe, J.A., Stoker, M.S., Stow, D.A.V., 1994. Late Cenozoic sediment drift complex, northeast Rockall Trough, North Atlantic. *Palaeoceanography* 9 (6), 989–999.
- Jakobsson, M., Mayer, L.A., Coakley, B., Dowdeswell, J.A., Forbes, Fridman, S.B., Hodnesdal, H., Noormets, R., Pedersen, R., Rebesco, M., Schenke, H.-W., Zarayskaya, Y., Accetella, A.D., Armstrong, A., Anderson, R.M., Bienhoff, P., Camerlenghi, A., Church, I., Edwards, M., Gardner, J.V., Hall, J.K., Hell, B., Hestvik, O.B., Kristoffersen, Y., Marcussen, C., Mohammad, R., Mosher, D., Nghiem, S.V., Pedrosa, M.T., Travaglini, P.G., Weatherall, P., 2012. The International Bathymetric Chart of the Arctic Ocean (IBCAO) Version 3.0. *Geophys. Res. Lett.* <https://doi.org/10.1029/2012GL052219>.
- Jansen, E., Raymo, M.E., Blum, P., et al., 1996. *Proceedings of the Ocean Drilling Program*. Ocean Drilling Program, College Station, TX, U.S.A.. <https://doi.org/10.2973/odp.proc.ir.162.1996>. Initial Reports, 162.
- Japsen, P., Green, P.F., Bonowa, J.M., Nielsen, T.F.D., Chalmers, J.A., 2014. From volcanic plains to glaciated peaks: Burial, uplift and exhumation history of southern East Greenland after opening of the NE Atlantic. *Glob. Planet. Chang.* 116, 91–114. 2014. <https://doi.org/10.1016/j.gloplacha.2014.01.012>.
- Jóhannesson, H., Semundsson, K., 1998. *Geologic Map of Iceland, 1:500,000*. Bedrock Geology. Icelandic Institute of Natural History and Iceland Geodetic Survey, Reykjavik.
- Johansen, B., Eldholm, O., Talwani, M., Stoffa, P.L., Buhl, P., 1988. Expanding spread profile at the northern Jan Mayen Ridge. *Polar Res.* 6, 95–104.
- Johnson, H., Ritchie, J.D., Hitchen, K., McInroy, D.B., Kimbell, G.S., 2005. Aspects of the Cenozoic deformational history of the northeast Faroe-Shetland Basin, Wyville-Thomson Ridge and Hatton Bank areas. In: Doré, A.G., Vining, B. (Eds.), *Petroleum Geology: NW Europe and Global Perspectives: Proceedings of the 6th Conference*. The Geological Society, London, pp. 993–1007.
- Kandilarov, A., Mjelde, R., Pedersen, R.B., Hellevang, B., Papenberg, C., Petersen, C.J., Planert, L., Flueh, E., 2012. The northern boundary of the Jan Mayen microcontinent, North Atlantic determined from ocean bottom seismic, multichannel seismic, and gravity data. *Mar. Geophys. Res.* 33, 55–76.
- Kharin, G.N., 1976. The petrology of magmatic rocks. In: In: Talwani (Ed.), *Initial Reports of the Deep Sea Drilling Project*, vol. 38. Publisher: Texas A & M University, Ocean Drilling Program, College Station, TX, United States, pp. 685–715. <https://doi.org/10.2973/dsdp.proc.38.110.1976>.
- Kimbell, G.S., Stewart, M.A., Gradmann, S., Shannon, P.M., Funck, T., Haase, C., Stoker, M.S., Hoper, J.R., 2016. Special Publications. Controls on the location of compressional deformation on the NW European margin, vol. 447 Geological Society, London. <https://doi.org/10.1144/SP447.3> first published on September 8, 2016.
- Kodaira, S., Mjelde, R., Gunnarsson, K., Shiohara, H., Shimamura, H., 1998. Structure of the Jan Mayen microcontinent and implications for its evolution. *Geophys. J. Int.* 132, 383–400 Blackwell Science Ltd, 1998.
- Laberg, J.S., et al., 2005. Cenozoic alongslope processes and sedimentation on the NW European Atlantic margin. *Mar. Petrol. Geol.* 22 (9–10), 1069–1088. <https://doi.org/10.1016/j.marpetgeo.2005.01.008>.
- Lamers, E., Carmichael, S.M.M., 1999. The Paleocene deepwater sandstone play West of Shetland. In: Fleet, A.J., Boldy, S.A.R. (Eds.), *Petroleum Geology of Northwest Europe: Proceedings of the 5th Conference*. Geological Society, London, pp. 645–659.
- Larsen, H.C., 1990. The East Greenland shelf. In: Grant, A. (Ed.), *The Geology of North America, The Arctic Ocean Region*. vol. 1. Geological Society of America, pp. 185–210.
- Larsen, H.C., Saunders, A.D., 1998. Tectonism and volcanism at the southeast Greenland rifted margin: A record of plume impact and later continental rapture. *Proc. Ocean Drill. Progr. Sci. Result* 152, 503–533. Retrieved from. http://www-odp.tamu.edu/publications/152_SR/VOLUME/CHAP.41.PDF.
- Larsen, L.M., Watt, S.W., Watt, M., 1989. Geology and petrology of the Lower Tertiary plateau basalts of the Scoresby Sund region, east Greenland. *Bulletin (Grønlands geologiske undersøgelse)* 157, 164 (ill., maps, Copenhagen, Denmark).
- Larsen, L.M., Waagstein, R., Pedersen, A.K., Storey, M., 1999a. Trans-Atlantic correlation of the Palaeogene volcanic successions in the Faeroe Islands and East Greenland. *Journal of the Geophysical Society* 156 (6), 1081–1095.
- Larsen, M., Hamberg, L., Olausson, S., Preuss, T., Stemmerik, L., 1999b. Sandstone wedges of the Cretaceous-Lower Tertiary Kangerlussuaq Basin, East Greenland - outcrop analogues to the offshore North Atlantic. In: Fleet, A.J., Boldy, S.A.R. (Eds.), *Petroleum Geology of Northwest Europe: Proceedings of the 5th Conference*. ©Petroleum Geology '86 Ltd, London, pp. 337–348 Published by the Geological Society.
- Larsen, M., Piasecki, S., Stemmerik, L., 2002. The post-basaltic Palaeogene and Neogene sediments at Kap Dalton and Savoia Halvo, East Greenland. *Geology of Greenland Survey Bulletin* 191, 103–110.
- Larsen, M., Heilmann-Clausen, C., Piasecki, S., Stemmerik, L., 2005. At the edge of a new ocean: post-volcanic evolution of the Palaeogene Kap Dalton Group, East Greenland. In: Doré, A.G., Vining, B.A. (Eds.), *Petroleum Geology: North-West Europe and Global Perspectives – Proceedings of the 6th Petroleum Geology Conference*. Geological Society of London, UK, pp. 923–932. <https://doi.org/10.1144/0060923>.
- Larsen, L.M., Pedersen, A.K., Sørensen, E.V., Watt, W.S., Duncan, R.A., 2013. Stratigraphy and age of the Eocene Igtertivå Formation basalts, alkaline pebbles and sediments of the Kap Dalton Group in the graben at Kap Dalton. *East Greenland. Bull. Geol. Soc. Den.* 61, 1–18.
- Larsen, L.M., Pedersen, A.K., Tegner, T., Duncan, R.A., 2014. Eocene to Miocene igneous activity in NE Greenland: northward younging of magmatism along the East Greenland margin. *J. Geol. Soc.* 171 (4), 539–553.
- Le Breton, E., Cobbold, P.R., Zanella, A., 2013. Cenozoic reactivation of the Great Glen Fault, Scotland: additional evidence and possible causes. *J. Geol. Soc.* 170, p403–415. <https://doi.org/10.1144/jgs2012-067>.
- Lí, W., Alvesc, T.M., Wu, S., Rebesco, M., Zhaoe, F., Mi, L., Ma, B., 2016. A giant, submarine creep zone as a precursor of large-scale slope instability offshore the Dongsha Islands (South China Sea). *Earth Planet. Sci. Lett.* 451, 272–284. <https://doi.org/10.1016/j.epsl.2016.07.007>.
- Lundin, E., Doré, A.G., 2002. Mid-Cenozoic post-breakup deformation in the 'passive' margins bordering the Norwegian-Greenland Sea. *Mar. Pet. Geol.* 19, 79–93.
- Lundin, E.R., Doré, A.G., 2005. NE Atlantic breakup: a re-examination of the Iceland mantle plume model and the Atlantic-Arctic linkage. In: Doré, A.G., Vining, B.A. (Eds.), *Petroleum Geology: North-West Europe and Global Perspectives*. Proceedings of the 6th Petroleum Geology Conference, pp. 739–754.
- Lundin, E.R., Doré, A.G., Rønning, K., Kyrkjebø, R., 2013. Repeated inversion and

- collapse in the Late Cretaceous–Cenozoic northern Vøring Basin, offshore Norway. *Petrol. Geosci.* 19, 329–341. <https://doi.org/10.1144/petgeo2012-022>.
- Manum, S.B., Schrader, H.J., 1976. Sites 346, 347, and 349. In: In: Talwani, M., Udintsev, G. (Eds.), Initial Reports of the Deep Sea Drilling Project, vol. 38. U.S. Government Printing Office, Washington, pp. 521–594.
- Manum, S.B., Raschka, H., Eckhardt, F.J., 1976a. Site 350. In: Talwani, M., Udintsev, G. (Eds.), Initial Reports of the Deep Sea Drilling Project. U.S. Government Printing Office, Washington, pp. 655.
- Manum, S.B., Raschka, H., Eckhardt, F.J., Schrader, H., Talwani, M., Udintsev, G., e.a., 1976b. Site 337 Initial Reports of the Deep Sea Drilling Project. 1976 In: In: Talwani, M., Udintsev, G. (Eds.), Initial Reports of the Deep Sea Drilling Project, vol. 38. U.S. Government Printing Office, Washington, pp. 117–150 Washington (U.S. Government Printing Office).
- Mathiesen, A., Bidstrup, T., Christensen, F.G., 2000. Denudation and uplift history of the Jameson Land Basin, East Greenland-constrained from maturity and apatite fission track data. *Glob. Planet. Chang.* 24, 275–301.
- McDougall, I., Kristjánsson, L., Sæmundsson, K., 1984. Magnetostratigraphy and geochronology of northwest Iceland. *J. Geophys. Res.* 89 (NB8), 7029–7060. <https://doi.org/10.1029/JB089iB08p07029>.
- Menke, W., Brandsdóttir, B., Einarsson, P., Bjarnason, I.T., 1996. Reinterpretation of the RRISP-77 Iceland shear-wave profiles. *Geophys. J. Int.* 126 (1), 166–172. <https://doi.org/10.1111/j.1365-246X.1996.tb05275.x>.
- Miller, K.G., Browning, J.V., Aubry, M.-P., Wade, B.S., Katz, M.E., Kulpecz, A.A., Wright, J.D., 2008. Eocene–Oligocene global climate and sea-level changes: St. Stephens Quarry, Alabama. *GSA Bulletin*; January/February 2008 120 (1/2), 34–53. <https://doi.org/10.1130/B26105.1>; 9 figures.
- Mitchum, R.M., Vail, P.R., Sangree, J.B., 1977. Seismic stratigraphy and global changes of sea level, part 6: stratigraphic interpretation of seismic reflection patterns in depositional sequences. In: In: Payton, C.E. (Ed.), *Seismic Stratigraphy – Applications to Hydrocarbon Exploration*, vol. 26. American Association of Petroleum Geologists, Memoir, pp. 117–133.
- Mjelde, R., Aurvåg, R., Kodaira, S., Shimamura, H., Gunnarsson, K., Nakanishi, A., Shiobara, H., 2002. Vp/Vs-ratios from the central Kolbeinsey Ridge to the Jan Mayen Basin, North Atlantic; implications for lithology, porosity and present-day stress field. *Mar. Geophys. Res.* 23, 123–145.
- Mjelde, R., Eckhoff, I., Solbakken, S., Kodaira, S., Shimamura, H., Gunnarsson, K., Nakanishi, A., Shiobara, H., 2007. Gravity and S-wave modelling across the Jan Mayen Ridge, North Atlantic; implications for crustal lithology. *Mar. Geophys. Res.* 28, 27–41.
- Mjelde, R., Breivik, A.J., Raum, T., Mittelstaedt, E., Ito, G., Faleide, J.I., 2008. Magmatic and tectonic evolution of the North Atlantic. *J. Geol. Soc.* 165, 31–42.
- Mjelde, R., Raum, T., Kandilarov, A., Murai, Y., Takanami, T., 2009. Crustal structure and evolution of the outer More Margin, NE Atlantic. *Tectonophysics* 468, 224–243.
- Mjelde, R., Kvarven, T., Faleide, J.I., Thybo, H., 2016. Lower crustal high-velocity bodies along North Atlantic passive margins, and their link to Caledonian suture zone eclogites and Early Cenozoic magmatism. *Tectonophysics* 670, 16–29. 2016. <https://doi.org/10.1016/j.tecto.2015.11.021>.
- Mordret, A., 2018. Uncovering the Iceland hot spot track beneath Greenland. *J. Geophys. Res.: Solid Earth* 123, 4922–4941. <https://doi.org/10.1029/2017JB015104>.
- Moreno-Vásquez, J., 1995. Neogene biofacies in eastern Venezuela and their calibration with seismic data. *Mar. Micropaleontol.* 26 (1–4), 287–302.
- Morgan, R.P.L., Barton, P.J., Warner, M., Morgan, J.V., Price, C., Jones, K., 2000. Lithospheric structure north of Scotland - I. P-wave modelling, deep reflection profiles and gravity-tx. *Geophys. J. Int.* 142 (3), 716–736. <https://doi.org/10.1046/j.1365-246x.2000.00151.x>.
- Morlighem, M., et al., 2017. BedMachine v3: Complete bed topography and ocean bathymetry mapping of Greenland from multi-beam echo sounding combined with mass conservation. *Geophys. Res. Lett.* 44 <https://doi.org/10.1002/2017GL074954>. <http://onlinelibrary.wiley.com/doi/10.1002/2017GL074954/full>.
- Mudge, D.C., 2015. Regional controls on Lower Tertiary sandstone distribution in the North Sea and NE Atlantic margin basins. 2015. In: In: McKie, T., Rose, P.T.S., Hartley, A.J., Jones, D.W., Armstrong, T.L. (Eds.), *Tertiary Deep-Marine Reservoirs of the North Sea Region*, vol. 403. Geological Society, London, pp. 17–42. Special Publications. <https://doi.org/10.1144/SP403.5>.
- Murray-Wallace, C., Woodroffe, C., 2014. Pleistocene sea-level changes. In: *Quaternary Sea-Level Changes: A Global Perspective*. Cambridge University Press, Cambridge, pp. 256–319. <https://doi.org/10.1017/CBO9781139024440.007>.
- Mutter, J.C., Talwani, M., Stoffa, P.L., 1982. Origin of seaward-dipping reflectors in oceanic crust off the Norwegian margin by "subaerial sea-floor spreading". *Geology* 10, 3–12.
- Mutter, J.C., Talwani, M., Stoffa, P.L., 1984. Evidence for a Thick Oceanic Crust Adjacent to the Norwegian Margin. *J. Geophys. Res.* 89 (B1), 483–502.
- Nasuti, A., Olesen, O., 2014. Magnetic Data. In: Hopper, J.R., Funck, T., Stoker, M.S., Ártung, U., Peron-Pinvidic, G., Doornenbal, H., Gaina, C. (Eds.), *Tectonostratigraphic Atlas of the North-East Atlantic Region*. GEUS, Copenhagen, Denmark.
- Nielsen, T., van Weering, T.C.E., 1998. Seismic stratigraphy and sedimentary processes at the Norwegian Sea margin northeast of the Faroe Islands. *Mar. Geol.* 152, 141–157.
- Nilsen, T.H., Kerr, D.R., Talwani, M., Udintsev, G. e.a. (Eds.), 1978. Turbidites, red beds, sedimentary structures, and trace fossils observed in DSDP Leg 38 cores and the sedimentary history of the Norwegian-Greenland Sea Initial Reports of the Deep Sea Drilling Project, vol. 38. U.S. Government Printing Office, Washington, pp. 259–288 Supplement to Volume.
- Nøhr-Hansen, H., 2003. Dinoflagellate cyst stratigraphy of the Palaeogene strata from the wells Hellefisk-1, Ikermiut-1, Kangamiut-1, Nukik-1, Nukik-2 and Qulleq-1, offshore West Greenland. *Mar. Petrol. Geol.* 20, 987–1016.
- Nøhr-Hansen, H., 2012. Palynostratigraphy of the Cretaceous–Lower Palaeogene sedimentary succession in the Kangerlussuaq Basin, southern East Greenland. *Rev. Palaeobot. Palynol.* 178, 59–90.
- Nøhr-Hansen, H., Piasecki, S., 2002. Paleocene sub-basaltic sediments on Savoia Halvo, East Greenland. *Geology of Greenland Survey Bulletin* 191, 111–116.
- Norwegian Petroleum Directorate, 2012. Submarine fieldwork on the Jan Mayen Ridge: integrated seismic and ROV-sampling. Norwegian Petroleum Directorate, Stavanger, Norway. <http://www.npd.no/en/Publications/Resource-Reports/2013/Chapter-7/>.
- Norwegian Petroleum Directorate, 2013. The Petroleum Resources on the Norwegian Continental Shelf. Norwegian Petroleum Directorate, Stavanger, Norway, pp. 63. <http://www.npd.no/en/Publications/Resource-Reports/2013/>.
- Nunns, A., 1983a. The structure and evolution of the Jan Mayen Ridge and surroundings regions. In: Watkins, J.S., Drake, C.L. (Eds.), *Studies in Continental Margin Geology*. American Association of Petroleum Geologists, memoir, pp. 193–208.
- Nunns, A.G., 1983c. Plate tectonic evolution of the Greenland-Scotland Ridge and surrounding regions. In: Bott, M.H.P., Saxov, S., Talwani, M., Thiede, J. (Eds.), *Structure and Development of the Greenland-Scotland Ridge*. Plenum, New York, New York, pp. 11–30.
- Nunns, A.G., Talwani, M., Lorentzen, G.N., Vogt, P.R., Sigurgeirsson, T., Kristjánsson, L., Larsen, H.C., Voppel, D., 1983. Magnetic anomalies over Iceland and surrounding seas. In: Bott, M.H.P., Saxov, S., Talwani, M., Thiede, J. (Eds.), *Structure and Development of the Greenland-Scotland Ridge*. Plenum, New York, pp. 661–678.
- Olafsson, I., Gunnarsson, K., 1989. The Jan Mayen ridge: velocity structure from analysis of sonobuoy data. *Orkustofnun, Reykjavík*. pp. 62 OS-89030/JHD-04.
- Ólavsdóttir, J., Stoker, M.S., Boldreel, L.O., Andersen, M.S., and Eidesgaard, O.R. (In preparation). The age of the Faroe Islands Basalt Group, Faroe-Shetland region, Northeast Atlantic Ocean.
- Ólavsdóttir, J., Boldreel, L.O., Andersen, M.S., 2010. Development of a shelf-margin delta due to uplift of Munkagrúnnut Ridge at the margin of Faroe-Shetland Basin: a seismic sequence stratigraphic study. *Petrol. Geosci.* 16, 91–103.
- Ólavsdóttir, J., Andersen, M.S., Boldreel, L.O., 2013. Seismic stratigraphic analysis of the Cenozoic sediments in the NW Faroe Shetland Basin e implications for inherited structural control of sediment distribution. *Mar. Petrol. Geol.* 46, 19–35. <https://doi.org/10.1016/j.marpetgeo.2013.05.012>.
- Ólavsdóttir, J., Eidesgaard, Ó.R., Stoker, M.S., 2017. The stratigraphy and structure of the Faeroese continental margin. In: In: Péron-Pinvidic, G., Hopper, J.R., Stoker, M.S., Gaina, C., Doornenbal, J.C., Funck, T., Ártung, U.E. (Eds.), *The NE Atlantic Region: A Reappraisal of Crustal Structure, Tectonostratigraphy and Magmatic Evolution*, vol. 447. Geological Society, London, pp. 339–356 Special Publications.
- Osmundsen, P.T., Andersen, T.B., 2001. The middle Devonian basins of western Norway: sedimentary response to large-scale transtensional tectonics. *Tectonophysics* 332 (1–2), 51–68.
- Osmundsen, P.T., Ebbing, J., 2008. Styles of extension offshore mid-Norway and implications for mechanisms of crustal thinning at passive margins. *Tectonics* 27 (6), TC6016.
- Ottesen, D., Rise, L., Andersen, E.S., Bugge, T., Eidvin, T., 2009. Geological evolution of the Norwegian continental shelf between 61 degrees N and 68 degrees N during the last 3 million years. *Norw. J. Geol.* 89 (4), 251–265.
- Owen, D.E., 1987. Commentary: usage of stratigraphic terminology in papers, illustrations and talks. *J. Sediment. Petrol.* 57, 363–372.
- Pálmason, G., 1980. A continuum model of crustal generation in Iceland: Kinematic aspects. *J. Geophys.* 47, 7–18.
- Pálmason, G., 1986. Model of crustal formation in Iceland, and application to submarine midoceanic ridges. In: Vogt, P.R., Tucholke, B.E. (Eds.), *The western Atlantic region*. Geological Society of America, *Geology of North America*, v. M, Boulder, Colorado, pp. 87–97.
- Parkin, C.J., White, R.S., 2008. Influence of the Iceland mantle plume on oceanic crust generation in the North Atlantic. *Geophys. J. Int.* 173 (1), 168–188. <https://doi.org/10.1111/j.1365-246X.2007.03689.x>.
- Parnell-Turner, R., White, N., Henstock, T., Murton, Murton, B.B., MacLennan, J., Jones, S.M., 2014. A continuous 55-million-year record of transient mantle plume activity beneath Iceland. *Nat. Geosci.* 7, 914–919. <https://doi.org/10.1038/ngeo2281>.
- Parsons, A.J., Whitham, A.G., Kelly, S.R.A., Vautravers, B.P.H., Dalton, T.J.S., Andrews, S.D., Pickles, C.S., Strogon, D.P., Braham, W., Jolley, D.W., Gregory, F.J., 2017. Structural evolution and basin architecture of the Traill Ø region, NE Greenland: A record of polyphase rifting of the East Greenland continental margin. *Geosphere* 13 (3), 1–38. <https://doi.org/10.1130/GES01382.1>.
- Passéy, S.R., 2009. Recognition of a faulted basalt lava flow sequence through the correlation of stratigraphic marker units, Skopunarfjørður, Faroe Islands. In: Varming, T., Ziska, H. (Eds.), *Faroe Islands Exploration Conference: Proceedings of the 2nd Conference*. Annales Societatis Scientiarum Færoensis, Tórshavn, pp. 174–204.
- Passéy, S.R., Bell, B.R., 2007. Morphologies and emplacement mechanisms of the lava flows of the Faroe Islands basalt group, Faroe Islands, NE Atlantic ocean. *Bull. Volcanol.* 70, 139–156. <https://doi.org/10.1007/s00445-007-0125-6>.
- Passéy, S.R., Hitchen, K., 2011. Cenozoic (igneous). In: Ritchie, J.D., Ziska, H., Johnson, H., Evans, D. (Eds.), *Geology of the Faroe-Shetland Basin and Adjacent Areas*. BGS Research Report, RR/11/01, Jarðfeingi Research Report, pp. 209–228 RR/11/01.
- Passéy, S.R., Jolley, D.W., 2009. A revised lithostratigraphic nomenclature for the Palaeogene Faroe Islands Basalt Group, NE Atlantic Ocean. *Earth and Environmental Science Transactions of the Royal Society of Edinburgh* 99, 127–158.
- Payros, A., Ortiz, S., Millán, I., Arostegi, J., Orue-Etxebarria, X., Apellaniz, E., 2015. Early Eocene climatic optimum: Environmental impact on the North Iberian continental margin. *GSA Bulletin* 127 (11–12), 1632–1644. <https://doi.org/10.1130/B31278.1>.
- Pedersen, A.K., Watt, M., Watt, W.S., Larsen, L.M., 1997. Structure and stratigraphy of the Early Tertiary basalts of the Bløseville Kyst, East Greenland. vol. 154. *Journal of the Geological Society, London*, pp. 565–570 7 fig.
- Peron-Pinvidic, G., Gernigon, L., Gaina, C., Ball, P., 2012a. Insights from the Jan Mayen

- system in the Norwegian-Greenland Sea - I: mapping of a microcontinent. *Geophys. J. Int.* 191, 385–412.
- Peron-Pinvidic, G., Gernigon, L., Gaina, C., Ball, P., 2012b. Insights from the Jan Mayen system in the Norwegian-Greenland Sea - II: architecture of a microcontinent. *Geophys. J. Int.* 191, 413–435.
- Peron-Pinvidic, G., Manatschal, G., Osmundsen, P.T., 2013. Structural comparison of archetypal Atlantic rifted margins: A review of observations and concepts. *Mar. Petrol. Geol.* 43 (0), 21–47.
- Planke, S., Eldholm, O., 1994. Seismic response and construction of seaward dipping wedges of flood basalts: Voring volcanic margin. *J. Geophys. Res.* 99 (B5), 9263–9278. <https://doi.org/10.1029/94JB00468>.
- Planke, S., Symonds, P.A., Alvestad, E., Skogseid, J., 2000. Seismic volcanostratigraphy of large-volume basaltic extrusive complexes on rifted margins. *J. Geophys. Res.* 105 (B8), 19335–19351. <https://doi.org/10.1029/1999JB900005>.
- Polteau, S., Mazzini, A., Trulsvik, M., Planke, S., 2012. JMRS11 – Jan Mayen Ridge Sampling Survey 2011. VBPR-TGS, Commercial report. February 2012.
- Polteau, S., Mazzini, A., Jerram, D.A., Millett, J., Planke, S., Abdelmalak, M.A., Hansen, G., Blischke, A., Mykklebus, R., 2018. The pre-breakup stratigraphy and petroleum system of the Southern Jan Mayen Ridge revealed by seafloor sampling. *Tectonophysics*. <https://doi.org/10.1016/j.tecto.2018.04.016>.
- Praeg, D., Stoker, M.S., Shannon, P.M., Ceramicola, S., Hjelstuen, B., Laberg, J.S., Mathiesen, A., 2005. Episodic Cenozoic tectonism and the development of the NW European "passive" continental margin. *Mar. Petrol. Geol.* 22 (9–10), 1007–1030. <https://doi.org/10.1016/j.marpetgeo.2005.03.014>.
- Pringle, M.S., Hardarson, B.S., Kristjánsson, L., Johannesson, H., 1997. Decrease in crustal production rate from established and dying rift: examples from western Iceland. *Eos* 78, 656.
- Raschka, H., Eckhardt, F.J., Manum, S.B., 1976. Site 348. In: Talwani, M., Udintsev, G. (Eds.), *Initial Reports of the Deep Sea Drilling Project*. U.S. Government Printing Office, Washington, pp. 595–654.
- Rasmussen, J., Noe-Nygaard, A., 1969. Beskrivelse til Geologisk Kort over Færøerne i målestok 1:50.000. C. A. Reitzels Forlag (Jørgen Sandal). (København).
- Rasmussen, J., Noe-Nygaard, A., 1970. Geology of the Faroe Islands (Pre-Quaternary). Geological Survey of Denmark, Copenhagen Trans: Henderson G 1/25.
- Raum, T., Mjelde, R., Digranes, P., Shimamura, H., Shiobara, H., Kodaira, S., Haatvedt, G., Sørensen, N., Thorbjørnsen, T., 2002. Crustal structure of the southern part of the Voring Basin, mid-Norway margin, from wide-angle seismic and gravity data. *Tectonophysics* 355 (1–4), 99–126. [https://doi.org/10.1016/s0040-1951\(02\)00136-1](https://doi.org/10.1016/s0040-1951(02)00136-1).
- Rey, S.S., Eldholm, O., Planke, S., 2003. Formation of the Jan Mayen Microcontinent, the Norwegian Sea. *Eos Trans. AGU* 84 Abstract T31D-0872.
- Rise, L., Ottesen, D., Berg, K., Lundin, E., 2005. Large-scale development of the mid-Norwegian margin during the last 3 million years. *Mar. Petrol. Geol.* 22 (1–2), 33–44. <https://doi.org/10.1016/j.marpetgeo.2004.10.010>.
- Rise, L., Chand, S., Hjelstuen, B.O., Hafliadason, H., Boe, R., 2010. Late Cenozoic geological development of the south Voring margin, mid-Norway. *Mar. Petrol. Geol.* 27 (9), 1789–1803.
- Ritchie, J.D., Johnson, H.D., Quinn, M.F., Gatiliff, R.W., 2008. Cenozoic compressional deformation within the Faroe-Shetland Basin and adjacent areas. In: In: Johnson, H.D., Doré, A.G., Holdsworth, R.E., Gatiliff, R.W., Lundin, E.R., Ritchie, J.D. (Eds.), *The Nature and Origin of Compression in Passive Margins*, vol. 306. Geological Society, London, pp. 121–136 Special Publications.
- Ritchie, D.K., Ziska, H., Johnson, H., Evans, D., 2011. Geology of the Faroe-Shetland Basin and adjacent areas. Rep. British Geological Survey Research Report, pp. 317 RR/11/01, Jarðfeingi Research Report, RR/11/01.
- Roberts, A.M., Corfield, R.I., Kusznir, N.J., Matthews, S.J., Hansen, E.K., Hooper, R.J., 2009. Mapping palaeostructure and palaeobathymetry along the Norwegian Atlantic continental margin: More and Voring basins. *Petrol. Geosci.* 15 2009, 27–43. <https://doi.org/10.1144/1354-079309-804>.
- Rogozhina, I., Petrunin, A.G., Vaughan, A.P.M., Steinberger, B., Johnson, J.V., Kaban, M.K., Calov, R., Rickers, F., Thomas, M., Koulakov, I., 2016. Melting at the base of the Greenland ice sheet explained by Iceland hotspot history. *Nat. Geosci.* 9 (5), 366–369. <https://doi.org/10.1038/ngeo2689>.
- Rotevatn, A., Kristensen, T.B., Ksienzyk, A.K., Wemmer, K., Henstra, G.A., Midtkandal, I., Grundvåg, S.-A., Andresen, A., 2018. Structural inheritance and rapid rift-length establishment in a multiphase rift: The East Greenland rift system and its Caledonian orogenic ancestry. *Tectonics* 37, 1858–1875. <https://doi.org/10.1029/2018TC005018>.
- Sandstå, N.R., Pedersen, R.B., Williams, R.D., Bering, D., Magnus, C., Sand, M., Brekke, H., 2012. Submarine fieldwork on the Jan Mayen Ridge; integrated seismic and ROV-sampling. Norwegian Petroleum Directorate. <http://www.npd.no/>.
- Sandstå, N.R., Sand, M., Brekke, H., 2013. Ressursrapporter 2013, Kapittel-7 Jan Mayen. Norwegian Petroleum Directorate, project web publication, Stavanger, Norway.
- Saunders, A.D., Fitton, J.G., Kerr, A.C., Norry, M.J., Kent, R.W., 2013. The North Atlantic Igneous Province. *Geophys. Res. Lett.* 40, 45–93. <https://doi.org/10.1029/GM100p0045>.
- Schiffer, C., Peace, A., Phethean, J., Gernigon, L., McCaffrey, K., Petersen, K.D., Foulger, G., 2018. The Jan Mayen Microplate Complex and the Wilson Cycle. Geological Society, London. <https://doi.org/10.1144/SP470.2> Special Publications.
- Schilling, 1976. Shipboard Scientific Party, 1996. Site 985. In: In: Jansen, E., Raymo, M.E., Blum, P. (Eds.), *Proc. ODP, Init. Repts.*, vol. 162. Ocean Drilling Program, College Station, TX, pp. 253–285. <https://doi.org/10.2973/odp.proc.ir.162.108.1996>.
- Schrader, H.J., Bjørklund, K., Manum, S., Martini, E., van Hinte, J., 1976. Cenozoic Biostratigraphy, Physical Stratigraphy and Paleooceanography in the Norwegian-Greenland Sea, DSDP Leg 38 Paleontological Synthesis. In: *Initial Reports of the Deep Sea Drilling Project*, vol. 38. Publisher: Texas A & M University, Ocean Drilling Program, College Station, TX, United States, pp. 1197–1211. <https://doi.org/10.2973/dsdp.proc.38.133.1976>.
- Scott, R.A., Ramsey, L.A., Jones, S.M., Sinclair, S., Pickles, C.S., 2005. Development of the Jan Mayen microcontinent by linked propagation and retreat of spreading ridges. In: Wandås, B.T.G., Nystuen, J.P., Eide, E., Gradstein, F. (Eds.), *Onshore-Offshore Relationships on the North Atlantic Margin*. Norwegian Petroleum Society, pp. 69–82.
- Shillington, D.J., Seeber, L., Sorlien, C.C., Steckler, M.S., Kurt, H., Dondurur, D., Çiğci, G., Imren, G.C., Cormier, M.-H., McHugh, C.M.G., Gürçay, S., Poyraz, D., Okay, S., Atgun, O., Diebold, J.B., 2012. Evidence for widespread creep on the flanks of the Sea of Marmara transform basin from marine geophysical data. *Geology* 40 (5), 439–442. <https://doi.org/10.1130/G32652.1>.
- Simonarson, L.A., Eiriksson, J., 2008. Tjornes - Pliocene and Pleistocene sediments and faunas. *Jökull* 58, 331–342.
- Skogseid, J., Planke, S., Faleide, J.I., Pedersen, T., Eldholm, O., Neverdal, F., 2000. NE Atlantic continental rifting and volcanic margin formation. Geological Society, London, Special Publications 167 (1), 295–326. <https://doi.org/10.1144/GSL.SP.2000.167.01.12>.
- Smallwood, J.R., Towns, M.J., White, R.S., 2001. The structure of the Faeroe-Shetland Trough from integrated deep seismic and potential field modelling. *J. Geol. Soc.* 158 (3), 409–412. <https://doi.org/10.1144/jgs.158.3.409>.
- Soper, N.J., Higgins, A.C., Downie, C., Matthews, D.W., Brown, P.E., 1976. Late Cretaceous-early Tertiary stratigraphy of the Kangerdlugssuaq area, east Greenland, and the age of opening of the north-east Atlantic. *J. Geol. Soc.* 132, 85–104 London.
- Staples, R.K., White, R.S., Brandsdóttir, B., Menke, W.P., Maguire, K.H., McBride, J.H., 1997. Faroe-Iceland Ridge Experiment 1. Crustal structure of northeastern Iceland. *J. Geophys. Res.* 102 (B4), 7849–7866. <https://doi.org/10.1029/96JB03911>.
- Stärz, M., Jokat, W., Knorr, G., Lohmann, G., 2017. Threshold in North Atlantic-Arctic Ocean circulation controlled by the subsidence of the Greenland-Scotland Ridge. *Nat. Commun.* 8, 15681.
- Stoker, M.S., Varming, T., 2011. Cenozoic (sedimentary). In: Ritchie, J.D., Ziska, H., Johnson, H., Evans, D. (Eds.), *Geology of the Faroe-Shetland Basin and Adjacent Areas*. BGS Research Report, RR/11/01, Jarðfeingi Research Report, pp. 151–208 RR/11/01.
- Stoker, M.S., Praeg, D., Shannon, P.M., Hjelstuen, B.O., Laberg, J.S., Nielsen, T., van Weering, T.C.E., Sejrup, H.P., Evans, D., 2005a. Neogene evolution of the Atlantic continental margin of NW Europe (Lofoten Islands to SE Ireland): anything but passive. In: In: Doré, A.G., Vining, B.A. (Eds.), *Petroleum Geology: North-West Europe and Global Perspectives*. Proceedings of the 6th Petroleum Geology Conference, vol. 6. Geological Society, London, pp. 1057–1076.
- Stoker, M.S., Hoult, R.J., Nielsen, T., Hjelstuen, J.S., Laberg, J.S., Shannon, P.M., Praeg, D., Mathiesen, A., van Weering, T.C.E., McDonnell, A.M., 2005b. Sedimentary and oceanographic responses to early Neogene compression on the NW European margin. *Mar. Petrol. Geol.* 22, 1031–1044.
- Stoker, M.S., Praeg, D., Hjelstuen, J.S., Laberg, J.S., Nielsen, T., Shannon, P.M., 2005c. Neogene stratigraphy and the sedimentary and oceanographic development of the NW European Atlantic margin. *Mar. Petrol. Geol.* 22, 977–1005.
- Stoker, M.S., Leslie, A.B., Smith, K., 2013. A record of Eocene (Stromsøy Group) sedimentation in BGS borehole 99/3, offshore NW Britain: Implications for early post-break-up development of the Faroe-Shetland Basin. *Scott. J. Geol.* 49 (2), 133–148. <https://doi.org/10.1144/sjg2013-001>.
- Stoker, M.S., Holford, S.P., Hillis, R.R., 2018. A rift-to-drift record of vertical crustal motions in the Faroe-Shetland Basin, NW European margin: establishing constraints on NE Atlantic evolution. *J. Geol. Soc.* 175, 263–274. <https://doi.org/10.1144/jgs2017-076>.
- Storey, M., Pedersen, A.K., Stecher, O., Bernstein, S., Larsen, H.C., Larsen, L.M., Baker, J.A., Duncan, R.A., 2004. Long-lived postbreakup magmatism along the East Greenland margin; evidence for shallow-mantle metasomatism by the Iceland Plume. *Geology* 32 (2), 173–176. <https://doi.org/10.1130/g19889.1>.
- Storey, M., Duncan, R.A., Tegner, C., 2007. Timing and duration of volcanism in the North Atlantic Igneous Province: Implications for geodynamics and links to the Iceland hotspot. *Chem. Geol.* 241, 264–281.
- Stow, D.A.V., Pudsey, C.J., Howe, J.A., Faugères, J.-C., Viana, A.R., 2002. Bottom currents, contourites and deep-sea sediment drifts: current state-of-the-art. In: In: Stow, D.A.V., Faugères, J.-C., Howe, J.A., Pudsey, C.J., Viana, A.R. (Eds.), *Deep-Water Contourite Systems: Modern Drifts and Ancient Series, Seismic and Sedimentary Characteristics*, vol. 22. Geological Society, London, Memoirs, pp. 7–20.
- Surlyk, F., Callomon, J.H., Bromley, R.G., Birkelund, T., 1973. Stratigraphy of the Lower Jurassic – Lower Cretaceous sediments of Jameson Land and Scoresby Land, East Greenland. *Bull. - Grøn. Geol. Undersøgelse* 105, 76.
- Svelling, W., Pedersen, R., 2003. Jan Mayen: A result of ridge-transform-micro-continent interaction. *Geophys. Res. Abstr.* 5, 12993.
- Sylvester, A., 1975. History and surveillance of volcanic activity on Jan Mayen island. *Bull. Volcanol.* 39, 313–335.
- Sylvester, A.G., 1978. Petrography of volcanic ashes in deep-sea cores near Jan-Mayen island: sites. In: paper presented at Initial Reports of the Deep Sea Drilling Project, vol. 338. U.S. Government Printing Office, Washington, pp. 345–350 dsdp leg 38.
- Sæmundsson, K., 1979. Outline of the geology of Iceland. *Jökull* 29, 7–28.
- Sæmundsson, K., Kristjánsson, L., McDougall, I., Watkins, N.D., 1980. K-Ar dating, geological and paleomagnetic study of a 5-km lava succession in Northern Iceland. *J. Geophys. Res.* 85, 3628–3646. <https://doi.org/10.1029/JB085IB07p03628>.
- Talwani, M., Eldholm, O., 1977. Evolution of the Norwegian-Greenland Sea. vol. 88. Geological Society of America Bulletin, pp. 969–999.
- Talwani, M., Udintsev, G., White, S.M., 1976a. Introduction and explanatory notes, Leg 38, Deep Sea Drilling Project. In: In: Talwani, M., Udintsev, G. (Eds.), *Initial Reports of the Deep Sea Drilling Project*, vol. 38. U.S. Government Printing Office,

- Washington, pp. 3–19.
- Talwani, M., Udintsev, G., Shirshov, P.R., 1976b. Tectonic synthesis. In: In: Talwani, M., Udintsev, G. (Eds.), *Initial Reports of the Deep Sea Drilling Project*, vol. 38. U.S. Government Printing Office, Washington, pp. 1213–1242.
- Talwani, M., Udintsev, G.B., Bjoerklund, K., Caston, V.N.D., Faas, R.W., van Hinte, J.E., Kharin, G.N., Morris, D.A., Mueller, C., Nilsen, T.H., Warnke, D.A., White, S.M., Manum, S.B., Schrader, H.-J., 1976c. *Initial Reports of the Deep Sea Drilling Project*, vol. 38. Publisher: Texas A & M University, Ocean Drilling Program, College Station, TX, United States, pp. 521–594. <https://doi.org/10.2973/dsdp.proc.38.107.1976>. ISSN: 0080-8334 CODEN: IDSDA6.
- Talwani, M., Udintsev, G.B., Bjoerklund, K., Caston, V.N.D., Faas, R.W., van Hinte, J.E., Kharin, G.N., Morris, D.A., Mueller, C., Nilsen, T.H., Warnke, D.A., White, S.M., Manum, S.B., Schrader, H.-J., 1976d. *Initial Reports of the Deep Sea Drilling Project*, vol. 38. Publisher: Texas A & M University, Ocean Drilling Program, College Station, TX, United States, pp. 655–682. <https://doi.org/10.2973/dsdp.proc.38.109.1976>. ISSN: 0080-8334 CODEN: IDSDA6.
- Talwani, M., Udintsev, G.B., Bjoerklund, K., Caston, V.N.D., Faas, R.W., van Hinte, J.E., Kharin, G.N., Morris, D.A., Mueller, C., Nilsen, T.H., Warnke, D.A., White, S.M., Manum, S.B., Schrader, H.-J., 1976e. *Initial Reports of the Deep Sea Drilling Project*, vol. 38. Publisher: Texas A & M University, Ocean Drilling Program, College Station, TX, United States, pp. 595–654. <https://doi.org/10.2973/dsdp.proc.38.108.1976>. ISSN: 0080-8334 CODEN: IDSDA6.
- Talwani, M., Mutter, J., Eldholm, O., 1981. The Initiation of Opening of the Norwegian Sea. *Oceanologica Acta* SP 23–30.
- Tegner, C., Brooks, C.K., Duncan, R.A., Heister, L.E., Bernstein, S., 2008. ^{40}Ar – ^{39}Ar ages of intrusions in East Greenland: Rift-to-drift transition over the Iceland hotspot. *Lithos* 101, 480–500.
- Theissen-Krah, S., Zastrozhnov, D., Abdelmalak, M.M., Schmid, D.W., Faleide, J.I., Gernignone, L., 2017. Tectonic evolution and extension at the Møre Margin – Offshore mid-Norway. *Tectonophysics* 721, 227–238. <https://doi.org/10.1016/j.tecto.2017.09.009>.
- Thiede, J., Firth, J.V. (Eds.), 1995. Site 907 Proceedings of the Ocean Drilling Program, vol. 151. Ocean Drilling Program, College Station, TX, pp. 57–111 Initial Reports.
- Thordarson, T., Höskuldsson, Á., 2008. Postglacial volcanism in Iceland. *Jokull* 58, 197–228.
- Torsvik, T.H., Amundsen, H.E.F., Trønnes, R.G., Doubrovine, P.V., Gaina, C., Kuszniir, N.J., Steinberger, B., Corfú, F., Ashwal, L.D., Griffin, W.L., Werner, S.C., Jamtveit, B., 2015. Continental crust beneath southeast Iceland. *Proc. Natl. Acad. Sci. Unit. States Am.* 112, 1818–1827.
- Tripati, A., Darby, D., 2018. Evidence for ephemeral middle Eocene to early Oligocene Greenland glacial ice and pan-Arctic sea ice. *Article number: 1038. Nat. Commun.* 9, 2041. <https://doi.org/10.1038/s41467-018-03180-5>. 1723. <https://doi.org/10.1038/s41467-018-03180-5>.
- Tuitt, A., Underhill, J.R., Ritchie, J.D., Johnson, H., Hitchen, K., 2010. In: *Timing, controls and consequences of compression in the Rockall-Faroe area of the NE Atlantic Margin*, vol. 7. pp. 963–977.
- Upton, B.G.J., Emeleus, C.H., Rex, D.C., Thirlwall, M.F., 1995. Early Tertiary magmatism in NE Greenland. *J. Geol. Soc.* 152 (6), 959–964. <https://doi.org/10.1144/gsl.jgs.1995.152.01.13>. London.
- Vail, P.R., 1987. Seismic Stratigraphy Interpretation Using Sequence Stratigraphy: Part 1: Seismic Stratigraphy Interpretation Procedure. *Atlas of Seismic Stratigraphy In: In: Bally, A.W. (Ed.), AAPG Studies in Geology #27*, vol. 1. pp. 1–10 1987.
- Van Sickle, W.A., Kominz, M.A., Miller, K.G., Browning, J.V., 2004. Late Cretaceous and Cenozoic sea-level estimates: backstripping analysis of borehole data, onshore New Jersey. *Basin Res.* 16, 451–465.
- Vogt, P.R., 1986. Magnetic anomalies of the North Atlantic Ocean. In: Vogt, P.R., Tucholke, B.E. (Eds.), *The Western North Atlantic Region*. Geological Society of America.
- Vogt, P.R., Anderson, C.N., Bracey, D.R., Schneider, E.M., 1970. North Atlantic Magnetic Smooth Zones. *J. Geophys. Res.* 75, 3955–3968.
- Walker, G.P.L., 1964. Geological investigations in eastern Iceland. *Bull. Volcanol* 27, 351–363.
- Weigel, W., Flüh, E., Miller, H., Butzke, A., Deghani, A., Gebhardt, V., Harder, I., Hepper, J., Jokat, W., Kläschen, D., Schübler, S., Zhao-Groekart, Z., 1995. Investigations of the East Greenland continental margin between 70° and 72° N by deep seismic sounding and gravity studies. *Mar. Geophys. Res.* 17 (2), 167–199. <https://doi.org/10.1007/bf01203425>.
- White, R.S., Smith, L.K., 2009. Crustal structure of the Hatton and the conjugate east Greenland rifted volcanic continental margins, NE Atlantic. *J. Geophys. Res. Solid Earth* 114, B02305. <https://doi.org/10.1029/2008jb005856>.
- Zastrozhnov, D., Gernignone, L., Gogin, I., Abdelmalak, M.M., Planke, S., Faleide, J.I., Eide, S., Myklebust, R., 2018. Cretaceous-Paleocene Evolution and Crustal Structure of the Northern Vøring Margin (Offshore Mid-Norway): Results from Integrated Geological and Geophysical Study. *Tectonics* 37. <https://doi.org/10.1002/2017TC004655>.

Paper III

Seismic volcanostratigraphic characteristics of the Jan Mayen microcontinent and Iceland Plateau Rift system

Blischke, A., Brandsdóttir, B., Stoker, M. S., Gaina, C., Erlendsson, Ö., Tegner, C., Halldórsson, S. A., Helgadóttir, H. M., Gautason, B., Planke, S. and Hopper, J. R
(in preparation)

Geochemistry, Geophysics, Geosystems, Wiley AGU publications

Copyright © The Authors 2020

Seismic volcanostratigraphic characteristics of the Jan Mayen microcontinent and Iceland Plateau Rift system

Anett Blischke^{1,2}, Bryndís Brandsdóttir¹, Martyn S. Stoker³, Carmen Gaina⁴, Ögmundur Erlendsson⁵, Christian Tegner⁶, Sæmundur A. Halldórsson¹, Helga M. Helgadóttir⁵, Bjarni Gautason², Sverre Planke^{7,4} & John R. Hopper⁸

- 1 Institute of Earth Sciences, Science Institute, University of Iceland, Askja, Sturlugata 7, 101 Reykjavík, Iceland
- 2 Iceland GeoSurvey, Branch at Akureyri, Rangárvöllum, 603 Akureyri, Iceland
- 3 Australian School of Petroleum and Energy Resources, University of Adelaide, Adelaide, South Australia 5005, Australia
- 4 Centre for Earth Evolution and Dynamics (CEED), University of Oslo, Box 1048, Blindern, 0316 Oslo, Norway
- 5 Iceland GeoSurvey, Grensásvegi 9, 108 Reykjavík, Iceland
- 6 Department of Geoscience - Earth System Petrology, Aarhus University, Høegh-Guldbergs Gade 2, 8000 Aarhus C, Denmark.
- 7 Volcanic Basin Petroleum Research AS, Oslo Science Park, 0349 Oslo, Norway
- 8 Geological Survey of Denmark and Greenland (GEUS), Øster Voldgade 10, DK1350 Copenhagen K, Denmark.

Corresponding author: **Anett Blischke** (anb@isor.is)

Key words: Dual-breakup igneous complex, kinematic model, Iceland plateau rift, Jan Mayen microcontinent, SDRs, volcanic seismic-stratigraphy

Key points:

- Detailed description of tectono-magmatic dual-breakup processes that created the Jan Mayen microcontinent.
- Firm link of the Iceland Plateau axial rift systems propagating into the Blossville Kyst in age, geochemistry and tectono-magmatic processes.
- Explains the nature of the fan-shaped southern ridge complex as the interlink to the propagating Iceland Plateau Rift domain.
- Proposes relationship of pre-breakup structural settings of main fracture zones to mantle anomaly locations that govern rift relocations and overlapping rift systems.

Abstract

Tectono-magmatic reconstruction of the Jan Mayen microcontinent (JMMC) and Iceland Plateau Rift (IPR) during the Northeast Atlantic region's dual-breakup process has been established by tectonic-kinematic modelling. Utilizing structural, volcano-stratigraphic and igneous-province-mapping that were based on vintage and new geological, geophysical, and geochemical datasets (1960s – 2017). A propagating rift system that developed from Eocene to Early Miocene through seven distinct tectono-magmatic phases, interlinking the microcontinent to its surrounding igneous provinces within the Northeast Atlantic setting, specifically to the Greenland-Iceland-Faroe ridge complex (GIFRC) tectono-magmatic anomalous region, and prior to Iceland's subaerial formation. Primary findings are evidence for non-uniform formation of tectono-magmatic rifted margins, with a clear north-south asymmetry to seaward dipping reflector formation along the eastern JMMC breakup margin and the Ægir rift system that formed preferentially linked to variations in the pre-rift lithospheric structure and very likely above a thermal mantle anomaly. Defining the formation of a second complex breakup margin along the JMMC southwestern to western flank during Late Oligocene to Early Miocene accompanied by emplacement of igneous complexes, and full opening of the JMB as a pull-apart basin and igneous domain accompanied by substantial dyke and sill intrusive activities, as part of a buried western Late Oligocene igneous breakup margin. Here reflected by the regionally extensive flood basalts during the final breakup phase and buried seaward-dipping formations and direct conjugate to the central East Greenland shelf margin. Furthermore, by establishing a firm linkage between the oblique IPR system and the Blossville Kyst igneous province regarding their timing and geochemistry data, as a propagating rift linked into the GIFRC. Thus, providing a reasonable explanation for the initiation of the fanned-out appearance of the oblique IPR rifting domain that interfingers with the JMMC's southern ridges due to deep crustal breaches and melt incursions that form several axial rift systems and volcanic ridges.

1 Introduction

This project is the final stage of a doctoral research project that combines the established structural and tectonic framework of the Jan Mayen microcontinent (JMMC) [Blischke *et al.*, 2017a] with a firm tectonostratigraphic framework, tying it into the Iceland plateau rift (IPR) [Blischke *et al.*, 2019], to observed and mapped tectono-magmatic features and processes. Aiming to provide a comprehensive understanding of the tectono-magmatic processes that affected and formed the JMMC and IPR throughout the Cenozoic in context to the opening of the Northeast Atlantic (73°N – 60°N and 5°E – 35°W) (Figure 1 and 2). Addressing the tectono-magmatic processes and spatial reconstruction of the igneous processes that interlink the study area to the Mid-Norwegian margin (Vøring- and Møre margins), the Faroe Islands, and the Greenland-Iceland-Faroe ridge complex (GIFRC), and especially in comparison to volcanic activities along the north-eastern margin of the Blossville Kyst of central East Greenland [Larsen *et al.* 1989, 2014; Tegner *et al.* (2008)].

In order to improve our understanding of igneous-facies, province relationships, and the timing of volcanic events of the JMMC-IPR area, a detailed interpretation was set out based on 2D MCS seismic reflection, seismic refraction, borehole and analogue field data. This enabled us to identify seismic stratigraphic signatures characteristic of landward flows, seaward dipping reflectors (SDR), igneous and volcanic complexes, intrusions (sills, dykes, vent structures) and volcanic ridges that were placed in their chronostratigraphic order, improving the understanding of the magmatic records in the JMMC-IPR areas. An investigation of available petrological datasets was undertaken together with the revision of ambiguous age dating of DSDP Leg 38 boreholes sites 350 and 348. The new petrologic analysis and age dating undertaken in this stage of the project provided a more confident fit of the igneous record into the regional model of tectono-magmatic evolution. Furthermore, was it important to address the issue of ridge – mantle anomalies that appear to develop along pre-existing structural complexes, specifically within the IPR area in connection to the GIFRC. Here, standard mid-oceanic ridge system could not easily develop, and rift jumps, or transfers occurred across the IPR region [Blischke *et al.*, 2017, 2019a]. Thus, reflecting multiple-branched crustal accretion zones that appeared across the IPR and along the GIFRC, details of which are the focus of this paper.

This has not previously been seen and demonstrated in such detail in the Northeast Atlantic region, where the JMMC-IPR represents a key component for understanding such a system. Research on tectono-magmatic processes north of Iceland associated with the opening of the Northeast Atlantic show that the tectonic evolution of the IPR and the JMMC regions has been considerably more complex than along the Reykjanes ridge south of Iceland, and the Mohns ridge north of the Jan Mayen fracture zone (JMFZ) since the onset of spreading in late Paleocene-early Eocene [Johnson and Heezen, 1967; Vogt and Avery, 1974; Talwani and Eldholm, 1977; Gairaud *et al.*, 1978; Vogt *et al.*, 1980; Eggen, 1984; Myhre *et al.*, 1984; Srivastava and Tapscott, 1986; Skogseid and Eldholm, 1987; Gudlaugsson *et al.*, 1988; Larsen and Jakobsdóttir, 1988; Ákermoen, 1989; Gunnarsson *et al.*, 1989; Eldholm *et al.*, 1990; Kuvaas & Kodaira, 1997; Hopper *et al.*, 2003; Scott *et al.*, 2005; Breivik *et al.*, 2003; 2008; 2012; Brandsdóttir *et al.*, 2008, 2015; Erlendsson, 2010; Peron-Pinvidic *et al.*, 2012a,b; Gernigon *et al.*, 2012, 2015; Gaina *et al.*, 2009, 2014, 2017a,b; Blischke *et al.*, 2017a; 2019]. Symmetric magnetic anomalies can be traced parallel to the Reykjanes ridge and Mohns ridge back to magnetic anomalies chrons C24n2r and C22 respectively [Gaina *et al.* 2009], whereas even high resolution geomagnetic data collected for the Jan Mayen fracture zone (EJMFZ) and the Ægir ridge areas revealed irregularities in

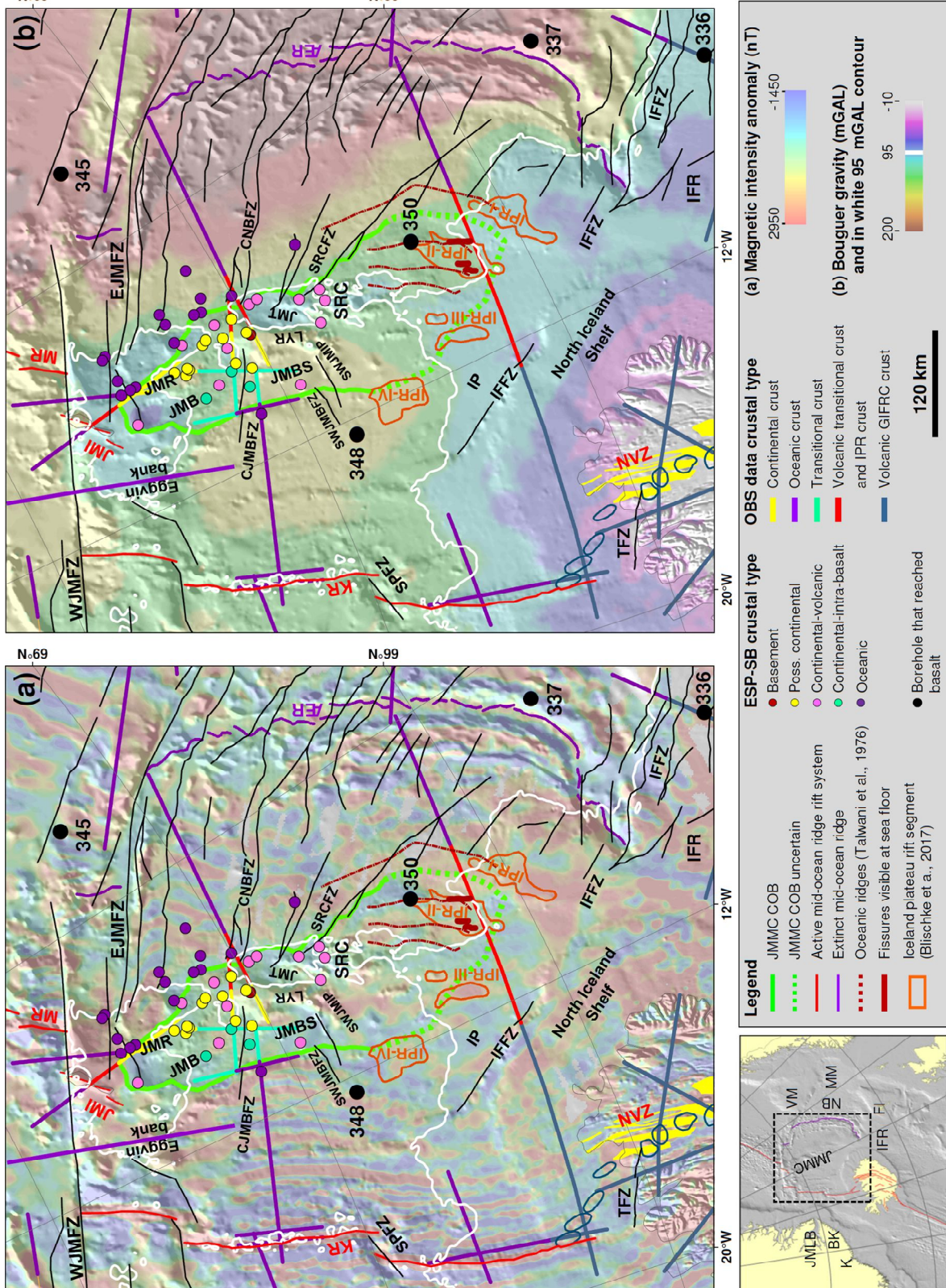
spreading rates within the Iceland plateau and the Ægir ridge in the Norway basin [Gernigon *et al.*, 2012, 2015] (Figure 1).

Results from early bathymetric, seismic reflection and refraction, magnetic and gravimetric surveys, alongside DSDP leg 38 boreholes identified the Jan Mayen ridge as a sliver of continental crust that is conjugated to the Møre margin of the Mid-Norwegian shelf edge, and formed as a result of a westward rift jump that activated the Kolbeinsey ridge at about 26 Ma (Chron C7) during Late Oligocene [Johnson and Heezen, 1967; Vogt *et al.*, 1970; Bott, 1971; Johnson and Tanner, 1972; Meyer *et al.*, 1972; Pitman and Talwani, 1972; Eldholm and Windisch, 1974; Vogt and Avery, 1974; Talwani and Udintsev, 1976k; Kharin *et al.*, 1976; Talwani and Eldholm, 1977; Grønlie *et al.*, 1979; Weigel *et al.*, 1995; Kodaira *et al.*, 1998a; Gradstein *et al.*, 2012]. Whether the initiation of the Kolbeinsey ridge took place in a single event or multiple phases has been debated in the literature [Johnson and Heezen, 1967; Johnson and Tanner, 1972; Talwani and Eldholm, 1977; Vogt *et al.*, 1980; Nunns, 1982, 1983a-c; Bott, 1985; Srivastava and Tapscott, 1986; Eldholm *et al.*, 1990; Kodaira *et al.*, 1998a, 1998b; Jung and Vogt, 1997; Müller *et al.*, 2001; Mjelde *et al.*, 2002, 2008] and plate boundary complications associated with rifting along the Ægir ridge have not been studied in any detail.

1.2 Geological setting

Bathymetrically, the JMMC comprises of a series of ridges with water depth ranging between 200–2500 m [e.g. Vogt *et al.*, 1970; Talwani *et al.*, 1976b]. The microcontinent is defined as a 400–450 km long and 100–310 km wide domain, between oceanic crustal margins formed by the extinct Ægir ridge to the east and the Kolbeinsey ridge to the west. The JMMC has been subdivided into the main Jan Mayen ridge (JMR), the Lyngvi ridge (LYR), the Jan Mayen basin (JMB), the Jan Mayen trough (JMT), and the Southern ridge complex (SRC) (Figure 1 and 2). The main northern JMR is well defined, continuous and flat-topped, whereas the SRC is composed of several smaller ridges, which become indistinct towards the south. The volcanic complex of the Jan Mayen Island lies at the northern end of the JMMC, linking the eastern and western segments of the JMFZ [Svelling and Pedersen, 2003]. The eastern margin of the JMMC developed as the outermost part of the continental shelf of central East Greenland and is characterized by eastward-thickening of Palaeogene strata and basaltic lava flows that dip steeply towards the Norway basin [e.g. Gairaud *et al.*, 1978; Skogseid and Eldholm, 1987; Åkermoen, 1989; Gunnarsson *et al.*, 1989; Erlendsson, 2010; Peron-Pinvidic *et al.*, 2012b; Blischke *et al.*, 2019]. The western margin of the JMMC developed by rifting within the Greenland continental shelf, in association with the Paleogene igneous province of the Bløseville Kyst and the Palaeozoic-Mesozoic Jameson Land basin.

Figure 1. Structural map of the Jan Mayen microcontinent with mapped fractures zones and lineaments based on this study. Also shown are gravity ridges defined by Talwani *et al.* [1976k]. Refraction velocity interpretations are based on wide-angle data (OBS) and crustal type interpretations [Kodaira *et al.*, 1998a; Mjelde *et al.*, 2008; Kandilarov *et al.*, 2012; Funck *et al.*, 2014, 2017; Brandsdóttir *et al.*, 2015; Tan *et al.*, 2017], as well as sonobuoy interpretations [Johansen *et al.*, 1988; Olafsson & Gunnarsson 1989; and Blischke *et al.*, 2017, 2018] and ESP interpretations of this study. The background is shaded bathymetry [IBCAO 3.0; Jakobsson *et al.*, 2012] beneath the (a) magnetic intensity anomaly data grid [Nasuti and Olesen, 2014] and (b) the Bouguer gravity anomaly grid data [Haase and Ebbing, 2014, 2017]. Abbreviations: CJMBFZ – Central Jan Mayen basin fracture zone; CNBFZ – Central Norway basin fracture zone; EJMFZ – East Jan Mayen fracture zone segments; IFFZ – Iceland-Faroe fracture zone; JMB – Jan Mayen basin; JMBS – Jan Mayen basin south; JMI – Jan Mayen Island complex; JMR – Jan Mayen ridge; JMT – Jan Mayen trough; KR – Kolbeinsey ridge; LYR – Lyngvi ridge; MR – Mohns ridge; NVZ – Northern volcanic zone; SPFZ – Spa fracture zone; SRC – Southern ridge complex; SRCFZ – Southern ridge complex fracture zone; SWJMBFZ – Southwest Jan Mayen basin fracture zone; SWJMIP – Southwestern Jan Mayen igneous province; TFZ – Tjörnes fracture zone; WJMFZ – Western Jan Mayen fracture zone; ÆR – Ægir ridge.



This margin is characterized by tilted extensional fault blocks that form mainly half-graben structures together with a complex of sills and/or lava flows, which cover the Jan Mayen basin west of the JMR [e.g. *Larsen et al., 2013; Hopper et al., 2014; Blischke and Erlendsson, 2018; Blischke et al., 2018*]. The southern extent of the microcontinent is largely obscured beneath Upper Paleogene and Neogene igneous and sedimentary rocks of the Iceland Plateau [*Brandsdóttir et al. 2015; Blischke et al., 2017b, 2019*]. The southern half of the microcontinent is generally described as a complex structural and volcanic domain with numerous extrusive and intrusive formations, blanking seismic reflection imaging of underlying structures, specifically within the JMT [e.g. *Talwani et al., 1976b; Scott et al., 2005; Gaina et al., 2009; Peron-Pinvidic et al., 2012a, b; Gernigon et al., 2012, 2015; Blischke et al., 2017a*].

Based on potential field and seismic data the broad fracture zones along the northern margin of the JMMC are geo-dynamically interpreted to have been active since ~55 Ma. At its centre lies the presently active Beerenberg volcanic system as the youngest part of the Jan Mayen Island igneous complex (JMI) [e.g. *Skogseid and Eldholm, 1987; Gaina et al. 2009; Geissler et al. 2017; Blischke et al., 2019*] (Figure 1).

The broad eastern volcanic margin of the JMMC, adjoining the Norway basin, which developed during the Early to Mid-Eocene, is characterised by the formation of volcanic escarpments and the emplacement of sills, larger-scale intrusive sections, and SDRs. The SDRs have not yet been fully delineated in reference to their association with the initiation of Early Eocene (chron C24n2r 53.36 Ma) seafloor spreading along the Ægir ridge [e.g. *Skogseid and Eldholm, 1987; Gaina et al., 2009; Peron-Pinvidic et al., 2012a,b; Gernigon et al., 2015; Blischke et al., 2017a, 2019*].

The evolution of the south-eastern and southern margins of the JMMC, SRC and IPR in respect to the Iceland-Faroe fracture zone (IFFZ), along the Iceland-Faroe ridge and north Iceland shelf remains ambiguous. Based on potential field data, the Iceland-Faroe ridge, and Iceland region are anomalous within the Northeast Atlantic reconstruction model [*Gaina et al., 2014, 2017*]. An area that has been affected by several igneous phases between Mid-Eocene (C22n ~49.3 Ma) and Late Oligocene (C13 ~33 Ma) [*Blischke et al. 2016, 2019*].

The western and southwestern margins of the JMMC and the Jan Mayen basin developed in response to the Late Oligocene (C13 ~33 Ma) to Early Miocene (C6 ~18.8 - 21.6 Ma) rift transfer and cessation of spreading along the Ægir ridge between 30-26 Ma [*Kharin et al., 1976; Gaina et al., 2009; Gernigon et al., 2015*]. This margin, encompassing the JMB and SRC, has been defined as a starved magmatic breakup margin [*Kodaira et al. 1998a*]; a distinct Iceland Plateau igneous province [*Talwani et al. 1977*]; or a pre-Kolbeinsey ridge igneous province and breakup margin characterized by extensive intrusive and extrusive formations within four distinct Iceland Plateau rift segments just south of the SRC [*Blischke et al., 2017a, 2019*].

The SRC consists of several smaller ridges created during extension and rift transfer associated with the formation of the Ægir ridge [e.g. *Gaina et al., 2009; Peron-Pinvidic et al., 2012a; Gernigon et al., 2015; Blischke et al., 2017a*]. The SRC segments may contain small, hyperextended pieces of continental crust between the volcanic ridges [e.g. *Peron-Pinvidic et al., 2012a; Blischke et al., 2017a, 2019*], whereas the Iceland Plateau is considered to be of primarily oceanic origin [*Talwani et al., 1977; Brandsdóttir et al., 2015*] with crustal thickness of 7-12 km based on seismic refraction and gravity data [*Brandsdóttir et al., 2015; Haase and Ebbing, 2014*] (Figure 1b).

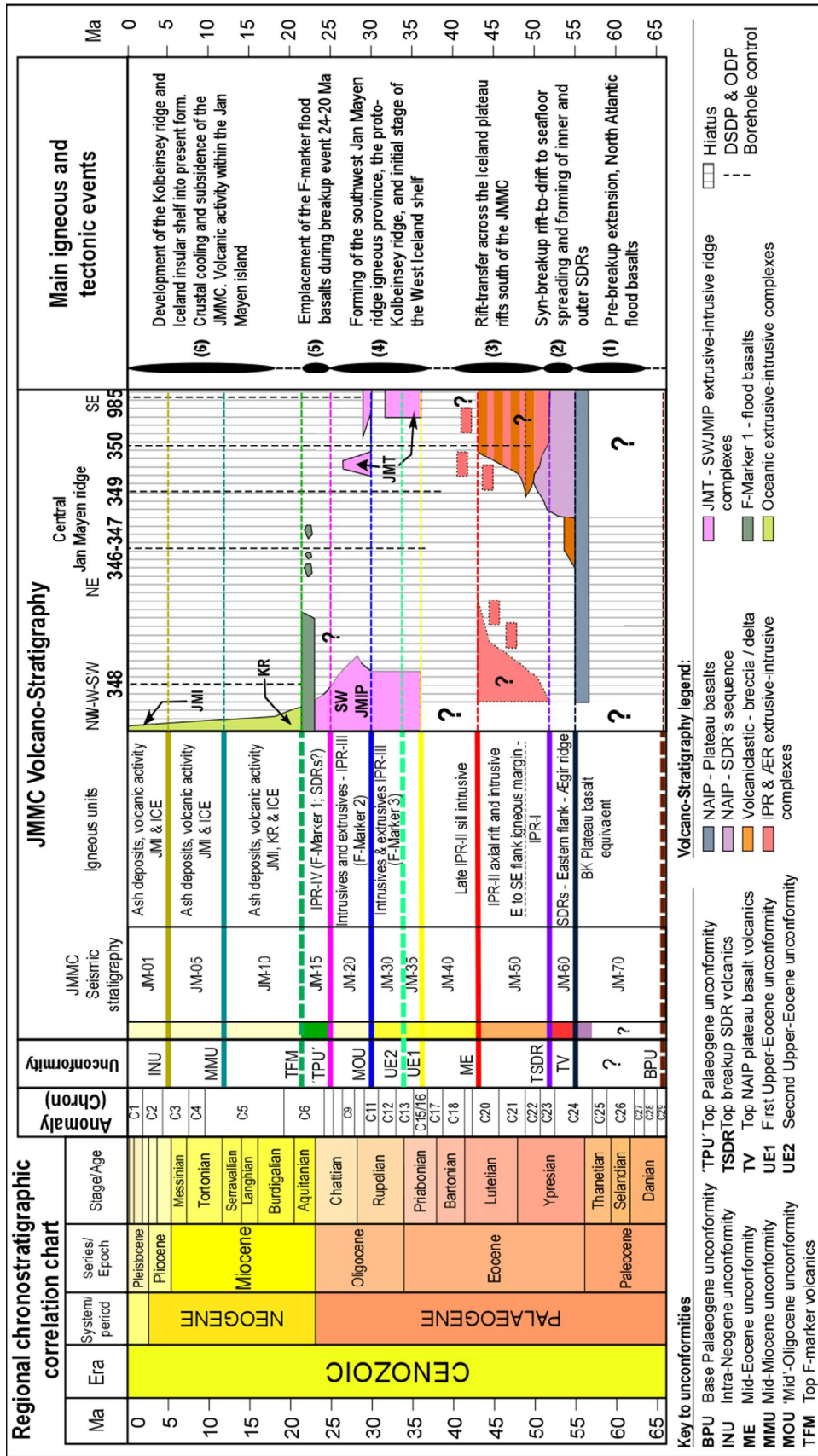


Figure 2. Volcano-chronostratigraphic chart of the JMMC modified after Blischke et al. [2017a, 2019] constrained by DSDP borehole and 2D reflection and refraction data [Tabwani et al., 1976a, b; Manum and Schrader, 1976; Manum et al., 1976a, b; Raschka et al., 1976; Nilsen et al., 1978; Thiede et al., 1995; Jansen et al., 1999a, b; Butt et al., 2001]. The time scale is based on Gradstein et al. [2012]. Abbreviations: ÆR – Ægir ridge; BK – Blossesville Kyst; JMI – Jan Mayen island igneous complex; JMT – Jan Mayen trough; KR – Kolbeinsey ridge; SDR – Seaward dipping reflectors; SWJIMP – Southwest Jan Mayen igneous province.

2 Data and methods

Vintage and new geological and geophysical datasets (1970's-2017) were used to build a comprehensive database including seismic reflection and refraction profiles, gravity and magnetic anomaly data, high-resolution multi-beam bathymetric imagery, borehole and seafloor sample information. Data from previous studies were included as well to build on to the volcano-stratigraphic interpretations [e.g. *Vogt et al., 1970, 1986; Talwani and Eldholm, 1977; Åkermoen, 1989; Doré et al., 1999; Lundin et al., 2005; Rey et al., 2003; Gaina et al., 2009; Gernigon et al., 2012; Hopper et al., 2014; Haase and Ebbing, 2014; Nasuti and Olesen, 2014; Funck et al., 2016, 2017; Blischke et al., 2017a*] (Figures 3 and 4; Supplements 1-7).

2.1 Dataset

2.1.1 Seismic data

Seismic reflection and refraction data were the primary dataset for this study (Figure 3; Supplement 1), consisting of vintage and recent surveys (1975-2012). Recently acquired and re-processed JMMC seismic reflection surveys (2008-2012) were included: JM-85 and JM-88 (re-processed 2009), IS-JMR-01 (2001), ICE-02 (2002), WI-JMR-08 (2008), NPD-11 (2011), and NPD-12 (2012). The 2011-2012 surveys were specifically useful, as they have a higher data quality and improved resolution of the deeper sub-strata and post-igneous strata. Still, these newest datasets did not improve the sub-basalt imaging for the youngest (Late Oligocene – Early Miocene) flood basalt domain of JMMC's western and southern flanks. The transition from the JMMC into the oceanic domain was evaluated through north Atlantic regional 2D MCS survey data that connect to the JMMC area: BGR-75, BGR-76 [*Hinz and Schlüter, 1978*], and RC2114 [*Talwani et al., 1981; Mutter et al., 1982; Talwani et al., 1977*].

Seismic-refraction datasets acquired since 1985 very summarized in *Blischke et al. [2017a; 2019]* consisting of ocean-bottom seismic (OBS) refraction surveys and sonobuoy experiments [*Johansen et al., 1988; Olafsson and Gunnarsson, 1989; Kodaira et al., 1998a,b; Mjelde et al., 2002, 2007; Breivik et al., 2012; Kandilarov et al., 2012; Brandsdóttir et al., 2015*]. Seismic velocity data were compared to the central East Greenland margin, Norwegian shelf and Faroe–Shetland regions in *Blischke et al. [2019]*, thereby enabling time-depth conversion and inferred correlations to deeper JMMC stratigraphic units. Information on crustal structure from refraction data was correlated with seismic reflection data, shallow offshore boreholes, and the seafloor database [*Peron-Pinvidic et al., 2012a; Blischke et al., 2017a; 2019*] in order to define stratigraphic sections. In this study expanded spread profile experiment data (ESP) was added to the velocity model, such as the ESP-5-L-DGO survey data by *Eldholm and Grue [1994]* and interpreted ESP data (ESP-121 to 128 on Figure 3). These profile datasets were analysed by travel-time-to-offset-ratio analysis [e.g. *Childs and Cooper, 1978*] and by the Tau-P velocity estimation methods of *Diebold and Stoffa [1981]*. The resulting average velocity values were tied into the existing seismic-reflection correlation datasets, assigning associated velocity values to the velocity facies domains of the JMMC. Velocity facies domains that guided the seismic volcano-facies interpretations on the seismic data distinguishing JMR domains versus igneous domains (Figure 1 and 4; Supplements 2 and 6b).

2.1.2 Geological data

Borehole and seafloor samples are sparse across the Northeast Atlantic, beyond the active mid-oceanic ridges (Figures 1 and 3; Supplements 1-5). Borehole sites 336, 337, 342, 343, 345, 346, 347, 349 and 350 of the deep-sea drilling program (DSDP) Leg 38 [Talwani and Udintsev, 1976a-j], site 642 of the ocean drilling program (ODP) Leg 104 [Eldholm et al., 1976a,b], and 985 for ODP Leg 162 [Jansen et al., 1996] serve as control sites for the overlying Cenozoic sediment cover, mapped unconformities and were tied into the stratigraphic framework for the JMMC [Blischke et al., 2019] (Supplements 2-5). The stratigraphic framework also includes interpretations based on seafloor sampling campaigns by Geodekyan et al. [1980], Sandstå et al. [2012, 2013], and Polteau et al. [2012, 2018] that were summarized in Blischke et al. [2017a, 2019].

2.1.3 Chronology

Igneous data controls are in DSDP Leg 38 boreholes 336, 337, 345, 348 and 350 and were reviewed in this study and boreholes 348 and 350 were re-analysed. New $^{40}\text{Ar}/^{39}\text{Ar}$ dating was needed to further constrain the timing of the ridge transition along the southern edge of the JMMC and the IPR due to K/Ar data analysis uncertainties. The radiometric dates were obtained for DSDP site 350, which sampled Middle Eocene basalts from the south-easternmost extent of the SRC, and site 348 that recovered Lower Miocene basalts from the western igneous margin of the microcontinent (Figures 3; Supplements 2-5 and 6b). Eight selected fine-grained, unaltered 115-513 mg whole-rock basalt samples were selected for ground-mass analysis at the argon geochronology lab at the Oregon State University. All samples were analysed from the DSDP core processed groundmass with the $^{40}\text{Ar}/^{39}\text{Ar}$ Heine resistance furnace on the MAP 215-50 through incremental heating. Three Early Miocene samples from DSDP 348 provided reliable results, and three out of five samples could be used for the Mid-Eocene core samples of DSDP 350 (Figure 5; Supplements 3 and 4). The results are presented in chapter 4.

2.1.4 Geochemical data

In order to further constrain our igneous-seismic-stratigraphic provinces we compiled available analyses of borehole and seafloor samples from geochemistry databases: PETDB [Lamont Doherty Earth Observatory, Columbia University, New York, <http://www.earthchem.org/petdb>], the GEOROC [Max Planck Institute for Chemistry, Mainz, <http://georo~mpch-mainz.gwdg.de/georoc/>], with data from Grönvold and Mäkipää [1978], Kharin et al. [1976], and Tegner, C. [unpublished] (Supplements 3 and 5; see full reference list under: Geochemistry data references).

Petrographic descriptions were used to constrain the volcano-facies environment during the emplacement of the sampled igneous sections. Seven selected samples from DSDP 348 and 350 were analysed at the University of Iceland (Supplement 5). Inductively coupled plasma-optical emission spectroscopy (ICP-OES) (SPECTRO CIROS) was used to identify major (SiO_2 , Al_2O_3 , FeO , MnO , MgO , CaO , Na_2O , K_2O , TiO_2 and P_2O_5). The methodology adopted is similar to that described by Govindaraju and Mevelle [1987] and additional details have been reported elsewhere [Halldórsson et al., 2008].

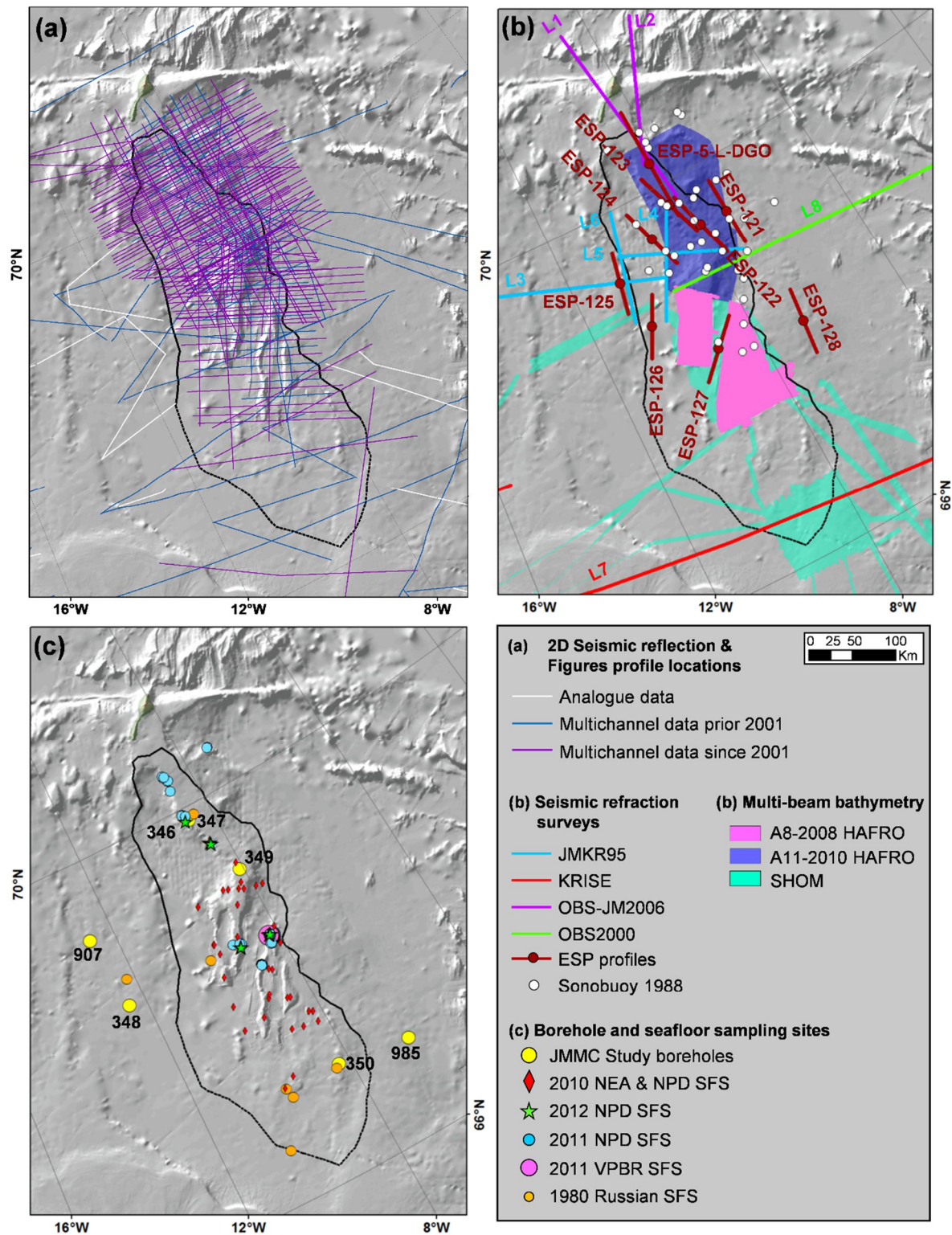


Figure 3. Hill shaded bathymetry map [Jakobsson et al., 2012] of the Jan Mayen region, showing (a) 2D seismic reflection lines (b) seismic refraction lines, OBS (ocean bottom seismic), and multibeam bathymetric maps [HAFRO – The Icelandic Marine and Fresh Water Research Institute; National Energy Authority of Iceland; Norwegian Petroleum Directorate; Spectrum ASA; TGS; SHOM - Service Hydrographique et Océanographique de la Marine]; (c) borehole and seafloor samples (SFS) [Volcanic Basin Petroleum Research AS].

2.1.5 Bathymetry

Satellite, ship-track and high-resolution multi-beam bathymetry data was used (Figure 3), such as the international bathymetric chart of the Arctic ocean (IBCAO) Version 3.0 with a 500 m x 500 m resolution [Jakobsson *et al.*, 2012] for the regional grid maps that was tied into the ship-track seafloor data, which was required for two-way-travel time-to-depth conversions of the 2D multi-channel seismic (MCS). Two high-resolution multi-beam echosounder surveys were conducted across the JMR and SRC areas in 2008 and 2010 with surveys A8-2008 and A11-2010 [Helgadóttir, 2008; Helgadóttir and Reynisson, 2010]

These seafloor data surveys highlight structural trends and features at the seafloor, which, in combination with seismic reflection data, enabled us to distinguish fault types, escarpments of the microcontinent's ridges, and volcanic features [Ákermoen, 1989; Gunnarsson *et al.*, 1989; Blischke *et al.*, 2017a; 2019].

Surveys A8-2008 and A11-2010 were planned and acquired by the National Energy Authority of Iceland (Orkustofnun), the Norwegian Petroleum Directorate (NPD), and the Marine Research Institute of Iceland (HAFRO). R/V Árni Friðriksson (HAFRO) conducted these two surveys acquiring 10,500 km² of bathymetric and seabed composition data that are available as 50 m x 50 m grid datasets with a depth range of 790-2210 m [Helgadóttir, 2008; Helgadóttir and Reynisson, 2010; Blischke *et al.*, 2017a, 2019]. The French Hydrographic and Oceanographic Office (SHOM) conducted a hydrographic and oceanographic cruise (NARVAL-2016) onboard R/V Beautemps-Beaupré in 2016 across the Jan Mayen trough, SRC and the IPR (Figure 1; Supplement 1), acquiring 35,000 km² multi-beam bathymetry data, available as a 50 m x 50 m grid dataset, alongside additionally sub-bottom profiles and magnetic data [Dupuy and Sogorb, 2017]. This high-resolution dataset was important not just for their 2D MCS data tie, but also for their seafloor imaging of structural trends and volcanic axial ridges (Figure 1).

2.1.6 Reconstruction work

Plate reconstructions and projections were calculated using an interactive fitting method utilizing GPlates [www.gplates.org; see also Gaina *et al.*, 2017b], compared and fitted within GIS for each reconstruction stage (~56-55 Ma; ~55-49 Ma; and 33-21 Ma). Rotation parameters for Greenland relative to Eurasia are based on Gaina *et al.* [2017b] and detailed kinematic reconstructions for the separate JMMC tectonic blocks are tied to the chronostratigraphic succession and best fit of fault and block topography in chronologic order are modified after Blischke *et al.* [2017a, 2019]. The geo-chron interpretation of the Ægir ridge system is based on the high-resolution magnetic data by Gernigon *et al.* [2015].

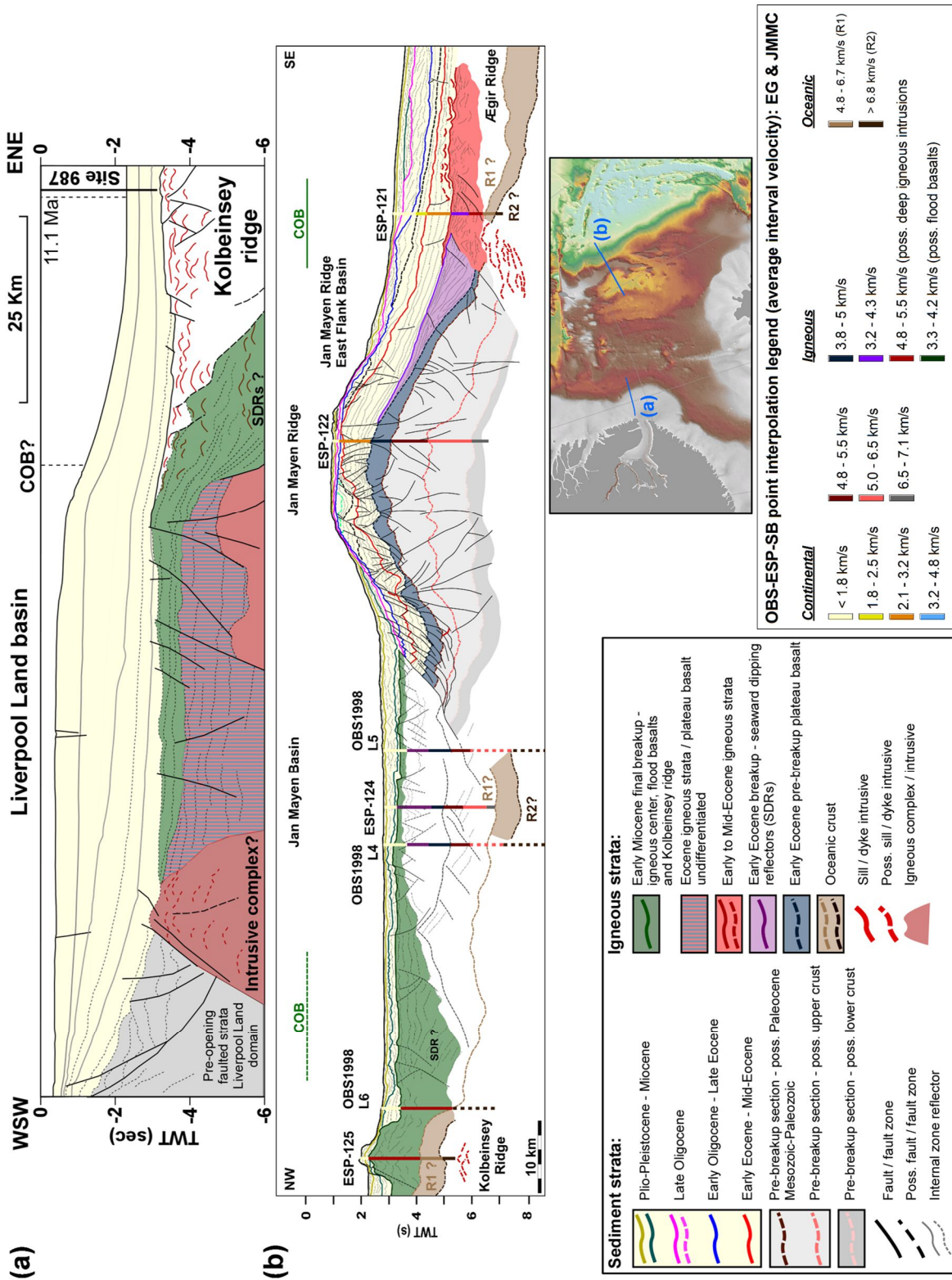


Figure 4. Tectonostratigraphic conjugate margin sections “b” and “d” of the Liverpool Land basin to JMMC transect type sections and detailed tectonostratigraphic type sections, tied to ESP velocity profiles, sonobuoy data and available borehole tie points. The pre-breakup section is inferred to contain Paleocene, Mesozoic to Paleozoic strata by direct comparison with the Jameson Land basin and the Liverpool Land high areas and seismic refraction data [Larsen, L.M. et al., 1989; Hopper et al., 2014; Blischke et al., 2017a; 2019; Blischke and Erlendsson 2018].

3. The JMMC seismic volcano-stratigraphic framework

The JMMC-IPR igneous formations are addressed through seismic volcano-stratigraphy interpretations, a method that has been utilized within the NE-Atlantic region by e.g. *Larsen and Jakobsdóttir* [1988]; *Symonds et al.* [1988] or *Planke et al.* [2000] to define seismic volcanic units by their shape, reflection patterns and boundary reflection signals, and by placing those into the chronological context. These seismic volcanic facies are sub-divided into different types, such as landward flows, SDR sequences, inner and outer SDRs, igneous centres, sills or dyke intrusive, and volcanic vent structures [e.g. *Hinz et al., 1981; Planke et al., 2000*] (Figures 2; 4-6; Supplements 2 and 6a,b).

The volcanic stratigraphic framework was primarily based on interpretation of seismic reflection data tied to seismic refraction velocity interpretations, geochemical analyses, and by comparison with the volcanic seismic-stratigraphic framework of adjacent areas (Figure 4). The method utilized for the definition of volcanic seismic facies is based on the work by *Self et al.* [1997]; *Symonds et al.* [1998] or *Planke et al.* [2000], who defined such units by their shape, reflection patterns and boundary reflection signals, and by placing those into the chronological context.

3.1 Volcano-stratigraphic facies

We defined six volcano-stratigraphic facies types: *extrusive landward flows* marking the plateau basalt equivalent and Oligocene-Miocene flood basalts (F-markers) that infilled low-lying topography of the JMT, the south-western basins and other low areas; *igneous-volcanic complexes* along JMMC's breakup margins and close to fracture zone segments; *intrusive features*, i.e. dykes, sills and connected vent structures across the JMMC; *oceanic crust* seaward of the JMMC continent ocean boundary; *seaward dipping reflector* (SDR) units that mark the initial breakup along the JMMC's eastern and western flank; and *volcanic axial ridges* that are visible south and southeast of, and within, the SRC and JMT, forming domal structures of volcanic material (Figures 1; 5).

3.1.1 Landward flows

The evenly layered landward flow sections that underlie the SDR wedges are here referred to as the Early Eocene plateau basalt equivalent stratigraphic units, which in places can be subdivided into subaerial and submarine flows (Figures 5 and 6; Supplements 2 and 6). These lavas form strong, relatively smooth and sheet-like seismic reflectors. Internally they vary locally but are overall sub-parallel in seismic reflection character. Prograding reflectors can be observed towards the northeast flank and basin ward margin of the JMR (Figure 6a-c). Younger and Early Miocene landward flow units related to the flat lying basaltic markers (F-Marker) in the JMB and within the low areas in between the SRC ridges and the JMT (Figures 5b-d; Supplements 2 and 6). These placed into the stratigraphic sequence confirm the overlapping systems of the IPR domains IPRI through IPR-IV from east to west (Figure 5c,d; Supplement 6)

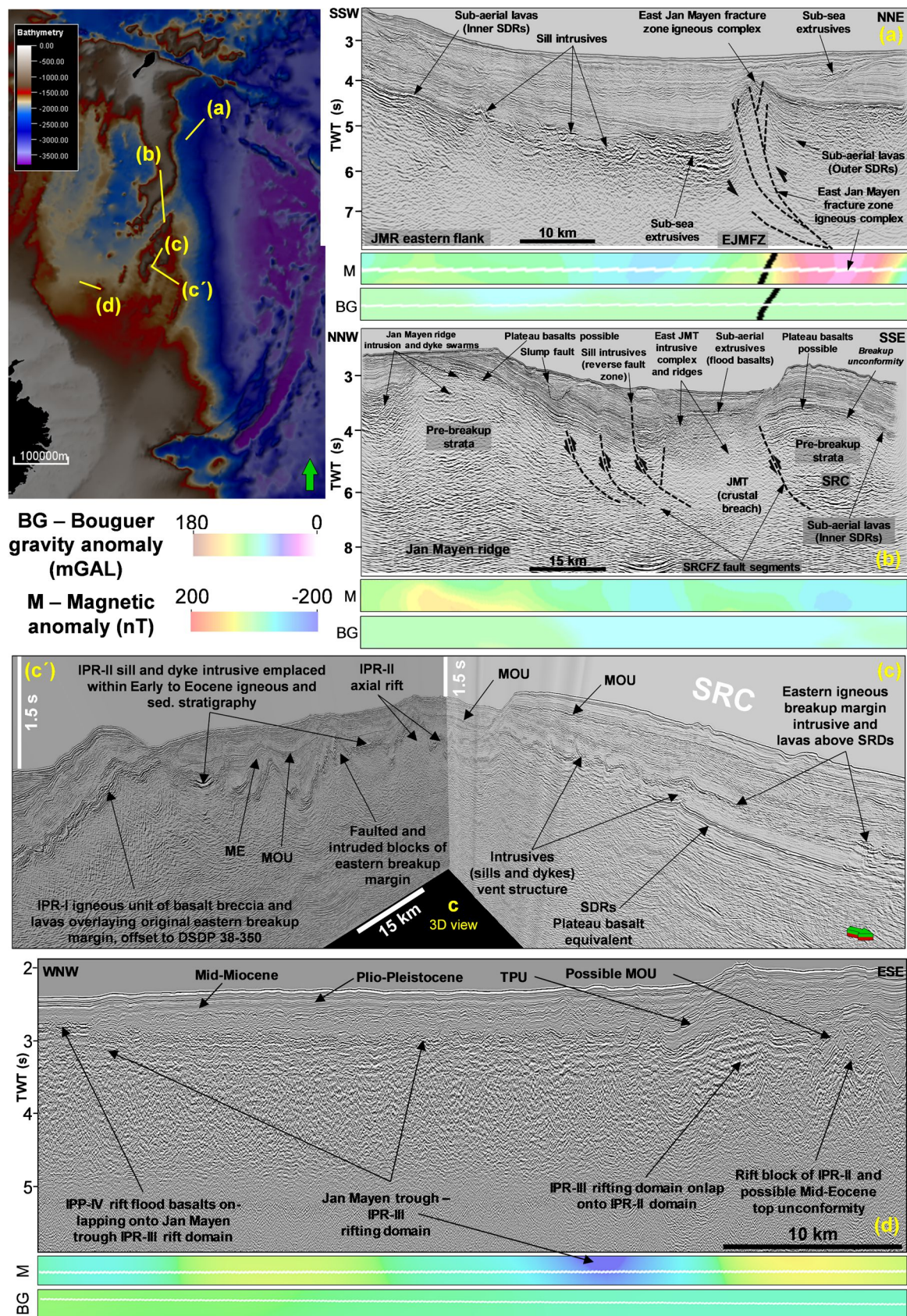


Figure 5. Examples of 2D seismic reflection profiles tied with magnetic (M) and Bouguer gravity anomaly (BG) data, outlining major fault and fracture zones in relationship to structural and igneous domain elements. Abbreviations: EJMfZ – Eastern Jan Mayen fracture zone, IPR – Iceland plateau rift, ME – Mid-Eocene unconformity, MOU – Mid-Oligocene unconformity, SRC – southern ridge complex, and TPU – Top Paleogene unconformity (see Figure 2).

3.1.2 Seaward dipping reflectors

SDR are subaerial to shallow submarine flood basalt units alternated with rift basin sediments that allow good reflection coefficient contrasts. They built distinct seaward dipping seismic reflector wedges that often have concave downwards shapes (Figures 5a and 6a,b; Supplement 2 and 6), are linked to initially forming volcanic rifted and breakup margins, and were first observed and defined by *Hinz* [1981], *Larsen and Jakobsdóttir* [1988], and *Planke et al.* [2000].

Therefore, these seismic reflection data features were a specific focus for this study, as they are commonly associated with rift axis and indicators for the first line of breakup along their inner set of SDR's that linked to an igneous centre located close to the continent-ocean boundary (COB) (Figure 6a-c). These igneous centres are referred to as outer highs by [*Planke et al.*, 2000]. These outer highs are followed seaward by deeper marine, much thinner and poorer developed outer SDR sets that are commonly located at the transition from breakup margin to ocean floor spreading and are located seaward of the COB. For the JMMC area a clear subdivision of Inner SDR – outer high – outer SDR appears well visible along the NE flank of the microcontinent and form a wide breakup margin that corresponds to the longer offset of the first clear magnetic anomaly and the location of the COB (Figure 6a). Towards the JMMC's south-east and southern extent the SDRs become indistinct and appear to form one clear SDR set only (Figure 6c). The seismic reflection pattern becomes more plateau basalt (landward flows) in character at the SRC south-easternmost extent (Figures 5b,c and 6c,d), and therefore are referred to as SDR-plateau basalt equivalent units. The outer SDRs appear to be well developed in two sets along the north-easternmost flank of the JMMC and align close to magnetic anomaly C24n.3n (~53.4 Ma) [*Gernigon et al.*, 2015; *Gaina et al.*, 2017b] (Figure 6a,b).

3.1.3 Igneous and volcanic complexes

The outer highs are one group of igneous centres that are specified by chaotic internal seismic reflection patterns, characterised by a strong top reflector, appear as mounded or sloping shapes, and can form circular features on magnetic or gravity datasets, specifically along the north-eastern JMR flank (Figure 6a,b; Supplement 6a). Here, such an igneous centre appears to have been active throughout a longer time interval, and apparently is linked to a segment of the EJMfz zone and is part of the *Jan Mayen eastern flank igneous complex* (Figures 5a and 6b) that are aligned with magnetic anomaly C24r (~55 Ma) [*Gaina et al.*, 2017b]. Another primary igneous complex is the Jan Mayen Island igneous complex with its homogenous and chaotic seismic reflection patterns, apparent deep-seated strong reflectors, and young volcanic cones that nearly reach up to the seabed (Figure 6a; Supplement 2).

A younger volcanic centre is located right along the western JMMC boundary and has a clear tie to seismic refraction data (Figure 4b; Supplement 2), relating to the Early Miocene proto-Kolbeinsey ridge volcanic breakup margin. Just as the probably Neogene to Pleistocene volcanic centres that can be seen along the north-western margin that cut through apparent Eocene igneous section, forming volcanic cone structures that are near or even above the seafloor (Figure 6a).

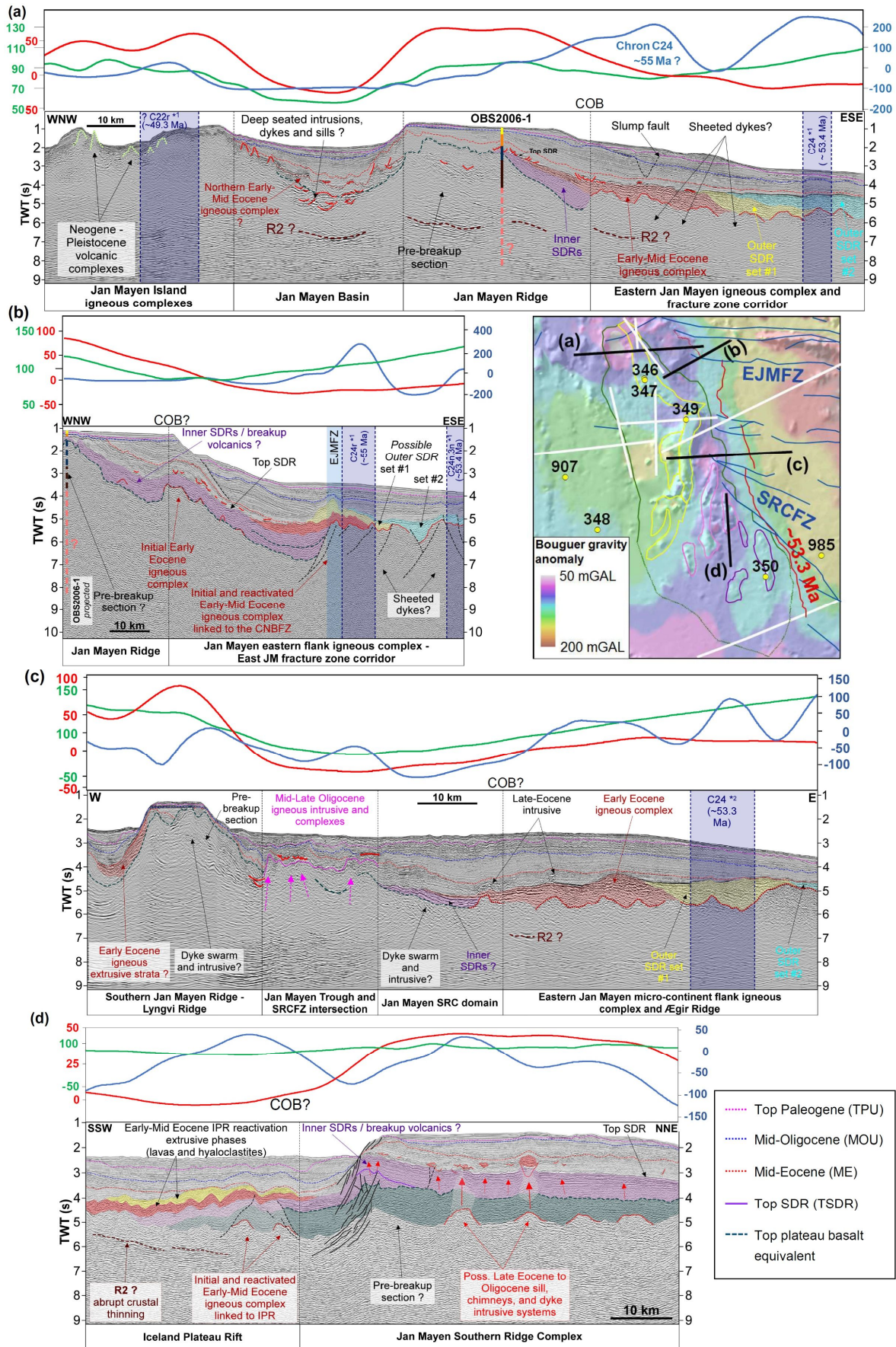


Figure 6. Key igneous domains of the JMMC: (a) E-W profile from the Jan Mayen Island igneous complex, across the northern Jan Mayen ridge and into the Eastern Jan Mayen fracture zone; (b) ENE-WSW profile across the eastern flank of the Jan Mayen ridge across the Eastern Jan Mayen fracture zone and Eocene volcanic complex; (c) E-W profile from the southern Jan Mayen ridge across the northern Jan Mayen trough across the southern ridge complex; and (d) N-S profile from the southern termination of the southern ridge complex into the Iceland Plateau rift system. Bold red lines represent sill or dyke intrusives, refraction velocities as in Figures 1 and 3. The 2D multi-channel seismic reflection data is based on NPD 2011, and 2009 reprocessed dataset of the JM-85, and WI-JMR-08 surveys. Base map: Bouguer gravity [Haase and Ebbing, 2014], magnetic anomaly chrons *1 Gaina et al. [2017b] for C24 (~55 Ma) and C24n3n (53.4 Ma), and *2 Gernigon et al. [2015] for C24n2r (53.3 Ma).

3.1.4 Intrusives

Smaller scale igneous intrusives are described in this study as dykes, sills and connected vent structures based on their seismic reflection data characteristics of their shape and acoustic impedance contrast between the intrusion and the sedimentary host rock (Figures 5 and 6; Supplement 6). The sill intrusion characteristics within the Jan Mayen ridge stratum are generally of relatively short segments with high amplitudes, abrupt terminations (sharp edges), and are often lying semi-parallel with stratigraphic layering or along fault plains. Some are clearly discordant and cross-cut the strata as “smiley” shaped features, specifically along JMMC’s eastern flank, the SRC (Figures 5a,b; 6), the JMT and within the JMB.

3.1.5 Volcanic ridges – axial rift zones

Volcanic ridges and axial rift zones are well visible structures south and southeast of and within the SRC and the Jan Mayen trough domains. They form up-doming structures of volcanic material, specifically close to fault or fracture zones, such as the IPR-II or along the northern end of the JMT (Figures 1; 5b,c; 6b). They appear both as centralized structures within the JMT and along large fault zones that serve as conduits of rising magma that leads to deformation and uplift of the overburden. Similar structures are described in the literature as a passage followed by magma in a volcanic system [Decker and Decker, 2005]. The increase of smaller scale intrusions within nearby sedimentary strata appears to be associated with these conduits. These up-doming structure are visible on seismic reflection data and bathymetry data (Figures 1; 5b,c; 6c,d). The volcanic ridges observed for the JMMC-IPR areas relate specifically to volcanic events and rifting during the IPR-II and IPR-III phases. Here crustal thickness decreases abruptly to 7-10 km [Haase and Ebbing, 2014] within the IPR rift graben structure in between and south of the SRC blocks, forming a southern microcontinent boundary straight to the south of the SRC (Figure 6d). An event that aligns with the on multibeam data identified fissure zones.

4. JMMC igneous sites

In order to constrain the established igneous framework, petrophysical parameters of igneous cores from DSDP boreholes 348 and 350 were conducted alongside radiometric dating (Figure 7-8; Supplements 3-5). The nearest onshore region of outcropping igneous rocks that might be analogous to the JMMC is in central East Greenland, specifically along the Blossesville Kyst coastline. These outcrops provide a potential stratigraphic analogue for the deeper Cenozoic and pre-breakup strata, e.g. the lower Palaeogene plateau basalt succession represents a direct analogue for the JMMC [e.g. *Pedersen et al.*, 1997; *Larsen, M et al.*, 2002, 2005; *Larsen, L.M. et al.*, 2013, 2014; *Blischke et al.*, 2017a, 2019]. Geochronological data from conjugate areas, compiled by *Storey et al.* [2007], *Hald and Tegner* [2000], *Tegner et al.* [2008], or *Ganerød et al.* [2014] were also used for comparison.

4.1 DSDP site 348

DSDP site 348 penetrated 17,4 m into fractured but homogenous basalt section at 526,6 m below the sea floor. The drilled interval is located within the assumed initial oceanic ridge basalt section of the Kolbeinsey ridge system and serves as a control site for comparison to mid-oceanic ridge basalt (MORB) west of the JMMC (Figure 1, Supplement 3a).

Existing DSDP core analysis by *Kharin* [1976], *Ridley et al.* [1976] and *Mohr* [1976] resulted placing site 348 within an abyssal tholeiites typical mid-oceanic ridge emplacement setting, probably as a sill intrusive located just east of a volcanic ridge seen on the seismic reflection site survey *Raschka et al.* [1976]. Core and thin-section analysis conducted as part of this study showed similarly that the uppermost drilled portion of the basalt consisted primarily of finely-crystalline olivine-tholeiite with volcanic glass (now replaced by smectite) closer to the basalt/sediment contact that would confirm an intrusive nature of the basalt into the sediments. In many cases, plagioclase crystals exhibit skeletal growth and 'swallow-tail'-morphology, which combined with the apparent glass content suggests that the basalt was rapidly cooled [e.g. *Lofgren*, 1974]. The basalt is slightly porphyritic, with micro-phenocrysts of plagioclase and olivine (now pseudomorphed and altered to iddingsite). Clinopyroxene and opaque minerals are unaltered but exhibit dendritic or feather-like morphology deeper in the cored section, which is common for ocean floor basalts [e.g. *Lofgren*, 1983]. The lowermost cored section consisted of fine- to medium-crystalline, aphyric olivine-tholeiite with large vesicles, possibly indicating that the basalt may have reached rapidly to the surface, as a sill or dyke intrusion, a conclusion also reached in the original analysis by *Kharin* [1976] and *White* [1978], who argued that the absence of lava-flow characteristics, including pillow structures and glassy rims, do not support a submarine extrusion.

The cored basaltic section's K₂O and Na₂O content fall within the typical MORB composition on the total-alkali-silica (TAS) classification diagram [*Le Bas*, 1989] (Figure 7a). It compares well to the MORB of the Ægir, Kolbeinsey and Mohns ridges, as well as the Tjörnes fracture zone (TFZ) (see purple field in Figure 7a) with a TiO₂ range of 1,29 - 1,65 wt%, a K₂O range of 0,02 - 0,08 wt%, and MgO range between 6,02 and 8,25 wt%. This contrasts with samples from the JMFZ, NVZ, Vesteris seamount and Vøring plateau.

Previous K-Ar radiometric dating from DSDP 348 ranged between $19,4 \pm 2,2$ Ma and $18,2 \pm 2,4$ Ma [Kharin *et al.*, 1976]. Our $^{40}\text{Ar}/^{39}\text{Ar}$ dating of the selected core samples resulted in three good cumulative ^{39}Ar release plateaus see Figure 8b, Supplements 3a and 4, with an age range between $22,15 \pm 0,26$ Ma to $23,19 \pm 0,61$ Ma. These new dates would fit magnetic anomaly C6b to C6c [Gradstein *et al.*, 2012].

4.2 DSDP site 350

The sampled basalt section of DSDP site 350 located at the southern tip of the easternmost SRC block (Figures 1; 7 and 8a; Supplements 3b; 4 and 5) was recovered from an acoustically opaque layer between 362 m and 388 m below seafloor. The 26 m-thick-section comprised a thick layer of highly altered tuff breccia with chlorite, zeolites, calcite, and doleritic basalt at the base of the cored section [Raschka *et al.*, 1976; Ridley *et al.*, 1976]; Kharin, 1976].

The basalt breccia consists of 95% basalt with angular fragments of altered and phyric hyalobasalt with plagioclase, pyroxene, altered olivine crystals, and possibly palagonite [Raschka *et al.*, 1976]. The basalt fragments have a thin chlorite-calcite-zeolite-smectite edging evenly on all sides. Furthermore, is the breccia cut by white-yellowish calcite veins with occasional pyrite occurrences. The calcite cement is layered, early formed calcite is yellowish and later formed calcite is white [Raschka *et al.*, 1976]. The during this study analysed geochemical samples show an elevated level in titanium and potassium with TiO_2 ranges between 2,09 – 3,09 wt%, a K_2O ranges of 0,45 – 1,41 wt%, and MgO ranges between 6,17 – 6,51 wt% (Figure 7b,c). Interestingly, the altered samples for well 350 align mostly within the geochemical trends for the Jan Mayen fracture zone, Jan Mayen island igneous complex, northern JMR and Vesteris seamount in Figure 7b.

The deeper basalt section is very fresh, holocrystalline, fine to medium grained, with rare plagioclase and pyroxene phenocrysts (2-5 mm), thin chlorite-calcite veins, and slickensides. A homogenous appearance is described, still with various textures such as micro-porphyritic and sub-ophitic, tholeiitic, and trachytoid [Raschka *et al.*, 1976]. The basalt core samples contain plagioclase (labradorite, twinned low-albite) interstitial pyroxene, altered olivine phenocrysts, amphibole, and rare brown glass. Opaque minerals are described as skeletal and sub-hedral crystals of magnetite that occur in a high concentration (8-10%) in comparison to all other DSDP Leg 38 sites [Raschka *et al.*, 1976].

Revisiting the core section during this study showed that the doleritic basalt intrusion has a distinct chilled margin against the basalt breccia and was emplaced into the basalt breccia seen in the core record, and as well as into overlying sediments, which can be seen on seismic reflection data (Supplement 6b). This would confirm the hypotheses of a later intrusion stated by [Raschka *et al.*, 1976]. Furthermore, based on combine core and seismic reflection data observations, does the stratigraphic unit directly overlying the basalt breccia unit consists of turbidite sedimentary rocks that are hydrothermally altered and lithified as well, clearly indicating igneous activity at different time and primarily after the emplacement of the turbidite section.

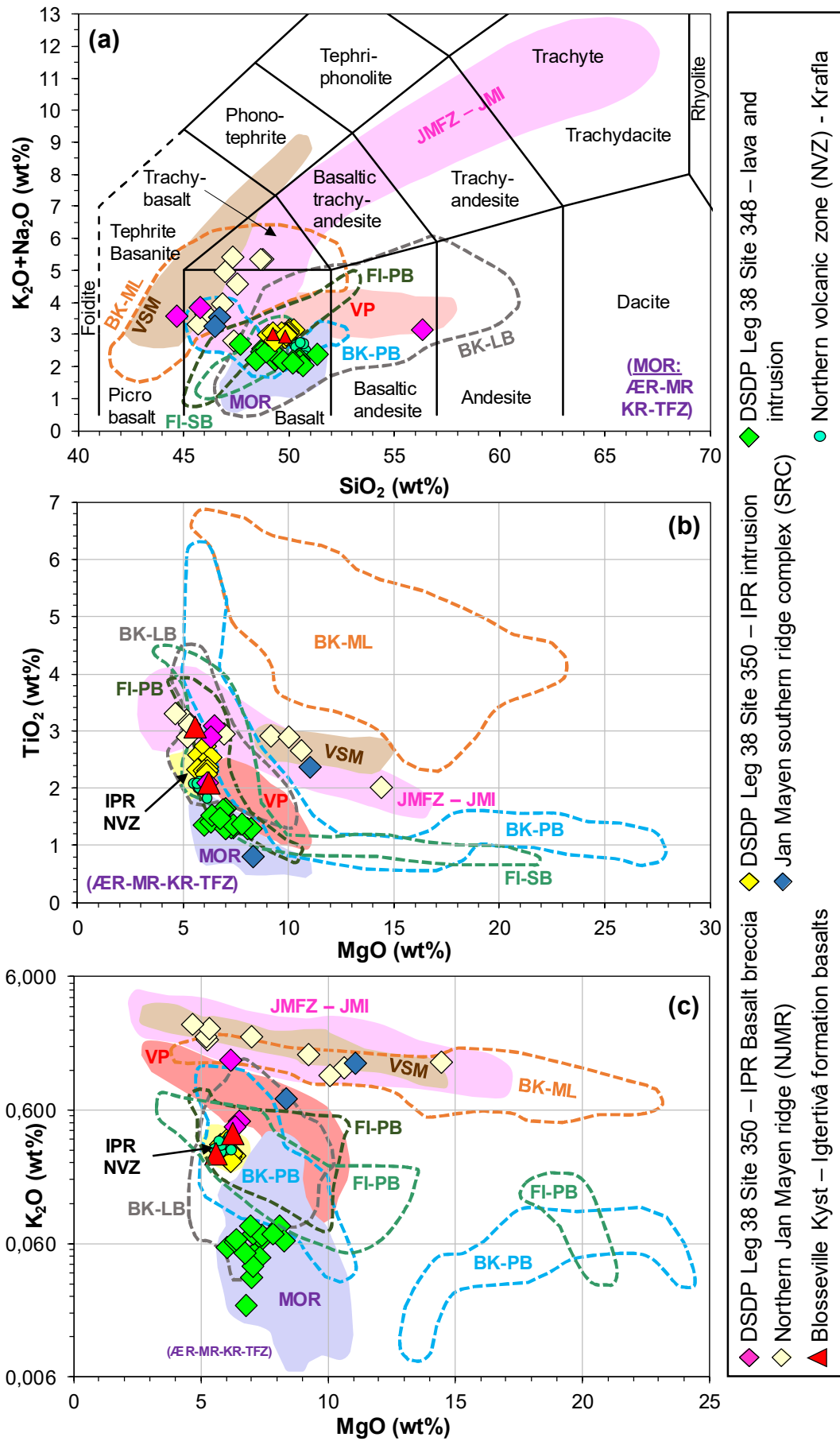


Figure 7. Geochemical composition of site 348 and 350 core samples (Figure 1; Supplements 3-5). (a) TAS classification diagram [Le Bas, 1989] showing comparison of data from DSDP and ODP boreholes within the JMFZ, with the Vøring and Blosseville Kyst igneous margins; Ægir-, Mohns- and Kolbeinsey ridges; and Iceland (TFZ and NVZ). Diagrams (b) (TiO₂ vs. MgO) and (c) (K₂O vs. MgO) show regional igneous provinces, based on data from PETDB [Lamont Doherty Earth Observatory, Columbia University, New York, <http://www.earthchem.org/petdb/>]; GEOROC [Max Planck Institute for Chemistry, Mainz, <http://georo-mpch-mainz.gwdg.de/georoc/>]; Grönvold and Måkipää, 1978; Kharin et al., 1976; and Tegner et al., unpublished]. Abbreviations: NK-ML – Blosseville Kyst Milne Land formation; BK-PB – Blosseville Kyst main plateau basalt; BK-LB – Blosseville Kyst – Lower basalt series; FI-PB – Faroe Islands pre-breakup series; FI-SB – Faroe Island syn-breakup series; IPR – Iceland plateau rift; JMFZ – Jan Mayen fracture zone; JMI – Jan Mayen Island; MOR – mid-oceanic ridges; NJMMC – northern Jan Mayen ridge; NVZ – Northern volcanic zone; SRC – Southern ridge complex; TFZ – Tjörnes fracture zone; VP – Vøring igneous margin; VSM – Vesteris Seamount.

The in this study analysed core samples resulted in a TiO₂ ranges between 2,34 – 2,75 wt%, a K₂O ranges of 0,27 – 0,37 wt%, and MgO ranges between 5,75 – 6,34 wt% (Figure 7b,c). The basalt intrusion is richer in plagioclase, which is reflected by the higher in K₂O and Na₂O content on the total-alkali-silica (TAS) classification diagram in comparison and a typical MOR basalts of site 348 (Figure 7a). The samples fall within the same areas as the Blosseville plateau basalts and in part the Vøring margin sample ranges (Figure 7a; Supplements 3b). Geochemically, the intrusive section compares mostly to the present-day northern volcanic zone basalts and the Vøring plateau-basalt samples that all exhibit higher concentration of titanium and potassium than typical MOR basalts, as seen in the samples of DSDP borehole 348. Thus, placing the IPR basalt-type closely within the present-day Iceland rift-type and Vøring plateau igneous complex domains in comparison.

Previous K/Ar age dating of DSDP site 350 produced highly unreliable results with an age range between 33,5 Ma ±2,8 Ma and 50,5 Ma ±5,5 Ma for the same sill intrusion [Kharin et al., 1976] (Figure 8a; Supplements 3b and 4). We therefore re-sampled and re-analysed the sill intrusion. New ⁴⁰Ar-³⁹Ar radiometric age ranges from ~49,28 ±0,3 Ma to 44,05 ±0,21 Ma that would correspond to magnetic anomaly chrons C22n (age range 48,57 – 49,34 Ma) to 20r (age range 43,43 – 45,72 Ma) [Gradstein et al., 2012] (Figure 8a; Supplement 4).

Although the core sample contained well visible plagioclase phenocryst in its matrix and expecting a reasonable cumulative ³⁹Ar gas release, did the recorded gas release not form as stable a plateau, as seen for DSDP site 348 (Figure 8). Cumulative gas release records that form a stable plateau for more than 50-70% of their heated interval over time are considered robust [Swindle and Weirich., 2017]. Shorter gas release plateaus are considered mini-plateaus resulting in a higher uncertainty. It has been discussed that if a rock samples that has been disturbed by a thermal event after its emplacement, the ages of the final steps are lower than the true original age [Swindle and Weirich, 2017]. Therefore, the DSDP site 350 ³⁹Ar gas release analysis has a higher uncertainty and age range than seen for site 348 but has improved in comparison to its original K/Ar method from a range of 17 Ma ±5,5 Ma down to 5,23 ±0,3 Ma, showing indications of later thermal events that affected the cored section.

4.3 Dredged seafloor samples

During the dredging and gravity coring survey by Polteau et al., [2018] did dredges number 7 (3% of total dredge content) and 8 (10% of total dredge content) return volcanic rocks from 15 sampling stations and 11,11m of sampled section in total. The sampled igneous rocks were described as freshly broken subaerial, vesicular, and altered basalt, brecciated volcanoclastic and dolerite basalt fragments. [Polteau et al., 2018].

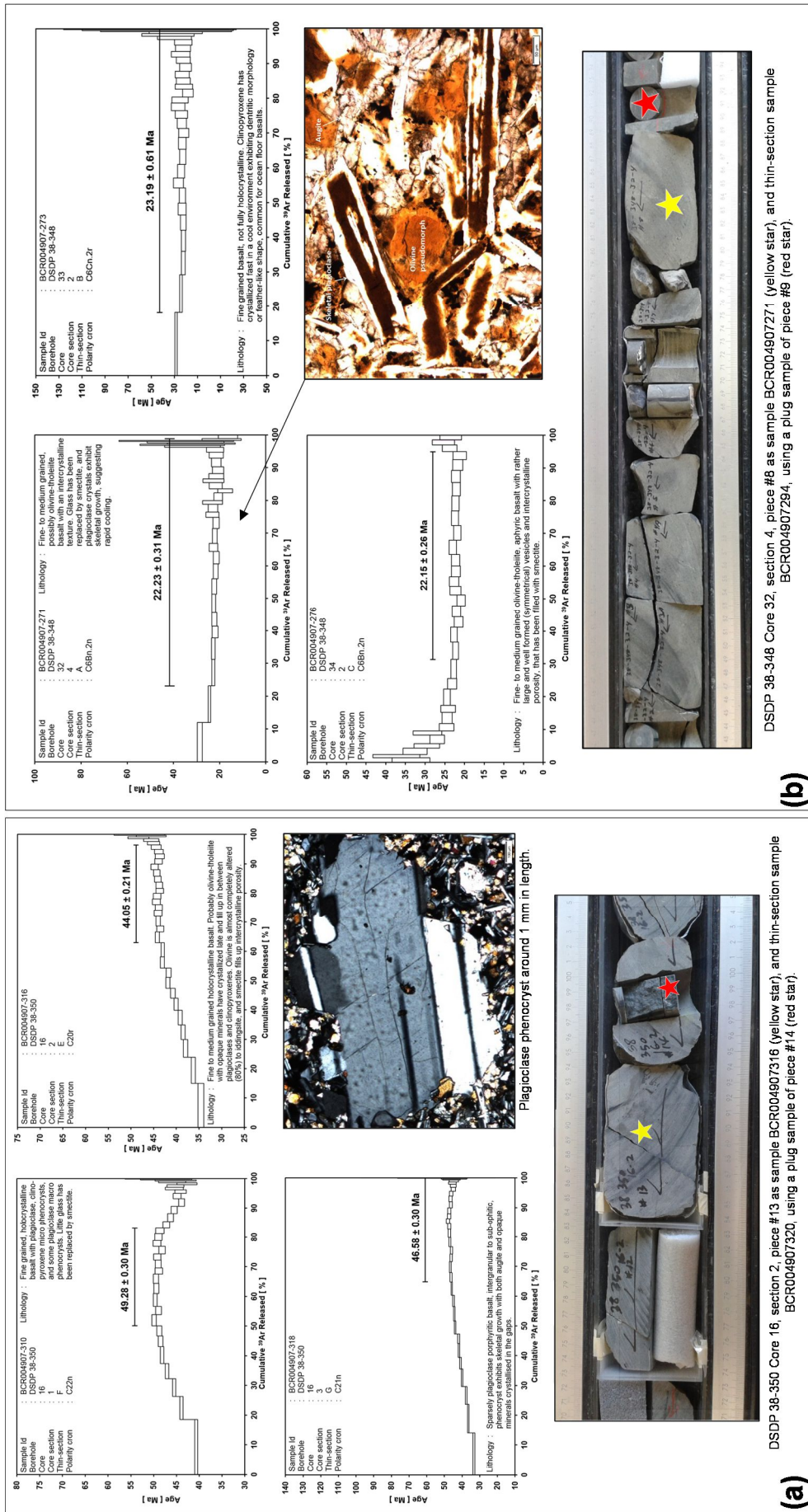


Figure 8. 40Ar/39Ar radiometric age estimate plateau displays for all samples for boreholes DSDP 38-350 and 348, (a) DSDP 38-350 and core sample 316, and thin-section analysis of sample 314, and (b) borehole DSDP 38-348 and core sample and thin-section analysis of sample.

Geochemical analysis resulted in weak to moderately altered basaltic rocks, which is based on their net weight percent losses of less than 0,7 - 3,8 wt% [Polteau *et al.*, 2018]. Two of the little-altered (<0,7 wt%) samples are plotted in comparison to offset borehole and seafloor samples on Figure 7. Both samples are magnesium-enriched basalts based on the TAS classification [Le Bas, 1989] (Figure 7a). However, they are divided into two different compositions based on their titanium and potassium content, one closer to the MORB type, and the other closer to the Blosseville Kyst Milne Land or the Faroe Island plateau basalt domains and syn-rift series (Figure 7b,c). This would be in line with the rare earth element trend described by Polteau *et al.*, [2018] to compare to the Enni formation of the Faroe Islands youngest exposed basalt formation [Larsen, L.M. *et al.*, 1989; Tegner *et al.*, 1998; Millett *et al.*, 2017].

Age determination of basaltic rock material dredged from the escarpment along the eastern flank of Lyngvi Ridge and the northwesternmost flank of the SRC has been problematic due to the altered state of the retrieved samples. The samples consist of partially unaltered vesicular basalt, volcanoclastic breccias and dolerite fragments. A varying degree of alteration was observed for the primary micro-crystalline basalt with mineralized vesicles. [Polteau *et al.*, 2012, 2018; Sandstå *et al.*, 2012, 2013]. Polteau *et al.* [2018] suggest an age range of basalt emplacement between ~59-47 Ma (Late Paleocene to Early Eocene), (Figure 2; Supplement 5a). The age is based on sediment dredge samples below and above the basaltic dredge section. Uncertainty remains regarding the in-situ nature of these samples, as allochthonous origin cannot be discounted [Blischke *et al.*, 2017b].

5. The formation of the JMMC igneous provinces

Based on seismic-stratigraphic mapping we defined seven distinct igneous phases within the JMMC region (Figures 2; 9; 10; Supplements 6; 7). The tectono-stratigraphy of each phases is discussed in chronological order below. Whereas our mapping is based primarily on the interpretation of seismic refraction and reflection data, we have also compared the geochemical composition of seafloor and borehole samples within (i.e. DSDP 348 and 350) and adjacent to the JMMC regions (Figures 1; 7; 8 and Supplements 3-5).

5.1 The Jan Mayen ridge – pre-breakup phase

The primary JMR with its igneous records is associated with pre-breakup volcanic activity during Late Paleocene to Early Eocene and relates to stratigraphic unit JM-70 (Figure 2). This unit onlaps the Jan Mayen igneous complex to the north and underlies the inner SDR units along the eastern flank areas of the JMMC (Figures 4; 6; Supplement 2). On seismic reflection data, this laterally continuous succession of parallel-bedded reflectors, interpreted as stacked plateau-basaltic flows [Blischke *et al.*, 2019], has been mapped across the JMR, Lyngvi ridge, SRC and partially along the eastern edge of the Jan Mayen basin areas (Figures 9 and 10). The uppermost 0,5 – 1,0 seconds of the sub-parallel-stratified Early-Eocene pre-breakup basalts has a velocity range between 3.8 km/s and 5.0 km/s, based on seismic refraction data, and a stratigraphic thickness close to 1,1 km across the central

JMR, increasing southwards to approximately 3,3 km on the southernmost Lyngvi ridge (dark grey layer in Figure 4b and Supplement 2a). As the JMMC has been subsequently affected by major erosive events, the original stratigraphic thickness of this layer cannot be determined. The Early-Eocene pre-breakup plateau basalts are comparable in stratigraphic architecture to equivalent strata exposed on the conjugate central East Greenland coast, and on offshore seismic reflection lines along its continental margin [Blischke and Erlendsson, 2018; Blischke et al., 2020a] (Figure 2a).

Locally disrupted zones of chaotic seismic reflection patterns, most likely representing sill intrusions and smaller intrusive centres, are embedded within the plateau basalt strata within the Lyngvi ridge and the northernmost segment of the SRC (Figures 6a-c; 9 and 10; Supplement 2a,c). These intrusive bodies appear to be focused within the Jan Mayen and Lyngvi ridge segments. They do not deform the post-break up formations and, thus, could be related to the pre-breakup volcanism.

5.2 The JMMC eastern margin igneous domain – syn-breakup phase

This syn-breakup igneous phase is linked to the development of stratigraphic unit JM-60, which comprises primarily of SDRs and is present along the eastern flank of the JMMC, covering the JMR ridge area, where it discordantly overlies the plateau-basalt-equivalent JM-70 strata [Blischke et al. 2017a, 2019] (Figures 2; 4-6; 9a-10; Supplements 2; 6; 7). The JM-60 unit's top surface (TSDR Figure 2) is a strong and continuous seismic reflector, which enabled reliable cross-correlation between structures that offset the SDR unit across faults or graben structures. Utilizing the denser seismic reflection data coverage these SDR units were clearly mappable and were delineated into three sets of SDRs along JMMC's NE margin and close to the EJMFZ (Figures 9a; 10). The inner and two outer sets of SDR's are subdivided by an igneous complex that represents the primary volcanic breakup margin (Figures 6a,b; 9a and 10), which represents the conjugate outer high to the Vøring margin that is located eastward in reference to that structure (Figure 11a). The Vøring is an analogue area for these volcanic deposits and a key reference unit [e.g. Hinz, 1981; Mutter et al., 1982; Skogseid and Eldholm, 1987; Planke et al., 2000] (Figure 11a; 12). Specifically, Skogseid and Eldholm, [1987] noticed a widened volcanic breakup margin that linked the JMMC across the EJMFZ to the Vøring margin with distinct sets of SDR wedges forming along both margins, during syn-breakup time.

The inner (older) SDRs – onlap westwards onto the JMR and SCR structural highs, where they pinch out onto the plateau basalt unit and its top unconformity (TV on Figures 2; 6; 9a). The inner SDR units exhibit a parallel to eastward-prograding seismic reflection as well as more local hummocky-lenticular patterns that tend to be thinner (< 1,5 km) and related by definition [Hinz, 1981; Mutter et al., 1982; Planke et al. 2000] to landward, subaerial lava flows (Figures 6a; 9a; 10; Supplements 2 and 6). Locally the SDRs increase convexly up to 4,2 km in stratigraphic thickness towards the primary volcanic margin which has been build up by igneous complexes (outer highs). The transition between the inner SDR wedge and the outer high is commonly parallel to the interpreted continent ocean boundary (COB) and limits the eastward extent of the JMR and SRC domains (e.g. Figure 6a,c; Supplement 2).

Traditionally, these volcanic margins have been mapped as continuous features [e.g. *Skogseid and Eldholm, 1987, Gaina et al., 2009, or Peron-Pinvidic et al., 2012a*] but our mapping suggests that they are formed by distinct igneous complexes and breakup segments (Figures 9a; 10; 11a). The igneous complexes along the margins are characterized by chaotic seismic reflection patterns, shallow sill and dyke intrusions, and possible sheeted dyke features (Figures 6; 9a; 10; 11; Supplement 6). Multiple reactivation of an igneous complex tied to fracture zones can be seen in Figure 6b, where deposits from several volcanic episodes are stacked vertically, rather than in a typical seaward progression as in Figure 6a,c. Some of these complexes appear semi-circular and have possibly formed volcanic cone structures in shallow marine environment, as they are covered by pro-grading reflectors that could relate hyaloclastite - volcanoclastic depositional patterns (Figure 10; Supplement 6).

The outer highs of the primary volcanic margin were correlated with the segmented Early Eocene chron C24 magnetic anomaly (Figure 6a,b), previously defined as geochron C24B (56-53 Ma) by [*Skogseid and Eldholm, 1987*]; or C24r (~55 Ma) by *Gaina et al.* [2009] and *Gernigon et al.* [2015]. The first continuous magnetic anomaly is interpreted as C24 or C24n3n (~53,4 Ma) by *Gaina et al.* [2009] and *Gernigon et al.* [2015] (Figure 6a-c). C24 straddles the two outer SDRs units (Figure 6a-c), which represent subsequent younger events during breakup, as they are onlapping onto the primary volcanic margin and the older SDR units. Close to the main segment of the EJMFZ the normally eastward pro-grading outer SDR units appear to stack on top of each other, as a distinct and longer-lived volcanic system developed right at the termination of that fracture zone (Figures 6b; 9a; 10). Typical SDR wedges disappear towards the south and south of the CNBFZ, and recognizable only across the northernmost two ridges of the SRC (Figures 6c; 9a; 10).

The primary volcanic margin and oldest oceanic basement has a seismic velocity range of 4,8 – 5,5 km/s, whereas the inner SDR units have a slightly lower velocity range of 3,2 – 4,3 km/s, comparable to the Vøring and Møre margins [*Blischke et al., 2019*]. A high velocity layer of 4,8 – 6,8 km/s between seismic reflection markers R1 and R2 might correspond to the oceanic layer 2 with irregular seismic reflectors right next to the COB (Figure 4b; 6; Supplement 2). Similar patterns and velocity ranges have been associated with lower crustal bodies (LCBs) observed beneath volcanic margins of the JMMC, East Greenland, Møre and Vøring [e.g. *Weigel et al., 1995; Breivik and Mjelde, 2003; Breivik et al., 2008, 2012; Faleide et al., 2010; Gernigon et al., 2015; Mjelde et al., 2016; Theissen-Krah et al., 2017; or Zastrozhnov et al., 2018*].

Seafloor samples from the northern JMR have no age assignment but appear related to younger volcanic activity as their basaltic to trachybasaltic composition (SiO₂ 45 – 49 wt%) aligns them with the JMFZ, Vesterise seamount, or Early Eocene Blosseville Kyst (Prinsen af Wales Bjerger formation) [*Haase et al., 1996; Debaille, V., 2009;*] (Figure 7). This correlates well with syn-breakup volcanic activity during the formation of the Early Eocene volcanic margin along the northern JMR domain and especially intrusive complexes within the JMB (Figures 6a).

The SRC seafloor samples were placed in a stratigraphically consistent order along the available dredge profile with an estimated age range between 59,2 and 47 Ma [*Polteau et al., 2012, 2018*]. This age range correlates the dredged igneous samples within the plateau and SDR basalts (see JMT flanks on Figure 6c) [*Blischke et al., 2019*]. Their geochemical composition however is different from the Vøring main SDR and Lower Series basalts, or the Blosseville Kyst lower basalt and plateau basalt series within the TAS classification diagram (Figure 7a).

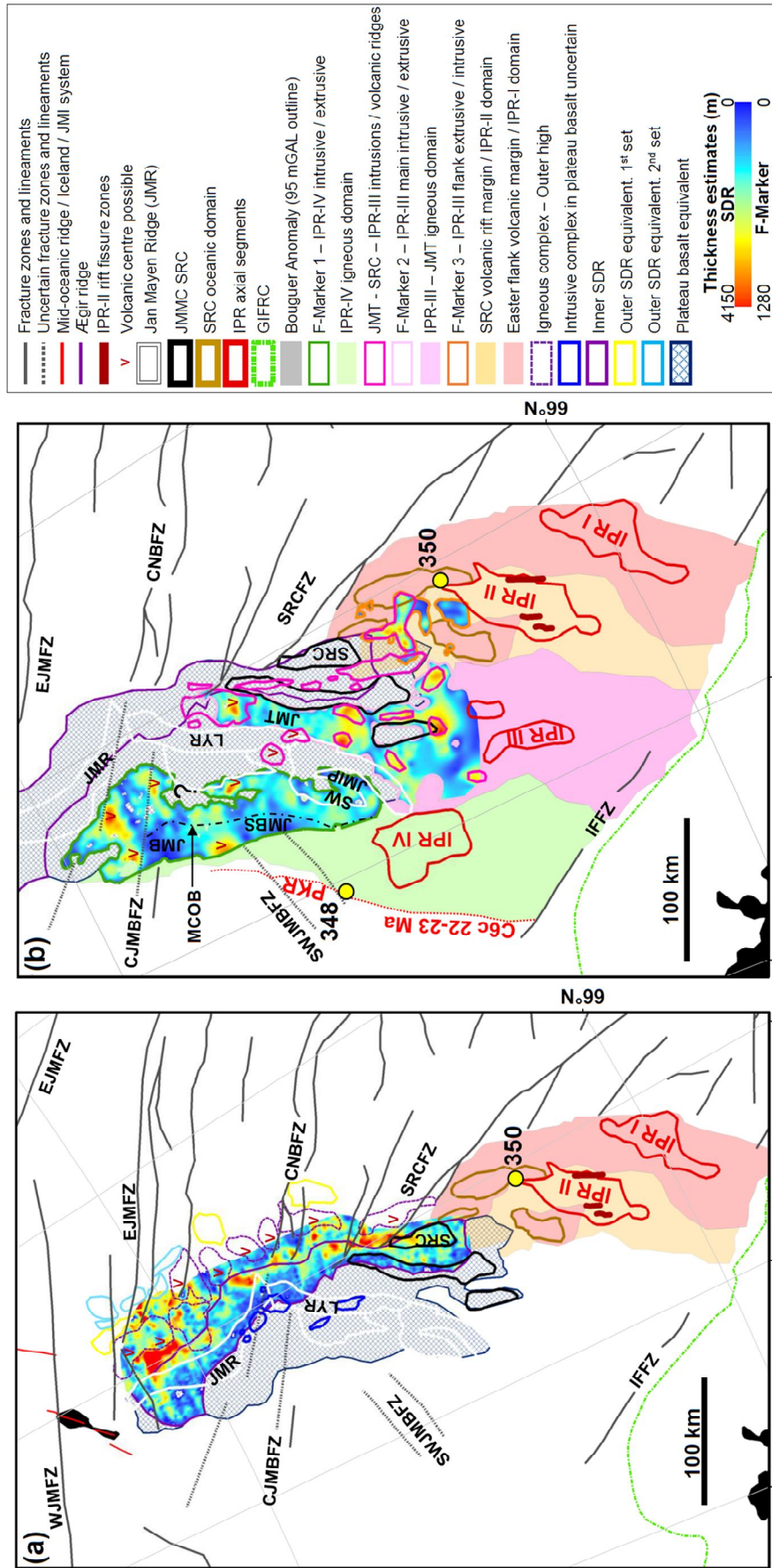


Figure 9. Stratigraphic thickness estimates of JMMC volcanic provinces on a magnetic intensity anomaly data grid [Nasuti and Olesen, 2014]. (a) Early Eocene breakup SDRs volcanic margin. (b) Thickness estimate of Eocene to Early Miocene flood basalts within the F-Marker region. Fracture zones modified from Gernigon et al. [2015] and Blischke et al. [2017a, 2019]. Abbreviations: CJMBFZ – central Jan Mayen basin fracture zone; CNBFZ – central Norway basin fracture zone; EJMFZ – East Jan Mayen fracture zone segments; IFFZ – Iceland-Faroe fracture zone; JMB – Jan Mayen basin; JMBS – Jan Mayen basin south; JMR – Jan Mayen ridge; JMT – Jan Mayen trough; MCOB – possible western microcontinent ocean boundary; PKR – proto-Kolbeinsey ridge; LYR – Lyngvi ridge; SRC – Southern ridge complex; SRCTFZ – Southern ridge complex transfer fracture zone; SWJMBFZ – Southwest Jan Mayen igneous province; SWJMBFZ – Southwestern Jan Mayen basin fracture zone; ÆR – Ægir ridge.

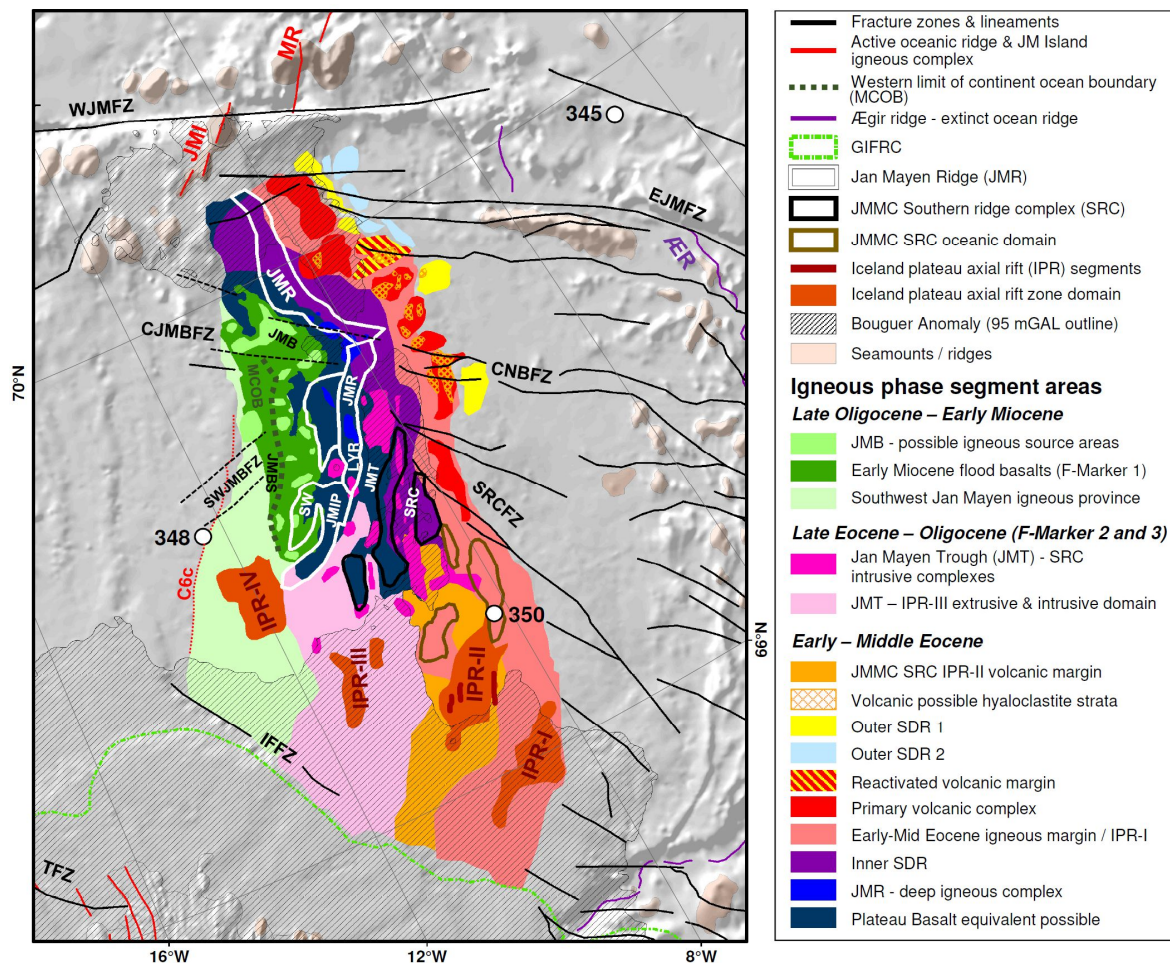


Figure 10. Jan Mayen microcontinent volcanic facies and provinces map in order of emplacement: Early-Middle Eocene; Late Eocene – Oligocene; and Late Oligocene – Early Miocene, showing the igneous facies types and units, such as intrusive and extrusive strata, plateau basalt equivalent, igneous centres, SDRs, hyaloclastite volcanic strata, flood basalts. Abbreviations: CJMBFZ – Central Jan Mayen basin fracture zone; CNBFZ – Central Norway basin fracture zone; EJMFZ – East Jan Mayen fracture zone segments; IFFZ – Iceland-Faroe fracture zone; IPR – Iceland plateau rift; JMI – Jan Mayen Island complex; JMB – Jan Mayen basin; JMBS – Jan Mayen basin southern segment; MCOB – Western margin continent ocean boundary; JMR – Jan Mayen ridge; JMT – Jan Mayen trough; LYR – Lyngvi ridge; MR – Mohns ridge; SRCFZ – Southern ridge complex fracture zone; SRC – Southern ridge complex; SWJMBFZ – Southwest Jan Mayen basin fracture zone; SWJMIP – Southwest Jan Mayen igneous province; TFZ – Tjörnes fracture zone; WJMFZ – Western Jan Mayen fracture zone; ÆR – Ægir ridge.

The SRC seafloor samples are best placed into the later-stage volcanism during the Early Eocene during the formation of the JMMC eastern flank volcanic margin and SDRs, and alike the northern JMR seafloor samples. Therefore, the placement of these samples within the syn-breakup igneous strata is inferred, and tentatively assigned an age range estimate in between $\sim 55\text{--}52 \pm 1$ Ma (Ypresian, Early Eocene) within the SDR sequence JM-60. This is correlative with the Prinsen of Wales Bjerge formation (54 – 53 Ma) of the Blosseville Kyst [Larsen, L.M. et al., 1985, 1989, 2013], or the intrusive phase (56–54 Ma) described by Tegner et al. [2008] just south of the Kangerlussuaq Fjord southwest of the JMMC (Figure 12). Based on this correlation, it seems probable that the SDR formations originally reached across the southern extent of the JMMC domain towards central East Greenland, which has since been affected by several erosive events that influenced the entire region by removing approximately 2-3 km volcanic section [Mathiesen et al., 2000; Japsen et al., 2014; Blischke et al., 2019] (Figures 4; 11a; 12).

5.3 The initial rift transfer phases of IPR-I and IPR-II

Along the eastern JMMC margin, a second and third phase of igneous activity coeval with seismic units JM-50 and JM-40 that overly the igneous complexes (outer highs) of the primary eastern volcanic margin, including the inner SDRs of stratigraphic unit JM-60. Here this unit is referred to as the Early-Mid Eocene igneous strata (Figures 2; 5c; 6; 9a; 10). This phase of igneous activity appears to represent a period of enhanced volcanism with post-SDR lava flows, volcanoclastic extrusion and sill and dyke intrusion along the entire eastern flank, around the SRC ridges, and specifically around the south-eastern and southern end of the JMMC.

5.3.1 The Eocene igneous strata and Iceland plateau rift I – IPR-I

The IPR-I rift system is considered to have formed the two southeasternmost blocks of the SRC. Thus, forming a volcanic margin that overlapped onto the three northern SRC blocks. A volcanic margin estimated to have been active during Early Eocene (52 to ~50 Ma) (lower JM-50 unit) (Figures 2; 6d; 9a; 10). This igneous phase included the extrusion of lava flows, possibly interlayered with volcanoclastics, dyke and sill intrusions associated with small scale faulting within the blocks of the JMR and SRC (e.g. Figures 5c; 6b,d; Supplement 6a-iii,a-iv; b). The IPR-I domain forms the south-eastern end of the SRC (Figure 9) and is characterised by high-amplitude irregular seismic reflective patterns that dip towards the Ægir ridge domain that shows an increase in seismic velocities 4,8 – 5,5 km/s within the basaltic strata [Blischke *et al.*, 2019] (Figures 5c; 6d; Supplement 6a-ii; b). This succession of the SRC volcanic margin overlies the SDR (JM-60) and plateau basalt units (JM-70) that would have been part of the original eastern breakup margin that is buried and hard to see below the IPR-I volcanic (Figures 6d; 9a; 10; Supplement 6b).

5.3.2 The Iceland plateau rift II – IPR-II

This was followed by the axial rift IPR-II that intersected into the Jan Mayen SRC, eastern volcanic margin, and the IPR-I domain during Early-Mid Eocene (~49 – 40 Ma) (upper JM-50 and JM-40 units) by normal and transpressional faulting followed by oblique extension, the forming of axial rift systems, wide spread dyke and sill intrusives into the adjacent blocks and strata, and small scale lava flows into the adjacent graben areas (Figures 1; 2; 5c; 6d; 9a; 10). Sills and small intrusive bodies are seen on seismic reflection data within the Early to Mid-Eocene sediment section that have deformed or uplifted the across the area mapped Mid-Eocene unconformity (ME on Figure 2) and are place within this IPR-II igneous activity time frame. This is primarily seen along the south-eastern and southern SRC margin, where the ME control marker is uplifted or deformed, and Late Eocene stratigraphic units are infilling these small features later in time (Figure 6d).

The ME unconformity therefore serves as a control marker that has been dated around 43 ± 3 Ma, which is based on seafloor samples recovered from the north-western Jan Mayen ridge [Sandstå *et al.*, 2012], the SRC [Talwani *et al.*, 1976e; Polteau, *et al.*, 2018], and tied to the stratigraphic framework of the JMMC [Blischke *et al.*, 2019]. IPR-II timed activity occurred furthermore coeval with the production and accumulation of ash deposits that are preserved in the sediment record of the surrounding DSDP boreholes [Talwani *et al.*, 1976a-e].

The IPR-II segment, located west of borehole DSDP site 350, is visible on gravity and magnetic data as well, which shows structural trends that are aligned with a faulted graben, with indications of increased volcanic activity of fault parallel dyke and shallow sill intrusives (Figures 1; 5c; Supplements 6b; 7). Across the same IPR segment high-resolution bathymetry data confirm these visible trends as volcanic ridges. These volcanic ridges vary in length between 20 km to about 40 km and up to 10 – 15 km in width, representing volcanic conduits that were probably localised source areas for these volcanic events (Figures 1; 5c; 6d).

5.3.3 Age and petrology

The IPR-I and IPR-II activity was originally placed combined into an age range between 50 – 33 Ma (Mid- to Late Eocene) based on the core data analysis of DSDP site 350 by *Kharin [1976]*. *Raschka et al. [1976]* inferred that by considering the paleontological record of the overlying sediments, the basalt most likely was emplaced no later than 40-44 Ma. This narrowed the age range of this igneous event to at least 50 and 40 Ma and fits into the overall volcano-stratigraphic framework for IPR-I and IPR-II combined.

The phase separation was assigned based on seismic reflection data records, where a clearly visible intersection of the IPR-II into the older domains of the SRC could be seen and DSDP site 350 was tied into that interpretation (Figures 7; 8; Supplements 3-5; 6b). Here, the core records show an IPR-II timed sill or dyke intrusive that is in contact with an apparently older and heavily altered basalt-breccia unit that is seismic stratigraphically assigned to IPR-I.

The DSDP site 350 age results of $\sim 49,28 \pm 0,3$ Ma to $44,05 \pm 0,21$ Ma is similar to the intrusive activity described by *Tegner et al. [2008]* for the Kangerlussuaq Fjord area of 50–47 Ma, or the Igtertivâ formation emplacement age range ($\sim 49 - 43$ Ma) at Kap Dalton [*Larsen, L.M., 2013*]. Evidence that all three areas were volcanically active during the Early to Mid-Eocene, when the oblique IPR-II and GIFRC systems formed (Figures 10b).

The sampled intrusive section of IPR-II compares geochemically to MOR basalts and the Blosseville Kyst plateau basalts (Figure 6a). The MgO vs. TiO₂ (wt%) and MgO vs. K₂O (wt%) comparison of the sill intrusion shows a good correlation to the data trends of the Blosseville Kyst with its the Igtertivâ formation, as well as more recent volcanics within the Northern volcanic zone of Iceland, and the Faroe Island syn-breakup series compositions (Figure 6b,c). The basalt breccia of the IPR-I is more influenced by alteration and aligns within the Jan Mayen fracture zone and Jan Mayen igneous complex trend (Figure 6).

5.4 Rift transfer and magmatic incursion of IPR-III

Rift transfer to the west of Iceland plateau rift I and II along the Iceland-Faroe fracture zone occurred between the Late Eocene and Late Oligocene in association with the formation of the igneous domains that are referred to as the Iceland plateau rift III (IPR III), the Jan Mayen trough, and the south-westernmost extent of the JMMC, also referred to as the south-western Jan Mayen igneous province (SWJMIP) that coeval with seismic units JM-35 to JM-20 (Figures 1; 2; 5b,d ; 6c; 9b; Supplements 2; 6a,c).

The IPR-III domain is aligned parallel to the JMT and SRC, specifically the JMT an extensional graben structure that became massively intruded by volcanic ridges into the Late Oligocene (Figures 5b; 6c; 9b). The alignment of these volcanic ridges with the underlying bouguer gravity anomaly implies that deeper intrusive activity extended from the Iceland shelf to the SRC domain (Figures 9b; 10; Supplement 7b), which suggests extensive igneous activity within the area during the rift relocation from east to west along the southern extent of the microcontinent.

During this time interval, there was a substantial increase in sill and dyke intrusions. Volcanic ridges close to major fault zones can be observed within the JMT and in between the SRC block that align with bouguer gravity and magnetic anomalies (Figures 5b; 6c; 9b; 10; Supplement 6a-viii), especially at the intersection of the Jan Mayen trough and the SRC transfer fracture zone (SRCTFZ on Figures 1; 5b; 6c).

Generally, the MOU is deformed by faulting and intrusive features and overlain by extrusive strata that is located below the Top Paleogene unconformity event (TPU) (Figures 6c; 9b). The Jan Mayen trough and the southern end of the Lyngvi ridge show increased intrusive complexes that appear to expand and cut into the JMMC domain by separating the SRC from the main ridge, thus forming the JMT and SWJMIP (Figures 8c, 9b; 10). This opening of the Jan Mayen trough – IPR-III and SRC block domains occurred in an oblique motion towards the southeast and parallel to the dextral SRC fracture zone that accommodated the formation of north-southerly striking fault and graben zones internally seen sinistral strike-slip faults that appear strike parallel to the volcanic ridges, as demonstrated by *Blischke et al.* [2020b].

5.4.1 Correlating key unconformities and igneous features

Key extrusive and intrusive bodies were mapped in reference to the MOU and TPU, as no age or petrological control from borehole data exists to otherwise correlate these events to each corresponding volcanic domain (Figures 2; 5b,d; 6c; Supplements 2; 6b,c). The formation of both the MOU and TPU created distinctive flat-topped topography across the main JMR as well as the highest parts of the SRC. Unconformities that were logged in borehole and seafloor records and tied to seismic stratigraphic data [*Talwani et al.*, 1976a, 1977; *Sandstå et al.*, 2012, 2013; *Blischke et al.*, 2017a, 2019] (Figures 6-8).

Volcanic ash layers are present within Late Eocene to Late Oligocene (~43-30 Ma \pm 4 Ma) sediments in DSDP boreholes 346, 347, 349 and 350. In contrast ash layers are absent in the Oligocene sediment sections of DSDP350 sites above that (~35-23 Ma), which is based on the core analysis by *Talwani et al.* [1976a-e, 1978] or *Sylvester* [1975, 1978]. This suggests that primary volcanic and phreatic activity shifted from east to west during that timeframe, which would also correlate to the third intrusive activity phase between ~37-35 Ma just south of the Kangerlussuaq Fjord area that was described by *Tegner et al.* [2008].

An east-to-west shift of igneous activity can be seen by tracing the extrusive horizons in reference to the key unconformities, here referred to as flood basalt events. The first flood basalt marker is called the “F-Marker 3”, a flat laying lava flow events within the Late Eocene to mid-Oligocene interval. The next shallower flood basalt or flat laying intrusives event is referred to as the “F-Marker 2” located within the mid- to Late Oligocene stratigraphic interval that is widely seen within the JMT – IPR-III rifting domain (Figures 2; 5d; Supplement 6d-viii;c).

F-Marker 3

Horizon “F-Marker 3” aligns to the undeformed MOU in between the SRC blocks and overlies the Early-Mid Eocene strata of the SRC volcanic margin and IPR-I and IPR-II domains but is obscured by younger igneous events within the JMT (Figures 2; 9b). Its mappable extent covers approximately 1250 km². On seismic profiles, F-Marker 3 is characterised by a relatively flat-lying hummocky-to-irregular seismic reflection that locally infills smaller graben areas connected to a series of small intrusive features. These grabens contain up to 2.5 km of fill including igneous material (Figure 9b). Possible Late Eocene to mid-Oligocene faulting, smaller-scale intrusions and vents can be observed within the faulted southernmost SRC segments, IPR-I and IPR-II domains during the same time interval, which implies that the IPR-III activity affected a wider area into the adjacent older SRC segments by faulting, intruding and deforming the older domains.

F-Marker 2

The mid- to Late Oligocene extrusive and intrusive features of horizon “F-Marker-2” (Figures 2; 5b,d; 9b; Supplement 6a-viii) spreads out within the JMT, and is manifest as a strong seismic reflection event covering an area of approximately 8100 km², which terminates against the rotated fault blocks and structural highs of the Lyngvi ridge, SRC western margin; and faulted blocks of the IPR-II (Figure 5b,d). The interval below F-marker 2 is almost opaque due to the strength of this reflector, masking most of the underlying structure. The true stratigraphic thickness for this interval ranges mostly from 0,1 to 1,8 km but increases up to 3,5 km close to possible igneous complexes or volcanic ridges within the Jan Mayen trough (Figure 9b).

The in-part irregular and hummocky structure of the F-Marker 2 is possibly related to flood basalt that were emplaced in a wet environment, or the flow intruded into unconsolidated and wet sediments, flowing along a consolidated unconform surface below it. As sub-basalt seismic reflection data imaging has not improved for this area, despite various re-surveying of the area since 1978 and no borehole control exists either, does this question remain unanswered. However, it is clear that this area forms its own seismic stratigraphic igneous domain belonging to the IPR-III phase.

5.5 The western igneous margin, and IPR-IV to the Kolbeinsey ridge transition

The last rift-transfer phase is tied to the western margin of the microcontinent and the Iceland plateau rift system IV (IPR-IV) at the south-westernmost extent of visible JMR segments. The western JMMC margin was rapidly stretched during the Late Oligocene which resulted in the formation of the northern and southern segments of the Jan Mayen basins (JMB and JMBS on Figure 1). The formation of this igneous domain represents the last rift-transfer phase between central East Greenland and the JMMC during Late Oligocene and Early Miocene (Figure 2). Its western boundary is marked by the first clear magnetic anomaly chron 6c (23,3-22,5 Ma), which is tied to DSDP borehole 348 (Figures 1; 7b; 10c; Supplement 4). Within this domain, dyke and sill intrusives, igneous complexes and regionally extensive flood basalts are identifiable on seismic reflection data (Figures 4b; 5d; Supplements 6a-vii; 6b). The IPR-IV represents the largest of the igneous centres within the

domain on seismic reflection data in comparison to gravity and magnetic anomalies that occur right across to the central East Greenland igneous centre that has been mapped on seismic reflection data, aligning with the igneous breakup margin along the Blosseville Kyst shelf that is estimated to have been active around ~24 Ma [e.g. *Talwani et al., 1977; Blischke et al., 2017a; 2018*] (Figures 1; 4; 9b; 10; 11; Supplement 7). The mapped flood basalts, herein referred to as “F-Marker 1” that is coeval with seismic unit JM-15, and onlaps onto the JMMC structures and older igneous domains (Figures 2; 4b; 5d Supplement 2b,c). These basalts formed prior to the first MORB of the Kolbeinsey ridge that were drilled in borehole 348 but overlie the IRP-III – Jan Mayen trough domain and older strata (Figures 4b; 5d; 9b; Supplements 2; 4; 5; 6b).

5.5.1 *The western igneous domain*

This domain is formed by the northern and southern Jan Mayen basin segments that are subdivided by the central Jan Mayen basin fracture zone (CJMBFZ), which is in alignment with the central Norway basin fracture zone (CNBFZ) (Figures 9; 10; 11). Both segments form part of the JMMC’s western breakup margin but are different in their structure, crustal thickness, and igneous character (Figures 1; 4b; 6a; Supplements 2b,c; 6b; 7). The entire western flank of the JMMC is strongly faulted into several westward-rotated fault blocks along fault segments that have partly slid into the Jan Mayen basin, forming half-graben and small graben structures. Most of the faults and tilted features are overprinted by intrusive strata [*Blischke et al., 2017a, 2019*] (Figures 4b; 6a). Within the Jan Mayen basin, the crustal thickness varies between 6-12 km based on different seismic refraction datasets [*Olafsson and Gunnarsson, 1989; Kodaira et al., 1998a; Blischke et al., 2017a, 2019*] and reflect a contrast to the JMR and the adjacent Kolbeinsey Ridge domain on gravity and magnetic datasets as well (Figure 1; Supplements 6b; 7). This deep and extended basin represents most likely a pull-apart basin that opened in between the nearly E-W striking CJMBFZ and the western Jan Mayen fracture zone (WJMFZ) during this phase, which aligns with the NE-SW stringing normal fault system and orientation of the north-western JMR margin (Figures 10-12).

A larger contrast in seismic-refraction velocity data has been recorded (>6,8 km/s) just beneath the heavily rotated and thinned western JMMC fault blocks within the southern segment of the Jan Mayen basin (JMBS) (Figure 1; 4b; Supplement 2b,c) that aligns with a negative magnetic anomaly change, and possible underplating underneath the JMMC’s western-southwestern flank. Additionally, there is an increase in bouguer gravity values (>130 mGAL) in contrast to the JMR (Figures 1b; Supplement 2b,c). These changes in geophysical properties outline an area of the JMBS that lies north of the IPR-IV and south of the CJMBFZ, along the western margin of the SWJMIP and Lyngi ridge areas and across the volcanic complexes of the initial Kolbeinsey ridge (Figures 10; Supplement 7). An area that is bound by the nearly east to west striking CJMBFZ to its north and cross-cut by the SW-NE striking southwestern Jan Mayen basin fracture zone (SWJMBFZ). That fracture zone has the same trend as the Spa fracture zone (SPFZ) at the Kolbeinsey ridge at present day and connected originally to the southern extend of the Blosseville Kyst at the time of breakup during Late Oligocene to Early Miocene (Figures 1; 10; 11; 12).

The flood basalts – F-Marker 1

The F-Marker 1 flood basalts mark the Early Miocene top of seismic-stratigraphic unit JM-15 in the Jan Mayen basin (F-Marker 1 on Figures 2; 5d; 9b; Supplements 6a-vii,b). These flood basalts were mapped on seismic reflection data as flat-lying and almost opaque reflectors that filled the low areas of the Jan Mayen basin with a mappable aerial extent of approximately 9400 km². Lateral continuity of the flood basalts was subsequently disrupted by faulting during further extension within the Jan Mayen basin and was filled with Lower Miocene sediments. Seismic refraction data indicate a velocity range of 3.3–4.2 km/s across the western- to south-western areas of the JMMC indicating a basalt layer thickness of 270–470 m that varies across the basin (Supplement 6b). Thickness estimates increase up to ~4 km at locations where possible igneous centres developed and most likely served as source areas for the F-Marker 1 flood basalts within the Jan Mayen basin as fissure or axial rift segments could not be found as is (Figures 4b; 9b).

The mapped distribution of the F-Marker 1 basalts represents a minimum extent based solely on available seismic reflection data; the true limit of the basalts might lie farther west, where the proto-Kolbeinsey ridge oceanic crust was first formed. The latter was drilled by DSDP borehole 348 which recorded sub-aerial basaltic lavas of fine- to medium-grained crystalline olivine-tholeiite composition (Figures 7;8; Supplement 3;5) that correlates to the same petrological group of MOR-basalts as the Kolbeinsey ridge, Ægir ridge and Tjörnes transfer zone sample data (Figures 8).

The initiation of the Kolbeinsey ridge

A wedge-shaped package comprising a sub-horizontal to inclined reflection character is visible on seismic reflection data (e.g. Figure 4b) that appear to onlap onto the severely extended and rotated fault blocks of the JMMC's western margin. The correlation of the F-Marker 1 to the top-most horizon of the wedge-shaped package might suggest that it represents SDR units. The latter might have been sourced from igneous complexes along the western breakup margin outlining a possible microcontinent ocean boundary (MCOB) (Figures 4b; 9b). The flood basalts are better imaged on post-2011 seismic reflection data and appear to be consistent across the central Jan Mayen basin, just south of the CJMBFZ (Figures 9b; 10). Here, a volcanic centre probably formed approximately at the northern extend of the SWJMBFZ intersection, right before, or during the first seafloor spreading on the Kolbeinsey Ridge. This feature aligns with chron 6c (23,3–22,5 Ma) and has a confirmed tie to an igneous complex system based on seismic refraction and reflection data (Figures 6b; 10; 11c). Furthermore, does the reconstruction to the central East Greenland shelf margin fit as a conjugate well into the arched shape of the western JMR-JMB margin. Thus, suggesting that the wide central East Greenland shelf margin represents a complex Eocene-Miocene igneous breakup margin that would move the location of the COB by definition eastward to the second breakup phase during Early Eocene (Figure 4).

5.6 The post-breakup Neogene-Quaternary oceanic phase

The oceanic domain west of the JMMC formed with the establishment of the Kolbeinsey ridge from the time of anomaly chron 6c (Figures 10; 11c). Igneous activity decreased along the microcontinent, which established its present structural and physiographic configuration (Figures 10; 11c). The record of Neogene volcanic activity is preserved in the DSDP and ODP borehole sites in the JMMC area, including interbedded volcanic ash and tuff layers within the deep-marine sediments [Talwani *et al.*, 1976a-e; 1977; Sandstå *et al.*, 2012, 2013; Blischke *et al.*, 2017a]. Seafloor basalt samples of the northern JMR fall into the same geo-chemical trends for the JMFZ and JMI (Figure 8). As no age data are available for these seafloor samples [Haase *et al.*, 1996], it is difficult to assign these to the youngest igneous domain. However, known seafloor sample age data for the JMMC's western-northwester breakup margin show an age range between 13,2-0,1 Ma [e.g. Fitch *et al.*, 1965; Campsie *et al.*, 1990; Davis *et al.*, 1996; Mertz *et al.*, 2004]. The provenance of these volcanic ash layers remains to be fully determined; i.e. whether they originated from the Beerenberg volcano of the JMI [Fitch *et al.*, 1964], the Kolbeinsey ridge system, or the early sub-aerial volcanic systems of Iceland [Sæmundsson, K., 1979; Hjartarson *et al.*, 2017].

Even though the Iceland igneous system is by far more dominant than the JMI, the northern igneous margin has had an impact on the JMMC throughout the Neogene and Quaternary, e.g. cone-shaped volcanic systems breaking through the older Early to Mid-Eocene igneous margin (Figure 6a). This continuous volcanic activity along the microcontinent's northern margin can also be noted along the north-western steep flank of the JMR, where increased gravitational slumping and faulting from the steep ridge flanks are observed, alongside up to the seafloor reaching present-day active transfer graben fault systems [Blischke *et al.*, 2019]. This segment of the northern JMR appears to be tied to the bouguer anomaly area underneath the Jan Mayen Island igneous complex. An area that has been interpreted as oceanic-Iceland type crust that reaches up to 22 km thickness, which is based on gravity and seismic refraction data inversion [Haase and Ebbing, 2014; Kandilarov *et al.*, 2012] (Figures 1; 10; Supplement 7). The north-western igneous margin of the JMMC and the Eggvin bank areas all lie within that bouguer anomaly adjacent to the JMI, indicating a variable domain in composition and crustal structure, with crustal thickness ranging between 8-13 km, an elevated mantle temperature, and enriched mantle sourced that feeds into the northern Kolbeinsey ridge area [Tan *et al.*, 2017].

Interestingly does the highly extended northernmost section of the JMB rift graben cross the lowermost Bouguer anomaly domain (50-60 mGAL) (Figure 6a). Such bouguer anomaly variations have been investigated within spreading regimes elsewhere, such as the East Pacific rise, where density variations have been analysed through 3D Bouguer gravity anomaly modelling including the effects of variations in crustal thickness and structures [Wang *et al.*, 1996]. Significant changes in Bouguer gravity anomaly patterns were interpreted as "subcrustal", showing distinct gravity lows centred over axial rift segments. Possibly such lower Bouguer gravity anomaly domains (<95 mGAL) could be located close to younger axial rift areas for the JMI area in the north and the IPR anomalous areas in the south of the JMMC study area that intersected older microcontinent and Early Eocene plateau basalt and rift domains (Figure 10).

6. The JMMC igneous development: implications for the opening of the Northeast Atlantic

Seismic volcano-stratigraphy, tectonic and palaeogeographic reconstruction of the JMMC has unravelled complex igneous processes of parallel rift-systems within the Iceland plateau, early Kolbeinsey ridge, and Greenland-Iceland-Faroe ridge complex. Three reconstructed igneous-province maps linked to a regional stratigraphic correlation chart are illustrated in Figures 11; 12 in order to outline the relationship, described below, between the JMMC and its conjugate margins during the breakup process, which spans the interval between ~55 Ma to ~22 Ma. Structural trends, fracture zones, rift zones, igneous complexes, and hotspot locations are based on present-day features mapped on potential field data, detailed kinematic reconstruction models [Blischke *et al.*, 2017b], and published work from adjacent margins [e.g. Larsen, L.M. *et al.*, 1989, 1999; Pedersen *et al.*, 1997; Planke *et al.*, 2000; Skogseid *et al.*, 2000; Henriksen, 2008; Doubrovine *et al.*, 2012; Funck *et al.*, 2014; Hopper *et al.*, 2014; Gernigon *et al.*, 2015; Blischke *et al.*, 2016; Gaina *et al.*, 2009, 2017; Geissler *et al.*, 2017; Hjartarson *et al.*, 2017 and Horni *et al.*, 2017].

6.1 Pre-breakup phase

Pre-breakup and primary breakup igneous units have been mapped on both sides of the NE-Atlantic region (Figure 11a and Figure 12). The “Lower series flows” along the Vøring conjugate margin formed by igneous activity from ~67 to 59 Ma [e.g. Planke *et al.*, 2000; Abdelmalak *et al.*, 2016]; the “Lower Basalt” sections along the central East Greenland margin between ~63 Ma and 56 Ma [e.g. Larsen, L.M. *et al.*, 1989; Pedersen *et al.*, 1997]; and the pre-breakup Lower Faroe Island basalt group (FIBG) comprising the Lopra and Beinisvørð formations within the Faroe-Shetland region, from ca. 61 to 56 Ma [e.g. Mudge *et al.*, 2015; Ólavsdóttir *et al.* 2019]. The base of these pre-breakup basalt successions is commonly poorly imaged or not visible in seismic reflection data and thus difficult to constrain [e.g. Abdelmalak *et al.*, 2016; Ólavsdóttir *et al.* 2019]. The pre-breakup section consists of a mixture of intrusive rocks, lavas, volcanoclastic and hyaloclastic units; the latter can often be mistaken for prograding sedimentary successions on seismic-reflection profiles.

Thick hyaloclastic units have been drilled on the Faroe shelf at the deepest levels of the pre-breakup FIBG, which has hindered accurate recognition of the base of the FIBG [Ólavsdóttir *et al.* 2019]. Such ambiguity is also reflected in the uncertainty across the main JMR as to where to place the top of the pre-basalt and breakup section (Figure 4b; 6; Supplement 2). Rocks from the conjugate areas fall into the alkaline, felsic-to- mafic composition that suggests contamination with continental crust [Parson *et al.*, 1989; Tegner *et al.*, 1998; Larsen, L.M. *et al.*, 1999; Meyer *et al.*, 2009; Kokfelt and Ártung, 2014]. These igneous units would lie within the JMMC’s Paleocene – Early Eocene JM-70 chronologic time interval, and similar volcanic units would be expected to be present within the pre-breakup strata of the JMR. This cannot be confirmed as no drilling data exists, but velocity contrasts, seismic reflection data characteristics, here specifically the intrusive dyke swarm features along the eastern breakup margin within the pre-breakup sections of the JMR show a close analogy based on geophysical data (Figures 4b; 8; Supplements 2; 6a-i).

Palaeogeographic reconstruction (Figure 11a), shows the JMMC area aligned with central East Greenland and pre-breakup structural trends as seen in the Jameson Land basin. The JMMC was located 300-400 km NNE along-strike of the Faroe Islands region, and just south of the Vøring volcanic margin across the Pre-EJMFZ. The JMMC plateau-basalt-equivalent section aligns with the Blosseville Kyst and appears to increase in stratigraphic thickness towards the south, which includes the SRC block (Figures 6; 11a). In contrast, the Blosseville Kyst plateau basalt section thins towards north and onlaps onto the Jan Mayen igneous complex, just south of the JMFZ. This was also observed onshore by *Brook* [2011], who described a south-westerly-increasing trend in plateau basalt thickness from the Jameson Land basin, Scoresby Sund and Blosseville Kyst towards the Kangerlussuaq basin. The inland and northern areas show regional onlap onto structural highs with subsequent erosion, estimated at 2-3 km in central East Greenland [*Larsen, L. M. et al., 1999, 2014; Mathiesen et al. 2000; Passey, 2009; Passey and Hitchen., 2011; Ártung et al., 2014*].

The marked north-to-south increase in thickness of the pre-breakup lower series and plateau basalt sections of the Blosseville Kyst, from ‘not present’ to up to 6-7 km might represent a primary “source-centre” for the pre-breakup succession being located at the intersection of the Blosseville Kyst and the pre-IFFZ (Figure 11a). As the initial area of breakup between East Greenland, the Faroe Islands and JMMC has several NE-SW striking magnetic lineaments aligned parallel to possible contemporary active onshore igneous centres (Figure 11a). This focal area formed the first segment of the GIFRC, the onset of the IFFZ, and would have covered the southern extension of the JMMC as well. An area that is presently unresolved, as no seismic data coverage exists, but may lie beneath the northeast Iceland shelf and eastern Iceland.

At the time of breakup, the JMR and Jan Mayen basin were juxtaposed with the Blosseville Kyst and Scoresby Sund. Fault trends and a southwest-to-northeast magnetic anomaly pattern across the Geikie plateau appear to terminate against the microcontinent in an area of several possibly time -parallel or older intrusive complexes located within the pre-breakup strata (Figures 8; 11a). One of those is a large igneous complex just north of Kap Brewster and at the mouth of the Scoresby Sund area aligning with a strong magnetic anomaly trend that was confirmed by seismic reflection mapping [*Blischke and Erlendsson, 2018*] (Figure 11a).

The Geikie plateau magnetic trends, although covered by massive lava fields and glacial ice, are parallel to numerous magnetic anomalies between the Kangerlussuaq area and the Faroe Islands, potentially marking deep-seated fracture systems that served as pathways for upwelling magma. The right-stepping alignment of these anomalies and potential fracture systems would correspond to a left-lateral opening of that area, as already pointed out for the pre-IFFZ by *Guarnieri et al. [2015]*, thus linking the tectonic fabric to rising magma and emplacement processes for the initial breakup phase (Figure 12).

Such fracture-zone-influenced magma emplacement can be seen on seismic reflection, gravity and magnetic anomaly data along the EJMFZ (e.g. Figure 5a; 6b), which was part of the early Jan Mayen Fracture Zone (JMFZ) system during Early Eocene (Figure 11a). In contrast to the south of JMMC, here the pre-IFFZ aligns with the Kangerlussuaq area across to the Faroe Islands platform and Fugloy ridge into the Møre margin. Associated with this trend are several possible igneous centres that might have formed an initial volcanic breakup margin that would have preceded the formation of syn-breakup SDR formations (Figure 11a,b).

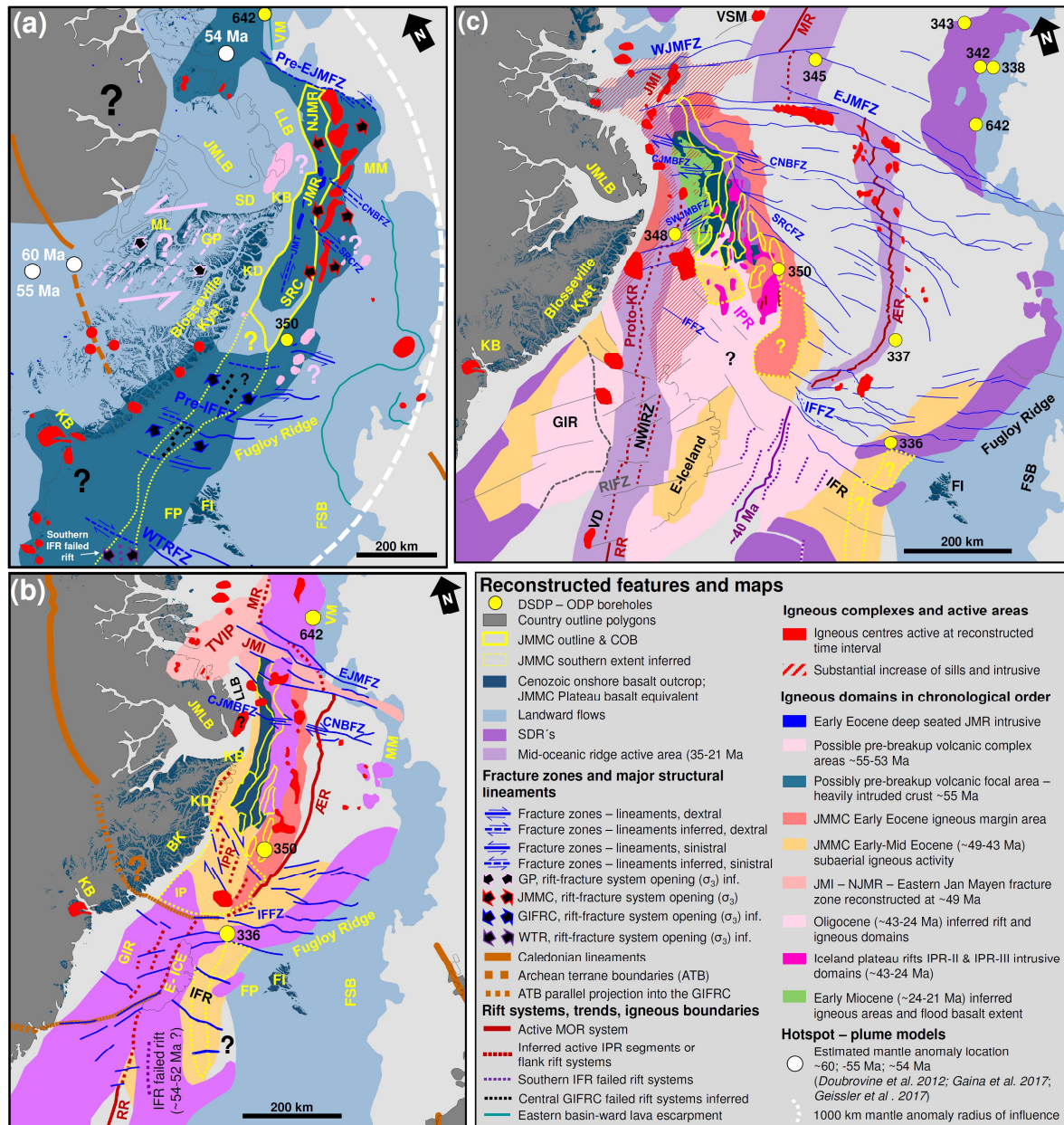


Figure 11. Reconstruction of the possible igneous province's maps for the Northeast Atlantic, where the positions of Eastern Greenland and the Jan Mayen main tectonic blocks are shown in an absolute position (relative to the mantle) according to kinematic parameters that were computed by carrying out visual fits (in GPlates 2.0.0; <https://www.gplates.org>) for the (a) pre-breakup (~60-54 Ma), (b) syn-breakup to drift phase (~55-49 Ma) and (c) final breakup phase along the western JMMC margin (~33-22 Ma) and the full formation of the Kolbeinsey Ridge. Features displayed are modified from data and interpretations by Larsen, L.M. et al. [1989, 1999]; Pedersen et al. [1997]; Planke et al. [2000]; Henriksen [2008]; Doubravine et al. [2012]; Funck et al. [2014]; Hopper et al. [2014]; Gernigon et al. [2015]; Blischke et al. [2016]; Gaina et al. [2009, 2017]; Geissler et al. [2017]; Hjartarson et al. [2017] and Horni et al. [2017]. Abbreviations: ÆR – Ægir ridge, CJMBFZ – central Jan Mayen basin fracture zone, CNBFZ – central Norway basin fracture zone, E-ICE – East Iceland, EJMFZ – East Jan Mayen fracture zone segments, FI – Faroe Islands, FSB – Faroe-Shetland basin, GIFRC – Greenland-Iceland-Faroe ridge complex, GIR – Greenland Iceland ridge, GP – Geikie plateau, IFFZ – Iceland-Faroe fracture zone, IFR – Iceland-Faroe ridge, JMB – Jan Mayen basin, JMBS – Jan Mayen basin south, JMI – Jan Mayen island igneous complex, JMLB – Jameson Land basin, JMR – Jan Mayen ridge, JMT – Jan Mayen trough, IPR – Iceland plateau rift, K – Kangerlussuaq, KB – Kap Brewster, KD – Kap Dalton, KR – Kolbeinsey ridge, LLB – Liverpool Land basin, MR – Mohn's ridge, NJMR – northern Jan Mayen ridge, NWIRZ – Northwest Iceland rift zone, RIFZ – Reykjanes-Iceland fracture zone; SD – Scoresby Sund, SRC – Southern ridge complex, SRCFZ – Southern ridge complex transfer fracture zone, SWJMBFZ – Southwest Jan Mayen basin fracture zone; TFZ – Tjörnes fracture zone, TVIP – Traill Ø-Vöring igneous complex, VD – Vesturdjúp rift zone; VSM – Vesteries seamount, VT – Vindtoppen formation, WJMFZ – Western Jan Mayen fracture zone and WTRFZ – Wyville-Thomson Ridge fracture zone.

Old structural trends and hyper-extended crust may represent potential zones of the mantle reaching up shallow, alongside magmatic material rising up through weaker and segmented crust, and thus may be preferred focal points for hot-spot upwelling and initial areas for mid-oceanic ridge segment formation [Schiffer *et al.*, 2018, 2019; Mordret *et al.*, 2018]. The plume or hot-spot locations modelled by *Dobrovine et al.* [2012] coincide with the starting point of the SW-NE-trending magnetic anomaly zone (Geikie plateau trend) that terminates right at the intersection point between the main Caledonian front and Archaean boundaries. This could suggest a deep structural weak zone that the upwelling mantle would have interacted with between 60-55 Ma [*Dobrovine et al.*, 2012] (Figure 11a).

The Trail-Ø region and Vøring margin were linked through the JMFZ and the northernmost area of the JMMC (Figure 11a,b). The SW-NE-striking Geikie plateau trend appears to align parallel to the magnetic trend seen at the Trail-Ø volcanic igneous province but is offset by the Proto-JMFZ. The modelled plume location for 54 Ma by *Gaina et al.* [2017] suggests a strong fluctuation of the mantle anomaly, thereby implying a much wider area of influence of the mantle anomaly piercing into the overlying weakened structural framework, and initiation of crustal rupture to the south and north of the JMMC. This being an area that has been described to show increased underplating, lower crustal body (LCB) formation, and large-scale fracture zone “magmatic leakage” [e.g. *Abdelmalak et al.*, 2017; *Gernigon et al.*, 2019]. Possible underplating has been recorded underneath the microcontinent as well adjacent to the projected microcontinent-ocean boundary and along its igneous breakup margins (Figure 4b; 6; Supplement 2).

Mapped igneous centres along the eastern flank of the JMMC appear semi-en-echelon in a left-stepping direction, which would require a linked right-lateral transfer system along the JMFZ (Figures 10, 11a). This could explain why the initial breakup margin formed along the north-eastern edge of the microcontinent, which later developed into the obliquely-opening Ægir ridge, with the Norwegian shelf margin moving south-eastward and the JMMC north-westward along the JMFZ. Consequently, this led to the formation of an extensional area south of the JMFZ with developing igneous centres and gradually subsiding eastern JMMC margin (Figure 11a,b). This hypothesis would require a transpressional region north of the JMFZ, which would be elevated just as the Vøring igneous margin remained a bathymetrically elevated area during Early Eocene, where the breakup unconformity of the top volcanics has been recorded around ~55 Ma (Figure 12).

6.2 Syn-breakup to drift phase

The syn-breakup to drift phase is dominated by the formation of SDRs and ocean crust along the Ægir ridge, within the Norway basin (Figure 11b). The eastern JMMC flank is overlapped by sets of SDRs and aligned by distinct igneous complexes that form the primary breakup margin. The geochron estimate of chron C24r (~55 Ma) matches the mapped inner SDR sets that are tied to the termination of one of the EJMFC segments. The first oceanic domain chron C24n.3n (~53,4 Ma) correlates to the outer SDR sets corresponding to the onset of ocean forming spreading and drift phase within the Norway basin [e.g. *Skogseid and Eldholm*, 1987; *Gaina et al.*, 2009; *Gernigon et al.*, 2015] (Figure 6a-c).

These early Ypresian (55–52 Ma) syn-breakup volcanics are well known from the conjugate areas of the microcontinent and have been confirmed by rock sample data of the Vøring plateau, and are mapped based on seismic reflection data for most breakup margin areas for the Northeast Atlantic area [e.g. *Planke et al., 1994; Passey and Jolley, 2009; Gaina et al., 2009; Gernigon et al., 2015; á Horni et al. 2017; Geissler et al., 2017*] (Figures 11b; 12).

The thickness variation of the JMMC's SDRs stratigraphic unit reflects the initial syn-breakup row of volcanic systems that formed along the eastern JMMC breakup margin and close to fracture zone segments (e.g. EJMFZ or SRCFZ) that facilitated the segmented separation of the microcontinent from the Norway basin (Figures 9; 10; 11b; 12). The southernmost blocks of the SRC are overlain by a younger Early- to Mid-Eocene volcanic margin, which obscures underlying igneous strata (Figures 5c; 6d; Supplement 2c). The underlying lava flow units have semi-parallel reflector signatures and amplitude contrasts of classic SDR's or landward flow lava units. Thus, the SRC Early- to Mid-Eocene igneous margin relates primarily to the formation of the southern Ægir ridge interaction with the developing IPR and southern JMMC. Furthermore, this area would have been the direct conjugate igneous margin to the Blosseville Kyst (Figure 11b).

The SDRs along the East Greenland Trail Ø coastline, the JMFZ, the northern Møre margin, and the western Faroe Islands margin are less apparent, but formed a wide igneous margin along the Fugloy ridge and the southern Møre margin (Figure 11b), indicating a clear asymmetry in the early opening of the Norway basin. Based on *Norcliffe et al. [2019]* asymmetric SDRs form preferentially above a waning thermal anomaly in the mantle, or due to variations in the pre-rift lithospheric structure, which clearly is the case for the eastern JMMC breakup margin and the Ægir rift system. This implies that the process of the JMMC's rift transfer was in place from breakup time, reflected within its rifting asymmetry and igneous activity across the IPR propagating into the central Blosseville Kyst region, and formation of the Trail-Ø volcanic igneous province north of the JMMC.

These processes appear to coincide with a change in spreading direction of the Northeast Atlantic system, i.e. a regional rather than a localized event [*Gaina et al., 2017*] (Figure 12). The south-eastern extent of the Iceland-Faroe ridge that forms the eastern part of the GIFRC is of interest in comparison to the south-easternmost extent of the JMMC's SRC, where indications of anomalous SDRs are marked by multiple stacked sets that indicate a vertical accretion of SDRs or volcanic rift systems, rather than the classical inner and outer SDR architecture during the same syn-breakup time interval [*Erlendsson and Blischke, 2013; Blischke et al., 2016; Hjartarson et al., 2017*] (Figures 11b; 12).

Such anomalous rifting activity is possibly linked to mantle upwelling anomalies, and/or pre-rift lithospheric structures, as seen in the complex pattern of magnetic anomalies, potential fracture zones, or structural lineaments across the GIFRC (Figure 11b). Archaean boundaries observed in East Greenland project into the GIFRC and connect directly into the trend of the pre-IFZ and Fugloy ridge structural domains, dividing two structural regions, the Caledonian to its north and Archaean to its south. Thus, two primary structural trends formed during this syn-breakup phase: a WNW-to-ESE trend across the main GIFRC; and a NW-to-SE trend as the IPR and Proto-EJMFZ systems developed north of the GIFRC. The IPR and GIFRC structural trends have been reactivated during later rift phases and possibly have affected rifting in Iceland (Figures 11b,c; 12).

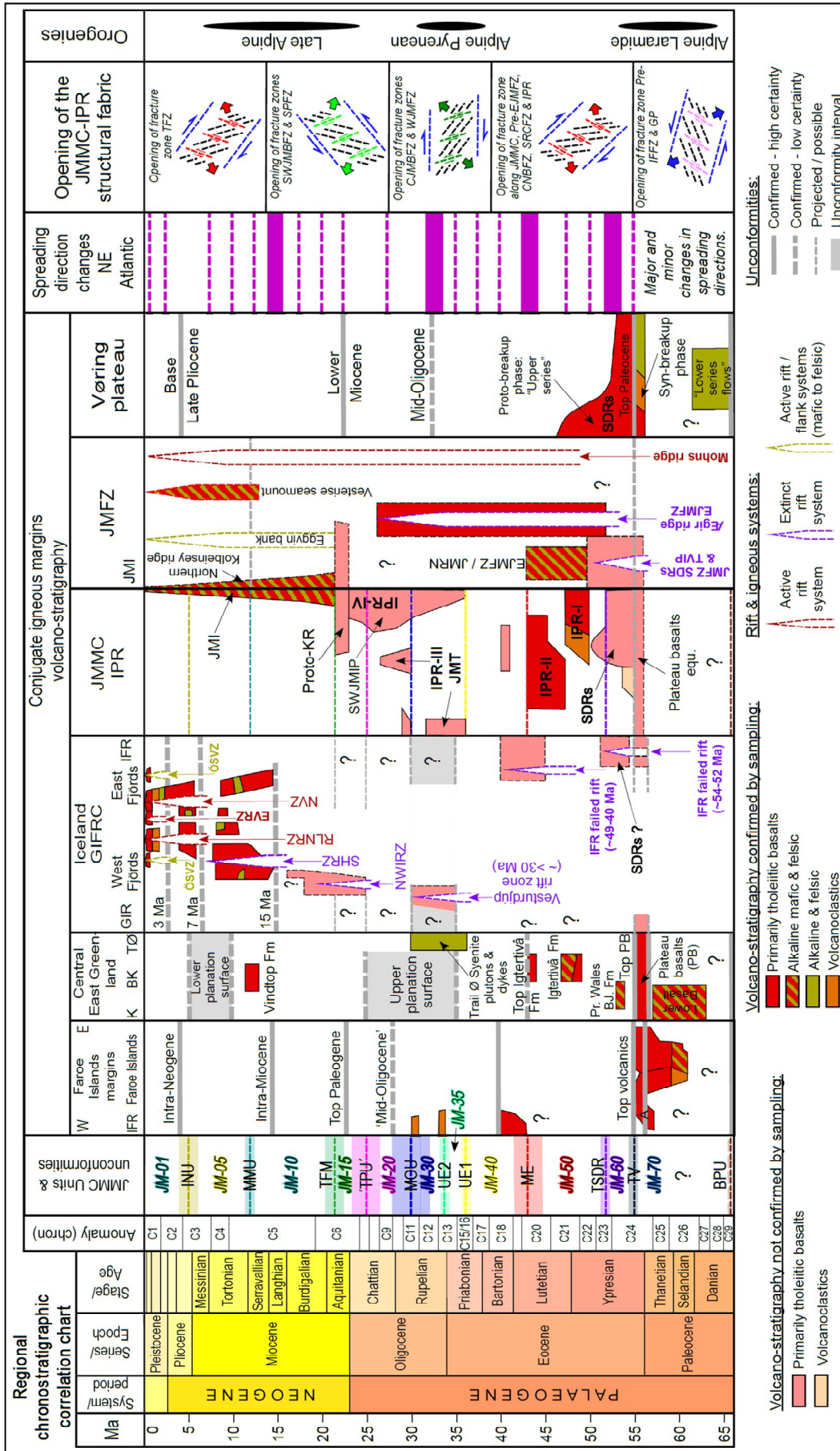


Figure 12. Regional chronostratigraphic summary chart in relationship of the JMMC's volcano-stratigraphy to its conjugate igneous margins in regards to Northeast Atlantic spreading direction changes modelled by *Gaina et al.* [2017a,b], main igneous provinces and rift relocations after *Sæmundsson* [1979], *Harðarson et al.* [1997, 2008], *Saunders et al.* [2013], *Thordarson and Höskuldsson* [2008], *Brandsdóttir et al.* [2015], *Blischke et al.* [2017a, 2019], *Geissler et al.* [2017], *Parson et al.* [2017], and *Hjartarson et al.* [2017], mid-oceanic ridge systems and orogenies modified after *Lundin and Doré* [2002]. Time scale from *Gradstein et al.* [2012]. Unconformity and JMMC abbreviations see Figure 1, and conjugate igneous margins, provinces, and rift relocations: GIFRC – Greenland-Iceland-Faroe ridge complex, IPR – Iceland plateau rift zone, NAIP – North Atlantic igneous province, SWJMIP – Southwest Jan Mayen igneous province, TVIP – Traill Ø-Vøring igneous complex; Iceland: EVZ – Eastern volcanic zone, NWIRZ – Northwest Iceland rift zone, RLNRZ – Reykjanes-Langjökull-North Iceland rift zone, SHRZ – Snæfellsnes-Húnaflói rift zone, SVB – Snæfellsnes intraplate volcanic belt, SWJMIP – Southwest Jan Mayen igneous province, and ÖVB – Örfæfi intraplate volcanic belt.

6.3 Rift-transfer phases

The rift-transfer phases involved the south-eastern JMMC igneous margin and the developing IPR segments I and II that interacted with the oblique spreading system of the Ægir ridge (Figures 11b,c; 12). The oldest continuous magnetic anomaly chron C21 (late Ypresian–early Lutetian, ~48–46 Ma) along the oblique spreading Ægir Ridge [*Gaina et al.*, 2009; *Ellis and Stoker*, 2014; *Blischke et al.*, 2017] formed just prior to the emplacement of the overlapping IPR-I volcanic succession (~52–50 Ma). The IPR-I is coeval with the JMMC seismic-stratigraphic unit JM-50, and most likely overlaps the syn-breakup JMMC Early Eocene igneous margin and SDRs (Figures 7d; 8d; 9; 11). The IPR domain segment “IPR-II” intersected the IPR-I segment and underlying JMMC Early Eocene igneous margin most likely between ~49 – 44 Ma, establishing a direct chronological and geochemical correlation with the Igtertivâ formation (~49 – 43 Ma) of Kap Dalton and the central Blosseville Kyst area. This overlap emphasises a tectono-magmatic connection between the areas along this propagating Iceland plateau rift system and the southern extent of the JMMC (Figures 11 and 12).

Volcanism continued throughout the Early- to Mid-Eocene (approximately 43-40 Ma) along the northern margin of the JMMC, EJMFZ, Jan Mayen Island, Trail-Ø igneous province, and within the GIFRC [e.g. *Gaina et al.*, 2009; *Geissler et al.*, 2017; *Blischke et al.*, 2019]. The Trail-Ø igneous province connected along the EJMFZ directly into the Vøring and Møre igneous domains forming a distinct segment of a mafic-to-alkaline igneous province that appears to have influenced the northernmost area of the JMR (Figures 11b; 12). Available geochemical data for the JMFZ, the JMI and the northern JMR suggest an igneous and magmatic connection along these systems. South of the JMMC, the GIFRC encompassed complex, parallel sub-aerial off-ridge volcanic systems connected by short fracture zone segments, including failed axial rift system across the Iceland-Faroe Ridge (~49-40 Ma) (Figures 11b,c; 12). Thus, the Ægir- and Reykjanes ridge systems were linked through a complex fracture zone region and off-ridge volcanic systems by the GIFRC. The Reykjanes ridge could therefore connected with the Blosseville Kyst igneous domain and the Ægir Ridge formed an overlapping spreading centre with the IPR (Figure 11a,b).

The Early to Mid-Eocene IPR rift transfer is in phase with an overall change in spreading direction, accompanied by decreased seafloor spreading rates within the Northeast Atlantic [*Gaina et al.*, 2017b] (Figure 12). As no major orogenic events occurred during this time period, this rift re-organisation most probably reflects the influence of large-scale magmatic processes, which resulted in regional uplift and development of the Mid-Eocene unconformity (Figure 12) [*Blischke et al.*, 2019]. This, most likely reflects processes of substantially increased magmatic activity underneath region that affected the adjacent rift system: the Reykjanes ridge to the south of the GIFRC, and the highly asymmetric Ægir

ridge and IPR system to the north. The IPR and Igtertivâ formation areas were part of the same rift system, indicating higher TiO₂ and K₂O contents and more developed magma sources in comparison to typical MORB (Figure 8). Thus, reflecting a mantle or hot-spot anomaly right below the GIFRC.

Asymmetric rift propagation across on the GIFRC or better across Iceland continues to present-day, specifically from the NVZ to the Kolbeinsey ridge and serves as an analogue for a hot-spot/plume – ridge interactive zone, geo-dynamically but also geochemically. Iceland-type basalts, as in the case of the NVZ, have a wide variation that could be linked to changes in mantle source composition, variation in mantle melting conditions, or variation in the extent of crustal assimilation. It is worth noting that the NVZ's increased depletion in comparison to other rift systems, reflecting heterogeneities in the Icelandic mantle that is described as a large-scale regional magmatic source that produced the NVZ sub-alkaline tholeiite basalts [e.g. *Fitton et al., 1997; Chauvel and Hémond, 2000; Thirlwall et al., 2004; Kokfelt et al., 2006*]. Interestingly, these basalts are very similar in geochemical composition to the IPR-II core samples and the Igtertivâ formation, when compared geochemically in terms of the MgO / K₂O (wt%) and MgO / TiO₂ (wt%) contents (Figure 8), suggesting a similar hot-spot influenced tectono-magmatic setting.

Anomalously thick crust reflected by the bouguer gravity anomaly data are specific for Iceland's older pre-Neogene eastern and western crustal domains (20-40 km), adjacent to younger volcanic zones and the plume locations, where crustal thickness decreases rapidly (< 20 km) [e.g. *Brandsdóttir and Menke, 2008; Brandsdóttir et al., 2015*]. The IPR-JMMC areas have, in contrast, a highly variable crustal thickness (6-22 km), including various ridge blocks that are separated by graben, and half graben structures and intersecting rift segments. This heterogeneity appears to reach far into the JMMC and especially the SRC, where the IPR-II intersects the IPR-I domain causes abrupt thinning (Figures 1; 9; 10; Supplement 7). In the case for the IPR-I area, a bouguer gravity anomaly that trends northwards possibly overlie a heavily intruded crustal sliver and intrusive complexes that was linked to the GIFRC across the pre-IFFZ domain northward into the SRC (Figures 9; 11b). The IPR-II segment intersected the IPR-I and the SRC possibly due to the rapid extension of the southern JMMC margin that counter acted the rapid extension of the Ægir ridge [e.g. *Gaina et al., 2009*]. Thus, due to this rapid extension, the SRC block started to be separated by graben structures with highly thinned crust that was intruded by dykes and sills and established axial rift segments as seen in IPR-II (Figures 11b,c). This represents a unique example of a multi-lateral and vertical igneous-margin that formed through a propagating rift system. A process that forms microplates along a complex igneous margin that can be observed in present-day Iceland as well [e.g. *Einarsson, 2008*].

6.4 Final breakup along the western JMMC margin

The breakup along the western margin of the JMMC commenced initially with a westward shift of IPR-III activity into the central graben that formed the Jan Mayen trough during the Oligocene (~35-25 Ma) (Figures 1; 5b; 6c; 9b; 11c; 12). This east-to-west rift transfer occurred as the Ægir ridge went into ultra-slow spreading and cessation mode [*Gernigon et al., 2015; Gaina et al., 2017b*]. This period of activity is accompanied by massive magmatic intrusive formations, such as the emplacement of volcanic ridges, dyke intrusions and flood basalts (F-markers 3 and 2). The intrusive phase aligns an apparent

Bouguer gravity anomaly trend within the JMT, the northern SRC, and the SWJMIP just south of the Lyngvi ridge structural domains. The emplacement of these volcanic ridges marks the complete breach of the fault and fracture zones that follow the Bouguer gravity trends, implying forced upwelling of magmatic material into available crustal and structural pathways, subsequently adding to the fan-shaped extent of the JMT and SRC domains (Figures 5b; 6c; 9b; 11; Supplements 7).

The final breakup phase (~25-22 Ma) occurred along the south-western and western flank of the JMMC, where evidence for increased volcanic activity is preserved, including the emplacement of igneous complexes, such as the IPR-IV or the formation of the Jan Mayen basin, increased dyke and sill intrusive activity, extrusive flood basalts (F-marker 1), and a possibly buried western SDR margin (Figures 4b; 9b; 10; 11c; Supplements 2; 6). This activity represents a distinct western igneous margin that formed as the JMMC fully separated from central East Greenland along the proto-Kolbeinsey ridge during magnetic anomaly C6c (23,3-22,5 Ma).

The eastern segment of the WJMFZ appears to have developed by forming / interlinking with the Eggvin bank, the north-western edge of JMMC, and the JMI that connected into the northernmost proto-Kolbeinsey ridge (Figures 8a; 11c; 12). The WJMFZ linked the JMI and the Trail Ø region that became partially inverted, with intrusion of a syenite pluton and dykes around 30 Ma [Parsons *et al.*, 2017; Geissler *et al.*, 2017; Blischke *et al.*, 2019] (Figure 12). The eastern segment of the WJMFZ was also connected with the Mohns ridge, forming a distinct igneous domain north of the JMMC, just as the GIFRC and Iceland formed as a larger counterpart to the south of the microcontinent.

Across the GIFRC, reconstructed magnetic and gravimetric anomalies suggest several rift and rift-flank segment systems that were offset by SW-NE striking fracture zones during the Late Oligocene to earliest Miocene interval (Figures 11c; 12). These aligned with the microcontinent's south-western and western volcanic margin just north of the GIFRC, and with the Reykjanes ridge south of the GIFRC (Figure 11c) [Blischke *et al.*, 2017a, 2019]. These anomalies correlate to known rift zones, such as the north-western Iceland rift zone that is proposed to represent the initial proto-Iceland rift zone approximately ~33-25 Ma that aligns with Iceland's present-day western shelf edge [Harðarsson *et al.*, 2008], and the volcanic complex of the Vesturdjúp (~30 Ma) at its southern extent [Hjartarson *et al.*, 2017] (Figures 11c; 12).

Global plate motion reorganizations are also believed to have triggered changes in spreading rates and directions from NNW-SSE to WNW-ESE between Greenland and the Eurasian plate (~33-21 Ma), just before the onset of the late Alpine orogeny and after cessation of ocean floor spreading within the Labrador Sea and Baffin Bay [Gaina *et al.*, 2017b] (Figure 12). The mid-Alpine Pyrenean orogeny occurred at the same time as this final phase of the Northeast Atlantic opening, placing the NW European plate margin in between the active ocean spreading ridges and the orogenic belt (Figures 11c; 12) [e.g. Lundin and Doré, 2002; Ritchie *et al.*, 2008].

This process forced a rearrangement of active spreading centres within the Northeast Atlantic region, as well as causing reactivation and compression along the south-eastern JMMC domain, and generated inversion structures within the SRC highs and within the Iceland-Faroe ridge area [Gaina *et al.*, 2009; Blischke *et al.*, 2016]. The modelled location of the Iceland hot-spot with the Northeast Atlantic ridge around 35-30 Ma [Dobrovine *et al.* 2012] correlates well with the apparent regional tilt of the entire GIFRC due east that opened ocean gateways in between the central East Greenland shelf and the subsiding Iceland-Faroe Ridge and Faroe-Islands plateau areas [Stärz *et al.*, 2017; Blischke *et al.*, 2019].

6.5 Iceland hot-spot and the JMMC igneous domains

Whether the Iceland and JMI mantle anomalies originate from a depleted upper mantle [Mertz *et al.*, 1991; Mertz and Haase, 1997; Hanan and Schilling, 1997; Hanan *et al.*, 2000; Stracke *et al.*, 2003], or from an active upwelling mantle or mantle plume based on geophysical and petrochemical data analysis [e.g. Fitton *et al.*, 1997; Chauvel and Hémond, 2000; Kempton *et al.*, 2000; Skovgaard *et al.*, 2001; Breddam, 2002; Kokfelt *et al.*, 2006; Parkin and White, 2008], has been debated. However, it has been clarified that the Icelandic and JMI-type basalts are different to typical MOR basalts, and show mixing towards their neighbouring ridge systems, giving proof to a petrochemical anomaly [e.g. Kokfelt and Árting, 2014].

Parnell-Turner *et al.* [2014] suggested that the Iceland hot-spot was active periodically from 55 to 35 Ma and that a pulsating plume has generated a V-shaped ridge every 3 Ma up to 35 Ma, continuing every 8 Ma into present times. Their formation along the Reykjanes ridge has been proposed to be influenced by axial rift propagation, which could be hot-spot pulse-driven but which might not be its primary cause [Hey *et al.*, 2010]. Deep-crustal melt-rich incursions have been described for the V-shaped Reykjanes ridge that is suggested to reflect the Iceland hotspot pulsing and influencing the ridge south of the GIFRC [White *et al.*, 1995; Abelson and Agnon, 2001; Ito, 2001; Rychert *et al.*, 2018].

A correlation of these interpreted regular hot-spot pulsing events south of the GIFRC to apparently regular changes in spreading directions, as suggested by Gaina *et al.* [2017b], do not line up in chronological time for the region north of the GIFRC [Blischke *et al.*, 2019]. Here, such regular pulsing events do not explain the major changes and unconformities that are primarily linked to regionally tectonic and magmatic events for the Northeast Atlantic region, and distinct hot-spot ridge interaction that resulted in the IPR propagation from the Ægir ridge to the Kolbeinsey ridge. Furthermore, the reconstructed geochronology of the Northeast Atlantic region, the mapped igneous domains of this study, in comparison with known modelled hot-spot rift interactions, and opening of the JMMC-IPR structural fabric suggest that the Iceland hot-spot influenced the JMMC-IPR domain system through 7 distinct tectono-magmatic phases, of which 5 are possible major phases that influenced the JMMC's breakup history (Figure 12): (1) Early Paleogene, possible pre-breakup magma-crust interaction underneath the central Blossville Kyst – JMMC area (>55 Ma); (2) Early-Mid Eocene forming of the GIFRC – IPR-I/IPR-II systems (~52-40 Ma); (3) the formation of the IPR-III, north-western Iceland rift zone system – proto-Kolbeinsey – JMMC western breakup margin (~35-22 Ma); (4) the Mid-Miocene rift transfer across Iceland Snæfellsnes-Húnaflói rift zone (~15-13 Ma) with increased magmatic activity in central East Greenland

(Vindtop Formation on Figure 12), the Eggvin bank – WJMFZ; and (5) formation of the Iceland multi-rift zone and intra-plate rift zone system since ~7 Ma.

These phases describe large-scale events linked to deep crustal incursions that are reflected as offset intrusive systems of neighbouring margins, similarly as described by V-shaped ridge systems. Elsewhere, asymmetric oceanic domains and “V-shaped” breakup development have been documented for the southernmost South Atlantic, which underwent south-to-north propagation of an initial asymmetric segmented rift margin and SDR formation, prior to the emplacement of the Parana Etendeka LIP and subsequent regular ocean floor emplacement [Koopmann, *H. et al.*, 2016]. Thus, several scenarios are possible that might explain deep intrusive incursions from one igneous domain into the other that relate to the interaction of mantle anomalies, lateral melt pollution, and structural settings that influence the complexity of a breakup margin.

Along the Early Eocene eastern JMMC breakup margin, a clear wedge shaped north to south asymmetric SDR formation formed that might be linked to variations in the pre-rift lithospheric structure and a thermal mantle anomaly. Connecting the second breakup, the JMI - Eggvin bank areas form the JMMC’s direct N-NW volcanic margin domains and have a strong influence on the microcontinent that differ in crustal structure and geochemical composition (Figures 1; 8; 10; 11c). Thus, this might reflect the JMI long-lived activity from ~55 Ma to present day.

The Jan Mayen island igneous geochemistry indicates more enriched and alkaline compositions that are similar to the Icelandic volcanic flank zones [Debaille *et al.*, 2009], but primarily align with samples from the northern Jan Mayen ridge, the Jan Mayen fracture zone, and in part with the Vesterise seamount (Figure 8). The Vesteris seamount’s origin has been suggested as a Mid-Miocene to present-day feature [Haase and Devey, 1994]. Jan Mayen island volcanism could have been developing around the northernmost WJMFZ fracture zone segment from Early Miocene (Figure 8c). The origin of the different compositions of this province is considered to either be related to a mantle plume or MORB melts that have been contaminated by continental lithosphere [Hanan *et al.*, 2000; Kokfelt and Ártíng, 2014]. Apparent crustal anomalies are seen on Bouguer gravity, magnetic, and refraction data around the JMI and the Eggvin bank along the WJMFZ (Figure 1; 9b; 10; 11c), with a thick crustal heterogenous segment along the northern extent of the JMMC, the JMI, and along the Kolbeinsey ridge [Tan *et al.*, 2017, 2018]. Here, the Kolbeinsey ridge might additionally function as a transitional conduit, as deeper levels of melting are suggested to have been influenced by mantle anomalies, and variation along the southernmost part of the ridge, indicated by geochemically-transitional signatures varying between typical depleted MORB and Icelandic basalts [Hart *et al.*, 1973; Sun, 1975; Schilling *et al.*, 1999; Thirlwall *et al.*, 2004; Kokfelt and Ártíng, 2014].

7. Conclusions

New details on the Northeast Atlantic opening mechanism have been mapped and delineated based on composite datasets of the JMMC-IPR region that clearly delineate the JMMC in between 2 breakup centres, the GIFRC to its south, and the JMI – JMFZ system to its north. The JMMC's volcanic seismic-stratigraphic record is characterized by seven separate tectono-magmatic and stratigraphic rift-transfer phases were defined as follows:

- (1) An initial breakup phase characterized by anomalous magmatic activity that followed a SW-NE opening fissure trend along WNW-ESE striking pre-existing fracture zones south and west of the JMMC, here inferred as an oblique opening of the Geikie plateau into the central JMR domain (~63-56 Ma);
- (2) Multiple SDR sets that formed along the JMMC eastern igneous margin during syn-breakup in the Early Eocene. SDR rift segments propagating from north to south in a general NNE-SSW strike direction represent a precursor for the Ægir ridge mid-oceanic ridge system's development that opened along the NW-SE striking EJMfZ, CNBFZ, and SRCfZ segments (~55-53 Ma);
- (3) Forming of JMMC's eastern breakup margin, the Iceland Plateau rift (IPR-I), and southernmost extent of the Ægir ridge system (~52-50 Ma);
- (4) SW to NE magmatic interaction of the Greenland-Iceland-Faroe ridge complex with the JMMC domain. The IPR-II segment intersecting the IPR-I segment and the southern extent of the SRC domains contemporary with the Ægir ridge. Volcanism was accompanied by axial rift segments, intrusives, flood basalts, shelf-margin deltaic sedimentation within a shallow shelf marine depositional environment (~49-36 Ma).
- (5) SW to NE magmatic incursion from the GIFRC into the JMMC systems that formed the IPR-III rift domain, severing the SRC from the main JMR (Lyngvi ridge) that formed the JMT and volcanic ridges within the SRC domain (~36-25 Ma);
- (6) The final breakup phase of the JMMC during the formation of the SWJMIP, the IPR-IV segment and western JMMC igneous margin that resulted in the formation of the proto-Kolbeinsey ridge and the WJMfZ segments (25-22 Ma);
- (7) Full separation of the JMMC and formation of the Kolbeinsey ridge that is linked to Iceland along its southern extent, and to the WJMfZ – Jan Mayen island igneous complex at its northern end (since 22 Ma), accompanied by tephra deposits within the Neogene deep marine sediments that possibly were sourced from both primary active volcanic systems.

The palaeo-geographic reconstruction clearly delineates the JMMC as the link between two separate breakup centres, the GIFRC to its south and the Jan Mayen island igneous complex – JMFZ system to its north. The key points are:

- A clear north-south asymmetric SDR formation along the eastern JMMC breakup margin and the Ægir rift system that preferentially formed in between pre-rift lithospheric structures above a thermal mantle anomaly.
- A firm link of the obliquely propagating Iceland plateau rift system into the Blossville Kyst, in regard to timing and available geochemistry data, emphasizing a tectono-magmatic connection.
- A reasonable explanation for the initiation of the fanned-out appearance of the oblique IPR rifting domain that interfingers with the southern ridges of the JMMC due to south-to-north directed deep crustal melt rich incursions that formed several axial rift systems and volcanic ridges.
- The formation of a second, complex breakup margin along the JMMC southwestern to western flank during Late Oligocene to Early Miocene, with emplacement of igneous complexes, such as the SW Jan Mayen igneous province; the full opening of the Jan Mayen basin as an igneous domain with massive dyke and sill intrusion, possibly as part of a buried western Late Oligocene SDR margin; and regionally extensive Miocene flood basalt.
- First observed and mapped dual breakup system of two opposed rifting complexes that created the JMMC through rift propagation.

In conclusion, the Northeast Atlantic region has not previously been observed and documented in such detail. Our study indicates that the JMMC is an important area for understanding ridge – mantle anomalies that appear to develop along pre-existing structurally complex areas. Our results suggest that rift relocations and the formation of overlapping volcanic systems might be a characteristic of breakup regions where symmetric mid-oceanic ridge systems cannot easily develop.

Acknowledgments

This work is a part of a research project at the University of Iceland and the Centre for Earth Evolution and Dynamics, University of Oslo, with funding by the National Energy Authority of Iceland (Orkustofnun), the Iceland GeoSurvey, and supported by the Norwegian Research Council by Centres of Excellence funding to CEED (project number 223272). Data permissions were provided by the National Energy Authority of Iceland (Orkustofnun), the Norwegian Petroleum Directorate (NPD), Spectrum ASA, TGS; the University of Oslo (UiO), the Bundesanstalt für Geowissenschaften und Rohstoffe (BGR), and Geological Survey of Denmark and Greenland (GEUS). Many thanks to Prof. emerit. Olav Eldholm for giving permission to use the unpublished JMMC ESP dataset. We additionally thank the Marine Research Institute of Iceland (MRI), for making the multibeam and backscatter data available and the Norwegian Petroleum Directorate (NPD) for use of their 2D multichannel reflection data sets from 2011 and 2012. Seafloor borehole core samples were obtained from the Bremen Core Repository of the International Ocean Discovery Program (IODP). Dating of core samples were carried out at the Oregon State University (OSU) Argon Geochronology Laboratory. Geochemical analyses were conducted at the University of Iceland, and the Aarhus University. Unpublished geochemical analyses of cores 32, 33 and 34 of DSDP site 348, and cores 14 and 15 of DSDP site 350 were kindly made available by Professor Godfrey Fitton at the University of Edinburgh and Prof. Christian Tegner at the Aarhus University. Martyn Stoker gratefully acknowledges the award of Visiting Research Fellow at the Australian School of Petroleum and Energy Resources at the University of Adelaide. In addition, the authors would like to thank Dr. Lotte Melchior Larsen for all the good advice and throughout this project.

References

- Abdelmalak, M. M., Meyer, R., Planke, S., Faleide, J. I., Gernigon, L., Frieling, J., et al. (2016). Pre-breakup magmatism on the Vøring Margin: Insight from new sub-basalt imaging and results from Ocean Drilling Program Hole 642E. *Tectonophysics*, *675*, 258–274. <https://doi.org/10.1016/J.TECTO.2016.02.037>
- Abdelmalak, M. M., Faleide, J. I., Planke, S., Gernigon, L., Zastrozhnov, D., Shephard, G. E., & Myklebust, R. (2017). The T-Reflection and the Deep Crustal Structure of the Vøring Margin, Offshore mid-Norway. *Tectonics*, *36*, 2497–2523. <https://doi.org/10.1002/2017TC004617>
- Abelson, M., & Agnon, A. (2001). Hotspot activity and plume pulses recorded by geometry of spreading axes. *Earth and Planetary Science Letters*, *189*, 31–47. [https://doi.org/10.1016/S0012-821X\(01\)00331-4](https://doi.org/10.1016/S0012-821X(01)00331-4)
- Åkermoen, T. (1989). Jan Mayen-ryggen: et seismisk stratigrafisk og strukturelt studium. Cand. scient. thesis, University of Oslo, 174 pp.
- Blischke, A., Planke, S., Tegner, C., Gaina, C., Brandsdóttir, B., Halldórsson, S. A., Helgadóttir, H. M., & Koppers, A. (2016). Seismic volcano-stratigraphic characteristics and igneous province assessment of the Jan Mayen microcontinent, central NE-Atlantic. *AGU Fall Meeting*, T33A-3008.
- Blischke, A., Gaina, C., Hopper, J. R., Péron-Pinvidic, G., Brandsdóttir, B., Guarnieri, P., et al. (2017a). The Jan Mayen microcontinent: an update of its architecture, structural development and role during the transition from the Ægir Ridge to the mid-oceanic Kolbeinsey Ridge. *Geological Society, London, Special Publications*, *447*(1), 299–337. <https://doi.org/10.1144/SP447.5>
- Blischke, A., Erlendsson, Ö., Einarsson, G. M., Ásgeirsson, V. L., & Árnadóttir, S. (2017b). *The Jan Mayen Microcontinent Project Database and Seafloor Mapping of the Dreki Area Input Data, Geological and Geomorphological Mapping and Analysis*. Iceland GeoSurvey, ÍSOR-2017/055, Reykjavik, Iceland.
- Blischke, A. & Erlendsson, Ö. (2018). *Central East Greenland – conjugate margin of the Jan Mayen microcontinent - Database, structural and stratigraphical mapping project*. Iceland GeoSurvey, ÍSOR-2018/024, 95 p., 2 maps, Appendices 1 to 5.
- Blischke, A., Erlendsson, Ö., Guarnieri, P., Brandsdóttir, B., & Gaina, C. (2018). Structural links between the Jan Mayen Microcontinent and the central East Greenland coast prior to, during, and after breakup, *The 33rd Nordic Geological Winter Meeting 2018*, The Geological Society of Denmark, Copenhagen.
- Blischke, A., Stoker, M. S., Brandsdóttir, B., Hopper, J. R., Peron-Pinvidic, G., Ólavsdóttir, J., & Japsen, P. (2019). The Jan Mayen microcontinent's Cenozoic stratigraphic succession and structural evolution within the NE-Atlantic. *Marine and Petroleum Geology*, *103*, 702–737. <https://doi.org/10.1016/J.MARPETGEO.2019.02.008>

- Blischke, A. (2020a). *The Jan Mayen microcontinent and Iceland plateau: Tectono-magmatic evolution and rift propagation*, PhD dissertation, Faculty of Earth Sciences, University of Iceland.
- Blischke, A., Erlendsson, Ö., Brandsdóttir, B., Hjartardóttir, Á.R. and Gautason, B. (2020b). *The Iceland Plateau – Jan Mayen volcanic breakup margin: An analogue for axial rift and transfer zone North Iceland*. Proceedings World Geothermal Congress 2020, 11175, 12.
- Blystad, P., Brekke, H., Færseth, R. B., Larsen, B. T., Skogseid, J., & Tærudbakken, B. (1995). Structural elements of the Norwegian continental shelf, Part II, The Norwegian Sea Region. *NPD Bulletin*, 8. Norwegian Petroleum Directorate.
- Bott, M. (1985). Plate tectonic evolution of the Icelandic transverse ridge and adjacent regions. *J. Geophys. Res.*, 90, 9953–9960.
- Bott, M. H. P., Browitt, C. W. A., & Stacey, A. P. (1971). The deep structure of the Iceland-Faeroe Ridge. *Marine Geophysical Researches*, 1(3), 328–351. <https://doi.org/10.1007/BF00338261>
- Brandsdóttir, B., Hooft, E. E. E., Mjelde, R., & Murai, Y. (2015). Origin and evolution of the Kolbeinsey Ridge and Iceland Plateau, N-Atlantic. *Geochemistry, Geophysics, Geosystems*, 16(3), 612–634. <https://doi.org/10.1002/2014GC005540>
- Brandsdóttir, B., & Menke, W. H. (2008). The seismic structure of Iceland. *Jökull*, 58, 17–34.
- Breddam, K. (2002). Kistufell: Primitive melt from the Iceland mantle plume. *Journal of Petrology*, 43(2), 345–373. doi: 10.1093/petrology/43.2.345
- Breivik, A., & Mjelde, R. (2003). *Modeling of profile 8 across the Jan Mayen Ridge*. Rep., Institute of Solid Earth Physics, University of Bergen, Bergen, Norway.
- Breivik, A. J., Faleide, J. I., & Mjelde, R. (2008). Neogene magmatism northeast of the Aegir and Kolbeinsey ridges, NE Atlantic: Spreading ridge–mantle plume interaction? *Geochemistry, Geophysics, Geosystems*, 9, Q02004, doi:[10.1029/2007GC001750](https://doi.org/10.1029/2007GC001750).
- Breivik, A. J., Mjelde, R., Faleide, J. I., & Murai, Y. (2012). The eastern Jan Mayen microcontinent volcanic margin. *Geophysical Journal International*, 188(3), 798–818. doi:10.1111/j.1365-246X.2011.05307.x
- Brooks, C. K. (2011). The East Greenland rifted volcanic margin. *Geological Survey of Denmark and Greenland Bulletin*, 24, 96.
- Butt, E. A., Elverhøi, A., Forsberg, C. F., & Solheim, A. (2001). Evolution of the Scoresby Sund Fan, central East Greenland - evidence from ODP Site 987. *Norwegian Journal Of Geology*, 81, 3–15.

- Campsie, J., Rasmussen, M. H., Kovacs, L. C., Dittmer, F., Bailey, J. C., Hansen, N. O., Laursen, J., & Johnson, L. (1990). Chronology and Evolution of the Northern Iceland Plateau. *Polar Research*, 8(2), 237–243. doi: 10.1111/j.1751-8369.1990.tb00386.x
- Channell, J. E. T., Amigo, A. E., Fronval, T., Rack, F., & Lehman, B. (1999a). Magnetic stratigraphy at Sites 907 and 985 in the Norwegian-Greenland Sea and a revision of the Site 907 composite section. *Proceedings of the Ocean Drilling Program, Scientific Results.*, 162, 131–148.
- Channell, J. E. T., Smelror, M., Jansen, E., Higgins, S. M., Lehman, B., Eidvin, T., & Solheim, A. (1999b). Age models for glacial fan deposits off East Greenland and Svalbard (sites 986 and 987). *Proceedings of the Ocean Drilling Program, Scientific Results.*, 162, 149–166.
- Chauvel, C., & Hémond, C. (2000). Melting of a complete section of recycled oceanic crust: Trace element and Pb isotopic evidence from Iceland. *Geochemistry, Geophysics, Geosystems*, 1(2), 31. <https://doi.org/10.1029/1999GC000002>
- Childs, J.R. and Cooper, A.K. (1978). *Collection, reduction and interpretation of marine seismic sonobuoy data*. U.S. Geological Survey, Department of interior, technical report, 78-442.
- Davis, L. L., & McIntosh, W. C. (1996). The petrology and (super 40) Ar/ (super 39) Ar age of tholeiitic basalt recovered from Hole 907A, Iceland. Plateau. *Proceedings of the Ocean Drilling Program, Scientific Results*, 151(Journal Article), 351–365. doi: 10.2973/odp.proc.sr.151.124.1996
- Debaille, V., Trønnes, R. G., Brandon, A. D., Waight, T. E., Graham, D. W., & Lee, C.-T. A. (2009). Primitive off-rift basalts from Iceland and Jan Mayen: Os-isotopic evidence for a mantle source containing enriched subcontinental lithosphere. *Geochimica et Cosmochimica Acta*, 73(11), 3423–3449. <https://doi.org/10.1016/J.GCA.2009.03.002>
- Decker, R., & Decker, B. (2005). *Volcanoes*, 4th ed., W. H. Freeman. ISBN 0-7167-8929-9
- Diebold, J.B. and Stoffa, P.L. (1981). The travelttime equation, tau-p mapping, and inversion of common midpoint data. *Geophysics* 46(3), 238-254.
- Doré, A. G., Lundin, E. R., Jensen, L. N., Birkeland, O., Eliassen, P. E., & Fichler, C. (1999). Principal tectonic events in the evolution of the northwest European Atlantic margin. (A. J. Fleet & S. A. R. Boldy, Eds.). UK: Geological Society of London, 41-61. <https://doi.org/https://doi.org/10.1144/0050041>
- Dobrovine, P. V, Steinberger, B., & Torsvik, T. H. (2012). Absolute plate motions in a reference frame defined by moving hot spots in the Pacific, Atlantic, and Indian oceans. *Journal of Geophysical Research: Solid Earth*, 117(B9). <https://doi.org/10.1029/2011JB009072>
- Dupuy, P.Y., & Sogorb, G. (2017). *Survey report - NARVAL 2016 hydrographic and oceanographic cruise onboard R/V Beautemps-Beaupré*. Groupe hydrographique et océanographique de l'Atlantique, N° 113 SHOM/GHOA/NP, Brest, France.

- Eggen, S.S. (1984). *Jan Mayen-ryggens geologi*. Norwegian Petroleum Directorate contribution 20, 29 p.
- Einarsson, P. (2008). Plate boundaries, rifts and transforms in Iceland. *Jökullkull*, 58, 35–58.
- Eldholm, O., & Windisch, C.C. (1974). Sediment distribution in the Norwegian-Greenland Sea. *Geological Society of America Bulletin*, 85, 1661-1676.
- Eldholm, O., Thiede, J., & Taylor, E. (1987a). *Evolution of the Norwegian continental margin: background and objectives*. In: Eldholm, O., Thiede, J., Taylor, E., et al., Proc. ODP, Init. Repts., 104, College Station, TX (Ocean Drilling Program), 5–25. doi:10.2973/odp.proc.ir.104.101.1987
- Eldholm, O., Thiede, J., Taylor, E., et al. (1987b). *Shipboard Scientific Party, 1987. Site 642: Norwegian Sea*. IN: *Proc. ODP, Init. Repts., 104: College Station, TX (Ocean Drilling Program)*, 53–453. doi:10.2973/odp.proc.ir.104.104.1987
- Eldholm, O., Karasik Deceased, A. M., & Reksnes, P. A. (1990). *The North American plate boundary*. (A. Grantz, L. Johnson, & J. F. Sweeney, Eds.), *The Arctic Ocean Region* (Vol. L), 171–185. Geological Society of America, Boulder, Colo. <https://doi.org/10.1130/DNAG-GNA-L.171>
- Eldholm, O., & Grue, K. (1994). North Atlantic volcanic margins: Dimensions and production rates. *Journal of Geophysical Research*, 99(B2), 2955–2968. <http://dx.doi.org/10.1029/93JB02879>
- Ellis, D., & Stoker, M.S. (2014). The Faroe–Shetland Basin: a regional perspective from the Paleocene to the present day and its relationship to the opening of the North Atlantic Ocean. In: S. J. C. Cannon, & D. Ellis (eds) *Hydrocarbon Exploration to Exploitation West of Shetlands*. *Geological Society, London, Special Publications*, 397. <http://dx.doi.org/10.1144/SP397.1>
- Erlendsson, Ö. (2010). *Seismic Investigation of the Jan Mayen Ridge – with a Close Study of Sill Intrusions*. MSc. thesis, Aarhus University, 111 pp + appendices.
- Erlendsson, Ö., & Blischke, A. (2013). *Haffréttarmál: hljóðendurvarps- og bylgjubrotsmælingar: skýrsla um stöðu mála á úrvinnslu og túlkun gagna (Law of the sea: seismic reflection and refraction database and interpretation status report)*. Iceland GeoSurvey, Report ÍSOR-2013/067.
- Faleide, J.I., Bjørlykke, K., & Gabrielsen, R.H. (2010). *Geology of the Norwegian continental shelf*. In: Bjørlykke, K. (ed.) *Petroleum Geoscience: From Sedimentary Environments to Rock Physics*. (New York: Springer), 467-499. doi: 10.1007/978-3-642-34132-8_25
- Fitch, F.J. (1964). The development of the Beerenberg volcano, Jan Mayen. *Proceedings of the Geologists' Association*. [https://doi.org/10.1016/S0016-7878\(64\)80002-X](https://doi.org/10.1016/S0016-7878(64)80002-X)
- Fitch, F.J., Grasty, R.L., & Miller, J.A. (1965). Potassium-Argon Ages of Rocks from Jan Mayen and an outline of its Volcanic History. *Nature*, 207, 1349-1351. doi: 10.1038/2071349a0

- Fitton, J. G., Saunders, A. D., Norry, M. J., Hardarson, B. S., & Taylor, R. N. (1997). Thermal and chemical structure of the Iceland plume. *Earth and Planetary Science Letters*, 153(3–4), 197–208. [https://doi.org/10.1016/s0012-821x\(97\)00170-2](https://doi.org/10.1016/s0012-821x(97)00170-2)
- Funck, T., Hopper, J. R., Fattah, R. A., Blischke, A., Ebbing, J., Erlendsson, Ö., Gaina, C., Geissler, W. H., Gradmann, S., Haase, C., Kimbell, G. S., McDermott, K. G., Peron-Pinvidic, G., Petersen, U., Shannon, P. M., & Voss, P. H. (2014). Crustal Structure. In: J. R. Hopper, T. Funck, M. S. Stoker, U. Ártíng, G. Peron-Pinvidic, H. Doornenbal, & C. Gaina (Eds.), *Tectonostratigraphic Atlas of the North-East Atlantic region* (1st ed., p. 340). Copenhagen, Denmark: The Geological Survey of Denmark and Greenland (GEUS).
- Funck, T., Erlendsson, Ö., Geissler, W. H., Gradmann, S., Kimbell, G. S., McDermott, K., & Petersen, U. K. (2016). A review of the NE Atlantic conjugate margins based on seismic refraction data. *Geological Society, London, Special Publications*, 447(1), 171–205. <http://doi.org/10.1144/SP447.9>
- Funck, T., Geissler, W. H., Kimbell, G. S., Gradmann, S., Erlendsson, Ö., McDermott, K., & Petersen, U. K. (2017). Moho and basement depth in the NE Atlantic Ocean based on seismic refraction data and receiver functions. *Geological Society, London, Special Publications*, 447(1), 207–231. <http://doi.org/10.1144/SP447.1>
- Gaina, C., Gernigon L., & Ball, P. (2009). Palaeocene - Recent plate boundaries in the NE Atlantic and the formation of the Jan Mayen microcontinent. *Journal of the Geological Society*, 166, 1–16. <https://doi.org/10.1144/0016-76492008-112>
- Gaina, C. (2014). Plate Reconstructions and Regional Kinematics. In J. R. Hopper, T. Funck, M. Stoker, U. Ártíng, G. Peron-Pinvidic, H. Doornenbal, & C. Gaina (Eds.), *Tectonostratigraphic Atlas of the North-East Atlantic region* (1st ed., p. 340). Copenhagen, Denmark: The Geological Survey of Denmark and Greenland (GEUS).
- Gaina, C., Blischke, A., Geissler, W. H., Kimbell, G. S., & Erlendsson, Ö. (2017a). Seamounts and oceanic igneous features in the NE Atlantic: a link between plate motions and mantle dynamics. *Geological Society, London, Special Publications*, 447(1), 419–442. <https://doi.org/10.1144/SP447.6>
- Gaina, C., Nasuti, A., Kimbell, G. S., & Blischke, A. (2017b). Break-up and seafloor spreading domains in the NE Atlantic. *Geological Society, London, Special Publications*, 447(1), SP447.12. <https://doi.org/10.1144/SP447.12>
- Ganerød, M., Wilkinson, C. M., & Hendriks, B. (2014). Geochronology. In J. R. Hopper, T. Funck, M. Stoker, U. Ártíng, G. Peron-Pinvidic, H. Doornenbal, & C. Gaina (Eds.), *Tectonostratigraphic Atlas of the North-East Atlantic region* (1st ed., p. 340). Copenhagen, Denmark: The Geological Survey of Denmark and Greenland (GEUS).
- Geissler, W. H., Gaina, C., Hopper, J. R., Funck, T., Blischke, A., Arting, U., á Horni, J., Péron-Pinvidic, G., & Abdelmalak, M. M. (2017). Seismic volcanostratigraphy of the NE Greenland continental margin. *Geological Society, London, Special Publications*, 447(1), 149–170. <https://doi.org/10.1144/SP447.11>

- Geodekyan, A. A., Verkhovskaya, Z. I., Sudin, A. V., & Ya., T. V. (1980). Gases in seawater and bottom sediments. In C. B. Udintsev (Ed.), *Iceland and Mid-Oceanic Ridge – Structure of the ocean-floor*. (pp. 19–36). USSR: Academy of Sciences of the USSR Soviet Geophysical Committee.
- Gairaud, H., Jacquart, G., Aubertin, F., & Beuzart, P. (1978). Jan Mayen Ridge synthesis of geological knowledge and new data. *Oceanologica Acta*, 1(3), 335–358.
- Gernigon, L., Gaina, C., Olesen, O., Ball, P. J., Péron-Pinvidic, G., & Yamasaki, T. (2012). The Norway Basin revisited: From continental breakup to spreading ridge extinction. *Marine and Petroleum Geology*, 35(1), 1–19. <https://doi.org/10.1016/j.marpetgeo.2012.02.015>
- Gernigon, L., Blischke, A., Nasuti, A., & Sand, M. (2015). Conjugate volcanic rifted margins, seafloor spreading, and microcontinent: Insights from new high-resolution aeromagnetic surveys in the Norway Basin. *Tectonics*, 34(5), 907–933. <https://doi.org/10.1002/2014TC003717>
- Gernigon, L., Franke, D., Geoffroy, L., Schiffer, C., Foulger, G. R., & Stoker, M. (2019). Crustal fragmentation, magmatism, and the diachronous opening of the Norwegian-Greenland Sea. *Earth-Science Reviews*. <https://doi.org/10.1016/J.EARSCIREV.2019.04.011>
- Govindaraju, K., & Mevelle, G. (1987). Fully automated dissolution and separation methods for inductively coupled plasma atomic emission spectrometry rock analysis. Application to the determination of rare earth elements. Plenary lecture. *Journal of Analytical Atomic Spectrometry*, 2(6), 615–621. <https://doi.org/10.1039/JA9870200615>
- Gradstein, F. M., Ogg, J. G., Schmitz, M. D., & Ogg, G. M. (2012). *The Geologic Time Scale* (1st ed.). Boston: Elsevier. <https://doi.org/https://doi.org/10.1016/C2011-1-08249-8>
- Grönvold, K., & Mäkipää, H. (1978). *Chemical composition of Krafla lavas 1975-1977*. Nordic volcanological institute, University of Iceland, Report 7816, 50, Reykjavik, Iceland.
- Guarnieri, P. (2015). Pre-break-up palaeostress state along the East Greenland margin. *Journal of the Geological Society*, 172, 727–739. <https://doi.org/https://doi.org/10.1144/jgs2015-053>
- Gunnarsson, K., Sand, M., & Gudlaugsson, S. T. (1989). *Geology and hydrocarbon potential of the Jan Mayen Ridge*. Orkustofnun, Report OS-98014, 143 pp., 5 appendices incl. 9 maps Reykjavik, Iceland.
- Gudlaugsson, S. T., Gunnarsson, K., Sand, M., & Skogseid, J. (1988). Tectonic and volcanic events at the Jan Mayen Ridge microcontinent. In A. C. Morton & L. M. Parson (Eds.), *Early Tertiary volcanism and the opening of the NE Atlantic* (Vol. 39, pp. 85–93). Geological Society of London.

- Haase, K. M., Devey, C. W., Mertz, D. F., Stoffers, P., & Garbe-Schonberg, D. (1996). Geochemistry of lavas from Mohns ridge, Norwegian-Greenland Sea: Implications for melting conditions and magma sources near Jan Mayen. *Contributions to Mineralogy and Petrology*, 123(3), 223–237. doi: 10.1007/s004100050152
- Haase, C., Ebbing, J., & Funck, T. (2017). A 3D regional crustal model of the NE Atlantic based on seismic and gravity data. *Geological Society, London, Special Publications*, 447(1), 233-247. <https://doi.org/10.1144/SP447.8>
- Haase, C., & Ebbing, J. (2014). Gravity Data. In J. R. Hopper, T. Funck, M. S. Stoker, U. Ártung, G. Peron-Pinvidic, H. Doornenbal, & C. Gaina (Eds.), *Tectonostratigraphic Atlas of the North-East Atlantic Region*. (pp. 29–38), Geological Survey of Denmark and Greenland (GEUS), Copenhagen, Denmark.
- Hald, N., & Tegner, C. (2000). Composition and age of tertiary sills and dykes, Jameson Land Basin, East Greenland: relation to regional flood volcanism. *Lithos*, 54(3–4), 207–233. [https://doi.org/10.1016/S0024-4937\(00\)00032-3](https://doi.org/10.1016/S0024-4937(00)00032-3)
- Halldorsson, S. A., Oskarsson, N., Gronvold, K., Sigurdsson, G., Sverrisdottir, G., & Steinthorsson, S. (2008). Isotopic-heterogeneity of the Thjorsa lava—Implications for mantle sources and crustal processes within the Eastern Rift Zone, Iceland. *Chemical Geology*, 255(3–4), 305–316. <https://doi.org/10.1016/J.CHEMGEO.2008.06.050>
- Hanan, B. B., Blichert-Toft, J., Kingsley, R., & Schilling, J. G. (2000). Depleted Iceland mantle plume geochemical signature: Artifact of multicomponent mixing? *Geochemistry Geophysics Geosystems*, 1(4), 19. <https://doi.org/10.1029/1999GC000009>
- Hanan, B. B., & Schilling, J.-G. (1997). The dynamic evolution of the Iceland mantle plume: the lead isotope perspective. *Earth and Planetary Science Letters*, 151(1–2), 43–60. [https://doi.org/10.1016/S0012-821X\(97\)00105-2](https://doi.org/10.1016/S0012-821X(97)00105-2)
- Harðarson, B. S., Fitton, J. G., & Hjartarson, A. (2008). Tertiary volcanism in Iceland. *Jökull*, 58, 161–178.
- Harðarson, B. S., Fitton, J. G., Ellam, R. M., & Pringle, M. S. (1997). Rift relocation — A geochemical and geochronological investigation of a palaeo-rift in northwest Iceland. *Earth and Planetary Science Letters*, 153(3), 181–196. [https://doi.org/https://doi.org/10.1016/S0012-821X\(97\)00145-3](https://doi.org/https://doi.org/10.1016/S0012-821X(97)00145-3)
- Hart, S. R., Schilling, J. G., & Powell, J. L. (1973). Basalts from Iceland and Along the Reykjanes Ridge: Sr Isotope Geochemistry. *Nature Physical Science*, 246, 104–107. <https://doi.org/10.1038/physci246104a0>
- Helgadóttir, G. (2008). Preliminary results from the 2008 Marine Research Institute multibeam survey in the Dreki area, with some examples of potential use. In *Iceland Exploration Conference 2008*. Reykjavik, Iceland.

- Helgadóttir, G., & Reynisson, P. (2010). *Setkjarnataka, fjölgeisla- og lágtíðnidýptarmælingar á Drekasvæði og Jan Mayen hryggárs. Árna Friðrikssyni RE 200 haustið 2010*. Prepared for Orkustofnun and Norsku Ólíustofnunina, Hafrannsóknastofnunin, Leiðangursskýrsla A201011, hluti 1 og 2, Reykjavík, Ísland.
- Henriksen, N. (2008). *Geological History of Greenland - Four billion years of earth evolution, (pp. 272)*. Geological Survey of Denmark and Greenland (GEUS), Copenhagen, Denmark.
- Hey, R., Martinez, F., Hoskuldsson, A., & Benediktsdóttir, A. (2010). Propagating rift model for the V-shaped ridges south of Iceland. *Geochemistry Geophysics Geosystems, 11*(3). doi: 10.1029/2009GC002865
- Hinz, K. (1981). An hypothesis on terrestrial catastrophes wedges of very thick oceanward dipping layers beneath passive continental margins; their origin and palaeoenvironmental significance. *Geologisches Jahrbuch, E2*, 3–28.
- Hinz, K., & Schlüter, H. U. (1978). The North Atlantic - results of geophysical investigations by the Federal Institute for Geosciences and Natural Resources on North Atlantic continental margins. *Erdoel-Erdgas-Zeitschrift, 94*, 271–280.
- Hjartarson, Á., Erlendsson, Ö., & Blischke, A. (2017). The Greenland–Iceland–Faroe Ridge Complex. *Geological Society, London, Special Publications, 447*(1). <https://doi.org/10.1144/SP447.14>
- Hopper, J. R., Funck, T., Stoker, M. S., Ártung, U., Peron-Pinvidic, G., Doornenbal, H., & Gaina, C. (2014). *Tectonostratigraphic Atlas of the North-East Atlantic Region*. (1st ed.) , (pp. 338). Copenhagen, Denmark: Geological Survey of Denmark-Greenland (GEUS).
- Hopper, J. R., Dahl-Jensen, T., Holbrook, W. S., Larsen, H. C., Lizarralde, D., Korenaga, J., et al. (2003). Structure of the SE Greenland margin from seismic reflection and refraction data: Implications for nascent spreading center subsidence and asymmetric crustal accretion during North Atlantic opening. *Journal of Geophysical Research, 108*(B5), 2269. <https://doi.org/10.1029/2002JB001996>
- á Horni, J., Hopper, J.R., Blischke, A., Geissler, W., Judge, M., McDermott, K., Erlendsson, Ö., Stewart, M. and Ártung, U. (2017). Regional Distribution of Volcanism within the North Atlantic Igneous Province. Geological Society, London, Special Publications, 447, 18, <http://dx.doi.org/10.1144/SP447.18>.
- Ito, G. (2001). Reykjanes 'V'-shaped ridges originating from a pulsing and dehydrating mantle plume. *Nature, 411*(6838). 681-684, doi: 10.1038/35079561.
- Jakobsson, M., Mayer, L.A., Coakley, B., Dowdeswell, J.A., Forbes, Fridman, S.B., Hodnesdal, H., Noormets, R., Pedersen, R., Rebecco, M., Schenke, H.-W., Zarayskaya, Y., Accettella, A.D., Armstrong, A., Anderson, R.M., Bienhoff, P., Camerlenghi, A., Church, I., Edwards, M., Gardner, J.V., Hall, J.K., Hell, B., Hestvik, O.B., Kristoffersen, Y., Marcussen, C., Mohammad, R., Mosher, D., Nghiem, S.V., Pedrosa, M.T., Travaglini, P.G. and Weatherall, P. (2012). The International Bathymetric Chart of the Arctic Ocean (IBCAO) Version 3.0, *Geophysical Research Letters*, doi: 10.1029/2012GL052219.

- Jansen, E., Raymo, M.E., Blum, P. et al. (1996). Proceedings of the Ocean Drilling Program, Initial Reports, 162. Ocean Drilling Program, College Station, TX, U.S.A., doi:10.2973/odp.proc.ir.162.1996.
- Japsen, P., Green, P.F., Bonowa, J.M., Nielsen, T.F.D. and Chalmers, J.A. (2014). From volcanic plains to glaciated peaks: Burial, uplift and exhumation history of southern East Greenland after opening of the NE Atlantic. *Global and Planetary Change* 116 (2014) 91–114, <http://dx.doi.org/10.1016/j.gloplacha.2014.01.012>.
- Johansen, B., Eldholm, O., Talwani, M., Stoffa, P.L. and Buhl, P. (1988). Expanding spread profile at the northern Jan Mayen Ridge. *Polar Research*, 6, pp. 95-104, <https://doi.org/10.1111/j.1751-8369.1988.tb00584.x>.
- Johnson, G. L. and Heezen, B.C. (1967). The morphology and evolution of the Norwegian-Greenland Sea. *Deep Sea Res. Oceanogr. Abstr.*, 14, 755–771.
- Johnson, G. L. and Tanner, B. (1972). Geophysical observations on the Iceland-Faeroe Ridge. *Jökull*, 21, 45–52.
- Jung W. and Vogt, P.R. (1997). A gravity and magnetic anomaly study of the extinct Aegir Ridge. Norwegian Sea, *J. Geophys. Res.*, 102, 5065–5089.
- Kandilarov, A., Mjelde, R., Pedersen, R.B., Hellevang, B., Papenberg, C., Petersen, C.J., Planert, L. and Flueh, E. (2012). The northern boundary of the Jan Mayen microcontinent, North Atlantic determined from ocean bottom seismic, multichannel seismic, and gravity data. *Marine Geophysical Research* 33, pp. 55-76.
- Kempton, P.D., Fitton, J.G., Saunders, A.D., Nowell, G.M., Taylor, R.N., Hardarson, B.S. and Pearson, G. (2000). The Iceland plume in space and time: a Sr–Nd–Pb–Hf study of the North Atlantic rifted margin. *Earth and Planetary Science Letters*, 177(3–4). 255-271, doi: 10.1016/S0012-821X(00)00047-9.
- Kharin, G.N., Udintsev, G.B., Bogatikov, O.A., Dmitriev, J.I., Raschka, H., Kreuzer, H., Mohr, M., Harre, W. and Eckhardt, F.J., (1976). K/AR ages of the basalts of the Norwegian-Greenland Sea DSDP Leg 38. doi:10.2973/dsdp.proc.38.116.1976.
- Kodaira, S., Mjelde, R., Gunnarsson, K., Shiobara, H. and Shimamura, H. (1998b). Evolution of oceanic crust on the Kolbeinsey Ridge, north of Iceland, over the past 22 Myr., *Terra Nova*, 10, 27–31, doi:10.1046/j.1365-3121.1998.00166.x.
- Kodaira, S., Mjelde, R., Gunnarsson, K., Shiobara, H. and Shimamura, H. (1998a). Structure of the Jan Mayen microcontinent and implications for its evolution. *Geophysical Journal International*, Blackwell Science Ltd, 1998, 132, pp. 383-400.
- Kokfelt, T.F. and Ártung, U. (2014). Geochemistry. In: Hopper, J.R., Funck, T., Stoker, M.S., Ártung, U., Peron-Pinvidic, G., Doornenbal, H. and Gaina, C. (eds.) *Tectonostratigraphic Atlas of the North-East Atlantic Region*. Geological Survey of Denmark and Greenland (GEUS). Copenhagen, Denmark.

- Kokfelt, T.F., Hoernle, K., Hauff, F., Fiebig, J., Werner, R. and Garbe-Schönberg, D. (2006). Combined Trace Element and Pb-Nd-Sr-O Isotope Evidence for Recycled Oceanic Crust (Upper and Lower) in the Iceland Mantle Plume. *Journal of Petrology*, 47(9). 1705-1749, doi: 10.1093/petrology/egl025.
- Koopmann, H., Schreckenberger, B., Franke, D., Becker, K. and Schnabel, M. (2016). The late rifting phase and continental break-up of the southern South Atlantic: the mode and timing of volcanic rifting and formation of earliest oceanic crust. *Geological Society, London, Special Publications*, 420, 315-340, 18 December 2014, <https://doi.org/10.1144/SP420.2>.
- Kuvaas, B., and S. Kodaira (1997). The formation of the Jan Mayen microcontinent: the missing piece in the continental puzzle between the Møre-Vøring basins and East Greenland. *First Break*, 15(7). 239–247.
- Larsen, H.C., and Jakobsdóttir, S. (1988). Distribution, crustal properties and significance of seawards-dipping sub-basement reflectors off East Greenland. In: Morton, A.C., and Parson, L.M., (eds.). *Early Tertiary Volcanism and the Opening of the Northeast Atlantic*. *Geol. Soc. London Spec. Publ.* 39, 95-114. <https://doi.org/10.1144/GSL.SP.1988.039.01.10>.
- Larsen, L.M., Pedersen, A.K., Tegner, T. and Duncan, R.A. (2014). Eocene to Miocene igneous activity in NE Greenland: northward younging of magmatism along the East Greenland margin. *Journal of the Geological Society*, 171, 4, pp. 539-553.
- Larsen, L.M., Pedersen, A.K., Sørensen, E.V., Watt, W.S. and Duncan, R.A. (2013). Stratigraphy and age of the Eocene Igtertivâ Formation basalts, alkaline pebbles and sediments of the Kap Dalton Group in the graben at Kap Dalton. East Greenland. *Bulletin of the Geological Society of Denmark*, 61, pp. 1-18.
- Larsen, L.M., Waagstein, R., Pedersen, A.K. and Storey, M. (1999). Trans-Atlantic correlation of the Palaeogene volcanic successions in the Faeroe Islands and East Greenland. *Journal of the Geophysical Society*, 156(6). pp. 1081-1095.
- Larsen, L.M., Watt, SW. and Watt, M. (1989). Geology and petrology of the Lower Tertiary plateau basalts of the Scoresby Sund region, east Greenland. *Bulletin (Grønlands geologiske undersøgelse)*; no. 157, 164 p.: ill., maps, Copenhagen, Denmark.
- Larsen, L.M. and Watt, W.S. (1985). Episodic volcanism during break-up of the North Atlantic: evidence from the East Greenland plateau basalts. *Earth and Planetary Science Letters*, Volume 73, Issue 1, 1985, Pages 105-116, ISSN 0012-821X, [https://doi.org/10.1016/0012-821X\(85\)90038-X](https://doi.org/10.1016/0012-821X(85)90038-X).
- Larsen, M., Heilmann-Clausen, C., Piasecki, S. and Stemmerik, L. (2005). At the edge of a new ocean: post-volcanic evolution of the Palaeogene Kap Dalton Group, East Greenland, in *Petroleum Geology: North-West Europe and Global Perspectives – Proceedings of the 6th Petroleum Geology Conference*, edited by A. G. Doré and B. A. Vining, pp. 923-932, Geological Society of London, UK, doi: 10.1144/0060923.

- Larsen, M., Piasecki, S. and Stemmerik, L. (2002). The post-basaltic Palaeogene and Neogene sediments at Kap Dalton and Savoia Halvø, East Greenland, *Geology of Greenland Survey Bulletin*, 191, 103-110.
- Le Bas, M.J., Le Maitre, R.W., Streckeisen, A. and Zanettini, B. (1989). IUGS Subcommission on the Systematics of Igneous Rocks. A Chemical Classification of Volcanic Rocks Based on the Total Alkali-Silica Diagram, *Journal of Petrology*, Volume 27, Issue 3, June 1986, Pages 745–750, <https://doi.org/10.1093/petrology/27.3.745>.
- Lofgren, G.E. (1983). Effect of Heterogeneous Nucleation on Basaltic Textures: A Dynamic Crystallization Study. *Journal of Petrology*, Volume 24, Issue 3, August 1983, Pages 229–255, <https://doi.org/10.1093/petrology/24.3.229>.
- Lofgren, G.E. (1974). An experimental study of plagioclase crystal morphology: Isothermal crystallization. *American Journal of Science*, vol. 274, pp. 243-273.
- Lundin, E.R. and Doré, A.G. (2005). NE Atlantic breakup: a re-examination of the Iceland mantle plume model and the Atlantic–Arctic linkage. In: Doré, A.G. and Vining, B.A. (eds) *Petroleum Geology: North-West Europe and Global Perspectives*. Proceedings of the 6th Petroleum Geology Conference, pp. 739-754.
- Lundin, E. and Doré, A.G. (2002). Mid-Cenozoic post-breakup deformation in the ‘passive’ margins bordering the Norwegian-Greenland Sea. *Mar. Pet. Geol.* 19, 79–93.
- Mathiesen A., Bidstrup T. and Christinsen F.G. (2000). Denudation and uplift history of the Jameson Land Basin, East Greenland-constrained from maturity and apatite fission track data. *Global and Planetary Change* 24, pp. 275-301.
- Manum, S.B., Raschka, H. and Eckhardt, F.J. (1976b). Site 350. In: Talwani, M. and Udintsev, G. (eds). *Initial Reports of the Deep Sea Drilling Project*. U.S. Government Printing Office, Washington, 655 pp.
- Manum, S.B. and Schrader, H.J. (1976). Sites 346, 347, and 349. In: Talwani, M. and Udintsev, G. (eds). *Initial Reports of the Deep Sea Drilling Project*. Volume 38, U.S. Government Printing Office, Washington, pp. 521-594.
- Manum S.B., Raschka H., Eckhardt F.J., Schrader, H., Talwani, M. and Udintsev, G., e.a. (eds) (1976a). Site 337 Initial Reports of the Deep Sea Drilling Project. In: Talwani, M., Udintsev, G., et al. 1976. *Initial Reports of the Deep Sea Drilling Project*. Volume 38, Washington (U.S. Government Printing Office). pp. 117-150, Washington (U.S. Government Printing Office).
- Mertz, D. F., Sharp, W.D. and Haase, K.M. (2004). Volcanism on the Eggvin Bank (central Norwegian-Greenland Sea, latitude approximately 71 degrees N); age, source, and relation-ship to the Iceland and putative Jan Mayen Plumes. *Journal of Geodynamics*, 38(1; 1). 57-84, doi: 10.1016/j.jog.2004.03.003.
- Mertz, D.F. and Haase, K.M. (1997). The radiogenic isotope composition of the high-latitude North Atlantic mantle. *Geology*, 25 (5). 411-414, doi: 10.1130/0091-7613(1997)025<0411:tricot>2.3.co;2.

- Mertz, D.F., Devey, C.W., Todt, W., Stoffers, P. and Hofmann, A.W. (1991). Sr-Nd-Pb isotope evidence against plume-asthenosphere mixing north of Iceland. *Earth and Planetary Science Letters*, 107 (2). 243-255, doi: 10.1016/0012-821X(91)90074-R.
- Meyer, R., Hertogen, J., Pedersen, R. B., Viereck-Götte, L. and Abratis, M. (2009). Interaction of mantle derived melts with crust during the emplacement of the Vøring Plateau, N.E. Atlantic. *Marine Geology: EUROMARGINS: Imaging, monitoring, and modelling the physical, chemical and biological processes in the European passive continental margins*, 261(1-4). 3-16.
- Meyer, O., Voppel, D., Fleischer, U., Gloss, H. and Gerke, K. (1972). Results of bathymetric, magnetic and gravimetric measurements between Iceland and 70°N, *Dtsch. Hydrogr. Z.*, 25, 193–201.
- Miller, K.G., Browning, J.V., Aubry, M.-P., Wade, B.S., Katz, M.E., Kulpecz, A.A. and Wright, J.D. (2008). Eocene–Oligocene global climate and sea-level changes: St. Stephens Quarry, Alabama. *GSA Bulletin*; January/February 2008; v. 120; no. 1/2; p. 34–53; doi: 10.1130/B26105.1; 9 figures.
- Millett, J.M., Hole, M.J., Jolley, D.W. and Passey, S.R. (2017). Geochemical stratigraphy and correlation within large igneous provinces: The final preserved stages of the Faroe Islands Basalt Group. *Lithos*, Volumes 286–287, 2017, Pages 1-15, ISSN 0024-4937, <https://doi.org/10.1016/j.lithos.2017.05.011>.
- Mjelde, R., Kvarven, T., Faleide, J.I. and Thybo, H. (2016). Lower crustal high-velocity bodies along North Atlantic passive margins, and their link to Caledonian suture zone eclogites and Early Cenozoic magmatism. *Tectonophysics* 670 (2016) 16–29, <http://dx.doi.org/10.1016/j.tecto.2015.11.021>.
- Mjelde, R., Raum, T., Breivik, A.J., Faleide, J.I., 2008. Crustal transect across the North Atlantic. *Mar. Geophys. Res.* 29, 73–87. <https://doi.org/DOI: 10.1007/s11001-008-9046-9>
- Mjelde, R., Eckhoff, I., Solbakken, S., Kodaira, S., Shimamura, H., Gunnarsson, K., Nakanishi, A. and Shiobara, H. (2007). Gravity and S-wave modelling across the Jan Mayen Ridge, North Atlantic; implications for crustal lithology. *Marine Geophysical Researches*, 28, pp. 27-41.
- Mjelde, R., Aurvåg, R., Kodaira, S., Shimamura, H., Gunnarsson, K., Nakanishi, A. and Shiobara, H. (2002). Vp/Vs-ratios from the central Kolbeinsey Ridge to the Jan Mayen Basin, North Atlantic; implications for lithology, porosity and present-day stress field. *Marine Geophysical Researches*, 23, pp. 123-145.
- Mohr, M (1976). Additional Petrographic Studies of Basalts, DSDP, Leg 38. doi:10.2973/dsdp.proc.38.111.1976.
- Mordret, A. (2018). Uncovering the Iceland hot spot track beneath Greenland. *Journal of Geophysical Research: Solid Earth*, 123, 4922–4941, <https://doi.org/10.1029/2017JB015104>.

- Mudge, D.C. (2015). Regional controls on Lower Tertiary sandstone distribution in the North Sea and NE Atlantic margin basins. IN: McKie, T., Rose, P.T.S., Hartley, A.J., Jones, D.W. and Armstrong, T.L. (eds) (2015). Tertiary Deep-Marine Reservoirs of the North Sea Region. Geological Society, London, Special Publications, 403, 17–42, <http://dx.doi.org/10.1144/SP403.5>.
- Murray-Wallace, C., and Woodroffe, C. (2014). Pleistocene sea-level changes. In Quaternary Sea-Level Changes: A Global Perspective (pp. 256-319). Cambridge: Cambridge University Press, doi:10.1017/CBO9781139024440.007.
- Mutter, J.C., Talwani, M. and Stoffa, P.L. (1982). Origin of seaward-dipping reflectors in oceanic crust off the Norwegian margin by "subaerial sea-floor spreading". *Geology*, 10, pp. 3-12.
- Müller, R.D., Gaina, G., Roest, W.R. and Hansen, D.L. (2001). A recipe for microcontinent formation. *Geology*, 29, 203–206.
- Myhre, A. M., O. Eldholm and E. Sundvor (1984). The Jan Mayen Ridge; present status. *Polar Research*, 2(1). 47–59.
- Nasuti, A. and Olesen, O. (2014). Magnetic Data. In: Hopper, J.R., Funck, T., Stoker, M.S., Ártung, U., Peron-Pinvidic, G., Doornenbal, H., Gaina, C. (Eds.). Tectonostratigraphic Atlas of the North-East Atlantic Region. Geological Survey of Denmark and Greenland (GEUS). Copenhagen, Denmark.
- Nilsen, T.H., Kerr, D.R., Talwani, M. and Udintsev, G. e.a. (eds) (1978). Turbidites, redbeds, sedimentary structures, and trace fossils observed in DSDP Leg 38 cores and the sedimentary history of the Norwegian-Greenland Sea Initial Reports of the Deep Sea Drilling Project. Washington (U.S. Government Printing Office). Supplement to Volume 38, pp. 259-288.
- Norcliffe, J., Paton, D., Mortimer, E., McCaig, A. and Rodriguez, K. (2019). Asymmetric emplacement of seaward dipping reflectors during rifting: where; when; how and why?. Vol. 21, EGU2019-10085, 2019.
- Norwegian Petroleum Directorate (2011). Submarine fieldwork on the Jan Mayen Ridge: integrated seismic and ROV-sampling. Norwegian Petroleum Directorate, Stavanger, Norway, <http://www.npd.no/en/Publications/Resource-Reports/2013/Chapter-7/>.
- Norwegian Petroleum Directorate (2013). The Petroleum Resources on the Norwegian Continental Shelf. Norwegian Petroleum Directorate, Stavanger, Norway, 63 pp., <http://www.npd.no/en/Publications/Resource-Reports/2013/>.
- Nunns, A. (1983a). The structure and evolution of the Jan Mayen Ridge and surroundings regions. In: Watkins, J.S. and Drake, C.L. (eds). Studies in Continental Margin Geology. American Association of Petroleum Geologists, memoir, pp. 193-208.
- Nunns, A.G., Talwani, M., Lorentzen, G.N., Vogt, P.R., Sigurgeirsson, T., Kristjánsson, L., Larsen, H.C. and Voppel, D. (1983b). Magnetic anomalies over Iceland and surrounding seas, in Structure and Development of the Greenland-Scotland Ridge. Edited by Bott, M.H.P., Saxov, S., Talwani, M. and Thiede, J., pp. 661-678, Plenum, New York.

- Nunns, A.G. (1983c). Plate tectonic evolution of the Greenland-Scotland Ridge and surrounding regions, in *Structure and Development of the Greenland-Scotland Ridge*. Edited by M.H. P. Bott, S. Saxov, M. Talwani and J. Thiede, pp. 11-30, Plenum, New York, New York.
- Nunns, A. (1982). The structure and evolution of the Jan Mayen Ridge and surrounding regions. In: *Studies in Continental Margin Geology*, vol. 34, edited by J. S. Watkins and C. L. Drake, pp. 193–208, AAPG Mem., Tulsa, Oklahoma, USA.
- Olafsson, I. and Gunnarsson, K. (1989). The Jan Mayen ridge: velocity structure from analysis of sonobuoy data. *Orkustofnun, Reykjavík*, OS-89030/JHD-04, 62 pp.
- Ólafsdóttir, J, Stoker, MS, Boldreel, LO, Andersen, MS, Eidesgaard, ÓR. Seismic-stratigraphic constraints on the age of the Faroe Islands Basalt Group, Faroe–Shetland region, Northeast Atlantic Ocean. *Basin Res.* 2019; 00: 1– 25. <https://doi.org/10.1111/bre.12348>.
- Parkin, C.J., and R.S. White (2008). Influence of the Iceland mantle plume on oceanic crust generation in the North Atlantic, *Geophysical Journal International*, 173(1). 168-188, doi: 10.1111/j.1365-246X.2007.03689.x.
- Parnell-Turner, R., White, N., Henstock, T., Murton, Murton, B.B., MacLennan, J. and Jones, S.M. (2014). A continuous 55-million-year record of transient mantle plume activity beneath Iceland. *Nature Geoscience*, 7, 914–919, doi:10.1038/ngeo2281.
- Parsons, A.J., Whitham, A.G., Kelly, S.R.A., Vautravers, B.P.H, Dalton, T.J.S., Andrews, S.D., Pickles, C.S., Strogen, D.P., Braham, W., Jolley, D.W. and Gregory, F.J. (2017). Structural evolution and basin architecture of the Traill Ø region, NE Greenland: A record of polyphase rifting of the East Greenland continental margin: *Geosphere*, v. 13, no. 3, p. 1–38, doi:10.1130/GES01382.1.
- Parson, L., Viereck, L., Love, D., Gibson, I., Morton, A. and Hertogen, J. (1989). The petrology of the lower series volcanics, ODP Site 642. In: Eldholm, O., Thiede, J., Taylor, E., et al., *Proc. ODP, Sci. Results*, 104: College Station, TX (Ocean Drilling Program). 419–428. doi:10.2973/odp.proc.sr.104.134.1989.
- Passey, S.R. (2009). Recognition of a faulted basalt lava flow sequence through the correlation of stratigraphic marker units, Skopunarfjørður, Faroe Islands. In: Varming, T. and Ziska, H. (eds.) *Faroe Islands Exploration Conference: Proceedings of the 2nd Conference*. *Annales Societatis Scientiarum Færoensis*, Tórshavn, 174-204.
- Passey, S.R., and Jolley, D.W. (2009). A revised lithostratigraphic nomenclature for the Palaeogene Faroe Islands Basalt Group, NE Atlantic Ocean. *Earth and Environmental Science Transactions of the Royal Society of Edinburgh*, 99, 127-158.
- Passey, S.R., and Hitchen, K. (2011). Cenozoic (igneous). In: Ritchie, J.D., Ziska, H., Johnson, H., and Evans, D. (eds). *Geology of the Faroe-Shetland Basin and Adjacent Areas*. BGS Research Report, RR/11/01, Jarðfeingi Research Report, RR/11/01, 209-228.

- Pedersen, A.K., Watt, M., Watt, W.S. and Larsen L.M. (1997). Structure and stratigraphy of the Early Tertiary basalts of the Blossville Kyst, East Greenland. *Journal of the Geological Society, London, Vol. 154, pp. 565-570, 7 fig., <https://dx.doi.org/10.1144/gsjgs.154.3.0565>.*
- Peron-Pinvidic, G., Gernigon, L., Gaina, C. and Ball, P. (2012a). Insights from the Jan Mayen system in the Norwegian-Greenland Sea - I: mapping of a microcontinent. *Geophysical Journal International, 191, pp. 385-412.*
- Peron-Pinvidic, G., Gernigon, L., Gaina, C. and Ball, P. (2012b). Insights from the Jan Mayen system in the Norwegian-Greenland Sea - II: architecture of a microcontinent. *Geophysical Journal International, 191, pp. 413-435.*
- Pitman, W.C I. and Talwani, M. (1972). Sea-floor spreading in the North Atlantic. *Geol. Soc. Am. Bull., 83, 619–646.*
- Planke, S., Symonds, P.A., Alvestad, E. and Skogseid, J. (2000). Seismic volcanostratigraphy of large-volume basaltic extrusive complexes on rifted margins. *Journal of Geophysical Research, 105(B8), pp. 19335-19351.*
- Planke, S. and Eldholm, O. (1994). Seismic response and construction of seaward dipping wedges of flood basalts: Voring volcanic margin. *J. Geophys. Res. 99 (B5), 9263–9278. <https://doi.org/10.1029/94JB00468>.*
- Polteau, S., Mazzini, A., Hansen, G., Planke, S., Jerram, D.A., Millett, J., Abdelmalak, M.M., Blischke, A. and Myklebust, R (2018). The pre-breakup stratigraphy and petroleum system of the Southern Jan Mayen Ridge revealed by seafloor sampling. *Tectonophysics. DOI: 10.1016/j.tecto.2018.04.016.*
- Polteau, S., Mazzini, A., Trulsvik, M. and Planke, S. (2012). JMRS11 – Jan Mayen Ridge Sampling Survey 2011. VBPR-TGS, Commercial report, February 2012.
- Raschka, H., Eckhardt, F.J. and Manum, S.B. (1976). Site 348. In: Talwani, M. and Udintsev, G. (eds). *Initial Reports of the Deep Sea Drilling Project. U.S. Government Printing Office, Washington, pp. 595-654.*
- Rey, S.S., Eldholm, O. and Planke, S. (2003). Formation of the Jan Mayen Microcontinent, the Norwegian Sea. *EOS Trans. AGU, 84, Abstract T31D-0872.*
- Ridley, W.I., Perfit, M.R., Adams, M.L. (1976). Petrology of basalts from deep sea drilling project, Leg 38, Initial reports DSDP, Volume 38, Pages 731-739, DOI: 10.2973/dsdp.proc.38.113.1976.
- Rychert, C.A., Harmon, N. and Armitage, J.J. (2018). Seismic imaging of thickened lithosphere resulting from plume pulsing beneath Iceland. *Geochemistry, Geophysics, Geosystems, 19, p. 1789–1799, <https://doi.org/10.1029/2018GC007501>.*

- Ritchie, J.D., Johnson, H., Quinn, M.F. and Gatliff, R.W. (2008). The effects of Cenozoic compression within the Faroe-Shetland Basin and adjacent areas. In: *The Nature and Origin of Compression in Passive Margins*, Geological Society of London, Special Publication 306, edited by Johnson, H., Doré, A.G., Gatliff, R.W., Holdsworth, R.W., Lundin, E.R. and Ritchie, J. D., pp. 121-136, doi: 10.1144/sp306.5.
- Sæmundsson, K. (1979). Outline of the geology of Iceland. *Jökull*, 29, 7–28.
- Sandstå, N.R., Sand, M. and Brekke, H. (2013). Ressursrapporter 2013, Kapittel-7 Jan Mayen. Norwegian Petroleum Directorate, project web publication, Stavanger, Norway.
- Sandstå, N.R., Pedersen, R.B., Williams, R.D., Bering, D., Magnus, C., Sand, M. and Brekke, H. (2012). Submarine fieldwork on the Jan Mayen Ridge; integrated seismic and ROV-sampling. Edited Norwegian Petroleum Directorate, <http://www.npd.no/>.
- Saunders, A.D., Fitton, J.G., Kerr, A.C., Norry, M.J. and Kent, R.W. (2013). The North Atlantic Igneous Province (pp. 45–93). <https://doi.org/10.1029/GM100p0045>.
- Schiffer, C., Peace, A., Phethean, J., Gernigon, L., McCaffrey, K., Petersen, K.D. and Foulger, G. (2018). The Jan Mayen Microplate Complex and the Wilson Cycle. Geological Society London Special Publications. 10.1144/SP470.2.
- Schiffer, C., Doré, A. G., Foulger, G. R., Franke, D., Geoffroy, L., Gernigon, L., et al. (2019). Structural inheritance in the North Atlantic. *Earth-Science Reviews*, 102975. <https://doi.org/https://doi.org/10.1016/j.earscirev.2019.102975>
- Schilling, J.G., Kingsley, R., Fontignie, D., Poreda, R. and Xue, S. (1999). Dispersion of the Jan Mayen and Iceland mantle plumes in the Arctic: A He-Pb-Nd-Sr isotope tracer study of basalts from the Kolbeinsey, Mohns, and Knipovich Ridges. *Journal of Geophysical Research*, 104(B5). 10543-10569, doi: 10.1029/1999jb900057.
- Scott, R.A., Ramsey, L.A., Jones, S.M., Sinclair, S. and Pickles, C.S. (2005). Development of the Jan Mayen microcontinent by linked propagation and retreat of spreading ridges. In: Wandås, B.T.G., Nystuen, J.P., Eide, E. and Gradstein, F. (eds). *Onshore–Offshore Relationships on the North Atlantic Margin*. Norwegian Petroleum Society, pp. 69-82.
- Self, S., Thordarson, T. and Keszthelyi, L. (1997). Emplacement of continental flood basalt lava flows, in *Large Igneous Provinces: Continental, Oceanic, and Planetary Flood Volcanism*, edited by Mahoney, J.J. and Coffin, M.L., pp. 381-410, American Geophysical Union, Geophysical Monographs.
- Skogseid, J. and Eldholm, O. (1987). Early Cenozoic crust at the Norwegian Continental Margin and the conjugate Jan Mayen Ridge. *Journal of Geophysical Research*, 921, 11471-11492, 10.1029/JB092iB11p11471.
- Skogseid, J., Planke, S., Faleide, J.I., Pedersen, T., Eldholm, O. and Neverdal, F. (2000). NE Atlantic continental rifting and volcanic margin formation. Geological Society, London, Special Publications, 167(1). 295–326. <https://doi.org/10.1144/GSL.SP.2000.167.01.12>.

- Skovgaard, A.C., Storey, M., Baker, J., Blusztajn, J. and S. R. Hart (2001). Osmium-oxygen isotopic evidence for a recycled and strongly depleted component in the Iceland mantle plume. *Earth and Planetary Science Letters*, 194(1). 259-275, doi: 10.1016/S0012-821X(01)00549-0.
- Srivastava, S.P. and Tapscott, C.R. (1986). Plate kinematics of the North Atlantic. In: *The Geology of North America, Vol. M, The Western North Atlantic Region*. pp. 379–404, Geol. Soc. of Am., Boulder, Colo.
- Stärz, M., Jokat, W., Knorr, G. and Lohmann, G. (2017). Threshold in North Atlantic-Arctic Ocean circulation controlled by the subsidence of the Greenland-Scotland Ridge. *Nat. Commun.* 8, 15681.
- Stoker, M.S., Houlst, R.J., Nielsen, T., Hjelstuen, J.S., Laberg, J.S., Shannon, P.M., Praeg, D., Mathiesen, A., van Weering, T.C.E. and McDonnell, A.M. (2005b). Sedimentary and oceanographic responses to early Neogene compression on the NW European margin. *Marine and Petroleum Geology*, 22, 1031–1044.
- Stoker, M.S., Praeg, D., Shannon, P.M., Hjelstuen, B.O., Laberg, J.S., Nielsen, T., van Weering, T.C.E., Sejrup, H.P., and Evans, D. (2005a). Neogene evolution of the Atlantic continental margin of NW Europe (Lofoten Islands to SE Ireland): anything but passive. In: Doré, A.G., and Vining, B.A. (eds). *Petroleum Geology: North-West Europe and Global Perspectives*. Proceedings of the 6th Petroleum Geology Conference, Volume 6. London, Geological Society, pp. 1057-1076.
- Storey, M., Duncan, R. and Tegner, C. (2007). Timing and duration of volcanism in the North Atlantic Igneous Province: Implications for geodynamics and links to the Iceland hotspot *Chemical Geology* 241(3-4). 264-281. <https://dx.doi.org/10.1016/j.chemgeo.2007.01.016>.
- Stracke, A., Zindler, A., Salters, V.J.M., McKenzie, D., Blichert-Toft, J., Albarède, F. and Grönvold, K. (2003). Theistareykir revisited. *Geochemistry, Geophysics, Geosystems*, 4(2). n/a-n/a, doi: 10.1029/2001GC000201.
- Sun, S.S., Tatsumoto, M. and Schilling, J.G. (1975). Mantle plume mixing along the Reykjanes ridge axis - Lead isotope evidence. *Science*, 190 (4210). p. 143-147, doi: 10.1126/science.190.4210.143.
- Svellingen, W. and Pedersen, R. (2003). Jan Mayen: A result of ridge-transform-micro-continent interaction. *Geophysical Research Abstracts*, Vol. 5, 12993 pp.
- Swindle, T.D. and Weirich, J.R. (2017). The effect of partial thermal resetting on ^{40}Ar - ^{39}Ar “Plateaus”. *Lunar and Planetary Science XLVIII* (2017).
- Sylvester, A. G. (1978). Petrography of volcanic ashes in deep-sea cores near Jan-Mayen island: sites 338, 345-350 dsdp leg 38, paper presented at Initial Reports of the Deep Sea Drilling Project, Washington (U.S. Government Printing Office).
- Sylvester, A. (1975). History and surveillance of volcanic activity on Jan Mayen island, *Bulletin of Volcanology*, 39, 313-335.

- Symonds, P.A., Planke, S., Frey, Ø. and Skogseid, J. (1998). Volcanic evolution of the western Australian continental margin and its implications for basin development. In: (ed) Purcell, R.R., *The Sedimentary Basins of Western Australia*. pp. 33-54, Perth.
- Talwani, M., Mutter, J. and Eldholm, O. (1981). The Initiation of Opening of the Norwegian Sea. *Oceanologica Acta SP*, 23-30.
- Talwani, M., Udintsev, G., Mirlin, E., Beresnev, A.F., Kanayev, V.F., Chapman, M., Groenlie, G. and Eldholm, O. (1978). Survey at sites 346, 347, 348, 349, and 350, the area of the Jan-Mayen Ridge and the Icelandic Plateau. doi: 10.2973/dsdp.proc.38394041s.127.1978.
- Talwani, M. and Eldholm, O. (1977). Evolution of the Norwegian-Greenland Sea. *Geological Society of America Bulletin*, 88, pp. 969-999.
- Talwani, M., Udintsev, G. (1976k). Tectonic Synthesis. *Initial Reports Deep Sea Drill. Proj.* 1214–1232.
- Talwani, M., Udintsev, G.B., Bjoerklund, K., Caston, V.N.D., Faas, R. W., van Hinte, J.E., Kharin, G.N., Morris, D.A., Mueller, C., Nilsen, T.H., Warnke, D.A., White, S.M., Manum, S.B. and Schrader, H.-J. (1976j). Sites 336 and 352. *Initial Reports of the Deep Sea Drilling Project, Vol.38*, p. 595-654. Publisher: Texas A & M University, Ocean Drilling Program, College Station, TX, United States. ISSN: 0080-8334 CODEN: IDSDA6. doi:10.2973/dsdp.proc.38.102.1976
- Talwani, M., Udintsev, G.B., Bjoerklund, K., Caston, V.N.D., Faas, R. W., van Hinte, J.E., Kharin, G.N., Morris, D.A., Mueller, C., Nilsen, T.H., Warnke, D.A., White, S.M., Manum, S.B. and Schrader, H.-J. (1976i). Site 337. *Initial Reports of the Deep Sea Drilling Project, Vol.38*, p. 595-654. Publisher: Texas A & M University, Ocean Drilling Program, College Station, TX, United States. ISSN: 0080-8334 CODEN: IDSDA6. doi:10.2973/dsdp.proc.38.103.1976
- Talwani, M., Udintsev, G.B., Bjoerklund, K., Caston, V.N.D., Faas, R. W., van Hinte, J.E., Kharin, G.N., Morris, D.A., Mueller, C., Nilsen, T.H., Warnke, D.A., White, S.M., Manum, S.B. and Schrader, H.-J. (1976h). Sites 338-343. *Initial Reports of the Deep Sea Drilling Project, Vol.38*, p. 595-654. Publisher: Texas A & M University, Ocean Drilling Program, College Station, TX, United States. ISSN: 0080-8334 CODEN: IDSDA6. doi:10.2973/dsdp.proc.38.104.1976
- Talwani, M., Udintsev, G.B., Bjoerklund, K., Caston, V.N.D., Faas, R. W., van Hinte, J.E., Kharin, G.N., Morris, D.A., Mueller, C., Nilsen, T.H., Warnke, D.A., White, S.M., Manum, S.B. and Schrader, H.-J. (1976g). Site 345. *Initial Reports of the Deep Sea Drilling Project, Vol.38*, p. 595-654. Publisher: Texas A & M University, Ocean Drilling Program, College Station, TX, United States. ISSN: 0080-8334 CODEN: IDSDA6. doi:10.2973/dsdp.proc.38.106.1976.

- Talwani, M., Udintsev, G.B., Bjoerklund, K., Caston, V.N.D., Faas, R. W., van Hinte, J.E., Kharin, G.N., Morris, D.A., Mueller, C., Nilsen, T.H., Warnke, D.A., White, S.M., Manum, S.B. and Schrader, H.-J. (1976f). Site 348. Initial Reports of the Deep Sea Drilling Project, Vol.38, p. 595-654. Publisher: Texas A & M University, Ocean Drilling Program, College Station, TX, United States. ISSN: 0080-8334 CODEN: IDSDA6. doi:10.2973/dsdp.proc.38.108.1976.
- Talwani, M., Udintsev, G.B., Bjoerklund, K., Caston, V.N.D., Faas, R. W., van Hinte, J.E., Kharin, G.N., Morris, D.A., Mueller, C., Nilsen, T.H., Warnke, D.A., White, S.M., Manum, S.B. and Schrader, H.-J. (1976e). Site 350. Initial Reports of the Deep Sea Drilling Project, Vol.38, p. 655-682. Publisher: Texas A & M University, Ocean Drilling Program, College Station, TX, United States. ISSN: 0080-8334 CODEN: IDSDA6. doi:10.2973/dsdp.proc.38.109.1976
- Talwani, M., Udintsev, G.B., Bjoerklund, K., Caston, V.N.D., Faas, R. W., van Hinte, J.E., Kharin, G.N., Morris, D.A., Mueller, C., Nilsen, T.H., Warnke, D.A., White, S.M., Manum, S.B., Schrader, H.-J. (1976c). Sites 346, 347, and 349. Initial Reports of the Deep Sea Drilling Project, Vol.38, p.521-594. Publisher: Texas A & M University, Ocean Drilling Program, College Station, TX, United States. ISSN: 0080-8334 CODEN: IDSDA6. doi: 10.2973/dsdp.proc.38.107.1976.
- Talwani, M., Udintsev, G. and Shirshov, P.R. (1976b). Tectonic synthesis. In: Talwani, M. and Udintsev, G. (eds). Initial Reports of the Deep Sea Drilling Project. Volume 38, U.S. Government Printing Office, Washington, pp. 1213-1242.
- Talwani, M., Udintsev, G. and White, S.M. (1976a). Introduction and explanatory notes, Leg 38, Deep Sea Drilling Project. In: Talwani, M. and Udintsev, G. (eds). Initial Reports of the Deep Sea Drilling Project. Volume 38, U.S. Government Printing Office, Washington, pp. 3-19.
- Tan, P., Sippel, J., Breivik, A.J., Meeßen, C. and Scheck-Wenderoth, M. (2018). Lithospheric control on asthenospheric flow from the Iceland plume: 3-D density modeling of the Jan Mayen-East Greenland Region, NE Atlantic. *Journal of Geophysical Research: Solid Earth*, 123, <https://doi.org/10.1029/2018JB015634>.
- Tan, P., Breivik, A.J., Trønnes, R.G., Mjelde, R., Azuma, R. and Eide, S. (2017). Crustal structure and origin of the Eggvin Bank west of Jan Mayen, NE Atlantic, *J. Geophys. Res. Solid Earth*, 122, 43–62, doi:10.1002/2016JB013495.
- Tegner, C., Brooks, C.K., Duncan, R.A., Heister, L.E. and Bernstein, S. (2008). ^{40}Ar – ^{39}Ar ages of intrusions in East Greenland: Rift-to-drift transition over the Iceland hotspot. *Lithos* 101, pp. 480-500.
- Tegner, C., Leshner, C.E., Larsen, L.M. and Watt, W.S. (1998). Evidence from the rareearth-element record of mantle melting for cooling of the Tertiary Iceland plume, *Nature*, 395(6702). 591-594.

- Theissen-Krah S., Zastrozhnov, D., Abdelmalak, M.M., Schmid, D.W., Faleide, J.I. and Gernigone, L. (2017). Tectonic evolution and extension at the Møre Margin – Offshore mid-Norway. *Tectonophysics* 721 (2017) 227–238, <http://dx.doi.org/10.1016/j.tecto.2017.09.009>.
- Thiede, J., Firth, J.V. et al. (eds) (1995). Site 907 Proceedings of the Ocean Drilling Program, Initial Reports. College Station, TX (Ocean Drilling Program). 151, pp. 57-111.
- Thirlwall, M.F., Gee, M.A.M., Taylor, R.N. and Murton, B.J. (2004). Mantle components in Iceland and adjacent ridges investigated using double-spike Pb isotope ratios. *Geochimica Et Cosmochimica Acta*, 68(2). 361-386, doi: 10.1016/S0016-7037(03)00424-1.
- Thordarson, T. and Höskuldsson, Á. (2008). Postglacial volcanism in Iceland. *JÖKULL* No. 58, p 197-228.
- Tripati, A. and Darby, D. (2018). Evidence for ephemeral middle Eocene to early Oligocene Greenland glacial ice and pan-Arctic sea ice. *Nature Communications* 9, Article number: 1038, pp. 2041-1723, <https://doi.org/10.1038/s41467-018-03180-5>.
- Van Sickel, W.A., Kominz, M.A., Miller, K.G., Browning, J. V., 2004. Late Cretaceous and Cenozoic sea-level estimates: backstripping analysis of borehole data, onshore New Jersey. *Basin Res.* 16, 451–465. <https://doi.org/10.1111/j.1365-2117.2004.00242.x>
- Vogt, P.R. (1986). Magnetic anomalies of the North Atlantic Ocean. IN: *The Western North Atlantic Region*. Edited by Vogt, P.R. and Tucholke, B.E., Geological Society of America.
- Vogt, P.R., Johnson, G.L. and Kristjansson, L. (1980). Morphology and magnetic anomalies north of Iceland. *J. Geophys. Res.*, 47, 67–80.
- Vogt, P.R. and Avery, O.E. (1974). Detailed magnetic surveys in the Northeast Atlantic and Labrador Sea. *J. Geophys. Res.*, 79, 363–389.
- Vogt, P.R., Anderson, C.N., Bracey, D.R. and Schneider, E.M. (1970). North Atlantic Magnetic Smooth Zones. *Journal of Geophysical Research*, 75, pp. 3955-3968.
- Wang, X., Cochran, J.R. and Barth, G.A. (1996). Gravity anomalies, crustal thickness, and the pattern of mantle flow at the fast spreading East Pacific Rise, 9°–10°N: Evidence for three-dimensional upwelling, *J. Geophys. Res.*, 101(B8). 17927– 17940, doi:10.1029/96JB00194.
- Weigel, W., Flüh, E., Miller, H., Butzke, A., Deghani, A., Gebbhardt, V., Harder, I., Hepper, J., Jokat, W., Kläschen, D., Schübler, S. and Zhao-Groekart, Z. (1995). Investigations of the East Greenland continental margin between 70° and 72° N by deep seismic sounding and gravity studies, *Marine Geophysical Research*, 17(2). 167-199, doi: 10.1007/bf01203425.
- White, R.S., Bown, J.W. and Smallwood, J.R. (1995). The temperature of the Iceland plume and origin of outward-propagating V-shaped ridges. *Journal of the Geological Society, London*, 152 (6). 1039-1045, doi: 10.1144/GSL.JGS.1995.152.01.26.

White, W.M. and Schilling, J.-G. (1978). The nature and origin of geochemical variation in Mid-Atlantic Ridge basalts from the Central North Atlantic. *Geochimica Et Cosmochimica Acta*, 42 (10). 1501-1516, doi: 10.1016/0016-7037(78)90021-2.

Zastrozhnov, D., Gernigon, L., Gogin, I., Abdelmalak, M.M., Planke, S., Faleide, J.I., Eide, S. and Myklebust, R. (2018). Cretaceous-Paleocene Evolution and Crustal Structure of the Northern Vøring Margin (Offshore Mid-Norway): Results from Integrated Geological and Geophysical Study. *Tectonics*, 37, <https://doi.org/10.1002/2017TC004655>.

Supplements

Supplement 1 JMMC study database summary table. JMMC study database [Blischke et al., 2019], reviewed and selected data and studies (Figure 3).

Supplement 2. Updated stratigraphic sections of the JMMC based on seismic reflection data by Blischke et al. [2019] tied to OBS, sonobuoy, ESP velocity profiles, and available boreholes, modified from Blischke et al. [2019]. Magnetic-, free air gravity data [Nasuti and Olesen, 2014 and Haase and Ebbing, 2014], and large fracture zone corridor intersections [e.g. Gaina et al., 2009; Kandilarov et al., 2012; Gernigon et al., 2015; Blischke et al. 2017a] plotted above the profiles highlight variations associated with major tectonic and igneous events.

Supplement 3. DSDP 38-348 & 350 Thin-section sample descriptions.

- (a) Icelandic Plateau thin-section analysis for 3 samples of borehole DSDP 38-348.
- (b) Icelandic Plateau thin-section analysis for 4 samples of borehole DSDP 38-350.

Supplement 4 $^{40}\text{Ar}/^{39}\text{Ar}$ radiometric age estimate sample results for boreholes DSDP 38-350 and 348.

Summary table of the $^{40}\text{Ar}/^{39}\text{Ar}$ age spectra dating estimate of core samples of wells DSDP-38-348 & 350 in comparison to the existing age K/Ar analysis (1) [Kharin et al., 1976], the new $^{40}\text{Ar}/^{39}\text{Ar}$ age analysis (2) [OSU Argon Geochronology Laboratory], and the magnetic polarity chron age model (3) [Gradstein et al. 2012].

Supplement 5 Geochemical database location map.

- (a) Borehole and seafloor sample locations map. The sites are labelled by sub-region or igneous provinces in comparison with geo-chronologic time zones and age dating model by Gaina et al. [2014]. Geochemistry data reference: PETDB [Lamont Doherty Earth Observatory, Columbia University, New York, <http://www.earthchem.org/petdb>], and GEOROC [Max Planck Institute for Chemistry, Mainz, <http://georo-mpch-mainz.gwdg.de/georoc/>]. Abbreviations: borehole numbers of DSDP Leg 38 sites 336 – 350, and Leg 104 site 642; BK – Blossville Kyst; EJMfZ – East Jan Mayen Fracture Zone; FI – Faroe Islands; GP – Geiko plateau; IFR – Iceland-Faroe Ridge; IPR – Iceland Plateau Rift; JMI – Jan Mayen Island complex; JMLB – Jameson Land Basin; JMR – Jan Mayen Ridge; K – Kangerlussuaq (central East Greenland); ML – Milne Land; NVZ – Northern Volcanic Zone; SRC – Southern Ridge Complex; TFZ – Tjörnes Fracture Zone; TØ – Trail Ø; VP – Vøring Plateau and Margin; and WJMfZ – West Jan Mayen Fracture Zone.
- (b) Geochemical ICP-OES analysis data for DSDP Leg 38 Sites 348 and 350.
- (c) Geochemistry data references.

Supplement 6 Mapped JMMC volcanic facies, stratigraphic horizons and igneous events.

- (a) Jan Mayen microcontinent area volcanic facies types example.
- (b) Data interpretation is based on 2D multi-channel seismic reflection data from surveys NPD-2011, ICE-02 in 2009 and reprocessed data from the JM-85, JMR-01, and JMR-08 surveys.
- (c) Summary of interpreted stratigraphic horizons and main igneous events.

Supplement 7 Present day JMMC volcanic facies and province interpretations in comparison with magnetic [Nasuti and Olesen, 2014], free air gravity and Bouguer gravity data [Haase and Ebbing, 2014].

Supplement 1

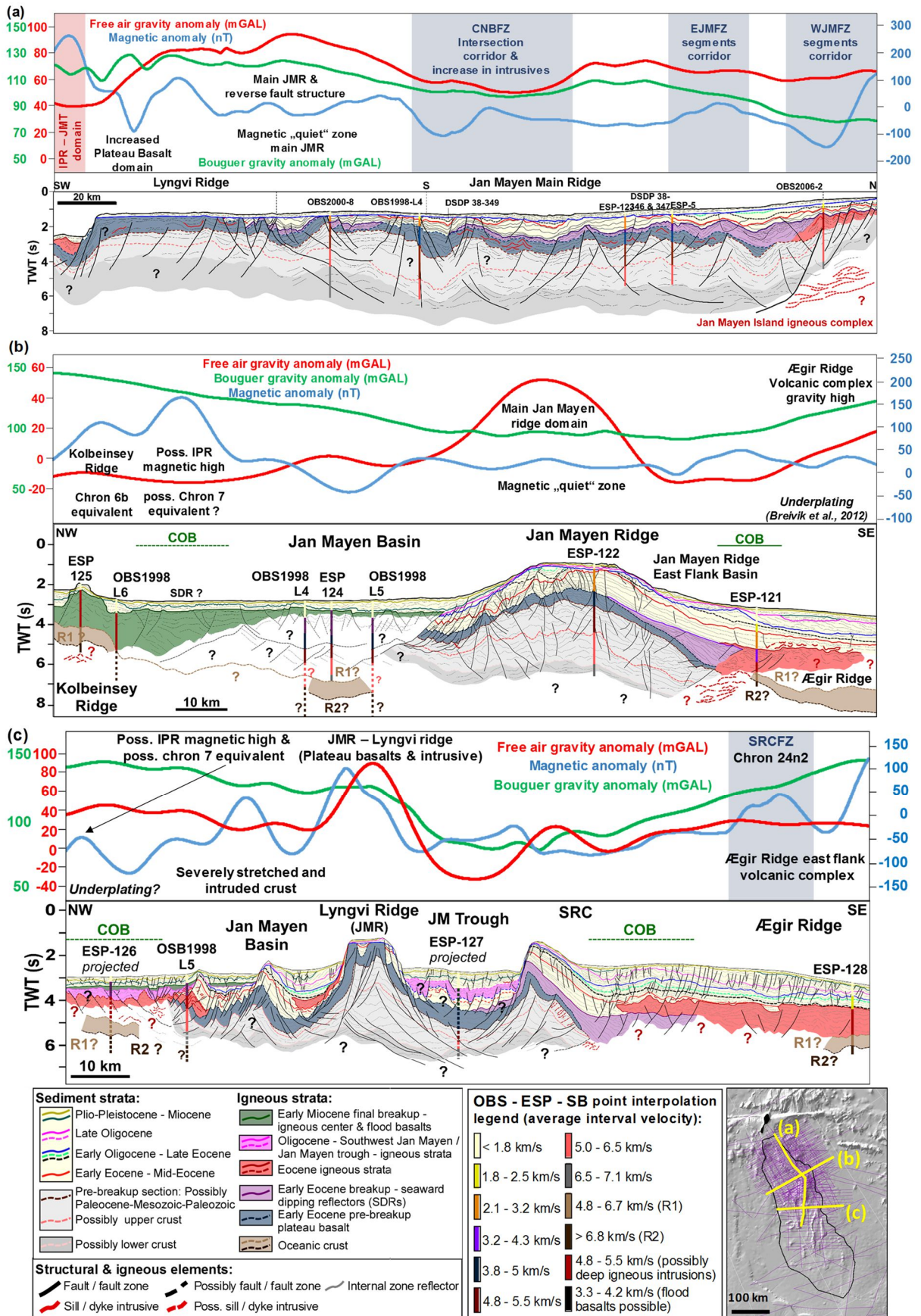
JMMC study database summary table.

JMMC study database [Blischke et al., 2019], reviewed and selected data and studies (Figure 3).

Year	Survey ID	Survey lead	Country	Platform name	Data repository	Data types
1974	DSDP Leg 38	DSDP		Glomar Challenger	IODP	Boreholes
1975	BGR-75	BGR	Germany	Longva	BGR	2D MCS
1976	BGR-76	BGR	Germany	Explora	BGR	2D MCS
1978	RC2114	L-DGO	USA/Norway	Robert Conrad	MGDS	Bathymetry; Magnetics; Gravity; 2D MCS; ESP-5
1979	J-79	NPD	Norway	GECCO alpha	NPD	Bathymetry; Magnetics; Gravity; 2D MCS
1980		PAH/SGC	USSR	Akademic Kurchatov		Seafloor sampling
1985	JM-85	NPD/NEA	Norway	Malene Østervold	NPD	Bathymetry; Magnetics; Free Air Gravity; Bouguer Gravity; Magnetic; 2D MCS
1986	Uio-86	Uio	Norway	Håkon Mosby	NPD	2D MCS
1986	Refranorge IV	IFP	France/Norway	Polarbjørn & Odys Echo	CGG/Uio	ESP; Velocity; Gravity
1988	JM-88	NPD/NEA	Norway	Håkon Mosby	NPD	Bathymetry; Magnetics; Gravity; 2D MCS; Sonobuoy
1995	JMKR95	UiB/UiH/NEA	Norway/Japan/NEA		UiB	Seismic refraction & 2D MCS
1995	ODP Leg 161	L-DGO	Norway/UK/USA	JOIDES Resolution	IODP	Boreholes
2000	KRISE	UiB	Norway	Håkon Mosby	UiB	Seismic refraction & 2D MCS
2000	OBS2000	UiB	Norway	Håkon Mosby	UiB	Seismic refraction & 2D MCS
2001	IS-JMR-01	InSeis	Norway	Polar Princess	CGG/Veritas	2D MCS
2002	ICE-02	TGS-Nopec	Iceland	Zephyr 1	TGS-NOPEC	2D MCS; Gravity
2006	OBS JM-06	UiB/Geomar	Norway/Germany	G. O. SARS	UiB	Seismic refraction & 2D MCS, gravity, magnetics
2008	WI-JMR-08	Wavefield InSeis	Norway	Malene Østervold	Spectrum	2D MCS
2008	A8-2008	HAFRO/NEA	Iceland	Arni Fridriksson	HAFRO/NEA	Multibeam
2009	JM-85-88	Spectrum	Norway	Re-processing	Spectrum	2D MCS
2010	A11-2010	HAFRO/NEA/NPD	Iceland	Arni Fridriksson	HAFRO/NEA/ NPD/Fugro Geolab	Multibeam; Seafloor sampling
2010	B11-2008	HAFRO/NEA	Iceland	Arni Fridriksson	HAFRO/NEA	Benthic survey
2011	NPD-11	NPD/UiB	Norway	Harrier Explorer	NPD/PGS	2D MCS; Seafloor sampling
2011	JMRS11	VPBR/TGS	Norway	TGS	VPBR/TGS	Seafloor sampling
2012	NPD-12	NPD/UiB	Norway	Nordic Explorer	NPD/PGS	2D MCS; Seafloor sampling
2016	NARVAL 2016	SHOM	France	R/V Beautemps-Beaupré	SHOM	Multibeam

Supplement 2

Updated stratigraphic sections of the JMMC based on seismic reflection data by Blischke et al. [2019] tied to OBS, sonobuoy, ESP velocity profiles, and available boreholes, modified from Blischke et al. [2019]. Magnetic-, free air gravity data [Nasuti and Olesen, 2014 and Haase and Ebbing, 2014], and large fracture zone corridor intersections [e.g. Gaina et al., 2009; Kandilarov et al., 2012; Gernigon et al., 2015; Blischke et al. 2017a] plotted above the profiles highlight variations associated with major tectonic and igneous events.



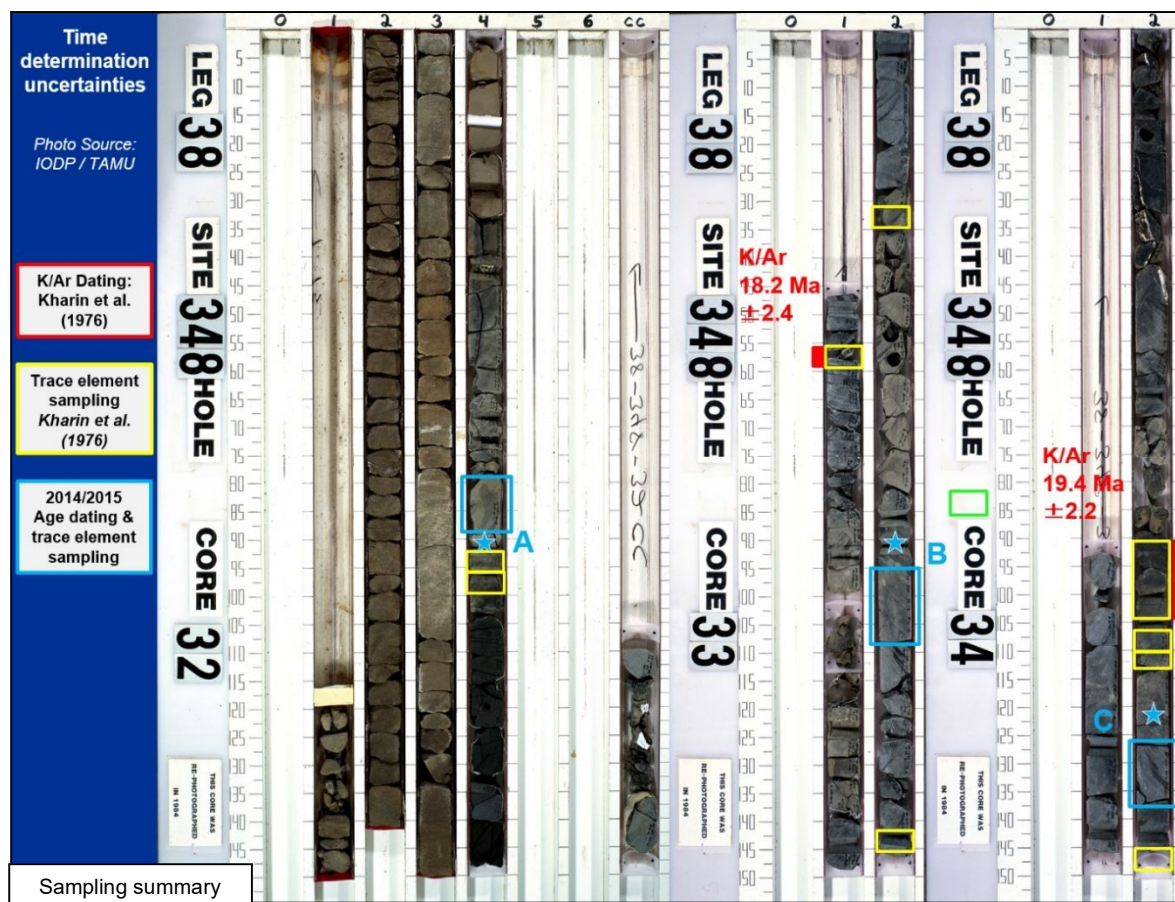
Supplement 3

DSDP 38-348 & 350 Thin-section sample descriptions.

The samples described here were used to selected samples for $^{40}\text{Ar}/^{39}\text{Ar}$ age analysis of unaltered plagioclase, which have been found in all 7 samples A-G, but are best seen in samples C, D, E, F and G.

The reviewed thin sections were analysed with 5x magnification in both plane polarized light (PPL) and with crossed polarized light (CP). A brief description of the selected thin sections follows with each sample.

(a) Icelandic Plateau thin-section analysis for 3 samples of borehole
DSDP 38-348



Site Summary

DSDP site 348 penetrated 17.4 m into fractured but homogenous basalt section at 526.6 m below the sea floor. The drilled interval is located within the assumed initial oceanic ridge basalt section of the Kolbeinsey ridge system and serves as a control site for comparison to Mid-oceanic ridge basalt (MORB) west of JMMC. The uppermost drilled basaltic section consisted primarily of finely-crystalline olivine-tholeiite with volcanic glass closer to the basalt/sediment contact, which has been replaced by smectite. In many cases, plagioclase crystals exhibit skeletal growth and 'swallow-tail'-morphology, which combined with the apparent glass content suggests that the basalt was rapidly cooled [e.g. Lofgren, 1974]. The basalt seems somewhat porphyritic, with micro-phenocrysts of plagioclase and olivine pseudomorphs that have fully altered to iddingsite. Plagioclase appears almost unaltered (~5-10% alteration), excluding some minor smectite fractures. Clinopyroxene and opaque minerals, such as augite, are unaltered but exhibit dendritic or feather-like morphology deeper in the cored section, which is common for ocean floor basalts [e.g. Lofgren, 1983]. The lowermost cored section consisted of fine- to medium-crystalline, aphyric olivine-tholeiite with rather large and well-formed, symmetrical vesicles with a porosity estimate of 5%. Considering the large vesicles, it is possible that the basalt may have reached close to the surface either as a sill or dyke intrusion, or as a subaerial lava flow; a conclusion also reached in the original analysis by Kharin [1976] and White [1978]. The absence of lava-

flow characteristics, including pillow structure and glassy rims, does not support a submarine extrusion.

Thin section sample BCR004907294 – Thin section A

Fine grained basalt, perhaps olivine-tholeiite (olivine in matrix, Fe-oxides both anhedral and euhedral, therefore forming rather late in the crystallization) although the texture is not sub-ophitic but rather intergranular. Glass, which has been replaced by smectite, seems to have been rather common within the matrix. In many cases, plagioclase crystals exhibit skeletal growth, represented e.g. by their centre filled with smectite altered glass, and also exhibiting „swallow-tail“ morphology (Figure S 3-1). These plagioclase shapes combined with the apparent glass content suggests that the basalt was rapidly cooled [e.g. *Lofgren, 1974*]. It cannot be excluded, however, that some of the smectite filled areas may have been inter-crystalline porosity, which is common in olivine-tholeiites. The basalt seems somewhat porphyritic, with micro phenocrysts of plagioclase and olivine pseudomorphs (fully altered to iddingsite). An example of this is shown in Figure S 3-2. The largest plagioclase crystals have a length of around 500 μm . It is highly likely that there was some glass content in this sample, but it has been completely replaced by smectite. Olivine is fully altered to iddingsite, but plagioclase seems almost completely fresh, excluding some minor smectite fractures (~5-10% alteration). Clinopyroxene and opaque minerals are unaltered. Hardly any vesicles are seen, but the few that are noted are filled with smectite and calcite.



Figure S 3-1. *Plagioclase exhibiting swallow-tail morphology and skeletal growth. View in PPL.*

Thin section sample BCR004907293 – Thin section B

Fine grained basalt, not fully holocrystalline. Clinopyroxene has crystallized fast in a cool environment exhibiting dendritic morphology or feather-like shape (Figure S 3-3). This is common for ocean floor basalts and has been described [e.g. *Lofgren, 1983*]. Plagioclase is rather finely crystallized, also showing signs of fast cooling such as skeletal growth and „swallow-tail“-morphology (Figure S 3-4). The sample is mostly aphyric, although some plagioclase crystals and olivine pseudomorphs (fully altered to iddingsite – Figure S 3-5) seem to be somewhat larger than the rest of the matrix (Figure S 3-6) indicating irregular crystallinity or micro-phenocrysts. There does not seem to be any fresh olivine left in the matrix of the basalt. The presence of olivine suggests that the basalt may be olivine-tholeiite, although sub-ophitic texture is not noted.



Figure S 3-2. *Plagioclase and olivine micro-phenocrysts. Olivine has been completely altered to iddingsite and plagioclase is skeletal, with glassy (smectite) centres. View in PPL.*



Figure S 3-3. *Augite that has crystallized fast in a cool environment commonly becomes dendritic. Here exhibiting curved, branching dendrites. View in PPL.*



Figure S 3-4. *Skeletal plagioclase, suggesting fast cooling. View in PPL.*



Figure S 3-5. *To the left: skeletal olivine pseudomorph – iddingsite. To the right: olivine pseudomorph – iddingsite and calcite. View in CP.*

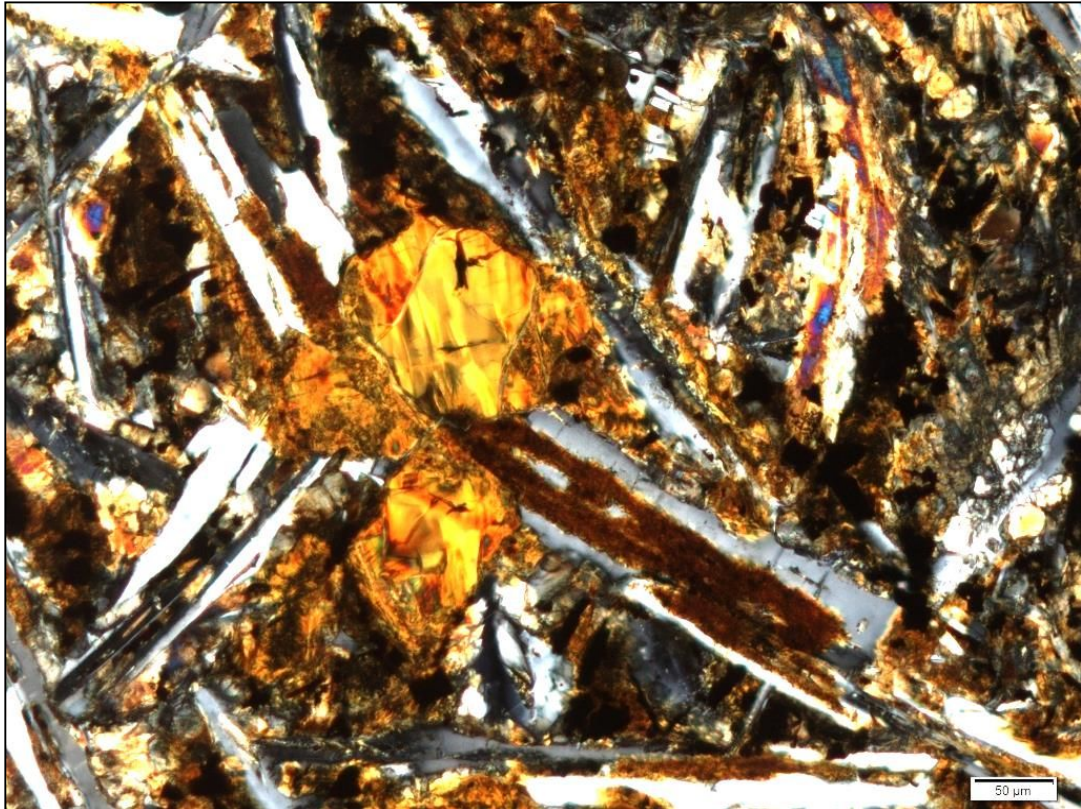


Figure S 3-6. *Olivine pseudomorphs and plagioclase crystals. View in CP.*



Figure S 3-7. *Altered glass in between plagioclase crystals. View in CP.*

Interstitial glass seems to be present, but it is fully altered to smectite and in some cases to calcite. The existence of glass within the sample is further proved by the signature of palagonite rims which are commonly exhibited on glass grains [e.g. *Jakobsson and Moore, 1986; Crovisier et al., 1992; Helgadóttir, 2006*]. Both can be seen in Figure S 3-7. Olivine is fully altered to iddingsite and in rare cases to calcite (Figure S 3-5). Some smectite alteration in tiny fractures is present in plagioclase (around 5% alteration). Clinopyroxene (augite) and opaque minerals are unaltered.

Thin section sample BCR004907296 – Thin section C

Fine- to medium grained, aphyric basalt with rather large and well formed (symmetrical) vesicles (Figure S 3-8). Porosity is estimated 5% (vesicular porosity). Considering the large vesicles, it is possible that the basalt may have reached surface and it may not have been erupted on the seafloor, but rather on land as a thick lava flow. It is however, also possible that this is an intrusive that may have intruded close to the surface, therefore releasing gas, forming vesicles. In any case, it seems likely that there was not much water involved, since the rock is well crystallized and if it were an intrusive the pressure would not have been substantial, allowing gas release.

The rock is holocrystalline, with some inter-crystalline porosity, that has been filled with smectite (Figure S 3-9). It seems rich in olivine pseudomorphs, especially in certain areas within the sample (Figure S 3-8) and is therefore likely to be rather primitive in composition. Although it is sometimes difficult to decide whether the supposed pseudomorphs are really olivine or if some of them could perhaps represent inter-crystalline porosity filled with smectite. The texture of the basalt is intergranular to sub-ophitic and opaque minerals are both anhedral and euhedral. This suggests that the basalt is olivine-tholeiite although. The largest plagioclase crystals are around 400 μm in length. No cross-cutting fractures were noted in this sample.

If glass was present it is fully altered to smectite. Olivine is also completely altered to iddingsite and plagioclase shows some minor alteration exhibiting smectite fractures or spots. The spots could perhaps show altered glass inclusions within the plagioclase. Vesicles are filled, or almost filled, with fine grained smectite.

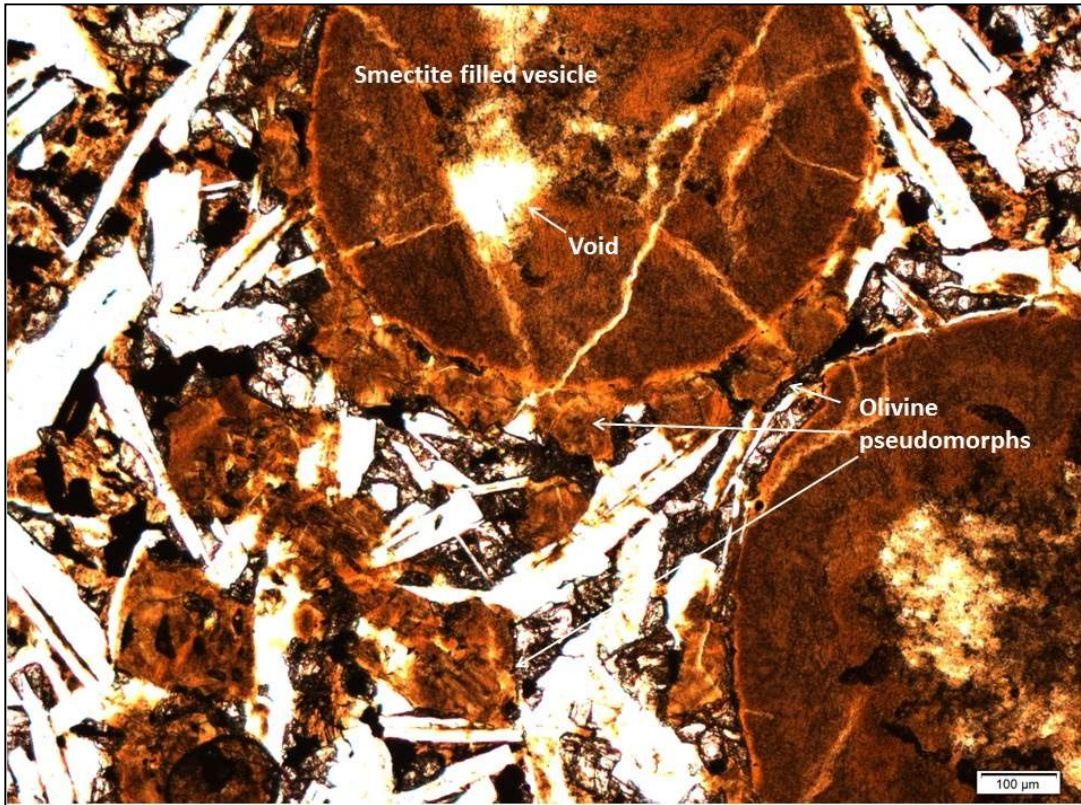


Figure S 3-8. *Vesicles in sample with olivine pseudomorphs. View in PPL.*

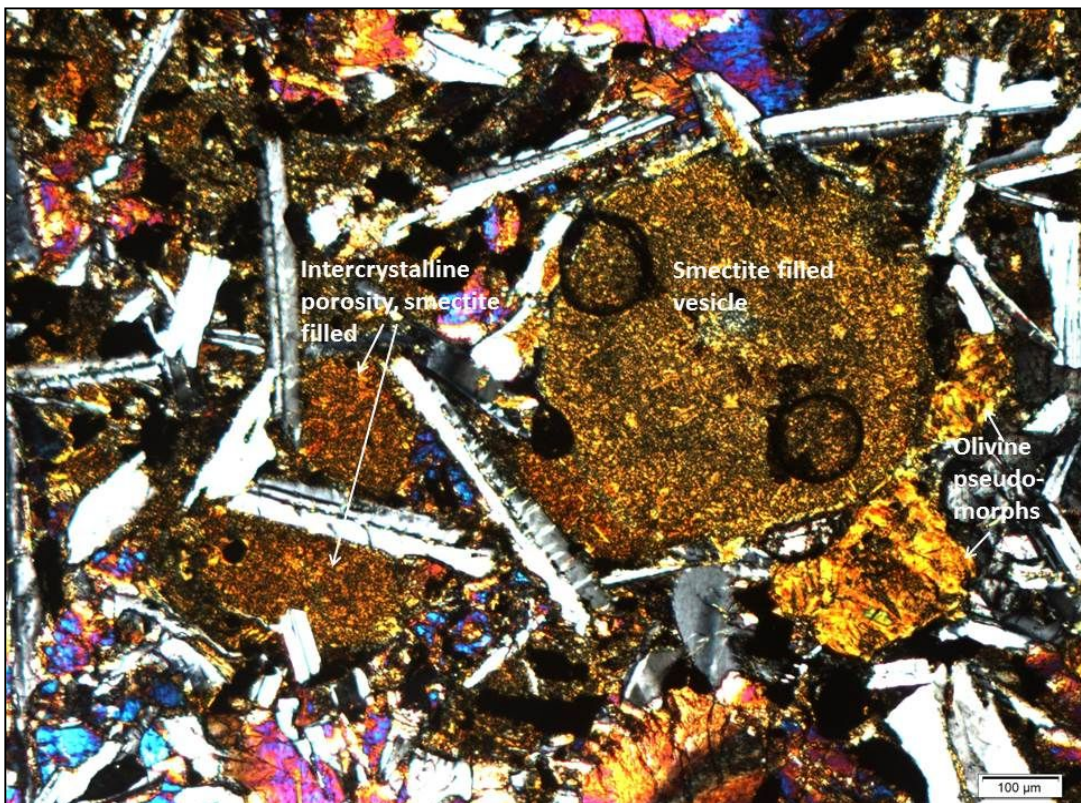
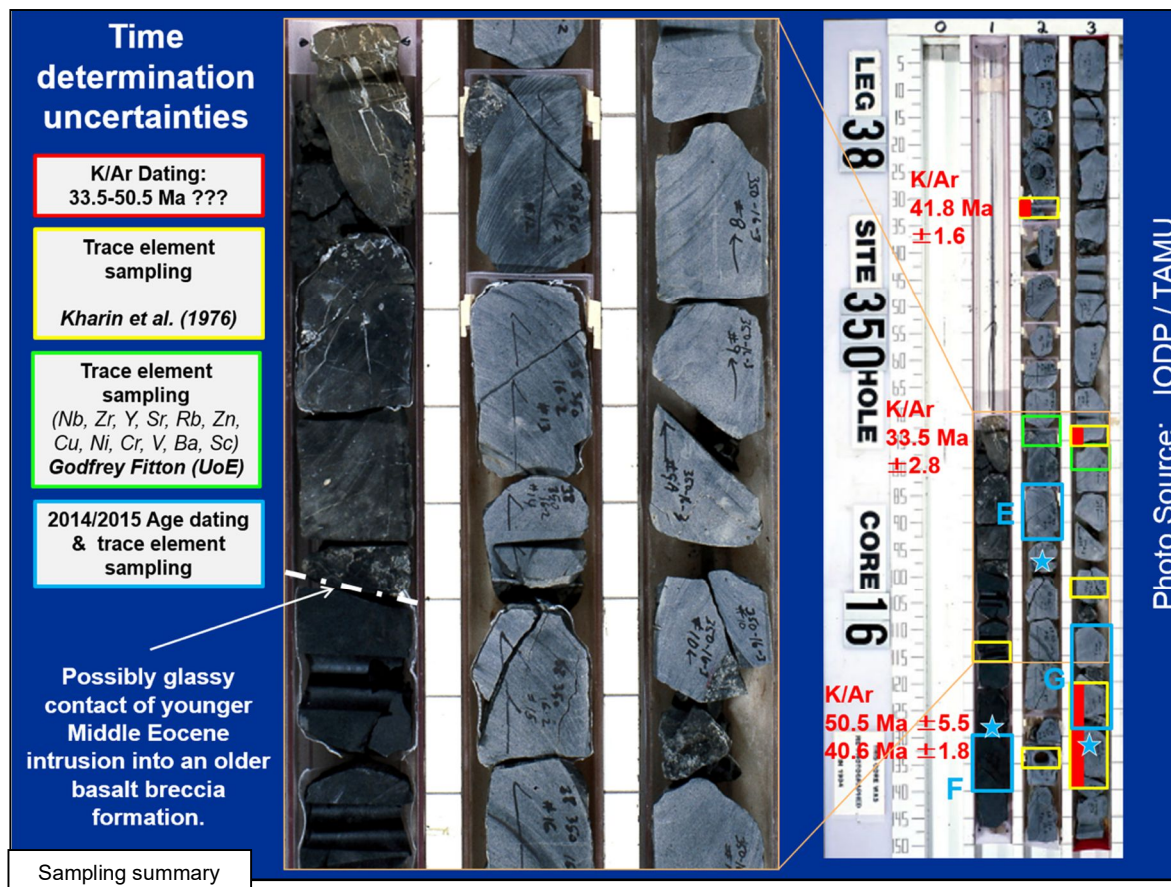


Figure S 3-9. *Inter-crystalline porosity. View in CP.*

(b) Icelandic Plateau thin-section analysis for 4 samples of borehole
DSDP 38-350



Site Summary

The sampled basalt section of DSDP site 350 at the southern tip of the easternmost SRC block was recovered from an acoustically opaque layer between 362 m and 388 m below seafloor. Samples from cores 14 and 16 were retrieved as the drilled section was heavily fractured and core 15 was not recovered. The samples revealed two different petrological units, a highly altered basaltic breccia and a basalt intrusion.

The younger intrusive basalt consists primarily of fine- to medium-grained holocrystalline olivine-tholeiitic basalt, with the deepest cored section consisting of a sub-ophitic to intergranular texture. Olivine is uneven in concentration and altered to iddingsite (75-80%), and in small amounts to mixed clay layers, accompanied by few but large unaltered plagioclase phenocrysts. Some inter-crystalline porosity can be seen in an otherwise dense rock that is filled with smectite, calcite, mixed layered clay, and quartz. Clinopyroxene, augite and secondary opaque minerals are unaltered in contrast to the inter-crystalline pores that also exhibit needle like or acicular crystals that may be zeolites secondary mineralization pore fills.

The breccia consists of dense, cryptocrystalline basalt with partially altered plagioclase, olivine pseudomorphs and large plagioclase phenocrysts. The basalt is rich in olivine and partially of picrite composition, which is also reflected by its geochemical composition for

potassium, sodium and silicaoxides. A few notable fractures were observed, sometimes with increased smectite and calcite alteration to in the adjacent rock. The glassy sample portions appear fully altered, and olivine has been completely altered to iddingsite and calcite, and plagioclase partially altered (around 50%) to calcite, perhaps mixed layer clay and probably albite.

Thin section sample BCR004907313 from borehole 350 – Thin section D

Dense, cryptocrystalline basalt with partially altered plagioclase and olivine pseudomorph phenocrysts (Figure S 3-10). Some fresh plagioclase phenocrysts are noted, around 500 μm in size (Figure S 3-11). There are large plagioclase phenocrysts and then smaller micro phenocrysts of plagioclase and olivine. The basalt is rich in olivine and is probably of picrite composition (Figure S 3-12).

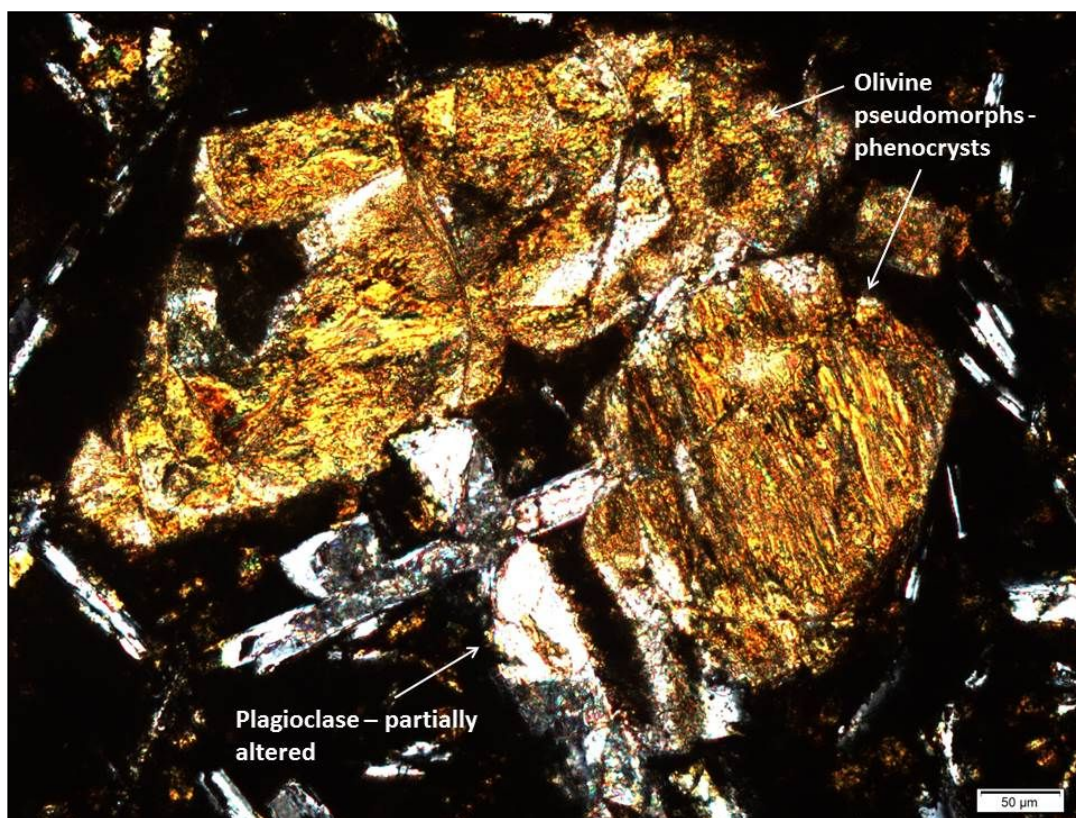


Figure S 3-10. *Olivine pseudomorphs and partially altered plagioclase in thin section D. View in CP.*

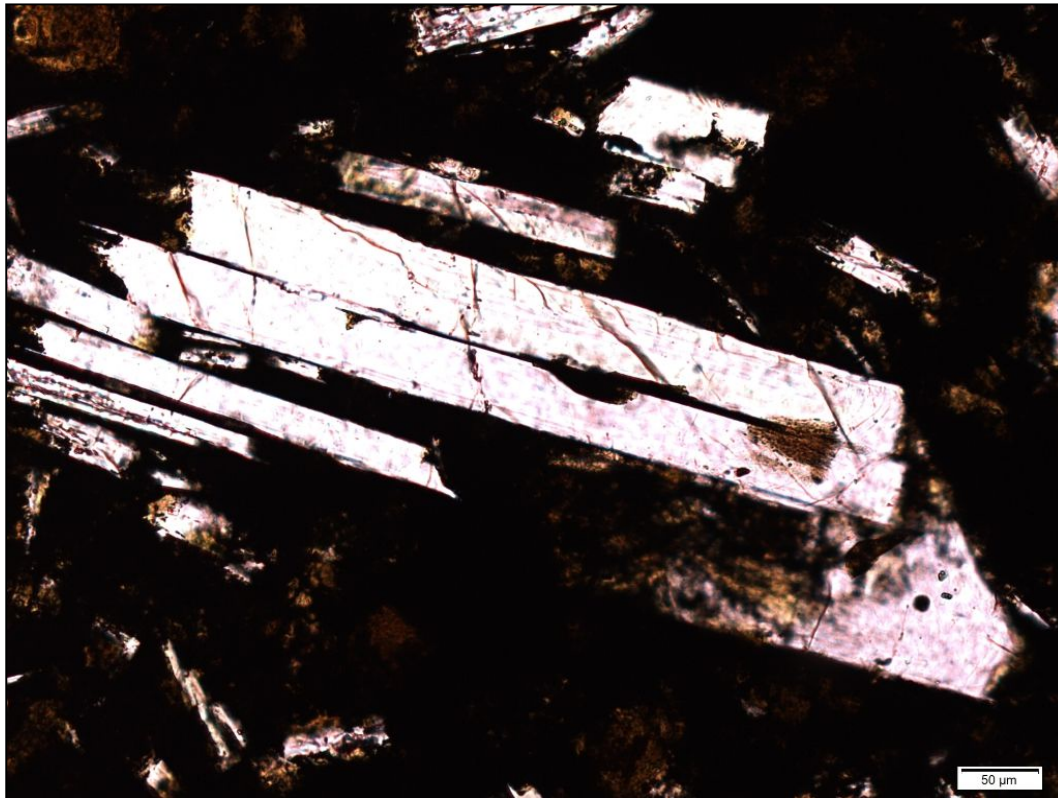


Figure S 3-11. *Unaltered plagioclase phenocryst. View in PPL.*

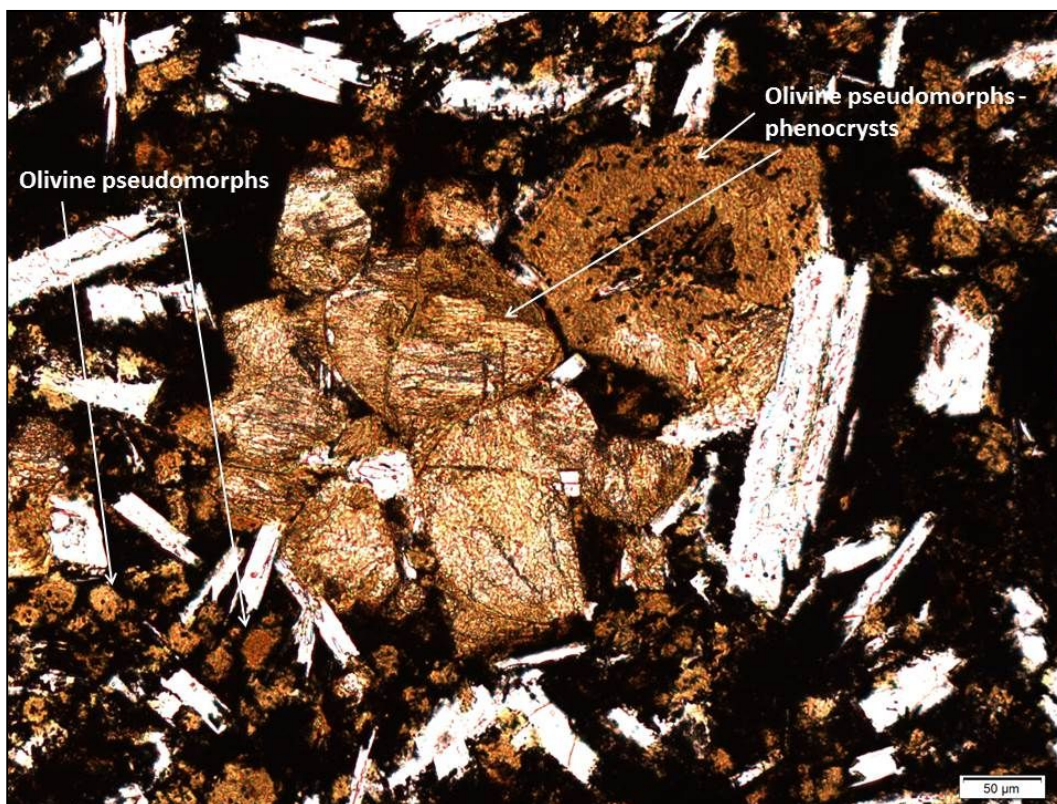


Figure S 3-12. *Olivine rich basalt with olivine pseudomorphs (iddingsite and calcite), both as phenocrysts and as part of the matrix. View in PPL.*



Figure S 3-13. *Albite altered plagioclase phenocryst in thin section D. View in CP.*

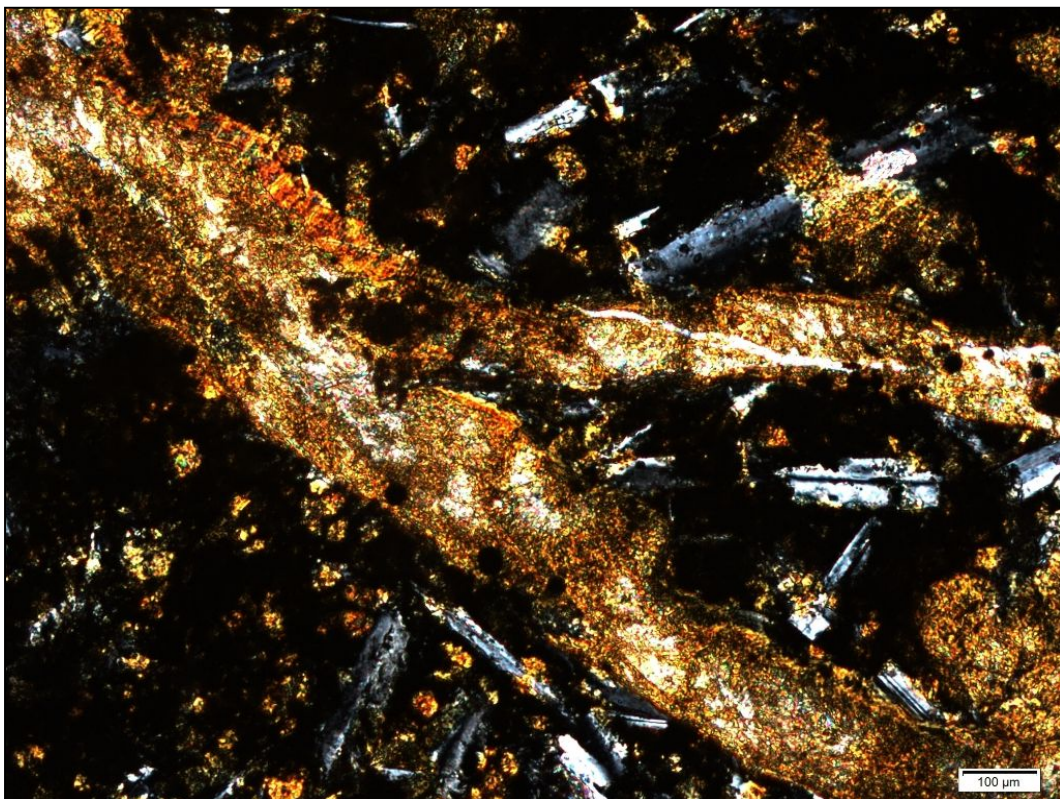


Figure S 3-14. *Fracture with smectite and calcite filling. View in CP.*

A few notable fractures are seen, sometimes exhibiting increased alteration in the adjacent rock. Plagioclase and olivine are the most prominent primary crystals but clinopyroxene is very poorly crystallized and can therefore hardly be seen. The same applies to opaque minerals.

It is hard to tell anything about the glass in the basalt since the glassy part is mostly black but when the overall alteration of the sample is considered it is likely that all glass in the sample is fully altered. Olivine is completely altered to iddingsite and calcite, and plagioclase partially altered (around 50%) to calcite, perhaps mixed layer clay and probably albite (Figure S 3-13). Alteration minerals in fractures (precipitation) are smectite and calcite (sequence in that order) (Figure S 3-14).

Thin section sample BCR004907320 – Thin section E

Fine to medium grained holocrystalline basalt. Probably olivine-tholeiite (opaque minerals have crystallized late and fill up in between plagioclases and clinopyroxenes). There is not much olivine, however, the ones that are seen are pseudomorphs (fully altered to iddingsite). In some areas the olivine seems a little bit more concentrated (Figure S 3-15). Large but few plagioclase phenocrysts are present (1-3 mm) (Figure S 3-16). Plagioclase in the matrix is also rather large (up to 400 μm). Some inter-crystalline porosity is noted (filled with smectite – Figure S 3-17) and very few vesicles (1-2).

Olivine is almost completely altered (80%) to iddingsite (where a hint of mixed layer clay (MLC) can be seen (Figure S 3-15). Some parts of olivine are still fresh, and plagioclase seems unaltered. Clinopyroxene and opaque minerals are unaltered.

Smectite fills up inter-crystalline porosity but MLC seems to be associated with olivine alteration (only a hint of MLC). The inter-crystalline pores also exhibit needle like or acicular crystals that may be zeolites of some sort (Figure S 3-18). It is not clear if some of the inter-crystalline pores show opal precipitation or if there are remains of fresh glass in between crystals in some cases.

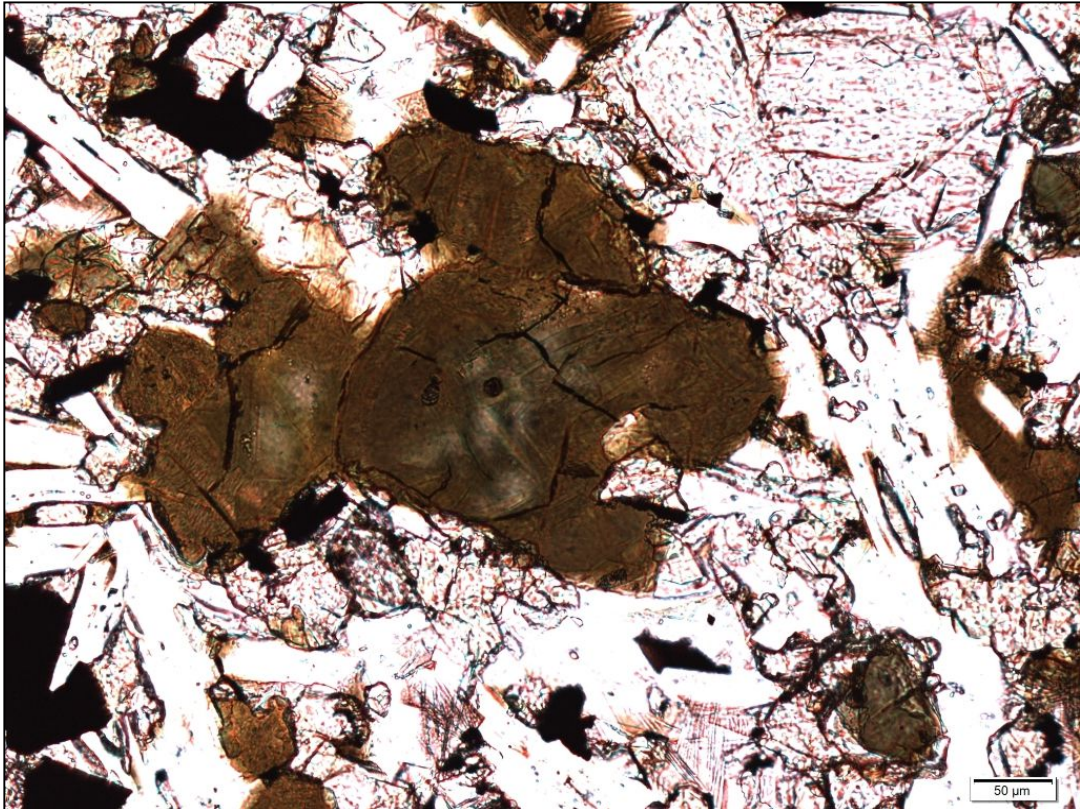


Figure S 3-15. *A few olivine pseudomorphs. View in PPL.*

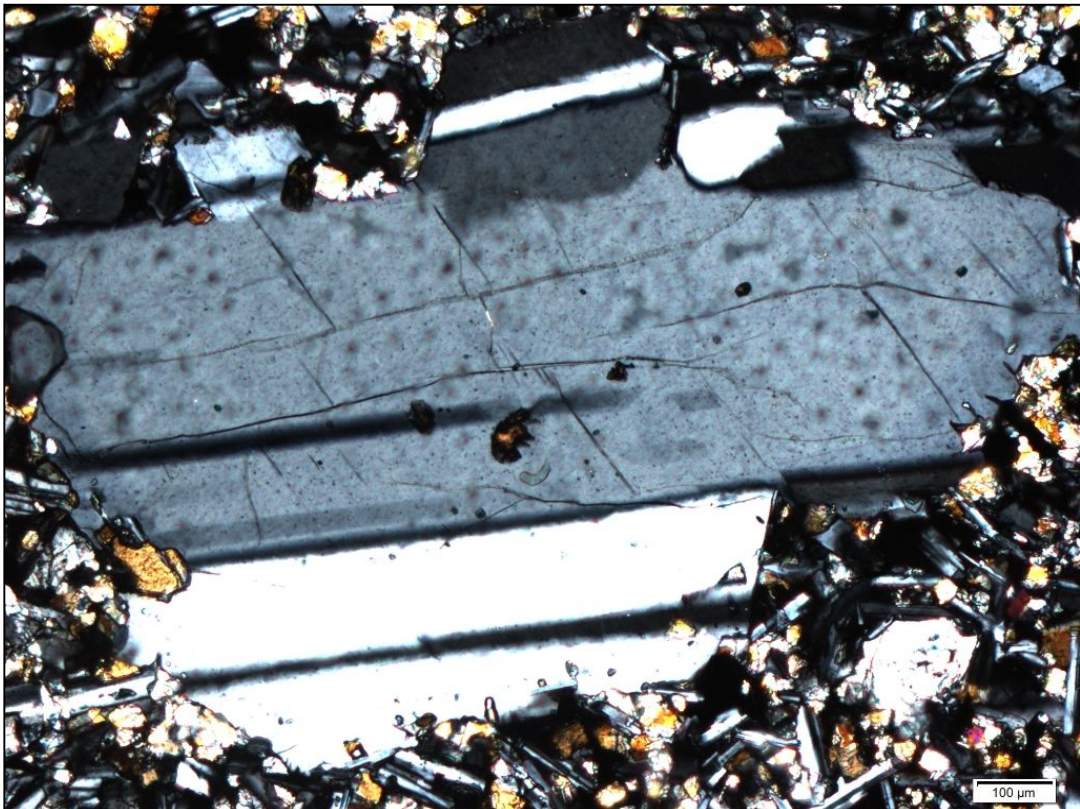


Figure S 3-16. *Plagioclase phenocryst around 1 mm in length. View in CP.*

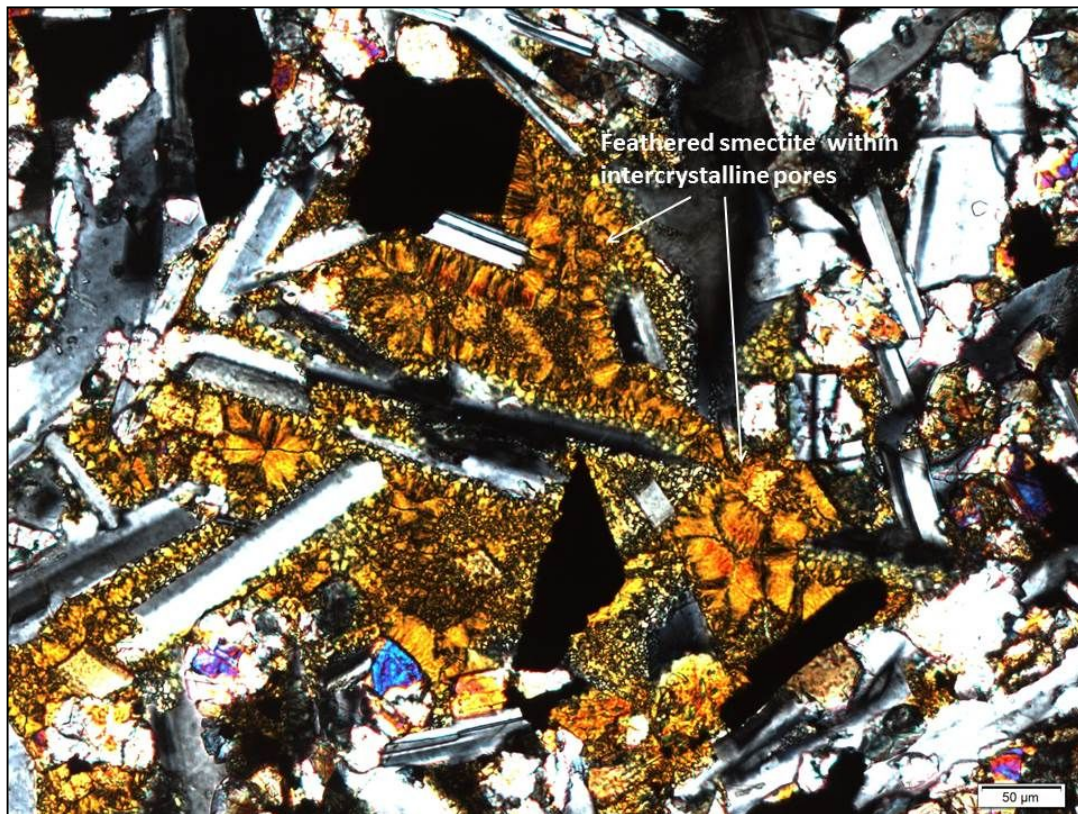


Figure S 3-17. *Inter-crystalline pores filled with feathered smectite, precipitating from the walls of the pores. View in CP.*

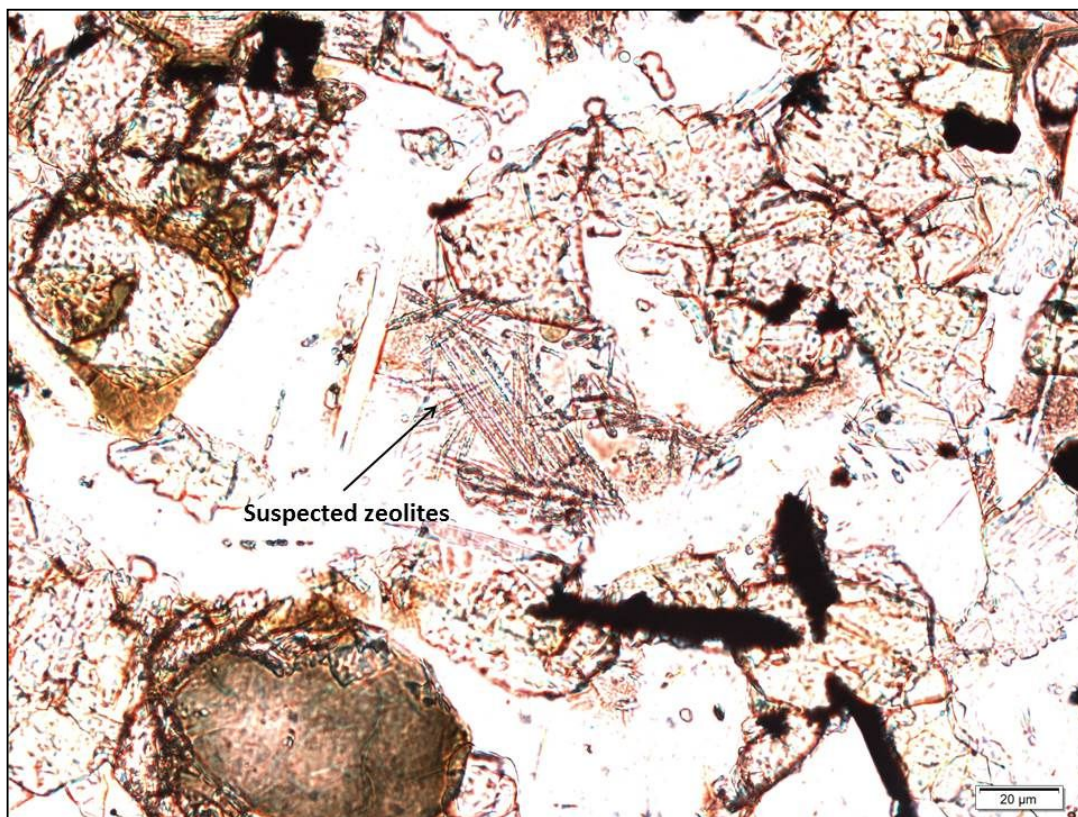


Figure S 3-18. *Suspected zeolites within inter-crystalline pores. View in PPL.*

Thin section sample BCR004907311 – Thin section F

Fine grained, holocrystalline basalt with plagioclase and clinopyroxene micro phenocrysts (or just irregular crystallisation – perhaps seriate texture) and some plagioclase macro phenocrysts (~700 μm , less than 5%). Opaque minerals are mostly euhedral but have probably crystallised later than plagioclase. There is substantial inter-crystalline porosity in some areas, filled with smectite. It is possible that some glass may have been present within the sample, now altered to smectite and calcite (a hint of palagonite rim turned to smectite is noted in one area within the sample – Figure S 3-19). Hardly any vesicles are seen, only 1-2 filled with calcite and smectite. Within the sample there is one large fracture with precipitations of smectite followed by calcite (Figure S 3-20).

If glass was present in between the primary crystals, then it is fully altered to smectite and in some cases to calcite. Olivine is also fully altered to smectite but other primary minerals (plagioclase, clinopyroxene and opaque minerals) remain unaltered.

Alteration minerals (precipitations) can be seen in one large fracture: smectite followed by calcite (including dogtooth calcite) and in the few vesicles.

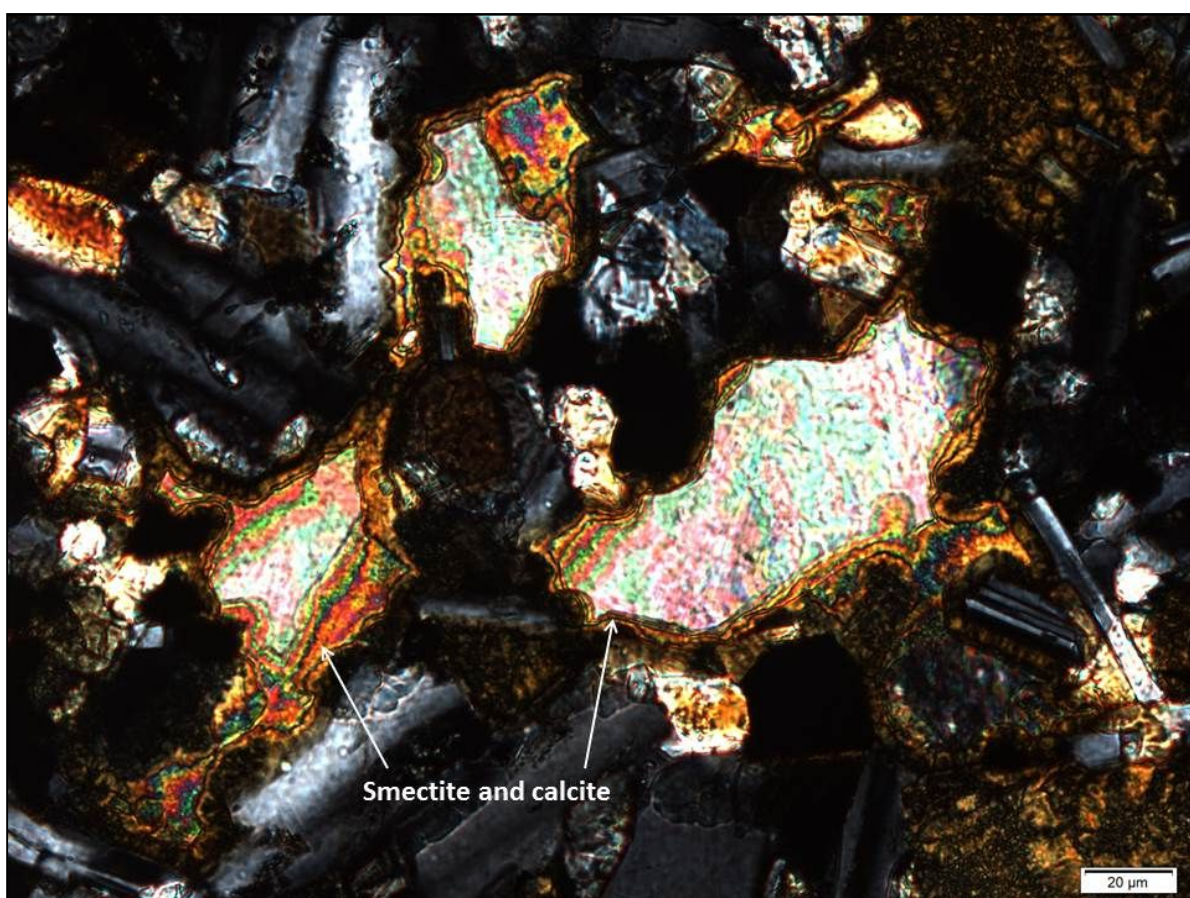


Figure S 3-19. *Either inter-crystalline pores filled with precipitations or glass that has altered to smectite and calcite. View in CP.*

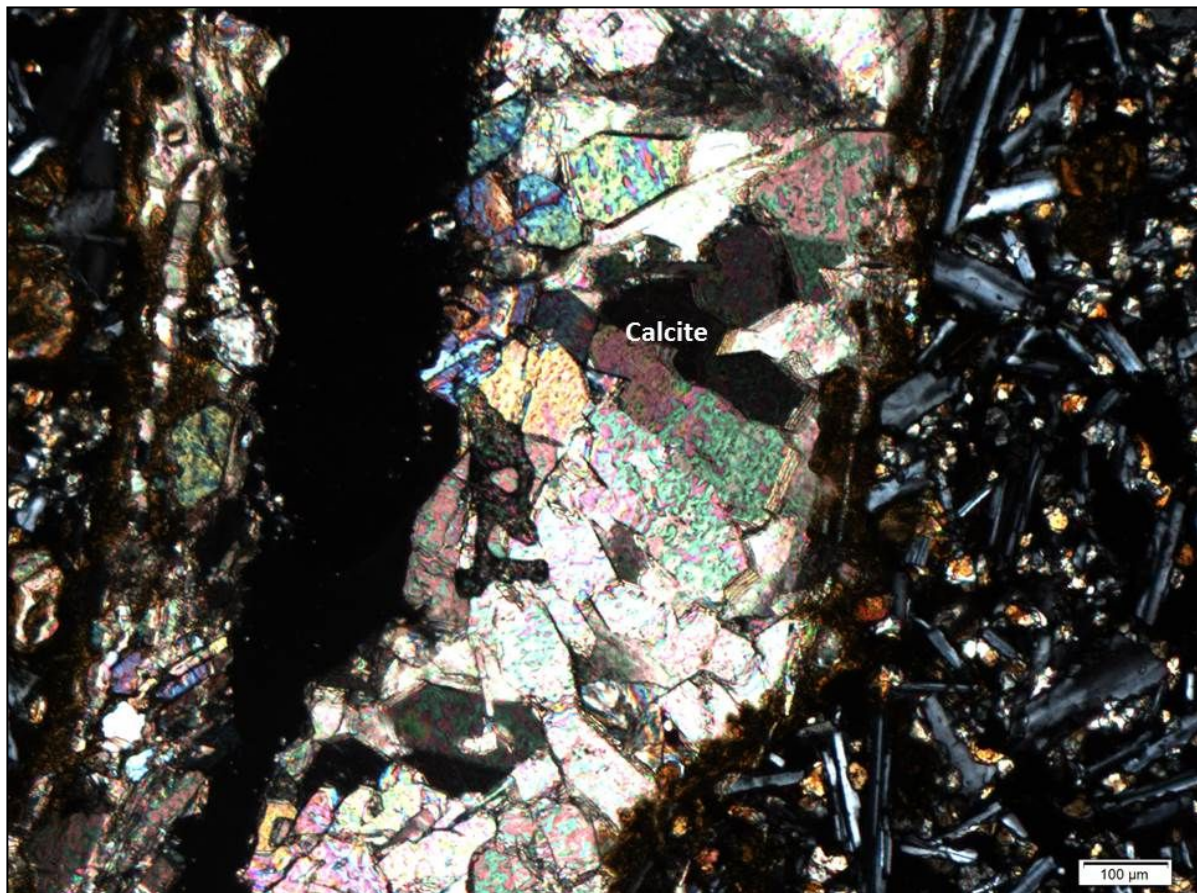


Figure S 3-20. *Fracture filling of smectite and calcite. View in CP.*

Thin section sample BCR004907321 from borehole 350 – Thin section G

Sparsely plagioclase porphyritic basalt, one phenocryst exhibits skeletal growth with both augite and opaque minerals crystallised in the gaps (Figure S 3-21). Plagioclase phenocrysts are up to ~400 μm in size. In between plagioclase crystals there are small clinopyroxene crystals, but some larger ones are seen in between. The texture of the basalt could therefore be described as sub-ophitic in some areas but in most cases, it is intergranular. Opaque minerals form late and are mostly irregular in form (anhedral or subhedral). Olivine (pseudomorphs mostly) is seen in the matrix and there are even some unaltered sections of olivine present. This combined suggests that the basalt may be of olivine-tholeiite composition. The rock is dense, no vesicles are seen but it does have some inter-crystalline porosity. A fracture filling is seen on one edge of the sample (Figure S 3-22).

Olivine is almost fully altered (~75%), but some of the olivine crystals are only partially altered to iddingsite. Plagioclase, clinopyroxene and opaque minerals are unaltered.

The fracture in the sample shows smectite, calcite, mixed layer clay and quartz (in that sequence). A part of the fracture filling can be seen in Figure S 3-22. Inter-crystalline pores seem to contain similar minerals as in thin section E, i.e. needle shaped suspected zeolites along with smectite (Figure S 3-23).

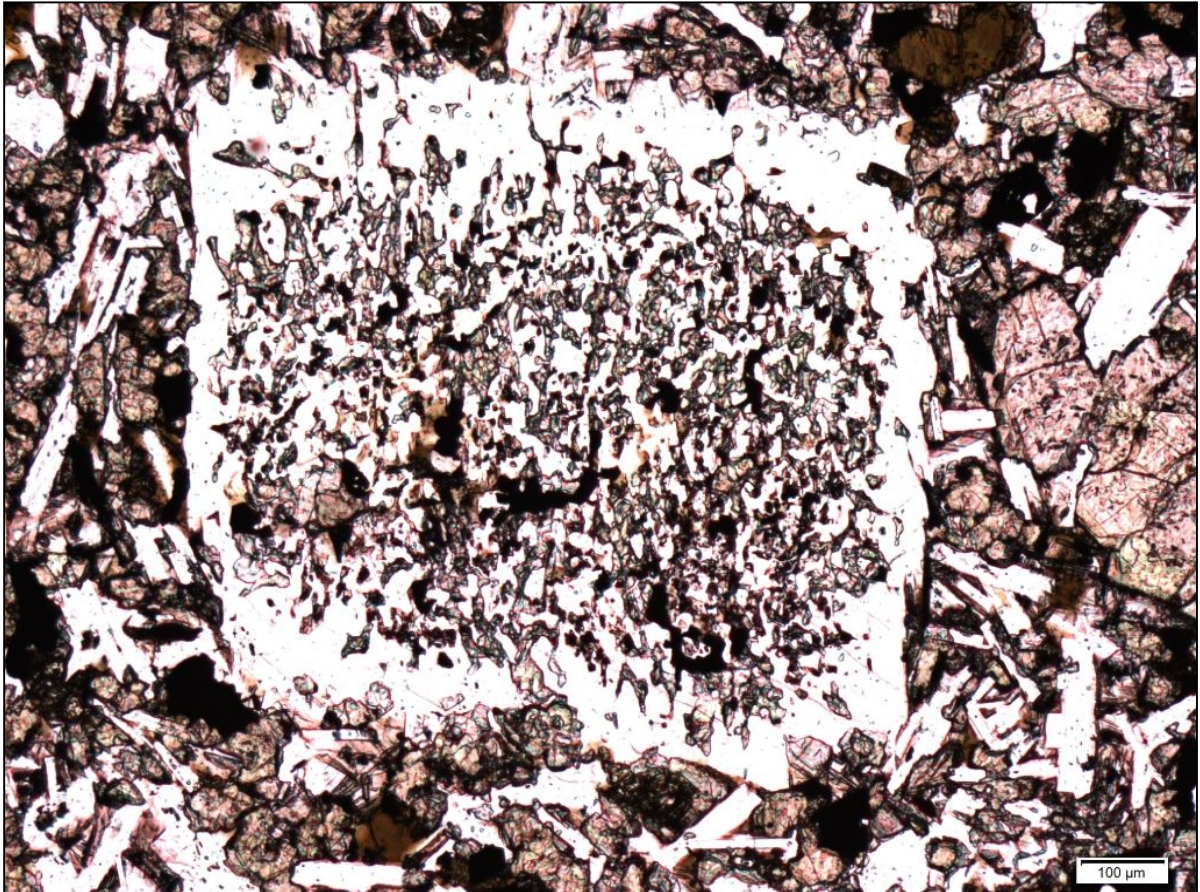


Figure S 3-21. *Skeletal plagioclase phenocryst. View in PPL.*

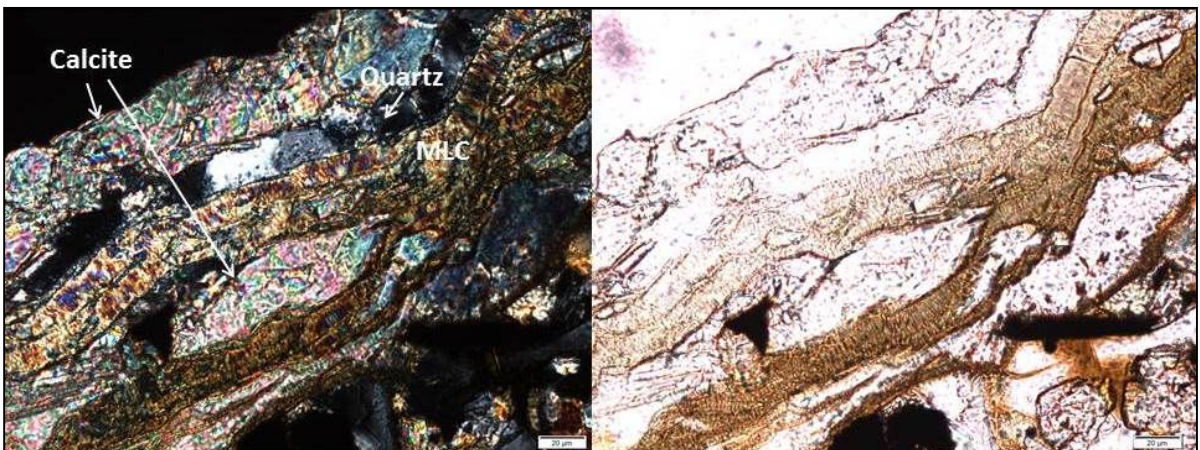


Figure S 3-22. *Fracture filling from one edge of the sample. To the left: view in PPL. To the right: view in CP.*

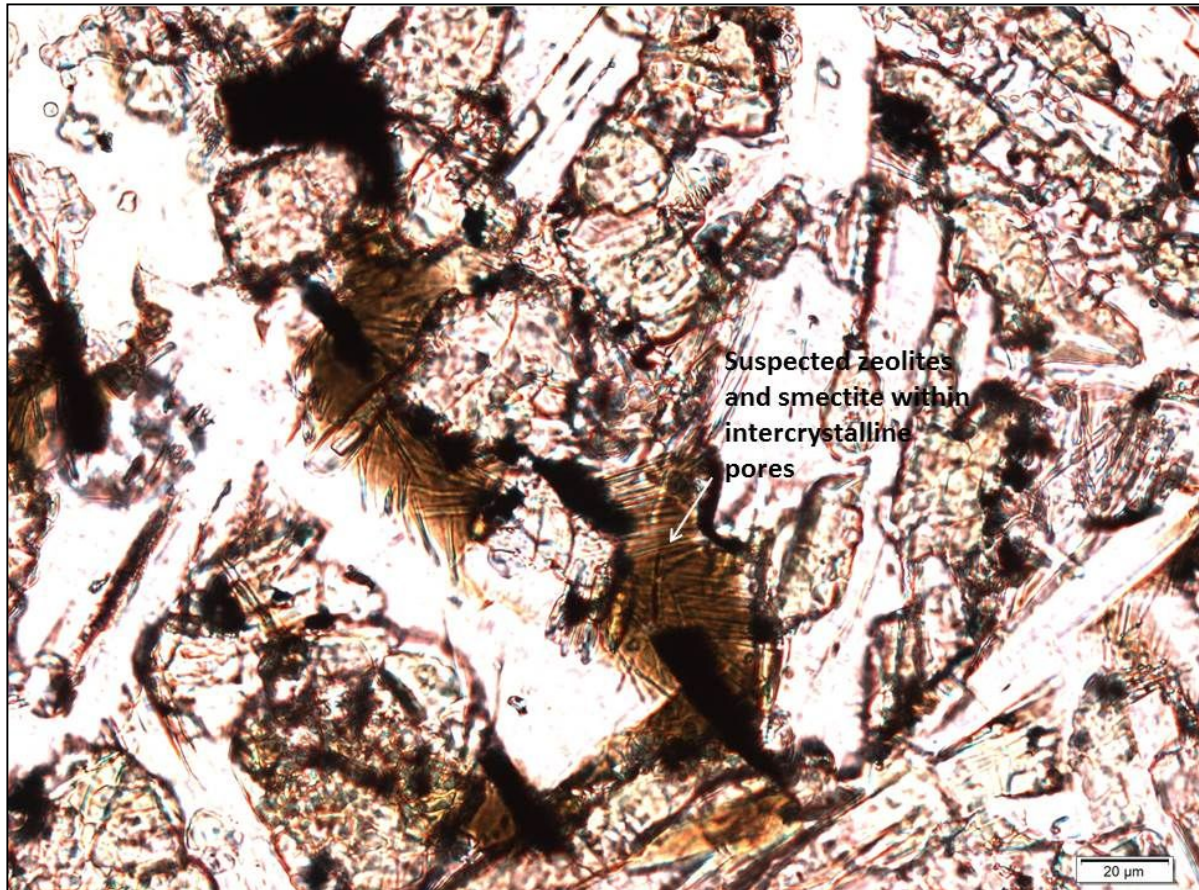


Figure S 3-23. *Inter-crystalline pores with smectite and suspected zeolites. View in PPL.*

References:

- Crovisier, J.-L., Honnorez, J. and Fritz, B. (1992). Dissolution of subglacial volcanic glasses from Iceland: laboratory study and modelling. *Applied Geochemistry*, Suppl. Issue No. 1: 55-81.
- Helgadóttir, H.M., 2006. Formation of Palagonite. Petrographic Analysis of Hyaloclastite Tuffs from the Western Volcanic Zone in Iceland. B.Sc. Thesis. Department of Geology and Geography, University of Iceland, 40 pp.
- Jakobsson, S.P. and Moore, J.G. (1986). Hydrothermal minerals and alteration rates at Surtsey volcano, Iceland. *Geological Society of America Bulletin* 97: 648-659.
- Lofgren, G.E. (1974). An experimental study of plagioclase crystal morphology: Isothermal crystallization. *American Journal of Science*, vol. 274, pp. 243-273.

Supplement 4

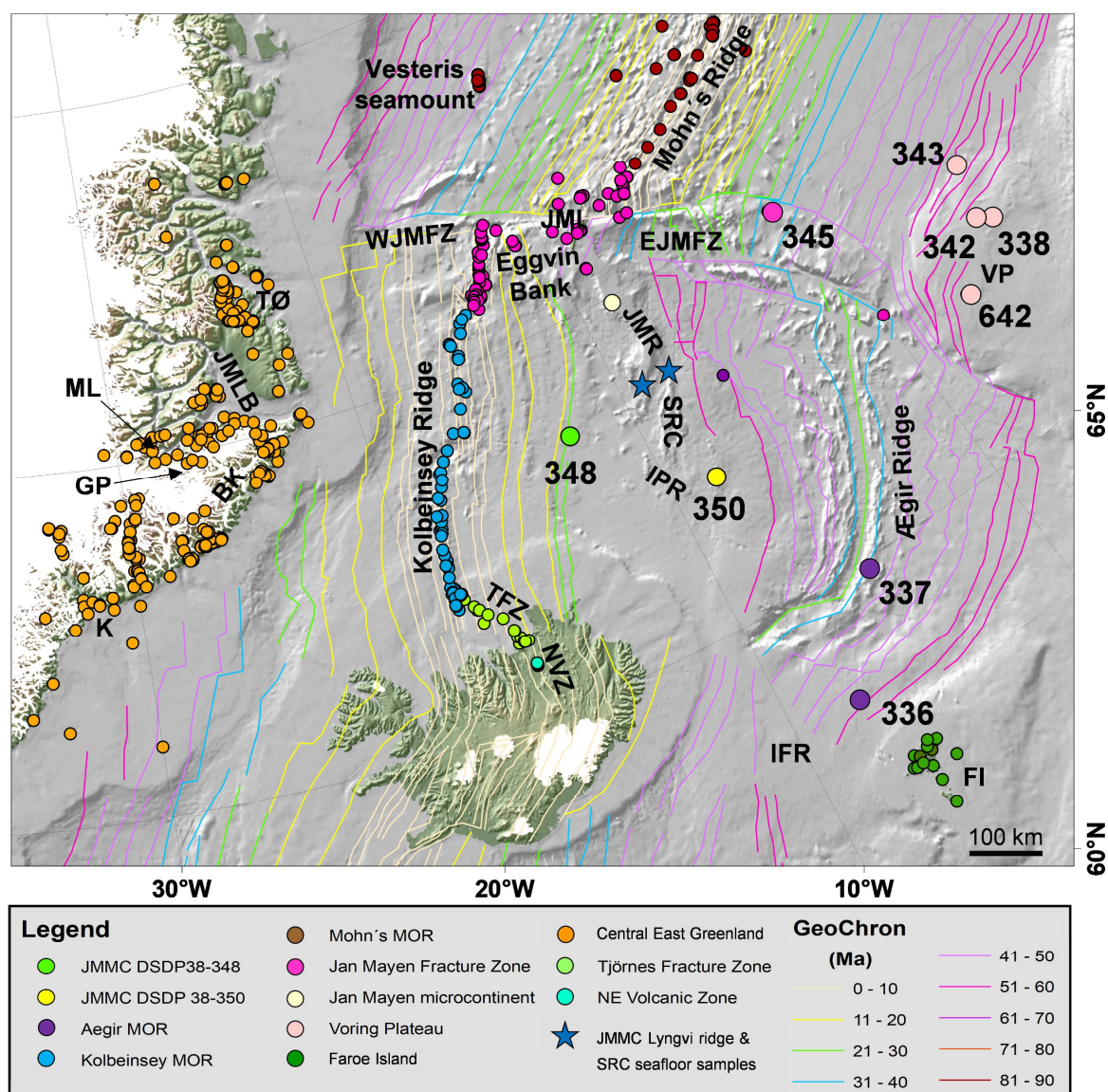
⁴⁰Ar/³⁹Ar radiometric age estimate sample results for boreholes DSDP 38-350 and 348.

Summary table of the $^{40}\text{Ar}/^{39}\text{Ar}$ age spectra dating estimate of core samples of wells DSDP-38-348 & 350 in comparison to the existing age K/Ar analysis (1) [Kharin *et al.*, 1976], the new $^{40}\text{Ar}/^{39}\text{Ar}$ age analysis (2) [OSU Argon Geochronology Laboratory], and the magnetic polarity chron age model (3) [Gradstein *et al.* 2012].

DSDP Well	Core; section	Sample Id	K/Ar age (1)	$^{40}\text{Ar}/^{39}\text{Ar}$ Age (2)	Polarity Chron (3)	Comment
35-348	32; Sec. 4	BCR004907 271	18.2 Ma ± 2.4 Ma	~ 22.23 Ma ± 0.31 Ma	C6Bn.2n	
35-348	33; Sec. 2	BCR004907 273	18.2 Ma ± 2.4 Ma	~ 23.19 Ma ± 0.61 Ma	C6Cn.2r	
35-348	34; Sec. 2	BCR004907 276	19.4 Ma ± 2.2 Ma	~ 22.15 Ma ± 0.26 Ma	C6Bn.2n	
35-350	14; Sec. 2	BCR004907 312	-	No Age	-	Very fine -crystalline to glassy basalt, segment is altered, and is part of the bed rock for the intrusive section just below.
35-350	14; Sec. 3	BCR004907 314		No Age		
35-350	16; Sec. 1	BCR004907 310	33.5 Ma ± 2.8 Ma	~ 49.28 Ma ± 0.30 Ma	C22n	New age dating connects this igneous events caused by the Iceland Plateau Rift I (<i>Brandsdóttir et al. 2015 & Blischke et al. 2017</i>).
35-350	16; Sec. 2	BCR004907 316	to	~ 44.05 Ma ± 0.21 Ma	C20r	
35-350	16; Sec. 3	BCR004907 318	50.5 Ma ± 5.5 Ma	~ 46.58 Ma ± 0.30 Ma	C21n	

Supplement 5

Geochemical data location map, study data and database references



(a) Borehole and seafloor sample location map.

The sites are labelled by sub-region or igneous provinces in comparison with geochronologic time zones and age dating model by Gaina et al. [2014]. Geochemistry data reference: PETDB [Lamont Doherty Earth Observatory, Columbia University, New York, <http://www.earthchem.org/petdb>], and GEOROC [Max Planck Institute for Chemistry, Mainz, <http://georo~mpch-mainz.gwdg.de/georoc/>]. Abbreviations: borehole numbers of DSDP Leg 38 sites 336 – 350, and Leg 104 site 642; BK – Blosseville Kyst; EJMfZ – East Jan Mayen Fracture Zone; FI – Faroe Islands; GP – Geiko plateau; IFR – Iceland-Faroe Ridge; IPR – Iceland Plateau Rift; JMI – Jan Mayen Island complex; JMLB – Jameson Land Basin; JMR – Jan Mayen Ridge; K – Kangerlussuaq (central East Greenland); ML – Milne Land; NVZ – Northern Volcanic Zone; SRC – Southern Ridge Complex; TFZ – Tjörnes Fracture Zone; TØ – Trail Ø; VP – Vøring Plateau and Margin; and WJMfZ – West Jan Mayen Fracture Zone.

Sample name	SiO ₂ (wt%)	Al ₂ O ₃ (wt%)	FeO ^T (wt%)	MnO (wt%)	MgO (wt%)	CaO (wt%)	Na ₂ O (wt%)	K ₂ O (wt%)	TiO ₂ (wt%)	P ₂ O ₅ (wt%)	Volatiler (wt%)	SUM-N	SUM-RUN
ISOR-Hí A: 348/88-91	48.722792	15.104225	13.091569	0.297533	6.391251	12.169669	2.482730	0.063742	1.542046	0.134444		100	93.79
ISOR-Hí B: 348/91-92	49.254061	14.718920	12.972664	0.264768	6.765535	12.099232	2.299322	0.020619	1.478914	0.125964		100	98.30
ISOR-Hí C: 348/120-120,5	50.480138	13.738551	12.394330	0.229850	7.819404	11.579404	2.185286	0.070964	1.388443	0.113630		100	100.22
ISOR-Hí E: 350/98-99	49.988566	14.062397	12.914342	0.212523	5.950520	10.973171	2.866783	0.301250	2.439078	0.291370		100	98.54
ISOR-Hí F: 350/128-129	50.228720	14.493527	12.009672	0.207002	5.737811	11.539787	2.870753	0.298592	2.340048	0.274087		100	97.66
ISOR-Hí G: 350/135-136	49.932078	13.943849	12.836850	0.216653	6.180112	11.111150	2.841404	0.269351	2.383590	0.284963		100	100.89
ISOR-Hí D: 350/142-143	45.799751	17.471490	16.043261	0.087811	6.519558	6.724145	3.371976	0.494068	3.096946	0.390994		100	94.44
UoAH: 348-32-4-142-150	50.382388	13.501386	13.304613	0.234238	7.393090	11.553085	2.132274	0.064340	1.315958	0.118627	1.056135	100	100.47
UoAH: 348-33-2-10-17	50.452039	13.611593	13.490045	0.247062	6.971177	11.635099	2.105572	0.03278	1.337159	0.116976	1.076220	100	100.21
UoAH: 348-34-1-127-135	50.494339	13.578633	13.441022	0.239837	7.087848	11.552666	2.127164	0.049587	1.314551	0.114353	1.096169	100	99.83
UoAH: 348-34-2-117-125	49.301145	13.693535	13.573870	0.233983	8.071915	11.483248	2.147021	0.080338	1.301468	0.113477	1.650298	100	100.41
UoAH: 348-34-2-48-58	49.405109	14.429559	13.431676	0.213749	7.016585	11.669890	2.249883	0.070246	1.393884	0.119418	1.375880	100	100.50
UoAH: 348-CORE-123-128	50.186893	13.742426	13.376666	0.232769	7.280064	11.574259	2.128034	0.047156	1.314345	0.117388	1.058446	100	100.72
UoAH: 350-14-2-140-148	44.660567	17.828688	16.574444	0.098038	6.334709	7.672525	3.128037	0.445258	2.899281	0.358453	5.160179	100	98.77
UoAH: 350-14-2-44-50	56.308835	14.728908	16.241094	0.032713	6.171461	0.902667	1.736842	1.407670	2.092593	0.377219	9.685523	100	98.65
UoAH: 350-16-1-142-148	49.956508	13.848121	13.798954	0.212800	5.705252	10.823540	2.735132	0.298525	2.341806	0.279363	1.118531	100	100.25
UoAH: 350-16-2-117-126	49.841035	13.839960	13.619249	0.210202	5.999842	10.902189	2.747780	0.259720	2.308176	0.271847	1.141853	100	100.04
UoAH: 350-16-3-139-144	49.821711	13.747815	13.573924	0.222878	6.177037	10.863517	2.731007	0.282379	2.306430	0.273302	0.950859	100	100.32
UoAH: 350-16-3-20-29	49.752051	13.981862	13.497908	0.208307	6.130906	10.888601	2.758554	0.247744	2.265088	0.268979	1.151836	100	99.98

(b) Geochemical ICP-OES analysis data for DSDP Leg 38 Sites 348 and 350.

Sample abbreviations: ISOR-HI – Iceland GeoSurvey and University of Iceland and UoAH – University of Aarhus.

Geochemistry data references:

Borehole core samples

DSDP Leg 38 borehole sites 336, 337, 338, 342, 343, 345, 348 & 350

Kempton, P.D., Fitton, J.G., Saunders, A.D., Nowell, G.M., Taylor, R.N., Hardarson, B.S. and Pearson G. (2000). The Iceland plume in space and time: a Sr–Nd–Pb–Hf study of the North Atlantic rifted margin, *Earth and Planetary Science Letters*, 177(3–4), 255–271, doi: 10.1016/S0012-821X(00)00047-9.

Kharin, G.N., Udintsev, G.B., Bogatikov, O.A., Dmitriev, J.I., Raschka, H., Kreuzer, H., Mohr, M., Harre, W. and Eckhardt, F.J., (1976). K/AR ages of the basalts of the Norwegian-Greenland sea DSDP Leg 38. doi:10.2973/dsdp.proc.38.116.1976.

Raschka, H., Eckhardt, F.J. and Manum, S.B. (1976). Site 348. In: Talwani, M. and Udintsev, G. (eds). *Initial Reports of the Deep Sea Drilling Project*. U.S. Government Printing Office, Washington, pp. 595–654.

Ridley, W.I., Perfit, M.R., Adams, M.L. (1976). Petrology of basalts from deep sea drilling project, Leg 38, *Initial reports DSDP, Volume 38, Pages 731–739*, DOI: 10.2973/dsdp.proc.38.113.1976.

ODP Leg 104 borehole site 642

Parson, L., Viereck, L., Love, D., Gibson, I., Morton, A. and Hertogen, J. (1989). The petrology of the lower series volcanics, ODP Site 642. In: Eldholm, O., Thiede, J., Taylor, E., et al., *Proc. ODP, Sci. Results, 104: College Station, TX (Ocean Drilling Program)*, 419–428. doi:10.2973/odp.proc.sr.104.134.1989.

Viereck, L.G., Hertogen, J., Parson, L.M., Morton, A.C., Love, D. and Gibson, I.L. (1989). Chemical stratigraphy and petrology of the Vøring Plateau: theoleiitic lavas and interlayered volcanoclastic sediments at ODP Hole 642E. In: Eldholm, O., Thiede, J., Taylor, E., et al., *Proc. ODP, Sci. Results, 104: College Station, TX (Ocean Drilling Program)*, 367–396. doi:10.2973/odp.proc.sr.104.135.1989.

Viereck, L., Taylor, P.N., Parson, L., Morton, A.C., Hertogen, J., Gibson, I.L. (1988). Origin of the Palaeogene Voring Plateau volcanic sequence. *Geological Society, London, Special Publications*. 39. 69–83. 10.1144/GSL.SP.1988.039.01.08.

Onshore samples

East Greenland – Blossville Kyst (BK)

- Danish Lithosphere Centre database (2014). In: Hopper, J.R., Funck, T., Stoker, M.S., Ártung, U., Peron-Pinvidic, G., Doornenbal, H. and Gaina, C. (eds) (2014). Tectonostratigraphic Atlas of the North-East Atlantic Region. Geological Survey of Denmark and Greenland, GEUS, Copenhagen, 338 pp.
- Brown, P.E., Evans, I.B. and Becker, S.M. (1996). The Prince of Wales Formation - Post-flood basalt alkali volcanism in the Tertiary of East Greenland. *Contributions to Mineralogy and Petrology*. 123. 424-434. 10.1007/s004100050166.
- Hansen, H., Pedersen, A.K., Duncan, R.A., Bird, D.K., Brooks, C.K., Fawcett, J.J., Gittins, J., Gorton, M. and O'Day, P. (2002). Volcanic stratigraphy of the southern Prinsen af Wales Bjerge region, East Greenland, in *The North Atlantic Igneous Province: Stratigraphy, Tectonic, Volcanic and Magmatic Processes*, Geological Society of London Special Publication 197, edited by Jolley, D.W. and Bell, B.R., pp. 183-218, doi: 10.1144/gsl.sp.2002.197.01.08.
- Holm, P.M. (1988). Nd, Sr and Pb isotope geochemistry of the Lower Lavas, E Greenland Tertiary Igneous Province, in *Early Tertiary Volcanism and the Opening of the NE Atlantic*, Geological Society of London Special Publication 39, edited by Morton, A.C. and Parson, L.M.
- Larsen, L.M., Watt, W.S. and Watt, M. (1989). Geology and petrology of the Lower Tertiary plateau basalts of the Scoresby Sund region, East Greenland, *Bulletin Grønlands Geologiske Undersøgelse*, 157, 164.
- Momme, P., Tegner, C., Brooks, K.C. and Keays, R.R. (2002). The behaviour of platinum-group elements in basalts from the East Greenland rifted margin. *Contributions to Mineralogy and Petrology*, Volume 143, numbe 2, pages 133-153.
- Peate, D.W., Baker, J.A., Blichert-Toft, J., Hilton, D.R., Storey, M., Kent, A.J.R., Brooks, C.K., Hansen, H., Pedersen, A.K. and Duncan R.A. (2003). The Prinsen af Wales Bjerge Formation Lavas, East Greenland: the Transition from Tholeiitic to Alkalic Magmatism during Palaeogene Continental Break-up, *Journal of Petrology*, 44(2), 279-304, doi: 10.1093/petrology/44.2.279.
- Tegner, C., Brooks, C.K., Duncan, R.A., Heister, L.E. and Bernstein, S. (2008). ^{40}Ar - ^{39}Ar ages of intrusions in East Greenland: Rift-to-drift transition over the Iceland hotspot. *Lithos* 101, pp. 480-500.
- Tegner, C., Leshner, C.E., Larsen, L.M. and Watt, W.S. (1998). Evidence from the rareearth-element record of mantle melting for cooling of the Tertiary Iceland plume, *Nature*, 395(6702), 591-594.

Seafloor samples

Jan Mayen Island igneous complex (JMI)

- Carmichael, I.S.E. (1967). The iron-titanium oxides of salic volcanic rocks and their associated ferromagnesian silicates. *Contrib. Mineral. Petrol.* 14, 36-64.
- Carstens, H. (1961). Cristobalite-trachytes of Jan mayen. *Norsk Polarinst., skrifter* 121, Oslo.
- Debaille, V., Trønnes, R.G., Brandon, A.D., Waight, T.E., Graham, D.W. and Lee, C.-T.A. (2009). Primitive off-rift basalts from Iceland and Jan Mayen: Os-isotopic evidence for a mantle source containing enriched subcontinental lithosphere, *Geochimica et Cosmochimica Acta*, 73(11), 3423-3449, doi: 10.1016/j.gca.2009.03.002.
- Gevorkyan, V.Kh., Lomakin, I.E. and Kasabov, R.V. (1981). Petrology of volcanic rocks of Jan Mayen (Northern Atlantic Ocean). *GEOL. ZH.*, 41 (4), p. 80-92.
- Hawkins, T.R.W. and Roberts, B. (1970). The petrology of the volcanic and intrusive rocks of Nord-Jan, Jan Mayen. *Norsk Polarinst. Arbok* 1970, p. 19-41.
- Imslund, P. (1986). The volcanic eruption on Jan Mayen, January 1985: Interaction between a volcanic island and a fracture zone. *Journal of Volcanology and Geothermal Research*, Volume 28, Issues 1-2, 1986, Pages 45-53, ISSN 0377-0273, [https://doi.org/10.1016/0377-0273\(86\)90004-1](https://doi.org/10.1016/0377-0273(86)90004-1).
- Imslund, P. (1984). Petrology, mineralogy and evolution of the Jan Mayen magma system. *Vísindafélag Íslendinga* 43, p. 1-328.
- Lussiaa-Berdou-Polve, M. and Vidal, P. (1973). Initial strontium composition of volcanic rocks from Jan Mayen and Spitzbergen. *Earth Planet Science Letters* 18 (2), pp. 333-338.
- Maaloe, S. Sørensen, J.B. and Hertogen, J. (1986). The trachybasaltic suite of Jan Mayen. *Journal of Petrology*, 27, p. 439-466.
- Roberts, B. and Hawkins, T.R.W. (1963). The geology of the area around Nordkapp, Jan Mayen. *Norsk Polarinst. Årbok* for 1963, p. 25-48.
- Weigand, P.W., Brunfelt, A.O., Heier, K.S., Sundvoll, B. and Steinnes, E. (1972). Geochemistry of Alkali Olivine Basalts from an Eruption on Jan Mayen. *Nature Physical Science*, volume 235, pages 31-33, doi: 10.1038/physci235031a0.
- Weigand, P.W. (1970). Bulk-rock and mineral chemistry of recent Jan Mayen basalts, *Norsk Polarinst Årbok* 1970, p. 42-52.

Jan Mayen fracture zone (JMFZ)

- Dittmer, F., Fine, S., Rasmussen, M., Bailey, J.C. and Campsie, J. (1975). Dredged basalts from the mid-oceanic ridge north of Iceland. *Nature*, 254, p. 298-301, doi: 10.1038/254298a0.
- Gevorkyan, V.Kh., Lomakin, I.E. and Kasabov, R.V. (1981). Petrology of volcanic rocks of Jan Mayen (Northern Atlantic Ocean). *GEOL. ZH.*, 41 (4), p. 80-92.
- Haase, K.M., Devey, C.W., Mertz, D.F., Stoffers, P. and Garbe-Schönberg, D. (1996). Geochemistry of lavas from Mohns Ridge, Norwegian-Greenland Sea: implications for melting conditions and magma sources near Jan Mayen, *Contributions to Mineralogy and Petrology*, 123(3), 223-237, doi: 10.1007/s004100050152.
- Hanan, B.B., Blichert-Toft, J., Kingsley, R. and Schilling, J. G. (2000). Depleted Iceland mantle plume geochemical signature: Artifact of multicomponent mixing?, *Geochemistry Geophysics Geosystems*, 1(4), doi: 10.1029/1999GC000009.
- Hawkins, T.R.W. and Roberts, B. (1970). The petrology of the volcanic and intrusive rocks of Nord-Jan, Jan Mayen. *Norsk Polarinst. Arbok 1970*, p. 19-41.
- Imslund, P. (1984). Petrology, mineralogy and evolution of the Jan Mayen magma system. *Vísindafélag Íslendinga* 43, p. 1-328.
- Kruber, C., Thorseth, I.H. and Pedersen, R.B. (2008). Seafloor alteration of basaltic glass: Textures, geochemistry, and endolithic microorganisms. *Geochemistry, Geophysics, Geosystems*, 9, Q12002, doi:10.1029/2008GC002119.
- Lussiaa-Berdou-Polve, M. and Vidal, P. (1973). Initial strontium composition of volcanic rocks from Jan Mayen and Spitzbergen. *Earth Planet Science Letters* 18 (2), pp. 333-338.
- Maaloe, S. Sørensen, J.B. and Hertogen, J. (1986). The trachybasaltic suite of Jan Mayen. *Journal of Petrology*, 27, p. 439-466.
- Magna, T., Wiechert, U.H., Stuart, F.M., Halliday, A.N. and Harrison, D. (2011). Combined Li-He isotopes in Iceland and Jan Mayen basalts and constraints on the nature of the North Atlantic mantle. *Geochim. Cosmochim. Acta* 75, p. 922-936, doi: 10.1016/j.gca.2010.11.007.
- Melson, W.G and O'Hearn, T. (2003). Smithsonian volcanic glass file.
- Mertz, D.F., and Haase, K.M. (1997). The radiogenic isotope composition of the high-latitude North Atlantic mantle. *Geology*, 25 (5), p. 411-414, doi: [https://doi.org/10.1130/0091-7613\(1997\)025<0411:TRICOT>2.3.CO;2](https://doi.org/10.1130/0091-7613(1997)025<0411:TRICOT>2.3.CO;2).
- Michael, P.J. (1995). Regionally distinctive sources of depleted MORB: Evidence from trace elements and H₂O. *Earth and Planetary Science Letters*, Volume 131, Issues 3-4, 1995, Pages 301-320, ISSN 0012-821X, [https://doi.org/10.1016/0012-821X\(95\)00023-6](https://doi.org/10.1016/0012-821X(95)00023-6).

- Neumann, E.-R., and Schilling, J.-G. (1984). Petrology of basalts from the Mohs-Knipovich Ridge; the Norwegian-Greenland Sea, *Contributions to Mineralogy and Petrology*, 85(3), 209-223, doi: 10.1007/BF00378101.
- O'Nions, R.K. and Pankhurst, R. J. (1974). Petrogenetic Significance of Isotope and Trace Element Variations in Volcanic Rocks from the Mid-Atlantic, *Journal of Petrology*, Volume 15, Issue 3, 1974, Pages 603–634, <https://doi.org/10.1093/petrology/15.3.603>.
- Pedersen, S., Larsen, O., Hald, N., Campsie, J. and Bailey, J.C. (1976). Strontium isotope and lithophile element values from the submarine Jan Mayen province. *Bulletine of the geological society of Denmark*, Volume 25, Pages 25-30.
- Poreda, R., Schilling, J.G. and Craig, H. (1986). Helium and hydrogen isotopes in ocean-ridge basalts north and south of Iceland, *Earth and Planetary Science Letters*, 78(1), 1-17, doi: 10.1016/0012-821X(86)90168-8.
- Roberts, B. and Hawkins, T.R.W. (1963). The geology of the area around Nordkapp, Jan Mayen. *Norsk Polarinst. Årbok for 1963*, p. 25-48.
- Schilling, J.G., Zajac, M., Evans, R., Johnston, T., White, W., Devine, J.D. and Kingsley, R. (1983). Petrologic and geochemical variations along the Mid-Atlantic Ridge from 29 degrees N to 73 degrees. *North American Journal of Science*, 283, pp. 510-586, doi: 10.2475/ajs.283.6.510.
- Sigurdsson, H. (1981). First-order major element variation in basalt glasses from the Mid-Atlantic Ridge: 29°N to 73°N. *Journal of Geophysical Research*, 86(B10), p. 9483– 9502, doi:10.1029/JB086iB10p09483.
- Stecher, O. (1998). Fluorine geochemistry in volcanic rock series: examples from Iceland and Jan Mayen. *Geochim. cosmochim. Acta* 62, p. 3117-3130, doi: 10.1016/S0016-7037(98)00210-5.
- Sun, S.S., Tatsumoto, M. and Schilling, J.G. (1975). Mantle plume mixing along the Reykjanes ridge axis - Lead isotope evidence, *Science*, 190(4210), 143-147, doi: 10.1126/science.190.4210.143.
- Troennes, R.G., Planke, S., Sundvoll, B. and Imsland, P. (1999). Recent volcanic rocks from Jan Mayen: Low-degree melt fractions of enriched Northeast Atlantic mantle. *J. Geophys. Res.*, B104, p. 7153-7168, doi: 10.1029/1999JB900007.
- Waggoner, D.G. (1989). An isotopic and trace element study of mantle heterogeneity beneath the Norwegian-Greenland Sea. Doctoral dissertation, University of Rhode Island, USA.
- Weigand, P.W., Brunfelt, A.O., Heier, K.S., Sundvoll, B. and Steinnes, E. (1972). Geochemistry of Alkali Olivine Basalts from an Eruption on Jan Mayen. *Nature Physical Science*, volume 235, pages 31–33, doi: 10.1038/physci235031a0.
- Weigand, P.W. (1970). Bulk-rock and mineral chemistry of recent Jan Mayen basalts, *Norsk Polarinst Årbok 1970*, p. 42-52.

Jan Mayen microcontinent (JMMC-SRC) seafloor samples

Polteau, S., Mazzini, A., Hansen, G., Planke, S., Jerram, D.A., Millett, J., Abdelmalak, M.M., Blischke, A. and Myklebust, R. (2018). The pre-breakup stratigraphy and petroleum system of the Southern Jan Mayen Ridge revealed by seafloor sampling. *Tectonophysics*. DOI: 10.1016/j.tecto.2018.04.016.

Kolbeinsey ridge (KR)

Devey, C.W., Garbe-Schönberg, C.-D., Stoffers, P., Chauvel, C. and Mertz, D.F. (1994). Geochemical effects of dynamic melting beneath ridges: Reconciling major and trace element variations in Kolbeinsey (and global) mid-ocean ridge basalt. *J. Geophys. Res.*, 99 (B5), p. 9077–9095, doi:10.1029/93JB03364.

Dittmer, F., Fine, S., Rasmussen, M., Bailey, J.C. and Campsie, J. (1975). Dredged basalts from the mid-oceanic ridge north of Iceland. *Nature*, volume 254, pages 298–301, <https://doi.org/10.1038/254298a0>.

Hanan, B.B., Blichert-Toft, J., Kingsley, R. and Schilling, J.G. (2000). Depleted Iceland mantle plume geochemical signature: Artifact of multicomponent mixing?, *Geochemistry Geophysics Geosystems*, 1(4), doi: 10.1029/1999GC000009.

Jochum, K.P., Hofmann, A.W. and Seufert, H.M. (1993). Tin in mantle-derived rocks: Constraints on Earth evolution, *Geochimica et Cosmochimica Acta*, Volume 57, Issue 15, Pages 3585-3595, ISSN 0016-7037, [https://doi.org/10.1016/0016-7037\(93\)90141-I](https://doi.org/10.1016/0016-7037(93)90141-I).

Mertz, D.F., Devey, C.W., Todt, W., Stoffers, P. and Hofmann, A.W. (1991). Sr-Nd-Pb isotope evidence against plume-asthenosphere mixing north of Iceland. *Earth and Planetary Science Letters*, Volume 107, Issue 2, Pages 243-255, ISSN 0012-821X, [https://doi.org/10.1016/0012-821X\(91\)90074-R](https://doi.org/10.1016/0012-821X(91)90074-R).

O'Nions, R.K. and Pankhurst, R. J. (1974). Petrogenetic Significance of Isotope and Trace Element Variations in Volcanic Rocks From the Mid-Atlantic, *Journal of Petrology*, Volume 15, Issue 3, 1974, Pages 603–634, <https://doi.org/10.1093/petrology/15.3.603>.

Schilling, J.G., Zajac, M., Evans, R., Johnston, T., White, W., Devine, J.D. and Kingsley, R. (1983). Petrologic and geochemical variations along the Mid-Atlantic Ridge from 29 degrees N to 73 degrees. *North American Journal of Science*, 283, pp. 510-586, doi: 10.2475/ajs.283.6.510.

Schilling, J.G., Kingsley, R., Fontignie, D., Poreda, R. and Xue, S. (1999). Dispersion of the Jan Mayen and Iceland mantle plumes in the Arctic: A He-Pb-Nd-Sr isotope tracer study of basalts from the Kolbeinsey, Mohns, and Knipovich Ridges, *Journal of Geophysical Research*, 104(B5), 10543-10569, doi: 10.1029/1999jb900057.

Sigurdsson, H. and Brown, G.M. (1970). An unusual enstatite-forsterite basalt from Kolbeinsey Island, north of Iceland. *J. Petrol.*, 11, p. 205-220, doi: 10.1093/petrology/11.2.205.

Sun, S-S., Nesbitt, R.W. and Sharaskin, A.Ya. (1979). Geochemical characteristics of mid-ocean ridge basalts. *Earth and Planetary Science Letters*, Volume 44, Issue 1, Pages 119-138, ISSN 0012-821X, [https://doi.org/10.1016/0012-821X\(79\)90013-X](https://doi.org/10.1016/0012-821X(79)90013-X).

Waggoner, D.G. (1989). An isotopic and trace element study of mantle heterogeneity beneath the Norwegian-Greenland Sea. Doctoral dissertation, University of Rhode Island, USA.

Mohns ridge (MR)

Blichert-Toft, J., Agranier, A., Andres, M., Kingsley, R., Schilling, J.-G. and Albarède, F. (2005). Geochemical segmentation of the Mid-Atlantic Ridge north of Iceland and ridge-hot spot interaction in the North Atlantic. *Geochemistry, Geophysics, Geosystems*, 6, Q01E19, doi:10.1029/2004GC000788.

Haase, K.M., Devey, C.W., Mertz, D.F., Stoffers, P. and Garbe-Schönberg, D. (1996). Geochemistry of lavas from Mohns Ridge, Norwegian-Greenland Sea: implications for melting conditions and magma sources near Jan Mayen, *Contributions to Mineralogy and Petrology*, 123(3), 223-237, doi: 10.1007/s004100050152.

Hanan, B.B., Blichert-Toft, J., Kingsley, R. and Schilling, J.G. (2000). Depleted Iceland mantle plume geochemical signature: Artifact of multicomponent mixing?, *Geochemistry Geophysics Geosystems*, 1(4), doi: 10.1029/1999GC000009.

Kingsley, R.H., Schilling, J.-G., Dixon, J.E., Swart, P., Poreda, R. and Simons, K. (2002). D/H ratios in basalt glasses from the Salas y Gomez mantle plume interacting with the East Pacific Rise: Water from old D-rich recycled crust or primordial water from the lower mantle? *Geochemistry, Geophysics, Geosystems*, 3(4), doi:10.1029/2001GC000199, 2002.

Kruber, C., Thorseth, I.H. and Pedersen, R.B. (2008). Seafloor alteration of basaltic glass: Textures, geochemistry, and endolithic microorganisms. *Geochemistry, Geophysics, Geosystems*, 9, Q12002, doi:10.1029/2008GC002119.

Melson, W.G and O'Hearn, T. (2003). Smithsonian volcanic glass file.

Mertz, D.F. and Haase, K.M. (1997). The radiogenic isotope composition of the high-latitude North Atlantic mantle. *Geology* ; 25 (5): 411–414, doi: [10.1130/0091-7613\(1997\)025<0411:TRICOT>2.3.CO;2](https://doi.org/10.1130/0091-7613(1997)025<0411:TRICOT>2.3.CO;2).

Michael, P.J. (1995). Regionally distinctive sources of depleted MORB: Evidence from trace elements and H₂O. *Earth and Planetary Science Letters*, Volume 131, Issues 3–4, 1995, Pages 301-320, ISSN 0012-821X, [https://doi.org/10.1016/0012-821X\(95\)00023-6](https://doi.org/10.1016/0012-821X(95)00023-6).

Neumann, E.-R. and Schilling, J.-G. (1984). Petrology of basalts from the Mohns-Knipovich Ridge; the Norwegian-Greenland Sea, *Contributions to Mineralogy and Petrology*, 85(3), 209-223, doi: 10.1007/BF00378101.

Poreda, R., Schilling, J.G. and Craig, H. (1986). Helium and hydrogen isotopes in ocean-ridge basalts north and south of Iceland, *Earth and Planetary Science Letters*, 78(1), 1-17, doi: 10.1016/0012-821X(86)90168-8.

Schilling, J.G., Kingsley, R., Fontignie, D., Poreda, R. and Xue, S. (1999). Dispersion of the Jan Mayen and Iceland mantle plumes in the Arctic: A He-Pb-Nd-Sr isotope tracer study of basalts from the Kolbeinsey, Mohns, and Knipovich Ridges, *Journal of Geophysical Research*, 104(B5), 10543-10569, doi: 10.1029/1999jb900057.

Waggoner, D.G. (1989). An isotopic and trace element study of mantle heterogeneity beneath the Norwegian-Greenland Sea. Doctoral dissertation, University of Rhode Island, USA.

Northern Jan Mayen Ridge (NJMR)

Debaille, V., R. G. Trønnes, A. D. Brandon, T. E. Waight, D. W. Graham, and C.-T. A. Lee (2009), Primitive off-rift basalts from Iceland and Jan Mayen: Os-isotopic evidence for a mantle source containing enriched subcontinental lithosphere, *Geochimica et Cosmochimica Acta*, 73(11), 3423-3449, doi: 10.1016/j.gca.2009.03.002.

Haase, K.M., Devey, C.W., Mertz, D.F., Stoffers, P. and Garbe-Schönberg, D. (1996). Geochemistry of lavas from Mohns Ridge, Norwegian-Greenland Sea: implications for melting conditions and magma sources near Jan Mayen, *Contributions to Mineralogy and Petrology*, 123(3), 223-237, doi: 10.1007/s004100050152.

Northern volcanic zone – Krafla (NVZ)

Grönvold, K. and Mäkipää (1978). Chemical composition of Krafla lavas 1975-1977. Nordic volcanological institute, University of Iceland, report 78 16.

Tjörnes fracture zone (TFZ)

Devey, C.W., Garbe-Schönberg, C.-D., Stoffers, P., Chauvel, C. and Mertz, D.F. (1994). Geochemical effects of dynamic melting beneath ridges: Reconciling major and trace element variations in Kolbeinsey (and global) mid-ocean ridge basalt. *J. Geophys. Res.*, 99 (B5), p. 9077– 9095, doi:10.1029/93JB03364.

Hemond, C., Condomines, M., Fourcade, S., Alegre, C.-J., Oskarsson, N. and Javoy M. (1988). Thorium, Strontium and oxygen isotopic geochemistry in recent tholeiites from Iceland: Crustal influence on mantle-derived magmas. *Earth Planet. Sci. Lett.* 87, p. 273-285, doi: 10.1016/0012-821X(88)90015-5.

Kokfelt, T.F., Hoernle, K., Hauff, F., Fiebig, J., Werner, R. and Garbe-Schönberg, D. (2006). Combined Trace Element and Pb-Nd–Sr-O Isotope Evidence for Recycled Oceanic Crust

(Upper and Lower) in the Iceland Mantle Plume, *Journal of Petrology*, 47(9), 1705-1749, doi: 10.1093/petrology/egl025.

Schilling, J.G., Zajac, M., Evans, R., Johnston, T., White, W., Devine, J.D. and Kingsley, R. (1983). Petrologic and geochemical variations along the Mid-Atlantic Ridge from 29 degrees N to 73 degrees. *North American Journal of Science*, 283, pp. 510-586, doi: 10.2475/ajs.283.6.510.

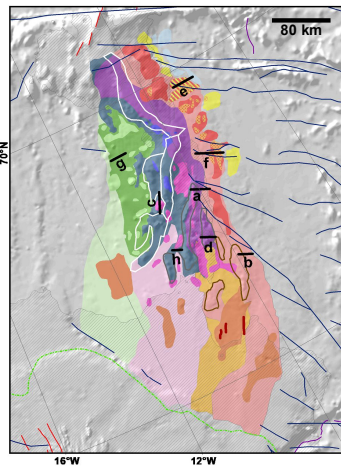
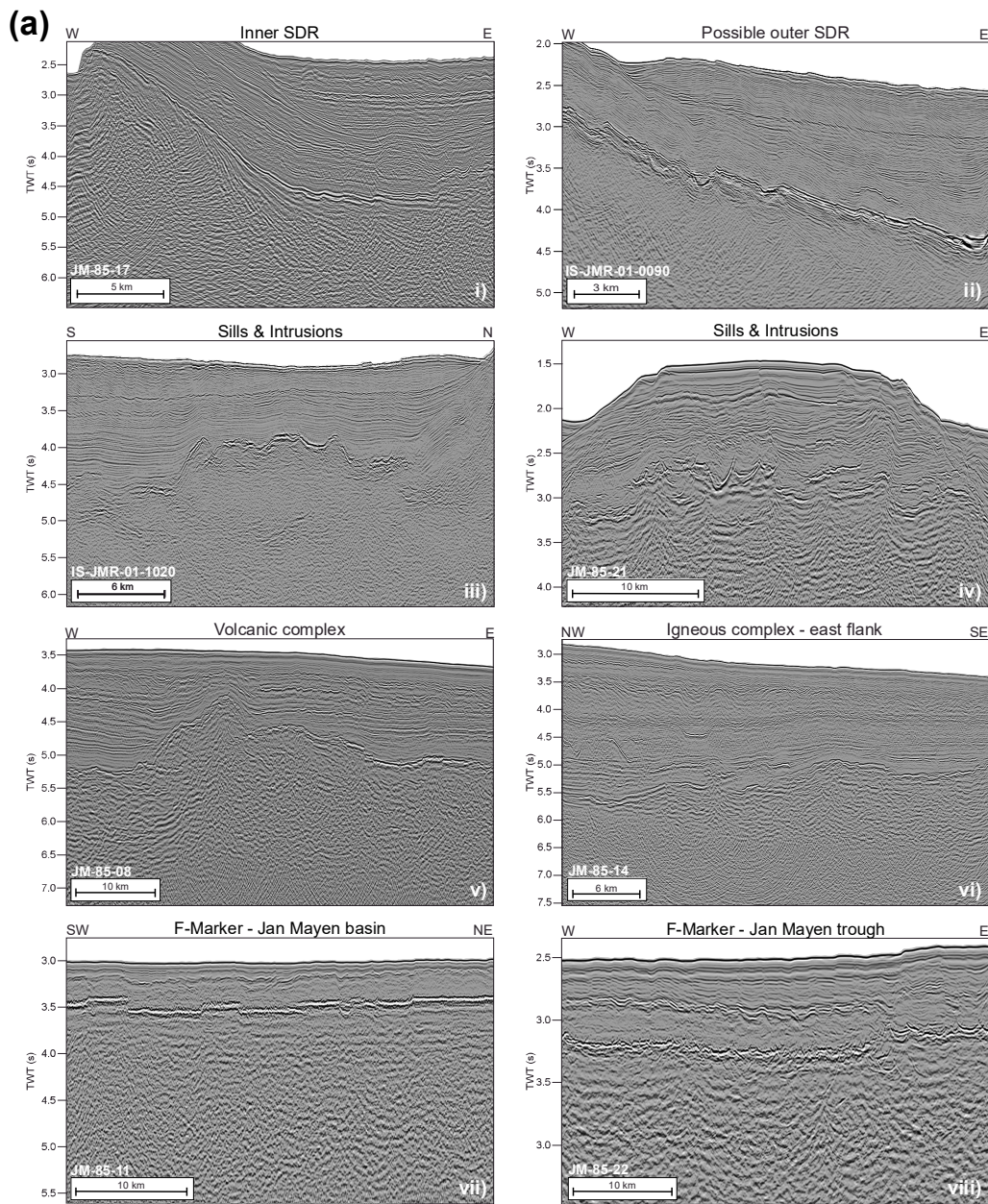
Sigvaldason, G.E. (1974). Basalt from the centre of the assumed Icelandic mantle plume. *J. Petrol.* 15, p. 497-524, doi: 10.1093/petrology/15.3.497.

Vesteris seamount (VSM)

Haase, K.M. and Devey, C.W. (1994). The Petrology and Geochemistry of Vesteris Seamount, Greenland Basin—an Intraplate Alkaline Volcano of Non-Plume Origin, *Journal of Petrology*, 35(2), 295-328, doi: 10.1093/petrology/35.2.295.

Supplement 6

Mapped JMMC volcanic facies, stratigraphic horizons and igneous events.



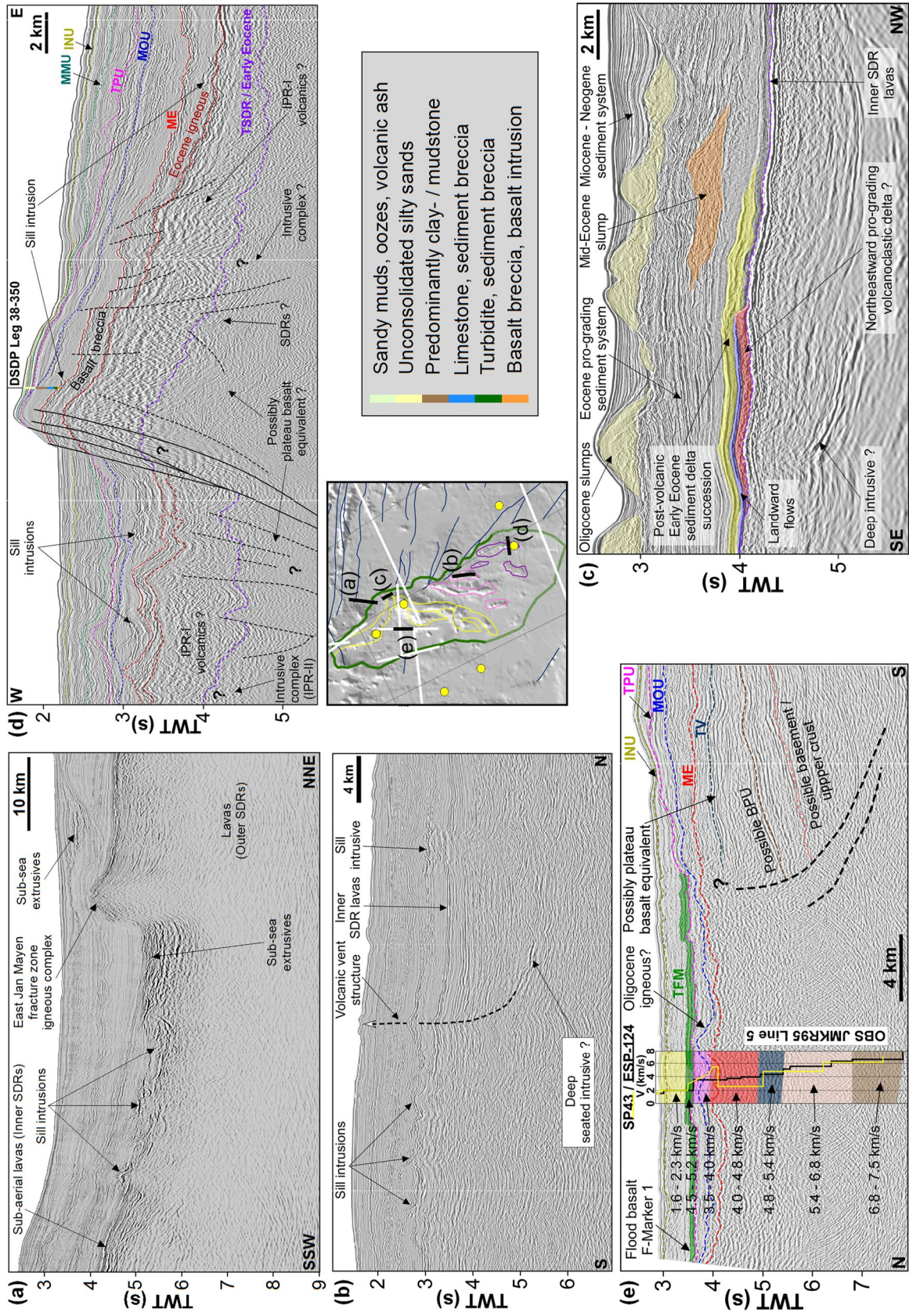
Jan Mayen microcontinent area volcanic facies types example:

- (i) **Seaward dipping reflector (SDR's) / Inner SDR:**
clearly visible wedge feature of eastward dipping reflectors into the Norway basin, discordantly overlaying the JMCC breakup margin.
- (ii) **Atypical seaward dipping reflector (SDR's) / Outer SDR:**
not clearly showing wedge shape units connected to the south-eastern SRC igneous margin (IPR-I) that has been heavily affected by later faulting during the rift transfer across the IPR.
- (iii & iv) **Sill and dyke intrusions:**
layer parallel, saucer-shaped, to fault parallel sill and dyke intrusions within the Eocene to Early Miocene strata.
- (v & vi) **Volcanic and igneous complexes:**
build up onto the SDR's and the firstly established oceanic crust along and east of the continent ocean boundary (COB).
- (vii & viii) **Shallow rift basalt - F-Marker:**
series of shallow intrusions and regional extensive lava flows, possibly in shallower water, occurred in different IPR activity phases during Late Oligocene within the Jan Mayen trough and during Early Miocene within the Jan Mayen basin, that relate to the rifting and separation of the western flank of the JMCC from the main land.

(b) Examples of volcanic and stratigraphic facies and related structures.

Data interpretation is based on 2D multi-channel seismic reflection data from surveys NPD-2011, ICE-02 in 2009 and reprocessed data from the JM-85, JMR-01, and JMR-08 surveys.

- (a) Fracture zone intrusive, sill and dyke intrusive – JMMC northeast flank;
- (b) Vent structures, sill and dyke intrusive – JMMC southeast flank;
- (c) Eocene terrestrial to shallow marine transition from landward flows to hyaloclastite delta and pro-grading sediment systems;
- (d) Early-Mid Eocene IPR basalt breccia and Eocene to Oligocene sill intrusive;
- (e) Oligocene F-Marker extrusive and intrusive.

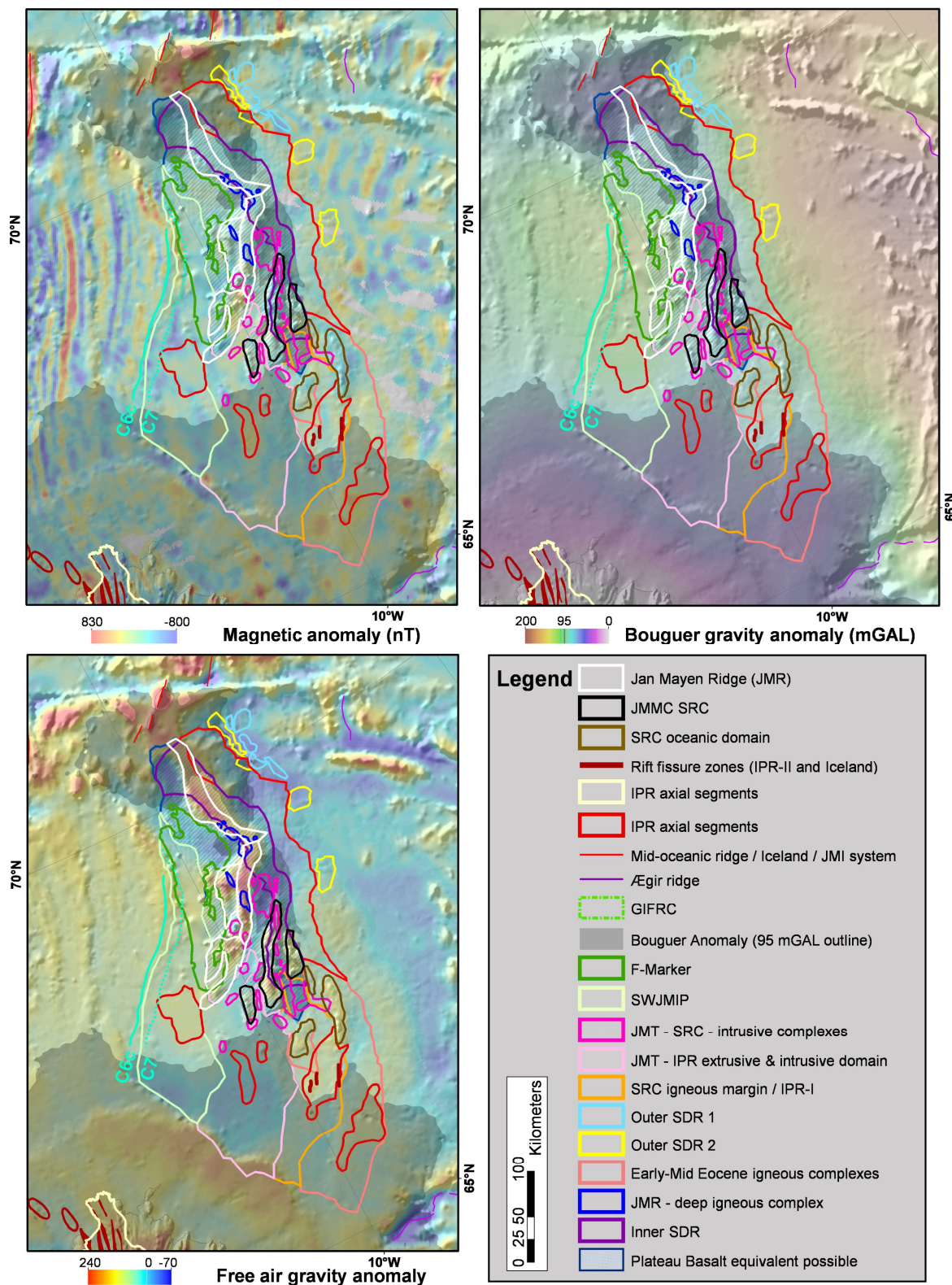


(c) Summary of interpreted stratigraphic horizons and main igneous events.

Horizon	Epoch	Igneous/ tectonic events
JM10	Plio-Pleistocene	Strong reflector. Unconformity. Continuous seafloor spreading on Kolbeinsey Ridge parallel to thermal subsidence affecting the Jan Mayen Ridge (deep marine environment).
JM15	Middle Miocene	Unconformity. Probably formed during last step of rifting, right before or during the first seafloor spreading on the Kolbeinsey Ridge
F-Marker 1	Early Miocene	2 nd breakup emplacement of Flood basalt (intrusive & extrusive formations) during a breakup event (JMB – west flank domain)
JM20	Top Paleogene	Unconformity. Uplift and erosion
Volcanic SW-W margin	Late Oligocene to Early Miocene	Rift transfer across IPR forming of large igneous complexes and forming of volcanic margin.
F-Marker 2	Late Oligocene	Emplacement of Flood basalt (intrusive & extrusive formations) during IPR rift transfer (JMT domain)
JM30	Middle to Late Oligocene	Unconformity. Onset of deposition after the main breakup within the Greenland margin
F-marker 3	Middle Oligocene	Emplacement of Flood basalt (intrusive & extrusive formations) during IPR rift transfer (SE SRC)
JM35	Early to Middle Oligocene	Unconformity. Onset of main rifting and breakup within the Greenland margin.
JM40	Late Eocene	Unconformity, intrusive complexes
JM45	Middle to Late Eocene	Seafloor spreading at the Ægir Ridge and accumulation of sediments at the Jan Mayen Ridge, derived from Greenland highlands.
JM50	Middle Eocene	Rift transfer across IPR forming of large igneous complexes and well-defined unconformity
Poss. Volcanic Conduit	Early to Middle Eocene	Rift transfer across IPR forming of large igneous complexes and forming of volcanic margin.
JM-60 SDR & poss. Plateau Basalt equivalent	Early Eocene	1 st breakup extension between Greenland and Norway. Forming of the plateau basalts and sub-joined with onset of seafloor spreading at the Ægir Ridge and forming of SDR's
JM70	Paleocene	Pre-rift strata

Supplement 7

Present day JMMC volcanic facies and province interpretations in comparison with magnetic [*Nasuti and Olesen, 2014*], free air gravity and Bouguer gravity data [*Haase and Ebbing, 2014*].



Appendix 1: Conference paper, the Iceland Plateau – Jan Mayen volcanic breakup margin

The Iceland Plateau – Jan Mayen volcanic breakup margin: An analogue for axial rift and transfer zone North Iceland.

Blischke, A., Erlendsson, Ö., Brandsdóttir, B., Hjartardóttir, Á. R. and Gautason, B. (2021)

*Proceedings World Geothermal Congress 2021, paper 11175, p. 12, Reykjavik, Iceland,
2021.*

Copyright © The Authors 2021

Proceedings World Geothermal Congress 2020
Reykjavik, Iceland, April 26 – May 2, 2020

The Iceland Plateau – Jan Mayen volcanic breakup margin: An analogue for axial rift and transfer zone North Iceland.

Anett Blischke^{1,2}, Ögmundur Erlendsson³ Bryndís Brandsdóttir¹, Ásta Rut Hjartardóttir¹ and Bjarni Gautason²

¹ Institute of Earth Sciences, Science Institute, University of Iceland, Askja, Sturlugata 7, 101 Reykjavík, Iceland

² Iceland GeoSurvey, Branch at Akureyri, Rangárvöllum, 603 Akureyri, Iceland

³ Iceland GeoSurvey, Grensásvegí 9, 108 Reykjavík, Iceland

E-mail: anett.blischke@isor.is, ogmundur.erlendsson@isor.is, bryndis@hi.is, astahj@hi.is, bg@isor.is

Keywords: Jan Mayen and Iceland Plateau igneous complexes, kinematic model, plateau basalts, rift transition, seaward dipping reflectors, seismic volcano-stratigraphy, dyke and sill intrusives, vent structures

ABSTRACT

Structural-, volcano-stratigraphic-, and igneous-province-mapping is a fundamental prerequisite for resource modelling and management, such as geothermal exploration or mining. Our tectonic-kinematic model of the Jan Mayen region was constructed utilizing gravity- and magnetic anomalies, multibeam bathymetric data, seismic reflection, and refraction data, borehole and seafloor samples. The Jan Mayen igneous complexes and the Iceland plateau rift portray the complexity of long-lived volcanic margins within an unstable rift-transfer tectonic setting from Eocene to Miocene times. Both regions are characterized by rift basins, en-echelon volcanic ridges, sill and dyke intrusive structures, and geothermal fluid venting structures such as chimneys, cutting through pre-existing crustal and sediment sections, commonly along re-activated fault planes. Using a dense seismic reflection dataset provides a unique opportunity to map intercalated igneous domains and rift zones of the Jan Mayen microcontinent in a three-dimensional space, enabling us to estimate the volcano-stratigraphic types, size, and extent of these rift and volcanic systems, as well as large-scale igneous features, such as deeper-seated intrusions, volcanic complexes, or rift valleys. The igneous Jan Mayen and Iceland Plateau regions represent a prime example of what is commonly referred to as Iceland type crust, i.e. the systematic build-up of thicker oceanic crust by rift-transfer processes, overlapping sub-aerial and sub-surface igneous activities in conjunction with localized microplates.

1. INTRODUCTION

Igneous complexes on the flanks of the Jan Mayen microcontinent (JMMC) and within the Iceland plateau (IP) constitute an analogue area for present day Iceland. Based on offshore potential field data and seismic reflection-refraction analysis (Blischke et al., 2017, 2019a,b) (Figure 1), we are able to construct a three-dimensional map of the JMMC-IP rift zones, including more detailed imaging of the type, size, and extent of individual rift and volcanic systems, as well as smaller scale igneous features, such as sill, dyke, or venting structures and their connection to deeper-seated intrusions that served as conduits for rising magmatic material and geothermal fluids. Our insight into Eocene-Miocene structures offshore may thus serve as analogues for present day processes within the volcanic rift zones of Iceland. Here we specifically address the complex volcanic and structural interaction represented in offshore seismic reflection data which generally present major challenges for on land geothermal field exploration.

2. DATA AND METHODS

Vintage and new JMMC-IP geological and geophysical datasets (1970's-2017), including seismic reflection and refraction profiles, gravity and magnetic anomaly data, high-resolution multibeam bathymetric imagery, and borehole and seafloor sample information were used to build a comprehensive volcano-stratigraphic model (e.g. Vogt et al., 1970, 1986; Talwani and Eldholm, 1977; Åkermoen, 1989; Doré et al., 1999; Lundin et al., 2005; Gaina et al., 2009, 2014, 2017a,b; Gernigon et al., 2012, 2015, 2019; Hopper et al., 2014; Haase and Ebbing, 2014; Nasuti and Olesen, 2014; Funck et al., 2014, 2016, 2017; Haase et al., 2017; Blischke et al., 2017a,b; 2019a,b). Datasets were processed using the Petrel software tool © Schlumberger, an integrated interpretation software for 3D mapping of geophysical and geological datasets, here specifically seismic reflection, borehole, or multibeam bathymetric datasets. JMMC-IPR microplate reconstructions and projections were adapted from Blischke et al. (2017; 2019a,b) utilizing GPlates, an interactive fitting method (www.gplates.org; Müller et al., 2018; Gaina et al., 2017b). Newly acquired, high-resolution multibeam bathymetric maps (Hélgadóttir, 2008; Hélgadóttir and Reynisson, 2010) were correlated with seismic reflection and potential field data, in order to constrain structural trends and igneous features, such as volcanic cones, axial ridges, or pockmarks. This combined with seismic reflection data enabled us to distinguish between normal and strike-slip faults, shallow volcanic activity, or slump fault systems that are still active along the steep JMMC escarpments. Volcano-stratigraphic seismic units were characterized by sedimentary and igneous stratigraphic units and seismic reflection characteristics in tie with available borehole and potential field data. Seaward dipping reflectors (SDR), volcanic ridges, igneous complexes, or extrusives, such as flood basalt domains were primary volcano-stratigraphic elements (Figures 1b; 2). Together this data formed the basis for establishing the three-dimensional stratigraphic framework of the JMMC-IP (Figure 3).

Gravity and magnetic anomaly mapping are effective methods to study areas where few seismic reflection profiles exist. A joint interpretation that combines seismic and potential field data thus produces a synergy that help to significantly improve and validate the geological and structural interpretations of potential prospects (Nasuti and Olesen, 2014). Gravity data are normally used to study the extent and depth of sedimentary basins, major tectonic features and to investigate variations in crustal thickness, segmentation and density across a region (Haase and Ebbing, 2014, 2016).

Blichke et al.

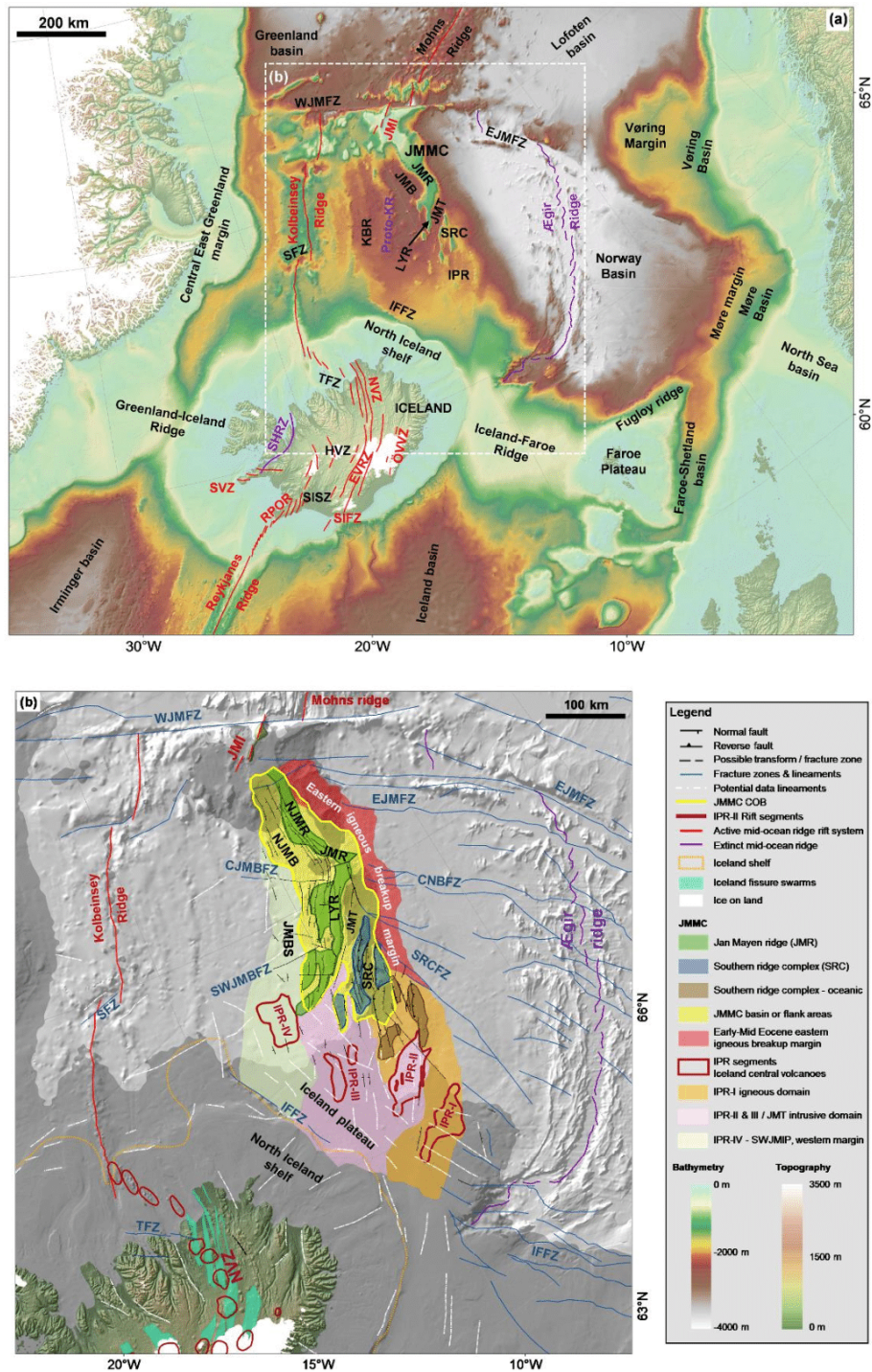


Figure 1: Central NE-Atlantic tectonic map showing faults, fractures zones and lineaments based on Einarsson and Sæmundsson (1987), Einarsson (2008), Hjartardóttir et al. (2013); Magnúsdóttir et al. (2015); Blichke et al. (2017a, 2019a,b). The background is a hill shade bathymetry map (IBCAO 3.0; Jakobsson et al., 2012). Abbreviations: CJMBFZ – Central Jan Mayen Basin Fracture Zone; CNBFZ – Central Norway Basin Fracture Zone; EJMfZ – East Jan Mayen Fracture Zone; EVZ – Eastern Volcanic Zone; HVZ – Hofsjökull Volcanic Zone; IFfZ – Iceland-Faroe Fracture Zone; IPR – Iceland Plateau Rift; JMMC – Jan Mayen Microcontinent (JMB – Jan Mayen Basin; JMBS – Jan Mayen Basin south; JMI – Jan Mayen Island igneous complex; JMR – Jan Mayen Ridge; JMT – Jan Mayen Trough; LYR – Lyngvi Ridge; SRC – Southern Ridge Complex; SRCfZ – Southern Ridge Complex Fracture Zone; SWJMBFZ – Southwest Jan Mayen basin fracture zone; KRB – Kolbeinsey Ridge Basin; NVZ – Northern Volcanic Zone; ÖSVZ – Örafajökull-Snafell Volcanic Zone, proto-KR – proto Kolbeinsey Ridge, RPOR – Reykjanes Peninsula Oblique Rift; SISZ – South Iceland Seismic Zone; SHRZ – Snæfellsnes-Húnaflói Rift Zone; SVfZ – Snæfellsnes Volcanic Zone; TFZ – Tjörnes Fracture Zone; WJMfZ – Western Jan Mayen Fracture Zone; WVZ – Western Volcanic Zone.

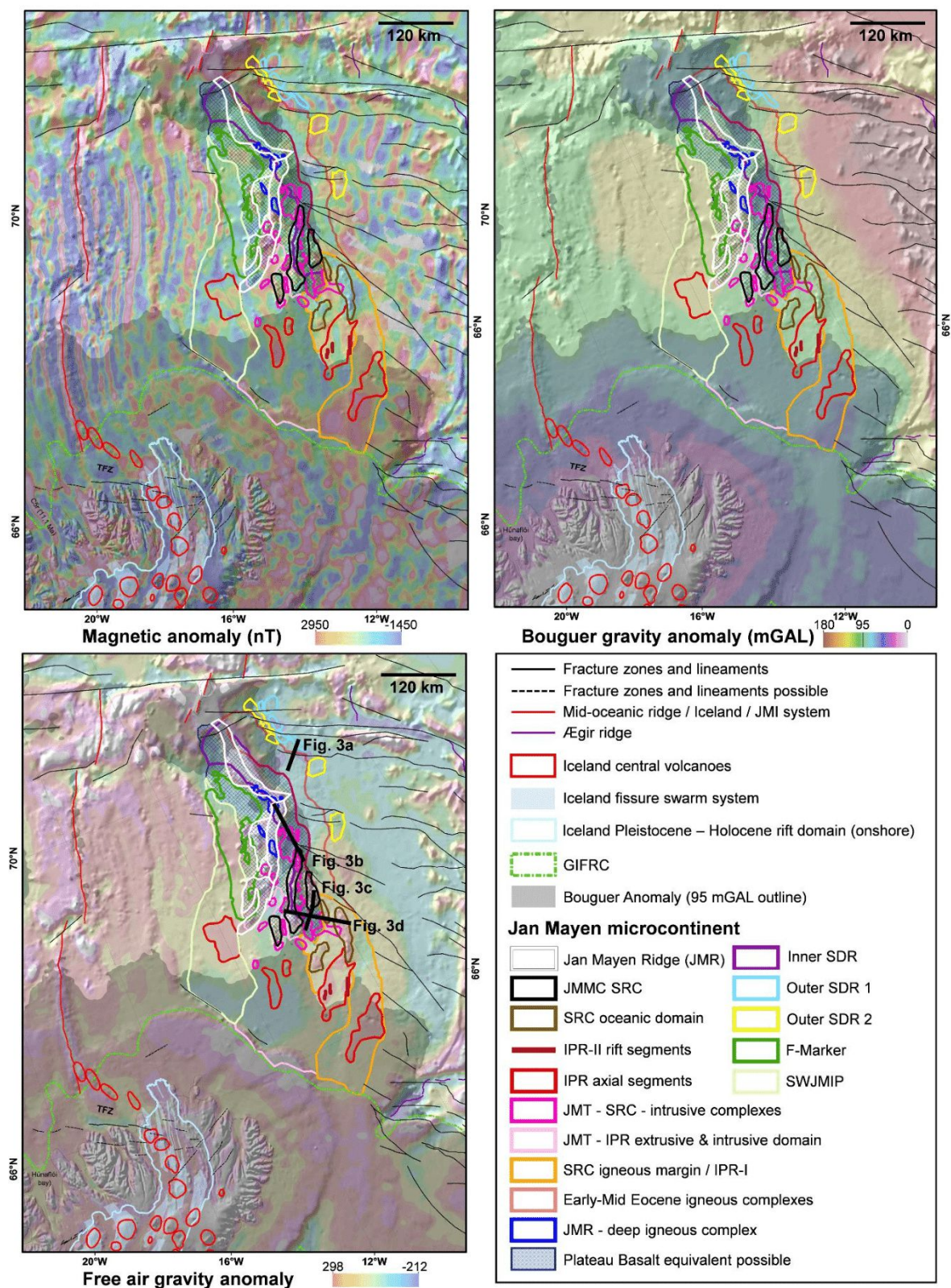


Figure 2: Present day JMMC. Volcanic facies and provinces map interpretations in comparison to magnetic anomaly data by Nasuti and Olesen (2014), free air gravity anomaly and bouguer gravity anomaly grid data modified by (Haase and Ebbing, 2014). Igneous domains and features are modified after Blischke et al. 2019b for the JMMC-IPR area, and Einarsson and Sæmundsson (1987), Einarsson (2008) and Sigmundsson et al., (2018) for Iceland.

Blischke et al.

Magnetic data are used to investigate subsurface geology based on anomalies in Earth's magnetic field that effected and preserved the field's orientation of the underlying rocks at its time of emplacement. Thus, providing a chronological mapping tool of magnetic anomalies across the ocean floor (Gaina, 2014). Magnetic data also provide information on hidden geological structures, especially in volcanic and metamorphic terrains and structures in non-magnetic sedimentary terrains (e.g. Gaina et al., 2017b; Blischke et al., 2019b). Several extrusive and intrusive features can be seen on gravity and magnetic maps (Figures 2-4).

3. GEOLOGICAL SETTING

Understanding the geological setting of an area is the basis for any exploration or development field work. The JMMC study was initially focused on the tectono-volcano-stratigraphic framework of the Lyngvi ridge and southern ridge complex (SRC), (Figure 3). To understand their formation, a comprehensive study the microcontinent and IPR region became necessary, in order to gain an understanding of the sub-areas and the forming of smaller scale volcano-stratigraphic features.

3.1 The Jan Mayen microcontinent (JMMC)

The JMMC and IPR area is defined as a 400-450 km long and 100-310 km wide domain located in the central NE Atlantic, between the extinct Ægir ridge to the east and the Kolbeinsey ridge to the west (Figure 1). The northern boundary comprises of the Jan Mayen fracture systems and the Jan Mayen island igneous complex, with leaky fracture zones, e.g. the eastern Jan Mayen Fracture Zone (EJMFZ) (Figure 4a). The region's southern boundary is formed by the Iceland-Faroe fracture zone (IFFZ) and the NE Iceland insular shelf. The JMMC comprises a series of bathymetric ridges with water depth ranging between 200-2500 m (e.g. Vogt et al., 1970; Talwani et al., 1977). The microcontinent has been subdivided into the main Jan Mayen Ridge (JMR), the Lyngvi Ridge, the Jan Mayen Basin with a northern and southern segment, the Jan Mayen Trough, and the Southern Ridge Complex (SRC). The main northern JMR is a well-defined, continuous and flat-topped structural feature. The SRC is comprised of several smaller ridges, which become more indistinct towards the south, where the fan-shaped, oblique IPR-domain intersects the JMMC's southern ridges (Figures 1-4).

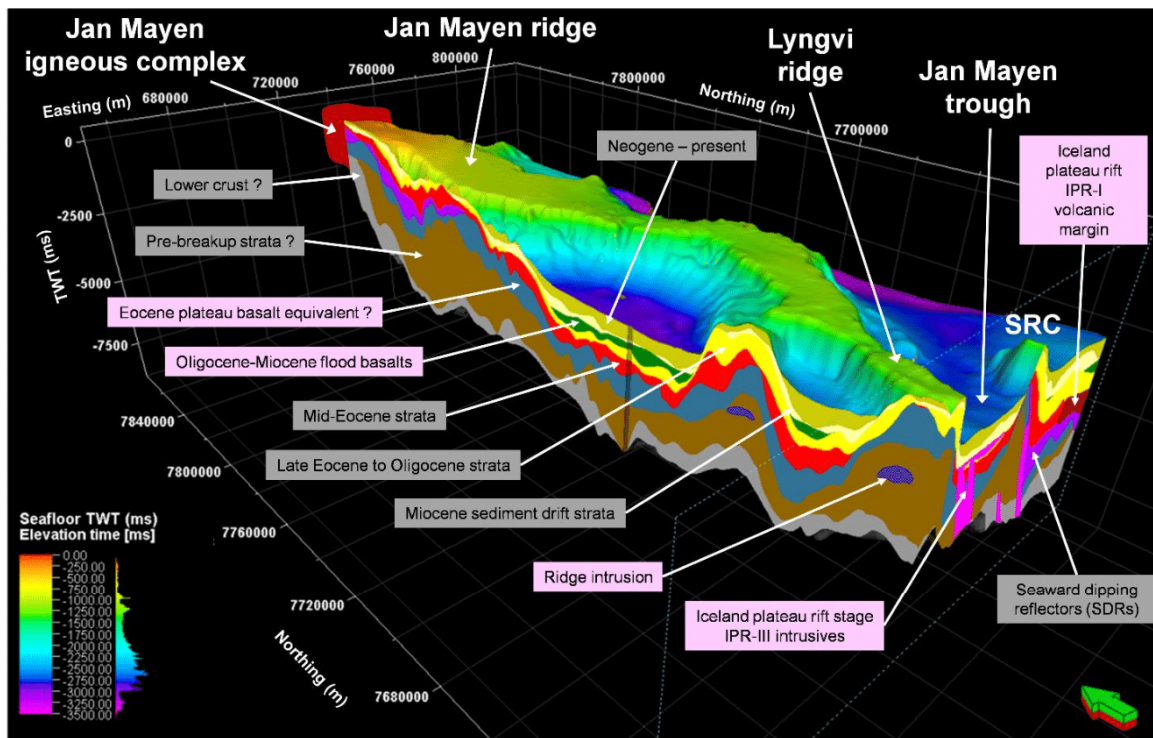


Figure 3: Present day three-dimensional JMMC primary volcano-stratigraphic framework after Blischke et al. 2019a,b. Abbreviations: SRC – Jan Mayen southern ridge complex.

These ridge structures resulted of microcontinent's location within a dual-breakup scenario, first from the central Norwegian shelf and the Vøring-Møre margin, and finally from the central East Greenland margin (e.g. Talwani et al., 1977; Gaina et al., 2009; Gernigon et al., 2015, 2019). The reconstructed geo-chronology of the central NE Atlantic region and mapped igneous domains was updated and indicates six major phases influencing the JMMC's breakup history by Blischke et al. (2017, 2019a,b) (Figures 1a; 2):

- (1) Early Paleogene: Possible pre-breakup magmatic intrusions underneath central East Greenland – JMMC (~63-55 Ma). Initial breakup phase and rupturing of the overlying lithosphere along SW-NE-striking, pre-existing fracture zones. During the initial rifting and breakup phase, overlapping igneous systems developed along the divergent plate boundary, with subaerial plateau basalt flows across the central NE Atlantic, including the JMMC region.
- (2) Early Eocene: North-to-south development of an inner and first set of seaward-dipping reflectors along the eastern margin of JMMC. Another two sets of outer seaward-dipping reflectors overlapped the first and inner SDR set, as a precursor to the formation of the Ægir ridge (55-52 Ma).

- (3) Early-Mid Eocene: Forming of JMMC's eastern volcanic margin that continued into the IPR-I. IPR-II segment intersects the IPR-I segment and the southern extent of the SRC. Creation of an overlapping spreading system of the IPR segments with the southern Ægir ridge connecting into the northern extent of the Greenland-Iceland-Faroe Ridge Complex (GIFRC) (~52-40 Ma).
- (4) Late Eocene-Oligocene: The formation of segment IPR-III and the Jan Mayen southern ridge complex, alongside extensions within the Jan Mayen trough and separation from the main Jan Mayen ridge (35-25 Ma).
- (5) Late-Oligocene-Early Miocene: Forming of the western igneous margin of the JMMC, along the proto-Kolbeinsey ridge that initiated the final breakup of the JMMC from Greenland (25-21 Ma).
- (6) Early Miocene: Spreading along the Kolbeinsey ridge with complete separation of the JMMC from the central East Greenland margin (since 21 Ma).

The JMMC-IPR area represents a unique area for research related to a dual breakup system of the two rifting complexes that created the Jan Mayen microcontinent, with a firm link of the oblique Iceland plateau rift system and the central East Greenland margin with respect to timing, geochemistry and tectono-magmatic processes, specifically in the Southern Ridge Complex and Jan Mayen Trough areas.

3.2 The Jan Mayen Southern Ridge Complex and Jan Mayen Trough

The Southern Ridge Complex (SRC) is a collection of several ridges that were formed during extension and rift transfer along the southern part of the microcontinent (Figures 1-4) (e.g. Talwani et al., 1977; Gaina et al., 2009; Peron-Pinvidic et al., 2012a; Gernigon et al., 2015; Blischke et al., 2017b). The SRC area initiated during the Ægir Ridge breakup phase by forming a wide igneous margin, which was broken into several smaller segments, forming several small basins with numerous post-breakup intrusives and vent structures along fault and fracture zones. The three northernmost SRC ridges appear similar in seismic characteristics to the eastern flank of the Jan Mayen ridge and are linked to the origin of the microcontinent. These blocks were not as much affected by post-breakup volcanism as the three southernmost SRC ridges, which are segments of the original Early-Eocene volcanic breakup margin, intersected by many intrusives (Figures 1a; 2; 3). Sill, dyke, and venting structures can be observed along fault- and fracture zones, nearly up to the seafloor, possibly indicating igneous activity over a longer duration (Figure 4c). The Jan Mayen Trough (JMT) separates the Lyngvi ridge from the SRC and widens towards the southwest with one segment of the SRC embedded within it (Figures 1b; 2). The entire JMT is covered by a flat-lying and almost opaque reflector on seismic reflection data and is chrono-stratigraphically placed within the Late-Oligocene flood basalts (Figures 2; 3; 4d). Even with the most recent, higher-resolution seismic reflection data, it is difficult to clearly define and map underlying deeper structures, though fault blocks can be seen that are separated by intrusives. These intrusives and fault blocks are correlated to the stratigraphic framework and to distinct changes in Bouguer gravity and magnetic anomaly values, indicating a potential grouping of these intrusive in order of emplacement in between the fault blocks (Figures 2-4).

3.3. Iceland Plateau Rift

The IPR formed an overlapping spreading system with the southernmost Ægir Ridge, tectonically compensating the southwards decrease in spreading rate along the Ægir ridge. Hyper-extended slivers of JMMC type crust were intersected by dyke and sill intrusions related to the Mid-Eocene to Late Oligocene formation of the IPR-I - IPR-IV volcanic ridges and flood basalts (Figures 2; 4c,d). The oblique IPR rifting domain, formed a fan-shaped intersection with the southern ridges of the JMMC, by crustal thinning and breaches where axial rift systems and volcanic ridges would develop (Blischke et al., 2019b). The total JMMC type crustal thickness varies between 7-12 km across the IPR segments based on seismic refraction data and gravity crustal thickness inversions (Haase and Ebbing, 2014; Brandsdóttir et al., 2015). The IPR, south and southeast of the SRC, is primarily of oceanic origin based on interpretation of seismic refraction velocity data (Talwani et al., 1977; Brandsdóttir et al., 2015), and detailed seismic reflection, magnetic and gravity data interpretations (Peron-Pinvidic et al., 2012a; Blischke et al., 2017b, 2019a,b) (Figures 1b, 2; 4c,d). The oblique IPR-I and II systems were linked to the Blossville Kyst of central East Greenland during the Eocene (52 – 40 Ma). The separation of the JMMC from the central East Greenland margin during Oligocene to early Miocene (~35 Ma – 21 Ma) was accompanied by extension, the formation of a distinct S-N oriented volcanic ridges and final breakup margin along the southwestern and western extend of the JMMC. The southwestern-western margin including the emplacement of igneous complexes, such as the SW Jan Mayen igneous province. The Jan Mayen basin is possibly part of a buried western Late Oligocene breakup margin that covered the basin with regionally extensive flood basalt (Figures 1b; 2; 3). The JMMC - IPR transition portrays the complexity of long-lived, active volcanic margins within an unstable rift-transfer tectonic setting, exhibiting both lateral and vertical crustal accretion throughout its formation in Eocene through Miocene times. Thus, accounting for some of the for oceanic type domain's anomalously thick crust due to overlapping systems and repeated reactivations that was accompanied by deep and shallow intrusive formations that preceded the present-day NE Iceland rift transfer system.

4. IGNEOUS AND STRUCUTRAL FEATURES OF THE JMMC AND IPR

This section briefly summarizes the JMMC and SRC-IPR areas focusing on volcanic and structural examples from seismic reflection data tied with potential field data (Figure 4), such as volcanic ridges – SRC-JMT igneous complexes, and structural examples of the Southern Ridge Complex fracture zone (SRCFZ) (Figure 5). The integrated data analysis was specifically applied to the JMFZ, SRC and IPR areas, focusing on volcanic ridges and other visible structures south, southeast and within the SRC and JMT, represented by up-doming structures of volcanic material within the seismic records. Up-doming structures, visible on some of the seismic reflection data (Figure 4b-d), are described in the literature as a crustal breach and passage followed by magma in a volcanic system (Decker and Decker, 2005). These structures are clearly identified for the rifting of the IPR-II and IPR-III systems inferred by Brandsdóttir et al. (2015); and described by Blischke et al. (2017a,b, 2019a,b); or Erlendsson and Blischke (2019) (Figure 4b-d). The volcanic ridges appear both as decentralized structures or along large faults or fault blocks that serve as conduits of rising magma along the fault zones that leads to deformation and uplift of the fault block. Often, an increase of intrusion events within sedimentary strata is associated with these conduits, lateral to and/or above the conduit structure.

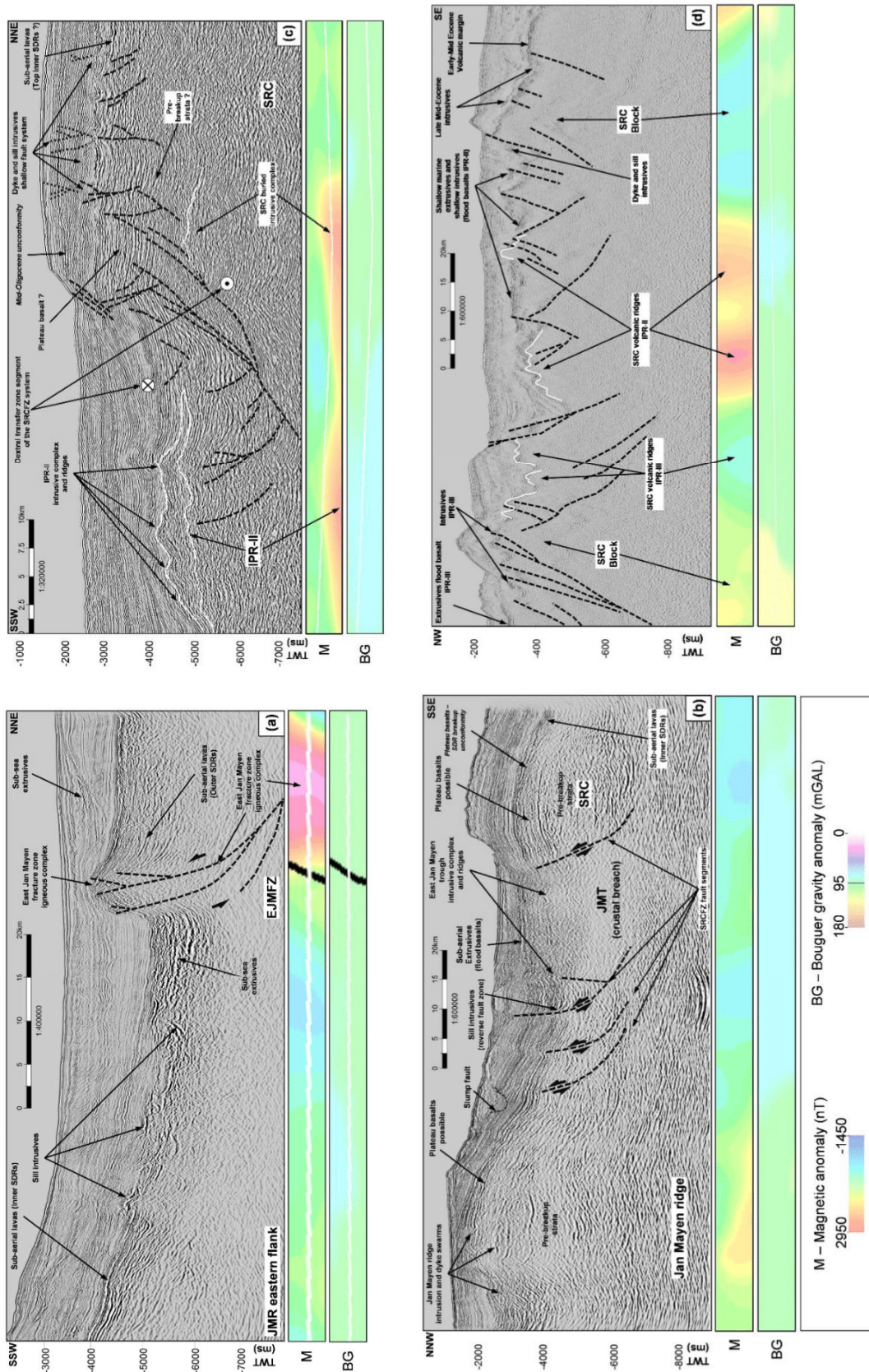


Figure 4: Examples of 2D seismic reflection profiles tied with magnetic (M) and Bouguer gravity anomaly data (Figure 2), outlining major fault and fracture zones in relationship to structural and igneous domain elements. For profile locations, see Figure 2 on the free air gravity map.

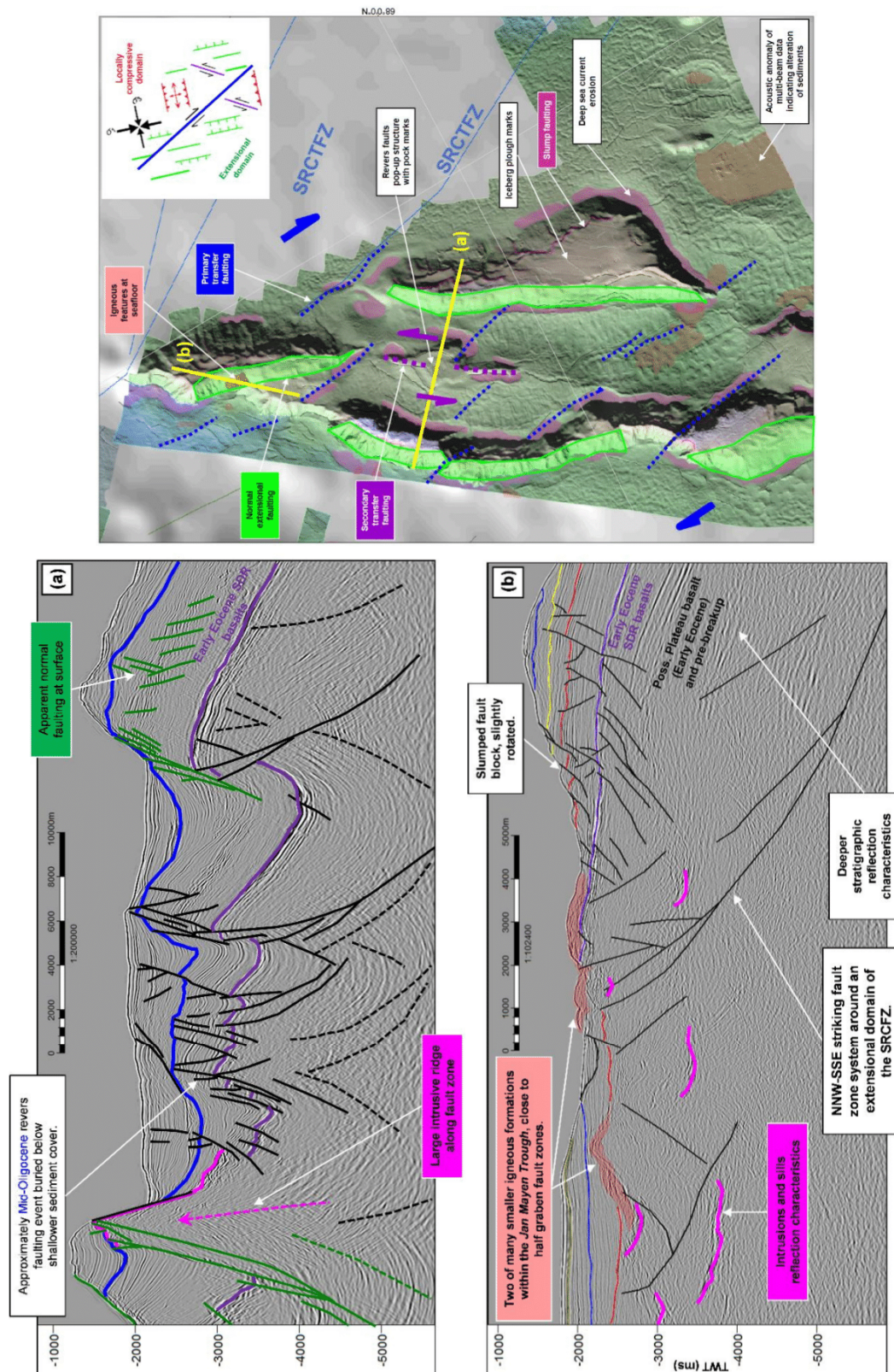


Figure 5: Detailed multibeam bathymetric map with structural features map of the JMMC, within the extensional domain of the Southern Ridge Complex Transfer Zone (SRCFZ), defining fault types, local fault patterns within a transfer system, and stress-field location that served as pathways for igneous features, such as intrusive dykes, sills or volcanic ridges, and seafloor extrusive lavas or build-ups. Viewing the depth dimension by seismic reflection profiles: (a) reverse fault structures within a transfer system, and (b) extensional fault patterns and intrusions crossing a transfer system modified after Blischke et al. (2017). Simplified stress field related fault type sketch modified after Lacazette, A. (2009).

Blischke et al.

The SRC is a collection of several ridges that were formed during extension and rift transfer along the southern part of the microcontinent in association with igneous activity along the IPR and the Southern Ridge Complex transfer zone (SRCFZ) (Figures 1b-5). The SRC area was created during the Ægir ridge breakup phase by the formation of a wide igneous margin, which was subsequently broken into several smaller segments, forming several small basins. The basins were heavily intruded by post-Eocene breakup sill and dyke intrusions, and vent structures along fault and fracture zones (Figure 4b-d).

Fracture zone segments of a dextral strike slip system and associated igneous intrusive complex are clearly visible within the Jan Mayen trough (JMT) and the northwesternmost segment of the SRCFZ (Figures 3; 4b). Structural elements, such as smaller scale fault system and fault-parallel sill and dyke complexes, enabled us to differentiate strike-slip from normal fault systems and slump faulting along the steep escarpments of the microcontinent's ridges (Figure 5a,b). The normal extensional fault system of the SRC blocks are aligned to the SRCFZ within an obliquely opening region. Parallel extensional and compression structural domains were formed by oblique WSW-ENE opening of the SRC along the SRCFZ trend. Mapped seafloor and subsurface fault types fit these systems and are linked with the minimum horizontal stress orientation of 75-80 deg. in an ENE direction that governs the direction of opening of the extensional fault system. Secondary sinistral strike-slip fault zones compensate the fault block rotation within the oblique opening along the SRCFZ, represented by pop-up structures within the center graben of the SRC (Figure 5). Our data underlines the study by Cianfara and Salvini (2015), which identified large regional scale lineament structures and segmentation in relationship to regional strike-slip corridors. Here, a comparison with the Tjörnes Fracture Zone system is highly interesting, which together with the connected Iceland oblique Northern Volcanic Rift Zone presents a striking similarity to the SRC – IPR area.

5. THE NORTHERN VOLCANIC RIFT ZONE OF ICELAND (NVZ) AND TJÖRNES FRACTURE ZONE (TFZ)

The Northern Volcanic Zone in northeast Iceland is a ~200-175 km long and ~50-100 km wide subaerial segment of the Mid-Atlantic ridge and located 200-300 km southwest of the JMMC-IPR domain (Figure 1). The NVZ is one segment of the onshore Iceland plate boundary that continues southwards into the Iceland hotspot, located beneath the Vatnajökull icecap and into the southward propagating Eastern Volcanic Zone. The offshore-onland Tjörnes Fracture Zone links the NVZ with the Kolbeinsey mid-oceanic ridge. The TFZ consists of the Dalvík seismic zone (DSZ), Húsavík-Flatey transfer zone (HFF), and the Grímsey oblique rift system (GOR) (Sæmundsson, 1974, 1978; Einarsson and Sæmundsson, 1987; Brandsdóttir and Menke, 2008; Einarsson, 2008; Thordarson and Höskuldsson, 2008; Magnúsdóttir et al., 2015; Brandsdóttir et al., 2015; Hjartardóttir et al., 2013, 2016, 2017; Drouin et al., 2017; or Sigmundsson et al., 2018). The NVZ is believed to have started to develop 6-7 million years ago following an eastward rift jump of the divergent plate boundary, towards the center of the Iceland hotspot (Sæmundsson 1978). The divergent NVZ is made up of 5-6 volcanic systems, consisting of central volcanoes with transecting fissure swarms, which form overlapping en-echelon domains up to 100 km in length and approximately 20 km in width. They have been subdivided and are monitored by seismicity activity, surface structural, geological and geothermal expressions (Björnsson et al. 1977; Sigurðsson and Sparks 1978; Einarsson 1991). Differences in fissure swarm width and elevation are believed to have been influenced by increased magma supply from the Iceland hotspot, which has a center below the western part of Vatnajökull glacier (Vogt 1971; Wolfe et al. 1997; Gaherty 2001). The hotspot can be seen as magnetic and gravity anomalies (Figure 2), and as low P- and S- seismic velocities (Wolfe et al., 1997).

Rifted depressions, as seen on the Mid-Atlantic ridges, characterize slow spreading (<3.5 cm/yr) divergent plate boundaries, while elevated volcanic edifices characterize fast spreading (>5 cm/yr) divergent plate boundaries (Mutter and Karson 1992). The structure of the divergent plate boundary across Iceland is in that sense more similar to fast spreading, rather than slow spreading divergent plate boundaries. Here reflected as well by the highly fractured and faulted fissure swarms and their episodic intrusives (Hjartardóttir et al., 2017). These indicate episodic deformation processes along fissure swarm zones and primarily along the central volcanoes that are the deep crustal links, which can be seen as localized magnetic and gravity anomalies (Jonsson et al., 1991). During rifting episodes, when magma is intruded into the fissure swarms as dike intrusions, the structural patterns changes abruptly, as intensive earthquake activity is felt and measured directly both within the central volcanoes, as well as in distinct parts of the linked fissure swarm (e.g. Brandsdóttir and Einarsson 1979; Einarsson and Brandsdóttir 1980; Buck et al. 2006). Thus, causing subsidence along grabens and accompanying fracture movements within the fissure swarms (Hjartardóttir et al., 2016; Sigurðsson, 1980). Detailed mapping is ongoing to increase the understanding of fissure swarms, rift zones, exact locations of eruptive centers, orientation of stress fields at eruption times, and their interaction with transform zones (e.g. Hjartardóttir et al. 2013, 2016, 2017; Magnúsdóttir et al., 2015; or Drouin et al., 2017). Here specifically transfer zones are complex structural systems that form complex sets of normal and reverse faulting, which are associated to strike-slip fault systems and challenging to resolve with surface data alone (Khodayar and Einarsson 2004; Guðmundsson et al. 2008). As detailed mapping works well for the present-day active parts of the NVZ, is it challenging to locate and map dormant or old inactive volcanic systems, fissure swarms, and fracture zone systems. Thus mapping, delineating, and timing those dormant volcanic systems and related structures with potential field and offshore seismic reflection data become useful.

5.1 Potential field data observations

As potential field data had been crucial for delineating the JMMC domain, magnetic anomalies may be used to define major anomalies on land Iceland as well (Figure 2), (Jonsson et al., 1991). The Pleistocene-Holocene boundary (2,6 Ma) correlates with a low negative magnetic anomaly domain onshore along its western limit (Figure 2a). However, this low magnetic anomaly domain appears much broader along the eastern Pleistocene-Holocene boundary that is based on surface geological exposures. The main positive magnetic anomaly that reflect the main breakup zone and plate boundary within the Pleistocene-Holocene time domain, appear to be segmented and subdivide by large scale, deeply buried transfer elements, as there are not clear at surface or seismicity data (Figure 2). Small positive magnetic anomaly segments can be observed, straddling the main positive anomaly within the 2,6 Ma negative magnetic anomaly domain. These small-scale anomalies possibly reflect blocks of older segments that are in-bedded within the Pleistocene time domain, or alternatively relate to present-day small-scale flank rift systems that are part of the Holocene and active fissure swarm within the NVZ. An apparent structural lineament trend appears across Iceland southwest to northeast that can be seen on magnetic and gravity anomalies data (Figure 2). This lineament is not seen on surface but appears to be deeply buried and offsets anomalies and aligns with Bouguer gravity trends. Interestingly does this trend align to the pre-breakup ridge trend that was present between central East Greenland and the Fugloy ridge area, which kept dominating the opening history of the Greenland-Iceland-Faroe ridge complex from Early Eocene onwards (Blischke et al., 2019b). Another well recognizable positive magnetic anomaly trend correlate

to chron C5r (11.1 Ma; Gaina et al., 2014) (Figure 2a). This anomaly aligns with the northern extend of the Snæfellsnes-Húnaflói rift zone that is estimated to have been active between ~15 Ma to ~7 Ma (Harðarson et al., 1997, 2008). Simultaneously magmatic activity reactivated in central East Greenland and the Kolbeinsey ridge had fully established as a mid-oceanic ridge system. East of the C5r anomaly that abruptly terminates in the Húnaflói bay, small scale NW-SE striking positive anomalies can be observed (Figure 2a) these appear to be linked by W-E trending anomaly signatures that align parallel to the present day active TFZ. A zone and trend that is even dominant on Bouguer gravity anomaly data (Figure 2b). As such, these observations might prompt to revisit the northern shelf area that has very limited seismic reflection or refraction data to be tied into potential field data or onshore geological field records.

6. REGIONAL COMPARISON

Apparent similarities between the JMMC-IPR region and the Northern Volcanic Zone are apparent, both containing oblique rift systems. Potential field data show good correlations to igneous centers and axial rift segments, structural offset of large-scale transfer and fracture zones, and the forming of micro-plates in between rift zones. Both regions have proven strike-slip zone structures that often are buried and difficult to assess. Many volcanic domains have been mapped across Iceland, such as axial and oblique rift systems, pre-Pleistocene-Holocene flexure zones, regional unconformities, tectonostratigraphic ties of local areas across Iceland indicating micro-plate and transfer zone formation. These are all features that also can be seen across the JMMC-IPR study area with observed opening fabric and mechanism based on mapped data compositions that clearly delineate the JMMC, such as: (1) clear north-south asymmetric SDR formation along the eastern JMMC breakup margin and the Ægir rift system that formed preferably linked to variations in the pre-rift lithospheric structure and very likely above a thermal mantle anomaly; (2) establishing a firm link of the oblique Iceland plateau rift system to offset margins in timing, geochemistry and tectono-magmatic connection; (3) reasonable explanation for the initiation of the fanned-out appearance of the oblique IPR rifting domain that inter-fingers with the southern ridges of the JMMC due to crustal thinning and breaching that allowed the formation of several axial rift systems and volcanic ridges; (4) the presence of a pre-breakup complex breakup margin along the JMMC southwestern to western flank, with emplacement of igneous complexes that precede the formation of the Kolbeinsey ridge system; (5) presence of dual breakup system of two opposed rifting complexes that created the JMMC; and (6) concentration of igneous centers, volcanic ridges, or flood basalts close to transfer zones that are linked to a complex fabric of strike-slip and normal fault structures.

High-temperature geothermal areas appear to be confined to active central volcanoes along the divergent plate boundary of Iceland, and most likely sustained by replenishment of shallow crustal magma chambers or intrusions, in form of sills, dykes, and venting structures. As these central volcanoes are also closely located to rift transfer systems, a comprehensive volcano-seismic stratigraphic mapping and sub-surface modelling approach would be highly important. This would increase the understanding of the internal rift graben settings of an area, their major structural elements, such as transfer zones and igneous complex structures that are accompanied by series of dykes and sills intruded at different time stages. As this is a challenging task onshore Iceland with limited seismic reflection data functionalities, would the focus lie in future 2D multi-channel deep seismic reflection data acquisitions close to Iceland's coast and across the Iceland shelf, where deep subsurface imaging is feasible.

Specifically, for low temperature areas in Iceland, knowing how an area was placed within a rift setting and how often it was impacted by consecutive volcanic activity is a crucial task for understanding geothermal systems and what fault fracture trends are most likely active. The understanding of the sub-division of Iceland in time with future $^{40}\text{Ar}/^{39}\text{Ar}$ age data analysis of pre-Pleistocene strata is of essence, in order to resolve tectono-stratigraphic reconstructions of onshore Iceland. Holocene tephrochronology can be used to chronologically stratify the youngest areas, however age analysis of younger igneous systems, e.g. Pleistocene - Pliocene are challenging, whereas would sequential stratigraphic analysis tied to subsurface structural segmentation and build-up be one approach for subsurface structural modelling. This includes the subsurface delineation of structural domains based on detailed seismic refraction, gravity and magnetic data acquisitions, which are feasibly option to improve subsurface imaging onshore Iceland.

7. CONCLUSION

The JMMC-IPR study portrays a none-uniform formation of tectono-magmatic rifted margins and domains that are in process comparison not dissimilar to Iceland. Igneous and structural domains, such as the north-south asymmetric and segmented SDRs formation along the eastern JMMC breakup margin, or the firm link of the oblique Iceland plateau rift system to the central East Greenland. A reasonable explanation was demonstrated for the initiation of the fanned-out appearance of the oblique IPR rifting domain that inter-fingers with the southern ridges of the JMMC due to several axial rift systems and volcanic ridge formation along over-stretched and breached crustal weak zones. The existence of a dual breakup scenario and the associated with a series of volcanic zones (fissure swarms and their central volcanoes) that are linked to transfer system has been imaged, as well as the full opening of the Jan Mayen basin as an igneous domain with massive dyke and sill intrusive activities and the regionally extensive flood basalt before final its final breakup. These observed processes are seen onshore Iceland, and are easier imaged within the active NVZ, but challenging for dormant volcanic systems and their fault and fracture trends. Thus, the applied methods and data compilations could improve the understanding of the Iceland onshore and shelf regions by focusing on: (1) primary use of all potential field data to better outline the underlying deep intrusive systems, thus aiding detailed tectonostratigraphic reconstruction of the central NE Atlantic region; (2) enables to differentiate between older structural trends vs. dominating known present-day trends, which is information that only becomes apparent by structural reconstructing an area; (3) focus on areas with direct volcanic rift influence vs. oblique rift system, such as the NVZ vs. TFZ domains; and (4) use nearby offshore areas to acquire seismic reflection and refraction data to more accurately map in detail subsurface structures that have much high resolution than commonly used methods onshore.

ACKNOWLEDGMENTS

This work is a part of a research project at the University of Iceland and the Centre for Earth Evolution and Dynamics, University of Oslo, with funding by the National Energy Authority of Iceland (Orkustofnun) and the Iceland GeoSurvey. Data permissions were provided by the National Energy Authority of Iceland (Orkustofnun), the Norwegian Petroleum Directorate (NPD), Spectrum ASA, TGS; the University of Oslo (UiO), the Bundesanstalt für Geowissenschaften und Rohstoffe (BGR), and Geological Survey of Denmark and Greenland (GEUS). We additionally thank the Marine Research Institute of Iceland (MRI), for making the multibeam and backscatter data available and the Norwegian Petroleum Directorate (NPD) for use of their 2D multichannel reflection data sets from 2011 and 2012.

Blischke et al.

REFERENCES

- Åkermoen, T.: Jan Mayen-ryggen: et seismisk stratigrafisk og strukturelt studium, *MSc. thesis*, (1989), University of Oslo, Oslo, Norway, 174 pp.
- Björnsson, A., Sæmundsson, K., Einarsson, P., Tryggvason, E. and Grönvold, K.: Current rifting episodes in North Iceland, *Nature* **266**, (1977), 318-323, doi:10.1038/266318a0.
- Blischke, A., Brandsdóttir, B., Erlendsson, Ö., Planke, S. and Gaina, C.: The Jan Mayen microcontinent and Iceland Plateau volcanic breakup margins, *EGU General Assembly 2019*, Vol. **21**, (2019b), EGU2019-14291-1.
- Blischke, A., Stoker, M.S., Brandsdóttir, B., Hopper, J.R., Peron-Pinvidic, G., Ólavsdóttir, J. and Japsen, P.: The Jan Mayen microcontinent's Cenozoic stratigraphic succession and structural evolution within the NE-Atlantic, *Marine and Petroleum Geology* **103** (2019a), 702–737, <https://doi.org/10.1016/j.marpetgeo.2019.02.008>.
- Blischke, A., Erlendsson, Ö., Brandsdóttir, B., Planke, S., Gaina, C., Stoker, M.S., Tegner, C., Gautason, B., Hopper, J.R., Helgadóttir, H.M. and Halldórsson, S.A.: Seismic volcano-stratigraphic characteristics of the Jan Mayen microcontinent and Iceland plateau rift system, *Geochemistry, Geophysics, Geosystems (G3)*, (To be submitted - 2019b).
- Blischke, A., Gaina, C., Hopper, J. R., Péron-Pinvidic, G., Brandsdóttir, B., Guarnieri, P., Erlendsson, Ö. and K. Gunnarsson: The Jan Mayen microcontinent: an update of its architecture, structural development and role during the transition from the Ægir Ridge to the mid-oceanic Kolbeinsey Ridge, In: Péron-Pinvidic, G., Hopper, J.R., Stoker, M.S., Gaina, C., Doornenbal, J.C., Funck, T. and Ártung, U.E. (eds), *The NE Atlantic Region: A Reappraisal of Crustal Structure, Tectonostratigraphy and Magmatic Evolution*, *Geological Society, London, Special Publications* **447**, (2017a), 299–337, <https://doi.org/10.1144/SP447.5>.
- Blischke, A., Erlendsson, Ö., Einarsson, G.M., Ásgeirsson, V.L. and Árnadóttir, S.: The Jan Mayen Microcontinent Project Database and Seafloor Mapping of the Dreki Area Input Data, Geological and Geomorphological Mapping and Analysis, prepared for Orkustofnun National Energy Authority of Iceland, *technical report ÍSOR-2017/055*, (2017b), Iceland.
- Brandsdóttir B., Hooft, E., Mjelde, R. and Murai, Y.: Origin and evolution of the Kolbeinsey Ridge and Iceland Plateau, N-Atlantic, *Geochemistry, Geophysics, Geosystems* **16**, (2015), 612-634, <https://doi.org/10.1002/2014GC005540>.
- Brandsdóttir, B. and Menke, W.H.: The seismic structure of Iceland, *Jökull* **58**, (2008), 17-34.
- Brandsdóttir, B. and Einarsson, P.: Seismic activity associated with the September 1977 deflation of the Krafla central volcano in northeastern Iceland, *Journal of Volcanology Geothermal Research* **6**, (1979), 197-212.
- Buck, W.R., Einarsson, P., Brandsdóttir, B.: Tectonic stress and magma chamber size as controls on dike propagation: Constraints from the 1975-1984 Krafla rifting episode, *Journal of Geophysical Research – Solid Earth* **111**, (2006), B12404, doi: 10.1029/2005JB003879.
- Cianfarra, P., and Salvini, F.: Lineament Domain of Regional Strike-Slip Corridor: Insight from the Neogene Transtensional De Geer Transform Fault in NW Spitsbergen, *Pure and Applied Geophysics* **172** (5), (2015), 1185–1201, <https://doi.org/10.1007/s00024-014-0869-9>.
- Decker, R. and Decker, B.: *Volcanoes*, 4th ed., W. H. Freeman, (2005), ISBN 0-7167-8929-9.
- Doré, A.G., Lundin, E.R., Jensen, L.N., Birkeland, Ø., Eliassen, P.E. and Fichler, C.: Principal tectonic events in the evolution of the northwest European Atlantic margin, In: Fleet, A.J., and Boldy, S.A. R (eds) *Petroleum Geology of Northwest Europe, Proceedings of the 5th Conference*, The Geological Society, London, (1999), 41-61.
- Drouin, V., Sigmundsson, F., Ófeigsson, B.G., Hreinsdóttir, S., Sturkell, E. and Einarsson, P.: Deformation in the Northern Volcanic Zone of Iceland 2008–2014: An interplay of tectonic, magmatic, and glacial isostatic deformation, *Journal of Geophysical Research, Solid Earth* **122**, (2017), 3158–3178, <http://doi.org/10.1002/2016JB013206>.
- Einarsson, P.: Plate boundaries, rifts and transforms in Iceland, *Jökull* **58**, (2008), 35–58.
- Einarsson, P.: Earthquakes and present-day tectonism in Iceland. *Tectonophysics* **189**, (1991), 261-279, doi: 10.1016/0040-1951(91)90501-I.
- Einarsson, P., Sæmundsson, K.: Earthquake epicenters 1982–1985 and volcanic systems in Iceland, map, In: Sigfússon, Th. (Ed.), *Í hlutarins edli, Festschrift for Thorbjörn Sigurgeirsson*, (1987), Menningarsjóður, Iceland.
- Einarsson, P. and Brandsdóttir, B.: Seismological evidence for lateral magma intrusion during the July 1978 deflation of the Krafla volcano in NE Iceland, *Journal of Geophysics* **47**, (1980), 160-165.
- Erlendsson, Ö., Blischke, A.: Review and Assessment of the CNOOC-JMR-2015 2D Seismic Reflection Dataset Data Quality Check and Preliminary Structural Mapping for the Dreki License Area, Prepared for Orkustofnun (OS), *technical report ÍSOR-2018/083*, (2019), Reykjavik Iceland, pp. 93.
- Funck, T., Geissler, W.H., Kimbell, G.S., Gradmann, S., Erlendsson, Ö., McDermott, K. and Petersen, U.K.: Moho and basement depth in the NE Atlantic Ocean based on seismic refraction data and receiver functions, In: Péron-Pinvidic, G., Hopper, J.R., Stoker, M.S., Gaina, C., Doornenbal, J.C., Funck, T. and Ártung, U.E. (eds), *The NE Atlantic Region: A Reappraisal of Crustal Structure, Tectonostratigraphy and Magmatic Evolution*, *Geological Society, London, Special Publications* **447**, (2017), 171-205, <http://doi.org/10.1144/SP447.1>.
- Funck, T., Erlendsson, Ö., Geissler, W.H., Gradmann, S., Kimbell, G.S., McDermott, K. and Petersen, U.K.: A review of the NE Atlantic conjugate margins based on seismic refraction data, In: Péron-Pinvidic, G., Hopper, J.R., Stoker, M.S., Gaina, C., Doornenbal, J.C., Funck, T. and Ártung, U.E. (eds), *The NE Atlantic Region: A Reappraisal of Crustal Structure*,

- Tectonostratigraphy and Magmatic Evolution, *Geological Society, London, Special Publications* **447**, (2016), 35 p., <http://doi.org/10.1144/SP447.9>.
- Funck, T., Hopper, J.R., Fattah, R.A., Blischke, A., Ebbing, J., Erlendsson, Ö., Gaina, C., Geissler, W.H., Gradmann, S., Haase, C., Kimbell, G.S., McDermott, K.G., Peron-Pinvidic, G., Petersen, U., Shannon, P.M. and Voss, P.H.: Crustal Structure. In: Hopper, J.R., Funck, T., Stoker, M., Ártíng, U., Peron-Pinvidic, G., Doornenbal, H. and Gaina, C. (eds), Tectonostratigraphic Atlas of the North-East Atlantic region, The Geological Survey of Denmark and Greenland (GEUS), Copenhagen, Denmark, *Atlas volume*, (2014), 340 pp.
- Gaherty, J.B.: Seismic evidence for hotspot-induced buoyant flow beneath the Reykjanes ridge, *Science* **293**, (2001), 1645-1647, doi: 10.1126/science.1061565.
- Gaina, C., Nasuti, A., Kimbell, G.S. and Blischke, A.: Break-up and seafloor spreading domains in the NE Atlantic. Geological Society, London, Special Publications, 447, (2017b), 25 p., doi:10.1144/SP447.12.
- Gaina, C., Blischke, A., Geissler, W.H., Kimbell, G.S. and Erlendsson, Ö. (2017a). Seamounts and oceanic igneous features in the NE Atlantic: a link between plate motions and mantle dynamics. Geological Society, London, Special Publications, 447, first published on September 8, 2016, doi:10.1144/SP447.6.
- Gaina, C.: Plate Reconstructions and Regional Kinematics, In: Hopper, J.R., Funck, T., Stoker, M.S., Ártíng, U., Peron-Pinvidic, G., Doornenbal, H. and Gaina, C. (eds.), Tectonostratigraphic Atlas of the North-East Atlantic Region, Geological Survey of Denmark and Greenland (GEUS), Copenhagen, Denmark, *Atlas volume*, (2014), 53-68.
- Gaina, C., Gernigon, L. and Ball, P.: Palaeocene - Recent plate boundaries in the NE Atlantic and the formation of the Jan Mayen microcontinent, *Journal of the Geological Society*, (2009), 166, pp. 1-16, <https://doi.org/10.1144/0016-76492008-112>.
- Ganerød, M., Wilkinson, C.M. and Hendriks, B.: Geochronology, In: Hopper, J.R., Funck, T., Stoker, M.S., Ártíng, U., Peron-Pinvidic, G., Doornenbal, H. and Gaina, C. (eds.), Tectonostratigraphic Atlas of the North-East Atlantic Region, Geological Survey of Denmark and Greenland (GEUS), Copenhagen, Denmark, *Atlas volume*, (2014), 252-261.
- Gernigon, L., Franke, D., Geoffroy, L., Schiffer, C., Foulger, G.R. and Stoker, M.: Crustal fragmentation, magmatism, and the diachronous opening of the Norwegian-Greenland Sea, *Earth-Science Reviews*, (2019), ISSN 0012-8252, <https://doi.org/10.1016/j.earscirev.2019.04.011>.
- Gernigon, L., Blischke, A., Nasuti, A., and Sand, M.: Conjugate volcanic rifted margins, seafloor spreading, and microcontinent: Insights from new high-resolution aeromagnetic surveys in the Norway Basin, *Tectonics* **34**, (2015), pp. 907-933, <https://doi.org/10.1002/2014TC003717>.
- Gernigon, L., Gaina, C., Olesen, O., Ball, P., Peron-Pinvidic, G. and Yamasaki, T.: The Norway Basin revisited: From continental breakup to spreading ridge extinction, *Marine and Petroleum Geology* **35**, (2012), pp. 1-19, <http://doi.org/10.1016/j.marpetgeo.2012.02.015>.
- Guðmundsson, Á., Friese, N., Galindo, I. and Philipp, S.L.: Dike-induced reverse faulting in a graben, *Geology* **36**, (2008), 123-126, doi: 10.1130/g24185a.1.
- Haase, C. and Ebbing, J.: Gravity data, In: Hopper, J.R., Funck, T., Stoker, M.S., Ártíng, U., Peron-Pinvidic, G., Doornenbal, H. and Gaina, C. (eds.), Tectonostratigraphic Atlas of the North-East Atlantic Region, Geological Survey of Denmark and Greenland (GEUS), Copenhagen, Denmark, *Atlas volume*, (2014), p 29-40.
- Haase, C., Ebbing, J. and Funck, T.: A 3D regional crustal model of the NE Atlantic based on seismic and gravity data, In: Péron-Pinvidic, G., Hopper, J.R., Stoker, M.S., Gaina, C., Doornenbal, J.C., Funck, T. and Ártíng, U.E. (eds), The NE Atlantic Region: A Reappraisal of Crustal Structure, Tectonostratigraphy and Magmatic Evolution, *Geological Society, London, Special Publications* **447** (2017), 15 p., <http://dx.doi.org/10.1144/SP447.8>.
- Helgadóttir, G.: Preliminary results from the 2008 Marine Research Institute multibeam survey in the Dreki area, with some examples of potential use, *Proceedings of the Iceland Exploration Conference 2008*, Reykjavík, Iceland, (2008).
- Helgadóttir, G. and Reynisson, P.: Setkjarnataka, fjölgeisla- og lágtíðni dýptar mælingar á Drekasvæði og Jan Mayen hrygg árs. Árna Friðrikssyni RE 200 haustið 2010, *technical report*, prepared for Orkustofnun and Norsku Olíustofnunina, Hafrannsóknastofnunin, Leiðangursskýrsla A201011, hluti 1 og 2, 17. ágúst –15. september 2010, Reykjavík, Ísland, (2010).
- Hjartardóttir, Á.R. and Einarsson, P.: Sprungusveimar Norðurgosbeltisins og umbrotin í Bárðarbungu 2014–2015 (in Icelandic), *Náttúrufræðingurinn*, Volume **87**, Issue 1-2, (2017), pp. 24-39.
- Hjartardóttir, Á.R., Einarsson, P., Magnúsdóttir, S., Björnsdóttir, Þ. and Brandsdóttir, B.: Fracture systems of the Northern Volcanic Rift Zone, Iceland - an onshore part of the Mid-Atlantic plate boundary, In: Wright, T.J., Ayele, A., Ferguson, D.J., Kidane, T., Vye-Brown, C. (Eds.), Magmatic Rifting and Active Volcanism, *The Geological Society of London*, (2016), pp. 297-314.
- Hjartardóttir, Á.R.: Fissure swarms of the Northern Volcanic Rift Zone, Iceland, PhD dissertation, Faculty of Earth Sciences, University of Iceland, (2013), pp. 138, ISBN 978-9935-9069-8-4.
- Hopper, J.R., Funck, T., Stoker, M.S., Ártíng, U., Peron-Pinvidic, G., Doornenbal, H. and Gaina, C. (eds): Tectonostratigraphic Atlas of the North-East Atlantic Region, Geological Survey of Denmark and Greenland, GEUS, Copenhagen, *Atlas volume*, (2014), 338 pp.
- Jakobsson, M., Mayer, L.A., Coakley, B., Dowdeswell, J.A., Forbes, Fridman, S.B., Hodnesdal, H., Noormets, R., Pedersen, R., Rebesco, M., Schenke, H.-W., Zarayskaya, Y., Accettella, A.D., Armstrong, A., Anderson, R.M., Bienhoff, P., Camerlenghi, A., Church, I., Edwards, M., Gardner, J.V., Hall, J.K., Hell, B., Hestvik, O.B., Kristoffersen, Y., Marcussen, C., Mohammad,

Blischke et al.

- R., Mosher, D., Nghiem, S.V., Pedrosa, M.T., Travaglini, P.G. and Weatherall, P.: The International Bathymetric Chart of the Arctic Ocean (IBCAO) Version 3.0, *Geophysical Research Letters*, (2012), doi: 10.1029/2012GL052219.
- Jancin, M., Young, K.D., Voight, B., Aronson, J.L. and Saemundsson, K.: Stratigraphy and K/AR ages across the west flank of the northeast Iceland axial rift-zone, in relation to the 7-MA volcano-tectonic reorganization of Iceland, (1985), *Journal of Geophysical Research – Solid Earth and Planets* **90**, (1985), 9961-9985, doi: 10.1029/JB090iB12p09961.
- Khodayar, M. and Einarsson, P.: Reverse-slip structures at oceanic diverging plate boundaries and their kinematic origin: data from Tertiary crust of west and south Iceland, *Journal of Structure Geology* **26**, (2004), 1945-1960, doi: 10.1016/j.jsg.2004.06.001.
- Lacazette, A.: Paleostress analysis from image logs using pinnate joints as slip indicators, *AAPG Bulletin* **93**, (2009), pp. 1489-1501, doi:10.1306/08110909087.
- Lundin, E.R. and Doré, A.G.: NE Atlantic breakup: a re-examination of the Iceland mantle plume model and the Atlantic–Arctic linkage, In: Doré, A.G. and Vining, B.A. (eds), *Petroleum Geology: North-West Europe and Global Perspectives. Proceedings of the 6th Petroleum Geology Conference*, (2005), pp. 739-754.
- Magnúsdóttir, S, Brandsdóttir, B., Driscoll, N. and Detrick, R.: Postglacial tectonic activity within the Skjálfandadjúp Basin, Tjörnes Fracture Zone, offshore Northern Iceland, based on high resolution seismic stratigraphy, *Marine Geology* **367**, (2015), 159–170, <http://dx.doi.org/10.1016/j.margeo.2015.06.004>.
- Müller, R.D., Cannon, J., Qin, X., Watson, R.J., Gurnis, M., Williams, S., et al.: GPlates: Building a virtual Earth through deep time, *Geochemistry, Geophysics, Geosystems* **19**, (2018), doi:10.1029/2018GC007584.
- Mutter, J.C. and Karson, J.A.: Structural processes at slow-spreading ridges, *Science* **257**, (1992), 627-634, doi: 10.2307/2877475.
- Nasuti, A. and Olesen, O. (2014). Magnetic Data. In: Hopper, J.R., Funck, T., Stoker, M.S., Ártung, U., Peron-Pinvidic, G., Doornbal, H., Gaina, C. (Eds.), *Tectonostratigraphic Atlas of the North-East Atlantic Region*. Geological Survey of Denmark and Greenland (GEUS), Copenhagen, Denmark.
- Sæmundsson, K.: Evolution of the axial rifting zone in northern Iceland and the Tjörnes fracture zone, *Geological Society of America, Bulletin* **85**, (1974), 495–504.
- Sæmundsson, K.: Fissure swarms and central volcanoes of the neovolcanic zones in Iceland, In: *Crustal evolution in northwestern Britain and adjacent regions*, Bowes, D.R. and Leake, B.E. (editors), Reprinted from *Geological Journal Special Issue* **10**, (1978), 415-432.
- Sigmundsson, F., Einarsson, P., Hjartardóttir, Á.R., Drouin, V., Jónsdóttir, K., Árnadóttir, T., Geirsson, H., Hreinsdóttir, S., Lia, S., Ófeigsson, B.G.: Geodynamics of Iceland and the signatures of plate spreading, *Journal of Volcanology and Geothermal Research*, (2018), <https://doi.org/10.1016/j.jvolgeores.2018.08.014>.
- Sigurðsson, H. and Sparks, S.R.J.: Rifting episode in North Iceland in 1874-1875 and the eruptions of Askja and Sveinagja, *Bulletin of Volcanology* **41**, (1978), 149-167, doi: 10.1007/BF02597219.
- Thordarson, T. and Höskuldsson, A.: Postglacial volcanism in Iceland. *Jökull* **58**, (2008).
- Talwani, M. and Eldholm, O.: Evolution of the Norwegian-Greenland Sea, *Geological Society of America Bulletin* **88**, (1977), pp. 969-999.
- Vogt, P.R.: Magnetic anomalies of the North Atlantic Ocean, In: *The Western North Atlantic Region*, edited by Vogt, P.R. and Tucholke, B.E., *Geological Society of America*, (1986).
- Vogt, P.R.: Asthenosphere motion recorded by the ocean floor south of Iceland, *Earth Planet Science Letter* **13**, (1971), 153-160, doi: 10.1016/0012-821X(71)90118-X.
- Vogt, P.R., Anderson, C.N., Bracey, D.R. and Schneider, E.M.: North Atlantic Magnetic Smooth Zones, *Journal of Geophysical Research* **75**, (1970), pp. 3955-3968.
- Wolfe, C.J., Bjarnason, I.T., VanDecar, J.C. and Solomon, S.C.: Seismic structure of the Iceland mantle plume, *Nature* **385**, (1997), 245-247.

Appendix 2 Seismic reflection survey data overview

Survey	BGR75	RC2114	JM-85 (2009)
Date	30th August, 1975 - 29th September, 1975	8th Aug 1978 – 7th Sept 1978	17th July 1985 – 2nd Sept 1985
Acquisition Vessel:	M/V LONGVA	M/V Robert D. Conrad	M/V Malene Østervold
Acquisition done by:	BGR	LDGO, Marek Truchan	Geco, D. Hill
Processing done by:	BGR	LDGO, Marek Truchan	Spectrum (AS)
References:	https://www.bgr.bund.de/EN/Themen/GG_Geophysik/Marine_Geophysik/Seismik/Messgebiete/arktis.html;jsessionid=9F2592B04BDCA398C092CC9300607BF0.1_cid321?nn=1541848#anker_bgr74	http://www-udc.ig.utexas.edu/sdc/cruise.php?cruise=rc2114	http://kortasia.os.is:8080/geoserver/www/landrunnssi/en/index.html
Type and frequency content of seismic source	Airgun array	AirGun BOLT:1500C 1864 cu.in	Airgun array 3564 cu.in
Streamer length and channel interval		3000 m / 50 m	3000 m / 50 m
Sample rate, record length, filters applied during recording	BGR - Federal Institute for Geosciences and Natural Resources (BGR), Hannover, David Diel Acquired by: BGR Vessel: M/V LONGVA Date: 30th August, 1975 - 29th September, 1975 Source: 1 Streamer: 1 Record length: 4796 ms Recording sample rate: 4 ms Samples per trace: 1200 High Cut Filter, all : 128 Hz (8-128 Hz) Slope: 18-70 dB/octave Number of channels: 48 Auxiliary traces/record: 5 SP interval: 50 m Source: Air gun array File type: File was converted using if2segy, netpbm, and Seismic Unix, author of if2segy script is Andrew MacRae (andrew.macrae at smu.ca). https://www.bgr.bund.de/EN/Themen/GG_Geophysik/Marine_Geophysik/Seismik/Messgebiete/arktis.html;jsessionid=9F2592B04BDCA398C092CC9300607BF0.1_cid321?nn=1541848#anker_bgr74	LAMONT-DOHERTY GEOLOGICAL OBSERVATORY OF COLUMBIA UNIVERSITY, PALISADES, NY acquisition, Marek Truchan Acquired by: LDGO Vessel: M/V Robert D. Conrad Date: 8th Aug 1978 – 7th Sept 1978 Source: 1 Streamer: 1 Record length: 12000 ms Recording sample rate: 4 ms Fold: 50 High Cut Filter, all : 10 Hz @ 70 dB/octave Low Cut Filter, hydrophone : 3 Hz @ 6 dB/octave Streamer length: 3000 m Number of channels: 100 Numbers of phones per group: 24 Group interval: 50 m Streamer depth: 10-12 m SP interval: 50 m (20 s) Source: Air guns - BOLT Sub-arrays: 4 Source volume: 1864 in3 Source pressure: 1850 psi Source depth: 10 m	Geco 2D acquisition Acquired by: Geco Vessel: M/V Malene Østervold Date: 17th July 1985 – 2nd Sept 1985 Source: 1 Streamer: 1 (Sercel Seal) Record length: 7200 ms (JM-85-16) & 15300 ms (JM-85-26) Recording sample rate: 4 ms Fold: 30 & 60 High Cut Filter, all : 90 Hz @ 72 dB/octave Low Cut Filter, hydrophone : 3.5 Hz @ 18 dB/octave Streamer length: 3000 m Number of channels: 120 Numbers of phones per group: 40 Group interval: 50 m Near offset: 111 m Streamer depth: 10 (lowered to 12-13 m during bad weather) SP interval: 25 m & 50 m Source: Air guns - Geco super wide Sub-arrays: 6 Source volume: 3564 in3 Source pressure: 1900 psi Source depth: 7.5 m +/- 1 m
Shot interval, CDP interval, fold	50 m / Fold: 24 ?	50 m (20 sec) / Fold: 50	25m / Fold: 30; 50m / Fold: 60
Processing sequence including information on filters and gains applied (at what stage, type filter flanks, type of gain)	BGR 2D processing Processed by: BGR Date: 1975 Processing sequence: 1. ALL GAINS 2. CONSTANTS APPLIED/REMOVED 3. ALL CHANNELS WERE OUTPUT 4. OUTPUT 4796 ms 5. VARIOUS TIME LENGTHS 6. AUX CHANNELS (-1,-2,...,5) AND SEIS 1-48 PER FIELD RECORD 7. NO TIME DELAYS WERE APPLIED OR RECORDED IN TRACE HEADERS	LDGO 2D processing Processed by: LDGO, Marek Truchan Date: 1978 Processing sequence: 1. ALL TRACES USED 2. Burg decon (some lines) 3. Filter: 220 ms 4. White noise: 100 5. Band pass: Low cut width: 6, 3; High cut width: 70, 10 6. Shade applied: 1 + 50 7. Times offset 8. Water velocity moveout 9. Moveout using vel analysis #1 10. Weiner filter: 200 ms 11. White noise: 0 12. PRED DIST: 0 ms 13. USE: 0 ms from 0 for filter 14. MINDEPTH: 200 15. P SCALE FACTOR: 0.89 16. PRED DIST BASED ON SEA FLOOR TIME 17. MINIMUM DIST: 0 ms 18. DIFFERENTIAL MOVEOUT USING VEL ANALYSIS # 1 19. TRACES STACKED	Geco 2D acquisition, D. Hill Acquired by: Geco Vessel: M/V Malene Østervold Date: 17th July 1985 – 2nd Sept 1985 Source: 1 Streamer: 1 (Sercel Seal) Record length: 7200 ms (JM-85-16) & 15300 ms (JM-85-26) Recording sample rate: 4 ms Fold: 30 (JM-85-26) & 60 (JM-85-16) High Cut Filter, all : 90 Hz @ 72 dB/octave Low Cut Filter, hydrophone : 3.5 Hz @ 18 dB/octave Streamer length: 3000 m Number of channels: 120 Numbers of phones per group: 40 Group interval: 50 m Near offset: 111 m Streamer depth: 10 (lowered to 12-13 m during bad weather) SP interval: 25 m & 50 m Source: Air guns - Geco super wide Sub-arrays: 6 Source volume: 3564 in3 Source pressure: 1900 psi Source depth: 7.5 m +/- 1 m
Static corrections	-	-	-

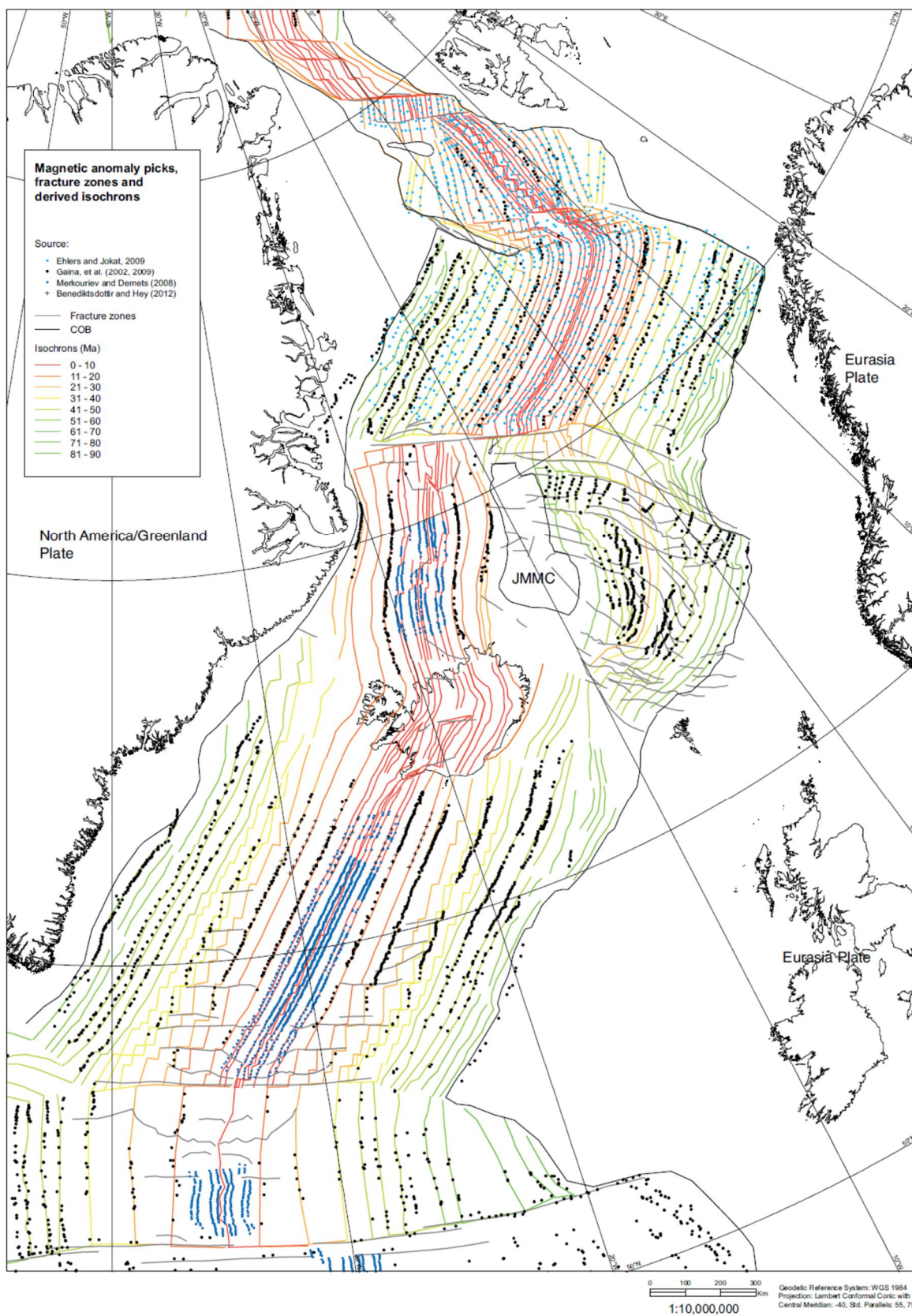
Survey	IS-JMR-01 (2001)	ICE02	IS-JMR-01 (2008)
Date	July 20th 2001 – 12th Aug 2001	June 2002	July 20th 2001 – 12th Aug 2001
Acquisition Vessel:	M/V Polar Princess	M/V Zephyr	M/V Polar Princess
Acquisition done by:	Multiwave Geophysical Company, Geir Valsvik	TGS	Multiwave Geophysical Company, Geir Valsvik
Processing done by:	Geotrace 2D Processing, Richard Goodchild	TGS, Tel:0044 (0)1234-272122	Geotrace 2D Processing, Richard Goodchild
References:	http://kortasia.os.is:8080/geoserver/www/landgrunnsja/en/index.html	http://kortasia.os.is:8080/geoserver/www/landgrunnsja/en/index.html	http://kortasia.os.is:8080/geoserver/www/landgrunnsja/en/index.html
Type and frequency content of seismic source	Bolt Airgun 4240 in3 / xx	Bolt gun type 1900 LL-X 4120 cu.in / xx	Bolt Airgun 4240 in3 / xx
Streamer length and channel interval	10000 m / 12.5 m	8081,5 m / 12,5 m	10000 m / 12,5 m
Sample rate, record length, filters applied during recording	<p>MGC 2D acquisition</p> <p>Acquired by: Multiwave Geophysical Company, Geir Valsvik Vessel: M/V Polar Princess Date: July 20th 2001 – 12th Aug 2001 Source: 1 Streamer: 1 (Sercel Seal) Record length: 10000 ms Recording sample rate: 2 ms High Cut Filter, all : 200 Hz @ 370 dB/octave Low Cut Filter, hydrophone : 3 Hz @ 12 dB/octave SODD: 50 ms Streamer length: 10050 m Number of channels: 804 Group interval: 12.5 m Near offset: 111 m Streamer depth: 8 m +/- 1 m SP interval: 25 m Subarrays: Single source / 4 strings Source volume: 4240 in3 Source pressure: 2000 psi Source depth: 6 m +/-1 m</p>	<p>TGS-NOPEC 2D acquisition</p> <p>#Acquired by: TGS-NOPEC, #Vessel: MV ZEPHYR-1 #Date: June 2002 #Source: 1 (Tuned Bolt Array) #Streamer: 1 (Syntrac 960-24) #Record length: 10240 ms #Recording sample rate: 2 ms #High Cut Filter, all : #Low Cut Filter, hydrophone : #Streamer length: 8000 m #Number of channels: 636 + 12 AUX (144m) #Group interval: 12.5 m #Nominal Fold: 106 Near offset: 111 m #Streamer depth: 9 m #SP interval: 37.5 m Subarrays: Single source / 4 strings #Source volume: 4120 in3 #Source pressure: 2000 psi #Source depth: 9 m</p>	<p>MGC 2D acquisition</p> <p>Acquired by: Multiwave Geophysical Company, Geir Valsvik Vessel: M/V Polar Princess Date: July 20th 2001 – 12th Aug 2001 Source: 1 Streamer: 1 (Sercel Seal) Record length: 10000 ms Recording sample rate: 2 ms High Cut Filter, all : 200 Hz @ 370 dB/octave Low Cut Filter, hydrophone : 3 Hz @ 12 dB/octave SODD: 50 ms Streamer length: 10050 m Number of channels: 804 Group interval: 12.5 m Near offset: 111 m Streamer depth: 8 m +/- 1 m SP interval: 25 m Subarrays: Single source / 4 strings Source volume: 4240 in3 Source pressure: 2000 psi Source depth: 6 m +/-1 m</p>
Shot interval, CDP interval, fold	Shot interval: 25 m / Fold: 201	Shot interval: 37,5 m / Fold: 106	Shot interval: 25 m / Fold: 201
Processing sequence including information on filters and gains applied (at what stage, type filter flanks, type of gain)	<p>Ensign Geophysics (AS) 2D processing</p> <p>Processed by: Ensign Geophysics (AS) Date: March 2002 Processing sequence: 1. Seg-d Reformat 2. SODD Correction -50ms 3. Amplitude Decay Recovery 4. Anit-Alias Filter 5. Resamp to 4ms 6. 3Hz Low Cut Filter 7. Spatial Anti-Alias Filter 8. Alternate Trace Drop 9. Prelim Velocity Analysis - 2km 10. Spike Removal 11. 2D CDP Sort - 201 fold 12. NMO Correction 13. Multiple Attenuation - Radon 14. Designature 15. DMO Correction - 1500m/s 16. Pre-Stack Stolt Migration - 1460 m/s 17. Final Velocity Analysis - 1km 18. Median Stack - 201 Fold 19. Demigrate 20. AGC Correction - 1000ms iterative 21. W-X Migration 22. FK Filter - +/-5ms dip/trace</p>	<p>TGS 2D processing proprietary</p> <p>Processed by: TGS Date: JULY-SEPT02 Processing sequence:</p>	<p>Geotrace 2D processing</p> <p>Processed by: Geotrace 2D acquisition, Richard Goodchild Date: March 2008 - Sept 2008 Processing sequence: 1. SEG-D reformat 2. 3Hz. low cut filter 3. SODD 4. Shot & chan edits 5. AAF & resample to 4ms 6. Desig. to Zero Phase 7. TT Sph. Div. 8. Automatic Despike 9. TFD Swell Noise attenuation in receiver domain 10. SAAF & Alternate Trace Drop 11. SRME at 25m 12. Preliminary NMO (1km) 13. FK dip filter on shots +/-12ms/tr 14. FX deconvolution in shot domain 15. FDNA diffracted multiple attenuation 16. TVF 17. Migration velocity analysis (1km) 18. Removal of T*T Gain 19. 2D Kirchhoff PreSTM 20. 1km residual velocity analysis 21. Radon demultiple</p>
Static corrections	-50 ms	-60 ms	+10 ms

Survey	WI-JMR-08	NPD-JM-11	NPD-1202
Date	21st June, 2008 - 28th Jun, 2008	8th June, 2011 - 03rd July, 2011	3rd June, 2012 - 10th Aug, 2012
Acquisition Vessel:	M/V Malene Østervold	M/V Harrier Explorer	M/V Nordic Explorer
Acquisition done by:	Wavefield Inseis ASA, Finn-Uwe Strumke	PGS 2DMCS, C. A. Syles	PGS 2DMCS, Gabriele Jones
Processing done by:	Geotrace 2D Processing, Richard Goodchild	PGS Geophysical DP (Oslo), Jørn K. Larsen	PGS Geophysical DP (Oslo), Jørn K. Larsen
References:	http://kortasia.os.is:8080/geoserver/www/landgunnssj/le/index.html	http://kortasia.os.is:8080/geoserver/www/landgunnssj/le/index.html	http://kortasia.os.is:8080/geoserver/www/landgunnssj/le/index.html
Type and frequency content of seismic source	Bolt Airgun 4100 in ³	Bolt 1900 LLXT 4130 in ³ / Air pressure: 2000 psi	Bolt 1900 LLXT 4130 in ³ / Air pressure: 2000 psi
Streamer length and channel interval	10050 m / 12,5 m	8100 m / 12,5 m	8100 m / 12,5 m
Sample rate, record length, filters applied during recording	<p>WI 2D acquisition</p> <p>Acquired by: Wavefield Inseis ASA, Finn-Uwe Strumke March to September 2008 Vessel: M/V MALENE ØSTERVOLD Date: June 8th 2011 – 3rd July 2011 Source: 1 Streamer: 1 (Sercel Fluid Seal-ALS) Record length: 10000 ms Recording sample rate: 2 ms Sample interval segy: 4 ms Low Cut Filter 3.0 Hz / -6 dB IIR = OUT Hi Cut Filter 200 Hz@ 370 dB/Oct SODD: 50 ms Streamer length: 10050 m Number of channels: 804 Group interval: 12.5 m Near offset: 216 m Streamer depth: 12 m +/- 1 m SP interval: 25 m Source volume: 4100 in³ Source pressure: 2000 psi Source depth: 10 m +/- 1 m Source first SP: 1001 Source last SP: 4814</p>	<p>PGS 2D acquisition</p> <p>Acquired by: PGS 2DMCS, Gabriele Jones Vessel: M/V HARRIER EXPLORER Date: June 8th 2011 – 3rd July 2011 Source: 1 Streamer: 1 (Geostreamer) Sensors: 2 Record length: 9216 ms Recording sample rate: 2 ms High Cut Filter, all : Low Cut Filter, hydrophone : Low Cut Filt, match geosens : Gain Setting, hydrophone : Streamer length: 8100 m Number of channels: 2 x 648 Group interval: 12.5 m Streamer depth: 25 m SP interval: 25 m Subarrays: 3 Source volume: 4130 in³ Source pressure: 2000 psi Source depth: 7M</p>	<p>PGS 2D acquisition</p> <p>Acquired by: PGS 2DMCS, Gabriele Jones Vessel: M/V NORDIC EXPLORER Date: 3rd Jun 2012 – 10th Aug 2012 Source: 1 Streamer: 1 (Geostreamer) Sensors: 2 Record length: 9216 ms Recording sample rate: 2 ms High Cut Filter, all: Low Cut Filter, hydrophone: Low Cut Filter, matched geosensor: Gain Setting, hydrophone: Streamer length: 8100 m Number of channels: 2 x 648 Group interval: 12.5 m Streamer depth: 25 m SP interval: 25 m Subarrays: 3 Source volume: 4130 in³ Source pressure: 2000 psi Source depth: 7 m</p>
Shot interval, CDP interval, fold	Shot interval: 25 m / Fold: 201	25 m / 11 traces = 1 CDP / 162	25 m / 11 traces = 1 CDP / 162
Processing sequence including information on filters and gains applied (at what stage, type filter flanks, type of gain)	<p>Geotrace 2D processing</p> <p>Processed by: Geotrace 2D Processing, Richard Goodchild Date: March 2008 - Sept 2008 Processing sequence: 1. SEG-D REFORMAT 2. 3HZ. LOW CUT FILTER 3. SODD 4. SHOT & CHAN EDITS 5. AAF & RESAMPLE TO 4MS 6. DESIG. TO ZERO PHASE 7. T*T SPH. DIV. 8. AUTOMATIC DESPIKE 9. TFD SWELL NOISE ATTENUATION IN RECEIVER DOMAIN 10. SAAF & ALTERNATE TRACE DROP 11. SRME AT 25M 12. PRELIMINARY NMO (1KM) 13. FK DIP FILTER ON SHOTS +/-12MS/TR 14. FX DECONVOLUTION IN SHOT DOMAIN 15. FDNA DIFFRACTED MULTIPLE ATTENUATION 16. TVF 17. MIGRATION VELOCITY ANALYSIS (1KM) 18. REMOVAL OF T*T GAIN 19. 2D KRCHHOFF PRESTM</p>	<p>PGS 2D proprietary</p> <p>Processed by: PGS Geophysical DP (Oslo), Jørn K. Larsen Date: Aug 2011 - Aug 2012 Processing sequence:</p>	<p>PGS 2D proprietary</p> <p>Processed by: PGS Geophysical DP (Oslo), Jørn K. Larsen Date: July 2012 - Feb 2013 Processing sequence:</p>
Static corrections	-15 ms	PGS: Gun and cable static correction: +21.62 ms / Recording system delay correction: -69.2 ms	PGS: Gun and cable static correction: +21.62 ms / Recording system delay correction: -69.2 ms

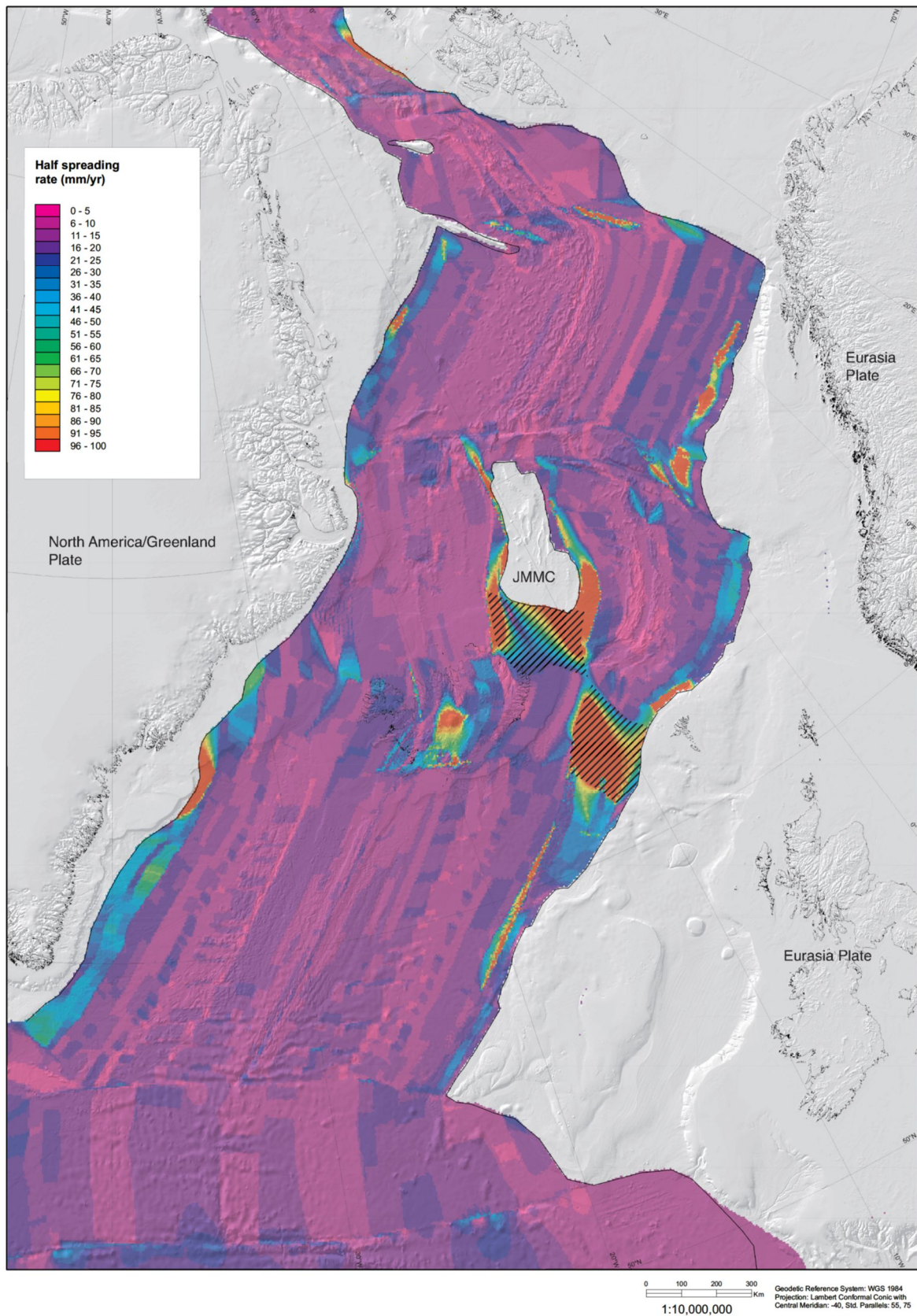
Appendix 3 Regional kinematic input data

From Gaina et al. (2014, 2017b)

Magnetic anomaly picks, fracture zones, and derived isochrons for the NAGTEC area. Additional picks and fracture zones from surrounding areas also constrain the kinematic model by Gaina et al. (2014, 2017b).



Half spreading rate grid for the oceanic crust based on the final kinematic model. Hachure regions around Jan Mayen and the Faroe Islands are unconstrained and misleadingly high by Gaina et al. (2014, 2017b).



Reconstruction of the residual bathymetry at Chron times C5 (11.1 Ma), C6 (19.722 Ma), C13 (33.16 Ma), C18 (40.32 Ma), C21 (47.329 Ma) and C24 (53.93 Ma) by Gaina et al. (2014, 2017b).

